REGULATION OF CENTROSOME DUPLICATION BY 14-3-3 PROTEINS AND ITS CONSEQUENCES FOR REGULATING NEOPLASTIC PROGRESSION

By

BOSE ARUNABHA HIREN SUREKHA

(LIFE09201204013)

Tata Memorial Centre, Mumbai

A thesis submitted to the

Board of Studies Life Sciences

In partial fulfillment of requirements

for the Degree of

DOCTOR OF PHILOSOPHY

of

HOMI BHABHA NATIONAL INSTITUTE

JULY, 2019

Homi Bhabha National Institute

Recommendations of the Viva Voce Committee

As members of the Viva Voce Committee, we certify that we have read the dissertation prepared by Ms. Arunabha Bose entitled "Regulation of centrosome duplication by 14-3-3 proteins and its consequences for regulating neoplastic progression" and recommend that it may be accepted as fulfilling the thesis requirement for the award of Degree of Doctor of Philosophy.

Chairperson – Dr. Neelam Shirsat — Date: 27th September 2019

Guide/Convener – Dr. Sorab N. Dalal — Date: 27th September 2019

External Examiner – Dr. B. J. Rao — Date: 27th September 2019

Member – Dr. Prasanna Venkatraman — Date: 27th September 2019

Member – Dr. Dibyendu Bhattacharyya — Date: 27th September 2019

Final approval and acceptance of this thesis is contingent upon the candidate's submission of the final copies of the thesis to HBNI.

I hereby certify that I have read this thesis prepared under my direction and recommend that it may be accepted as fulfilling the thesis requirement.

Date: 27th September 2019
Place: Navi Mumbai

Dr. Sorab N. Dalal
Guide

STATEMENT BY AUTHOR

This dissertation has been submitted in partial fulfillment of requirements for an advanced degree at Homi Bhabha National Institute (HBNI) and is deposited in the Library to be made available to borrowers under rules of the HBNI.

Brief quotations from this dissertation are allowable without special permission, provided that accurate acknowledgement of source is made. Requests for permission for extended quotation from or reproduction of this manuscript in whole or in part may be granted by the Competent Authority of HBNI when in his or her judgment the proposed use of the material is in the interests of scholarship. In all other instances, however, permission must be obtained from the author.

Arunabha Bose.

DECLARATION

I, hereby declare that the investigation presented in the thesis has been carried out by me. The work is original and has not been submitted earlier as a whole or in part for a degree / diploma at this or any other Institution / University.

Arunabha Bose.

List of Publications arising from the thesis

Journal

1. **Bose, A.** & Dalal, S. N. 14-3-3 proteins mediate the localization of Centrin2 to centrosome. *Journal of Biosciences*, (2019), *44*, 1-10 .

2. Mukhopadhyay, A., Sehgal, L.*, **Bose, A***. *et al.* 14-3-3γ Prevents Centrosome Amplification and Neoplastic Progression. *Sci. Rep.*, (2016), *6*, 1–19 (*indicates equal contribution).

3. **Bose, A.,** et. al, 14-3-3γ prevents centrosome duplication by inhibiting NPM1 function (manuscript submitted).

Chapters in books and lectures notes

1. **Bose, A.** and Dalal, S.N. Centrosome amplification and tumorigenesis – cause or effect? (2019) in "*The Golgi apparatus and Centriole - Functions, interactions and role in disease"*, Springer Publications.

Conference/Symposium

1. Presented a poster titled, "Regulation of centrosome duplication by 14-3-3γ" at the **EMBO – Centrosome and Spindle Bodies conference** held in Heidelberg, Germany from the 24th – 27th of September, 2017.

2. Participated in the "STED imaging workshop" organized by Leica, at IISER Pune, from the 25th – 27th of October, 2016.

3. Participated in the workshop on "Transmission Electron Microscopy" organized by ACTREC and JEOL India, from the 6th – 7th of October 2016.

4. Presented a poster titled, “Regulation of centrosome duplication by 14-3-3 proteins” at the XXXIX All India Cell Biology Conference (**AICBC**) – Cellular Organization and Dynamics, from the 04th – 10th of December, 2015.

5. Participated in the 12th National Research Scholar’s Meet, held at ACTREC from the 15th – 16th of November 2015

6. Presented a poster titled, “Regulation of centrosome duplication by 14-3-3 proteins and its consequences for regulating neoplastic progression” at the international conference, “Carcinogenesis”, held at ACTREC from the 11th – 13th of February 2015.

This Thesis is dedicated to my family who have taught me everything I know and always believed in me.

ACKNOWLEDGEMENTS

The work that is presented in this thesis would be absolutely impossible without the presence and support of a lot of people. I am glad I have this opportunity to thank all of them here, because I know I won't be able to say all of this in person.

When I think about all the people who have helped me on this journey, there is no one who has had as huge an impact on me as my PhD supervisor, Sorab. Sorab has taught me so much in so many ways (he will of course say that I've forgotten everything). He has been a guide, a friend, a mentor and a tough task master. His best quality is his ability to always cheer us up when we go to him deflated with failed experiments, while also making us rein in our enthusiasm when we get too excited about a good result. Even when he gets mad at us, it is mostly because he genuinely believes that we can be better. He has taught me the importance of designing well controlled experiments and the value of being dispassionate while assessing data. I'm not exaggerating when I say that he is one of the kindest people I know. Thank you for everything.

I thank Dr. Sudeep Gupta (Director, ACTREC), Dr. Shubhada Chiplunkar (ex-Director, ACTREC), and Dr. Rajiv Sarin (ex-Director, ACTREC) for providing us with good infrastructure, academic and technical support. I would like to thank Dr. Neelam Shirsat (DC Chairperson), Dr. G.B. Maru (ex-DC Chairperson), Dr. Prasanna Venkatraman and Dr. Dibyendu Bhattacharyya (my DC members) for all their valuable suggestions during my PhD. A special thanks to Dr. Venkatraman for all the 14-3-3 collaboration work and kudos for being an all-round star and inspiration (I know everyone from my lab will agree).

I thank ACTREC for providing me with the PhD fellowship all these years and Sorab for funding me these past two years. I also thank DBT for funding this project.

I would like to thank Prasanna lab members, Kruti, Somavally and Mukund for all the 14-3-3 related work. Dr. Tapas Kundu and Suchismita, I thank for all your help with the NPM1 experiments.

This project involved a lot of imaging work, for which I will be eternally grateful to Vaishali Ma'am, Tanuja Ma'am and Jayraj at the ACTREC imaging facility. I have learnt a lot from Vaishali Ma'am and admire her curiosity and constant endeavour to get better at everything she does. I would like to thank all the members from Common instrument facility (Mr. Uday Dandekar, always ready to help, no matter the time), EM facility (Siddhi and Dr. Vinita Sawant), Flow Cytometry facility (Mrs. Rekha and Mrs. Shyamal), DNA sequencing facility, IT facility (Anand Sir), Library (Mrs. Mugdha, Mrs. Swati), SCOPE Cell (Dr. Nalini Hasgekar, Dr. Aparna Bagwe, and Dr. Ojaswini Upasini), Administration (Mrs. Sharvari, Mrs. Chitra, Mrs. Alka and Mr. Anil), Accounts and Program office (Mrs. Maya Dolas) for their help.

My time in the lab was made so much more memorable by all the members of Sorab lab. Srikanta, Sonali, Sarika, Kumar, Mansa, Neelima, Lalit, Amitabha, Mugdha, Nazia, Rahul, Amol, Monika, Bhagyashree, Neha, Poonam, Rajan, Suruchi, Pawar Kaka, Arun, Vishal and all the trainees in the lab, especially the trainees who have worked with me, Prafull, Keerthana, Teja, Shreya, Sufi, Harshini and Sveta. I have to thank Basu for lighting up the lab with his ready humour and songs and for being someone I could always turn to for help. Sarika (Wifey), thank you for being the "hero" of my life, for listening to all my ramblings

and bringing so much “clarity” to my thoughts. Sonali, for being the best friend one could ask for and a great source of comfort in some tough times.

I thank ACTREC for the giving me the opportunity to forge some life-long friendships. Asmi, Ram, Manish, Usha and Mayuri have always brought a smile to my face and I have enjoyed stealing food from all of you. I thank my batchmates, Saujanya, Niru, Pratik, Gopal, Bhavik, Sameer, Jacinth, Prajish, Bhushan and Mukul for all their warmth and camaraderie. This work would be impossible without the constant lending and borrowing of reagents and instruments from all the labs in ACTREC, for which I have to thank the entire ACTREC student community.

There’s not much I can say that can describe the depth of gratitude I feel towards my family. I thank Awwa and Baba for instilling in me a sense of curiosity and wonder at all things, since as long as I can remember. They are the voice in my head and my conscience, that I take everywhere with me. My sister, Poorvi, is the light of my life and I thank her and my parents for all their restraint and unconditional love in putting up with my temper. My husband, Patanjali, is a gift to me in every way and I cherish (and unfortunately, sometimes take advantage of) his patience and kindness. I have to thank my in-laws for giving me so much love and understanding. My one friend and enemy, Neha, you know how important you are to me, so I’m not going to say more. It fills me with great joy to imagine how happy you all would be to hold this thesis in your hands!

INDEX

Synopsis

Homi Bhabha National Institute

SYNOPSIS OF Ph. D. THESIS

1. **Name of the Student: Arunabha Bose**
2. **Name of the Constituent Institution: Tata Memorial Centre, ACTREC**
3. **Enrolment No.: LIFE09201204013**
4. **Title of the Thesis: Regulation of centrosome duplication by 14-3-3 proteins and its consequences for regulating neoplastic progression.**
5. **Board of Studies: Life Sciences**

SYNOPSIS

(Limited to 10 pages in double spacing)

SYNOPSIS

Introduction

The cell cycle ensures that duplicated DNA is divided equally into two daughter cells. Progression through a cell cycle involves the sequential activation and deactivation of cyclin-dependent kinases (CDKs) (1). CDK activity is dependent on the partner cyclins and is regulated both positively and negatively by phosphorylation (reviewed in (2)). CDK inhibitors (CKIs) bind to and inactivate CDK–cyclin complexes (2). Sequential activation of different CDKs is responsible for controlling the onset of S

phase and mitosis, and for ensuring that, with certain notable exceptions, S-phase always alternates with M-phase in each cell cycle (3).

Accurate genome segregation in the cell-division cycle is mediated by the microtubule organizing function of the centrosome. The centrosome is a membrane-less organelle, comprising of two centrioles, a mother and a daughter, surrounded by a proteinaceous cloud, the pericentriolar matrix (PCM) (4,5). The two centrioles differ in age, maturity and the amount of PCM they nucleate. Centrosome duplication is initiated at the G1–S transition of the cycle, at the same time at which DNA replication is initiated, and is coincident with cdk2-dependent phosphorylation of centrosomal substrates and the subsequent moving apart or 'splitting' of the centriole pair (6). Procentriole nucleation occurs orthogonal to each mother centriole during S phase (7). These nascent procentrioles become mature full-length structures by the end of G2 (8). By M-phase both centrosomes have acquired the maximal amount of PCM and migrate to the two ends of the spindle to form the poles (9,10). Following cytokinesis, a normal diploid cell inherits one centrosome. Centrosome amplification contributes to tumorigenesis while the presence of less than two centrosomes in a mitotic cell leads to errors in genome segregation (11-14). Therefore, regulation of centrosome duplication is an essential process that is required for accurate genome segregation.

14-3-3 proteins are a group of small, dimeric, acidic proteins with seven isoforms in mammalian cells (15). Most 14-3-3 proteins bind to their ligands via one of two consensus motifs, RSXpSXP or RXYFXpSXP, although a number of ligands bind to 14-3-3 in a phospho-independent manner (16-18). Previous studies have shown that only two isoforms, 14-3-3ε and 14-3-3 γ, can bind to and inhibit cdc25C function (19). 14-3-3 binding to cdc25C controls both cdc25C localization and cdc25C activity (20,21). Previous studies have also shown that the loss of 14-3-3γ leads to an increase in centrosome number, chromosome instability and tumorigenesis (22).

One of the goals of this study is to understand how loss of 14-3-3γ leads to centrosome duplication, as the mechanisms that mediate centriole licensing and duplication are still unclear. In order to answer this question, we have undertaken two approaches. In the first approach, we have attempted to identify which centrosomal proteins 14-3-3 proteins bind to. Upon identifying these proteins, we have tried to map the 14-3-3 binding site on these proteins and tested for the phenotypes that occur upon loss of 14-3-3 binding. In the second approach, we have endeavoured to understand which residues in 14-3-3 proteins are important for mediating ligand binding.

Also, it has been shown that with an increase in passage of cells harbouring a knockdown of 14-3-3γ, there is an increase in centrosome clustering (22). Clustering of multiple centrosomes furnishes an adaptive advantage to cancer cells, which are usually aneuploidy (23,24). These experiments have been performed in fixed samples, so one of the goals of this study is to study how clustering occurs in the 14-3-3γ knockdown cells in a live cell imaging system.

Objectives

1. Does 14-3-3 binding to centrosomal proteins inhibit centrosome licensing and duplication?

2. Does centrosome clustering increase upon 14-3-3γ knockdown?

Results and discussion

1. *Does 14-3-3 binding to centrosomal proteins inhibit centrosome licensing and duplication?*

1.1 *Which centrosomal proteins do 14-3-3 proteins bind to?*

Previous results have demonstrated that 14-3-3γ binds to centrosomal proteins such as γ-tubulin and centrin using FRET (22). This was confirmed in GST pull-down assays, in which it was demonstrated that 14-3-3 proteins formed a complex with γ-tubulin, Centrin2, Cep-170, and GCP2, all centrosomal proteins. Based on these results, a

motif scan was performed to identify putative 14-3-3 binding sites on these proteins. However, the scan did not generate any positive results for the proteins Centrin2, GCP2 and γ-tubulin. To address this question, several deletions of the centrosomal proteins described above were designed and were tested for their ability to form a complex with 14-3-3 proteins.

Centrin2 is the most ubiquitously expressed isoform of the centrin family of proteins (25). In mammalian cells, Centrin-2 is essential for centriole biogenesis (26). Centrin2 localizes to the distal lumen of centrioles throughout the cell cycle (27) and has four EF hand domains. An analysis of several N and C-terminal deletions of Centrin2 demonstrated that 14-3-3 proteins bind to Centrin2 via the first EF hand domain. The 14-3-3 binding deficient mutant is also unable to localize to the centrosome. Based on our results, we hypothesize that binding to 14-3-3 proteins is essential for the centrosomal localisation of Centrin2 (28).

Three mutants of γ-tubulin, each with a deletion of progressive C terminal domains were cloned into pECFP-N1 vector. All the mutants express correctly and localize to the centrosome. We then performed GST pull-down assays using GST tagged 14-3-3γ in order to map the 14-3-3γ binding site on γ tubulin. We mapped the binding to the first domain of γ tubulin, i.e., the FtsZ / GTPase domain. In order to confirm this, we are generating a mutant that does not express this FtsZ/GTPase domain.

Three mutants of GCP2, each with a deletion of progressive C terminal domains were cloned into ECFP-N1 vector. All the mutants express correctly and localize to the centrosome. Further, GST pulldowns and Co-IP assays need to be standardised in order to map the 14-3-3 binding site.

Upon performing a bioinformatics scan to search for putative 14-3-3 binding sites on Cep170, we found that there were three such sites; Thr-644, Thr-1078 and Thr-1259. We have generated site directed mutants of Cep170 and are testing their binding with 14-3-3γ. We have found that the levels of Cep170 are decreased in HCT116 derived

14-3-3γ knockdown cells in Western blot experiments. However, we were unable to observe the same in immunofluorescence experiments.

1.2 *How do negatively charged residues in the peptide binding groove of 14-3-3 proteins regulate ligand function?*

Most ligands of 14-3-3 proteins bind via a phosphorylated serine at a defined motif, RSXpSXP or RXYFXpSXP, although a number of ligands bind to 14-3-3 in a phospho-independent manner (16-18). It has been demonstrated that the 14-3-3 residues important for phosphor-peptide binding are conserved within all 14-3-3 isoforms. The binding site for the phosphor-serine consists of a basic pocket composed of Lys-50, Arg-57 and Arg-128 and Tyr-129, within the third and fifth helices (16,17,29). We wanted to understand if there are other residues with the 14-3-3 peptide binding groove that also contribute to ligand binding. A sequence alignment of the seven 14-3-3 isoforms demonstrated that there are two negatively charged residues, an Aspartate 129 (D129) and a Glutamate 136 (E136) in 14-3-3γ, that are conserved within the peptide binding groove of all 14-3-3 isoforms. It has been demonstrated that 14-3-3 possess ATPase activity and that mutation of the Aspartate 129 to an Alanine (D129A) results in an increase in ATPase activity and oligomerization (30). Therefore, we decided to test the contribution of these two negatively charged residues to ligand binding by mutating them to Alanine.

To this end, site directed mutants of 14-3-3γ, D129A, E136A and D129AE136A were generated and cloned into an mOrange CMV vector. As a knockdown of 14-3-3γ leads to an increase in centrosome number (22), we wished to determine the effect of these mutant 14-3-3 proteins on centrosome duplication by over-expressing them in HCT116 cells. Centrosome number was determined in 100 transfected mitotic cells as described previously (22). Cells transfected with either the vector control or the WT construct showed the presence of two centrosomes in mitotic cells. In contrast, a statistically significant proportion of mitotic cells expressing the D129A construct

contained a single centrosome while expression of the E136A mutant led to the presence of >2 centrosomes in mitotic cells. Expression of the double mutant, D129AE136A leads to the presence of two centrosomes in mitosis, an example of intragenic complementation suggesting that each of these mutants can suppress the phenotype of the other mutant. Similar results were observed in the HCT116 derived vector control and 14-3-3γ knockdown cells and in other cell lines such as HEK293 and HaCaT cells. Given that the phenotypes were observed in all cell types all further experiments were performed in HCT116 cells.

In order to determine centriolar organization in cells containing single or multiple centrosomes, HCT116 cells were co-transfected with each of the mOrange 14-3-3γ constructs and EGFP centrin2 to visualise centrioles. After synchronization at mitosis, the cells were stained with antibodies to pericentrin and DAPI to visualize DNA. Cells transfected with either mOrange alone or the WT construct showed two Centrin2 dots in each pericentrin cloud. In contrast, cells transfected with the D129A mutant, which contained single centrosomes based on pericentrin staining, showed the presence of 2 Centrin2 dots within the single pericentrin cloud. This suggested that there could be a defect in duplication or disjunction of the centriolar pair. Cells transfected with the E136A mutant, which showed multiple pericentrin dots also displayed two Centrin2 dots contained within each pericentrin cloud. A similar phenotype was observed in cells expressing the D129AE136A mutant.

To test whether the two centrioles seen in the single centrosomes observed upon expression of the D129A mutant had a defect in duplication or disjunction, we stained for Cep68, an intercentrosomal linker protein. We observed the presence of two dots for Cep68, colocalising with each of the 2 Centrin2 dots. Therefore, we can conclude that the single centrosomes seen in cells expressing the D129A mutant are due to a defect in duplication. We also stained for Ninein, a subdistal appendage marker, in order to test the age of the two centrioles seen in cells expressing the D129A mutant.

Ninein localises specifically to the older of the two mother centrioles in interphase. We observed that the two Centrin2 dots seen in cells expressing the D129A mutant co-localised with a single ninein dot. Given the results of the Cep68 and the ninein staining, it means that the single centrosome observed in cells expressing the D129A mutant is a centrosome with disengaged centrioles that are unable to duplicate.

Based on the data obtained, we concluded that there is a centrosome duplication defect in cells with a single centrosome expressing the 14-3-3γ D129A mutant, i.e. they were unable to form procentrioles. In order to rescue the single centrosome defect, we overexpressed certain proteins that are extremely essential for procentriole formation. Overexpression of Plk4 increases centriole numbers and leads to de novo centrosome formation (31). Over-expression of either Cdk1 or Cdk1-AF resulted in an increase in centrosome over-duplication in HCT116 cells (22). Increased Cdk2 activity allows cells to accumulate multiple centrosomes (32). However, when tested, these constructs were unable to reverse the single centrosome phenotype.

Another protein required for centriole duplication is Nucleophosmin 1(NPM1) (33,34). Phosphorylation of NPM1 at a Threonine 199 (T199) residue by cdk2 releases NPM1 from the centrosome (34). This acts as a licensing factor for centriole duplication and triggers centriole biogenesis. HCT116 cells were co-transfected with each of the mOrange tagged 14-3-3γ mutants and either Flag epitope tagged WT NPM1 a phosphor-deficient mutant (T199A) or a phosphor-mimetic mutant (T199D) to determine if NPM1 expression could lead to an override of the single centrosome or multiple centrosome phenotype observed with the 14-3-3γ mutants. We observed that wild type NPM1 (WT) was able to partially rescue the single centrosome phenotype seen in cells expressing the D129A mutant. Expression of the T199D mutant was able to completely rescue the single centrosome phenotype seen in cells expressing the D129A mutant. Expression of the T199A mutant was able to rescue the multiple centrosome phenotype in cells expressing the E136A construct. These results

suggested that the phenotypes observed in cells expressing the D129A and E136A mutants might be due to the interaction between NPM1 and 14-3-3γ.

The WT and 14-3-3γ mutant constructs were cloned into HA pcDNA3 transfected into HCT116 cells. Co-immunoprecipitation assays demonstrated that the D129A mutant bound with greater efficiency to NPM1 as compared to the WT. The E136A mutant did not bind to NPM1. The D129AE136A mutant bound to NPM1 with a lower affinity as compared to WT.

A motif scan identified three putative 14-3-3 binding sites on NPM1 S48, S143 and S292. We performed site directed mutagenesis to convert each of the serine residues to alanine so that they can no longer be phosphorylated. Upon testing their binding to 14-3-3γ using a GST pull-down assay, we determined that only the S48A mutant was unable to bind to 14-3-3γ. We tested the effect of the S48A mutant on centrosome number by co-transfecting it into HCT116 cells along with each of the 14-3-3γ mutants. We found that the S48A is able to rescue the single centrosome phenotype seen upon expression of D129A.

Since the NPM1 S48A mutant is able to reverse the single centrosome phenotype seen upon expression of D129A, we performed site directed mutagenesis to create an NPM1 S48E mutant. It is hypothesized that the S48E is a phosphomimetic mutant. We observed that the S48E mutant binds to 14-3-3γ. We tested the effect of the S48E mutant on centrosome number and found that it reverses the multiple centrosome phenotype observed upon expression of E136A.

The T199 phosphorylation status of the NPM1 WT, S48A and S48E mutants was also tested. To this end, HCT116 cells were transfected with each of the ECFP tagged NPM1 constructs and T199A was used as a negative control for T199 phosphorylation. We hypothesized that since the S48A mutant is able to rescue the single centrosome phenotype, it should be highly phosphorylated at T199. Conversely, since the S48E mutant is able to rescue the multiple centrosome

phenotype, it should have T199 phospho levels comparable to that seen upon expression of NPM1 T199A. And that is what we observed.

Our results suggest that the centrosome phenotypes observed upon expression of the different 14-3-3γ mutants are due to differential binding of these mutants to NPM1. In case of the D129A mutant, it binds to NPM1 with a high affinity. This inhibits the ability of NPM1 to dissociate from the centrosome upon phosphorylation by CDK2 at T199. Expression of 14-3-3γ binding deficient mutant, NPM1 S48A, is therefore able to reverse this phenotype. In case of the E136A mutant, which is unable to bind to NPM1, NPM1 dissociates from the centrosome prematurely, which leads to centrosome amplification. Expression of the S48E mutant, which binds to 14-3-3γ, is thus able to reverse this phenotype. The D129AE136A mutant behaves like WT 14-3-3γ due to intragenic complementation.

2. *Does centrosome clustering increase upon 14-3-3γ knockdown?*

Normal cells with multiple centrosomes undergo a multipolar mitosis. A multipolar mitosis leads to massive aneuploidy and has negative consequences on the viability of cells (35). However, most transformed cells with multiple centrosomes undergo a clustered mitosis (6). It has been proven that the clustering phenotype shown by cells with multiple centrosomes is a mechanism leading to increased survival of transformed cells (23,24).

It has been demonstrated that a loss of 14-3-3γ gives rise to multiple centrosomes (22). Further, it has also been demonstrated that with an increase in passage of the 14-3-3γ, there is an increase in the percentage of cells undergoing a clustered mitosis (22). However, these experiments were performed in fixed samples and the cells counted were mainly prophase cells. Centrosome clustering is a phenomenon that can be truly tested only in anaphase cells.

In order to perform the above experiments and to follow the 14-3-3γ knockdown cells across the cell cycle, we tried to generate HeLa cells with a stable 14-3-3γ

knockdown. These cells already express H2B-mCherry and α-tubulin GFP. For this purpose, previously verified 14-3-3γ shRNA was cloned into a pLKO Hygro vector (20). Several Hygromycin resistant 14-3-3γ knockdown clones were obtained. However, most of the clones with a knockdown of 14-3-3γ did not survive. And the clones that did survive did not harbour a knockdown of 14-3-3γ. According to a paper published shortly thereafter, upon depletion of 14-3-3γ, HeLa cells display a delay of the cell cycle in the G2/M phase and a decrease in cell proliferation (36). Therefore, we concluded that HeLa cells are not a good model system for our experiments.

To follow the fate of the 14-3-3γ knockdown cells across the cell cycle, using live cell imaging, the following construct was generated. We cloned the H2B-mCherry – IRES -- γ-tubulin-GFP into a pcDNA3 puro vector. Based on a transient transfection of this construct into the vector control and the 14-3-3γ knockdown cells, we were able to observe centrosome amplification in the 14-3-3γ knockdown cell line in an interphase cell. More experiments are needed to verify if the 14-3-3γ knockdown cells with multiple centrosomes prefer a clustered mitosis over a multipolar one with an increase in passage. Also, stable cell lines can be prepared to study the same.

Bibliography

1. Nurse, P. (1997) Checkpoint pathways come of age. *Cell* **91**, 865-867
2. Lim, S., and Kaldis, P. (2013) Cdks, cyclins and CKIs: roles beyond cell cycle regulation. *Development* **140**, 3079-3093
3. Obaya, A. J., and Sedivy, J. M. (2002) Regulation of cyclin-Cdk activity in mammalian cells. *Cellular and molecular life sciences : CMLS* **59**, 126-142
4. Winey, M., and O'Toole, E. (2014) Centriole structure. *Philosophical transactions of the Royal Society of London. Series B, Biological sciences* **369**
5. Conduit, P. T., Wainman, A., and Raff, J. W. (2015) Centrosome function and assembly in animal cells. *Nature reviews. Molecular cell biology* **16**, 611-624

6. Marthiens, V., Piel, M., and Basto, R. (2012) Never tear us apart--the importance of centrosome clustering. *J Cell Sci* **125**, 3281-3292

7. Nigg, E. A., and Holland, A. J. (2018) Once and only once: mechanisms of centriole duplication and their deregulation in disease. *Nature reviews. Molecular cell biology* **19**, 297-312

8. Wang, W. J., Soni, R. K., Uryu, K., and Tsou, M. F. (2011) The conversion of centrioles to centrosomes: essential coupling of duplication with segregation. *J Cell Biol* **193**, 727-739

9. Brinkley, B. R., Cox, S. M., Pepper, D. A., Wible, L., Brenner, S. L., and Pardue, R. L. (1981) Tubulin assembly sites and the organization of cytoplasmic microtubules in cultured mammalian cells. *J Cell Biol* **90**, 554-562

10. Tang, C. J., Fu, R. H., Wu, K. S., Hsu, W. B., and Tang, T. K. (2009) CPAP is a cell-cycle regulated protein that controls centriole length. *Nat Cell Biol* **11**, 825-831

11. Basto, R., Brunk, K., Vinadogrova, T., Peel, N., Franz, A., Khodjakov, A., and Raff, J. W. (2008) Centrosome amplification can initiate tumorigenesis in flies. *Cell* **133**, 1032-1042

12. Levine, M. S., Bakker, B., Boeckx, B., Moyett, J., Lu, J., Vitre, B., Spierings, D. C., Lansdorp, P. M., Cleveland, D. W., Lambrechts, D., Foijer, F., and Holland, A. J. (2017) Centrosome Amplification Is Sufficient to Promote Spontaneous Tumorigenesis in Mammals. *Developmental cell* **40**, 313-322.e315

13. Kazazian, K., Go, C., Wu, H., Brashavitskaya, O., Xu, R., Dennis, J. W., Gingras, A. C., and Swallow, C. J. (2017) Plk4 Promotes Cancer Invasion and Metastasis through Arp2/3 Complex Regulation of the Actin Cytoskeleton. *Cancer Res* **77**, 434-447

14. Sir, J. H., Putz, M., Daly, O., Morrison, C. G., Dunning, M., Kilmartin, J. V., and Gergely, F. (2013) Loss of centrioles causes chromosomal instability in vertebrate somatic cells. *J Cell Biol* **203**, 747-756

15. Aitken, A. (2006) 14-3-3 proteins: a historic overview. *Seminars in cancer biology* **16**, 162-172

16. Yaffe, M. B., Rittinger, K., Volinia, S., Caron, P. R., Aitken, A., Leffers, H., Gamblin, S. J., Smerdon, S. J., and Cantley, L. C. (1997) The structural basis for 14-3-3:phosphopeptide binding specificity. *Cell* **91**, 961-971

17. Rittinger, K., Budman, J., Xu, J., Volinia, S., Cantley, L. C., Smerdon, S. J., Gamblin, S. J., and Yaffe, M. B. (1999) Structural analysis of 14-3-3 phosphopeptide complexes identifies a dual role for the nuclear export signal of 14-3-3 in ligand binding. *Molecular cell* **4**, 153-166

18. Coblitz, B., Shikano, S., Wu, M., Gabelli, S. B., Cockrell, L. M., Spieker, M., Hanyu, Y., Fu, H., Amzel, L. M., and Li, M. (2005) C-terminal recognition by 14-3-3 proteins for surface expression of membrane receptors. *The Journal of biological chemistry* **280**, 36263-36272

19. Dalal, S. N., Yaffe, M. B., and DeCaprio, J. A. (2004) 14-3-3 family members act coordinately to regulate mitotic progression. *Cell cycle (Georgetown, Tex.)* **3**, 672-677

20. Hosing, A. S., Kundu, S. T., and Dalal, S. N. (2008) 14-3-3 Gamma is required to enforce both the incomplete S phase and G2 DNA damage checkpoints. *Cell cycle (Georgetown, Tex.)* **7**, 3171-3179

21. Telles, E., Hosing, A. S., Kundu, S. T., Venkatraman, P., and Dalal, S. N. (2009) A novel pocket in 14-3-3epsilon is required to mediate specific complex formation with cdc25C and to inhibit cell cycle progression upon activation of checkpoint pathways. *Exp Cell Res* **315**, 1448-1457

22. Mukhopadhyay, A., Sehgal, L., Bose, A., Gulvady, A., Senapati, P., Thorat, R., Basu, S., Bhatt, K., Hosing, A. S., Balyan, R., Borde, L., Kundu, T. K., and Dalal, S. N. (2016) 14-3-3 gamma Prevents Centrosome Amplification and Neoplastic Progression. *Sci Rep* **6**, 26580

23. Kwon, M., Godinho, S. A., Chandhok, N. S., Ganem, N. J., Azioune, A., Thery, M., and Pellman, D. (2008) Mechanisms to suppress multipolar divisions in cancer cells with extra centrosomes. *Genes & development* **22**, 2189-2203

24. Ganem, N. J., Godinho, S. A., and Pellman, D. (2009) A mechanism linking extra centrosomes to chromosomal instability. *Nature* **460**, 278-282

25. Wolfrum, U., and Salisbury, J. L. (1998) Expression of centrin isoforms in the mammalian retina. *Exp Cell Res* **242**, 10-17

26. Salisbury, J. L., Suino, K. M., Busby, R., and Springett, M. (2002) Centrin-2 is required for centriole duplication in mammalian cells. *Current biology : CB* **12**, 1287-1292

27. Paoletti, A., Moudjou, M., Paintrand, M., Salisbury, J. L., and Bornens, M. (1996) Most of centrin in animal cells is not centrosome-associated and centrosomal centrin is confined to the distal lumen of centrioles. *J Cell Sci* **109 (Pt 13)**, 3089-3102

28. Bose, A., and Dalal, S. N. (2019) 14-3-3 proteins mediate the localization of Centrin2 to centrosome. *Journal of Biosciences* **44**, 42

29. Brunet, A., Kanai, F., Stehn, J., Xu, J., Sarbassova, D., Frangioni, J. V., Dalal, S. N., DeCaprio, J. A., Greenberg, M. E., and Yaffe, M. B. (2002) 14-3-3 transits to the nucleus and participates in dynamic nucleo-cytoplasmic transport. *J. Cell Biol.* **156**, 817-828

30. Ramteke, M. P., Shelke, P., Ramamoorthy, V., Somavarapu, A. K., Gautam, A. K., Nanaware, P. P., Karanam, S., Mukhopadhyay, S., and Venkatraman, P.

(2014) Identification of a novel ATPase activity in 14-3-3 proteins--evidence from enzyme kinetics, structure guided modeling and mutagenesis studies. *FEBS letters* **588**, 71-78

31. Habedanck, R., Stierhof, Y. D., Wilkinson, C. J., and Nigg, E. A. (2005) The Polo kinase Plk4 functions in centriole duplication. *Nat Cell Biol* **7**, 1140-1146
32. Mantel, C., Braun, S. E., Reid, S., Henegariu, O., Liu, L., Hangoc, G., and Broxmeyer, H. E. (1999) p21(cip-1/waf-1) deficiency causes deformed nuclear architecture, centriole overduplication, polyploidy, and relaxed microtubule damage checkpoints in human hematopoietic cells. *Blood* **93**, 1390-1398
33. Okuda, M., Horn, H. F., Tarapore, P., Tokuyama, Y., Smulian, A. G., Chan, P. K., Knudsen, E. S., Hofmann, I. A., Snyder, J. D., Bove, K. E., and Fukasawa, K. (2000) Nucleophosmin/B23 is a target of CDK2/cyclin E in centrosome duplication. *Cell* **103**, 127-140
34. Tokuyama, Y., Horn, H. F., Kawamura, K., Tarapore, P., and Fukasawa, K. (2001) Specific phosphorylation of nucleophosmin on Thr(199) by cyclin-dependent kinase 2-cyclin E and its role in centrosome duplication. *The Journal of biological chemistry* **276**, 21529-21537
35. Ring, D., Hubble, R., and Kirschner, M. (1982) Mitosis in a cell with multiple centrioles. *J Cell Biol* **94**, 549-556
36. Dar, A., Wu, D., Lee, N., Shibata, E., and Dutta, A. (2014) 14-3-3 proteins play a role in the cell cycle by shielding cdt2 from ubiquitin-mediated degradation. *Mol Cell Biol* **34**, 4049-4061

Publications in Refereed Journal:

a. Published: -

- **Bose, A.** & Dalal, S. N. 14-3-3 proteins mediate the localization of Centrin2 to centrosome. *Journal of Biosciences* **44**, 42, (2019).

- Mukhopadhyay, A., Sehgal, L.*, **Bose, A***. *et al.* 14-3-3γ Prevents Centrosome Amplification and Neoplastic Progression. *Sci. Rep.* **6,** 1–19 (2016) (*indicates equal contribution).

b. Accepted:

c. Communicated: **Bose, A**., et. al, 14-3-3γ inhibits centrosome duplication by inhibiting NPM1 function.

Other Publications:

Book/Book Chapter: **Bose, A.** and Dalal, S.N. Centrosome amplification and tumorigenesis – cause or effect? (2019) in "*The Golgi apparatus and Centriole - Functions, interactions and role in disease",* Springer Publications.

Conference/Symposium:

- Presented a poster titled, "Regulation of centrosome duplication by 14-3-3γ" at the **EMBO – Centrosome and Spindle Bodies conference** held in Heidelberg, Germany from the 24th – 27th of September, 2017.

- Participated in the "STED imaging workshop" organized by Leica, at IISER Pune, from the 25th – 27th of October, 2016.

- Participated in the workshop on "Transmission Electron Microscopy" organized by ACTREC and JEOL India, from the 6th – 7th of October 2016.

- Presented a poster titled, "Regulation of centrosome duplication by 14-3-3 proteins" at the XXXIX All India Cell Biology Conference (**AICBC**) – Cellular Organization and Dynamics, from the 04th – 10th of December, 2015.

- Participated in the 12th National Research Scholar's Meet, held at ACTREC from the 15th – 16th of November 2015

- Presented a poster titled, "Regulation of centrosome duplication by 14-3-3 proteins and its consequences for regulating neoplastic progression" at the international conference, "Carcinogenesis", held at ACTREC from the 11th – 13th of February 2015.

Signature of Student:

Date: 25/04/19

Doctoral Committee:

S. No.	Name	Designation	Signature	Date
1.	Dr. Neelam Shirsat	Chairman		25/4/19
2.	Dr. Sorab N. Dalal	Guide/ Convener		25/4/19
3.	Dr. Prasanna Venkataraman	Member		25/4/19
4.	Dr. Dibyendu Bhattacharrya	Member		25/4/19

Forwarded Through:

S.V. Chiplunkar 03/05/2019

Prof. S.V. Chiplunkar,
Chairperson, Academic &
Training Programme, ACTREC

(Prof. Dr. S. V. Chiplunkar)
Chairperson, Academic &
Training Programme , ACTREC

6/5/19

Prof. S. D. Banavali,
Dean (Academics)
T.M.C.

PROF. S. D. BANAVALI, MD
DEAN (ACADEMICS)
TATA MEMORIAL CENTRE
MUMBAI – 400 012.

LIST OF TABLES

LIST OF FIGURES

1. Introduction

1. Introduction

1.1 The cell cycle

The cell cycle is a structured series of events which ensures that replicated DNA is separated accurately into two daughter cells (fig. 1.1) [reviewed in (1,2)]. Two of the most important events that occur during the cell cycle are; precise copying of the genome (S phase), and segregation of the duplicated genome into daughter cells (M phase) [reviewed in (2,3)]. These two phases are temporally distinct and are divided due to the existence of two gap phases (G1 and G2) (4). It is extremely essential that the replication and segregation phases are distinct and alternate, to ensure the maintenance of ploidy. This ordered progression is ensured by the unidirectional nature of the cell cycle; once a cell crosses the G1/S transition, it is committed to replicate its DNA [reviewed in (5)]. Similarly, once a cell has crossed the G2/M transition, it is committed to completing mitosis and will not usually revert to a second G2 [reviewed in (5)].

Mammalian cells are sensitive to mitogenic stimuli in their environment during a specific time in the early G1 phase of the cell cycle, known as the restriction point (R) (6). Here, the cell assesses the cumulative effect of all growth factor stimuli, or the absence of them. If the signals are favourable to growth, then the cell enters the cell cycle. Under certain conditions, including high cell density and an absence of growth factors, mammalian cells will accumulate in a state of $2n$ DNA content. This is known as the G0 phase or quiescence, which is an out-of-cycle phase and could be one of minimal metabolism [reviewed in (7)]. At other times during the cell cycle, the absence of mitogens does not

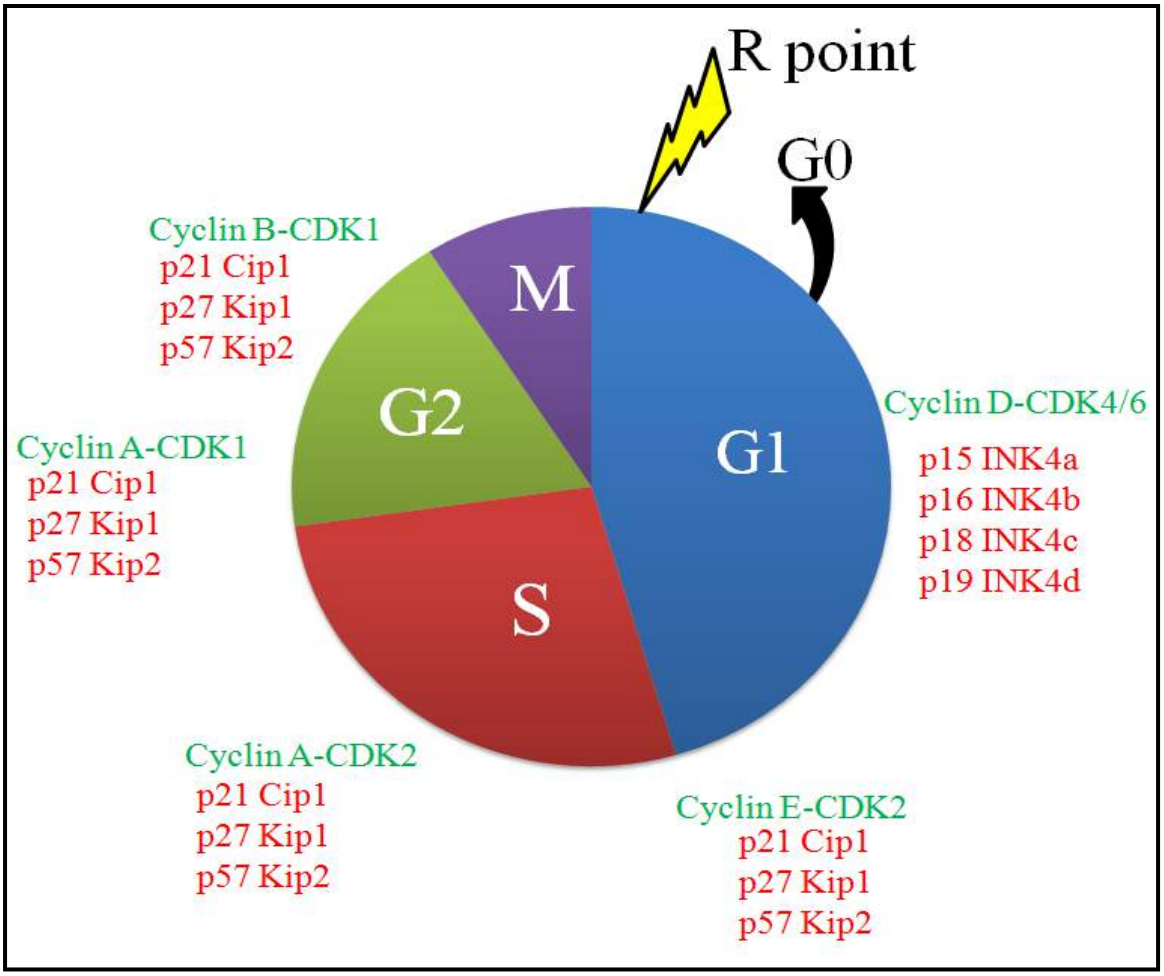

Fig. 1. 1 The cell cycle *– The restriction point (R) — is the point after which cells are unable to respond to extracellular signals and are committed to completion of the cell cycle. Cells may enter a quiescent, or the G0 phase, which is an out-of-cycle state at a point in G1 before the restriction point. Transition through G1 is mediated by cyclin D-cdk4/6 complexes, which are inhibited by the INK family of CDK inhibitors (8-10). Transition from G1 to S is mediated by cyclin E/CDK2 complexes (11). Progression through S to and entry into G2 is mediated by the cyclin A-CDK2 complex (12). Progression through G2 and entry into mitosis is mediated by cyclin A-CDK1 and cyclin B-CDK1 complexes (13). All the cyclin-CDK complexes besides the cyclin D-cdk4/6 complex, are inhibited by KIP family of CDK inhibitors. Activating complexes are shown in green and inhibitory in red.*

affect cell-cycle progression and the cells will proceed through the cell cycle, back to the responsive period. There are four phases in the cell cycle; G1, S, G2 and M (fig. 1.1).

G1 – This is the first gap phase in the cell cycle. During this phase, the cell can either be committed to division or withdraw from the cell cycle and enter a resting, G0 phase. This decision depends on a number of extracellular growth signals (14). The cell also synthesizes proteins necessary for DNA replication.

S – This is the synthesis phase of the cell cycle, during which the cell replicates its DNA. During S phase, the cell also duplicates its centrosome, an organelle essential for chromosome segregation.

G2 – This is the second gap phase in the cell cycle where the cell prepares for the next phase, mitosis. Organelles and proteins essential for mitosis are synthesized in this phase.

M – Mitosis is that phase of the cell cycle where separation of DNA into two daughter cells occurs. It is further divided into (fig. 1.2) –

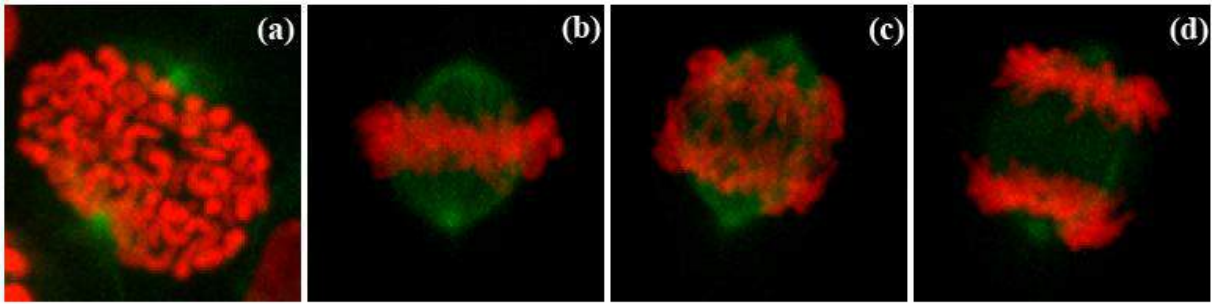

Fig. 1.2 Phases of mitosis. *HeLa Kyoto cell line stably expressing H2B-mCherry and α-tubulin-GFP were synchronized in mitosis and imaged on an Olympus Spinning Disk Confocal microscope after Nocodazole release. (a) Prophase, (b) Metaphase, (c) Anaphase and (d) Telophase.*

Prophase – Here, chromatin condensation into chromosomes occurs (fig. 1.2 (a)).

Metaphase – Spindle assembly occurs and the chromosomes align at the metaphase plate. Each kinetochore has to be attached to a spindle microtubule before the next phase can begin (fig. 1.2 (b)).

Anaphase – The spindle starts shortening, and the paired chromatids are pulled apart towards each end of the bipolar spindle (fig. 1.2 (c)).

Telophase – The single chromatids reach the poles of the spindle and cell division is initiated (fig. 1.2 (d)).

Cytokinesis – The cell divides into two daughter cells, each with a full complement of the genome.

There are exceptions to this ordered cell cycle. The development of the endosperm in plants occurs due to formation of a syncytium, a large cell comprising 100 nuclei post fertilization (15). The *Drosophila* embryo also develops as a syncytium, as a series of nuclear duplications without cell divisions (16). Salivary glands of *Chironomous* contain Polytene chromosomes, which are created due to repeated rounds of chromosome duplication without segregation (17). Previously, it was believed that neurons exist in a post-mitotic state; however, recent reports indicate tetraploidization in neurons (18).

1.1.1 Regulation of the cell cycle

Ordered succession through a cell cycle is mediated by the activity of a heterodimer made of two classes of proteins; the cyclins and the cyclin dependent kinases (CDK's). The cyclins are the regulatory subunit, while the cyclin dependent kinases are the catalytic subunit (19). Physical interaction with the cyclin controls the catalytic activity of the CDK (20,21). Multiple CDK's are bound by multiple cyclins in animal cells, the abundance of the cyclins is the determining factor. The expression of cyclins is cyclic in nature; cyclins are expressed

and undergo degradation, depending on the cell cycle phase. Each of the cyclins is under different transcriptional and proteolytic controls. Activation of a CDK by a cyclin, thus lends temporal control of its activity and confers substrate specificity via the bound cyclin.

Different cyclin-CDK complexes are active during distinct phases of the cell cycle. The cyclin D-CDK4/6 complex is active during G1, the cyclin E-CDK2 complex during the G1-S transition, cyclin A-CDK2 during S phase and cyclin A/B-CDK1 prior to and during mitosis up to the end of metaphase (fig. 1.1) (22-24). In mammals, each cyclin has multiple family members, A1, A2, A3, B1, B2, D1, D2, D3, E1 and E2 (19).

1.1.2 Regulation of CDK's.

Regulation of the CDKs occurs at many levels. These include, increased cyclin concentration, leading to binding to CDKs, activating and inhibitory phosphorylation (T14Y15 and T161), Cdk inhibitors (CIP/KIP and INK4), and SCF (Skp1/Cul1/F-box protein) ubiquitin ligase and the APC/C (Anaphase Promoting Complex/Cyclosome) mediated ubiquitination and subsequent degradation of cyclins and Cdk inhibitors (fig. 1.3).

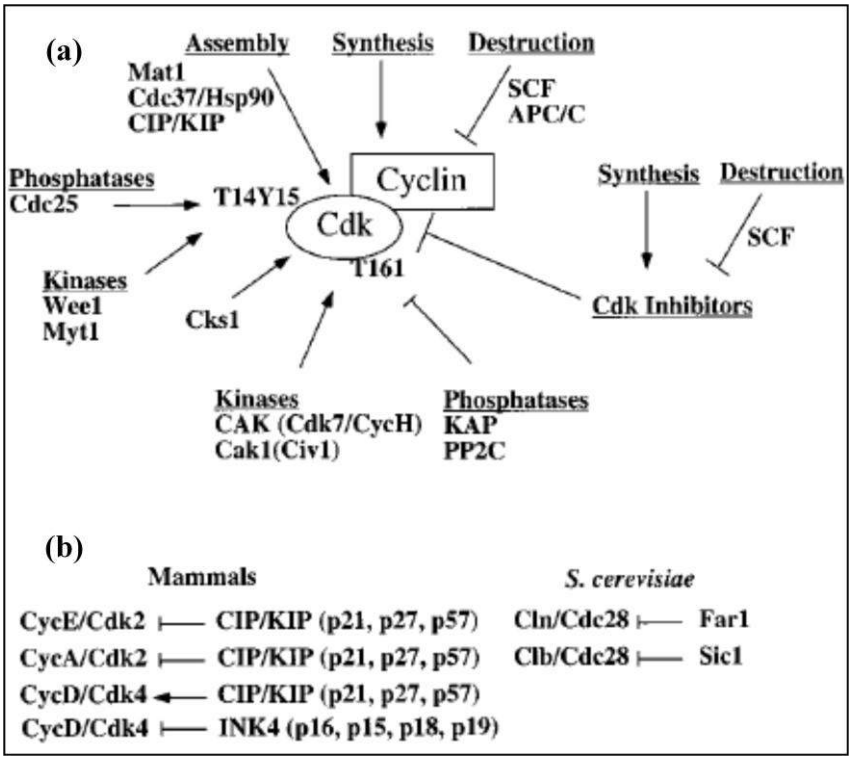

Fig. 1.3 Regulation of the CDKs (19). *(a) Mechanism of regulation of the CDK's, (b) Interaction of CDK's by CKI's (19).*

1.1.2.1 Regulation of the CDK's by phosphorylation.

The catalytic activity of the Cyclin dependent kinases is initiated by phosphorylation of residues on their T loop; a threonine residue (T172 in CDK4, T160 in CDK2 and T161 in CDK1). The CDK7–cyclin-H complex (also known as CAK; CDK activating kinase), a serine/threonine kinase that is also involved in transcription and DNA repair, is responsible for this acitivity (25). Dual specificity kinases (WEE1 and MYT1) phosphorylate adjacent threonine and tyrosine residues (T14/Y15 in CDK1), which are inhibitory in nature. The CDC25 phosphatases (CDC25A, CDC25B and CDC25C) dephosphorylate these residues and relieve the inhibition (26,27).

1.1.1.2 Regulation of cdk's by the CKI's.

Another level at which the CDKs are regulated is via the CDK kinase inhibitors (CKIs). The CKIs restrain CDK activity. They are divided into two groups (28). The first group includes the INK4 proteins, which specifically bind to and inhibit only monomeric CDK4 and CDK6 proteins (28). Four INK4 proteins have been identified: p16INK4a (also known as CDK inhibitor 2A or CDKN2A), p15INK4b (CDKN2B), p18INK4c (CDKN2C) and p19INK4d (CDKN2D) (8,9,29-31).

The second group of CKIs includes the Cip/Kip (*C*DK-*i*nteracting *p*rotein/CD*K*-*i*nteracting *p*rotein) family of proteins which bind to cyclin-CDK complexes (32). Cip and Kip inhibitors have a more extensive effect on cell cycle progression by blocking CDK activity by forming inactive trimeric complexes with the cyclin-CDK complex (33-37). The Cip/Kip family of CKIs consists of three members: p21Cip1 (also called CDK inhibitor 1A or CDKN1A), p27Kip1 (CDKN1B), and p57Kip2 (CDKN1C) [reviewed in (38)].

Cyclin D-CDK4/6 – The Cyclin D-CDK4/6 complex is active during entry into G1. CDK4 and CDK6 are bound by three D-type cyclins: D1, D2 and D3. Cyclin D levels increase due to mitogenic stimuli through receptor tyrosine kinases, Map and ras kinases (39-42). This results in its binding to CDK4/6, which activates the catalytic function of CDK4/6. pRb and related proteins are the key targets of these complexes (27). The control of the phosphorylation state of the Retinoblastoma (Rb) is extremely essential for cells to cycle from G1 to S [reviewed in (41)]. Rb is hypophosphorylated in early G1 or growth arrested cells and binds to transcription factors of the E2F family, repressing transcription by recruiting histone deacetylase (HDAC) (43,44). Phosphorylation by the cyclin D-CDK4/6 complex disrupts the binding of Rb to the E2F family of transcription factors. This results in initiation of the DNA synthesis phase by suspending the E2F-Rb-HDAC complex formation.

The effects of a knockout of cyclin D are most observed in tissues that express only one D-type cyclin (45,46). Cyclin D1 is expressed at high levels in the retina and breast and it was observed that mice lacking cyclin D1 exhibited developmental anomalies confined largely to the retina and developing breast tissue during pregnancy, but were otherwise viable (46). CDK4 (-/-) mice survived embryogenesis but exhibited delayed growth, with both male and female mice being infertile (47). *Cdk4*-null mutant mice are liable to harbor neurological abnormalities, imapired thymocyte maturation and allergen response, and defective adipocyte differentiation and function (45,46,48). *Cdk6*-deficient mice show thymic atrophy and are defective in Notch-dependent survival, proliferation and differentiation. (49). The Cyclin D/CDK4/6 complex is therefore, required for growth and development but not for viability.

Cyclin E-CDK2 – Transition from G1 to S mainly requires the activity of the Cyclin E-CDK2 complex. The expression of cyclin E begins during late G1 and continues till cells enter S phase (11,50). Activation of the cyclin E-CDK2 complex occurs via two mechanisms. First, the E2F family of proteins, no longer bound to Rb; mediate the synthesis of Cyclin E which leads to an increase in Cyclin E levels (51,52). Second, binding of the cyclin D-CDK4/6 complex to WAF1/KIP inhibitors renders them unable to bind to and inhibit the cyclin E-CDK2 complex (28). This is important because cells from mice with a knockout of CDK4 are defective in activating cyclin-E–CDK2 complexes via the redistribution of p27 to cyclin-D–Cdk4 complexes (47). They are thus delayed in entering the cell cycle.

The substrates of the cyclin E-CDK2 complex include proteins required for DNA replication, licensing of replication origin and centrosome duplication (53-56). Cyclin E-CDK2 mediates the phosphorylation of the CDK inhibitor Kip1, which permits cells to transition from G1 to S (57). When cells enter S phase, cyclin E undergoes degradation via the ubiquitin proteasome pathway (58-61).

Cdk2-null mice are viable and have no defects apart from male and female sterility due to meiotic defects, with a life span of 2 yrs (62,63). It is possible that other cdk's might compensate for its absence. Cyclin E1 or E2 deletion is also as harmless as cdk2 deletion, as the male knockout mice have reduced fertility, but no other phenotype (64,65). However, defects in duplication cycles in placental trophoblast giant cells resulted in embryonic lethality by E11.5, in mice with a double knockout of both cyclin E1 and E2 (65). Cyclin E is therefore, not essential for mitotic cells in embryonic development, but for endoreplicating cells. Also, it is possible that the cyclin E proteins have redundant functions within a class and a dual knockout is thus, fatal.

Cyclin A-CDK2 and Cyclin A/CDK1 – The cyclin A-CDK2 complex is responsible for cells to go through S phase, whereas the cyclin A-CDK1 mediates entry into mitosis. Cyclin A unbound CDK is inactive as it is inaccessible to substrate due to the presence of an unphosphorylated T-loop region (20). Also, the catalytic residues in the CDK are not arranged in the correct conformation for catalysis (12,66). Upon Cyclin A binding, CDK2 and CDK1 undergo a conformational change that makes them accessible to the substrate, ATP (67). Substrates of the kinase activity of the cyclin A-CDK2 complex in S phase initiate DNA replication (68-70). Cyclin A-CDK2 is also necessary for the synchronization of the end of the S phase with activation of the mitotic cyclin-CDKs (71). The cyclin A-CDK1 complex promotes mitotic entry by phosphorylating Bora, which mediates Aurora-A dependent Plk1 phosphorylation (72). Myosin phosphatase targeting subunit 1 (MYPT1) is also a cyclin A-CDK1 substrate that modulates Plk1 at kinetochores in prometaphase (73). The Anaphase Promoting Complex (APC) mediated proteolysis of cyclin A is essential for mitotic exit (74).

Cyclin A function is required for the division of hematopoietic and embryonic stem cells, as germline Cyclin A2 knockout mice die at embryonic stage E5.5 (75,76). The importance of

CDK1 in development is elucidated by the fact that deletion of Cdk1 arrests of embryonic development around the blastocyst stage (77).

Cyclin B1-CDK1 – During G2, cyclin A is degraded and cyclin B levels rise, which initiates mitosis (74,78). There are two cyclin B family members which are expressed in mammals, B1 and B2, but only cyclin B1 is essential for viability in mice (79). After the degradation of cyclin A, rising levels of cyclin B1 promote its binding to CDK1. Active cyclin B1-CDK1 complexes regulate the phosphorylation of several proteins required for centrosome separation, chromosome condensation and nuclear envelop breakdown (80-82). Inactivation of the cyclin B1-CDK1 complex drives exit from mitosis and this is brought about by APC/C mediated degradation of cyclin B1 [reviewed in (83,84)]. The substrates of the cyclin B1 CDK1 complex include CDC25C, Rad2, Sgo2 and Orc1 (85,86).

The two B type cyclins have different roles. Cyclin B2 knockout mice do not have any phenotype and are fertile, while Cyclin B1 knockout mice die *in utero* (79). Cyclin B1, may therefore, be able to compensate for the loss of Cyclin B2, but not vice versa.

1.1.2 Cell cycle checkpoints.

To ensure the completion of critical events in each phase of the cell cycle before progression to the next phase, each transition has to be monitored to ascertain that fidelity of the previous phase. DNA is prone to various stresses and insults that might affect the viability of a cell [reviewed in (87)]. In order to respond to these stresses, eukaryotic cells have evolved regulatory circuits, called checkpoints, to co-ordinate surveillance mechanisms with transition of the cell cycle from one phase to the subsequent one. Checkpoints are non-essential regulatory pathways that prevent the succession of the cell cycle in response to stresses such as damaged DNA or incomplete S-phase (88). These pathways also coordinate the activation of DNA damage repair responses (89-91).

Checkpoints are present at specific points during the cell cycle to detect the presence of defects such as DNA damage and to initiate repair pathways. “Sensor” proteins detect the presence of damaged DNA and relay this information to “transducer” proteins. Further, cell signaling pathways then transmit this information to “effector proteins” which lead to – 1) Arrest of the cell cycle and 2) Initiation of DNA damage repair pathways. If repair pathways are unable to repair the severely damaged DNA, the cell undergoes apoptosis. This is essential, because a cell harbouring damaged DNA or chromosomal instability will pass on these defects to daughter cells (92). Over a number of generations, these defective daughter cells may then contribute to tumorigenesis (92).

There are four checkpoints in a mammalian cell cycle. G1/S, incomplete S and G2/M are checkpoints that detect and respond to DNA damage. The fourth checkpoint, called the Spindle Assembly Checkpoint (SAC), detects improper connections between the spindle microtubules and the kinetochores and arrests cells at metaphase. Once a cell is arrested at a checkpoint, it can proceed to the next phase once only once it has repaired the damage that led to checkpoint initiation.

Loss of checkpoint function can affect the cell in various ways, depending on the severity of the defect. These defects are caused due to mutations in genes required for checkpoint function, the most studied of which are mutations in the p53 gene. Dominant negative mutations in the p53 gene cause a loss of WT p53 function. This leads to deregulation of its downstream effectors, such as p21. p21 is thus unable to regulate CDK function, and this causes an abrogation of the G1/S arrest (93). Oncogenic mutations in cyclin D1 cause cells to enter the cell cycle independent of mitogenic stimuli, which can lead to uncontrolled growth of cells (94,95).

G1/S checkpoint – This checkpoint is present just before the cell can enter S phase and prevents replication of damaged DNA. It also prevents the synthesis of proteins required for S phase progression. The checkpoint can be initiated by exposure to Ionizing Radiation (IR) or DNA damaging agents such as lovastatin, cisplatin and bleomycin (96-98). Upon exposure to DNA damaging agents, ATM (ataxia telangiectasia, mutated) and ATR (ataxia telangiectasia and Rad3-related) kinases phosphorylate the checkpoint serine/ threonine kinases, CHK1 (checkpoint kinase 1) and CHK2 (checkpoint kinase 2) (99). These kinases then phosphorylate CDC25A, leading to its ubiquitination and degradation (100-102). Inactivation of CDC25A prevents activation of cyclin E-CDK2 complexes, thus inhibiting G1/S transition (100). Activated ATM and ATR also stabilise p53 levels (103-105). Increased p53 levels lead to an increase in the levels of its downstream effector protein, p21, which inhibits the cyclin E-CDK2 complex (106,107).

Another mechanism for ensuring G1/S arrest is via the INK4 and Cip/Kip families of CKIs. Expression of INK4 titrates CDK4 away from the cyclin D-CDK4 complex and cyclin D is degraded via the ubiquitin proteasome pathway (8,108). Also, in early G1 phase, binding of p21Cip1 and p27Kip1 inhibits the cyclin E-CDK2 and cyclin A-CDK2 (10,93,109). For entry in S phase, the cyclin D-CDK4/6 complex must sequester the p21Cip1 and p27Kip1 away from the cyclin E-CDK2 and cyclin A-CDK2 complexes. Degradation of D-type cyclins therefore prevents the titration of p21Cip1 and p27Kip1 by cyclin D-CDK4/6 complexes. The Cip/Kip bound cyclin E-CDK2 and cyclin A-CDK2 complexes thus prevent S phase entry (110).

Incomplete S-phase checkpoint – This checkpoint monitors DNA replication and the presence of stalled replication forks. When the incomplete S-phase checkpoint is initiated, it prevents replication initiation and fork progression, and therefore, slows down DNA replication (111-113). The cell thus has time to repair damaged DNA and complete DNA replication. Loss of

the incomplete S-phase checkpoint results in cells entering mitosis prematurely, via Premature Chromatin Condensation (PCC), which can be lethal (114). The incomplete S-phase checkpoint is activated upon exposure to UV radiation, X-rays or chemical mutagens such as hydroxyurea. Exposure to these agents leads to the formation of pyrimidine dimers, DNA methylation, depletion of deoxyribonucleotides and damaged DNA (115,116).

ATR senses the presence of single stranded DNA lesions and stalled replication forks, which lead to its activation and phosphorylates and activates Chk1 and Chk2. This results in the inhibition of CDC25A, CDC25B and CDC25C, which averts the activation of cyclin E-CDK2, cyclinA-CDK2 and cyclin A-CDK1 and thus, G2 entry. It also prevents activation of CDK1 by its dephosphorylation on Thr 14 and Tyr 15. This prevents cyclin B1-CDK1 complex activation and inhibits progression into mitosis (117-125).

G2/M checkpoint – The G2/M checkpoint is activated upon DNA damage to cells that are in G2 or cells that acquired DNA damage in previous cell cycle phases but escaped checkpoint activity (126,127). It is activated by agents such as ionizing radiation, Adriamycin and Bleomycin, that cause double strand breaks. The G2/M is the last checkpoint that monitors DNA damage before cells enter mitosis. It has been shown that cells lacking the p53, which are unable to arrest at the G1/S checkpoint, might depend on the G2/M checkpoint to repair DNA damage (128). Inability of cells to undergo the G2/M arrest upon DNA damage can result in the production of daughter cells with defective DNA and can contribute to tumourigenesis.

This checkpoint is activated by the rad family of proteins that sense double strand DNA damage (129). This results in the activation of the ATM and ATR family of kinases, which phosphorylate Chk1 and Chk2 kinases (117,130). The ultimate objective of this checkpoint is preventing the activation of the cyclin B1-CDK1 complex. This is achieved by the

inactivation of the CDC25 phosphatases A, B and C, due to phosphorylation by Chk1, Chk2 and C-TAK1 (117-125,131,132). This phosphorylation results in the generation of a 14-3-3 binding site on CDC25C at a serine 216 residue (121,133). 14-3-3 proteins sequester CDC25C in the cytoplasm and prevents its nuclear localisation. This inhibits its ability to activate the cyclin B1-CDK1 complex and thus prevents mitotic progression. The inhibitory phosphorylation on CDK1 is further accentuated by the association of Wee1 with 14-3-3 proteins. This binding activates Wee1 and maintains the inhibitory phosphorylation of CDK1 (134,135).

Spindle Assembly Checkpoint (SAC) – During mitosis, replicated chromosomes have to be divided into two daughter cells. The paired chromosomes are attached to the spindle microtubules via kinetochores at the metaphase plate, followed by segregation during anaphase into two daughter cells. Inability of the chromosomes to attach correctly to the spindle microtubules can result in the two daughter cells receiving unequal complements of the genome, which may lead to apoptosis or disease. The Spindle Assembly Checkpoint (SAC) prevents the anaphase transition of a cell in metaphase with incorrect attachment between the kinetochores and the mitotic spindle [reviewed in (136)]. It delays anaphase transition until all the chromosomes are properly attached to the mitotic spindle.

The SAC is activated upon loss of spindle pole tension, unattached kinetochores at metaphase or by certain spindle poisons such as nocodazole (137). The goal of the SAC is preventing the degradation of the APC/C. Several proteins regulate the SAC - BUB1 (budding uninhibited by benzimidazole 1) and the MAD (mitotic-arrest deficient) family of proteins, MAD1, MAD2 and MAD3 (BUBR1 in humans) (138-140). The target of the SAC is the co-factor of the ubiquitin ligase APC/C, CDC20 (141-144). Activation of the SAC hinders the ability of CDC20 to stimulate APC/C-mediated ubiquitination of two key substrates, cyclin B and Securin, thus preventing their degradation by the 26S proteosome. Cyclin B degradation is

required for mitotic exit (84). Destruction of Securin leads to activation of Separase, which results in anaphase onset by cleaving the cohesion complex that holding sister chromatids together (145-147). Thus, by controlling CDC20 function, the SAC allows chromosomes to align properly on the metaphase plate and attach to the spindle poles via microtubules. The checkpoint is quenched when the chromosomes are oriented correctly. This releases the cell from a mitotic arrest, allowing anaphase to begin.

1.2 14-3-3 proteins.

14-3-3 proteins are a family of small, dimeric, acidic, regulatory proteins [reviewed in (148)]. They were first isolated as abundant, soluble proteins from bovine brain tissue lysates and were theorized to be brain specific (149). 14-3-3 proteins derive their name from the elution fraction of bovine brain tissue lysates containing these proteins following DEAE-cellulose chromatography and their migration position after starch gel electrophoresis (149). The 14-3-3 proteins were extracted by the authors' from the 14th fraction of bovine brain lysate in a DEAE cellulose column and fractions 3.3 of the final step (149). Subsequent research has revealed that 14-3-3 proteins contribute to regulation of the cell cycle, cellular metabolism, apoptosis, cell-cell adhesion, protein transport, transcription and malignant transformation (150-156).

14-3-3 proteins were the first proteins demonstrated to bind to phosphorylated Serine or Threonine residues (157,158). There are seven isoforms of 14-3-3 proteins in mammalian cells; β, γ, ε, σ, η, τ (or θ) and ζ, with δ and α being the phosphoforms of β and ζ, respectively (148,159). These isoforms were named with respect to their order of elution on HPLC (160,161). The different isoforms are quite homologous, but contain a few regions of variation. 14-3-3 proteins are found in most eukaryotic organisms, from fungi to mammals [reviewed in (162)]. Multiple 14-3-3 isoforms are expressed across eukaryotes, from two in

the yeast *Saccharomyces cerevisiae* (BMH1 and BMH2), to at least 13 in the plant *Arabidopsis thaliana* (GRF1-GRF13) (163-165). Most isoforms of 14-3-3 proteins are ubiquitously expressed, barring 14-3-3σ, which is expressed solely in epithelial cells and 14-3-3τ, expressed predominantly in T cells (166,167).

1.2.1 Structure of 14-3-3 proteins.

All the different 14-3-3 isoforms function as either homodimers or heterodimers, with 14-3-3σ acting exclusively as a homodimer and 14-3-3γ and 14-3-3ε preferentially forming heterodimers (168-170). Initial crystallization studies with the ζ and τ isoforms demonstrated that the 14-3-3 proteins are helical and dimeric in nature (171-173) (fig. 1.4). The monomer comprises of 9 anti-parallel α-helices, with an N terminal and a C terminal domain. The biologically functional dimer is a shrunken "ω" shaped structure. Four of the α-helices are involved in dimer formation, with the remaining helices making up the sides and top of the "ω" (171-173). All 14-3-3 isoforms consist of a target binding region and a dimerization domain at the N-terminus.

The current consensus is that the rigid "ω" shape contributes to deformation of the target protein but does not largely change the 14-3-3 dimer structure (174,175). The exception to this model is 14-3-3ζ, with a flexible carboxyl-terminal region. Phosphorylation of this region changes its conformation (176). This relatively unconserved region is theorized to have an isoform specific auto inhibitory role in ligand binding (176,177).

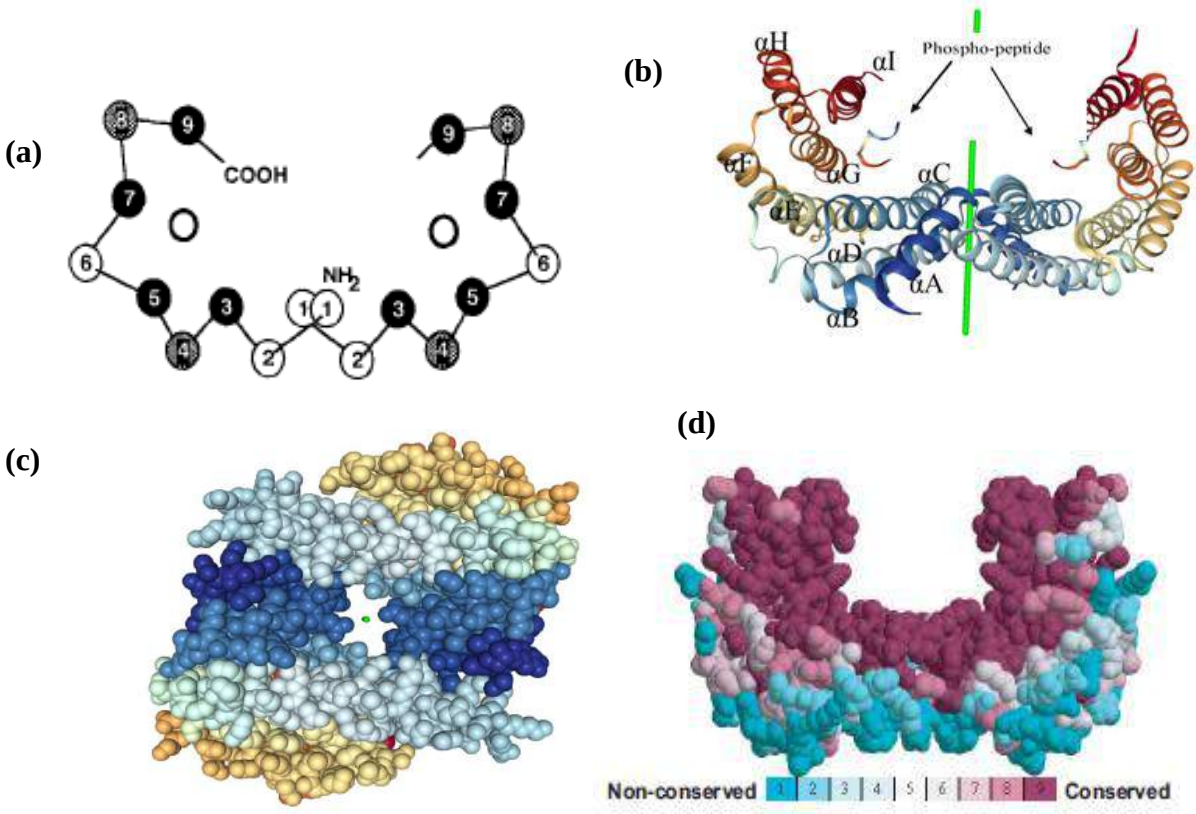

Fig. 1.4 Structure of 14-3-3 proteins*. (a) Schematic representation of the 14-3-3 dimer (178). The more conserved alpha helices are shaded. The hypothetical docking positions of helices from interacting proteins are represented by the two central unnumbered circles. PDB ID code 1QJB (b) The ribbon representation, of 14-3-3ζ bound to two Mode I phospho-peptides, with the central green stick indicating the axis of symmetry. Each monomer is coloured in red to blue from the C to N terminus (αA- αB) (173), (c) The spacefill representation of the homodimer with 90° rotation. An aperture is present at the central dimeric interface, marked here with a green dot, (d) Structure of 14-3-3ζ shaded according to residue conservation across species (179). Legend denotes relative conservation levels in the protein, with teal representing the least-conserved residues and burgundy representing the most highly conserved residues.*

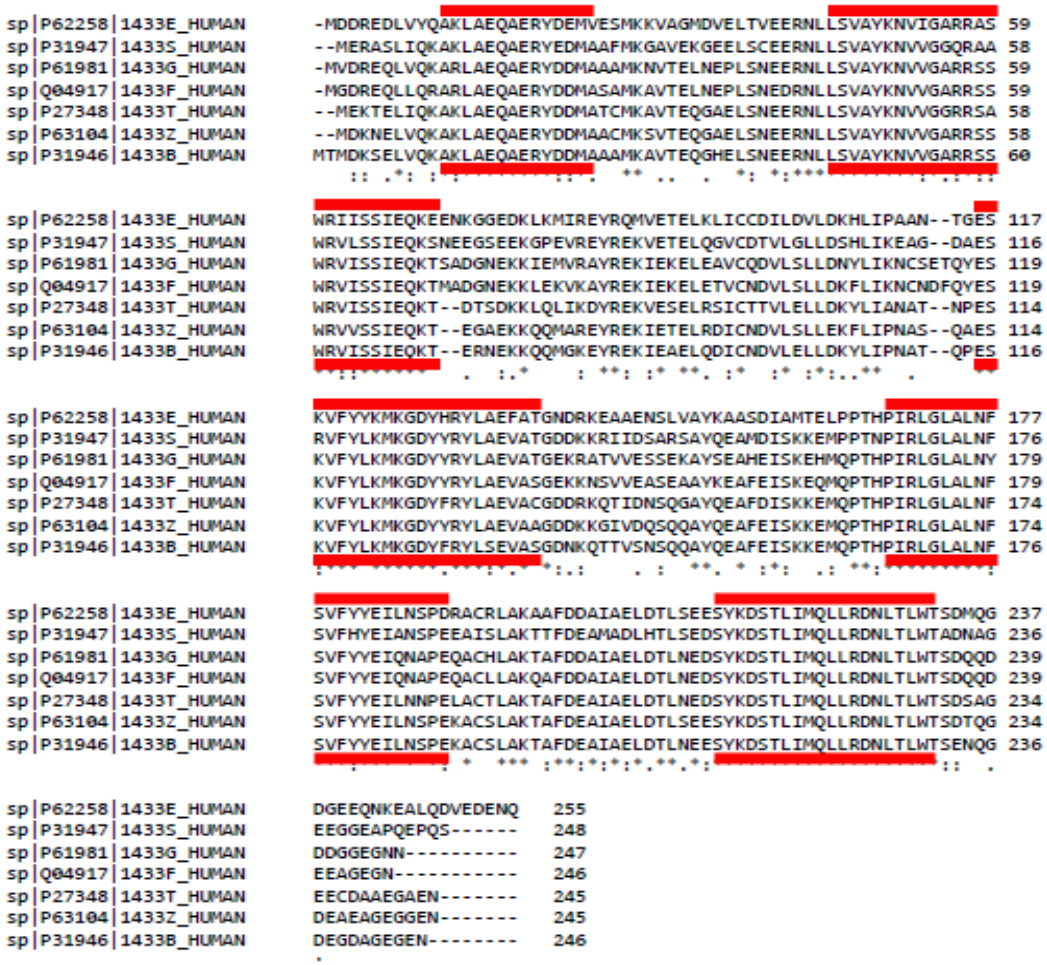

Fig. 1.5 Sequence alignment of human 14-3-3 isoforms*. Conserved residues are highlighted by a red line in the sequence alignment.*

There are five conserved sequence blocks within the 14-3-3 family of proteins. These blocks comprise the end of helix αA, the αA/αB-connecting loop, the helices involved in ligand binding (αC, αG, αE and αI), and the start of helix αB, that constitute an essential element of the dimer interface (174,178) (fig. 1.5). A large negatively charged channel is created due to the dimer. Invariant regions that are conserved throughout isoforms mainly line the interior of this channel with variable residues present on the exterior side of the protein. This channel is important for the recognition of target proteins.

The specificity of interaction of each of the 14-3-3 isoforms and their ligands involves the outer surface of the protein. Each monomer encodes an amphipathic groove that forms a structure for interacting with ligands. The 14-3-3 dimer can therefore, interact with two ligands (171-173,175,180). Direct interactions between the phosphate and Lys-49 and Arg-56 in helix αC, and Arg-127 and Tyr-128 in helix αE are required for the binding of 14-3-3 to phospho- Serine/Threonine containing motifs. These residues form a basic compartment in a mainly acidic molecule. Substrate serine/threonine phosphorylation can thus function as molecular switches controlling ligand binding.

1.2.2 Target recognition by 14-3-3 proteins.

Recognition of consensus phosphorylated binding motifs.

Initial studies suggested that 14-3-3 proteins bind to their ligands only when the ligand protein is phosphorylated at a serine or threonine residue (173,180). Muslin, et. al, illustrated the archetype phosphorylated serine recognition motif, RSxpSxP, from a 15-mer Raf-1 peptide containing RQRS^{257}TS^{259} TP (157). When phosphorylated on S259, this peptide bound directly to 14-3-3ζ with a K_d of 122 nM. The binding is site specific, because when unphosphorylated, the same peptide could not interact efficiently with 14-3-3 or when phosphorylated at S257 or at S257 and S259 together. The Arg residue in the –3 or –4 position relative to the phosphoSerine is essential for 14-3-3 binding. The Proline residue at +2 is important, but this position can be substituted by other residues (173). Further screening of phosphoSerine-oriented peptide libraries identified two alternative consensus motifs with one (mode 1) closely related to the RSxpSxP motif (180). There are preferences for certain amino acids in the –1, –2, and +1 positions. Thus, the 14-3-3 recognition motif has been refined to R[S/Ar][+/Ar]pS[L/E/A/ M]P, where Ar represents an aromatic residue and + indicates a basic residue. The second identified motif (mode 2) uses the most favorable

sequence Rx[Ar][+]pS[LE/A/M]P. The phosphorylated residue can also be a Threonine, though many identified 14-3-3 binding partners contained a phosphorylated Serine residue within the motif. For example, phosphorylation at a Thr231 site modulates the binding of 14-3-3 to serotonin N-acetyltransferase (AANAT) (175,181). Similarly, phosphorylation by AKT at Thr28 and Ser193 generates a 14-3-3 binding site on the protein FOXO4 (182-184). The defined 14- 3-3 consensus motifs can be used to identify putative 14-3-3 binding sites, as several proteins that were anticipated to bind 14-3-3 based on these recognition sequences were then experimentally verified, including Cdc25 and Bad (121,157,180,185-187). However, further experiments are required to completely elucidate this mode of interaction due to the vast range of substitutions tolerated in these motifs.

Recognition of consensus unphosphorylated binding motifs.

There is a third consensus binding motif (pS/pT-X1–2-COOH), which is C-terminal and phosphorylation independent (188). The interactions of 14-3-3 with unphosphorylated ligands are of high affinity, similar to those with phosphorylated proteins. These targets bind to 14-3-3 proteins in the same location as phosphorylated targets and can compete with phosphopeptides for binding, adding a level of complexity to 14-3-3 target recognition (189).There are structural homologies between the two classes of ligands in cases such as 5-phosphatase, which displays an RSxSxP-like motif, RSESEE (190). This C-terminal motif could result in binding of an additional small molecule that closes a gap remaining in the 14-3-3 ligand binding groove, and hence significantly stabilize the resulting ternary complex. An example of such a compound is an activator of the H (+) –ATPase, the fungal phytotoxin Fusicoccin. Fusicoccin binds to the 14-3-3:H (+)-ATPase complex and facilitates the binding of 14-3-3 to the unphosphorylated C terminus of the H (+)-ATPase (191). Two new compounds structurally unrelated to Fusicoccin, Pyrrolidone 1 and Epibestatin, were recently

identified and they can selectively activate the H (+)-ATPase by stabilizing its complex with the 14-3-3 protein (192,193).

1.2.3 14-3-3 proteins and dimerization.

Deletion experiments have determined that the N terminal is essential for dimerization. Work by Gu and Du, 1998, demonstrated that deletion of even the first 32 amino acids can disrupt the dimerization of 14-3-3ζ (194). Several monomeric forms of 14-3-3 proteins bind to their phosphorylated ligands with unchanged affinity as compared to the dimeric forms in vitro (194-197). But in vivo, dimerization deficient mutants of 14-3-3 are unable to associate with phosphorylated ligands as well as wild type protein (198). A ligand binding deficient mutant of 14-3-3, K49E, is capable of forming heterodimers with endogenous WT 14-3-3 (199,200). However, this heterodimer is also unable to bind ligands, which elucidates the importance of the 14-3-3 dimer for ligand binding (200). In at least some cases, the dimer of 14-3-3 is essential for it to perform its functions (197). Dimerization deficient mutants of 14-3-3 proteins can bind phosphorylated Raf-1 (197). Yet, the kinase exists in an inactive conformation, as its activity requires the "bridging" function of the dimeric 14-3-3 proteins (197).

A single polypeptide with two 14-3-3 binding sites can bind to 14-3-3 with a 30-fold increase in binding affinity (180). Therefore, a single polypeptide harbouring two 14-3-3 binding sites of low affinity sites will be able to bind to dimeric 14-3-3. This has been demonstrated in the case of 14-3-3 ligands such as Wee1, keratin 18, Cbl, IGF-I receptor and IRS-1, which all need multiple phosphorylation sites for stable binding to 14-3-3 (201-205). Recently, it has been demonstrated that the inhibition of 14-3-3 dimerization can be used in anti-cancer therapy. Woodcock, J. et. al., have identified sphingosine mimetics that can result in mitochondrial-mediated apoptosis by making dimeric 14-3-3 susceptible to phosphorylation

at a site within the dimer interface. RB-011 and RB-012 are compounds that can induce apoptosis in human A549 lung cancer cells, with RB-012 reducing tumour voulmes in mice through disruption of MAPK signalling (206).

1.2.4 Modes of action of 14-3-3 proteins (fig. 1.6).

Structural change of the protein – 14-3-3 binding can regulate enzymatic activity. Plant nitrate reductase (NR) can be inactivated by phosphorylation followed by 14-3-3 binding (207-209). Phosphorylation of NR at a Ser543 site generates a 14-3-3 binding site on this

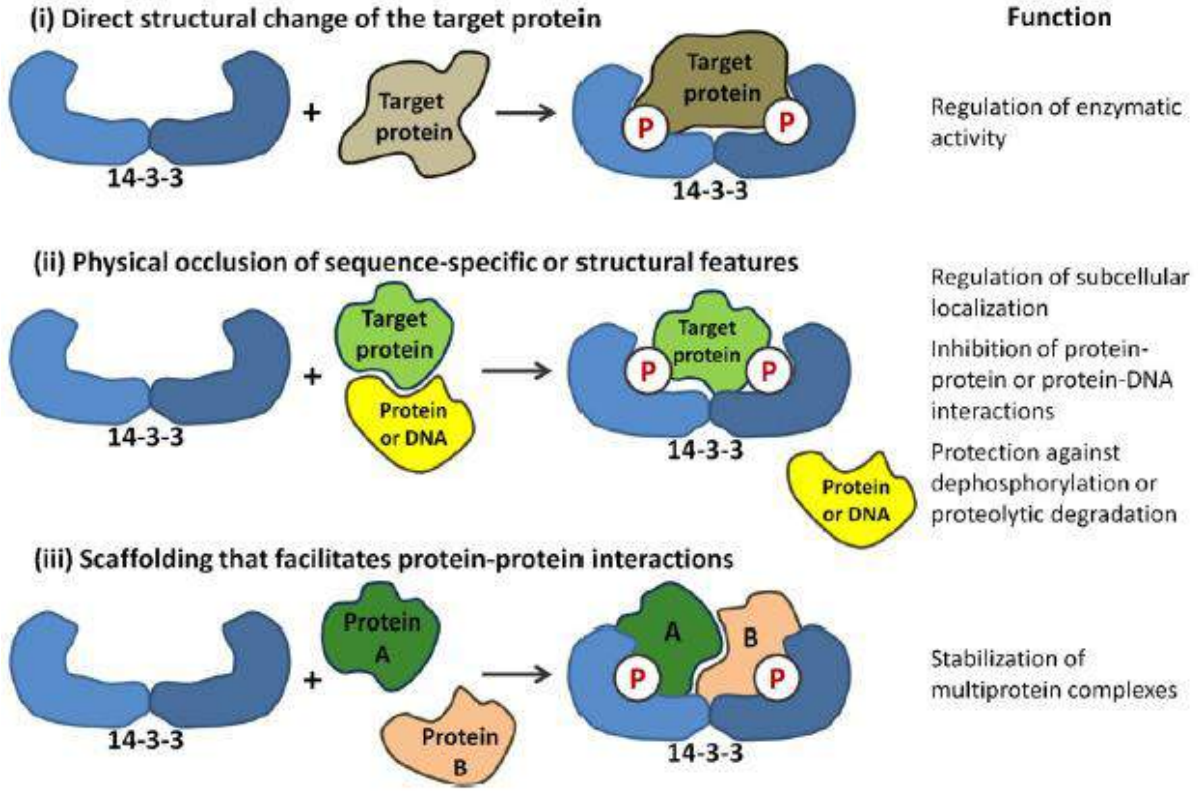

Fig. 1.6 Modes of action of 14-3-3 proteins *(210).*

protein (207). Binding of 14-3-3 induces a conformational change in NR that disrupts the Electron Transfer Chain within its cofactors and thus inhibits the enzyme (208). 14-3-3 bound NR is also a more stable dimer which further undergoes degradation (211). 14-3-3ζ has been demonstrated to inhibit the activity of the pro-apoptotic protein apoptosis signal-regulating

kinase 1 (ASK-1) (212). Tumour necrosis factor (TNF) mediated phosphorylation of ASK-1 at a Ser 966 site results in its kinase domain being bound by 14-3-3ζ, which blocks its accessibility and negatively affects its conformation (212,213).

On the other hand, 14-3-3 binding can also activate enzymes. For example, tryptophan and tyrosine hydroxylases are phosphorylated in the presence of Ca^{2+}, followed by 14-3-3η binding resulting in a conformational change and full activity (160,195). For serotonin-N-acetyltransferase (AANAT), phosphorylation of the residue Thr31 leads to binding of 14-3-3ζ and a conformational change, which releases the "fly-casting" mechanism and activates the protein (175,214).

Regulation of the Raf- 1 protein kinase by 14-3-3ζ is complex and three 14-3-3 binding sites are involved. In cells non-stimulated EGF or serum, 14-3-3ζ keeps Raf-1 in an inactive conformation by binding to two sites, Ser 259 and Ser621 (197). Upon stimulation, 14-3-3ζ is displaced from the Ser259 site, but it remains attached to the Ser621 site. This results in intermediate activation of Raf-1. For full catalytic activity, the 14-3-3ζ protein binds to two different phosphorylated serines, thus stabilizing the active conformation (197).

Scaffolding as a means to modulate protein-protein interaction – Both Raf-1 and Bcr protein kinases can bind to a single 14-3-3β dimer resulting in interaction between the two protein kinases (215). 14-3-3β acts as a bridge, connecting Raf-1 and Bcr, which are unable to interact in the absence of 14-3-3β (215). 14-3-3 also affects the binding of BAD to Bcl-XL. During survival conditions, BAD is phosphorylated on S112, S136 and S155 (186,187,216-218). 14-3-3ζ binding maintains BAD in the cytoplasm and aids in the phosphorylation of the S155 site (186,216). This phosphorylation prevents binding of BAD to the anti-apoptic proteins Bcl-2 and Bcl-XL (216-218).

Chibby (Cby), a conserved antagonist of β-catenin, has a vital role in the canonical Wnt signalling pathway [106]. Cby interacts with the C-terminal activation domain of β-catenin and inhibits its ability to be transcriptionally activated. Mass spectrometry studies have shown that 14-3-3ε and 14-3-3ζ recognize a Ser20 phosphorylated residue on Cby and sequester it in the cytoplasm (219). 14-3-3, Cby and β-catenin form a stable, tripartite complex, which leads to the nuclear export of β-catenin and terminates its signalling (219).

Tertramerization of the tumour suppressor protein p53 is required for its activity, in this conformation it binds to DNA with high affinity or interact more proficiently with its ligands [reviewed in (220)]. 14-3-3 proteins bind to a site in its intrinsically disordered C-terminal domain and activate the DNA binding affinity and increase the stability of p53 (221-223). In vitro studies indicate, that 14-3-3γ and 14-3-3ε can accelerate the tetramerization of p53 even at low p53 dimer concentration (224). This augments the binding p53 to sequence-specific DNA and thus controls p53 activity (224).

Sequestering of structural or sequence-specific features - It has been demonstrated in vitro that 14-3-3 β, ε, γ, σ and ζ can bind to wild type CDC25C (152). In vivo, only 14-3-3γ and 14-3-3ε can bind to CDC25C (152). Binding of 14-3-3γ or 14-3-3ε at a Ser216 residue sequesters CDC25C phosphatase in the cytoplasm, whereas they cannot bind to the mutant S216A (152). Disruption of 14-3-3 binding to CDC25C, exposes a nuclear localization sequence on CDC25C. This results in its translocation to the nucleus where it activates CDK1 and leads to mitotic entry (121,133,225,226).

Another group of proteins that undergoes this type of regulation are the FOXO proteins, a subgroup of forkhead transcription factors that play a central role in cell-cycle regulation, differentiation, stress response and apoptosis [reviewed in (227)]. Akt kinase phosphorylation creates two 14-3-3 binding motifs on FOXO4, Thr28and Ser193; one of which is embedded

within the NLS (182,228). Several studies demonstrated that upon binding to 14-3-3ζ, the resulting FOXO4:14-3-3ζ complex is translocated to the cytosol where the bound 14-3-3 protein masks the NLS of FOXO4 and inhibits its re-entry into the nucleus (182,184,200,229,230).

1.3 14-3-3γ

14-3-3γ (known as YWHAG in humans) is one of the isoforms of 14-3-3 proteins that was first isolated in 1991 by Isobe T. et. al., while performing a fractionation of bovine brain lysates (231). This isoform was theorised to be expressed only in the brain, but has since been isolated from a number of different tissues, such as skeletal muscle and the heart (231,232).

1.3.1 Functions of 14-3-3γ

14-3-3γ performs various functions in a cell by participating in different cellular pathways. Some of these are described below.

1.3.1.1 Regulation of cell cycle checkpoint control.

One of the ways by which 14-3-3 proteins regulate the G2/M transition is via binding to CDC25C (121,131,225,226). CDC25C, a dual specificity phosphatase activates the mitotic complex, CyclinB-CDK1, leading to the entry of cells into mitosis (233). During interphase or cell cycle arrest, to prevent the entry of cells into mitosis, CDC25C is phosphorylated at a Serine residue at position 216 (S216) which leads to the creation of a 14-3-3 binding site (121). 14-3-3 then sequesters CDC25C in the cytoplasm, prevents activation of the mitotic complex, cyclinB-CDK1 and thus, mitotic entry (226). Of the different isoforms of 14-3-3, only 14-3-3γ and 14-3-3ε were found to interact with CDC25C in vivo (152). To test whether 14-3-3γ binding to CDC25C had any effect on CDC25C function, the 14-3-3γ-CDC25C complex formation was disrupted by expressing an S216A CDC25C mutant which failed to

bind 14-3-3γ (152). The cells expressing S216A CDC25C mutant showed premature chromatin condensation (152). PCC is seen in S phase cells in which premature mitosis is induced by the override of the incomplete S phase and G2 checkpoint pathways (152). In HCT116 cells, disruption of endogenous 14-3-3γ-CDC25C complex by loss of 14-3-3γ also resulted in premature activation of cyclinB-CDK1 complex by CDC25C and increased PCC (234).

14-3-3γ also regulates the G2/M transition by interacting with Cdt2 (cell division cycle protein 2) (235). Cdt2 has a role in the cell cycle due to its function as the substrate recognition adaptor of the $CRL4^{Cdt2}$ E3 ubiquitin ligase complex. This complex is required for the proteasomal degradation of Cdt1 (DNA replication licensing factor), p21 (cyclin-dependent kinase [CDK] inhibitor), and Set8 (histone methyltransferase) in S phase [reviewed in (236)]. Cdt2 itself is regulated by SCF^{FbxO11}-mediated proteasomal degradation. It has been reported that 14-3-3γ interacts with Cdt2 phosphorylated at threonine 464 (T464) and shields it from proteasomal degradation (235). Further, loss of 14-3-3γ leads to a delay of the cell cycle in the G2/M phase and a decrease in cell proliferation (235). This occurs due to the accumulation of the CRL4Cdt2 substrate, Set8 methyltransferase.

One of the kinases that phosphorylate CDC25 proteins and generate a 14-3-3 binding site is Chk1 (124). Upon DNA damage, activation of Chk1 prevents cell cycle progression and causes a G2/M arrest via CDC25C (237,238). Phosphorylation of Chk1 at Ser317 and Ser345 by ATR, in response to DNA damage mediates autophosphorylation of Chk1 at Ser296 (239). This is a binding site for 14-3-3γ (239). The 14-3-3γ dimer is able to bind to both Chk1 and CDC25A which leads to phosphorylation of CDC25A at a Ser76 residue by Chk1 (239). This further leads to degradation of CDC25A in a β-TRCP dependent manner. 14-3-3γ is thus required for checkpoint activation via Chk1 (239).

1.3.1.2 Regulation of cell-cell adhesion.

Mice harbouring a knockdown of 14-3-3γ are sterile, due to defects in cell-cell adhesion (154). It has been demonstrated that loss of 14-3-3γ inhibits desmosome formation in HCT116 cells. Under normal conditions, PKCμ phosphorylated plakoglobin (PG) at a Ser236 residue, which is a 14-3-3 binding site (154). 14-3-3γ then loads PG onto the KIF5B-KLC1 complex, which is then transported to the desmosome (154). However, upon loss of 14-3-3γ, this pathway is affected and desmosome formation cannot be inititated, leading to defects in cell adhesion (154). This can be restored by artificially targeting PG to the desmosome (240).

1.3.1.3 Regulation of adeno-associated virus type 2 replication.

Adeno-associated virus type 2 is a non-pathogenic human parvovirus which requires a helper virus for efficient DNA replication. One of the proteins expressed by the virus is Rep68, the function of which is to replicate DNA and site specific integration. It was found that phosphorylation of Rep68 at Ser535 induces its binding to a 14-3-3γ-14-3-3ε to form a ternary complex (241,242). A Rep68 mutant which is unable to bind to 14-3-3 proteins has increased affinity for DNA and is more efficient in viral DNA replication (243).

1.3.1.4 Regulation of smooth muscle activation.

14-3-3γ levels have been shown to rise in rat carotid arteries, post surgery (243). Arteries are composed of vascular smooth muscle cells (VMSCs), hyper proliferation of which leads to the harmful narrowing of arteries post surgery. 14-3-3γ might have a function in muscle tissue, given its high expression in VSMCs and skeletal and heart muscle (243). It has been demonstrated that upon exposure of VSMCs to growth stimuli such as Platelet Derived Growth Factor (PDGF), different isoforms of PKC phosphorylate 14-3-3γ, which then

interacts with Raf (244). This interaction might promote the activation and proliferation of the VSMCs, resulting in the formation of lesions.

1.3.1.5 Regulation of p53 activity by 14-3-3γ and suppression of 14-3-3γ expression by p53.

p53 initiates the transcription of genes involved in cell-cycle arrest, senescence, apoptosis and DNA repair, and is thus important for the preservation of genome integrity. p53 activity can be regulated by both post-translational modifications and protein–protein interactions. It is a tumor suppressor protein, which is frequently mutated in cancers. It was observed that 14-3-3γ binds to p53 in vitro and in vivo (245). The 14-3-3 binding deficient mutants of p53 were unable to induce cell cycle arrest in response to IR, which implies that the p53 binding to 14-3-3 is important for p53 function (245). 14-3-3γ helps in oligomerization of p53 and the 14-3-3γ-p53 complex had higher affinity to bind DNA when compared to p53 alone (222,224,246). Conversely, it has been demonstrated that in non-small cell lung cancers, that loss of functional p53 correlates with an increase in 14-3-3γ levels (247). Upon exposure to IR, p53 binds to the promoter of 14-3-3γ and suppresses its expression (247). p53 also enhances the ubiquitination of 14-3-3γ and thus regulates its levels (248).

1.3.1.6 ATPase activity

Recent reports have shown that 14-3-3 proteins possess ATPase activity (249). Pure recombinant human 14-3-3 ζ, γ, ε and τ isoforms hydrolyze ATP with similar Km and kcat values. This activity can be altered by mutation of Asp124 or Arg55 to Alanine and results in a gain or loss of function. The activity could be due to the presence of an as yet unknown binding pocket (249).

1.3.1.7 Role in neurodegenerative disorders

14-3-3γ levels are often deregulated in different neurodegenerative disorders. Mutations in α-synuclein are the cause of aggregate formation (Lewy bodies), which are a hallmark of Parkinson's disease. 14-3-3 proteins interact with α-synuclein and are seen in α-syn inclusion bodies (250). Over-expression of α-synuclein in mouse model revealed a reduction in the levels of 14-3-3γ, 14-3-3ζ and 14-3-3ε (251). Conversely, over-expression of 14-3-3γ, 14-3-3ε and 14-3-3ζ in a neuroglioma cell line led to the reduction of the α-synuclein aggregates. 14-3-3γ overexpression in dooaminergic cells also provided protection against cytotoxicity due to drugs such as Rotenone and 1-Methyl-4- phenyl pyridinium (251). Thus, 14-3-3γ might have a protective function against Parkinson's disease.

Leucine rich repeat kinase-2 (LRRK2) is a multidomain protein and is mutated in familial Parkinsons's disease. PKA mediated binding of 14-3-3γ at a S1444 site regulates the kinase activity of LRRK2 (252). Mutation of 14-3-3 interaction with LRRK2 is hampered in R1441C/G/H-mediated PD pathogenesis. LRRK2 is phosphorylated by protein kinase A at multiple sites. LRRK2 phosphorylated at S1444 residue serves as binding site for 14-3-3γ. The kinase activity of LRRK2 is attenuated by binding to 14-3-3γ. Mutation of this binding site to an alanine results in loss of 14-3-3 binding. This is important, because a LRRK2 overexpression knock-in model showed lysosomal dysfunction and accumulation of α-synuclein enriched Lewy Bodies (253). Further, increased levels of 14-3-3γ in the cersbrospinal fluid are a diagnostic marker for the transmissible spongiform encephalopathy (TSE) Creutzfeldt-Jakob disease (CJD) (254,255).

1.3.1.8 Regulation of class switching in B cells by 14-3-3γ

14-3-3 proteins bind to supercoiled as well as cruciform DNA (256,257). 14-3-3γ specifically binds to the multiple 5'-AGCT-3' repeats in the IgH locus switch (S) regions, which is where

B-cell class switching occurs. This binding aids in the recruitment or stabilization of activation-induced cytidine deaminase (AID), protein kinase A (PKA) and uracil DNA glycosylase (258,259). Moreover, binding of 14-3-3γ, 14-3-3ζ and 14-3-3δ enhances the activity of AID and inhibition of recruitment of 14-3-3γ and AID inhibits class switch DNA recombination (259).

Besides these functions, 14-3-3γ is also postulated to have a role in the regulation of mRNA stability, transcription of synaptic genes, ion channel activation, regulation of P-Body formation and mitochondrial metabolism. However, the exact mechanism of this regulation is unknown.

1.3.2 Expression of 14-3-3γ in cancers

14-3-3γ is ubiquitously expressed in the cytoplasm as well as the nucleus. Its levels can vary across cancers.

Cancer subtype	Levels	Assay	Outcome	Reference
Non-Small Cell Lung Carcinoma (NSCLC)	Increased	IHC, Invasion assay, qRT-PCR, Western Blot	Poor survival, lymph node metastasis, increased invasion	(247,260)
Breast Cancer	Increased	Western Blot, IHC, MALDI TOF	Tumour progression, poor prognosis	(261,262)
Lung Cancer	Increased	RT-PCR,	Tumour	(263)

		Western Blot, IHC	progression	
Cholangiocarcinoma	Increased	IHC	Poor survival	(264)
Hepatocellular Carcinoma	Increased	IHC	Poor survival, extra hepatic metastases	(265)
Uterine leiomyoma	Decreased	Two - dimensional electrophoresis (2DE), Western blot, RT-PCR, IHC and mass spectrometry	NA	(266)

Table 1.1 Expression of 14-3-3γ in cancers

1.3.3 Mouse models of 14-3-3γ

In order to study the role of 14-3-3γ in vivo, Steinacker et al., developed 14-3-3γ knockout mice by introducing a neomycin resistance cassette in exon2 of the 14-3-3γ coding sequence (267). These mice did not have any physiological or developmental abnormalities. Given that levels of 14-3-3γ increase in the cerebrospinal fluid of patients with CJD, the 14-3-3γ knockout mice were injected with prions to study the effect of the loss of 14-3-3γ on the progression of CJD. However, there was no change in disease progression in wild type, heterozygous and knockout mice (267). There was no change in the levels of other 14-3-3 isoforms either. In another model, 14-3-3γ in the lateral ventricles of the brains of embryonic

mice was knocked down using shRNA (268). These mice had thicker stems and highly branched processes (268). Interestingly, the over-expression of 14-3-3γ in electroporated embryos also led to a delay in neuronal migration (269).

Mouse models with a partial loss of function of the gene of interest are essential in order to study the effect of genes which are involved in multiple pathways. Such mutants are called hypomorphic mutants. In order to generate a hypomorphic mutant of 14-3-3γ, lentiviruses harbouring 14-3-3γ shRNA were injected into the testes of pre-pubescent male mice (154). These pre-founder male mice were sterile and the testis section of these mice showed loss of cell-cell adhesion, and cell-matrix adhesion leading to collapse of the blood-testis barrier (BTB) and defects in spermatogonial stem cell differentiation and spermatocyte development and maturation (154).

1.4 The centrosome.

Error-free segregation of chromosomes in mitosis depends on the correct organization of the mitotic spindle. In mammalian cells, this is dependent on centrosome function. The centrosome is a membrane-less organelle, composed of two centrioles surrounded by a proteinaceous toroid, the pericentriolar matrix (PCM). Initially identified by Flemming and van Beneden, the name centrosome was given to this organelle by T. Boveri and literally means “central body”, alluding to its close association with the nucleus [reviewed in (270)]. It is the principal microtubule organizing centre (MTOC) in a mammalian cell. Due to its ability to organise microtubules, the centrosome exerts an influence on various processes in a cell; cellular trafficking, mediating an immune response, cellular signaling, cell polarity and cell cycle progression [reviewed in (271-274)]. Given their contribution to numerous cellular processes, any defects in centrosome structure or number can lead to several disease conditions [reviewed in (275)].

A mature centrosome in a mammalian cell in interphase is composed of two centrioles, a mother and a daughter, that differ in age and maturity (fig. 1.7). The older of the two centrioles, the mother centriole can be identified by the presence of distal and sub-distal appendages. Distal appendages are essential for anchoring the mother centriole at the cell membrane during ciliogenesis (276). Sub-distal appendages are essential for the microtubule organizing function of the centrosome [reviewed in (277)]. The mother centriole also has the ability to organize PCM, which is an electron dense layer of proteins surrounding the two centrioles (278). The PCM is responsible for all the microtubule organizing function of the centrosome. Several papers using 3D-SIM and STED nanoscopy have determined that PCM proteins are arranged into concentric layers that surround the mother centriole in a tube-like organization (279-282).

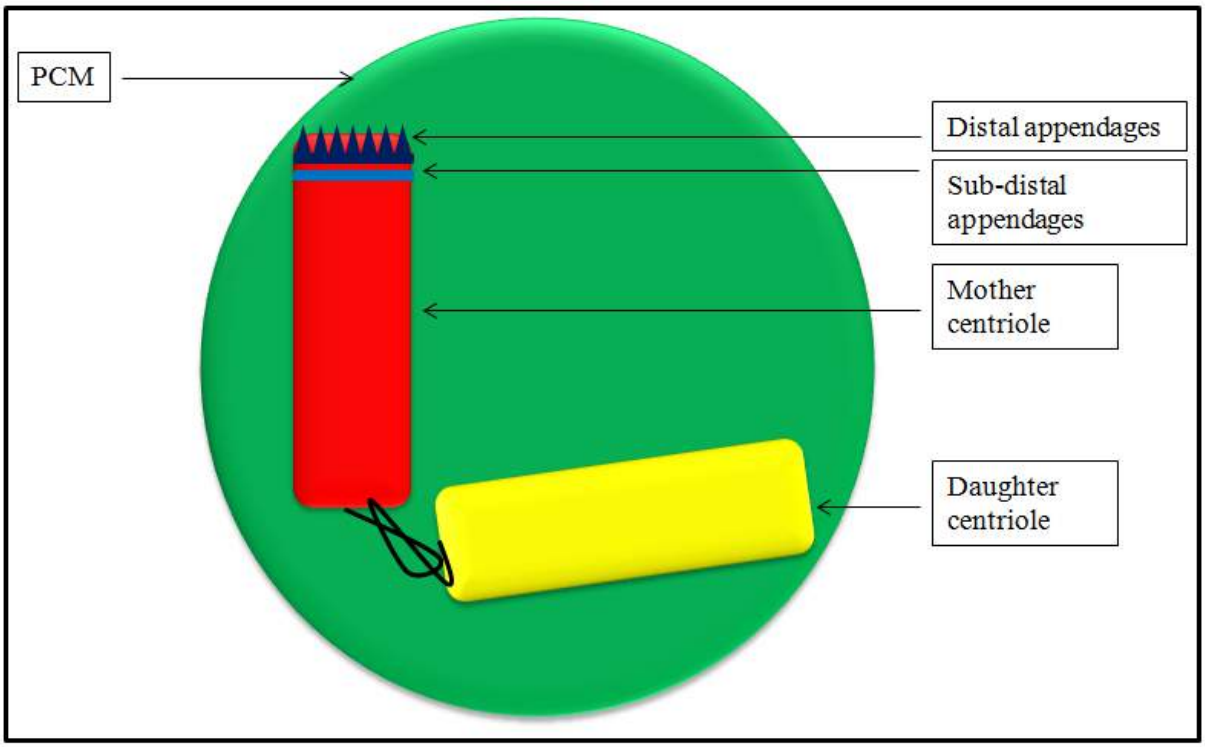

1.7 The centrosome *– The centrosome consists of two centrioles, the mother (shown in red) and the daughter (shown in yellow). The mother centriole possesses distal and sub-distal appendages. The two centrioles are surrounded by the PCM.*

1.4.1 Centriolar architecture

Most centrioles are made up of nine circularly organized triplet microtubules around a central cartwheel, in a typical 9+3 structure [reviewed in (283)]. This cartwheel consists of a central hub that is approx. 25 nm in diameter, and radial spokes, which are made of 9 homodimers of Sas-6 (284). The spokes emanating from the hub bind to the first microtubule of each triplet at a pinhead through an interaction between Cep135 and the microtubule (51).

The triplet microtubule has a complete A microtubule, onto which two additional partial microtubules (the B- and the C-tubules, respectively) are assembled. In humans and other organisms, the triplets are arranged in a circle with a diameter of approximately ~450 nm in height with inner and outer diameters of ~130 nm and ~250 nm, respectively. The triplet microtubules form the cylindrical cask of centrioles and basal bodies. They are arranged at a small angle off the circumference, giving the centrioles the look of a turbine. In humans, assembly of the triplets occurs sequentially, starting with the A-tubule, followed by the B- and C-tubules, respectively (285).

Made of microtubules, the centriole is an intrinsically polar structure with a proximal and a distal end. The proximal end is where the minus ends of the microtubule are positioned. A procentriole is built from the proximal end, using the SAS-6 cartwheel as a template (51). As demonstrated using CrSAS-6, the cartwheel is assembled from a seed of a single Sas-6 protein (51,284). Pairs of SAS-6 rings are then recruited in a step-wise manner (51). Recently, live analysis of GFP-tagged Drosophila Sas-6 via 3D-structured illumination microscopy (SIM) has also demonstrated that Sas-6 is incorporated from the proximal end of the cartwheel (286). Once the Sas-6 rings are assembled in a stack, peripheral components can be added to form the centriole. Cep135 has been postulated to act as the pinhead connecting the cartwheel with the microtubules, although its necessity can vary across

systems (51,287,288). Triplet microtubules are added along the central cartwheel. Cryotomography experiments have indicated that only the A-MT is complete and contains 13 protofilaments, while the B- and C-MTs share protofilaments with A- and B-MTs, respectively (51,289).

(a)

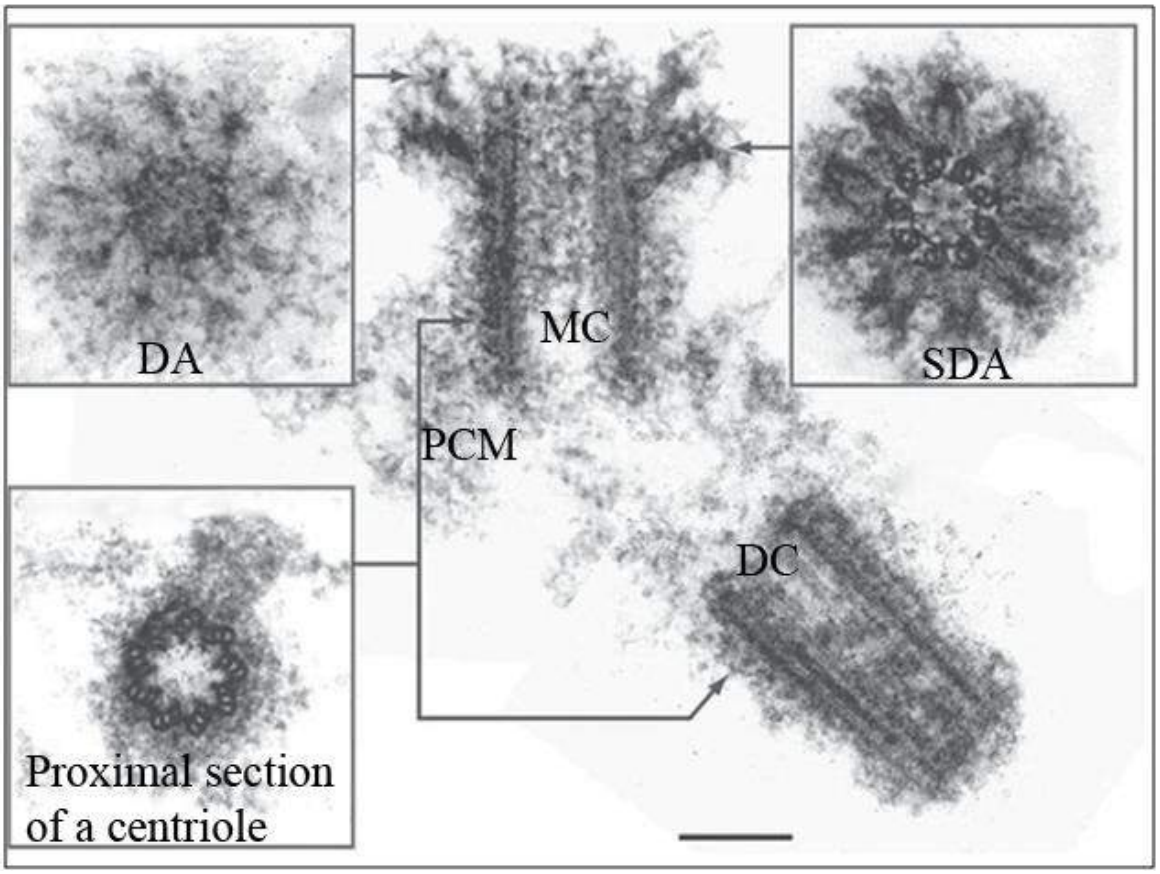

(b)

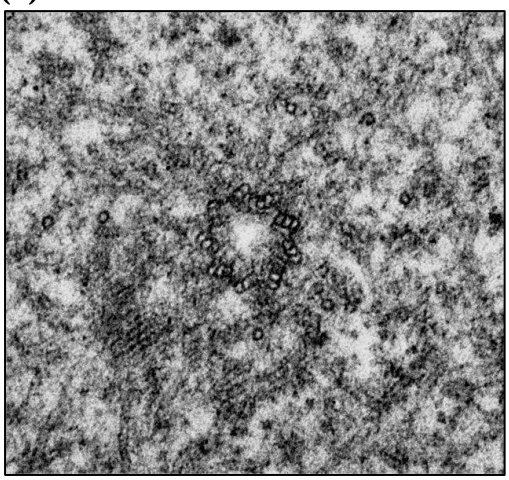

(c)

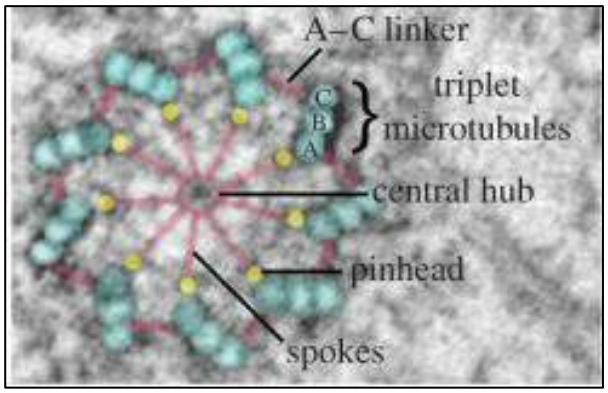

Fig. 1.8 Centriolar and cartwheel architecture *– (a) Electron micrographs of centrioles in isolated centrosomes shown in longitudinal section and cross sections highlighting the distal and subdistal appendages (MC – mother centriole, DC – daughter centriole, PCM – pericentriolar matrix, DA – distal appendages and SDA – sub-distal appendages (290), (b) Section of a centriole in HCT116 cells displaying the typical 9+3 structure, (c) Electron micrograph of a centriole superimposed with a cartoon representing the organisation of the central cartwheel and triplet microtubules (290).*

The centriole is made of different proteins that regulate its size, shape, length and assembly (fig. 1.9). CEP192, CEP63 and CEP152 which are present on the proximal end of the centriole, form a scaffold that recruits Plk4 (291). Plk4 marks the site of procentriole biogenesis on the proximal end of the mother centriole via a process of symmetry breaking (292-294). Plk4 interacts with and recruits STIL to this site, which then forms a complex with SAS6, initiating procentriole biogenesis (295,296). CPAP (centrosomal P4.1-associated protein), present within the procentriole and centriole and is essential for microtubule rescruitment via its interaction with Sas-4 (297-299). The protein SPICE (spindle and centriole-associated protein) has not be localized with precision (denoted with a question mark), but is theorized to be present below centrin in both the procentriole and centriole (297,298). At the distal end of the centrioles are proteins such as CP110 and centrin. CP110 (centriolar coiled-coil protein of 110 kDa) is present at the very distal tip of both centriolar cylinders. CEP120, CEP192 and CEP135 are found near microtubules in the procentriole and centriole, while Centrobin is only found in the vicinity of microtubules in the procentriole.

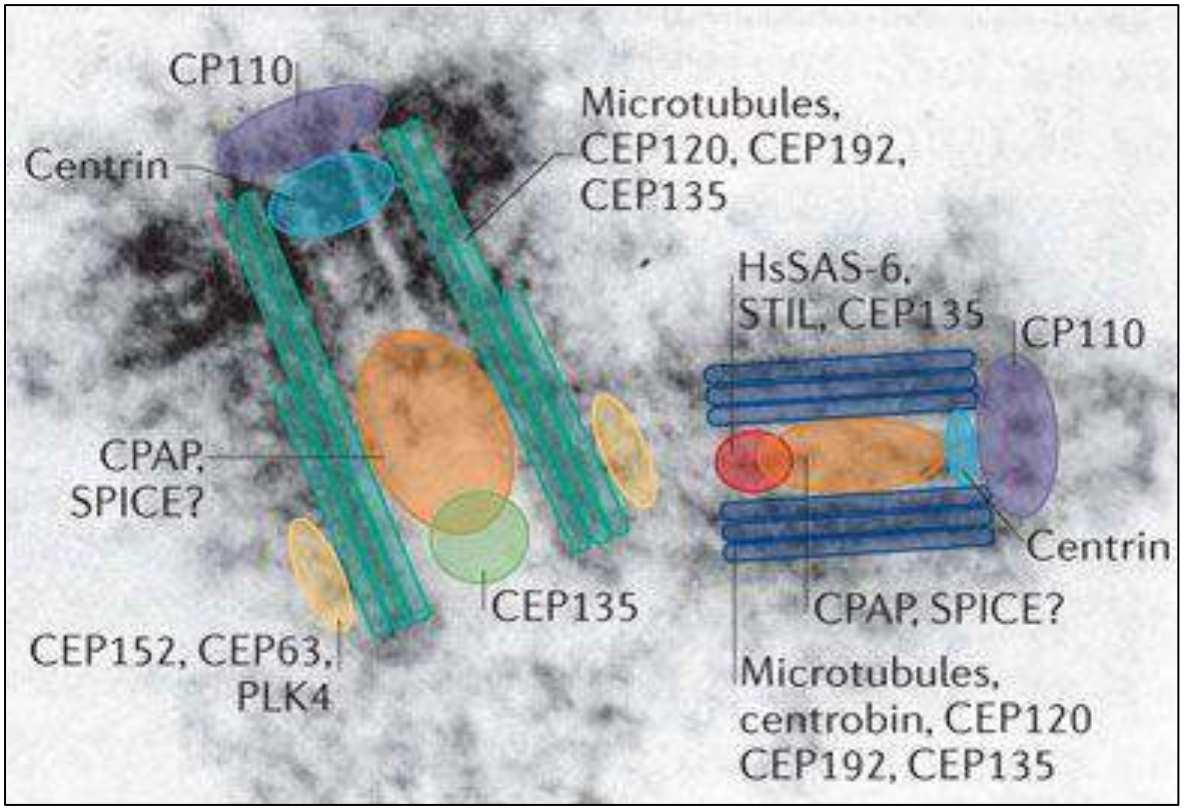

Fig. 1.9 Localisation of different proteins within the centriole and the procentriole *– Electron micrograph of a centrosome superimposed with a cartoon representing the localisation of different centriolar proteins (300).*

1.4.2 Centriolar appendages

Centriolar appendage proteins localise exclusively to the distal end of the mother centrioles and consist of distal and sub-distal appendages (table 1.2). These are present only on the mother centriole, and are acquired when the mother centriole undergoes maturation during the G2 phase of the cell cycle.

Centriolar appendage	Localisation	Reference
CEP83	Distal	(301)
CEP89	Distal	(302)

CEP164	Distal	(303)
FBF1	Distal	(276)
p150 Glued	Distal	(304)
SCLT1	Distal	(276)
Ninein	Sub-Distal	(305)
CEP170	Sub-Distal	(306)
CEP110	Sub-Distal	(305)
Nlp	Sub-Distal	(307)
ODF2	Sub-Distal	(308)
CEP128	Sub-Distal	(309)
CEP19	Sub-Distal	(310)

Table 1.2 List of centriole appendage proteins

1.4.2.1 Distal appendages

Distal appendage proteins (DAPs) are essential for cilia formation. Using knockdown experiments, it was shown that CEP164, which localises to the very end of the mother centriole, is necessary for the cilia formation (303). Furthermore, immunogold labelling showed that CEP164 localized to the very tip of the mother centriole at the distal appendages, and above the subdistal appendages.CEP164 is important for the targeting of RAB8 to the mother centriole, which promotes the formation of the ciliary membrane (311).

CEP83 recruits CEP89 and SCLT1 to the distal appendages, subsequently, SCLT1 targets CEP164 and FBF1 to DAPs. CEP164 and FBF1 are the downstream components in the DAP assembly pathway and their localization to the centrioles is not required for targeting of other DAPs (276).

1.4.2.2 Sub-distal appendages

Sub-distal appendage proteins (SDAPs) help the mother centriole to nucleate microtubules. ODF2 was shown to be required for the formation of both DAPs and SDAPs (312). Knockdown experiments have demonstrated that loss of NIN, DCTN1 and KIF3A (all localizing to the SDAP region), resulted in MT disorganization and loss of focused MT asters at the mother centriole (304,313). Knockout experiments have shown that there exists a heirarchy between proteins localising at the SDAP region. The first set of proteins named the ODF2 group consists of ODF2, CEP128, and Centriolin, with ODF2 being the most upstream component (309). The second subgroup, termed the NIN group, consists of NIN, CEP170, DCTN1, and KIF2A, with NIN being the most upstream component. Importantly, depletion of any member of the ODF2 group can abolish the localization of every component of the NIN group to the distal end of the mother centriole, but not vice versa.

1.4.3 G1-G2 tether

The G1-G2 tether is a proteinaceous linker that connects the proximal end of the two centrioles upon disengagement. C-NAP1 is present at the proximal end of the mother centrioles and the each pool of C-NAP1 is connected to the other by rootletin fibres (314,315). It is postulated that LRRC45 helps to link the rootletin fibres with C-NAP1 (316). STED nanoscopy experiments have demonstrated that a network of Cep68 binds to rootletin and increases the thickness of the rootletin fibres (315). Prior to centrosome separation, the degradation of the tether is initiated by the activity of the NIMA related kinase, Nek2 (317).

1.4.4 The centrosome duplication cycle

For ensuring the accurate segregation of the genome to the two daughter cells, the canonical centrosome duplication cycle is synchronized with the DNA replication cycle. Similar to the DNA duplication cycle, the typical centrosome duplication cycle is also semi-conservative; the new centrioles are formed using the previously existing centrioles as a template. There are two rules that govern the centrosome cycle -

1. Copy number control - This regulates how many centrioles can form adjacent to a previously existing centriole. This is essential, because the presence of more than one pro-centriole perpendicular to the mother centriole can affect the organization of the spindle.
2. Cell cycle control - This regulates the number of times in a cell cycle the centrosome can duplicate. Centrosome amplification is one of the results of loss of this control and is frequently observed in transformed cells.

The centrosome duplication cycle consists of four different phases; 1) Disengagement, 2) Duplication, 3) Maturation and 4) Separation. The four steps are discussed below (fig. 1.10).

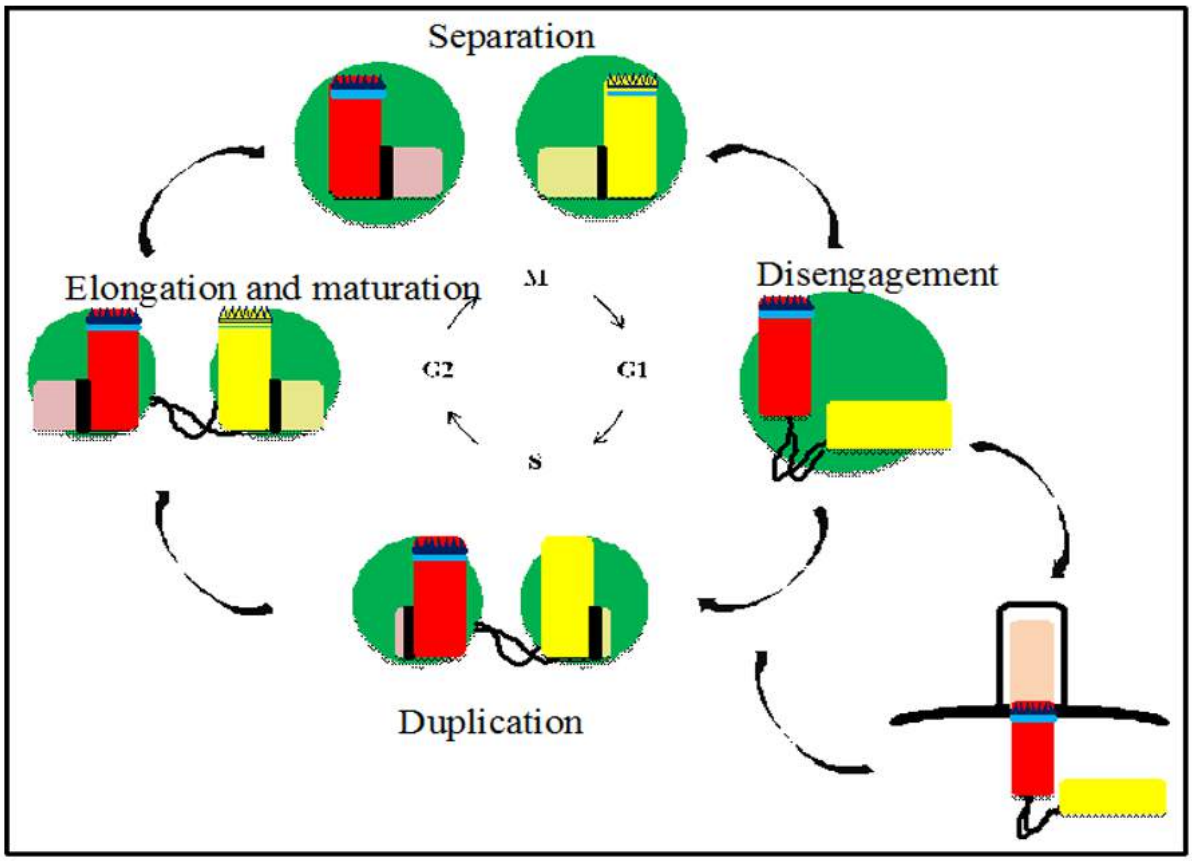

Fig. 1.10 The centrosome cycle. *The centrosome cycle consists of four distinct phases – Disengagement, Duplication, Elongation and maturation and Separation.*

1) Disengagement - The orthogonal arrangement of the mother and the daughter centriole from the beginning of the S phase to the beginning of mitosis, is referred to as centriole engagement. The mother centriole and its corresponding daughter centriole are orthogonally attached to each other via an S-M linker, the exact composition of which is currently unknown [reviewed in (318)]. For the initiation of pro-centriole biogenesis in the next cell cycle, it is essential that this orthogonal arrangement be lost, as it exerts a steric barrier on the same. This is known as *disengagement*. This disengagement step licenses both centrioles to begin the assembly of one procentriole at the next cell cycle. Dissolution of the S-M linker and establishment of the G1-G2 tether is one of the licensing factors for the initiation of centriole duplication. Disengagement requires the activity of enzymes such as Plk1 and

Separase (319). Both these enzymes act to facilitate the loss of the S-M linker, although their substrates are unknown. Pericentrin is postulated to be one of the substrates of Separase, as expression of a Pericentrin B mutant that cannot be cleaved by Separase results in an absence of disengagement in HeLa cells(320,321). Also, Separase is active only once in the cell cycle; during anaphase transition (322). This ensures the copy number control of the centrosome cycle. Inhibition of Plk1 activity using the small molecule BI2536, inhibits centriole disengagement during late G2 or early mitosis (319).

Nucleophosmin1 (NPM1) is a nucleolar protein that has been demonstrated to have a role to play in centriole disengagement. NPM1 has been demonstrated to localise between the paired centrioles of unduplicated centrosomes (323). It has been shown that phosphorylation of NPM1 at a Thr199 residue by CDK2 or CDK1 results in its displacement from the centrosome (56,324). Expression of a phospho-deficient mutant of NPM1 (T199A) has been demonstrated to inhibit centrosome duplication, while a phospho-mimetic mutant (T199D), promotes centrosome amplification (325,326).

Several recent reports have suggested that there might be other factors that govern centriole disengagement, apart from the loss of the orthogonal configuration (327-329). One of them has been demonstrated to be the distance between the mother and daughter centriole. Using light microscopy in HeLa cells, it has been demonstrated that centrioles are competent for duplication when they are at a distance of ~80 nm (330).

Before procentriole biogenesis can occur, the daughter centriole that is disengaged needs to become proficient at functioning as a mother centriole in the next cycle. This includes its ability to become duplication competent and being able to nucleate microtubules. This is achieved via a process called, “centriole to centrosome conversion”. This process is mediated by CDK1 and starts with the initial loss of the central cartwheel comprising of SAS6 dimers

(331). Next, the cartwheel-less centriole needs to be stabilized via the acquisition of Cep295 due to PLK1 activity (332). Further, the centrioles recruit Cep63, Cep152 and Cep192 to form a scaffold at the proximal end and are ready for procentriole biogenesis (291,333,334).

2) Duplication - Duplication is regulated by proteins such as Plk4, STIL, SAS6, Cep152, Cep192 and CDK2. As per the rule of copy number control in the centrosome cycle, only one procentriole must form adjacent to each mother centriole. This is brought about in the following manner. As the first step, Cep152 and Cep192 are recruited to the pre-existing centrioles that will serve as templates for the formation of the daughter centrioles. These two proteins form a scaffold around the centrioles (291). This scaffold recruits Plk4 to the centrioles. Plk4 is known as the master regulator of centriole duplication and its over-expression can result in centrosome amplification and in the generation of several procentrioles from a single mother centriole (335). Upon recruitment at the centriole, Plk4 initially localises in a ring-like manner around the centriole (292,293). To ensure the formation of only one procentriole from the mother centriole, this ring is focused into a single dot. One of the ways this is theorized to occur is due to its stabilization by STIL (294). Several such Plk4-STIL complexes are formed and there is a competition for the highest concentration of the Plk4-STIL complex (294). The point with the highest concentration of this complex marks the site of procentriole biogenesis (294). Another model suggests that the auto-activation and lateral inhibition activity of Plk4 determines where the ring will coalesce into a spot marking the site of procentriole biogenesis (295,296).

CDK1 is also essential for centrosome duplication. Recent studies in *Xenopus* egg extracts and HeLa cells indicate that Cyclin B1-CDK1 competes with Plk4 for binding to STIL (336). The Cyclin B1- CDK1 complex binds to STIL at the same site as Plk4. Therefore, when its levels are high during mitosis, it blocks the interaction between Plk4 and STIL by sequestering STIL. Once Cyclin B1 levels decrease after anaphase transition, Plk4 can bind

to STIL and participate in procentriole biogenesis. CDK1 thus prevents centrosome amplification by preventing premature complex formation between Plk4 and STIL (336). After recruitment of Plk4 and STIL marks the site of pro-centriole formation, SAS6 dimers localise to the same site and initiate pro-centriole assembly by assembling into higher order oligomers (337). SAS6 oligomerization is the building block for the 9-fold symmetrical centriole.

3) Elongation and Maturation - During late S to G2, once Plk4 has marked the site of pro-centriole biogenesis, centriole elongation is carried out by proteins such as CPAP, CP110 and SAS6 (338). Dimers of SAS6, the 9-fold symmetrical cartwheel protein, assemble into higher order oligomers and stack at the procentriole. Due to its nine-fold symmetry, it is able to act as a scaffold around which microtubules are assembled (337). CPAP is a tubulin dimer binding capping protein that, along with CP110, promotes microtubule assembly and controls centriolar length (298). CPAP and CP110 have opposing roles in the control of centriolar length (Schmidt, 2009, Current Biology). Unusually long centrioles can form due to overexpression of CPAP or by a reduction in the levels of CP110 (339). The growing microtubule triplets are linked to the SAS6 cartwheel via Cep135 (297). Centrin and hPOC5 localise to the distal lumen of centrioles and are essential for elongation at the distal end (340).

Along with procentriolar elongation, another event that occurs is the expansion of the PCM. This is necessary so that each of the two centrosomes can function as an independent MTOC. This includes the recruitment of γ-Tubulin Ring Complexes (γ-TURCs), which nucleate microtubules. In cultured vertebrate cells, PLK1 phosphorylates Pericentrin to initiate the centrosomal recruitment of several PCM proteins such as Aurora A and Cep192 (341). PLK1 phosphorylation of NEK9 leads to the phosphorylation of NEDD1 (also known as GCP-WD), which induces the recruitment of γ-tubulin to centrosomes at mitosis (342,343). CDK5

regulatory subunit-associated protein 2 (CDK5RAP2), Pericentrin and CEP192 mediated phosphorylation of NEDD1 can recruit γ-TURCs into the PCM (342). CEP192 is an important activator of centrosomal Aurora A and helps to coordinate the feedback activation of Aurora A and PLK1. Plk1 activity also recruits Cep215, a PCM protein, to the two centrosomes (342). Aurora A kinase, in conjunction with Plk1, phosphorylates components of the γ-TURCs, thus making them competent for the recruitment of microtubules (341). Experiments in *C. elegans* and *D. melanogaster* have demonstrated that loss of Aurora A can lead to abnormalities in centrosome maturation, with a reduction in the accumulation of α-tubulin and γ-tubulin at the centrosome (344,345). Centriole maturation also involves the acquisition of distal and sub distal appendages by the newly formed mother centriole. The recruitment of the sub-distal appendage protein ODF2 is one of the steps of this process (312). Ninein and Cep170 also function as sub-distal appendages and bind microtubules (346). Distal appendages such as Cep164, Cep89, Cep 83, FBF1 and SCLT1 are essential for membrane docking and ciliogenesis (276)

4**) Separation** – The G1-G2 tether is made of proteins such as C-Nap1 (Cep250), rootletin, Cep68 and LRRC45 (314,315,317,347-349). For the formation of a mitotic spindle, it is essential that the G1-G2 tether connecting the two centrosomes be degraded. This is brought about by the phosphorylation of C-NAP1 and rootletin by the NIMA related kinase, Nek2 (317). This phosphorylation leads to their displacement from the proximal end of the mother centrioles (314). Plk1 mediated degradation of Cep68, further displaces Cep215, a PCM protein, from the centrosome, resulting in loss of the G1-G2 tether (349).

Once the G1-G2 tether has undergone dissolution, the two centrosomes have to be separated, so as to form the mitotic spindle. This occurs primarily via the anti-parallel sliding action of the plus-end directed motor protein, Eg5 (350,351). Inhibition of Eg5 results in the presence of a monopolar spindle, with two centrosomes at a single pole (351). Additionally, proteins

such as dynein, Lis1 and CLIP-70, which are minus-end directed, contribute to spindle formation by inducing microtubule sliding in the direction opposite to that of Eg5. The combined action of these motor proteins and their binding partners promotes migration of the centrosomes to the two poles (352,353). Once the centrosomes are separated, they migrate to each end of the cell and form the mitotic spindle.

Fate of the centrioles upon exit from the cell cycle.

In post mitotic cells that have exited the cell cycle, formation of the primary cilium occurs. This is a single cilium that is observed only in resting or G0 cells. It is essential for sensing extracellular growth stimuli and is involved in many crucial pathways such as Hedgehog, Wnt and platelet- derived growth factor (PDGF) signaling. In a quiescent cell, the two centrioles in a centrosome can migrate to the plasma membrane, where the mother centriole – also referred to as the basal body – docks below the plasma membrane via the fusion of vesicles that cap the distal appendages [reviewed in (354)]. Then, lengthening of nine MT doublets of the mother centriole occurs and they form the nine doublets of the axoneme respectively. Centrioles are also required to begin the formation of motile cilia and flagella [reviewed in (355,356)]. Here, there are two additional centrally located MTs that form in the transition zone.

1.4.5 Functions of the centrosome.

Centrosomes can bind more than 100 regulatory proteins, which implies its functions in a several cellular processes.

1.4.5.1 Microtubule organization.

The cellular functions of microtubules, such an intracellular transport and the formation of a mitotic spindle, depend on microtubules being arranged in an ordered array. To assemble and

re-organize these arrays during different phases of the cell cycle or for different processes, cells need to be able to control their growth. This control is achieved by tethering them at an organizing centre, the predominant of which in a mammalian cell is the centrosome. The main microtubule nucleator is the γ-TURC, which forms a template for microtubule assembly [reviewed in (357)]. γ-TURCs present at the centrosome anchor the minus end of microtubules. The MTOC function of the centrosome is most apparent in its role in formation of the spindle. The number of centrosomes in a cell determines how many poles a mitotic spindle can have. The presence of less than two centrosomes in a mitotic cell leads to mitotic delay and a high rate of chromosomal instability (358). Centrosome amplification leads to the organization of a multipolar spindle, which is deleterious to normal cells (359,360). Mice overexpressing Plk4 in the developing CNS displayed centrosome amplification and a multipolar mitosis which results in aneuploidy and microcephaly (361). However, transformed cells are able to bypass the massive aneuploidy brought about by multiple centrosomes, by clustering their centrosomes and forming a pseudo-bipolar spindle (360).

1.4.5.2 Regulation of the cell cycle.

Due to the coupling of the cell cycle with the centrosome cycle, there are several cell cycle proteins that play a role in the centrosome cycle and vice versa. It has been demonstrated in Chinese Hamster Ovary (CHO) cells that Cyclin E and cyclin A contain a centrosomal localisation sequence (CLS) and that expression of a cyclin E mutant with a deletion of the CLS results in an inhibition of DNA replication (362). Expression of a mutant cyclin E that harboured the CLS but was unable to bind to CDK2 accelerated S phase entry (362). The accelerated S-phase entry is due to the centrosomal recruitment of MCM5 and Orc1 via the cyclin A CLS (363). Experiments in *C. elegans* embryos have shown that Aurora A at the centrosome controls nuclear envelope breakdown, which might occur due to its effect on the actomyosin networks (364-366). Further, it has also been demonstrated that the cyclin B-

CDK1 complex is first phosphorylated by Plk1 at the centrosome during prophase (367). The centrosome thus acts as an integration point for several cell cycle processes.

1.4.5.3 Immune response.

Centrosomes have been observed to move to the contact site of immune cell function. When immune cells such as T-cell lymphocytes first contact an antigen, the centrosome is positioned at that site. This re-orients the organization of the microtubule and its associated proteins. Due to the microtubules being aligned at the point of contact, microtubule associated organelles and secretory cytolytic vesicles can now access secretory sites and the cell is able to give rise to an immune reaction. Upon movement of the centrosome form the site of contact, the microtubules are re-organized again and the immune reaction is halted [reviewed in (273)]. The centrosome plays an important role in the initiation of an immune response.

1.4.5.4 Cellular signaling.

Several proteins involved in the DNA damage response, such as p53, Chk1, Chk2, Brca1 and Brca2 localize to centrosomes, in addition to their cytoplasmic and / or nuclear localizations [reviewed in (368)]. Centrin, a protein that is essential for procentriole biogenesis, interacts with a core component of nucleotide excision repair (NER), Xeroderma Pigmentosum group C protein, (369). A knockout of all Centrin isoforms in chicken DT40 cells resulted in delays in NER, but no discernible centrosome phenotype (370). A single nucleotide change in the Pericentrin gene ($PCNT^{3109G>T}$) causes Seckel syndrome and results in its loss from the centrosome (371,372). Cells isolated from patients with Seckel syndrome also exhibit a defect in ATR checkpoint signalling (371,372). Similarly, a knockdown of Cep164 in *Zebrafish* was shown to cause nephronophthisis-related ciliopathies and dysregulated DDR

(373). All these reports elucidate the role of the centrosome as a cellular signalling integration point.

1.4.5.5 Actin organization.

Microtubules and actin are two of the main cytoskeletal elements in a cell regulating cellular architecture. The centrosome is the fundamental MTOC in a cell. However, several studies suggest that it plays a role in organizing the actin network too. Centrosomes purified from the human T-lymphocyte Jurkat cell line could generate large radial arrays of actin filaments, when seeded on glass coverslips in the presence of 1 μM purified actin monomers (374). It was further demonstrated that this nucleation was modulated by PCM1 via its recruitment of the nucleation promoting factor WASH and Arp2/3 complex at the centrosome (374). Centrosome-associated Arp2/3 locally concentrates F-actin in resting lymphocytes (375). This is essential for tethering the centrosome to the nucleus. Upon lymphocyte activation, Arp2/3 levels at the centrosome decrease, which releases the centrosome from being bound to the centrosome so that it can migrate to the synapse (375). An inverse co-relation exists between actin and microtubule nucleation at the centrosome (376). The centrosome thus has a dual role in organizing the cytoskeleton.

1.4.5.6 Cell migration and polarity.

In wound healing assays using fibroblast monolayers, the centrosome is localized between the nucleus and the leading edge of cells (377). Due to this, both the Golgi complex and the endocytic recycling compartment are positioned between the nucleus and the leading edge (377). Cells lining the tissue periphery lose cell-cell contact to be able to migrate during epithelial-to-mesenchymal transition (EMT). This involves a change in polarity from apico-basal to migratory front and rear end polarity. In developing mouse embryos, cultured 3D cell aggregates and micro-patterned cell doublets, the change in polarity involves the movement

of centrosomes from their off-centered position next to intercellular junctions, toward extracellular matrix adhesions on the opposite side of the nucleus, results in the reversal of internal polarity (378). This movement also included the disassembly of the microtubule network (378).

1.4.5.7 Asymmetric cell division.

Asymmetric cell division is essential for the maintenance of a stem cell pool. One daughter cell continues as the stem cell, whereas the other undergoes differentiation. It was first demonstrated using Drosophila neuroblasts that there is a preference for centrosome inheritance between the two daughter cells of a stem cell (379). When centrosomes split in *Drosophila* neuroblasts, the younger centrosome is retained by the stem cells. The older centrosome is inherited by the differentiating daughter cell and lacks PCM. This centrosome migrates away to the other side of the cell before it begins rebuilding its PCM (379). This inheritance pattern is cell-type specific, as in the case of Drosophila male germline stem cells, the mother centriole is the one that is retained by the stem cell (380). The functional consequences of these inheritance patterns are unknown.

1.4.6 Centrosomes and cancer

Deregulation of any step of the centrosome cycle can result in centrosome abnormalities. These can be classified into two types – a) structural, and b) numerical. Both these abnormalities can contribute to neoplastic progression.

The overexpression of Ninein like protein (Nlp) in MCF10A derived 3D acini can lead to excessive cell proliferation and formation of defective acini (381). The overexpression of Nlp results in a diffuse localization of E cadherin at adherens junctions (382). The adherens junctions are thus, weak and lead to increased mechanical stress when a cell in the epithelial

tissue enters mitosis (382). Also the microtubules in such cells are more stabilized (382). When such a cell enters mitosis, due to the excessive mechanical stress, it buds out from the original site and might become metastatic (382). In addition to the increased invasion, structural alterations to the centrosome, could also lead to aneuploidy which often contributes to tumour progression (383).

Copy number changes in centrosome number can occur due to centrosome over-duplication, defects in cytokinesis or due to the *de novo* formation of centrosomes. Several tumour cells show centrosome amplification, suggesting that the change in centrosome number could drive aneuploidy and thus, tumour progression (384). However, it is only recently that the causative link between centrosome amplification and tumour progression has been established. The first evidence was derived from experiments in Drosophila. No spontaneous tumours formed in transgenic flies overexpressing Plk4 and they were also viable (385). However, in a tissue transplantation assay, brain tissue from flies overexpressing Plk4 was transplanted into the abdomen of WT hosts (385). It was observed that that a significant percentage of the hosts developed tumours with multiple centrosomes and metastatic colonies (385). In a similar transplantation assay, Castellanos et. al., screened for the ability of mutants of different centrosomal proteins to affect tumour formation in Drosphila (386). They were able to demonstrate that 2% of the WT hosts with wing discs from flies overexpressing Sak transplanted into their abdomen could develop tumours (386).

Studies on Plk4 overexpression have shown significant centrosome amplification in the liver and skin, but not in the lung or kidney (387). Despite the centrosome amplification, there was no increase in spontaneous tumor formation or decreased survival compared to controls. Decreasing p53 levels alone induced many tumors, but Plk4 overexpression did not enhance the same (387). It was observed that there was an increase in the speed of tumour initiation in

p53-/- mice with either tissue wide or only an epidermis specific overexpression of Plk4 (388,389).

Inversely, overexpression of Plk4 can initiate tumorigenesis, in a mouse intestinal neoplasia model (390). In a recent study, widespread overexpression of Plk4 in mice demonstrated for the first time that centrosome amplification can initiate tumourigenesis (390). Mice were followed for more than 35 weeks post Plk4 overexpression and it was found that from 35 weeks of age, the mice exhibited a dramatic increase in the spontaneous formation of lymphomas, squamous cell carcinomas, and sarcomas. Like many human tumours, these also exhibited aneuploidy and chromosomal instability. There was also a reduction in the levels of p53 and its target genes (390). These results suggest that centrosome amplification, in conjunction with p53 inactivation over time, can result in tumour formation.

1.4.7 Centrosome clustering

Normal cells with centrosome amplification undergo a multipolar mitosis and eventual apoptosis (391). A multi-polar mitosis in most tumour cells also leads to cell death, ostensibly due to loss of genes that are absolutely required for cell viability. Experiments in a transgenic *Zebrafish* line overexpressing Plk4 under a heat shock promoter demonstrate that neuroepithelial cells harbouring centrosome amplification undergo apoptosis (392). Similarly mice with centrosome amplification in the CNS due to conditional overexpression of Plk4 exhibit microcephaly, due to increased apoptosis (393). It is interesting to study how transformed cells harbouring multiple centrosomes prevent the massive aneuploidy resulting from multi-polar mitoses. In order to tolerate the burden of extra centrosomes, transformed cells have developed a mechanism called clustering (391). In transformed cells with multiple centrosomes, during mitosis, centrosomes are not organized in a multipolar spindle. in fact, they migrate to and cluster at two poles leading to the formation of a pseudobipolar spindle

during metaphase (360,385,394). This pseudobipolar spindle is less efficient at separating chromosomes and contributes to errors in kinetochore-microtubule attachments, especially the formation of merotelic attachments, which contributes to the presence of lagging chromosomes and an increase in chromosome instability (CIN) (359,395). However, the CIN is still at a low enough rate, that the tumor cells survive and give rise to neoplastic clones.

Multiple studies have attempted to identify gene products/molecular pathways required for centrosome clustering. This could lead to the identification of small molecules that inhibit clustering, as this might result in multi-polar mitoses resulting in killing of tumour cells. A screen developed by Kwon et al attempted to identify genes required for clustering using *Drosophila* S2 cells (360). siRNA mediated knockdown of the motor protein HSET, induced the formation of multipolar spindles in human cancer cells harbouring multiple centrosomes (360). A reduction in the levels of proteins that are essential for the Spindle Assembly Checkpoint (SAC); Mad2, BubR1 (human Bub1), and CENP-E can also generate multi-polar spindles in S2 cells (360). Several actin binding proteins were also identified in these screens suggesting that disruption of actin dynamics could inhibit centrosome clustering (360,396). This is consistent with recent data from the Godinho laboratory, which suggests that normal cells are unable to cluster centrosomes due to the presence of E-cadherin, which confers less actin contractility on these cells (397).

Proteins that are a part of the chromosomal passenger complex (CPC), proteins of the Ndc80 complex, Cep164, and Aurora B, which all contribute to spindle tension, are also required for centrosome clustering, as shown in a genome wide RNAi screen in UPCI:SCC114, a human Oral Squamous Cell Carcinoma (OSCC) cell line (396). Depletion of Aurora A in a panel of

Acute Myeloid Leukemia cell lines also results in formation of a multipolar spindle and non-proliferation (398).

Several drugs that bind to cytoskeletal elements, such as Griseofulvin, CP-673451 and crenolanib, inhibit clustering demonstrating the contribution of the cytoskeleton towards clustering (399,400). CCB02, a drug that inhibits the interaction of CPAP and tubulin activates extra centrosomes to undergo increased PCM expansion (299). This causes cells to undergo revert from a clustered mitosis to a multipolar one, prolonging mitosis, and eventual cell death. 3D-organotypic invasion assays using tyrosine kinase inhibitor (TKI)-resistant EGFR-mutant non-small-cell lung cancers show that CCB02 has anti-invasive activity (299).

Loss of 14-3-3γ leads to premature CDC25C activation and hence cdk1 activation, which leads to an increase in centrosome number. This is accompanied by an increase in the number of cells with pseudo-bipolar spindles with passage, an increase in aneuploidy and tumour formation (326). However, expression of a CDC25C S216A mutant, that is deficient for 14-3-3 binding, in 14-3-3γ knockdown cells, leads to a reversal of the clustering phenotype and a decrease in tumour growth and cell viability, presumably due to prematurely high levels of cdk1 activity in interphase and mitosis (326). All of these results suggest that centrosome clustering is a complex phenotype that requires multiple cellular pathways.

2. Aims and Objectives

2. Aims and objectives

- Does 14-3-3 binding to centrosomal proteins inhibit centrosome licensing and duplication?
- How do 14-3-3 proteins regulate centrosome clustering?

3. Materials and Methods

3. Materials and methods

3.1 Plasmids and constructs

The pGEX4T1 14-3-3γ WT plasmid has been described previously (401). pcDNA3 Plk4 (Sak) wt (Nigg HR9) was a gift from Erich Nigg (Addgene plasmid #41165; http://n2t.net/addgene:41165: RRID:Addgene_41165). Cdk2-HA was a gift from Sander van den Heuvel (Addgene plasmid #1884; http://n2t.net/addgene:1884; RRID:Addgene_1884). The CDK1 WT and CDK1 AF constructs have been described previously (326). pSLIK CA ROCK2 was a gift from Sanjay Kumar (Addgene plasmid #84649; http://n2t.net/addgene:84649; RRID:Addgene_84649). pEGFPCentrin2 (Nigg UK185) was a gift from Erich Nigg (Addgene plasmid #41147; http://n2t.net/addgene:41147; RRID:Addgene_41147).

All the primers used in generating the following constructs are given in Table 3.1. All the DNA constructs described in this section were sequenced before being used for expression and other studies. All the vector maps were created using SnapGene Viewer software.

Name of gene	**Sequence**
Centrin2 5' Xho	CTCGAGCTATGGCCTCCAACTTTAAGAAGGCA
Centrin2 C1 3'	TTAAGCTTTTCAAAGCCCAGGGCCCT
Centrin2 C2 3'	TTAGGATCCCTCAGACATTTTCTGGGTCATCAC
Centrin2 C3 3'	TTAGGATCCGTTCTCACCCAACTCCTTGG
Centrin2 C4 3'	GGATCCTTAATAGAGGCTGGTCTTTTTCA
Centrin2 64 5'	CTCGAGCTATGCCCAAGAAAGAAGAAATTAAGA

Centrin2 37 3’	GGGATCCAAAAGCTTCCCGGATCTC
Centrin2 47 3’	TGGATCCGGTGCCAGTTCCATCCGC
Centrin2 28 5’	GGCTCGAGATGGAGCAAAAGCAGGAG
Centrin2 38 5’	CTCGAGCTATGGATCTTTTCGATGCGGAT
Centrin2 48 5’	CTCGAGCTATGATAGATGTTAAAGAACTGA
Centrin2 D39 5’	GCAGGAGATCCGGGAAGCTTTTGCGCTTTTCGATGCGGATGGAACTGGCA
Centrin2 D39 3’	TGCCAGTTCCATCCGCATCGAAAAGCGCCAAAAGCTTCCCGGATCTCCTGC
Centrin2 T45A 5’	GATCTTTTCGATGCGGATGGCGCCGGCACCATAGATGTTAAAGAACTG
Centrin2 T45A 3’	CAGTTCTTTAACATCTATGGTGCCGGCGCCATCCGCATCGAAAAGATC
Centrin2 T47A 5’	CTTTTCGATGCGGATGGAACTGGCGCCATAGATGTTAAAGAACTGAAG
Centrin2 T47A 3’	CTTCAGTTCTTTAACATCTATGGCGCCAGTTCCATCCGCATCGAAAAG
Centrin2 T45/T47A 5’	ATCTTTTCGATGCGGATGGCGCCGGCGCCATAGATGTTAAAGAACTGAAG
Centrin2 T45/T47A 3’	CTTCAGTTCTTTAACATCTATGGCGCCGGCGCCATCCGCATCGAAAAGAT
NPM1 Xho 5’	CTCGAGATGGAAGATTCGATGGACATG
NPM1 EcoRI 3’	AAAGAGACTTCCTCCACTGC
NPM1 S48A 5’	GTTATCTTTAAGAACGGTAGCGCTCGGGGCTGGTGCAAAGGATGAGTTGC

NPM1 S48A 3’	GCAACTCATCCTTTGCACCAGCCCCGAGCGCTACCGTTCTTAAAGATAAC
NPM1 S218A 5’	GAAAAGACTCAAAACCATCAGCAACACCAAGATCTAAAGGACAAGAATCC
NPM1 S218A 3’	GGATTCTTGTCCTTTAGATCTTGGTGTTGCTGATGGTTTTGAGTCTTTTC
NPM1 S293A 5’	AGAGGCTATTCAAGAGCTCTGGCAGTGGAGGAAGGCTCTTTAA
NPM1 S293A 3’	TTAAAGAGCCTTCCTCCACTGCCAGAGCTCTTGAATAGCCTCT
NPM1 S48E 5’	CCAGTTATCTTTAAGAACGGTCGAGCTCGGGGCTGGTGCAAAGGATGAGT
NPM1 S48E 3’	ACTCATCCTTTGCACCAGCCCCGAGCTCGACCGTTCTTAAAGATAACTGG
14-3-3γ EcoRI 5’	GGAATTCATGGTGGACCGCGAGC
14-3-3γ XhoI 3’	TCCTCGAGATTGTTGCCTTCGCCGC
14-3-3γ D129A 5’	GAAGATGAAAGGGGCCTACTATCGATACCTGGCTGAAGTGGC
14-3-3γ D129A 5’	GCCACTTCAGCCAGGTATCGATAGTAGGCCCCTTTCATCTTC
14-3-3γ E136A 5’	TACTACCGCTACCTGGCTGCAGTGGCCACCGGTGAGAAAAGGGCGACGGT
14-3-3γ E136A 3’	ACCGTCGCCCTTTTCTCACCGGTGGCCACTGCAGCCAGGTAGCGGTAGTA
14-3-3γ R56A 5’	AAGAACGTTGTGGGGGCAGCAAGATCTTCCTGGAGGGTC
14-3-3γ R56A 3’	GACCCTCCAGGAAGATCTTGCTGCCCCCACAACGTTCTT

γ-tubulin 5’	CTCGAGATGCCGAGGGAAATCA
γ-tubulin G3 3’	GAAGCTTCTGCTCCTGGGTGCCC
γ-tubulin G2 3’	TAAGCTTCTGGCGACAGGTTCTCT
γ-tubulin G1 3’	CAGAAGCTTGATCTGGGAGAAGGATGG
CDK2 T14 SFO 5’	GTGGAAAAGATCGGAGAGGGCGCCTACGGAGTTGTGTACAAAGCCAGAAA
CDK2 T14 SFO 3’	TTTCTGGCTTTGTACACAACTCCGTAGGCGCCCTCTCCGATCTTTTCCAC
CDK2Y15 BSRG 5’	AAAAGATCGGAGAGGGCACGTTCGGAGTTGTGTAAAAAGCCAGAAACAAG
CDK2Y15 BSRG 3’	CTTGTTTCTGGCTTTGTTCACAACTCCGAACGTGCCCTCTCCGATCTTTT
GCP2 5’	CCTCGAGATGAGTGAATTTCGGATTCA
GCP2 GC3 3’	GAAGCTTCTGTGCGGTGACTGCG
GCP2 GC2 3’	GCAAGCTTCATGCAGTCCTTCAGGCAG
GCP2 GC1 3’	TAAAGCTTGTCCTCCACCACGGCCG
14-3-3γ shRNA 5’	CCGGAGGGTCATCAGTAGCATTGAAAGTTCTCTTCAATGCTACTGATGACCCTCCTTTTTTC
14-3-3γ shRNA 3’	TCGAGAAAAAAGGAGGGTCATCAGTAGCATTGAAGAGAACTTTCAATGCTACTGATGACCCT

Table 3.1 Oligonucleotides used.

3.1.1 Generation of deletion constructs of Centrin2.

To generate the C-terminal and N terminal deletion constructs of Centrin2, we amplified the different sequences from the EGFP-Centrin2 construct (fig. 3.1) (402). Forward primers with an XhoI site and reverse primers with a BamHI site were used to amplify the various

sequences and clone them into a TA vector. Then, using XhoI and BamHI restriction sites, these sequences were cloned into an EGFP-C1 vector. For the N terminal deletions, the forward primer included a sequence encoding the start codon, AUG.

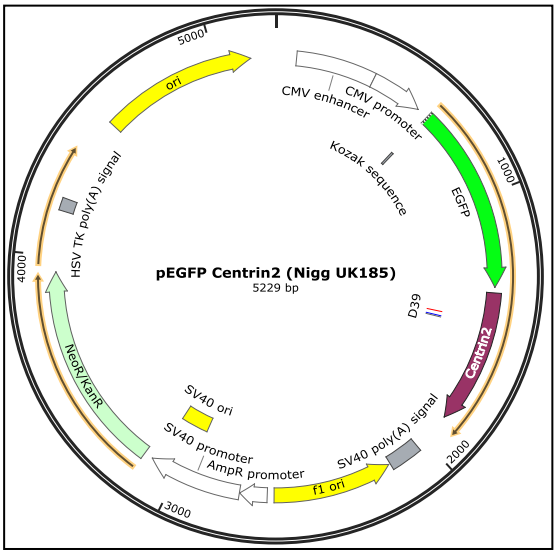

Fig. 3.1 Map of the EGFP-Centrin2 construct.

3.1.2 Site Directed Mutagenesis to generate the point mutants of Centrin2.

To discover possible 14-3-3 binding sites on Centrin2, a web based prediction server was used (403).Two putative sites were identified; T45 and T47. These two residues were altered to generate T45A, T47A and T4547A. Mutation of T45A would lead to the generation of a NaeI site and mutation of T47A would generate a SfoI site. We also hypothesized that a D39 residue might function as a phosphomimetic 14-3-3 binding site and mutated it to Ala, to generate a HhaI site. The EGFP-Centrin2 construct was used as the template.

PCR components	**Forward Mix (µL)**	**Reverse Mix (µL)**
HF Buffer 5X	5.0	5.0

Fwd primer (25 pmol)	1.0	0.0
Rev primer (25 pmol)	0.0	1.0
dNTPs 10mM	0.5	0.5
DMSO (100%)	0.75	0.75
Template (100 ng/µL)	1.0	1.0
Phusion polymerase (2U/µL) (Thermo Fisher Scientific)	0.25	0.25
Milli Q	17.0	17.0

Table 3.2 List of components used in making sited directed mutagenesis (SDM) PCR mix.

SDM PCR program:

1) Initial denaturation at 95°C for 5 minutes.

2) Denaturation at 95°C for 1 minute.

3) Annealing at 50°C for 1 minute.

4) Extension at 72°C for 4 minutes. (2kb/min)

5) Repeat from step 2 for 9 cycles.

6) Hold at 4°C forever.

For the first 9 cycles, the forward and reverse mixes were incubated in different tubes. After 9 cycles, forward and reverse PCR mixtures were mixed and the above PCR program was repeated. A control reaction was also set up, using only the template DNA and MQ. The final PCR product and the control were then digested with DpnI (NEB) to degrade template DNA

(methylated DNA). After digestion with DpnI, the PCR product was used for transforming competent DH5α cells. The transformants were grown at 37°C. The clones obtained were screened using the respective restriction enzymes.

3.1.3. Generation of deletion constructs of γ-tubulin.

To generate the C-terminal deletion constructs of γ-tubulin, we amplified the different sequences from the EGFP-γ-tubulin construct. Forward primers with an XhoI site and reverse primers with a HindIII site were used to amplify the various sequences and clone them into a TA vector. Then, using XhoI and HindIII restriction sites, these sequences were cloned into an ECFP-N1 vector.

3.1.4 Generation of deletion constructs of GCP2.

To generate the C-terminal deletion constructs of GCP2, we amplified the different sequences from the FLAG-GCP2. Forward primers with an XhoI site and reverse primers with a HindIII site were used to amplify the various sequences and clone them into a TA vector. Then, using XhoI and HindIII restriction sites, these sequences were cloned into an ECFP-N1 vector.

3.1.5 Site Directed Mutagenesis to generate the point mutants of 14-3-3γ.

For the generation of point mutants of 14-3-3γ, an shRNA resistant WT 14-3-3γ cDNA (234) was amplified and cloned into pCMV mOrange digested with EcoRI and XhoI (New England Biolabs) (fig. 3.2). A web based prediction server was used to identify possible 14-3-3 binding sites (403). The following mutant versions of 14-3-3γ, D129A, E136A, R56A, R56AD129A, R56AE136A, D129AE136A and R56AD129AE136A were generated by site directed mutagenesis (SDM) (404). For D129A, the SDM primers were designed so that the D129A mutation would lead to the generation of a ClaI site. For E136A, mutation would lead to the generation of an AgeI site. For R56A, mutation would generate a BglII site. The PCR

reaction was the same as that described in table 3.2. The final PCR product and the control were then digested with DpnI (NEB) to degrade template DNA (methylated DNA). After digestion with DpnI, the PCR product was used for transforming competent DH5α cells. The transformants were grown at 37°C. The clones obtained were screened using the respective restriction enzymes.

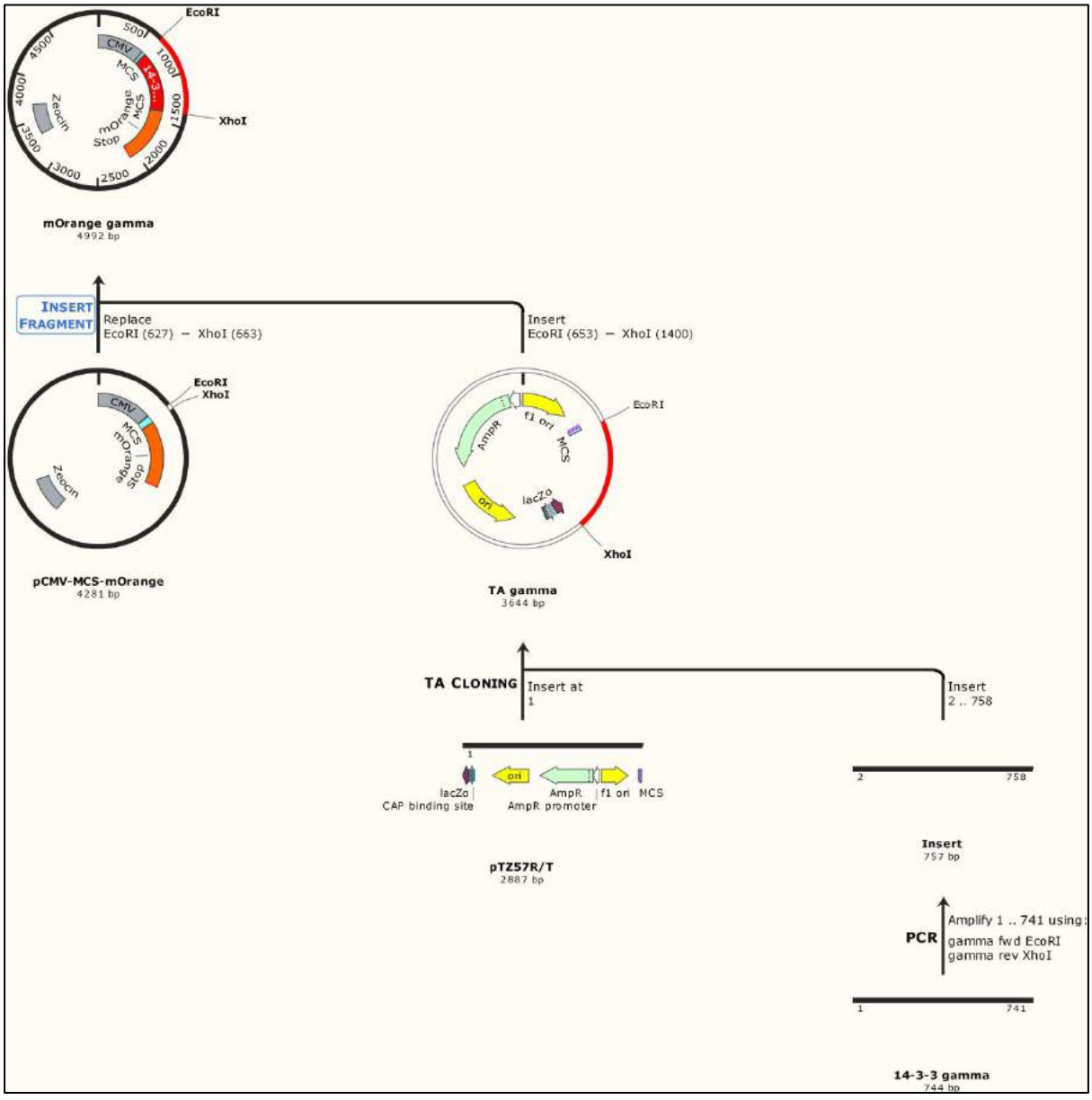

Fig. 3.2 Cloning strategy for generating mOrange tagged 14-3-3γ.

3.1.6. CFP tagged NPM1.

In order to generate CFP tagged WT NPM1, FLAG tagged NPM1 was used. Using a forward primer with an XhoI site and a reverse primer with a BamHII site, NPM1 was first subcloned into a TA vector. Then, we digested the positive TA – NPM1 clone with XhoI and BamHI to excise the NPM1 fragment and clone it into the ECFP-N1 NPM1 construct (fig. 3.3).

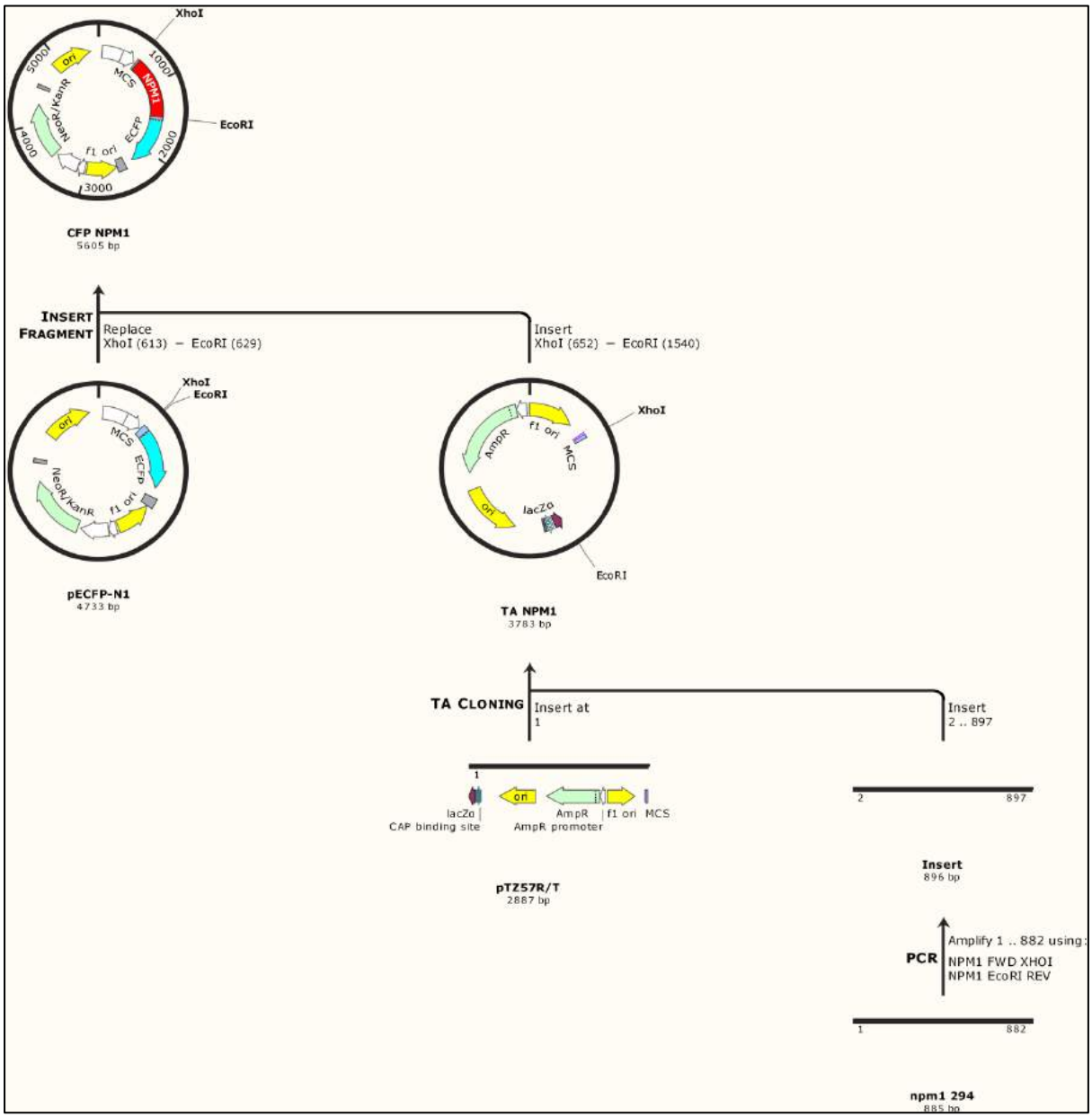

Fig. 3.3 Cloning strategy for generating ECFP tagged NPM1.

Reagent	Volume (µL)
FLAG tagged NPM1 (100 ng/µL)	1.0
Forward primer (20pM)	1.0
Reverse primer (20pM)	1.0
Taq polymerase (NEB)	0.2
dNTPs (20mM)	0.5
MgCl2 (Fermentas)	1.5
DMSO	1.0
Buffer 10X (NEB)	2.0
MQ	11.8
Total	20.0

Table 3.3 List of components used in making PCR mix.

PCR program:

1) Initial denaturation at 95°C for 5 minutes.

2) Denaturation at 95°C for 1 minute.

3) Annealing at 60°C for 1 minute.

4) Extension at 72°C for 1 minutes. (1 kb/min)

5) Repeat from step 2 for 29 cycles.

6) Hold at 4°C forever.

3.1.7 Site Directed Mutagenesis to generate point mutants of NPM1.

For generating the point mutants of NPM1, the CFP tagged NPM1 was used as the template. The following mutant versions of NPM1, S48A, S48E, S143A and S293A were generated. The S48A mutation would generate an AgeI site, S48E, a SacI site, S293A, a SacI site and S143A, an EagI site. The SDM PCR reaction components were the same as that given in table 3.2. The PCR program was the same as that described in section 3.1.2, except that the annealing was performed at 55°C.

3.1.8 Generation of HA-tagged 14-3-3γ mutants.

The 14-3-3γ mutants were cloned downstream of the HA epitope tag in pCDNA3 HA 14-3-3γ (152) by replacing the WT construct using BamHI and XhoI (New England Biolabs). All primer sequences are listed in table 1.

3.1.9 Generation of HA CDK2 AF.

In order to generate HA-CDK2 AF, HA-CDK2 was used as the template (fig. 3.4). To convert HA-CDK2 WT to HA-CDK2 AF, SDM was performed using the same components as that given in table 3.2. T14 and Y15 in the WT sequence were converted to Ala and Phe respectively. Mutation of T14A would generate a SfoI site and mutation of Y15F would generate a BsrgI site. The PCR program was the same as that described in section 3.1.2, except that the annealing was performed at 60 °C. The final PCR product and the control were then digested with DpnI (NEB) to degrade template DNA (methylated DNA). After digestion with DpnI, the PCR product was used for transforming competent DH5α cells. The transformants were grown at 37°C. The clones obtained were screened using the respective restriction enzymes.

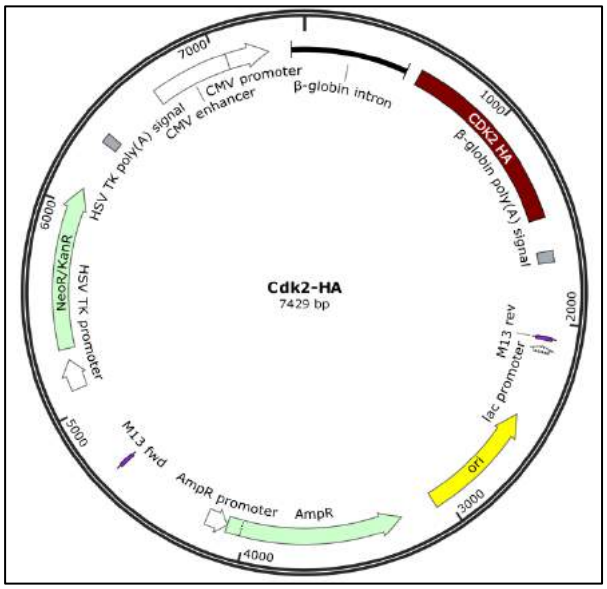

Fig. 3.4 Map of the CDK2-HA construct.

3.1.10 Cloning of 14-3-3γ shRNA into pLKO.1 Hygro vector

In order to generate a knockdown of 14-3-3γ in HeLa cells, we needed to clone the shRNA targeting 14-3-3γ into a pLKO.1 Hygro vector. For this purpose, we used previously validated shRNA sequences (234). The shRNA sequences contained an AgeI site in the forward primer and an EcoRI site in the reverse primer. In the pLKO.1 Hygro vector, these two sites are at a distance of 24 bps, which would make it difficult to screen for positive clones. Therefore, we first excised RFP from the pTRIPz vector using AgeI and EcoRI restriction enzymes and ligated it with the pLKO.1 Hygro vector also digested with the same enzymes. The pLKO.1 Hygro-RFP clones were then digested with AgeI and EcoRI and the pLKO.1 Hygro backbone ligated with the shRNA. Positive clones would have a fragment of ~65 bps and negative clones would have a fragment of ~700 bps (the size of RFP).

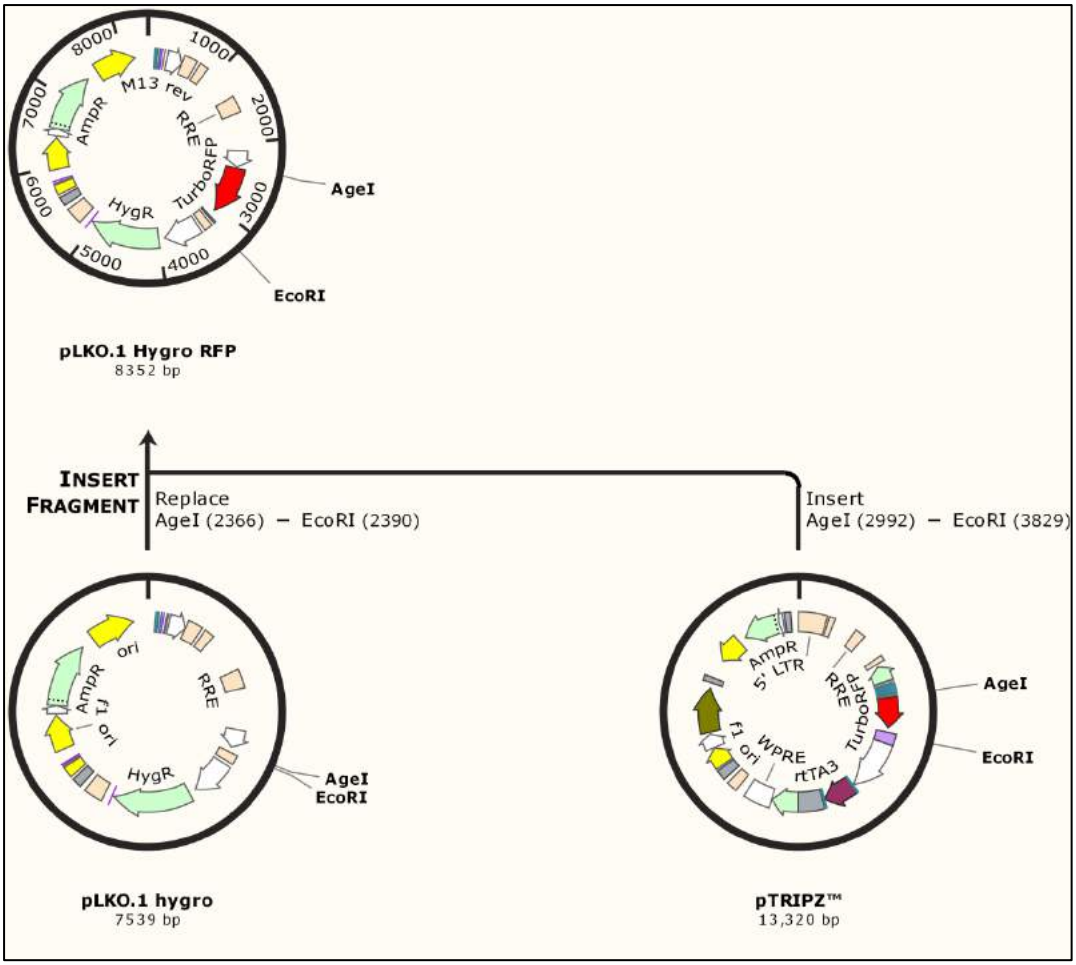

Fig. 3.5 Cloning strategy to generate pLKO.1 Hygro vector containing shRNA targeting 14-3-3γ.

For annealing of the shRNA,

- 5 µL Forward oligo (20pmols)
- 5 µL Reverse oligo (20pmols)
- 5 µL 10x NEB buffer 2
- to 35 µL MQ

The above mixture was incubated at 95°C for 4 minutes followed by incubation at 70°C for 10 minutes and the reaction was gradually cooled to room temperature. 2µl of annealed oligonucleotides mix were phosphorylated by T4 Polynucleotide Kinase (T4 PNK) enzyme at 37°C. After phosphorylation, T4 PNK enzyme was inactivated by incubating the reaction

mixture at 70°C for 10 minutes. After heat inactivation, shRNA was ligated to the AgeI and EcoRI digested vector using T4 DNA ligase (NEB) at 16°C for 16 hours. The ligation mixture was incubated at 65°C for 10 minutes to heat inactivate T4 DNA ligase and then used for transforming DH5α competent cells. All the lentiviral vector transformants were grown at 30°C to avoid recombination.

3.1.11 Generation of the pcDNA3.1-H2B-mCherry-IRES-γ-tubulin GFP construct.

In order to generate this construct, initially the IRES sequence was amplified from the TRIPz vector using forward primers containing a BamHI site and reverse primers containing an EcoRI site. This fragment was first sub-cloned into a TA vector and then inserted into the pcDNA3.1 Puro vector using BamHI and EcoRI restriction enzymes. Then H2B-mCherry was amplified from the genomic DNA of the HeLa Kyoto EGFP-α-tubulin/H2B-mCherry cell line (405). This fragment was also sub-cloned into a TA vector. Positive clones were digested with NheI and KpnI and cloned into the pcDNA3.1 IRES clone. Further, γ-tubulin GFP was amplified from a γ-tubulin GFP plasmid and sub-cloned into a TA vector. Positive clones were digested using EcoRV and NotI and the resulting fragment was cloned into the pcDNA3.1-H2B-mCherry-IRES construct (fig. 3.5). Components of the PCR mix are given in table 3.4.

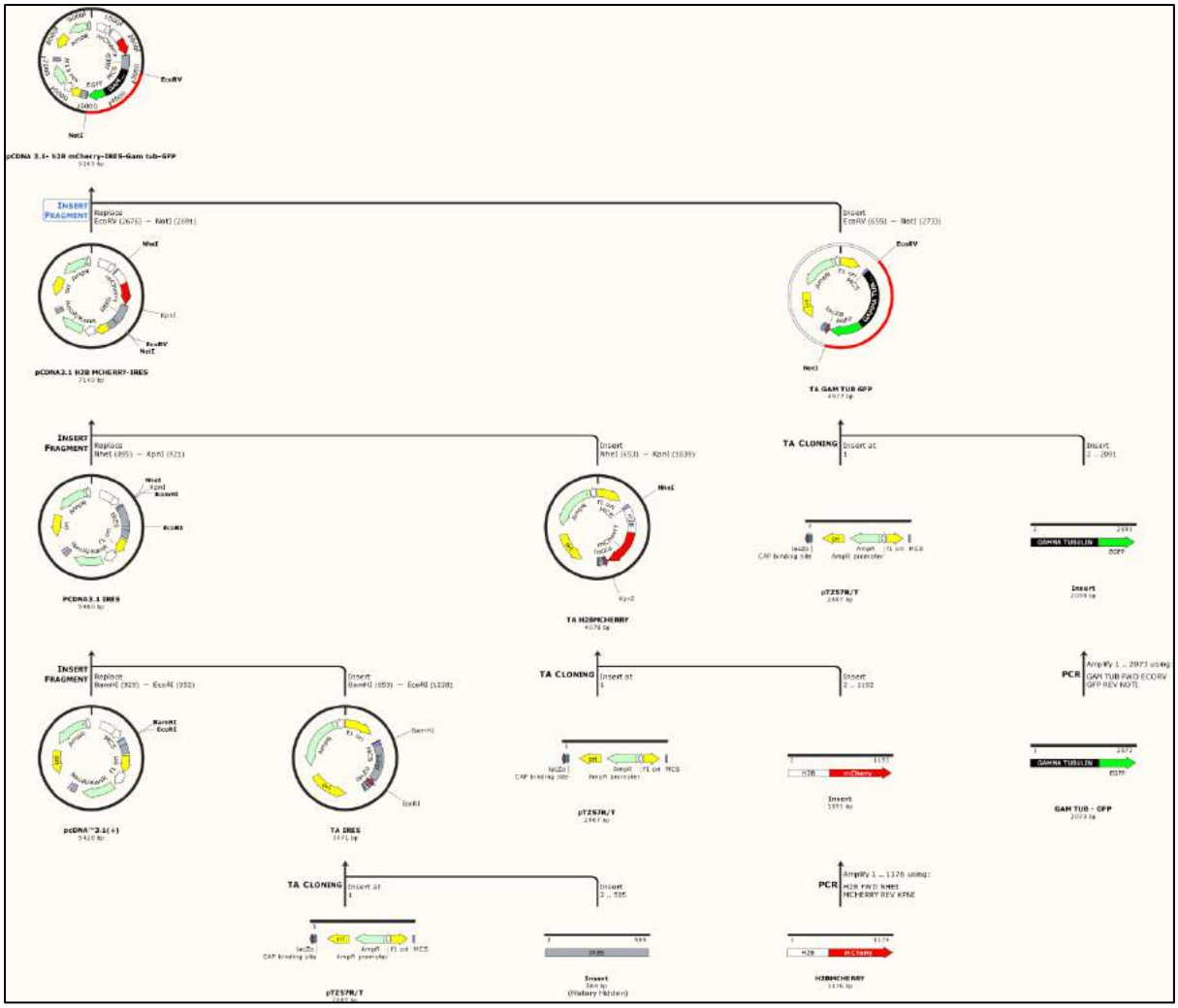

Fig. 3.6 Cloning strategy for generating pcDNA3.1 H2B-mCherry-IRES-γ-tubulin-GFP.

Reagent	Volume (µL)
Template (100 ng/µL)	1.0
Forward primer (20pM)	1.0
Reverse primer (20pM)	1.0
Taq polymerase (NEB)	0.2
dNTPs (20mM)	0.5

MgCl2 (Fermentas)	1.5
Buffer 10X (NEB)	2.0
MQ	11.8
Total	20.0

Table 3.4 List of components used in making PCR mix.

PCR program:

1) Initial denaturation at 95°C for 5 minutes.

2) Denaturation at 95°C for 1 minute.

3) Annealing for 1 minute at

- 52°C for IRES

- 55°C for H2B-mCherry

- 53°C for γ-tubulin-GFP

4) Extension at 72°C for

- 50 secs for IRES (1 kb/min)

- 1 minute 20 secs for H2B-mCherry

- 2 minutes 20 secs for γ-tubulin-GFP

5) Repeat from step 2 for 29 cycles.

6) Hold at 4°C forever.

3.1.12 Common reagents used for cloning

3.1.12.1 Luria Bertoni (LB) media

LB is required for optimal bacterial growth. For preparing 1 litre of LB media, the reagents required are:

Component	Volume or Amount
Tryptone (Himedia)	10 g
Yeast extract (Himedia)	5 g
NaCl	10 g
Tris pH 7.5 1 M	10 mL
MQ	Make volume to 1 L

Table 3.5 Composition of LB media

In order to make LB agar, agar powder (Himedia) was added – 20 g/L. The media was autoclaved and used.

3.1.12.2 Antibiotics

Antibiotic	Stock concentration	Final concentration
Ampicillin	100 mg/mL	100 µg/mL
Kanamycin	50 mg/mL	50 µg/mL
Zeocin	100 mg/mL	25 µg/mL

Table 3.6. Antibiotics used for selection

Antibiotics were added to the LB media for selection of bacteria harbouring the plasmid of interest.

3.2 Cell lines and transfection

Human colorectal carcinoma cell line, HCT116 (ATCC CCL-247), Human immortalized keratinocyte cell line, HaCaT (RRID:CVCL_0038) (406) and Human embryonic kidney cell line, HEK293 (ATCC CRL-1573), were cultured in Dulbecco's Modified Eagles Medium (GIBCO), as described previously (407). The media was supplemented with 10% Fetal Bovine Serum (FBS) (GIBCO), 100 U Penicillin, 100µg/ml of Streptomycin and 2µg/ml of Amphotericin B (407-409). The HCT116 derived vector control, 14-3-3γ knockdown and 14-3-3ε knockdown clones were maintained in a selection media containing 5µg/ml of Blasticidin.

The different methods of DNA transfection used in this study are described below:

1. Lipofectamine LTX (Invitrogen) transfection method:

Diameter of the tissue culture dish	**DMEM(-FBS, -Antibiotics) (µL)**	**Plasmid DNA (1 µg/µl) (µL)**	**Plus Reagent (µL)**	**Lipofectamine LTX (µL)**
35 mm	190.0	2.0	2.0	5.0
60 mm	480.0	5.0	5.0	12.5
100 mm	930.0	15.0	15.0	40.0

Table 3.7 A table describing the different components used in making DNA : Lipofectamine LTX transfection mix.

Cells were at ~60-70% confluency. One – four hours before transfection, the culture media was changed to DMEM (+FBS, -Antibiotics). For transfection, the DNA was added to DMEM (-FBS, - Antibiotics) in an eppendorf. The mixture was resuspended and PLUS reagent was added and mixed again. This mix was incubated at room temperature for 5 minutes, and then Lipofectamine LTX was added. The transfection mix was incubated at room temperature for 30 minutes before adding this transfection mix in a dropwise manner to the cells. After adding transfection mix cells were incubated at 37°C with 5% CO2. 16 hours post transfection, cells were washed with 1x PBS and DMEM + 10% FBS with antibiotics was added.

2. PEI (Polysciences, Inc.) transfection method:

Diameter of the tissue culture dish	**DMEM (-FBS, -Antibiotics) (µL)**	**Plasmid DNA (1µ/µL)**	**PEI (µL)**
35 mm	190.0	2.5	7.5
60 mm	480.0	5.0	15.0
100 mm	940.0	15.0	45.0

Table 3.8: A table describing different components used for making DNA:PEI transfection mix.

Confluency of the cells should be around 60-70% for transfection and cells should be fed with DMEM + 10% FBS medium 1-4 hours before adding transfection mix. Incubate the transfection mix at room temperature for 30 minutes before adding dropwise to the cells.

After adding transfection mix cells were incubated at 37°C with 5% CO2. 16 hours post transfection, cells were washed with 1x PBS and DMEM + 10% FBS with antibiotics was added.

3.3 Antibodies and Western blotting

Cell extracts were prepared using 1X sample buffer (Table 3.9) and protein concentration was determined using Folin-Lowry's method of protein estimation. 50 to 100 μg of protein was resolved on a 10% resolving polyacrylamide gel (table 3.10). Proteins on the SDS-PAGE gel were transferred to nitrocellulose membranes of 0.45 μm pore size (MDI) in a wet transfer apparatus (Bio-Rad) using 100 constant volts for 1 hour for a minigel and 55 constant volts for 3 hours for a maxi gel (table 3.11). Depending on the antibody being used, membranes were incubated overnight with the primary antibody at 4°C or for 2 hours at room temperature. Post incubation in primary antibody, membranes were washed thrice with TBS-T for 10 minutes each. Membranes were incubated with the secondary HRP antibody for 1 hour at room temperature. Membranes were washed thrice with TBS-T for 10 minutes each. Membranes were flooded with either PicoWest (Thermoscientific) or Clarity (Bio-Rad) Western blot chemiluminescent substrates and the signal captured onto X-ray films (Kodak) or a Bio-Rad gel-doc system. For Western blotting, the details of the different antibodies used are given in Table 3.12.

Components	Stock concentration	Volume
Tris pH 6.8	1.0 M	500 μL

Glycerol	100%	1.0 mL
Sodium Dodecyl Sulphate	10%	2.0 mL
Distilled water		6.5 mL

Table 3.9 Composition of 1X loading buffer.

Component	**Final concentration**	**Volume**
Tris base	250 mM	30 g
Glycine	2.5 M	187.7 g
SDS	10%	10 g
MQ		Make up volume to 1L

Table 3.10 Composition of 1X running buffer

Component	**Final amount**
Tris base	12.1 g
Glycine	57.6 g
10% SDS	4 mL
Methanol	800 mL
RO water	Make volume upto 4 L

Table 3.11 Composition of transfer buffer

Antibody	Cat.no.	Incubation conditions	Dilution
14-3-3γ	Abcam ab137106	4°C O/N	1:500
14-3-3γ	Enzo Life Sciences CG31	4°C O/N	1:500
β-actin	Sigma A5316	4°C O/N	1:2500
GFP	Clontech 632375	4°C O/N	1:15000
NPM1	Invitrogen 325200	4°C O/N	1:2000
Phospho-T199	Abcam ab81551	4°C O/N	1:2000
ROCK2	Santacruz sc-398519	4°C O/N	1:200
Phospho-MLC 2	Cell signaling 3671	4°C O/N	1:1000
FLAG	Sigma F-1804	4°C O/N	1:500
HA	12CA5 hybridoma supernatant	4°C O/N	1:100
CDK1	Cell Signalling 9116	4°C O/N	1:1000
14-3-3ε	Santacruz sc-1020	4°C O/N	1:500
Centrin2	Santacruz sc-27793-R	RT for 2 hours	1:500
CDC25C	Santacruz sc-327	RT for 2 hours	1:500

γ-tubulin	Santacruz sc-17787	4°C O/N	1:1000
GCP2	Santacruz sc-390116	4°C O/N	1:500
Cep170	Invitrogen 41-3200	4°C O/N	1:500
Aurora A	Invitrogen 458900	4°C O/N	1:1000
Phospho-T288 Aurora A	Cell signaling 3079	4°C O/N	1:1000
Sas-6	(298)	4°C O/N	1:3000
myc	9E10 hybridoma supernatant	4°C O/N	1:100

Table 3.12 Antibodies used for Western Blotting.

These antibodies were diluted in 1% BSA solution in TBS-T containing 0.2% Sodium Azide. The membrane was blocking using 5% milk in TBS-T. The composition of TBS-T is given in Table 3.13.

Components	**Stock concentration**	**Volume**
Sodium Chloride	2.5 M	60 mL
TRIS pH 8.0	1.0 M	10 mL
Tween-20	100%	1 mL
DW		929 mL

Table 3.13 Composition of TBS-T.

The secondary goat anti-mouse HRP (Pierce) and goat anti-rabbit HRP (Pierce) antibodies were used at a dilution of 1:2500 for Western blots. The secondary antibodies were diluted in 2.5% milk in TBST containing 1% goat serum.

3.4 Immunofluorescence

For immunofluorescence analysis, cells were seeded on 22 mm coverslips (table 3.14). Post-transfection and synchronization, cells were fixed with 4% paraformaldehyde for 20 minutes at room temperature. After fixation, the coverslips were washed twice with 1X PBS. Then, permeabilization was carried out with 0.3% Triton X-100 in 0.1 NP-40 in 1X PBS for 17 minutes. Then the cells were washed carefully with 0.1% NP-40 in 1X PBS twice, taking care to not remove the second wash. Primary antibodies were prepared in 3% BSA in 1X PBS + 0.1% NP-40 solution. 30µL of the primary antibody solution was added on a parafilm and the coverslips were inverted onto the solution. These parafilms with the coverslips were then kept inside a humidified chamber for 2 hours at room temperature in a humidity chamber. Thereafter, the coverslips were inverted to have the cells facing upwards. The cells were then washed with 1X PBS and 1X PBS + 0.1% NP-40 six times alternatively. Secondary antibodies were prepared in 3% BSA in 1X PBS + 0.1% NP-40 solution. 30µL of the secondary antibody solution was added on a parafilm and the coverslips were inverted onto the solution. Cells were incubated in secondary antibody solution for one hour at room temperature in the humidity chamber. Secondary antibodies (conjugated with Alexafluor-568, Alexafluor-488 and Alexafluor-633 from Molecular probes, Invitrogen; dilution 1:100) were used for immunofluorescence studies. After incubation, the cells were again washed with 1X PBS and 1X PBS + 0.1% NP-40 six times alternatively. DNA was labeled using DAPI and cells were mounted on glass slides using Vectashield (Vector Laboratories H-1000). A list of the primary antibodies used is in table 3.16.

DNA	Amount of DNA transfected (µg)
14-3-3γ-mOrange	1.0
EGFP-Centrin2	1.0
ECFP-NPM1	0.5
FLAG-NPM1	1.0
myc-Plk4	1.0
HA-CDK2	0.5
CDK1	0.5

Table 3.14 Amount of DNA used

Component	Volume or amount
NaCl	8 g
KH_2PO_4	0.2
KCl	0.2
Na_2HPO_4	2.18
MQ	Make up volume to 1L

Table 3.15 Composition of 1X PBS

Antibody	Cat. No.	Dilution
Pericentrin	Abcam ab4448	1:1000

α-tubulin	Abcam ab7291,	1:200
Ninein	Cloudclone PAC657Hu01	1:200
Cep68	Abcam ab91455	1:200

Table 3.16 Antibodies used for immunofluorescence.

3.4.1 Assaying centrosome number

In order to count centrosome number, cells were synchronized in mitosis. To this end, cells transfected with the various constructs were treated with Nocodazole (10μM #M1404 Sigma-Aldrich) for 18 hours (410). Post 18 hours, the Nocodazole was washed off, with 3 washes with1X PBS. These washes were given by adding the PBS dropwise with a 1 mL pipette. After washing off Nocodazole, complete medium was added to the cells. Then, the cells were further incubated for another 20 minutes. This was to ensure the recovery of cells from mitotic arrest. The cells were then fixed and stained with antibodies against Pericentrin and co-stained for DNA using DAPI. The number of centrosomes in 100 mitotic cells expressing the respective constructs was determined in three independent experiments. Images were acquired on an LSM 780 confocal microscope at a 630X magnification with a 4X digital zoom. 0.75 μm thin sections of the entire cell were captured. Images are represented as a projection of the entire Z stack. Images were processed on the LSM software.

3.4.2 Spindle formation assay.

In order to assess the ability of cells expressing the various constructs to nucleate microtubules, HCT116 cells were transfected with the respective constructs using PEI. 24 hours post transfection, media was changed and Nocodazole was added in order to synchronize cells in mitosis. 18 hours post incubation in Nocodazole, cells were treated as

described in section 3.4.2. Post fixation, cells were stained with antibodies against Pericentrin and α-tubulin and costained for DNA using DAPI. Images were acquired on a Leica SP8 confocal microscope at a 630X magnification with a 4X digital zoom. 0.75 μm thin sections of the entire cell were captured. Images are represented as a projection of the entire Z stack. Images were processed on the Leica LASX software.

3.4.3 Synchronization in G2 using RO3306.

To visualize the organization of the intercentrosomal linker protein Cep68 and to determine the age of the two centrioles in cells expressing the different mOrange tagged 14-3-3γ constructs, cells needed to be arrested in G2. Therefore, we used the cdk1 inhibitor, RO3306 (9μM #SML0569 Sigma-Aldrich) (411). HCT116 cells were co-transfected with each of the mOrange tagged 14-3-3γ constructs and EGFP-Centrin2. 24 hours post transfection, the medium was changed and cells were treated with RO3306 for 24 hours (411). After synchronization in mitosis, cells were fixed and stained using Cep68 or Ninein. Synchronization was confirmed using flow cytometry. Images were acquired on a Leica SP8 confocal microscope at a 630X magnification with a 4X digital zoom. 0.75 μm thin sections of the entire cell were captured. Images are represented as a projection of the entire Z stack. Images were processed on the Leica LASX software.

3.4.4 ROCK2 activation and Calpeptin treatment

To test the effect of ROCK2 activation using the Doxycycline inducible ROCK2 CA construct, cells were first transfected with the mOrange constructs. 24 hours post transfection, medium was changed and Doxycyline was added to the medium at a concentration of 2μg/mL. 6 hours post Doxycycline treatment, Nocodazole was added to synchronize the cells in mitois. 18 hours post Nocodazole treatment, cells were fixed and stained with antibodies against Pericentrin and centrosome number counted.

To test the effect of ROCK2 activation using Calpeptin, transfected cells were first synchronized to G1/S using Mimosine (80µM Sigma Aldrich (#M0253)) for 20 hours (410). 6 hours post-release from Mimosine, when the cells were at S phase, cells were treated with Calpeptin (5µM Santacruz (#202516)) for 30 minutes. Calpeptin was washed off and Nocodazole was added to synchronize cells in mitosis (410). 18 hours post Nocodazole treatment, cells were fixed and stained with antibodies against Pericentrin and centrosome number counted. The synchronization was confirmed using flow cytometry as described (326).

3.4.5 Determination of the localization of tagged constructs

In order to determine the localization of the different deletion constructs of Centrin2, γ-tubulin and GCP2, HCT116 cells were transfected with each of the deletion constructs. 24 hours post transfection, medium was changed. 48 hours post transfection, cells were fixed and stained with antibodies against Pericentrin as a centrosomal marker and costained for DNA using DAPI.

For assessing the localization of the mOrange-14-3-3γ constructs, HCT116 cells were transfected with each of the constructs. 24 hours post transfection, cells were treated with mimosine (80µM Sigma Aldrich (#M0253)) for 20 hours (410). After synchronization in G1/S, cells were harvested at different time points to obtain cells in S phase and G2 phase. Harvested cells were processed for immunofluorescence and flow cytometry.

3.5 GST pulldown

3.5.1 GST protein preparation

BL21 cells were transformed with pGEX4T1 (GST) vector, pGEX4T1-14-3-3γ or pGEX4T1-14-3-3ε. A single colony of the transformed cells was inoculated in 10 ml of LB broth

containing Ampicillin (100mg/ml) and incubated at 37°C O/N at 200 rpm (rotations per minute). This culture broth was used to inoculate 100 ml LB broth (10 times the volume of the inoculum) containing Ampicillin in a 1.0 L flask followed by incubation at 37°C for 1 hour at 200 rpm. After 1 hour of incubation, 10 µL of 1M IPTG was added to this culture and the flasks were further incubated at 37°C for 3 hours at 200 rpm. After 3 hours the cells were harvested by centrifugation at 4000 rpm for 10 minutes at 4°C. The supernatant was discarded and cells were suspended gently in ice cold 0.1% Triton X-100 in PBS, using a 10ml pipette while ensuring that the frothing is minimum. To lyse the bacterial cells, this suspension was sonicated using a sonicator (Branson) at 50 duty cycles for 10 seconds and then placed on ice for 10 seconds. The sonication was repeated 4 times (totally sonicated 5 times). The suspension was centrifuged at 10,000 rpm for 15 minutes at 4°C. The pellet was then discarded and the supernatant was transferred to 15mL screw cap conical tubes and 150 µL of a 50% slurry of Glutathione Sepharose beads (Amersham) was added and incubated on a rocker at 4°C for 1 hour. After 1 hour, the beads were pelleted by centrifugation at 1000 rpm for 3 minutes at 4°C. The supernatant was discarded, 1ml of NET-N buffer (composition given in Table 3.17) was added and beads were transferred to a 1.5mL Eppendorf using a cut-tip. The beads were pelleted by centrifugation at 1000 rpm for 3 minutes at 4°C. Beads were washed thrice with NET-N. After the wash, beads were re-suspended in 150µl of NET-N. to determine the purity of the GST tagged proteins, 5µl of the concentrate was resolved on a 10% SDS-PAGE gel and stained with Coomassie blue.

3.5.2 GST pulldown

To determine the ability of 14-3-3γ and 14-3-3ε to interact with various centrosomal proteins, EBC extracts of HCT116 cells from one 100 mm plate were prepared (table 3.18). 5% of the extract was used as Whole Cell Extract (WCE) and the rest was incubated with the various GST fusion proteins as indicated O/N. 16 hours post incubation, the beads were washed

thrice with 1 mL NET-N. The complexes were resolved on a 10% SDS-PAGE gel and Western blotted with antibodies against the indicated proteins.

To map the 14-3-3 binding site of 14-3-3 on NPM1 and to test the interaction of 14-3-3γ with NPM1 S48E, HCT116 cells were transfected with 15µg of each of the CFP tagged NPM1 constructs and CFP vector alone. Two 100 mm plates were used per transfection. 48 hours post transfection, EBC extracts of HCT116 cells were prepared. 5% of the extract was used as WCE and the rest was incubated with the various GST fusion proteins as indicated O/N. 16 hours post incubation, the beads were washed thrice with 1 mL NET-N. The complexes were resolved on a 10% SDS-PAGE gel and Western blotted with GFP antibody.

Component	Stock concentration	Volume
Tris pH 8.0	1 M	2000 µL
Sodium Chloride	2.5 M	4000 µL
EDTA pH 8.0	0.5 M	200 µL
MgCl2	25mM	120 µL
NP-40	100%	500 µL
DW		93.3 mL

Table 3.17 Composition of NET-N buffer.

Component	Final concentration	Volume
Tris pH 8.0 1 M	0.50 mM	50 mL
2.5 M NaCl	125 mM	50 mL

NP-40	0.5%	5 mL
MQ		895 mL

Table 3.18 Composition of EBC lysis buffer

The EBC lysis buffer was stored at 4°C and protease inhibitors were added just before use.

Inhibitor	**Stock concentration**	**Final concentration**	**Volume**
Leupeptin	1 mg/mL	10 µg/mL	100 µL
Aprotinin	2 mg/mL	20 µg/mL	100 µL
Sodium Fluoride	1 M	50 mM	500 µL
Sodium Orthovanadate	0.2 M	1 mM	50 µL
Pepstatin A	100 mg/mL	10 µg/mL	10 µL
PMSF	500 mM	1 mM	20 µL

Table 3.19 Composition of protease inhibitors per 10 mL of EBC lysis buffer

3.6 Co-Immunoprecipitation

For the co-immunoprecipitation assays, HCT116 cells were transfected with 15µg of the HA tagged 14-3-3γ constructs. Two 100 mm plates were used per transfection. 48 hours after transfection, the cell culture medium was decanted from both the plates and 1mL of cold PBS (pre-cooled to 4ºC) was added to each plate. The cells on each plate were scraped using a cell scraper and collected in separate 1.5 mL eppendorfs kept on ice. The cells were then pelleted by centrifugation at 2500 rpm for 3 minutes and the PBS was decanted. PBS washes were

given so as to remove all traces of media. Thereafter, 1ml of EBC lysis buffer containing protease inhibitors (as mentioned in 3.19) was added to the cells and incubated for 15 minutes on ice. This was followed by centrifugation at 13,000 rpm for 15 minutes at 4ºC. The supernatant was transferred to a new 1.5 ml eppendorf. 50 µL of this supernatant was kept separately and used as 5% whole cell extract. To this, 25µL of 3X sample buffer was added, boiled in a water bath for 7 minutes and stored at -80ºC. The rest of the supernatant was incubated with 100 µL of anti-HA antibody (12CA5 hybridoma supernatant) for 4 hours. After 4 hours, 30 µL of a 50% slurry of Protein-G-Sepharose was used to precipitate the HA-tagged 14-3-3γ proteins. After 1 hour, the beads were washed thrice with 1 mL NET-N. after boiling with 3X sample buffer, the complexes were resolved on a 10% SDS-PAGE gel and Western blotted with antibodies against the indicated proteins.

3.7 Live cell imaging

To estimate the duration of mitosis, HCT116 cells seeded in a glass-bottomed dish were co-transfected with the respective constructs. 48 hours post-transfection, and 2 hours before imaging, cells were treated with nocodazole (410). One hour prior to imaging, ascorbic acid (100 µM) was added to the media, to reduce photo-bleaching (412,413). Just before imaging, nocodazole was removed and the cells were fed with media containing ascorbic acid again. During imaging, cells were maintained at 5% CO_2 and 95% RH. All images were acquired on a Leica SP8 confocal microscope at 1000X magnification with 4X optical zoom. Images were acquired at 20-minute intervals. Images were processed using the Leica LASX software.

3.8 Electron microscopy

To study centrosome amplification and organization at higher magnification in cells expressing the different 14-3-3γ mutants, the cells were visualized under a transmission electron microscope. Cells synchronized at M-phase were fixed with 3% glutaraldehyde,

washed with 0.1 M of sodium cacodylate pH 7.4, and post-fixed with 1% osmium tetroxide (Tedpella). Cells were then dehydrated and processed. Grids were contrasted with alcoholic uranyl acetate for 30 seconds and dipped once in lead citrate. The grids were observed under a JEOL 1400Plus transmission electron microscope, at an accelerating voltage of 120 KeV and at 10000X.

3.9 Effect of overexpression of CDC25C in the sh-14-3-3ε cells.

In order to assess the effect of the overexpression of CDC25C in the sh-14-3-3ε cells on centrosome number, HCT116 cells were co-transfected with 1 µg each of the previously described pTU6 and pTU6 E7 vector and GFP or GFP CDC25C (234). sh-14-3-3γ cells were used as the positive control. 48 hours post transfection, the cells were treated with Nocodazole to synchronize them in mitosis. Post synchronization, the cells were processed for Western blotting or immunofluorescence and centrosome number was determined as described previously.

3.10 RT-PCR to determine mRNA levels of Cep170 in the sh-14-3-3γ cells.

HCT116 derived vector control and sh-14-3-3γ cells were washed with 1X PBS and TRIZOL (Thermo Fisher Scientific) was added to the cells (1ml for 35 mm tissue culture plate) and incubated at room temperature for 5 minutes for dissociation of nucleoprotein complex. Samples were collected in an eppendorf, 200µl of chloroform was added, vortexed and incubated at room temperature for 2-3 minutes. Samples were centrifuged at 13000 rpm for 15 minutes at 4°C. The aqueous phase was collected in another Eppendorf and 500µl of isopropanol was added and incubated at room temperature for 10 minutes to precipitate the RNA. Samples were centrifuged at 13000 rpm for 15 minutes at 4°C followed by 75% ethanol wash (75ml 100% Ethanol and 25 ml nuclease free water) at 10000 rpm for 5 minutes at 4°C. The RNA pellet was dried for 10 minutes at room temperature and 25µl of

commercial water was added. To dissolve the RNA, samples were incubated at 55°C for 10 minutes. RNA was stored at -70°C. For mRNA to cDNA conversion, High capacity cDNA reverse transcription kit (Applied Biosystems) was used.

PCR components	Volume (µL)
RT buffer 10X	2.0
RT Random Primers 10X	0.8
dNTPs 10mM	0.4
Template (100 ng/µl)	10.0
Reverse Transcriptase	1.0
Nuclease free water	6.0

Table 3.20 PCR components for mRNA to cDNA conversion.

PCR program:

1) 25°C for 10 minutes.

2) 37°C for 2 hours.

3) 85°C for 5 minutes.

4) Hold at 4°C forever.

1µl of the cDNA was used for the PCR amplification using Taq polymerase. Annealing temperature was 60°C. PCR for GAPDH served as a loading control. The sequence of the primers used is given in Table 3.14.

Name of oligonucleotide	Sequence
GAPDH 5’	TGCACCACCAACTGCTTAGC
GAPDH 3’	GGCATGGACTGTGGTCATGAG
Cep170 5’	CACCGTGTTACTAGCTCTGCG
Cep 170 3’	CCATCTCCTGGCTTGGTCTG
14-3-3γ 5’	GAGCCACTGTCGAATG
14-3-3γ 3’	CGCTGCAATTCTTGATC

Table 3.21 Sequence of oligonucleotides used for the RT-PCR reaction.

3.11 Soft agar assay.

The soft agar colony formation assay is performed to determine the ability of cells to grow independent of anchorage (407). Low melting point (LMP) agarose of two different concentrations were prepared, 1.6% and 0.8%, and autoclaved to maintain sterility. After autoclaving, both the LMP agarose solutions were kept on a float in a water bath set at 40ºC to prevent the agarose from solidifying. The 1.6% LMP agarose was then mixed with equal volumes of 2X DMEM + antibiotic + FBS mix (a mixture of sterile 2X concentrated DMEM solution, 2X concentrated relevant antibiotic and 20% FBS). Upon mixing, the final concentration of agarose became 0.8%, the concentration of DMEM and antibiotic becomes 1X and concentration of FBS became 10% (which is the concentration required for optimal growth of cells). Now 2 ml of this solution was poured onto 35mm cell culture plates slowly

and allowed to form a thick solid layer on the plate. This was called the lower layer of the soft agar plate.

Next, the cells of the relevant clones were trypsinized and resuspended in 1ml of 2X DMEM media. The cells are then counted using a haemocytometer to determine the concentration of the cells in the solution. Meanwhile, the 0.8% LMP agarose was mixed with equal volumes of the 2X DMEM + antibiotic + FBS mix to make a final volume of 0.4% LMP agarose + DMEM solution. To 1 ml of this solution, 2500 cells were resuspended slowly to form a homogenous suspension and spread evenly on top of the lower layer of soft agar plate and allowed to settle down and form a semi-solid upper layer. Thereafter, the plates were kept in a tissue culture incubator maintained at 37ºC, 5% CO2, for three weeks. A volume of 150µl to 200µl of fresh DMEM media with the relevant antibiotics were added on top of the soft agar plates every 2 days during these three weeks of incubation. Thereafter the total number of colonies formed on the soft agar plate was counted by making grids at the bottom of the soft agar plate. Three independent experiments were performed in triplicates for each clone.

4. Results

4. Results

4.1 Does 14-3-3 binding to centrosomal proteins inhibit centrosome licensing and duplication?

4.1.1 Are the multiple centrosomes observed upon loss of 14-3-3γ able to function as MTOCs?

Previous studies from our lab have demonstrated that a knockdown of 14-3-3γ results in the presence of excess γ-tubulin positive dots (234). Further experiments demonstrated that loss of 14-3-3γ lead to the presence of multiple Centrin, Cep170 and Ninein foci (326). It was also shown that the multiple γ-tubulin foci were able to function as centrosomes, by performing dual staining for α- and γ-tubulin. We wished to confirm this phenotype using another centrosomal marker and performed dual staining for the centrosome using Centrin and Pericentrin (a PCM protein) (280,281). We transfected HCT116 derived vector control and sh-14-3-3γ cells with GFP Centrin and synchronized the cells in mitosis using nocodazole. 48 hours post transfection, we fixed the cells and stained for Pericentrin and counterstained for DNA using DAPI. The number of centrosomes in a 100 transfected mitotic cells was determined. In both the vector control and the sh-14-3-3γ cells, we observed that each GFP Centrin1 foci co-localized with Pericentrin staining. In case of the sh-14-3-3γ cells, multiple Centrin1 foci were found to co-localize with the Pericentrin staining. This demonstrates that the multiple Centrin dots observed in the sh-14-3-3γ cells are able to function as MTOC's (326) (fig. 4.1).

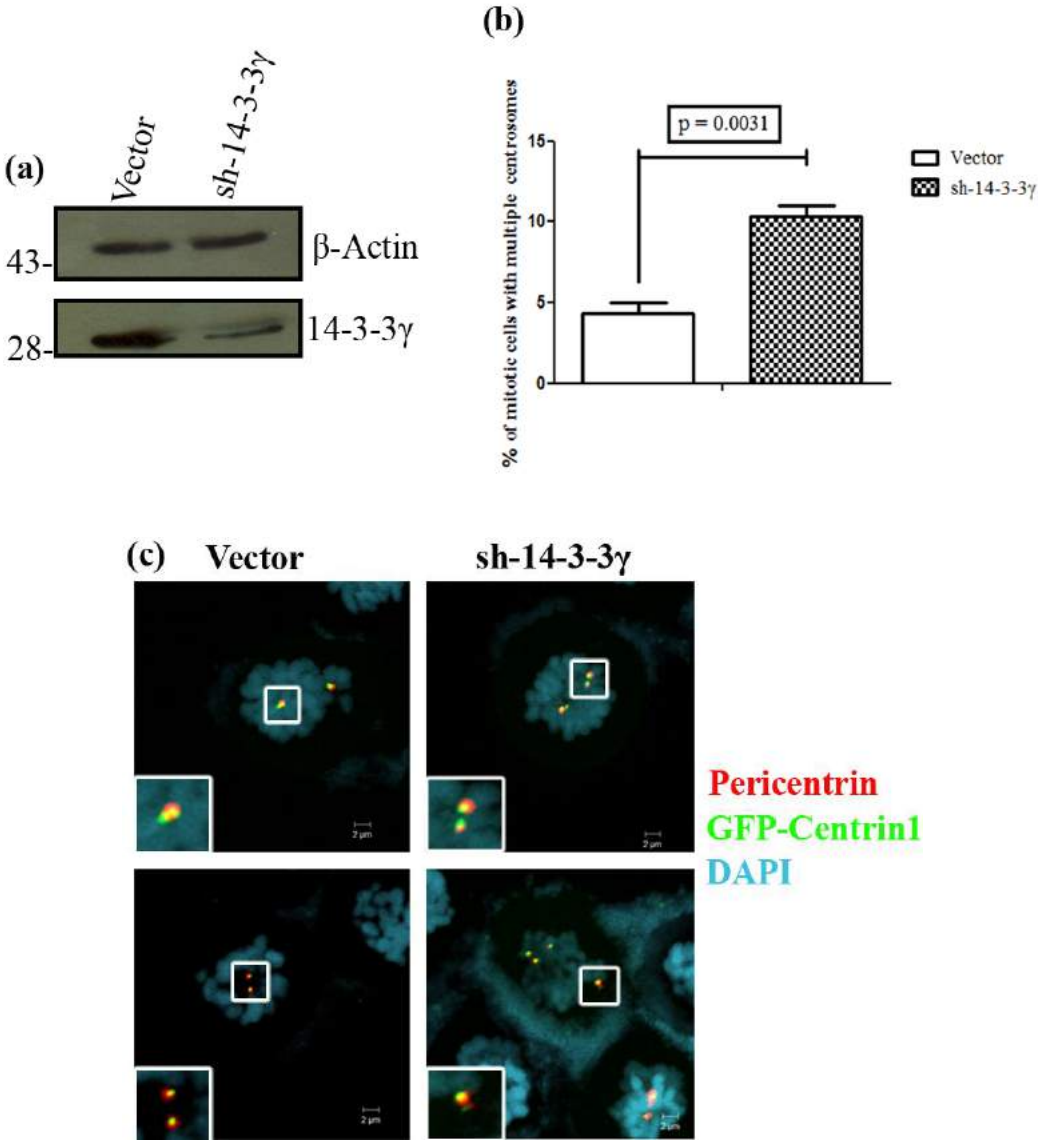

Fig. 4.1 The multiple centrosomes in the sh-14-3-3γ cells are mature. *Vector control or sh-14-3-3γ cells were transfected with GFP-Centrin. 48 hours post transfection, cells were processed for IF or lysates prepared for Western Blots. (a) Lysates were resolved on a 10% SDS-PAGE gel and Western blot performed for the indicated proteins, (b) Quantitation of centrosome number upon performing dual staining with Centrin and Pericentrin. The mean and standard deviation from three independent experiments is plotted. Significance was derived using a Student's t-test with p< 0.05., (c) The cells were stained with antibodies to Pericentrin, co-stained with DAPI followed by confocal microscopy and centrosome number was determined. Representative images are shown. The insert is a zoomed image of the box*

in the main field. Images were captured at 630X magnification and 4X digital zoom under confocal microscope. Scale bar indicates 2μm, unless mentioned.

4.1.2 Loss of 14-3-3γ leads to increased levels of activated Aurora A kinase and SAS6.

In order to characterize the centrosome amplification observed upon depletion of 14-3-3γ, we decided to check the expression of proteins involved in the centrosome cycle. Overexpression of SAS6, the central cartwheel protein can drive extra rounds of centriole replication within a single cell cycle (414). Aurora A kinase is a protein that has functions in centrosome maturation and separation. Overexpression of Aurora A causes defects in cytokinesis and gives rise to centrosome amplification (415). Phosphorylation of Aurora A at Thr288 in its catalytic domain increases its kinase activity (416).

Lysates were prepared from HCT116 derived vector control and sh-14-3-3γ cells at passage 15 and passage 52 and the levels of hSAS6 determined. We found that there was a minor increase in hSAS6 levels in the sh-14-3-3γ cells across passage (fig. 4.2 (a)). We also observed an increase in the levels of p-T288 levels of Aurora A, indicating increased Aurora A activation, in the sh-14-3-3γ cells (fig. 4.2 (b)). β-Actin was used as a loading control. This suggests that centrosome amplification in the sh-14-3-3γ cells is accompanied by an increase in the activation of Aurora A and the levels of SAS6 (326).

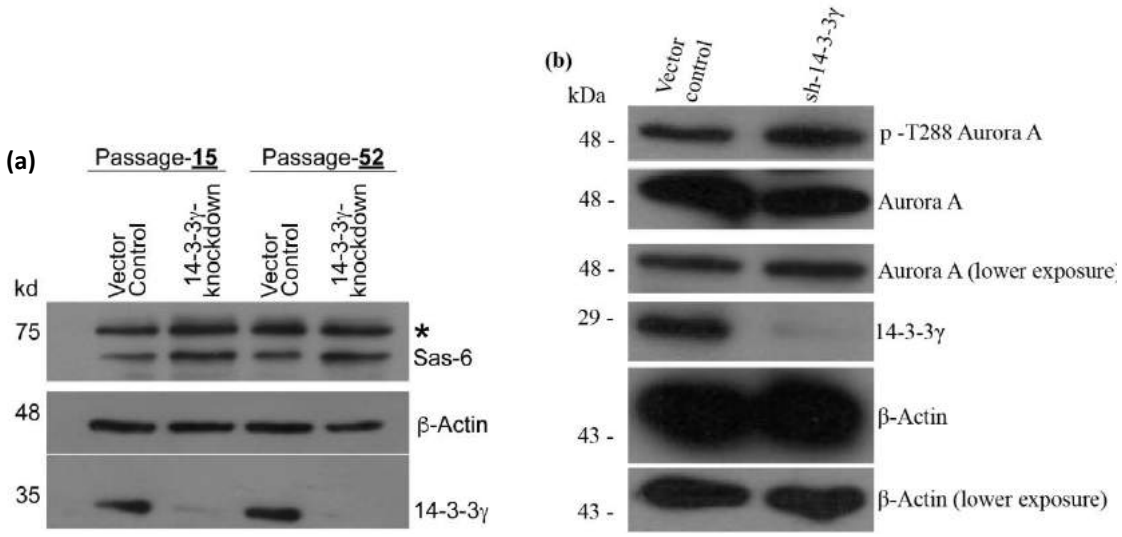

Fig. 4.2 Determination of the levels of proteins involved in centrosome duplication upon depletion of 14-3-3γ. *(**a**) Protein extracts from the vector control or 14-3-3γ-knockdown cells were resolved on SDS-PAGE gels followed by Western blotting with the indicated antibodies. * indicates a non-specific band identified by the Sas-6 antibody. Western blots for β-Actin served as a loading control. (**b**) Protein extracts from the vector control or 14-3-3γ knockdown cells synchronized in mitosis by treatment with nocodazole were resolved on SDS-PAGE gels followed by Western blotting with the indicated antibodies. Note the increase in the levels of activated Aurora A (pT288) while the levels of total Aurora A remain unchanged. Western blots for β-Actin served as a loading control.*

4.1.3 Increased anchorage independence of the higher passage 14-3-3-γ knockdown cells

Anchorage independence and aneuploidy are markers of transformation of cells. Given that the loss of 14-3-3γ leads to increased aneuploidy across passage, due to centrosome amplification, we wanted to observe the effect of loss of 14-3-3γ on anchorage independence. Therefore, we seeded HCT116 derived vector control and sh-14-3-3γ cells, at p15 and p52, on soft agar and counted the number of colonies formed after 3 weeks (fig. 4.3). We observed

that the sh-14-3-3γ cells formed more number of colonies across passage. This indicates that the sh-14-3-3γ cells become more anchorage independent with an increase in passage.

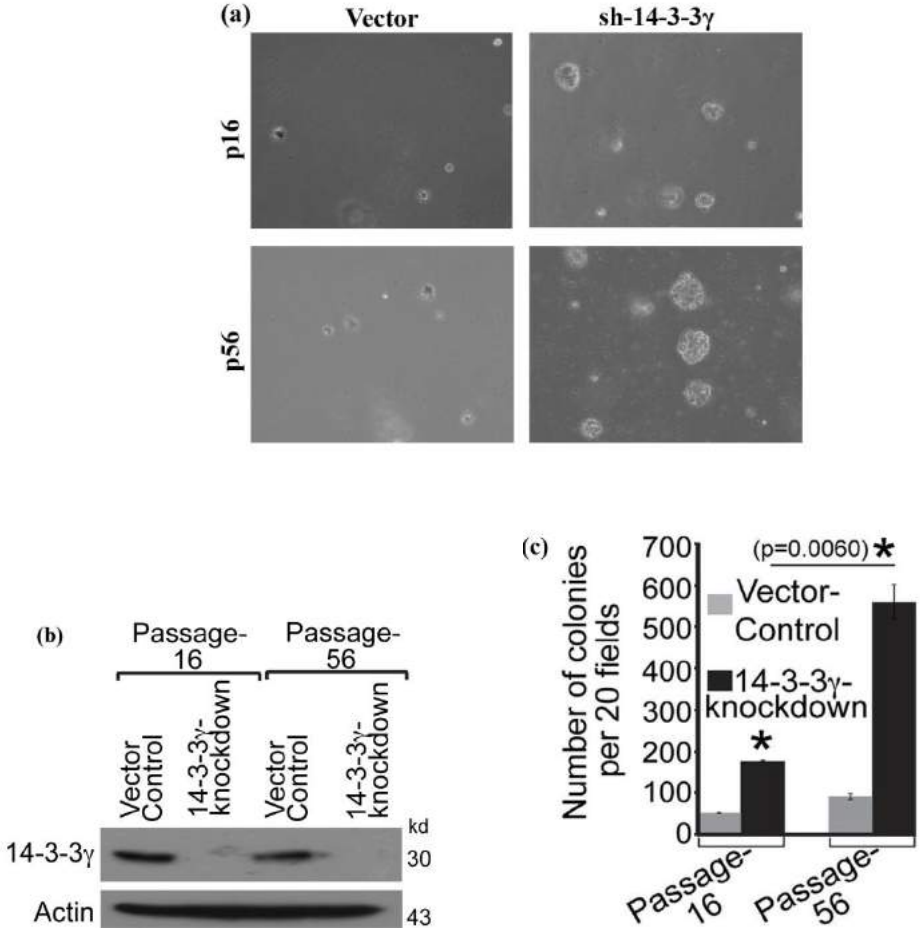

Fig. 4.3 Increased anchorage independence in the sh-14-3-3γ cells across passage. (a) *Representative images of early and late passage 14-3-3γ -knockdown and vector control cells plated in soft agar,* ***(b)*** *Cell lysates of vector-control and sh-14-3-3γ cells from passage-16 and passage-56 were resolved by SDS-PAGE and immuno-blotted with antibodies to 14-3-3γ. The levels of 14-3-3γ were reduced in 14-3-3γ-knockdown cells at passage - 16 and passage-56. β-Actin served as a loading control,* ***(c)*** *2-3 weeks after seeding the cells, colonies were counted from 20 fields (at 10X magnification) and the mean and standard deviation from three independent experiments is plotted.*

4.1.4 Centrosome amplification in the sh-14-3-3γ cells occurs due to premature phosphorylation of NPM1 at T199.

Nucleophosmin 1 (NPM1) is an oligomeric, nucleolar phosphoprotein that functions as a molecular chaperone for both proteins and nucleic acids [reviewed in (417)]. Wild-type NPM1 forms pentameric oligomers through interactions at the amino-terminal core domain.

Previous studies have demonstrated that changes in the oligomerization state of NPM1 may affect its function (418). NPM1 is phosphorylated by cdk2/cyclin E at the G1/S transition at a Threonine 199 residue, which acts as a licensing factor for centrosome duplication (325). NPM1 associates with unduplicated centrosomes, but upon phosphorylation at Thr199 by CDK2/cyclin E at the G1/S transition, it dissociates from the centrosome, leading to centrosome duplication (325). In vitro kinase assays determined that the cyclin B1/CDK1 could also phosphorylate NPM1 at T199 (326). It has been demonstrated that a depletion of 14-3-3γ leads to an increase in p-T199 levels of NPM1 (326). Overexpression of WT NPM1 and a phosphomimetic T199D mutant leads to increased centrosome amplification in both the vector control and the sh-14-3-3γ cells (326). Expression of a T199A mutant was able to decrease centrosome amplification.

It had been demonstrated that the centrosome amplification observed in the sh-14-3-3γ cells begins in the S-phase. If the increased levels of p-T199 were the cause of the centrosome amplification, levels of p-T199 NPM1 would also increase from S-phase onwards. In order to test the same, we synchronized HCT116 derived vector control and sh-14-3-3γ cells cells at the G1/S phase using mimosine and harvested them at different time points (fig. 4.4 (a and b)). Then, we prepared lysates and performed a Western blot for cyclin B1 total NPM1 and p-T199 NPM1. We found that p-T199 NPM1 in the vector control cells first appears at 10 hours post release from mimosine, when the majority of the cells are in G2 phase. Whereas,

in the sh-14-3-3γ cells, NPM1 phosphorylation appears at the six hour time point and coincides with the increased expression of cyclin B1 (fig. 4.4 (c)). We had demonstrated that premature activation of CDK1 occurs in the sh-14-3-3γ cells (326). Given the observation that phosphorylation of NPM1 at T199 occurs prematurely in the sh-14-3-3γ cells, it suggests that CDK1 kinase might be the major kinase phosphorylating NPM1 in the sh-14-3-3γ cells. Therefore, this implies that premature activation of CDK1 in the sh-14-3-3γ cells leads to premature phosphorylation of NPM1 at T199, which leads to centrosome amplification.

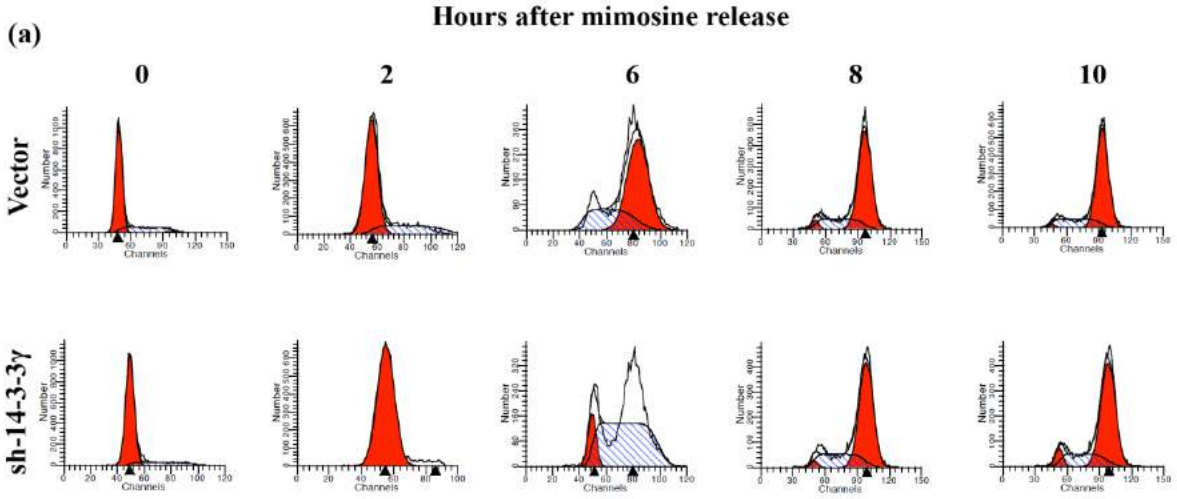

(b)

Time point (hours)	vec-control			sh-14-3-3γ		
	% G0/G1	% S	% G2/GM	% G0/G1	% S	% G2/GM
0	74.88	24.01	1.11	85.58	14.42	0.00
2	74.66	25.34	0.00	100.00	0.00	0.00
6	0.00	32.07	67.93	15.54	84.46	0.00
8	3.36	23.01	73.63	2.42	27.08	70.5
10	1.35	21.04	77.61	6.19	22.41	71.4

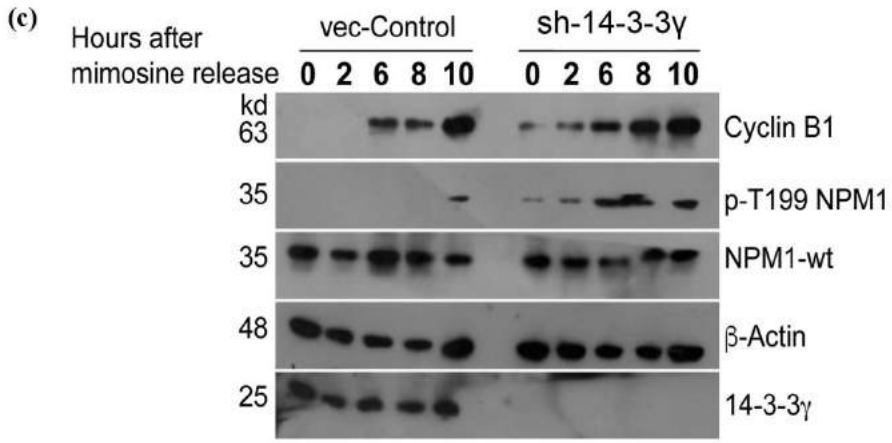

Fig. 4.4 NPM1 phosphorylation peaks during early S-phase in the sh-14-3-3γ cells. *Vector control and sh-14-3-3γ cells were synchronized in G1/S using mimosine. At various time points post mimosine withdrawal (0 hours), cells were either processed for FACS analysis or protein extracts prepared from synchronized cell populations.* ***(a)*** *The cell cycle histograms are shown,* ***(b)*** *The percentage of cells in the different cell cycle phases is shown in the table, and* ***(c)*** *The extracts were then resolved on SDS-PAGE gels followed by Western blotting with the indicated antibodies. Western blots for β-Actin served as a loading control.*

4.1.5 Effect of overexpression of CDC25C in 14-3-3ε knockdown cells

It has been demonstrated that a knockdown of 14-3-3γ leads to centrosome amplification (326). This phenotype is enhanced by the expression of WT CDC25C and CDC25C S216A (a 14-3-3 binding defective mutant of CDC25C). Further, a double knockdown of 14-3-3γ and 14-3-3ε also leads to an increase in centrosome amplification. Given these data, we wanted to know the effect of overexpression of CDC25C in 14-3-3ε knockdown cells. Therefore, we transfected HCT116 derived vector control, sh-14-3-3γ and sh-14-3-3ε cells with GFP, GFP CDC25C WT and GFP CDC25C S216A constructs. Upon synchronization of the cells in mitosis, we counted the number of centrosomes in 100, transfected mitotic cells.

We found that overexpression of CDC25C in the sh-14-3-3ε cells also leads to an increase in centrosome number, though not as much as that observed in the sh-14-3-3γ cells (fig. 4.5).

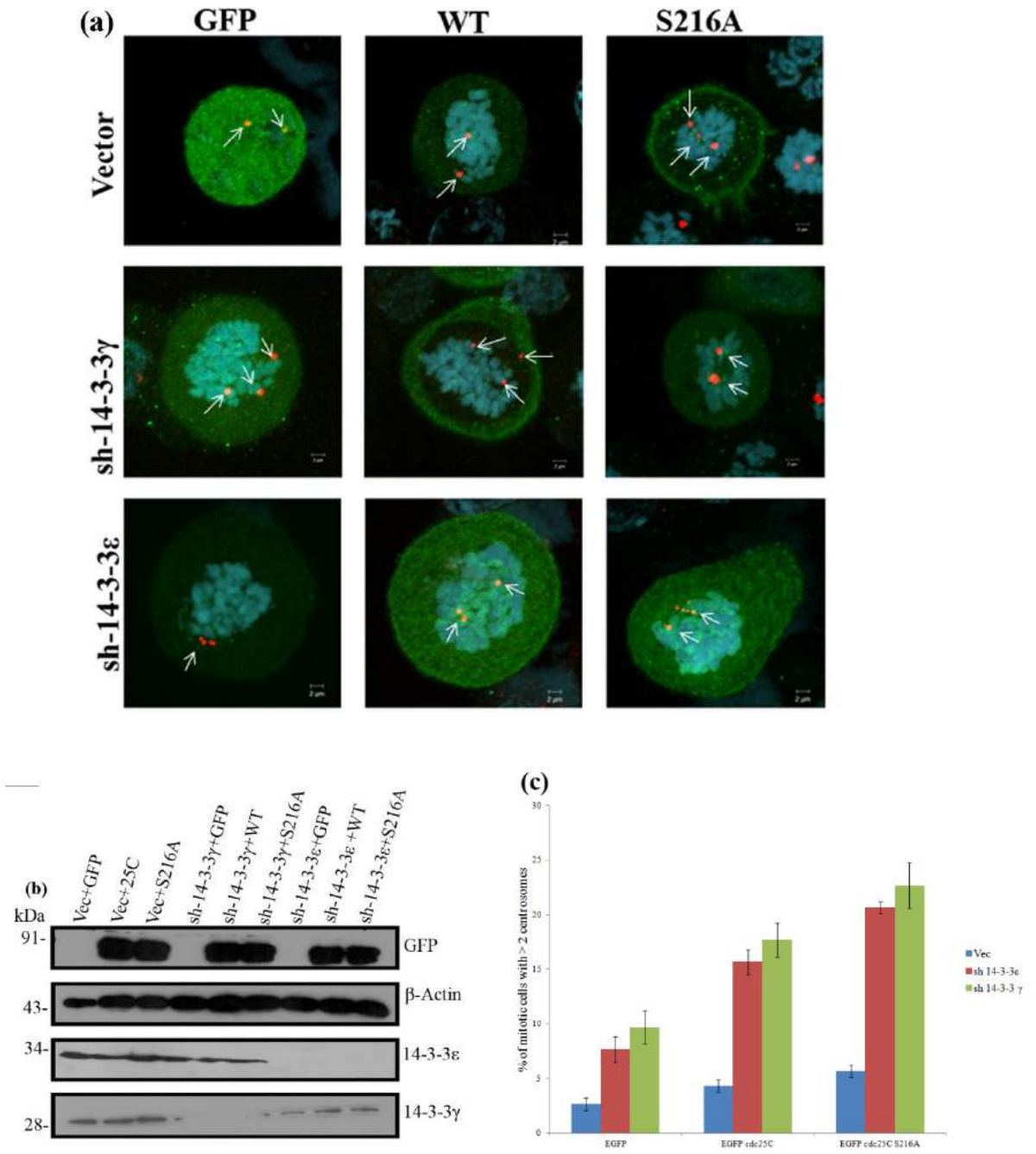

Fig. 4.5 Effect of overexpression of CDC25C in sh-14-3-3ε cells. *Vector control, sh-14-3-3γ and sh-14-3-3ε cells were transfected with GFP, GFP CDC25C WT or GFP CDC25C S216A. (a) Representative images of the respective transfections. Images were captured at 630X magnification and 4x digital zoom under confocal microscope. Scale bar indicate 2μm,*

(b) 48 hours post transfection, lysates were prepared and resolved on SDS-PAGE gels. Western blot was performed using the indicated antibodies, and (c) Quantitation of centrosome number upon depletion of 14-3-3γ or 14-3-3ε.

4.1.6 Do 14-3-3 proteins form a complex with centrosomal proteins?

Previous results from our lab have demonstrated that a loss of 14-3-3γ in HCT116, HEK293 and U2OS cell lines and a loss of 14-3-3ε in HCT116 cell line leads to centrosome amplification (326). Further, it has also been shown that 14-3-3γ and 14-3-3ε bind to centrosomal proteins such as γ-tubulin and Centrin using a GST pulldown (326,419). In order to confirm the same and to identify other possible 14-3-3 binding proteins, we performed a GST pulldown assay. We were able to demonstrate that 14-3-3γ and 14-3-3ε bind to the centrosomal proteins Centrin2, GCP2, γ-tubulin and Cep170 (fig. 4.6 (*a* and *b*)).

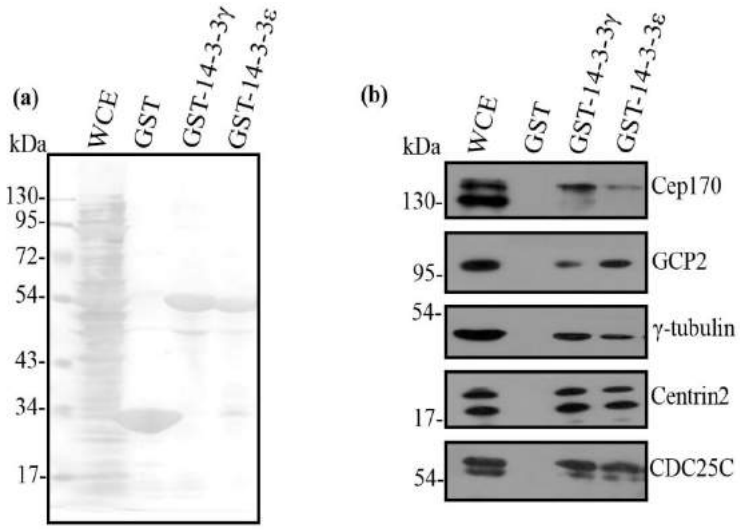

Fig. 4.6 Interaction of 14-3-3γ and 14-3-3ε with centrosomal proteins. *Protein extracts prepared from HCT116 cells were incubated with the indicated GST fusion proteins. The complexes were resolved on 10% SDS-PAGE gels and Western blots performed with antibodies against Cep170, GCP2, γ-tubulin and Centrin2. CDC25C was used as a positive*

control. Note that all the proteins form a complex with GST-14-3-3γ and GST-14-3-3ε but not GST alone. (a) Indicates Poonceau S stained membrane and (b) is the Western blot.

Further, in order to understand how 14-3-3 proteins might regulate the centrosome cycle, we decided to map the 14-3-3 binding site on these proteins. In order to do so, we used the Scansite motif prediction webserver (420). We were unable to detect any putative 14-3-3 binding sites on the proteins Centrin2, γ-tubulin or GCP2. However, we found three potential 14-3-3 binding sites on the protein Cep170. Based on these results, in order to map the 14-3-3 binding sites, we decided to generate domain deletion constructs of proteins that did not possess a consensus 14-3-3 binding site. Cep170, we decided to generate site directed mutants of the potential 14-3-3 binding sites. Also, given that 14-3-3ε did not interact with Centrin and γ-tubulin in a FRET based assay, but 14-3-3γ did, we decided to study the interaction of 14-3-3γ with centrosomal proteins (326).

4.1.7 Centrin2

Centrins are small, highly conserved members of the EF-hand superfamily of calcium-binding proteins that are expressed throughout eukaryotes. They have a role in ensuring the duplication and appropriate functioning of the ciliary basal bodies in ciliated cells (reviewed in (421)). They have been localized to the distal end of centrioles and are essential for centriole duplication (422).

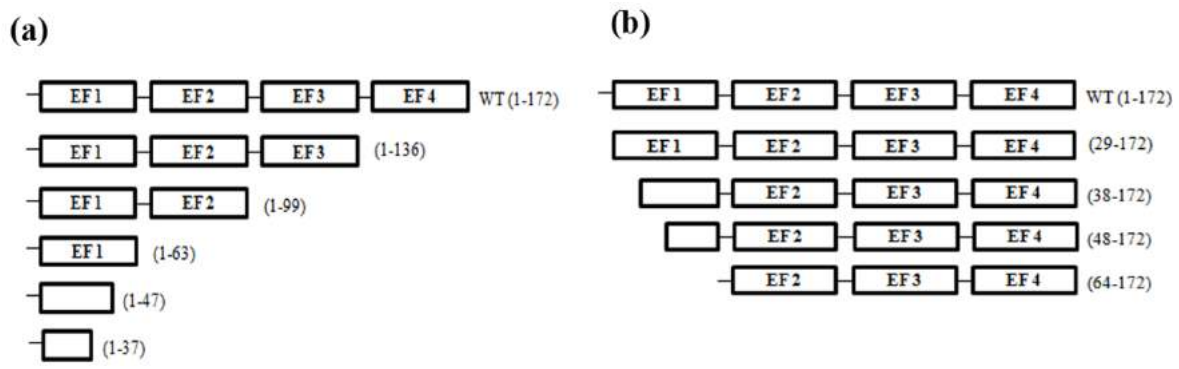

Fig. 4.7 Cartoon of the various deletion mutants of Centrin2. *The C and N terminal deletion constructs of Centrin2 were generated by sequentially deleting a domain from each terminal.*

4.1.7.1 The N terminal EF-1 of Centrin2 is sufficient for binding to 14-3-3γ.

In order to test the ability of these mutants to bind 14-3-3γ, we transfected the WT and the mutant constructs into HCT116 cells, with EGFP as the vector control. 48 hours post transfection, we prepared proteins extracts from the transfected cells and subjected them to a GST pulldown assay using GST 14-3-3γ. GST alone was used as the vector control. We found that all mutant constructs as well as the WT construct were capable of binding to GST 14-3-3γ (fig. 4.8). GFP alone did not bind to GST 14-3-3γ and none of the constructs bound to GST alone. This suggests that the first EF hand domain construct, 1-63, was sufficient for mediating binding of centrin2 to 14-3-3γ. Shorter C terminal constructs, 1-37 and 1-47 were also tested, and we found that they were also able to bind to 14-3-3γ (fig. 4.8). This implies that the 14-3-3 binding site lies within the first 37 amino acids of Centrin2.

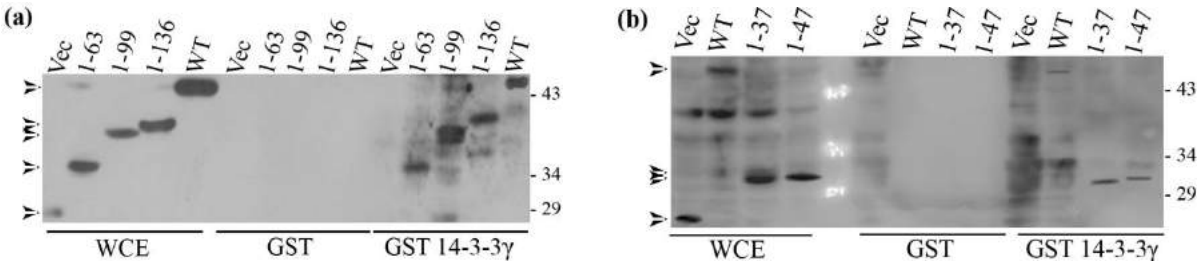

Fig. 4.8 The N terminal EF 1 hand domain of Centrin2 is sufficient for binding to 14-3-3γ. ***(a and b)*** *HCT116 cells were transfected with the indicated EGFP or EGFP tagged Centrin2 deletion constructs. 48 hours post transfection, protein extracts prepared from HCT116 cells were incubated with the indicated GST fusion proteins. The complexes were resolved on 10% SDS-PAGE gels and Western blots performed with antibodies against GFP.*

4.1.7.3 Localization of the C-terminal deletion constructs of Centrin2

In order to assess the localization of these mutants, we transfected them into HCT116 cells. 48 hours post transfection, we fixed and stained these cells for Pericentrin, a PCM marker and DAPI, in order to visualize the nucleus (fig. 4.9). We observed that the EGFP vector control had a pan-cellular localization, as expected. The WT Centrin2 construct localized as either two or four Centrin2 dots (depending on the stage of the cell cycle) and co-localized with Pericentrin (423). The three C-terminal deletion constructs of Centrin2 also co-localized with Pericentrin. However, as opposed to what was observed in the WT Centrin2 construct, we were unable to observe the typical two or four dots Centrin2 localization in any of the mutants in spite of an enrichment at the centrosome and co-localization with Pericentrin. It is possible that sequences in the last C terminal EF hand domain (EF-4) are necessary for the correct organization of Centrin2 at the centrosome.

Additionally, the mutant expressing amino acids 1-136 showed increased nuclear localization. This is similar to the localization of only the C terminal region of Centrin2 (aa. 95-172), when co-expressed with XPC, observed previously (424). The aa. 95-172 region is hypothesized to be important for binding to XPC and the nuclear localization of Centrin2. Nuclear sequestration of Centrin2 has been shown to play control centrosome amplification

in response to DNA damage response, irrespective of p53 status (425). It is possible that the third EF hand domain of Centrin2, from aa. 99-136 is sufficient for its nuclear localization.

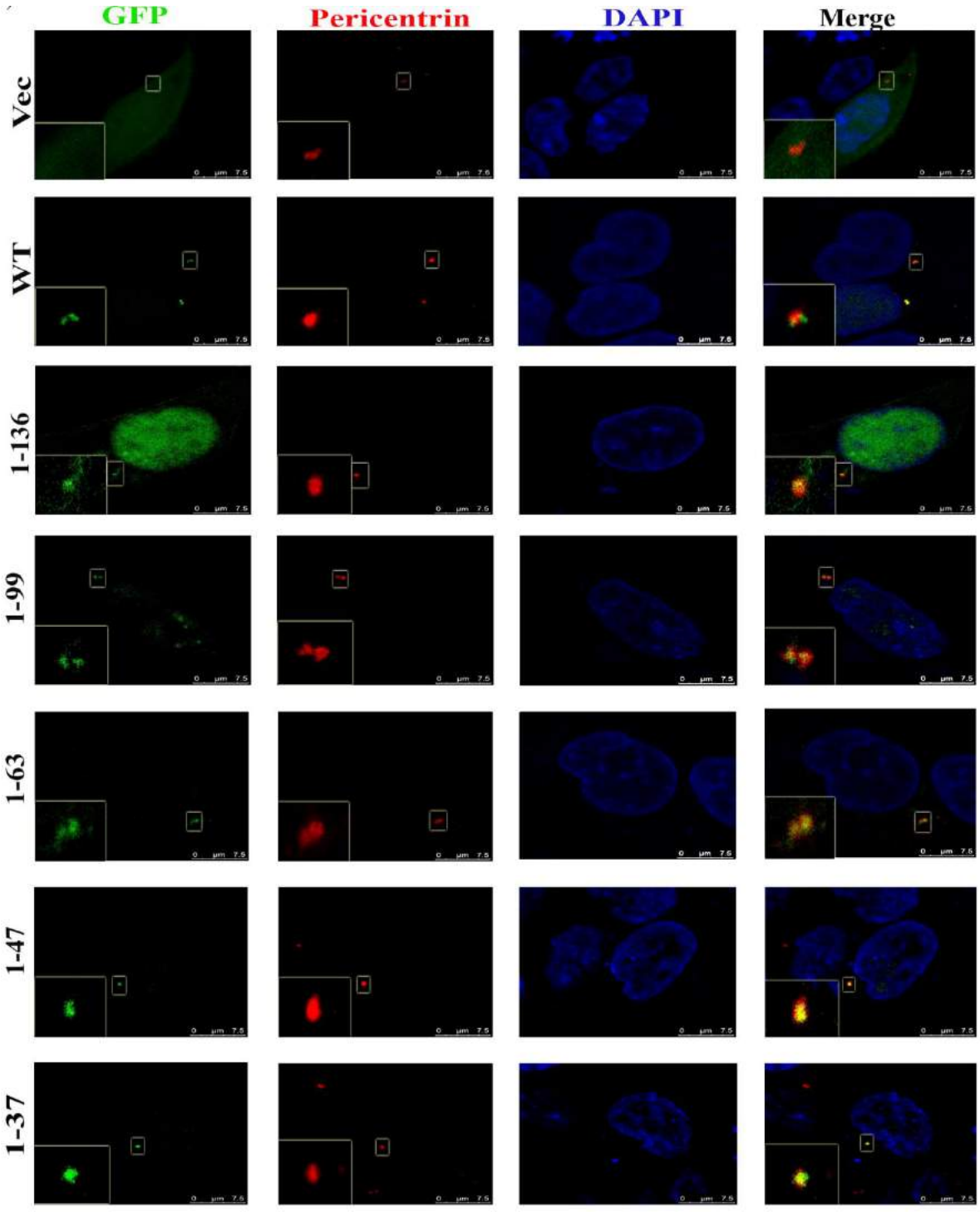

Fig. 4.9 Localization of the C-terminal deletion constructs of Centrin2. *HCT116 cells were transfected with each of the GFP tagged Centrin2 constructs. 48 hours post transfection, the cells were fixed and stained for pericentrin and counterstained with DAPI. The insert is a zoomed image of the box in the main field. Note that the mutant constructs do not show the typical orthogonal arrangement observed with the WT construct. Magnification was a 1000X with 4X digital zoom and scale bars indicate distance in μm.*

4.1.7.4 The EF1 domain of Centrin2 is essential for binding to 14-3-3γ

There are two scenarios, given that even the construct expressing the shortest stretch of N – terminal amino acids was capable of binding to 14-3-3γ. First, the 14-3-3 binding sequence lies within the first 37 amino acids of Centrin2. Second there are multiple 14-3-3 binding sites on Centrin2. To test which one of these is true, we generated two kinds of constructs. In the first kind, we generated partial deletions of the first EF1 hand domain. In the second, we deleted the first 28 amino acids of Centrin2, which have been demonstrated to be required for the self assembly of Centrin2 (426,427).

All these mutants, WT centrin2 and GFP alone were transfected into HCT1116 cells and a GST pulldown was performed 48 hours post transfection (fig. 4.10). We found that the construct with a deletion of the EF1 hand domain (64-172) was unable to bind to 14-3-3γ. Given that the construct with a deletion of the first 28 amino acids could bind to 14-3-3γ, it means that the 14-3-3 binding site lies within the first EF hand domain of Centrin2. Surprisingly, the constructs with a shorter deletion of the EF1 hand domain, 37-172 and 48-172, were also able to bind to 14-3-3γ. This suggests the presence of multiple 14-3-3 binding sites on Centrin2.

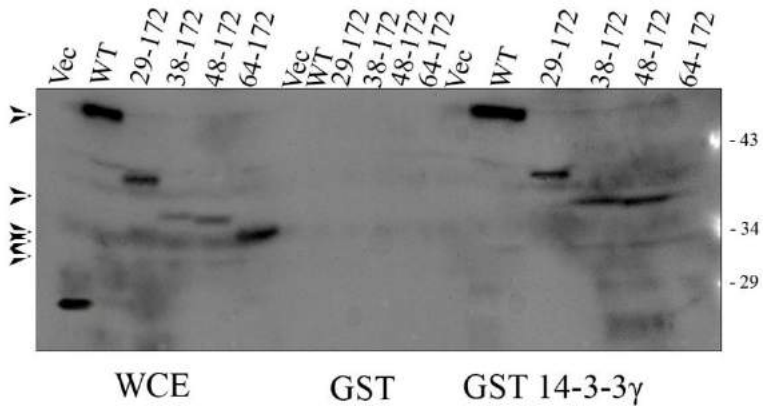

Fig. 4.10 The N terminal EF1 hand domain of Centrin2 is essential for binding to 14-3-3γ

HCT116 cells were transfected with the EGFP or EGFP tagged Centrin2 deletion constructs. 48 hours post transfection, protein extracts prepared from HCT116 cells were incubated with the indicated GST fusion proteins. The complexes were resolved on 10% SDS-PAGE gels and Western blots performed with antibodies against GFP. Note that only the deletion of the entire EF1 hand domain of Centrin2 results in loss of binding to 14-3-3γ.

4.1.7.5 Deletion of the EF1 hand domain of Centrin2 results in the loss of its centrosomal localization.

When we tested the localisation of the N terminal deletion constructs of Centrin2, we found that the 28-172, 38-172 and 48-172 constructs all co-localized with Pericentrin. They were not organized in the typical two or four dot arrangement of Centrin2, though, as seen with other C terminal mutants, they were enriched at the centrosome. This implies that expression of the full length protein of Centrin2 is required for its proper organization at the centrosome, even though it is not necessary for it to be enriched at the centrosome. Therefore, there could be multiple sites within the sequence of Centrin2 that mediate its correct organization at the centrosome. Interestingly, the mutant that was unable to bind to 14-3-3γ, 64-172, was also unable to localize to the centrosome. Instead, it was observed in a cytoplasmic punctuate localisation, which did not co-localize with Pericentrin. This suggests that the EF1 hand

domain of Centrin2 is necessary both for binding to 14-3-3γ and for its centrosomal localization (fig. 4.11).

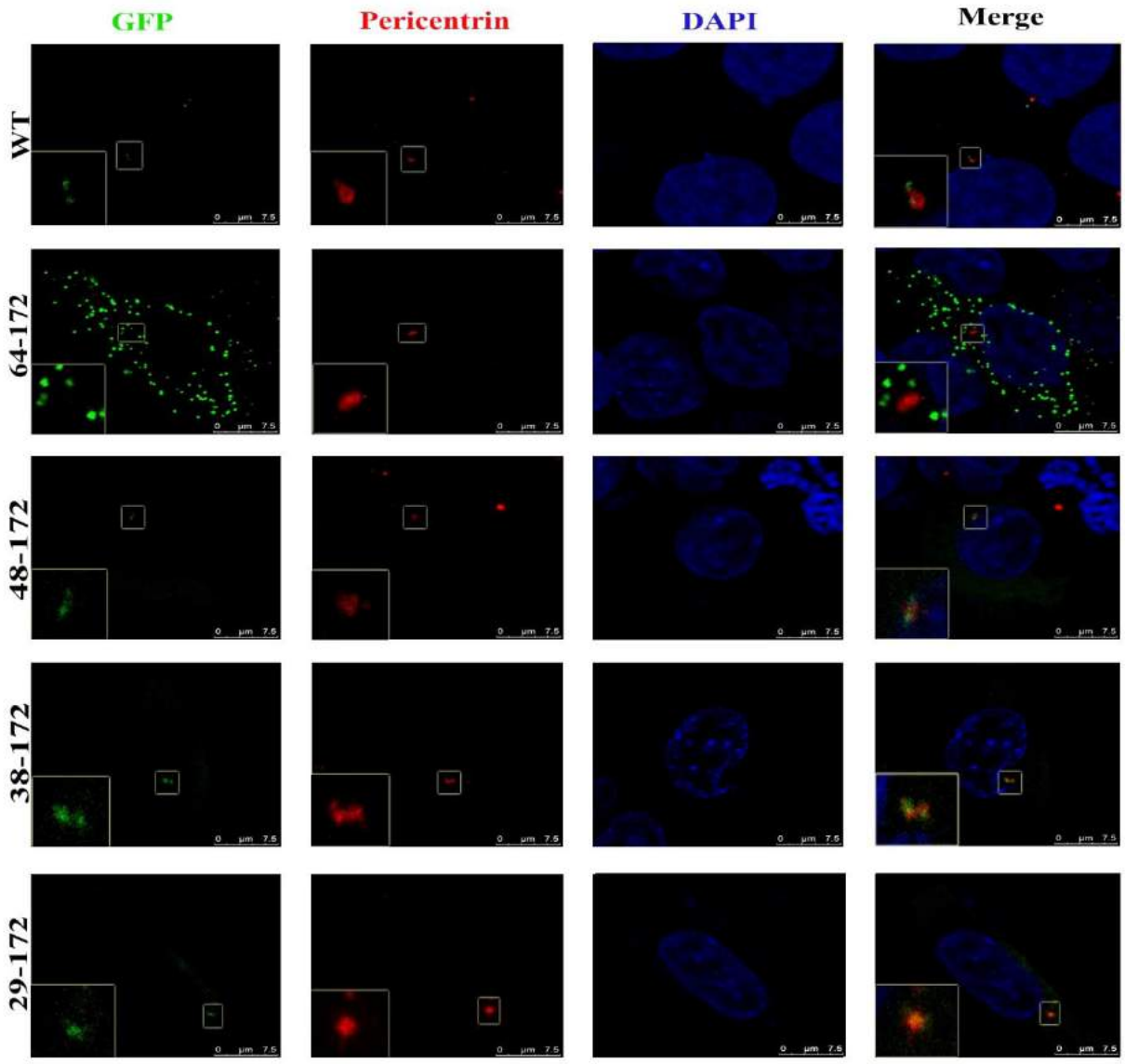

Fig. 4.11 Deletion of the first EF hand domain of Centrin2 leads to loss of the centrosomal localization of Centrin2.*HCT116 cells seeded on coverslips were transfected with the GFP tagged WT or mutant Centrin2 constructs. 48 hours post transfection, the cells were fixed and stained for pericentrin and DAPI. The insert is a zoomed image of the box in the main field. Note that the 64-172 construct does not localize to the centrosome unlike the WT or other mutant constructs. None of the Centrin2 deletion mutants show the typical orthogonal*

arrangement observed with the WT construct. Magnification was a 1000X with 4X digital zoom and scale bars indicate distance in µm.

4.1.7.6 Point mutants within the first EF1 hand domain of Centrin2 are able to bind to 14-3-3γ.

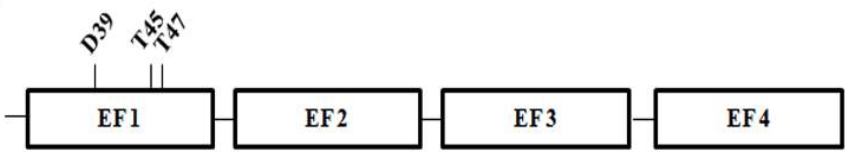

Fig. 4.12. Cartoon of the point mutants potential 14-3-3 binding sites of Centrin2

Based on our results, we hypothesized that there could be multiple 14-3-3 binding sites within the EF1 hand domain of Centrin2. So, using the prediction web server (http://www.compbio.dundee.ac.uk/1433pred) we identified two potential 14-3-3 binding sites within EF1 in Centrin2; T45 and T47 (403). We altered these two Threonine residues that could be possible phosphate acceptors in these potential 14-3-3 binding sites to Alanine (T45A and T47A). We also generated a double mutant, T45/47A. Additionally, we hypothesized that an Aspartic acid residue at position 39 (D39) might function as a phospho-mimetic residue in a potential 14-3-3 binding site. This residue was altered to Alanine (D39A) (fig. 4.12).

All these point mutants were tested for their ability to form a complex with 14-3-3γ in GST pull-down assays. It was observed that all of the point mutants were able to form a complex with 14-3-3γ (fig. 4.13). The double mutant (T45/47A) also formed a complex with 14-3-3γ (fig. 4.13). These results suggested that none of these potential 14-3-3γ binding sites in Centrin2 was required for complex formation with 14-3-3γ.

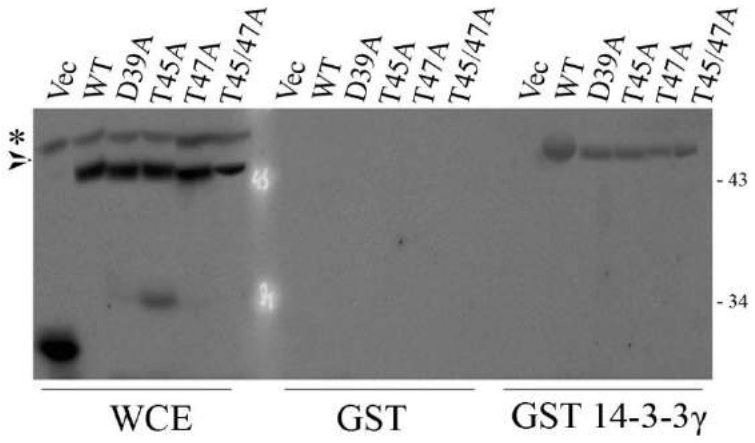

Fig. 4.13. Point mutants of potential 14-3-3 binding sites of Centrin2 are able to bind to 14-3-3γ *HCT116 cells were transfected with the indicated GFP tagged WT or Centrin2 point mutants constructs and GFP as a vector control. At 48 h post transfection, EBC extracts of HCT116 cells were incubated with the various GST fusion proteins as indicated. The complexes were resolved on a 10% SDS-PAGE gel and Western blots performed with antibodies against GFP. * Indicates a non-specific band. Arrows indicate the positions of the GFP fusion proteins and the position of molecular weight markers in kDa is indicated.*

4.1.7.7 Point mutants of the putative 14-3-3 binding sites of Centrin2 are able to localize to the centrosome.

The point mutants within the EF1 hand domain we generated were able to localise to the centrosome and were organized in the typical two or four dots of Centrin2 as seen in the WT protein (fig. 4.14). This suggests that none of these residues are essential for the localisation of Centrin2 at the centrosome.

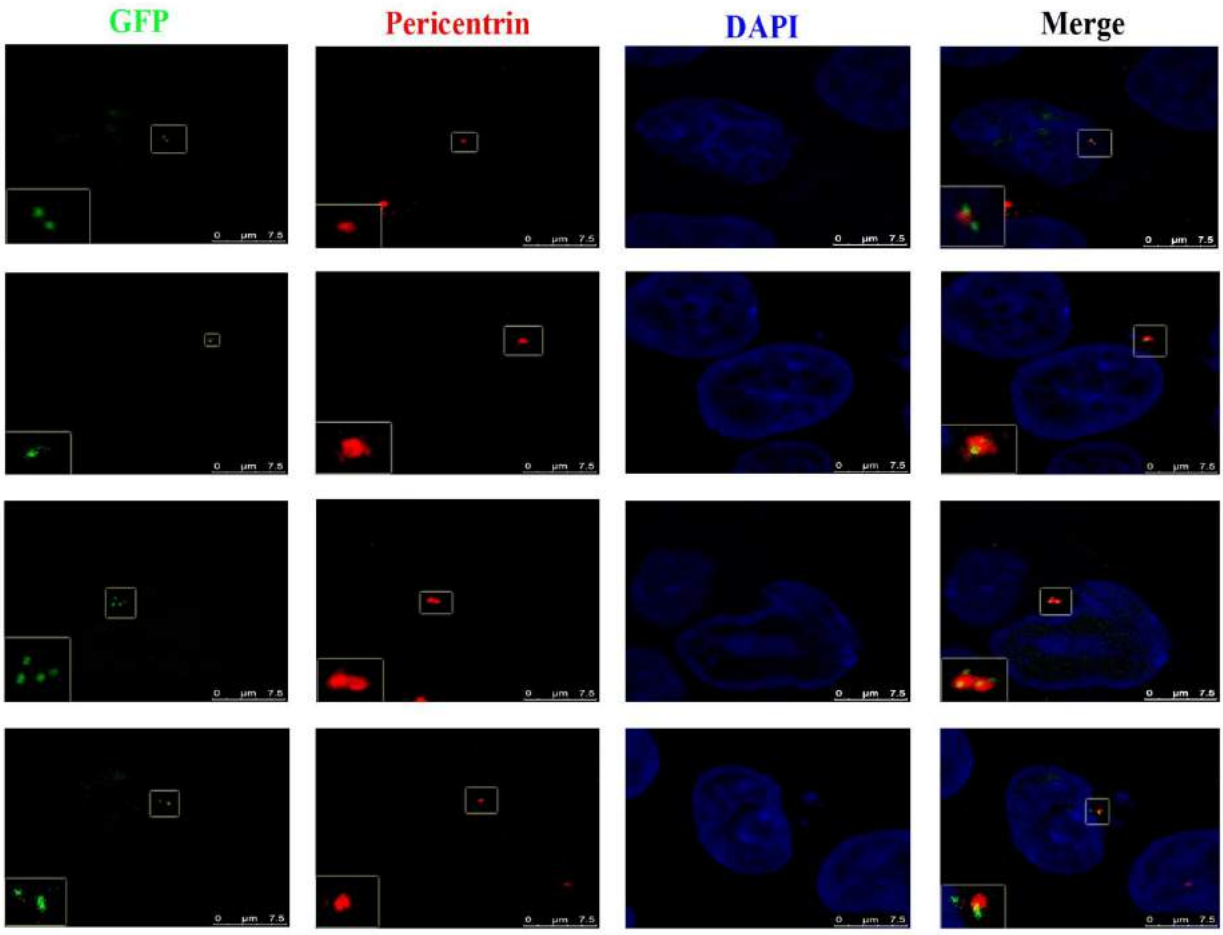

Fig. 4.14. Point mutants of potential 14-3-3 binding sites of Centrin2 are able to localize to the centrosome. *To determine the localisation of the point mutants, HCT116 cells seeded on coverslips were transfected with GFP, GFP Centrin2 WT and each of the GFP tagged Centrin2 point mutant constructs. 48 hours post transfection, the cells were fixed and stained for Pericentrin and counterstained with DAPI as described (428). The insert is a zoomed image of the box in the main field. Note that the mutant constructs show the typical orthogonal arrangement observed with the WT construct. Magnification was a 1000X with 4X digital zoom and scale bars indicate distance in µm. Images are represented as a projection of the entire Z stack.*

4.1.7.8 14-3-3γ and 14-3-3ε bind to the same region in Centrin2

As 14-3-3γ and 14-3-3ε are both capable of binding to Centrin2, we wanted to test if they bind to the same region in Centrin2 (fig. 4.15). Therefore, we transfected HCT116 cells with constructs expressing GFP, GFP Centrin2 WT, 64-172 and 1-63 and performed a GST pulldown assay using GST, GST 14-3-3γ and GST 14-3-3ε. We found that both GST 14-3-3γ and GST 14-3-3ε are able to bind to the full length and the mutant expressing aa. 1-63. However, neither of the 14-3-3 isoforms could bind to the mutant expressing aa. 64-172. This suggests that both isoforms bind to the same region in Centrin2. Also β-actin was used as a negative control to demonstrate the specificity of binding of 14-3-3 proteins.

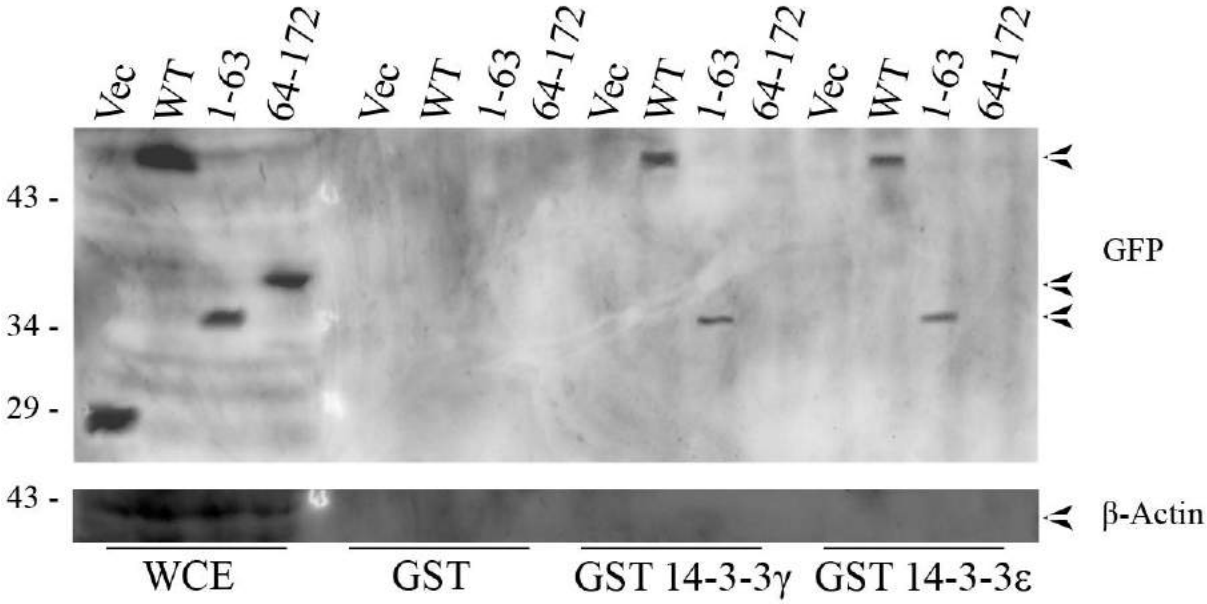

Fig. 4.15 14-3-3γ and 14-3-3ε bind to the same region in Centrin2. *HCT116 cells were transfected with the indicated GFP tagged WT or Centrin2 mutant constructs and GFP as a vector control. At 48 h post transfection, EBC extracts of HCT116 cells were incubated with the various GST fusion proteins. The complexes were resolved on a 10% SDS-PAGE gel and western blots performed with antibodies against GFP or β-Actin. Note that 64-172 does not form a complex with GST-14-3-3e or GST-14-3-3γ in contrast to the WT or the 1-63 mutant.*

Arrows indicate the positions of the GFP fusion proteins and the position of molecular weight markers in kDa is indicated. β-Actin serves as a negative control.

4.1.7.9 Depletion of both 14-3-3γ and 14-3-3ε does not alter the centrosomal localization of Centrin2

Next, we wished to determine if the loss of 14-3-3γ, 14-3-3ε or both could result in a loss of the centrosomal localisation of Centrin2. To this end, we co-transfected previously described shRNA constructs of 14-3-3γ and 14-3-3ε and GFP Centrin2 in HCT116 cells (234,401). At 72 hours post transfection, the cells were fixed and stained for pericentrin and counterstained with DAPI (fig. 4.16 (a)). We determined that the constructs were functional by performing a Western blot for both proteins and using β-actin as a loading control (fig. 4.16 (b)). We found that there was a decrease in the levels of both proteins. In addition, as has been previously reported, centrosome amplification was observed upon loss of these proteins, suggesting that these constructs are functional and there was an inhibition of CDC25C function (fig. 4.16 (c)) (326). Loss of 14-3-3γ, 14-3-3ε or both proteins did not result in an alteration in the localization of Centrin2. It is possible that due to an incomplete knockdown of both 14-3-3γ and 14-3-3ε, there is sufficient 14-3-3 protein available to mediate Centrin2 localization. Alternatively, it is possible that loss of one or more isoforms is not sufficient to induce a defect in Centrin2 localization, as, like Raf and CDC25C, Centrin2 binds to multiple 14-3-3 isoforms (152,429).

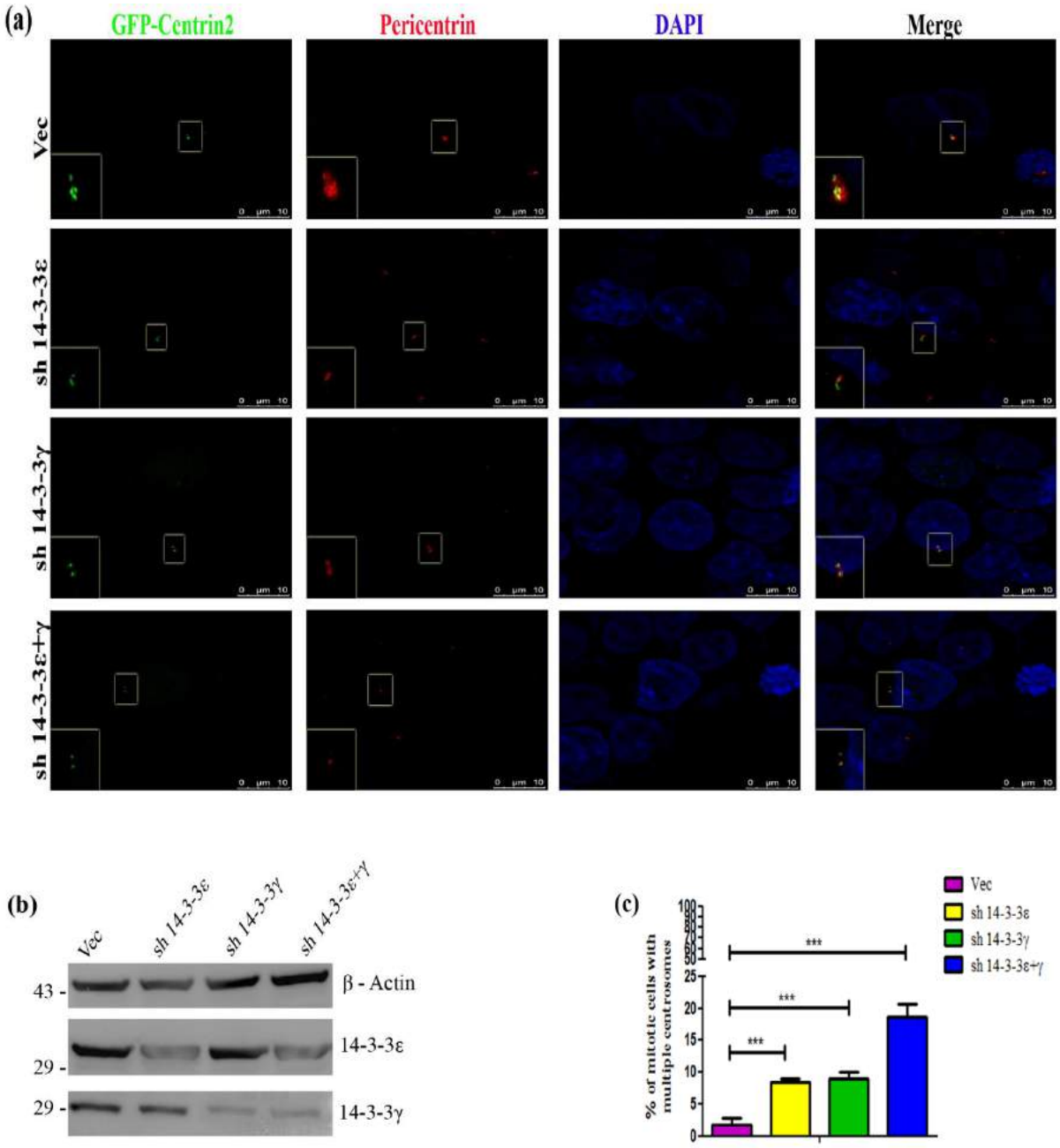

Fig. 4.16 Loss of both 14-3-3γ and 14-3-3ε does not alter the centrosomal localization of Centrin2. *(a) HCT116 cells seeded on coverslips were transfected with the GFP tagged WT Centrin2 and either the vector control or the indicated 14-3-3 shRNA constructs. At 72 h post transfection, the cells were fixed and stained for Pericentrin and DAPI. The inset is a zoomed image of the box in the main field. Magnification was a 630X with 4X digital zoom and scale bars indicate distance in µm. Note that loss of both 14-3-3e and 14-3-3γ does not lead to an alteration in Centrin2 localization, (b) Western blots indicated that the knockdown constructs*

*were effective, and (c) HCT116 cells transfected with the indicated shRNA constructs were synchronized in mitosis with nocodazole and centrosome number determined by staining the cells with antibodies to Pericentrin and counterstaining with DAPI. Note that loss of either 14-3-3ε or 14-3-3γ leads to centrosome amplification with an additive increase in centrosome amplification when the expression of both genes is inhibited. *** Indicates a p-value<0.001 and all p values were generated using the Student's t-test.*

4.1.7.10 Centrin2 mutants that are unable to bind to 14-3-3 proteins do not anchor microtubules

It has been demonstrated that overexpression of fluorescently tagged Centrin2 results in the overduplication of centrioles in S-phase arrested HeLa and CHO cells (430). However, this might be a cell specific phenotype, as this phenotype was not observed in U2OS or RPE-1 cells (430). Overduplication of centrioles or centrosome amplification can result in the generation of a multipolar spindle (395). Given our observation that the 14-3-3 binding deficient Centrin2 mutant, 64-172, exhibited a punctate cytoplasmic localisation, we wished to test if this mutant could anchor microtubules. We transfected HCT116 cells with GFP, Centrin2 WT and the 64-172 mutant and synchronized the cells in mitosis using nocodazole. We fixed the cells after nocodazole release and stained for Pericentrin and α-tubulin and counterstained for DNA with DAPI. We observed that spindle formation in these cells was comparable to that seen in cells expressing the WT or the vector control constructs (fig. 4.17). However, the puncta formed by the 64-172 mutant did not nucleate microtubules or function as spindle poles. Therefore, expression of a 14-3-3 binding-deficient mutant of Centrin2 does not interfere with spindle organization.

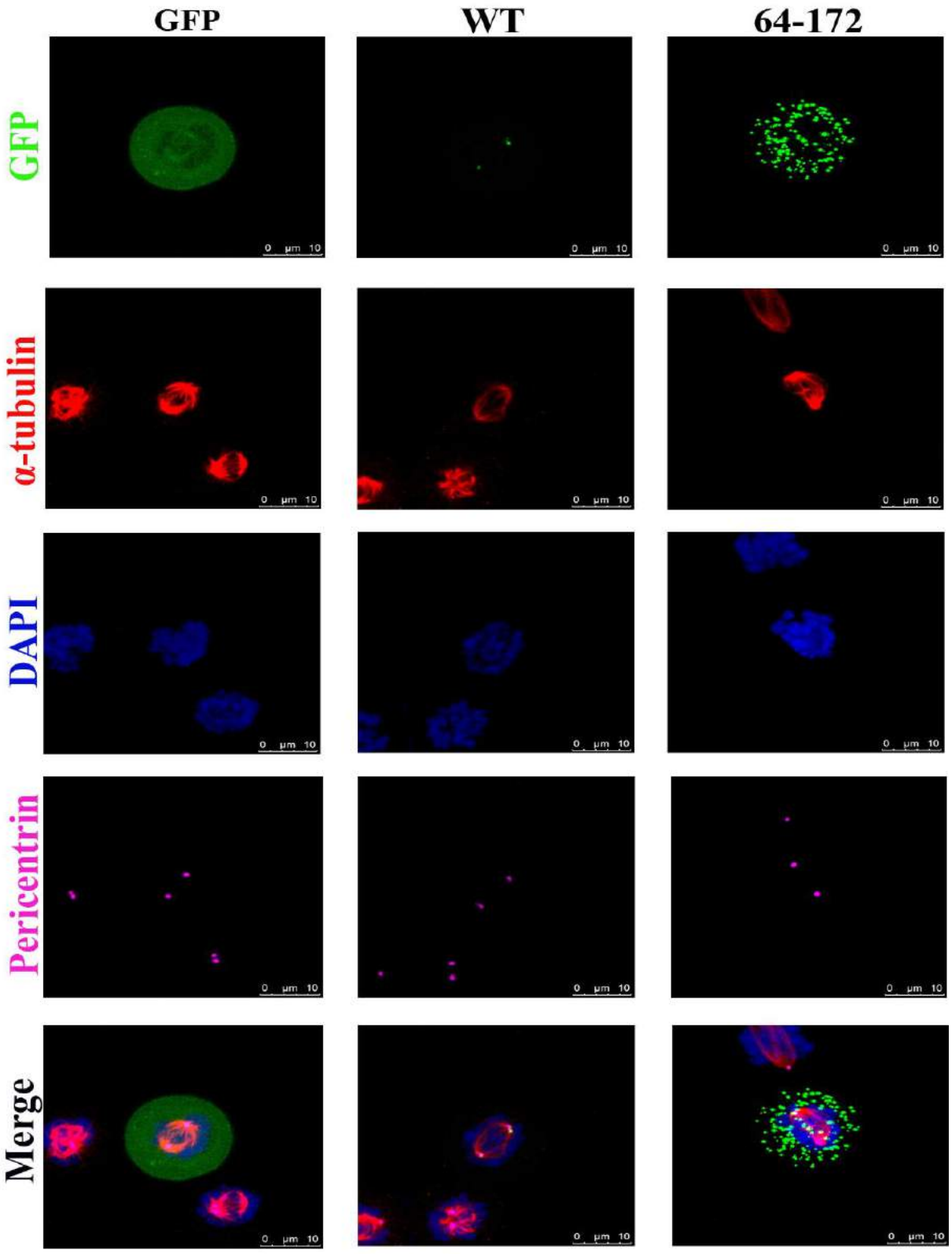

Fig. 4.17 Expression of a 14-3-3 binding-deficient mutant of Centrin2 does not interfere with spindle organization. *To test the effect of the 64-172 mutant of Centrin2 on spindle*

formation, HCT116 cells were transfected with either GFP alone or the GFP tagged WT or 64-172 constructs. Post synchronization in mitosis, the cells were fixed and stained with antibodies to Pericentrin and α-tubulin and counterstained with DAPI. Note that the 64-172 construct does not anchor microtubules. Magnification was a 630X with 4X digital zoom and scale bars indicate distance in μm.

4.1.7.11 Centrin2 mutants that are unable to bind to 14-3-3 proteins do not hamper mitotic progression

We observed that the 14-3-3 binding deficient mutant of Centrin2 was unable to nucleate microtubules. However, given its strong cytoplasmic punctate localisation, we wished to determine if it affected the duration of mitosis. We transfected HCT116 cells with the Centrin2 WT or 64-172 construct and synchronized the cells in mitosis as described in the Materials and methods section. We found that cells transfected with either construct completed mitosis in approximately the same amount of time, i.e ~40 minutes (fig. 4.18). This suggests that the 64-172 mutant does not act as a dominant negative mutant and is unable to hinder mitotic progression.

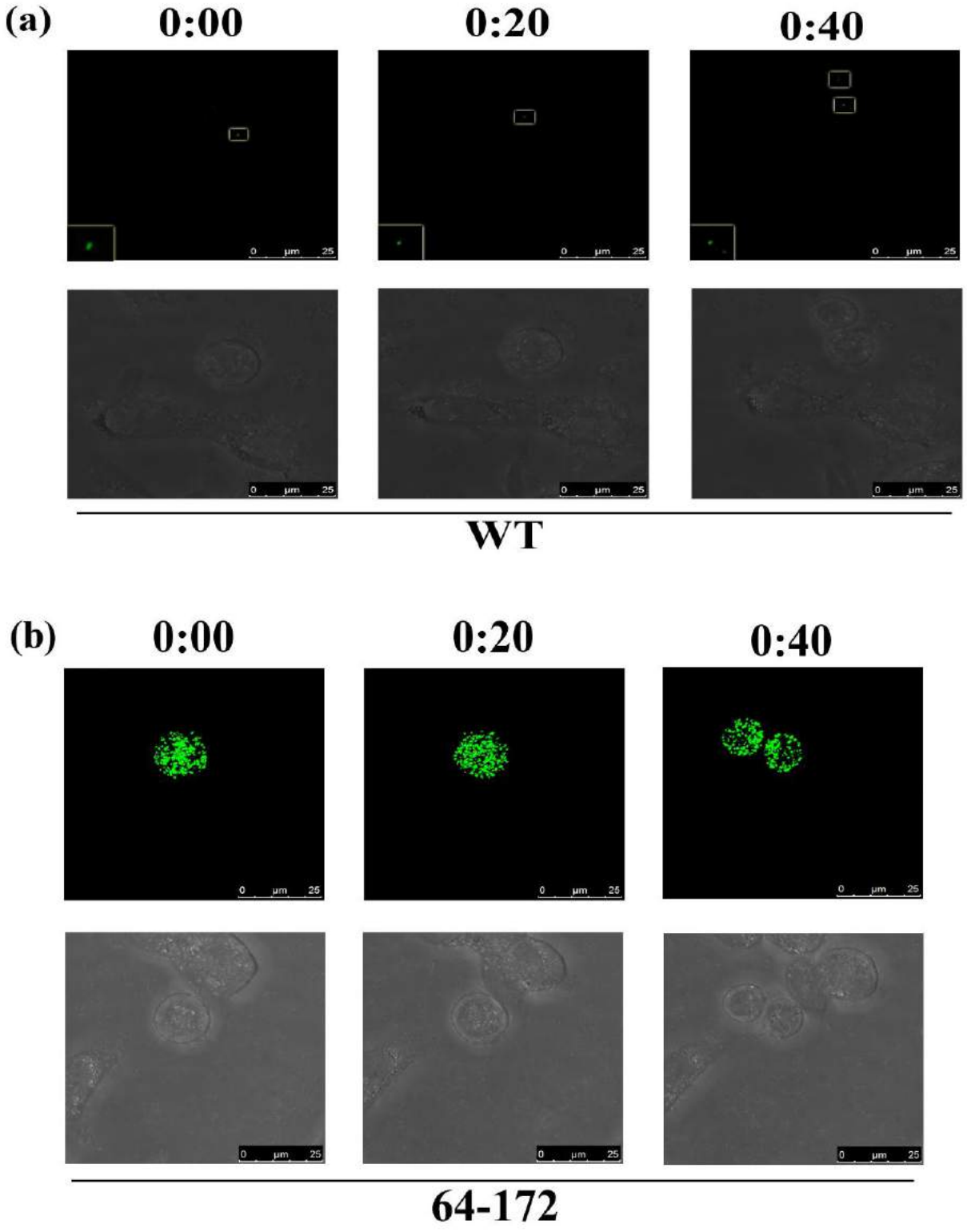

Fig. 4.18 Expression of a 14-3-3 binding-deficient mutant of Centrin2 does not interfere with mitotic progression. *In order to determine the duration of mitosis in cells expressing the 14-3-3 binding defective mutant of Centrin2, HCT116 cells were transfected with GFP*

tagged WT or mutant Centrin2 constructs. 48 hours post transfection, the cells were imaged on a Leica SP8 time lapse confocal microscope. The insert is a zoomed image of the box in the main field. Magnification was a 630X with 4X digital zoom and scale bars indicate distance in μm.

4.1.8 γ-tubulin

γ-tubulin is a part of the pericentriolar matrix (PCM). It plays a central role in PCM organization by providing a template for the initiation of polymerization of α- and β-tubulin heterodimers into growing microtubules and is essential for microtubule nucleation by an MTOC [reviewed in (357)]. It is a component of the γ-tubulin ring complex (γ-TURC) along with GCP2-6, MOZART1, MOZART2A, MOZART2B and NEDD1 (431). The γ-tubulin small complex (γ-TUSC), made of γ-tubulin, GCP2 and GCP3 is conserved in all eukaryotes, whereas the γ-TURC is found in fewer eukaryotes (432). γ-tubulin is essential for development in mice, as TUBG1 (γ-tubulin) knockout embryos failed to develop post the morula/blastocyst stage due to defects in the mitotic spindle; the mitotic spindle was highly disorganized, and disorganized spindles showed one or two pole-like foci of bundled MTs that were surrounded by condensed chromosomes (433).

γ-tubulin contains a FtsZ/GTPase domain at the N terminus, a middle Tubulin/FtsZ, 2 layer sandwich domain and a C-terminal domain. We decided to generate C-terminal deletion constructs of γ-tubulin – G1- only the first FtsZ/GTPase domain, G2 – FtsZ/GTPase + Tubulin/FtsZ 2 layer sandwich domain and G3 – full length construct. They were all cloned into a pECFP-N1 vector (fig. 4.19). In order to test the expression of the γ-tubulin deletion constructs, we transfected them into HCT116 cells. 48 hours post transfection, we harvested the cells and prepared lysates and loaded it on an SDS-PAGE gel. When we performed a

Western Blot using GFP antibody, we observed that the deletion mutants expressed properly at the right size (fig. 4.19).

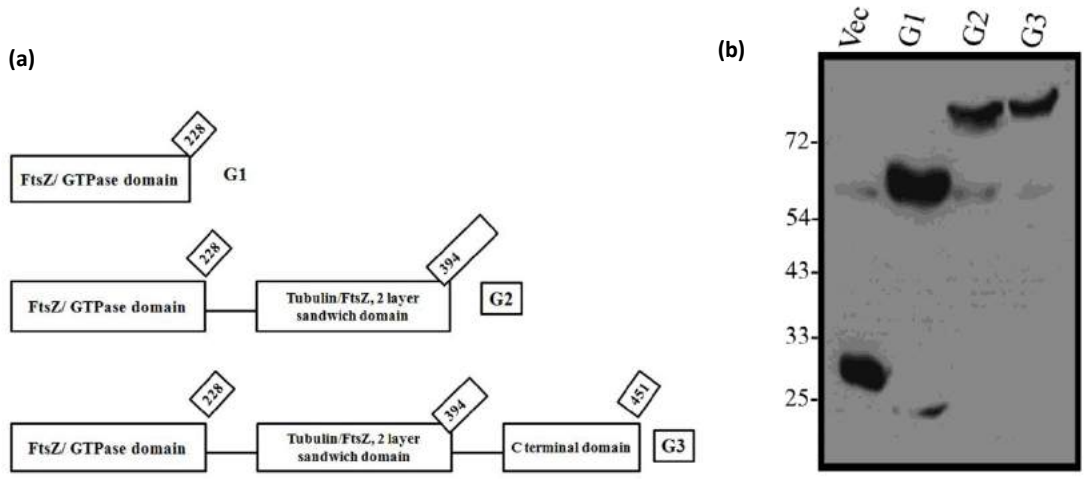

Fig. 4.19 The deletion constructs of γ-tubulin. *(a) We generated C-terminal domain deletions of γ-tubulin and cloned them into an ECFP-N1 vector. The numbered boxes indicate the number of amino acids encoded by that domain, (b) HCT116 cells were transfected with the γ-tubulin deletion constructs. 48 hours post transfection, lysates were prepared and resolved on a 10% SDS-PAGE gel. Western Blot was performed using GFP antibody.*

4.1.8.1 Localization of the γ-tubulin deletion constructs

In order to observe the localization of the γ-tubulin constructs, we transfected them into HCT116 cells. 48 hours post transfection, we fixed and stained the cell using antibodies against Pericentrin to stain the centrosome and counterstained for DNA using DAPI (fig. 4.20). We observed that the full length construct (G3) and the G2 construct were able to localize to the centrosome, as seen with Pericentrin staining. However, the G1 construct,

which expressed only the FtsZ/GTPase domain, was unable to localize to the centrosome. This indicates that the Tubulin/FtsZ 2 layer sandwich domain is necessary for the centrosomal localization of γ-tubulin.

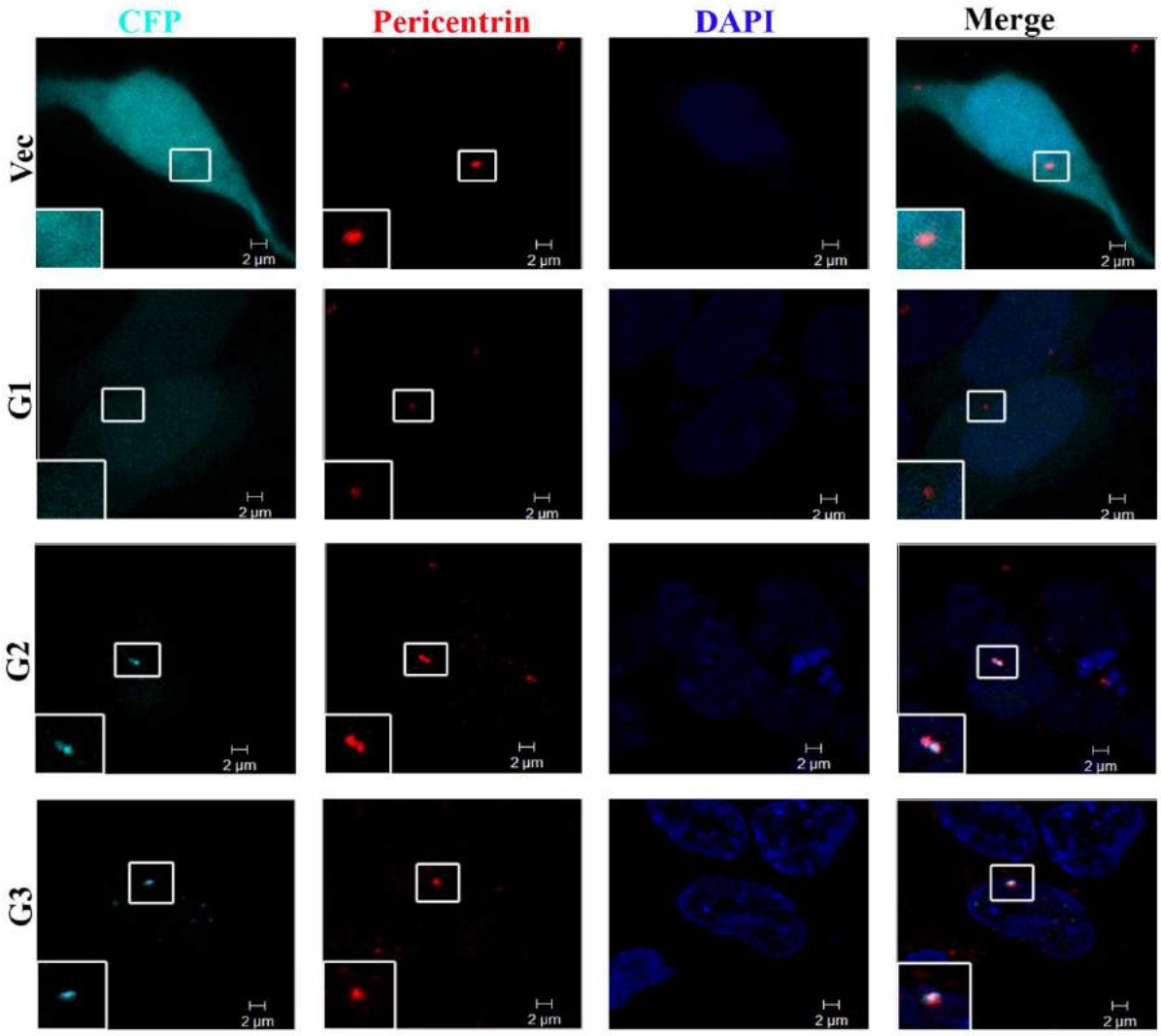

Fig. 4.20 Localization of the γ-tubulin deletion constructs. *To determine the localisation of the deletion constructs, HCT116 cells seeded on coverslips were transfected with ECFP, G1, G2 and G3 constructs. 48 hours post transfection, the cells were fixed and stained for Pericentrin and counterstained with DAPI as described (428). The insert is a zoomed image of the box in the main field. Note that the G3 (full length) and G2 mutant constructs colocalised with Pericentrin. However, the G1 construct had a pan cellular localisation.*

Magnification was a 630X with 4X digital zoom and scale bars indicate distance in µm. Images are represented as a projection of the entire Z stack.

4.1.8.2 The N terminal of γ-tubulin mediates interaction with 14-3-3γ

We wanted to determine the binding site of 14-3-3 proteins on γ-tubulin. So, we transfected HCT116 cells with the ECFP-N1, G1, G2 and G3. 48 hours post transfection, we performed a GST pulldown assay to determine which domain in γ-tubulin is essential for binding to 14-3-3γ. We found that the ECFP-N1 is unable to bind to 14-3-3γ whereas; all the deletion constructs are able to bind to 14-3-3γ (fig. 4.21). This led us to conclude that the N-terminal FtsZ/GTPase domain of γ-tubulin is sufficient for its interaction with 14-3-3γ. However, binding to 14-3-3γ might not be essential for its localisation at the centrosome.

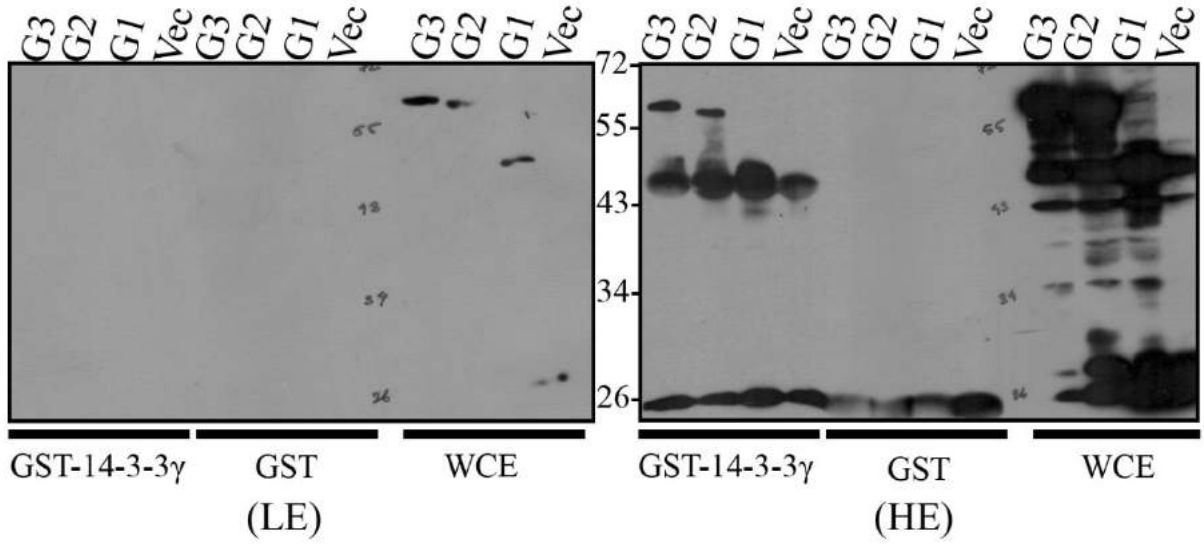

Fig. 4.21 Mapping the 14-3-3γ binding site on γ-tubulin. *HCT116 cells were transfected with the indicated CFP vector or G1, G2 and G3 construct. At 48 h post transfection, EBC extracts of HCT116 cells were incubated with the various GST fusion proteins. The complexes were resolved on a 10% SDS-PAGE gel and western blots performed with antibodies against GFP. The position of molecular weight markers in kDa is indicated. Note that all the deletion constructs bind to γ-tubulin. The GFP antibody detects GST, non-*

specifically, and the band for G1 appears just above the GST-14-3-3γ band. LE indicates a Lower Exposure and HE indicates a Higher Exposure.

4.1.9 γ-tubulin complex protein 2 (GCP2)

GCP2 is one of the three proteins that form the γ-TUSC, with γ-tubulin and GCP3. It is a homologue of the yeast spindle pole body protein Spc97p (434). Since it is a component of the γ-TUSC, it is essential for microtubule nucleation. A null mutation of *Arabidopsis* GCP2 severely impaired the development of male and female gametophytes (435). A knockdown of GCP2 in the glioblastoma cell line T98G led to an accumulation of cells in G2/M phase (436). This was accompanied by mitotic delay, although the cells were able to complete mitosis (436). Structurally, GCP2 consists of the domain that bears homology to the Spc97p protein. We decided to generate C terminal truncated mutants that did not express the Spc97p domain. We generated two deletion mutants; GC1 – aa. 1 – 220 and GC2 – aa. 1 – 738. Both these sequences were cloned into the ECFP-N1 vector, along with the full length cDNA.

In order to test the expression of the GCP2 deletion constructs, we transfected them into HCT116 cells. 48 hours post transfection, we harvested the cells and prepared lysates and loaded it on an SDS-PAGE gel. When we performed a Western Blot using GFP antibody, we observed that the deletion mutants expressed properly at the expected size (fig. 4.22).

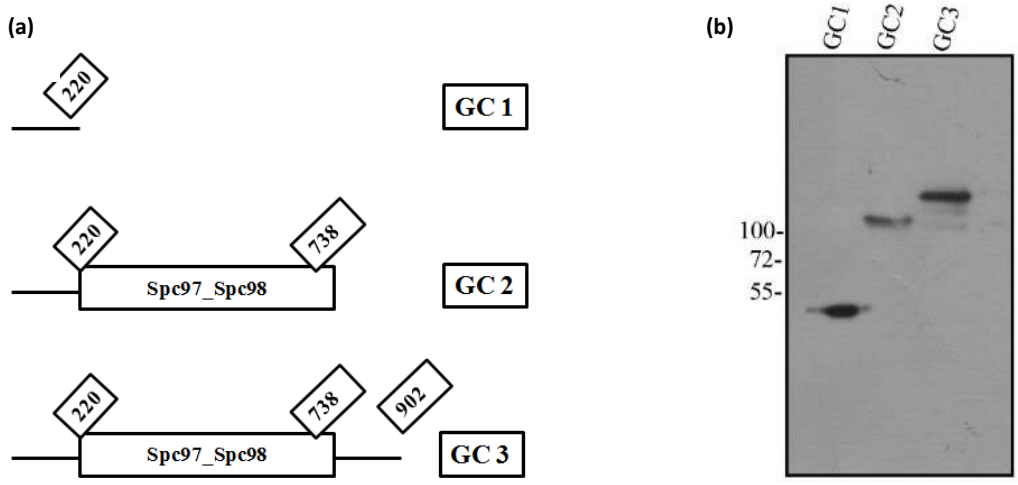

Fig. 4.22 Deletion constructs of GCP2. *(a) Cartoon representing the deletion constructs of GCP2. We generated C-terminal domain deletions of GCP2 and cloned them into an ECFP-N1 vector. The numbered boxes indicate the number of amino acids encoded by that domain, (b) Expression of the deletion constructs. HCT116 cells were transfected with the GCP2 deletion constructs. 48 hours post transfection, lysates were prepared and resolved on a 10% SDS-PAGE gel. Western Blot was performed using GFP antibody.*

4.1.9.1 Localization of the GCP2 deletion constructs

In order to observe the localization of the GCP2 constructs, we transfected them into HCT116 cells. 48 hours post transfection, we fixed and stained the cell using antibodies against Pericentrin to stain the centrosome and counterstained for DNA using DAPI. We observed that each of the deletion constructs co-localized with the Pericentrin staining (fig. 4.23). This suggests that Spc97p domain is not essential for the centrosomal localisation of GCP2. However, the intensity of the GC1 construct at the centrosome was much weaker as compared to the other constructs. Deletion of the Spc97p domain might therefore, affect the centrosomal recruitment of GCP2.

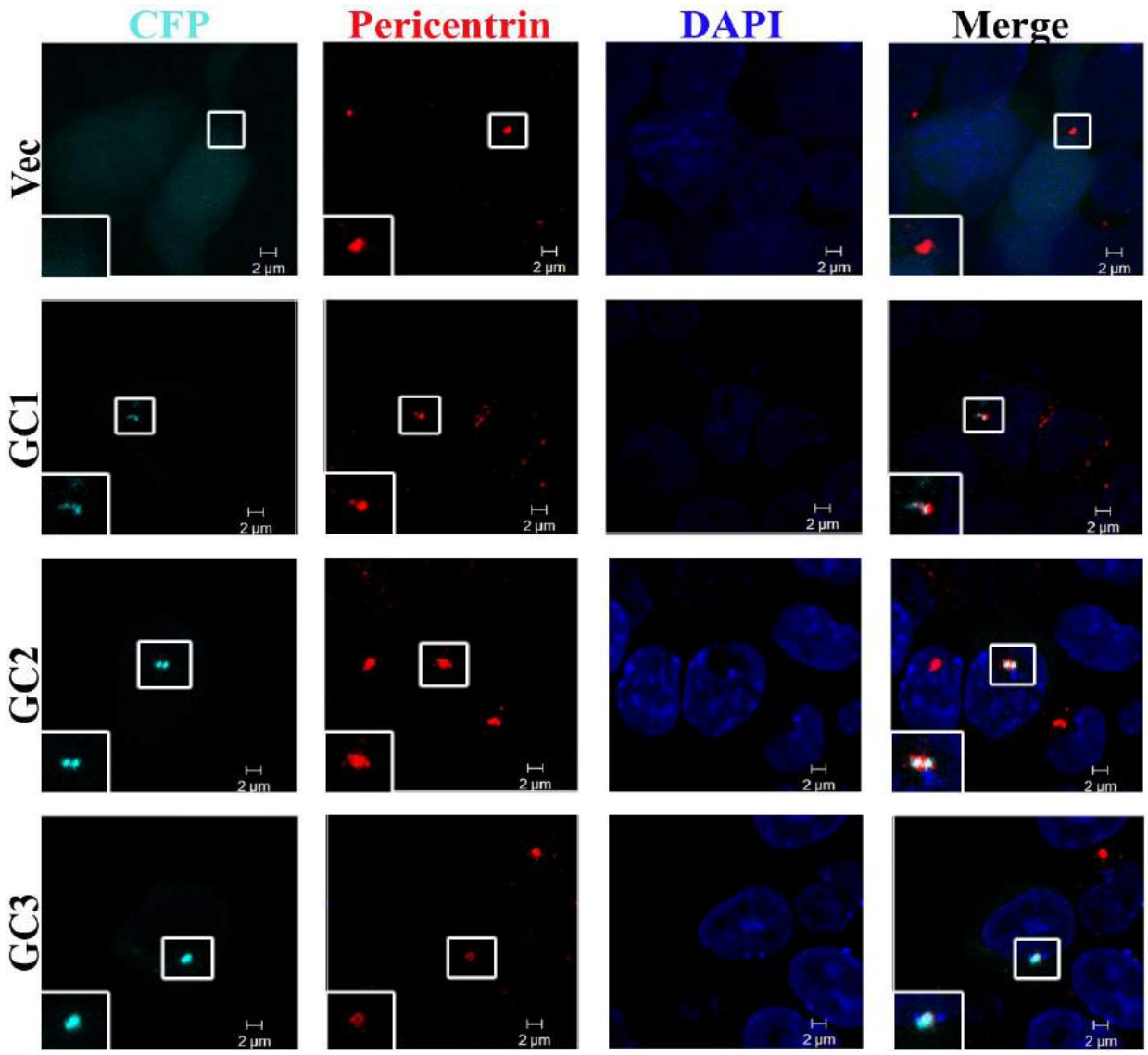

Fig. 4.23 Localization of the GCP2 deletion mutants. *To determine the localisation of the deletion constructs, HCT116 cells seeded on coverslips were transfected with ECFP, GC1, GC2 and GC3 constructs. 48 hours post transfection, the cells were fixed and stained for Pericentrin and counterstained with DAPI as described (428). The insert is a zoomed image of the box in the main field. Note that the GC3 (full length) and GC2 mutant constructs colocalised very strongly with Pericentrin. However, the GC1 construct had a weaker intensity at the centrosome. Magnification was a 630X with 4X digital zoom and scale bars indicate distance in µm. Images are represented as a projection of the entire Z stack.*

4.1.10 Cep170

Centrosomal protein of 170 kD (Cep170) localises to the subdistal appendages and hence serves as a marker for the mother centriole (306). It has been demonstrated that Cep170 is recruited to the centrosome by CCDC120 and CCDC68, which are also components of the sub-distal appendages (437). It has also been demonstrated that the non-canonical IκB kinase, TANK Binding Kinase 1 (TBK1), is essential for the centrosomal localization of Cep170 (438). Expression of phosphosite mutants of Cep170 that cannot be phosphorylated by TBK1 lead to mitotic defects, such as multipolar spindles (438). It has a forkhead associated domain (FHA domain), which is a phosphopeptide recognition domain found in many regulatory proteins (306).

Upon screening for possible 14-3-3 binding sites on Cep170, we found three sites at high stringency, T644, T1078 and T1259. These residues were altered to Alanine to determine if they are required for 14-3-3 binding.

Phosphoserine/threonine binding group (pST_bind)				
14-3-3 Mode 1			Gene Card YWHAZ	
Site	Score	Percentile	Sequence	SA
T644	0.2050	0.012 %	QGERRRRTLPQLPNE	2.802
14-3-3 Mode 1			Gene Card YWHAZ	
Site	Score	Percentile	Sequence	SA
T1078	0.3444	0.194 %	SKVTKSKTSPVVSGS	1.363
14-3-3 Mode 1			Gene Card YWHAZ	
Site	Score	Percentile	Sequence	SA
T1259	0.3125	0.107 %	PKHTRLRTSPALKTT	1.118

Fig. 4.24. Putative 14-3-3 binding sites on Cep170

4.1.10.1 Are levels of centrosomal proteins altered in the sh-14-3-3γ cells?

The levels of several proteins involved in the centrosome cycle are altered in various cancers (439). We wished to determine if there was an alteration in the levels of the proteins that we identified as interactors of 14-3-3 proteins. We observed that there was no change in the protein levels of Centrin2, GCP2, and γ-tubulin in the vector control vs the sh-14-3-3γ cells. However, there was a decrease in the protein levels of Cep170 in the sh-14-3-3γ cells (fig. 4.25). Given that total protein levels of Cep170 are decreased in the sh-14-3-3γ cells, we wished to determine if the mRNA levels are also affected. So, we performed an RT-PCR to determine the mRNA levels. We observed that the mRNA levels of Cep170 are also decreased in the sh-14-3-3γ cells (fig. 4.25).

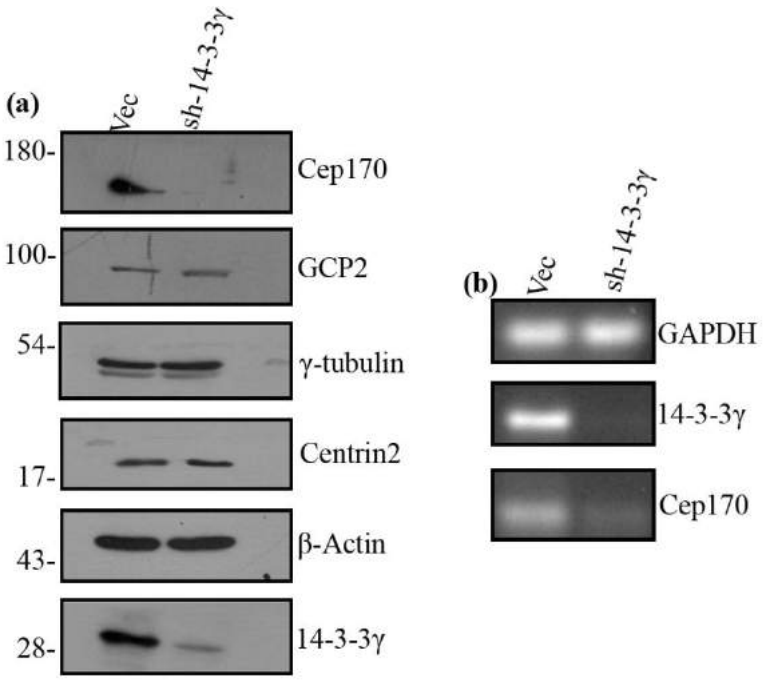

Fig. 4.25. Loss of 14-3-3γ results in the decrease of Cep170 at both protein and mRNA levels. *(a) Lysates of the vector control and sh-14-3-3γ cells were prepared and resolved on a 10% SDS-PAGE gel. Western blot was performed for the indicated proteins. β-Actin served as the loading control, (b) RT-PCR was performed to determine mRNA levels of Cep170 in the vector control vs the sh-14-3-3γ cells. GAPDH was used as the loading control.*

4.1.10.2 The decrease in total levels of Cep170 in the sh-14-3-3γ cells does not affect the intensity of Cep170 at the centrosome.

In order to find the functional consequences of this phenotype, we wished to determine if the intensity of Cep170 staining at the centrosome was affected. We observed that there was no significant change in Cep170 intensity at the centrosome in the vector control vs the sh-14-3-3γ cells (fig. 4.26).

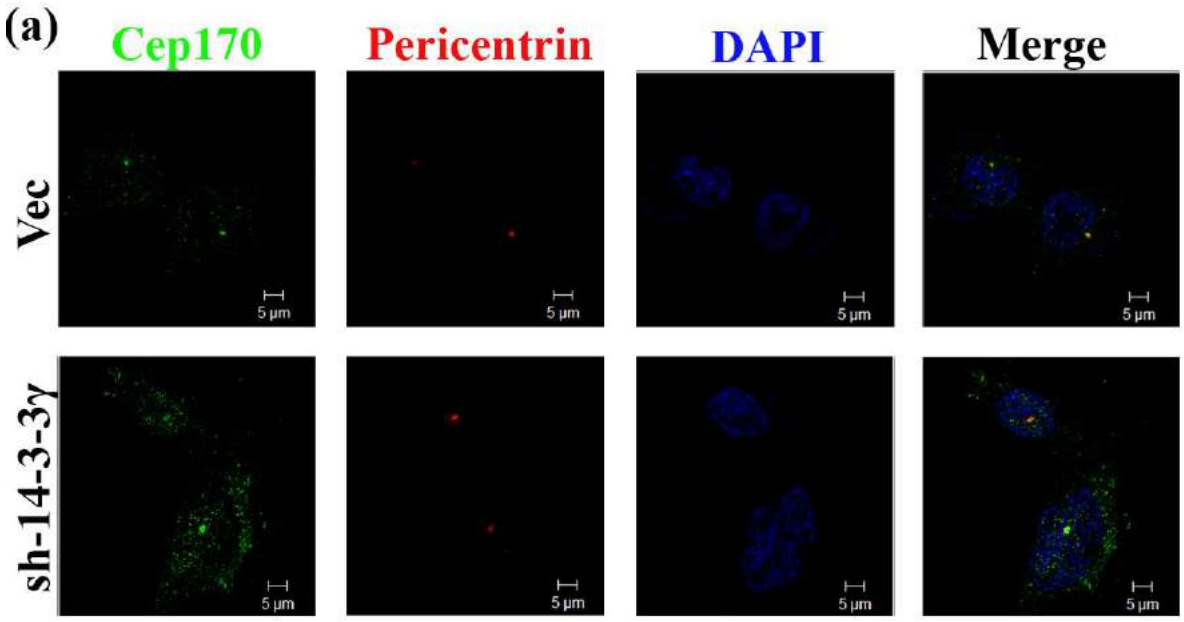

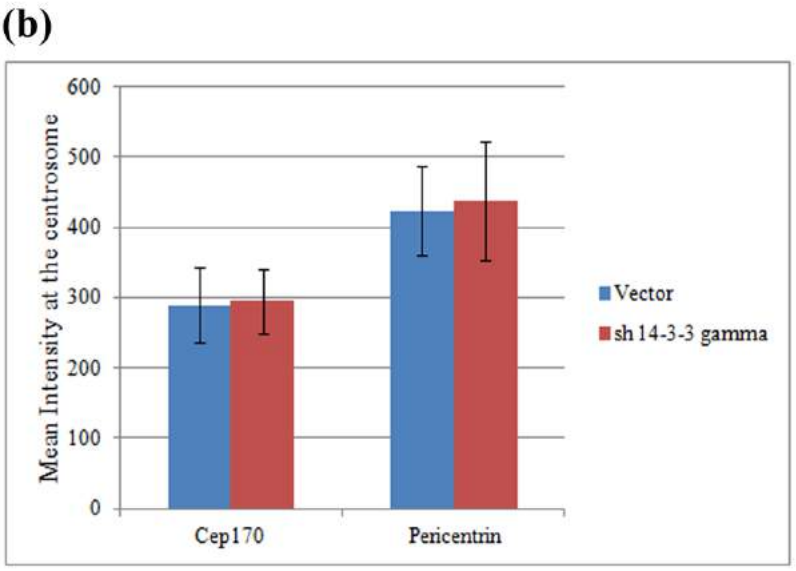

Fig. 4.26. Intensity of Cep170 at the centrosome in sh-14-3-3γ cells is not altered. *(a) Vector control and the sh-14-3-3γ cells were stained with antibodies against Cep170 and Pericentrin and costained using DAPI. Magnification was a 630X with 2X digital zoom and scale bars indicate distance in μm. Images are represented as a projection of the entire Z stack, (b) Mean intensity at the centrosome was determined. GAPDH was used as the loading control.*

4.1.11 How do negatively charged residues in the peptide binding groove of 14-3-3 proteins regulate ligand function?

Most 14-3-3 ligands are phosphorylated at a serine or threonine residue, though there are some ligands that bind in a phospho-independent manner (157,173,180,188). The phosphorylated ligands bind via either a Mode I consensus sequence (R[S/Ar][+/Ar]pS[L/E/A/ M]P), or a Mode II consensus sequence Rx[Ar][+]pS[LE/A/M]P, where Ar represents an aromatic residue and + indicates a basic residue (157,173,180). Previous studies have indicated that a number of positively charged residues, such as Lys49, Arg56, Arg127 and Tyr128, in the amphipathic peptide binding groove of 14-3-3 proteins are essential for binding to ligands. These residues form a basic compartment in an acidic molecule, giving substrate serine/threonine phosphorylations the ability to act as a molecular switch controlling ligand binding. Careful examination of the peptide-binding grove of 14-3-3 proteins revealed the presence of two conserved negatively charged residues, Asp129 and Glu136 (fig. 4.27). This was interesting because as mentioned previously, positively charged amino acids are needed within the peptide-binding groove for ligand binding. We wished to test the contribution of these negatively charged residues to ligand binding.

Fig. 4.27 Sequence alignment of the peptide binding groove of 14-3-3 isoforms.

4.1.11.1 Site directed mutagenesis of 14-3-3γ WT

We have demonstrated previously, that a loss of 14-3-3γ leads to centrosome amplification (326). Therefore, we decided to test the effect of these mutants on centrosome number. Using Site Directed Mutagenesis (SDM), we mutated the Asp129 and Glu136 to obtain D129A and E136A. We also generated a double mutant – D129AE136A. Arg56 has been demonstrated to be important for ligand binding (180). We mutated this to Alanine, as a residue known to have an effect on ligand binding. We finally generated multiple mutants, R56A, D129A, E136A, R56AD129A, R56AE136A, D129AE136A and R56AD129AE136A. shRNA resistant WT 14-3-3γ was cloned into a pCMV-mOrange vector. Then, SDM was performed to generate the various combinations of mutant proteins. The clones were sequenced and verified.

4.1.11.2 Testing the expression of the 14-3-3γ mutants

In order to test the expression of the 14-3-3γ mutants, we transfected HCT116 cells with each of the constructs. 48 hours post transfection, we harvested the cells and performed protein estimation. Equal concentrations of the lysates were loaded onto an SDS-PAGE gel and

Western Blot performed with antibody GFP that detected mOrange. We found that the mutant proteins expressed at the correct molecular weight, ~54 kDa (fig. 4.28).

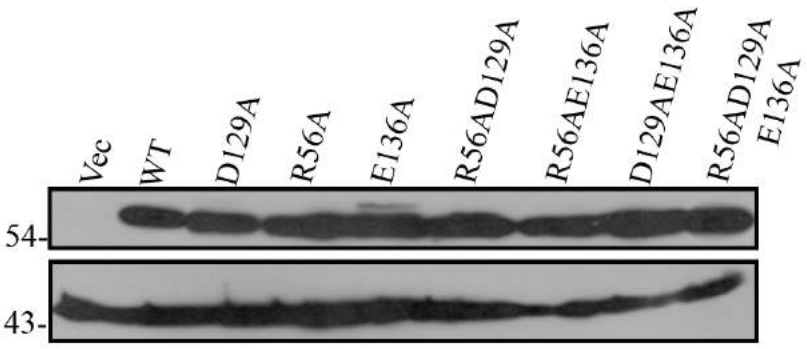

Fig. 4.28 Expression of the mOrange tagged 14-3-3γ constructs. *HCT116 cells were transfected with the mOrange tagged 14-3-3γ constructs. 48 hours post transfection, lysates were prepared and resolved on a 10% SDS-PAGE gel. Western Blot was performed using 14-3-3γ antibody.*

4.1.11.3 Effect of the expression of the 14-3-3γ mutants on centrosome number

In order to test the effect of the mutants on centrosome number, we transfected HCT116 cells with each of the mutants. 48 hours post transfection and synchronization in mitosis with nocodazole, we fixed the cells and stained with antibodies against pericentrin and counterstained for DNA using DAPI. We counted centrosome number in a 100 transfected mitotic cells. We observed that expression of the vector control or the WT 14-3-3γ construct did not affect centrosome number. The R56A construct alone also had no effect on centrosome number. However, expression of the D129A mutant resulted in an increase in the percentage of cells with a single centrosome in mitosis. Conversely, expression of the E136A mutant gave rise to an increase in the percentage of cells with multiple centrosomes in mitosis. Expression of the D129AE126A mutant restored centrosome number to that seen

upon expression of the WT construct, as an example of intragenic complementation (fig. 4.29).

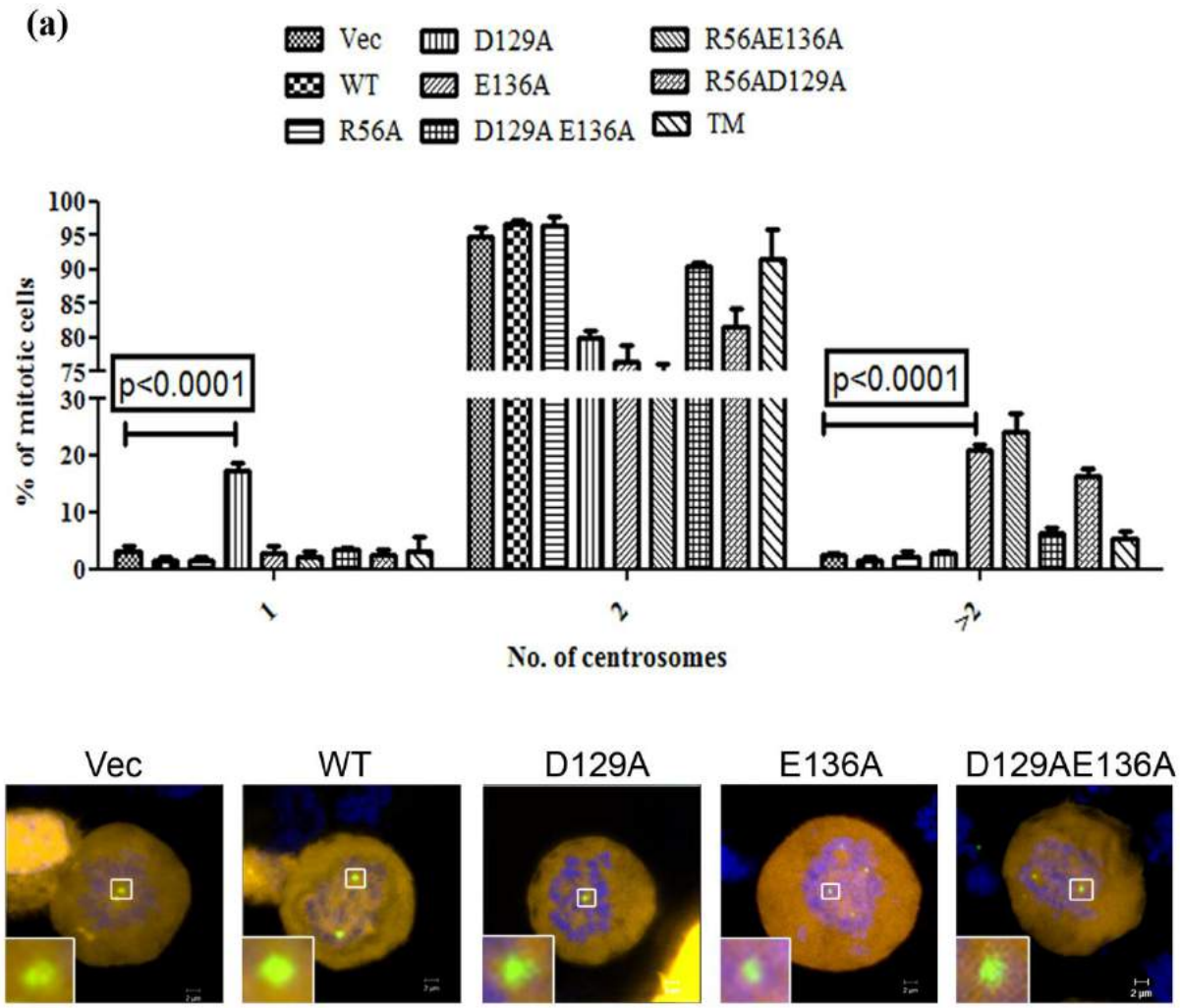

Fig. 4.29 Effect of the expression of the 14-3-3γ mutants on centrosome number. *HCT116 cells were transfected with 1 µg of constructs expressing either the vector control (mOrange) or the mOrange tagged WT and mutant 14-3-3γ constructs. (a) The graph shows the percentage of mitotic cells with 1, 2 or >2 centrosomes, (b) The transfected cells were fixed, permeabilized and stained with antibodies to Pericentrin (green) and counterstained with DAPI. Original magnification 630X with 4X optical zoom. Scale bar indicates 2µm.*

Expression of the R56AD129A mutant also gave rise to multiple centrosomes. The R56AE136A behaved like the E136A alone and the triple mutant gave rise to a phenotype similar to that of the WT. Given that the expression of the R56A alone did not result in any significant change in centrosome number when compared to the WT and also that R56 has already been demonstrated to be involved in ligand binding, we decided to focus on the D129A, E136A and the double mutant D129AE136A (180).

4.1.11.4 Effect of the 14-3-3γ mutants in the sh-14-3-3γ cells.

As described earlier, loss of 14-3-3γ leads to centrosome amplification (326). Given that the 14-3-3γ mutants were overexpression constructs, we wanted to know if endogenous 14-3-3γ modulates the phenotype observed. So, we decided to determine the effect of the 14-3-3γ mutants on cells harboring a knockdown of 14-3-3γ (fig. 4.31). As observed before, there was an increase in the percentage of cells with multiple centrosomes in the sh-14-3-3γ cells when compared to the vector control (fig. 4.30 (a)). Expression of the D129A mutant in both the vector control and the sh-14-3-3γ cells resulted in a significant increase in the percentage of cells with a single centrosome as compared to cells transfected with the WT construct or the vector control (fig. 4.30 (a)). Expression of E136A led to a significant increase in the percentage of cells with >2 centrosomes in both the vector control and sh-14-3-3γ cells. Expression of the D129AE136A mutant did not result in a significant change in centrosome number. This could be due to intragenic complementation. All proteins were expressed at equivalent levels (fig. 4.30 (b)). These results suggest that the D129 and E136 residues affect centrosome number even in the presence of endogenous protein and are dominant over the endogenous protein in human cells.

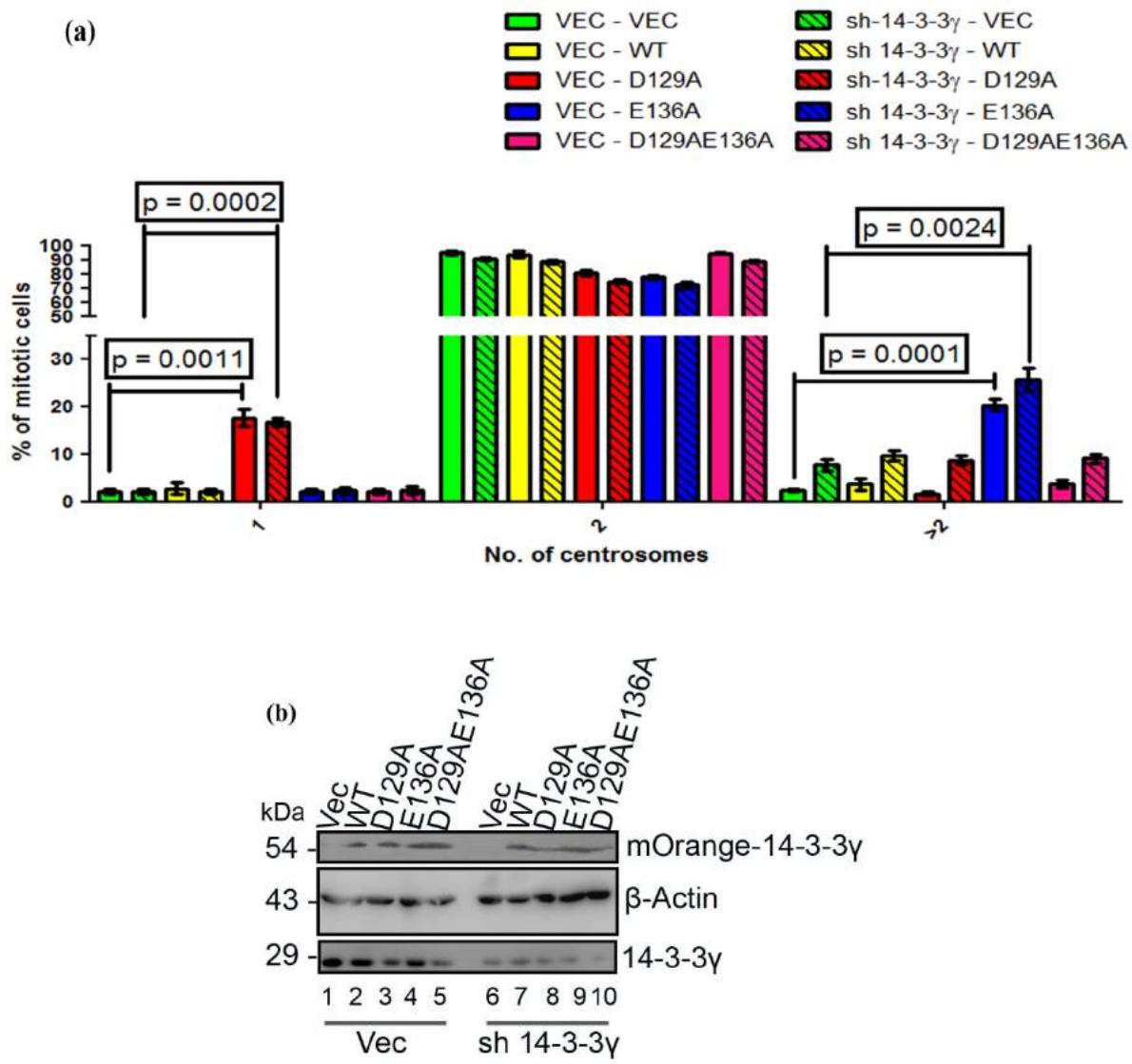

Fig. 4.30. Effect of the 14-3-3γ mutants in the sh-14-3-3γ cells. *The HCT116 derived vector control or 14-3-3γ knockdown clones (sh14-3-3γ) were transfected with the indicated constructs and centrosome number determined in mitotic cells. (a) Note that D129A inhibits centrosome duplication in both the vector control and 14-3-3γ knockdown cells while E136A promotes centrosome duplication in both cell types. The graph shows the percentage of mitotic cells with 1, 2 or >2 centrosomes, (b) 48 hours post transfection, protein extracts were prepared from the transfected cells and Western blots were performed with the indicated antibodies. Western blot for β-actin served as a loading control. Note that all proteins were expressed at equivalent levels in both cell types.*

4.1.11.5 The effect of the 14-3-3γ mutants on centrosome number is independent of cell type.

We wanted to know if the phenotype we observed was dependent on the cell line being used. To this end, we expressed these constructs in HaCaT and HEK293 cell lines and observed that the phenotype was conserved and independent of the cell line being used (fig. 4.31).

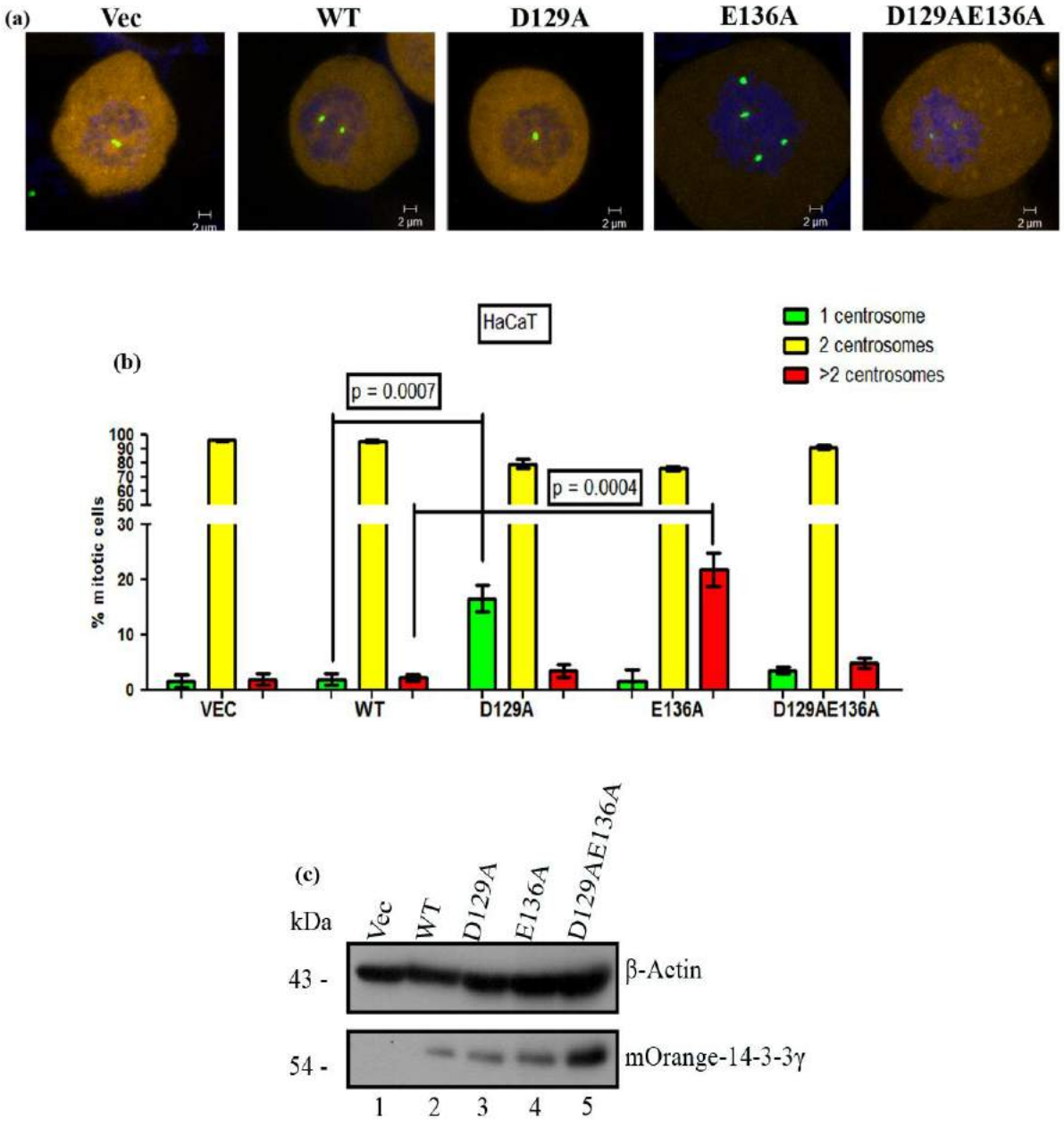

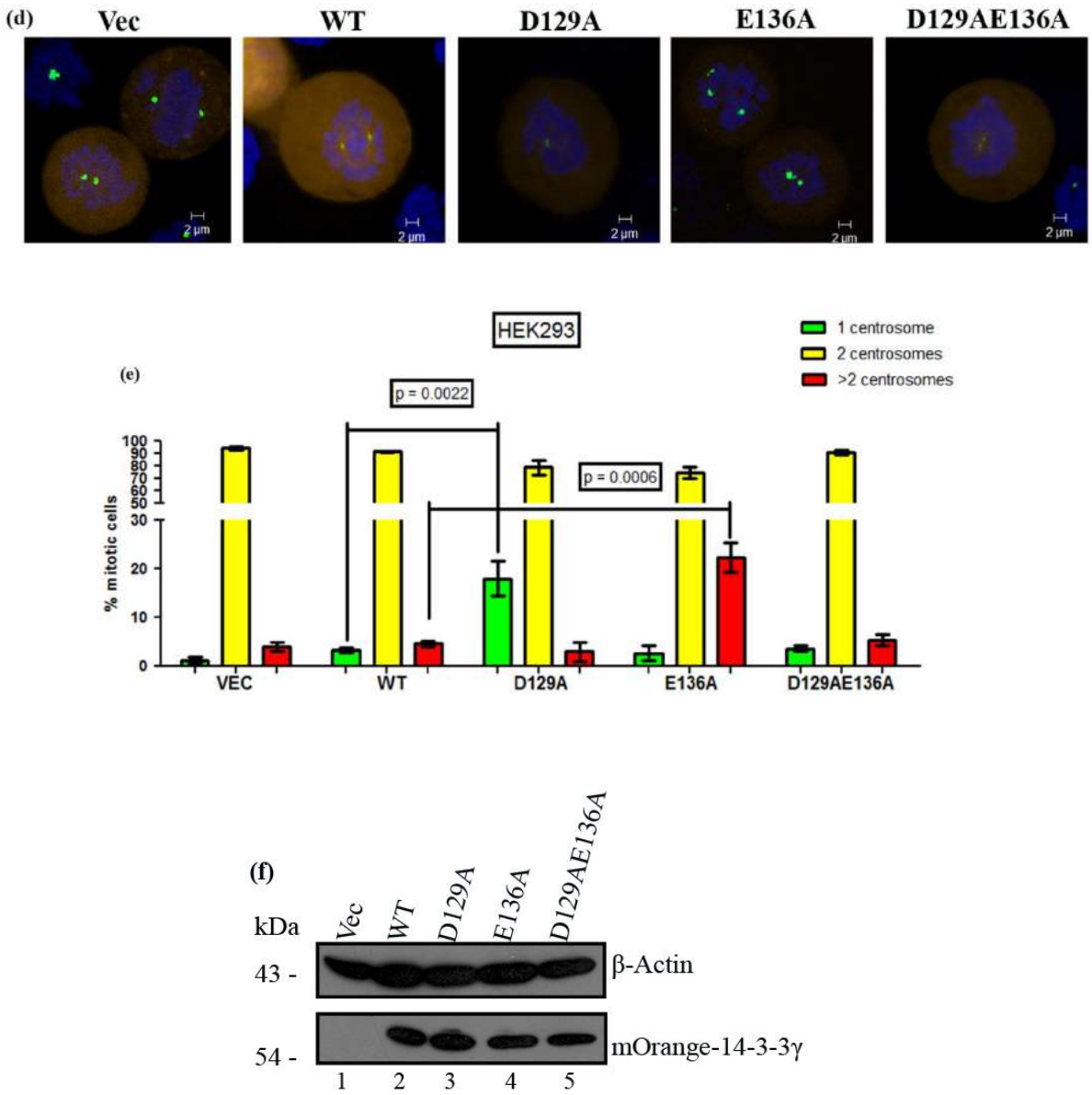

Fig. 4.31. Effect of the mutants is conserved in HaCat and HEK293 cell lines. *HaCaT or HEK293 cell lines were transfected with the vector control or the indicated 14-3-3γ constructs. 48 hours post transfection, protein extracts were prepared from the transfected cells and Western blots were performed with the indicated antibodies or centrosome number determined in mitotic cells. Western blots for β-actin served as a loading control. The graph shows the percentage of mitotic cells with 1, 2 or >2 centrosomes. (a-c) – HaCat and (d-f) – HEK293.*

4.1.11.6 Centriolar organization in cells expressing the mutants

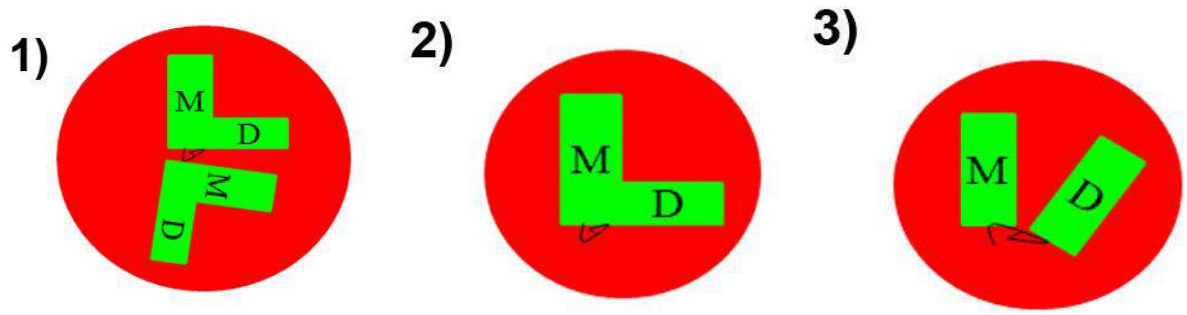

Fig. 4.32. The three possibilities that can lead to the presence of a single centrosome in mitosis. (1) defect in separation, (2) defect in disengagement and (3) defect in duplication.

There are three scenarios that can explain the presence of a single centrosome in mitosis. One, a defect in centrosome separation, two, a defect in centriole disengagement, and three, a defect in centriole duplication (fig. 4.32). In order to understand the phenotype further, we had to determine the centriolar structure of the cells with the single and multiple centrosomes. So, we co-transfected HCT116 cells with each of the mOrange 14-3-3γ constructs and EGFP centrin2 to help us visualise the centrioles. 24 hours post transfection, nocodazole was added to synchronize cells at mitosis. After synchronization, the cells were stained for Pericentrin and DNA (fig. 4.33). We observed that cells transfected with the D129A mutant, which had single centrosomes based on Pericentrin staining, showed the presence of 2 centrin2 dots within the single Pericentrin cloud. This means that there could be a defect in duplication or disjunction of the centriolar pair. Cells transfected with the E136A mutant, which showed multiple pericentrin dots also displayed two Centrin2 dots. The D129AE136A mutant showed a phenotype similar to the WT, with two pericentrin clouds, each harbouring two Centrin2 dots.

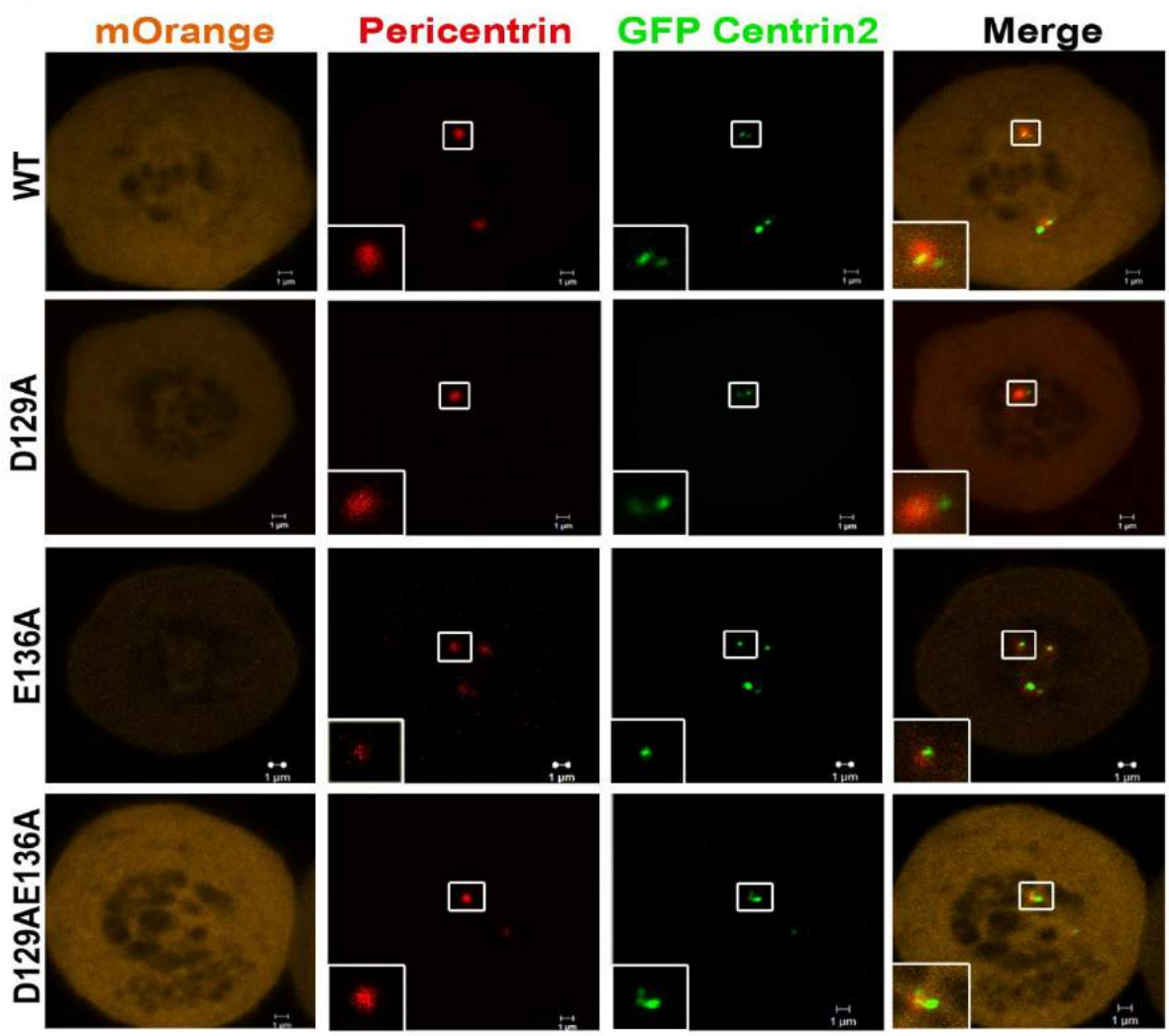

Fig. 4.33 Centriolar organization in cells expressing the different 14-3-3γ mutants. *HCT116 cells were transfected with the indicated 14-3-3γ constructs and GFP Centrin2, synchronized in mitosis with nocodazole, fixed and stained with antibodies to Pericentrin. Note that cells expressing the D129A mutant, with a single centrosome show the presence of two Centrin2 dots within the single Pericentrin dot. Original magnification 1000X with 2X optical zoom. Scale bar indicates 1 µm.*

4.1.11.7 Ultrastructure of the centrioles.

Further, we decided to determine the ultrastructure of the centrioles observed in the single centrosome. In order to do so, the mOrange tagged WT or mutant 14-3-3γ constructs were transfected into HCT116 cells followed by selection of transfected cells in puromycin. The puromycin resistant cells were synchronized in mitosis and imaged using electron microscopy. As shown in figure 4.34, cells expressing WT 14-3-3γ, E136A and D129AE136A showed the typical orthogonal arrangement of centrioles, while in cells expressing the D129A mutant cells the two centrioles were parallel to one another. This suggested that cells with a single centrosome did not have the typical orthogonal arrangement of centrioles, which is seen in mitotic cells.

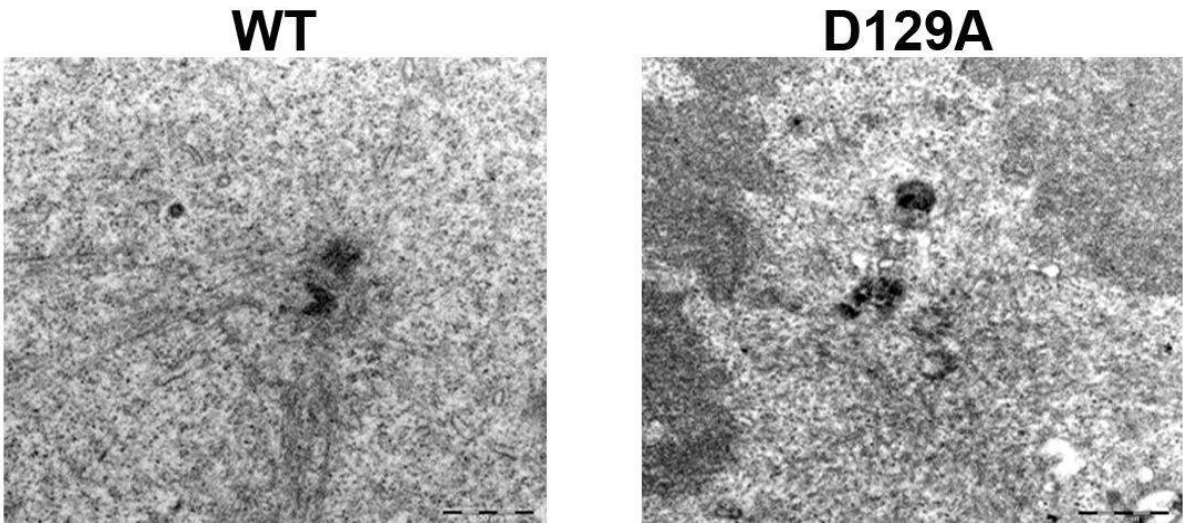

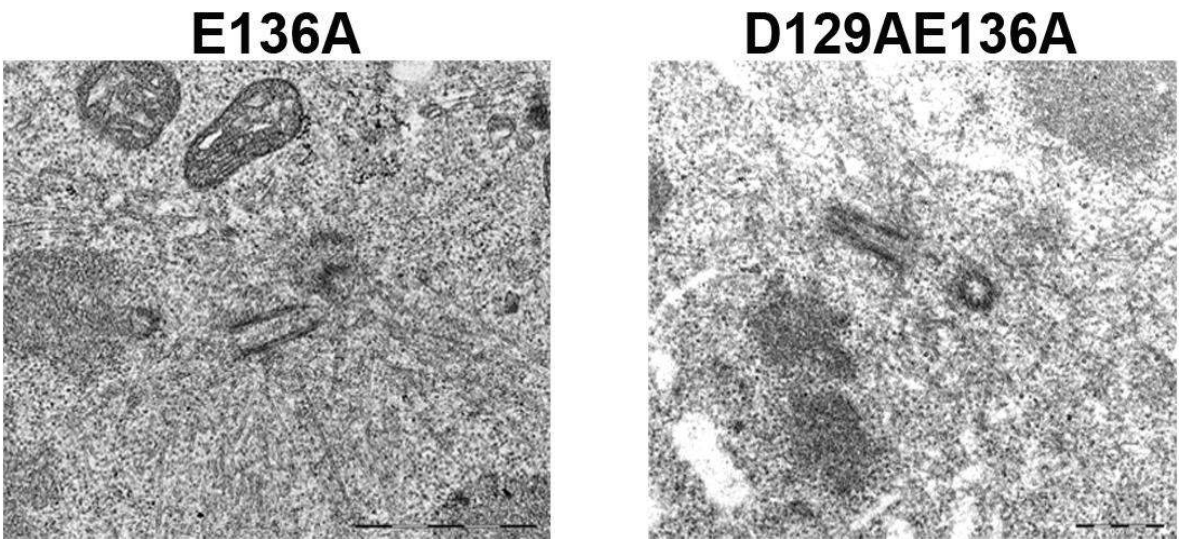

Fig. 4.34 Ultrastructure of the centrosomes*. HCT116 cells were transfected with the indicated constructs, synchronized in mitosis with nocodazole and fixed and stained with Osmium tetroxide and visualized using a transmission electron microscope. Representative images are shown. Magnification is 10000X and the bar indicates 500 nm, except in E136A, where the bar indicates 1000 nm.*

4.1.11.8 Cells with a single centrosome due to the expression of 14-3-3γ D129A have a defect in duplication

To test whether the two centrioles seen in the single centrosome observed upon expression of the D129A mutant had a defect in duplication or disjunction, we stained for Cep68, an inter-centrosomal linker protein (315,440). Disengagement is a licensing event for centriole duplication, which results in the establishment of a G1-G2 tether, which loosely connects the two centrioles that are ready to participate in procentriole biogenesis (330). Cep68 is a part of the G1-G2 tether and localises to the proximal end disengaged centrioles (315). Its degradation begins by the end of G2, when the centrosomes begin to separate (349,440). If centriolar disengagement had occurred, we would observe one Cep68 dot for each Centrin2

dot, in a 1:1 ratio. HCT116 cells were co-tranfected with each of the mOrange constructs and GFP Centrin2. 48 hours post transfection and synchronization in G2 with RO3306 (a CDK1 inhibitor), we fixed and stained the cells with antibodies against Cep68 and counterstained for DNA with DAPI (411,441). We observed that in cells expressing the WT, E136A and the D129AE136A mutant, that each contained 4 centrioles, there was a 2:1 ratio for Centrin2:Cep68 signal; 2 pairs of Centrin2 dots each with one Cep68 dot (fig. 4.36). In cells expressing the D129A mutant, with a single centrosome, there was a 1:1 ratio for Centrin2:Cep68 staining; each Centrin2 dot was associated with a Cep68 dot (fig. 4.35). This suggests that the two centrioles observed in the cells expressing the D129A mutant had undergone disengagement, but were unable to initiate duplication.

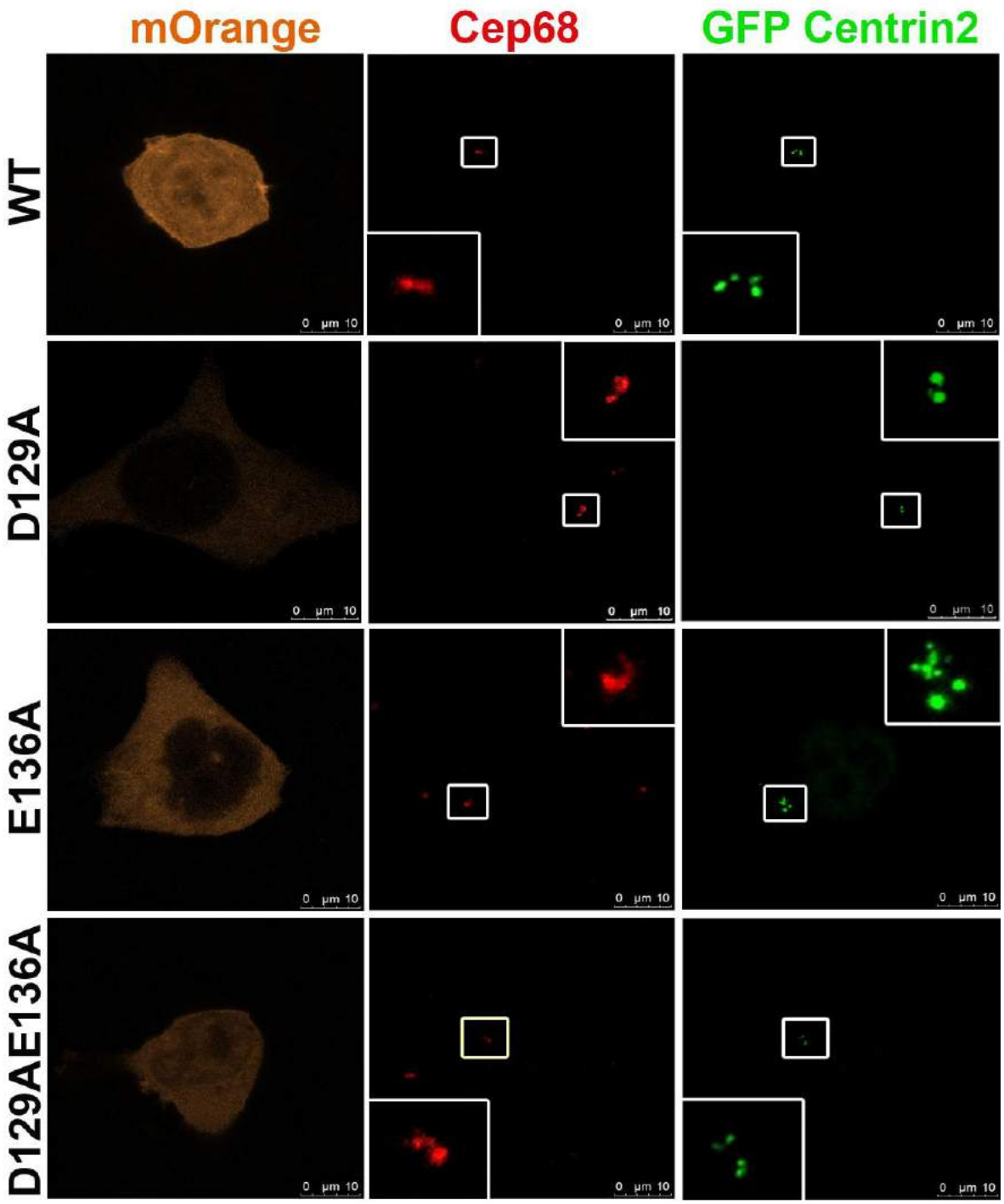

4.35. Organization of intercentriolar linker proteins in cells expressing the mutants. *HCT116 cells were transfected with the indicated 14-3-3γ constructs and GFP Centrin2, synchronized in G2 with a CDK1 inhibitor, fixed and stained with Cep68. Each single centrosome is associated two Cep68 dots suggesting that disengagement has occurred.*

Original magnification 630X with 4X optical zoom. Scale bar indicates 10 μm unless mentioned.

4.1.11.9 The two centrioles in cells expressing the D129A differ in age.

Newly formed centrioles in cycling cells need to undergo a maturation process for almost two cell cycles before they can be competent to function as microtubule-organizing centers and basal bodies. Hence, each cell contains three generations of centrioles, only one of which is able to form cilia. Ninein, a sub-distal appendage protein, is one such protein that is localized only on the grandmother centriole (313,442). We co-transfected HCT116 cells with each of the mOrange constructs and GFP Centrin2 and harvested the cells after synchronization in G2 (411,441). In cells expressing WT 14-3-3γ or the E136A and D129AE136A mutants, only one of the centriole pairs is associated with a Ninein dot (fig. 4.36)). The two Centrin2 dots seen in cells expressing the D129A mutant co-localized with a single Ninein dot. This suggests that this single centrosome consists of one mother and one daughter centriole, with the mother centriole having undergone at least two consecutive cycles (443). Given the results of the Cep68 and the Ninein staining, it means that the single centrosome observed in cells expressing the D129A mutant is a centrosome with disengaged centrioles that are unable to duplicate.

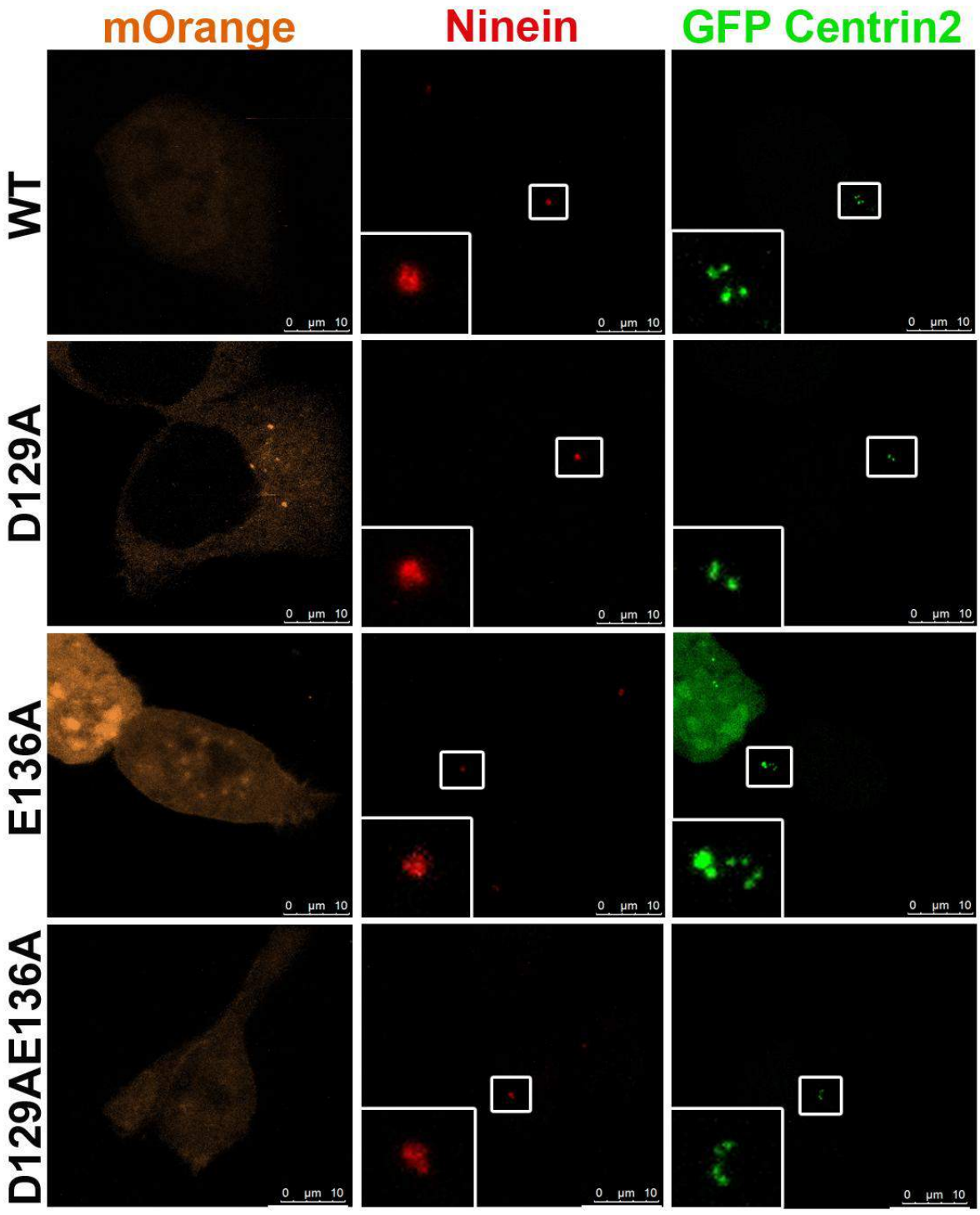

Fig. 4.36. Determination of centriolar age in cells expressing the mutants. *HCT116 cells were transfected with the indicated 14-3-3γ constructs and GFP Centrin2, synchronized in G2 with a CDK1 inhibitor, fixed and stained with Ninein. Only a single centrosome is associated a single Ninein dot indicating the presence of the grandmother centriole. Note that*

in case of cells expressing the D129A mutant, the two centrioles are associated with a single Ninein dot, indicating that the centrosome has undergone at least two rounds of duplication. Original magnification 630X with 4X optical zoom. Scale bar indicates 10 µm unless mentioned.

4.1.11.10 Organization of the spindle in cells expressing the 14-3-3γ mutants

Next, we wished to find out if the cells with a single centrosome are capable of organizing microtubules. In order to observe the structure of the spindle in cells expressing the 14-3-3γ mutants, we transfected HCT116 cells with the mOrange tagged 14-3-3γ constructs, synchronized them in mitosis and stained for α-tubulin and Pericentrin (fig. 4.37). In cells expressing the WT and D129AE136A construct, we could observe the presence of a bipolar spindle. We observed that in cells with single centrosomes, expressing the D129A construct, the organization of the spindle was flawed. The single centrosome was able to nucleate microtubules, but it was unable to form a bipolar or pseudo bipolar spindle. Also, cells transfected with the E136A construct, showed the presence of multiple centrosomes, with each centrosome functioning as an MTOC.

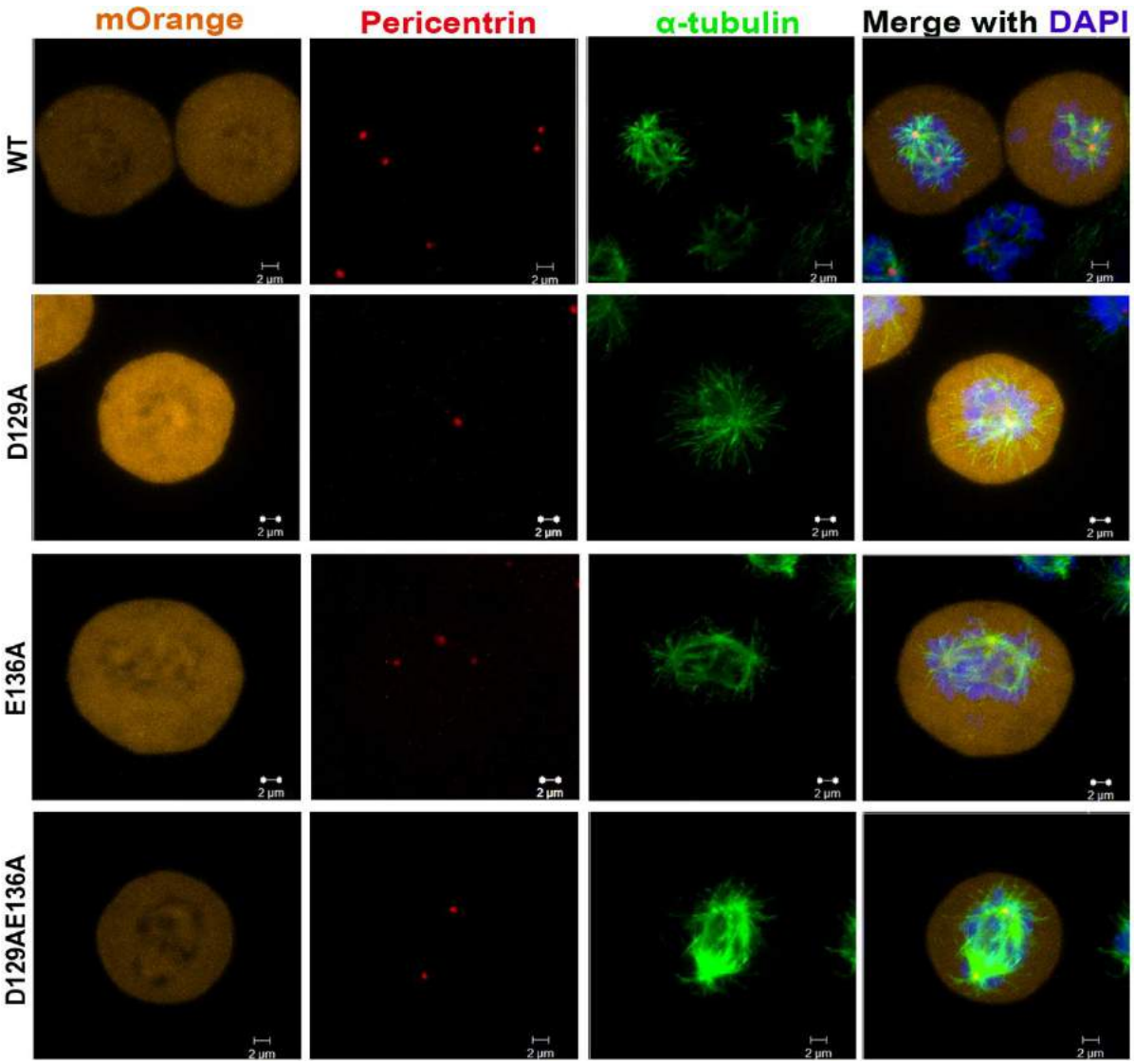

Fig. 4.37. Spindle organization in cells expressing the mutants. *HCT116 cells were transfected with the indicated 14-3-3γ constructs, synchronized in mitosis with nocodazole, fixed and stained with antibodies to Pericentrin and α-tubulin. Original magnification 630X with 4X optical zoom. Scale bar indicates 2 µm.*

4.1.11.11 Duration of mitosis in cells expressing the 14-3-3γ mutants

Cells with improperly organized centrioles have been demonstrated to undergo a prolonged mitosis, while transformed cells with multiple centrosomes have been shown to undergo centrosome clustering (444,445). Given that expression of mOrange tagged 14-3-3γ D129A led to the formation of a single centrosome in mitosis, with the lack of a bipolar spindle, we

decided to study if they completed mitosis by tracking these cells using live cell imaging,. In order to do so, we co-transfected HCT116 cells with each of the mOrange 14-3-3γ mutants and EGFP Centrin2. 48 hours post transfection, the cells were synchronized in mitosis with nocadozole, treated with ascorbic acid to reduce phototoxicity and imaged at 20 minute intervals. We observed that cells expressing the mOrange tagged 14-3-3γ WT construct, with 2 centrosomes, were able to complete mitosis in 40 minutes, on average (fig. 4.38 (a)). Cells transfected with the D129A construct, that had 2 centrosomes were also able to do the same. However, cells with single centrosomes did not complete mitosis even after 80 minutes (fig. 4.38 (b)). In fact, we were able to track only one cell expressing the D129A mutant with a single centrosome that completed mitosis and only the cell that inherited the original centrosome survived (fig. 4.38 (c)). Also, cells transfected with the E136A construct, which had multiple centrosomes, displayed a clustered centrosome phenotype and were able to complete mitosis in slightly more than 40 minutes (fig. 4.38 (d)).

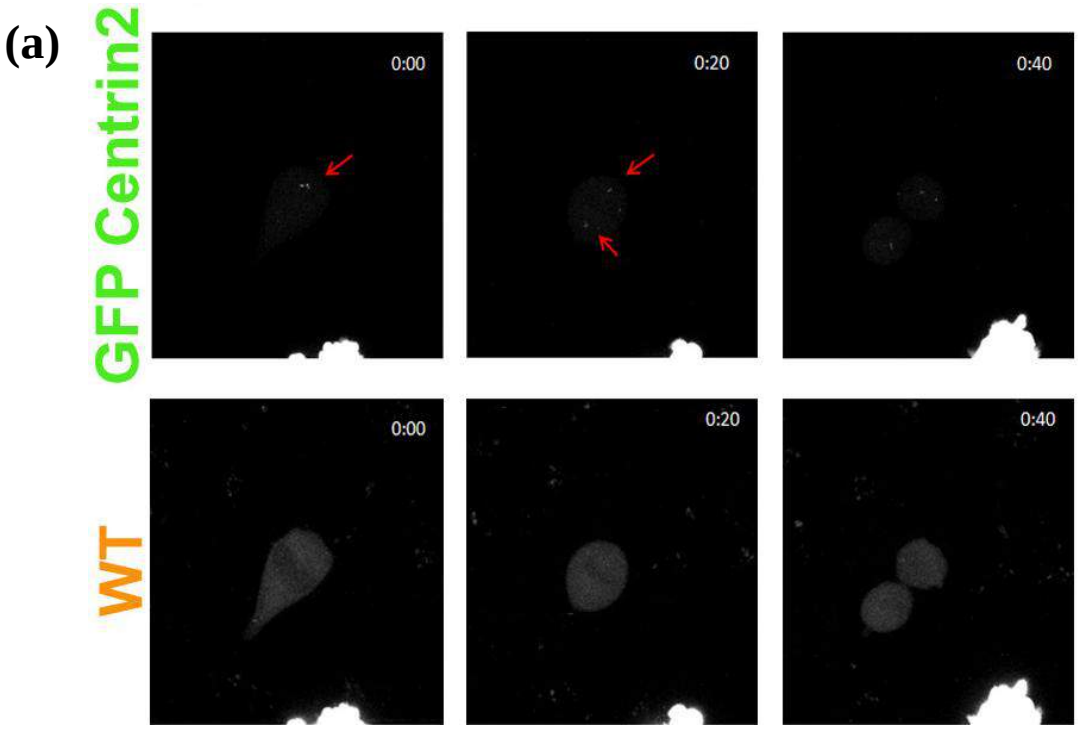

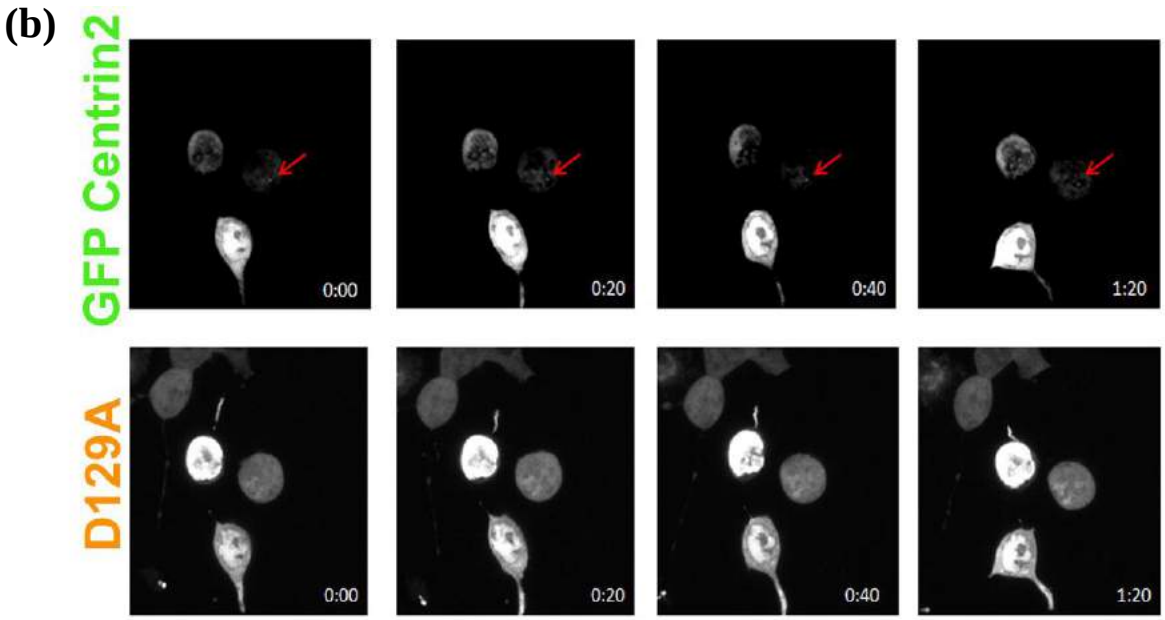
(b)
GFP Centrin2
D129A
0:00
0:20
0:40
1:20
0:00
0:20
0:40
1:20

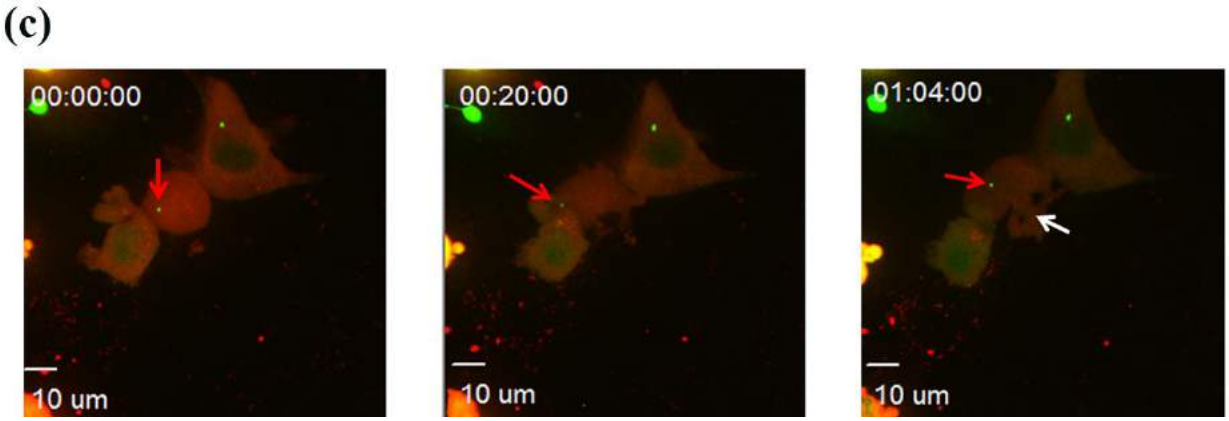
(c)
00:00:00
00:20:00
01:04:00
10 um
10 um
10 um

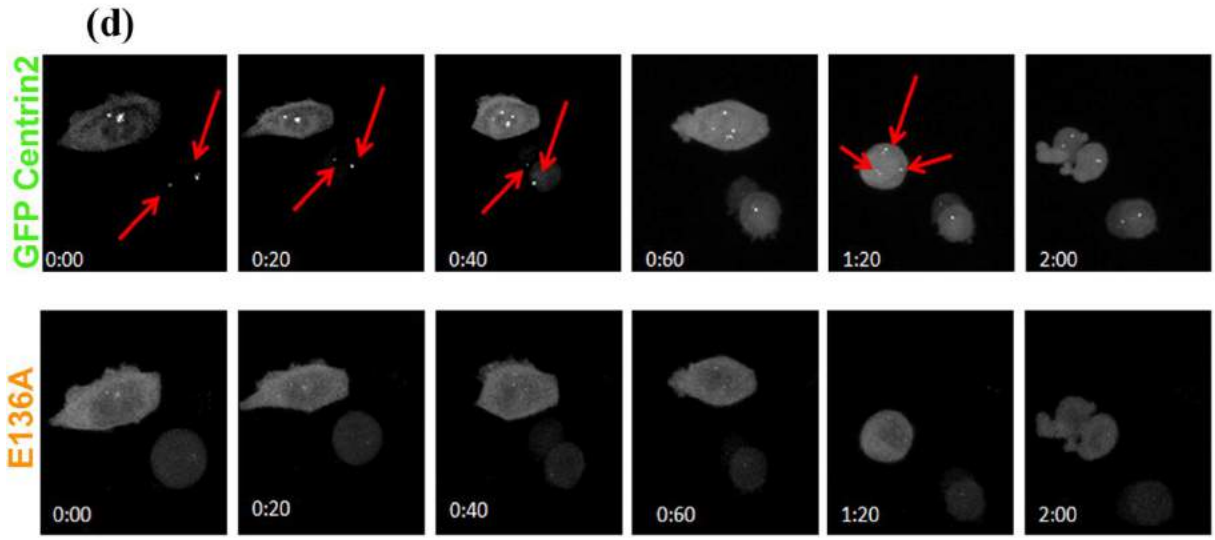
(d)
GFP Centrin2
E136A
0:00
0:20
0:40
0:60
1:20
2:00
0:00
0:20
0:40
0:60
1:20
2:00

Fig. 4.38. Duration of mitosis in cells expressing the mutants. *HCT116 cells transfected with the indicated constructs and GFP Centrin2 were synchronized in mitosis with nocodazole. After washing out the nocodazole the cells were imaged using live cell microscopy as described in materials and methods. Note that cells expressing D129A fail to complete cell division. Arrows indicate transfected cells. Original magnification 630X with 4X optical zoom. Scale bar indicates 1 µm unless mentioned.*

4.1.11.12 Localization of the 14-3-3 mutants in interphase

Previous reports indicate that a 14-3-3ε mutant that was defective for ligand binding accumulated in the nucleus (200). We wished to determine if we could infer anything about the difference in phenotypes seen upon expression of these 14-3-3γ mutants based on their localization. In order to determine if the centrosome phenotype was due to a difference in cellular localization of each of the mutants, we transfected each of the 14-3-3γ constructs into HCT116 cells and synchronized with mimosine. We harvested and fixed the cells at different stages of the cell cycle, to analyze if there was a difference in the cellular localization of the mutants as compared to the wild type, and if the difference is dependent on the stage of the cell cycle. We observed that as opposed to the 14-3-3γ WT, which had a pan cellular localization, each of the mutants; D129A, E136A and D129AE136A had a predominantly cytoplasmic localization during all stages of the cell cycle. Hence, we can conclude that the cellular localization of the mutants probably does not affect the centrosome cycle (fig. 4.39).

(a)

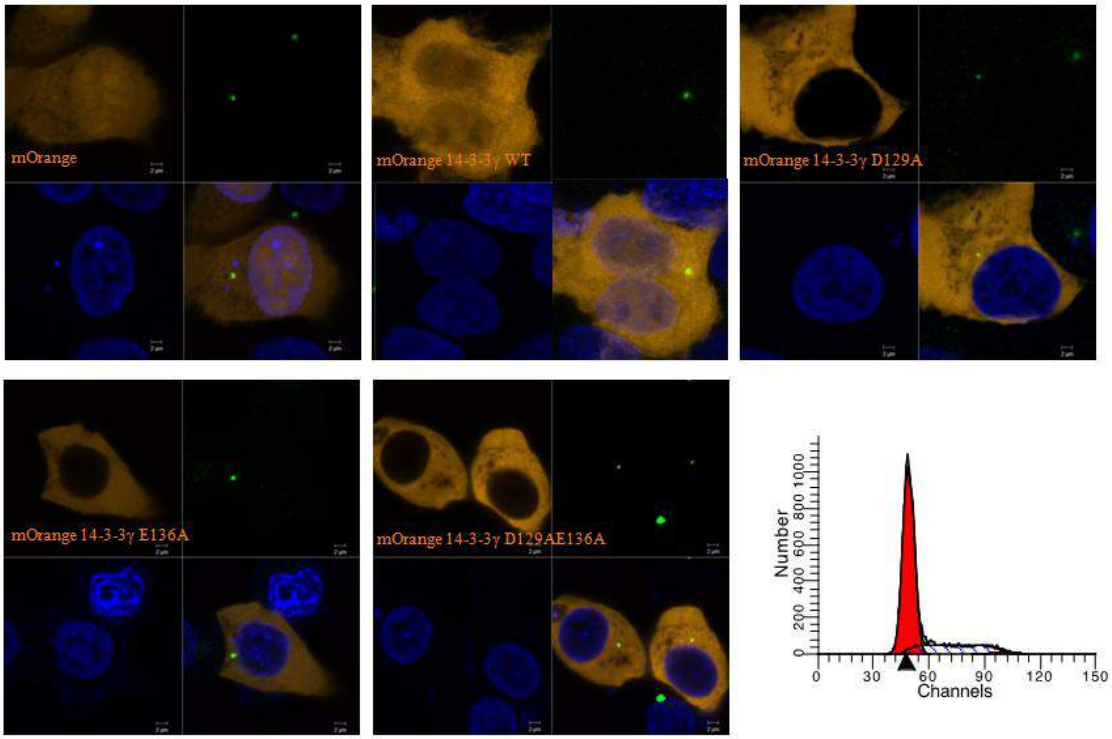
mOrange
mOrange 14-3-3γ WT
mOrange 14-3-3γ D129A
mOrange 14-3-3γ E136A
mOrange 14-3-3γ D129AE136A
Number
0 200 400 600 800 1000
0 30 60 90 120 150
Channels

(b)

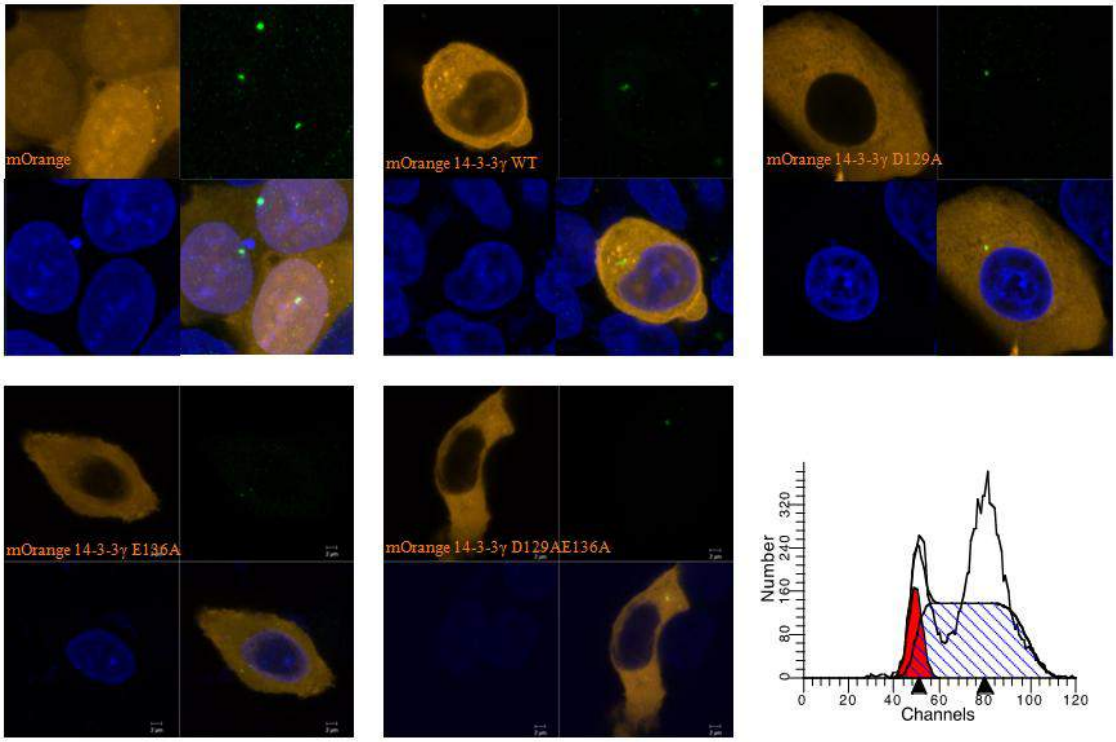
mOrange
mOrange 14-3-3γ WT
mOrange 14-3-3γ D129A
mOrange 14-3-3γ E136A
mOrange 14-3-3γ D129AE136A
Number
0 80 160 240 320
0 20 40 60 80 100 120
Channels

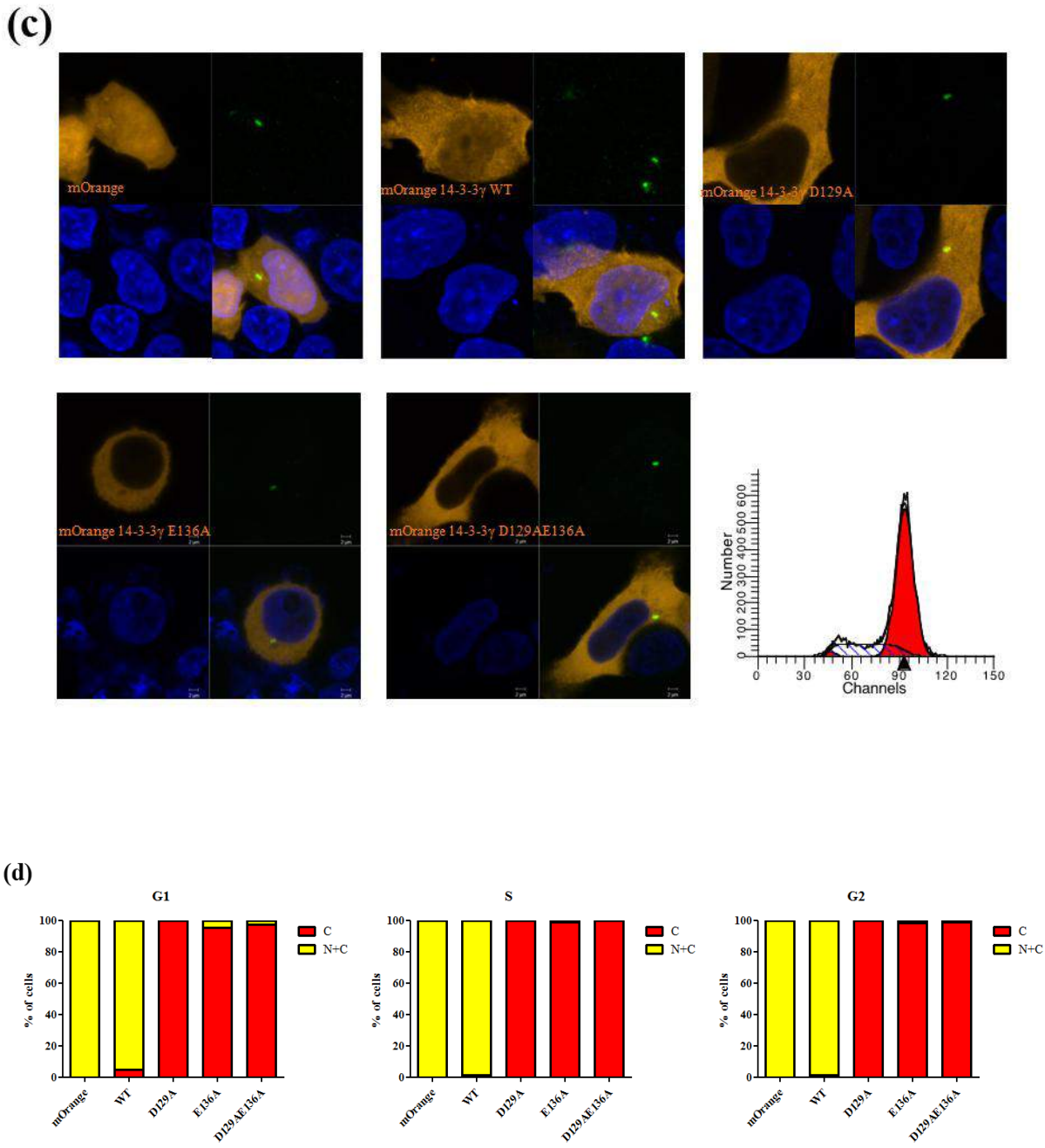

Fig. 4.39 Localization of the mutants in interphase. *HCT116 cells were synchronized in G1/S using mimosine. Cells were harvested at various time points post mimosine release, to obtain them at G1, S and G2. Cells were processed for cell cycle analysis and immunofluorescence. Cells were stained with antibodies against Pericentrin, as a centrosomal marker and costained with DAPI for DNA. Original magnification 630X with 4X*

optical zoom. Scale bar indicates 2 µm unless mentioned (a-c). Quantitation of the localisation of the mutants across cell cycle phases.

4.1.11.13 Overxpression of Plk4, CDK2 and CDK1 does not reverse the single centrosome phenotype

Based on the data obtained, we concluded that there is a centrosome duplication defect in cells with a single centrosome expressing the 14-3-3γ D129A mutant (they were unable to form procentrioles). In order to rescue the single centrosome defect, we overexpressed certain proteins that are extremely essential for procentriole formation. Overexpression of Plk4 increases centriole numbers and leads to de novo centrosome formation (402). Over-expression of either cdk1 or cdk1-AF resulted in an increase in centrosome over-duplication in HCT116 cells (326). Increased Cdk2 activity allowed the cells to accumulate multiple centrosomes (446).

Therefore, we co-transfected HCT116 cells with mOrange tagged 14-3-3γ constructs and the myc Plk4 construct and a myc vector control. 48 hours post transfection and synchronization in mitosis, we prepared lysates of the cells and loaded them on SDS-PAGE gels. Upon performing a Western blot, we were able to ascertain that the proteins were expressing correctly. In order to test the effect of overexpression of Plk4, we fixed the cells after synchronization and stained for the centrosome using antibodies against Pericentrin and counterstained for DNA using DAPI. We counted the number of centrosomes per cell in a 100 mitotic cells. We found that overexpression of Plk4 is able to induce the formation of multiple centrosomes in mitosis, as is expected. However, the overexpression was unable to decrease the number of cells with a single centrosome in cells expressing the mOrange 14-3-3γ D129A. This suggests that the single centrosome phenotype is not due to a defect in Plk4 function (fig. 4.40 (a)).

CDK2 and CDK1 are cell cycle regulated kinases that have been demonstrated to play a role in the centrosome cycle. CDK2 is said to link the cell cycle and the centrosome cycle by initiating both DNA replication and centrosome duplication (447,448). CDK1 overexpression has also been demonstrated to lead to centrosome overduplication (80,81,367). When we overexpressed CDK1 and CDK1 AF, or CDK2 and CDK2 AF in HCT116 cells, we were able to observe an increase in the percentage of cells with multiple centrosomes. However, there was no reduction in the percentage of cells with a single centrosome. Western blots prove that the proteins were all expressed correctly. These data suggest that the single centrosome phenotype is also not due to loss of CDK1 or CDK2 function (fig. 4.40).

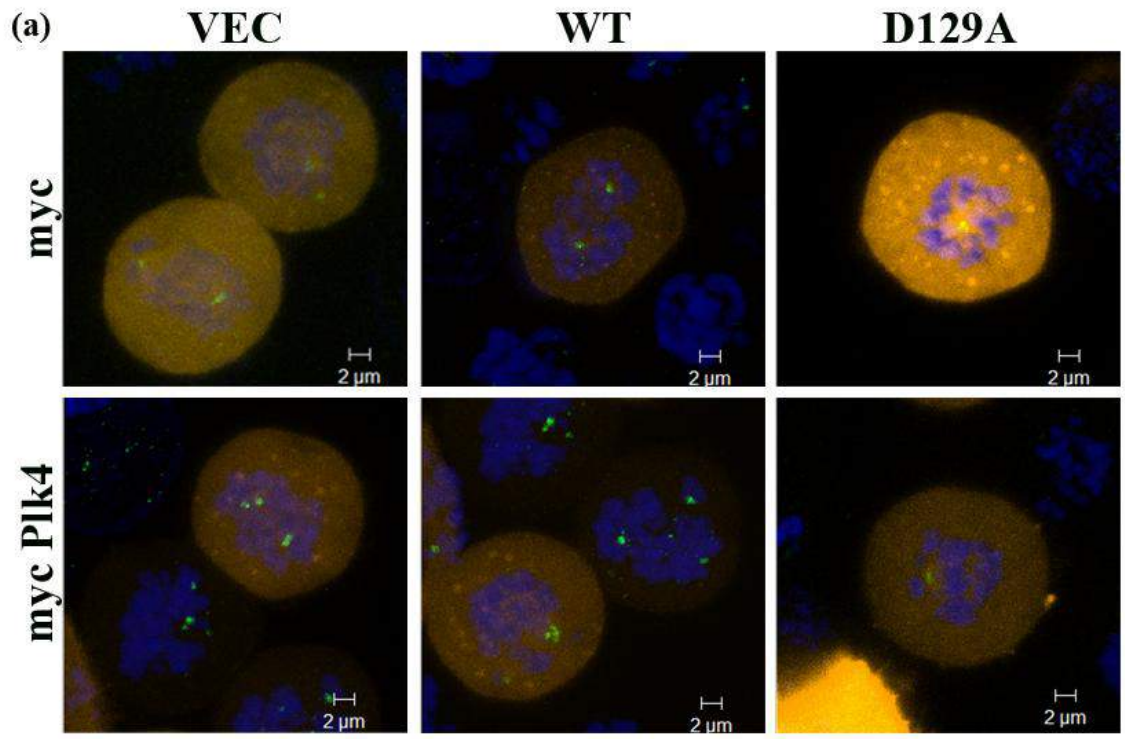

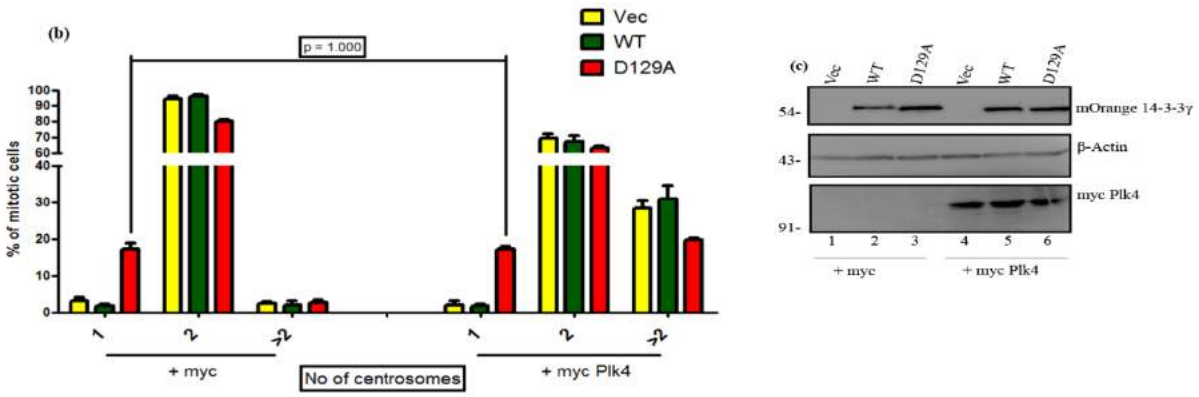
(b)
Vec
WT
D129A
p = 1.000
% of mitotic cells
+ myc
No of centrosomes
+ myc Plk4
(c)
Vec
WT
D129A
54-
43-
91-
mOrange 14-3-3γ
β-Actin
myc Plk4
+ myc
+ myc Plk4

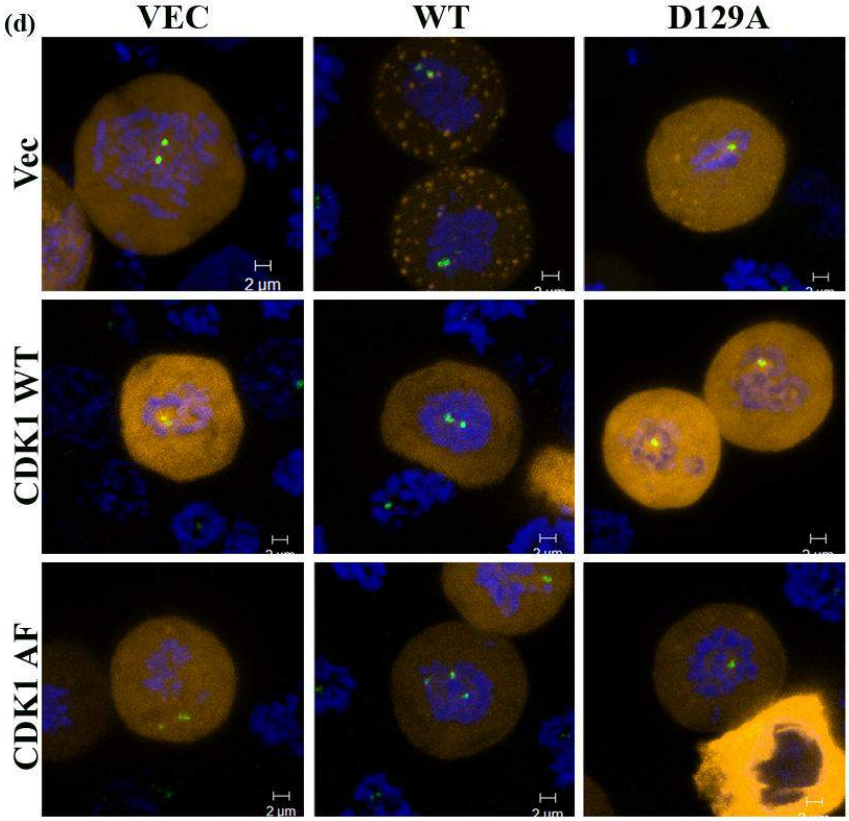
(d)
VEC
WT
D129A
Vec
CDK1 WT
CDK1 AF
2 µm

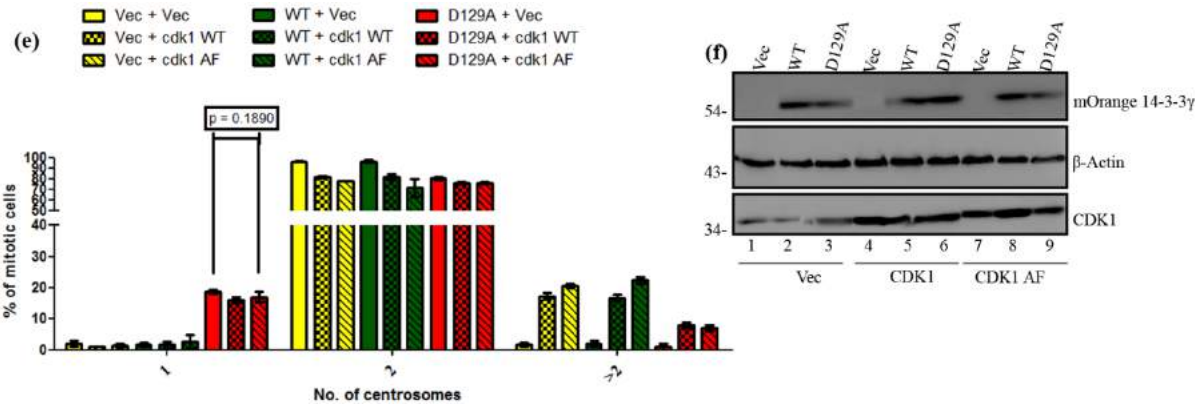
(e)
Vec + Vec
Vec + cdk1 WT
Vec + cdk1 AF
WT + Vec
WT + cdk1 WT
WT + cdk1 AF
D129A + Vec
D129A + cdk1 WT
D129A + cdk1 AF
p = 0.1890
% of mitotic cells
No. of centrosomes
(f)
54-
43-
34-
mOrange 14-3-3γ
β-Actin
CDK1
Vec
CDK1
CDK1 AF

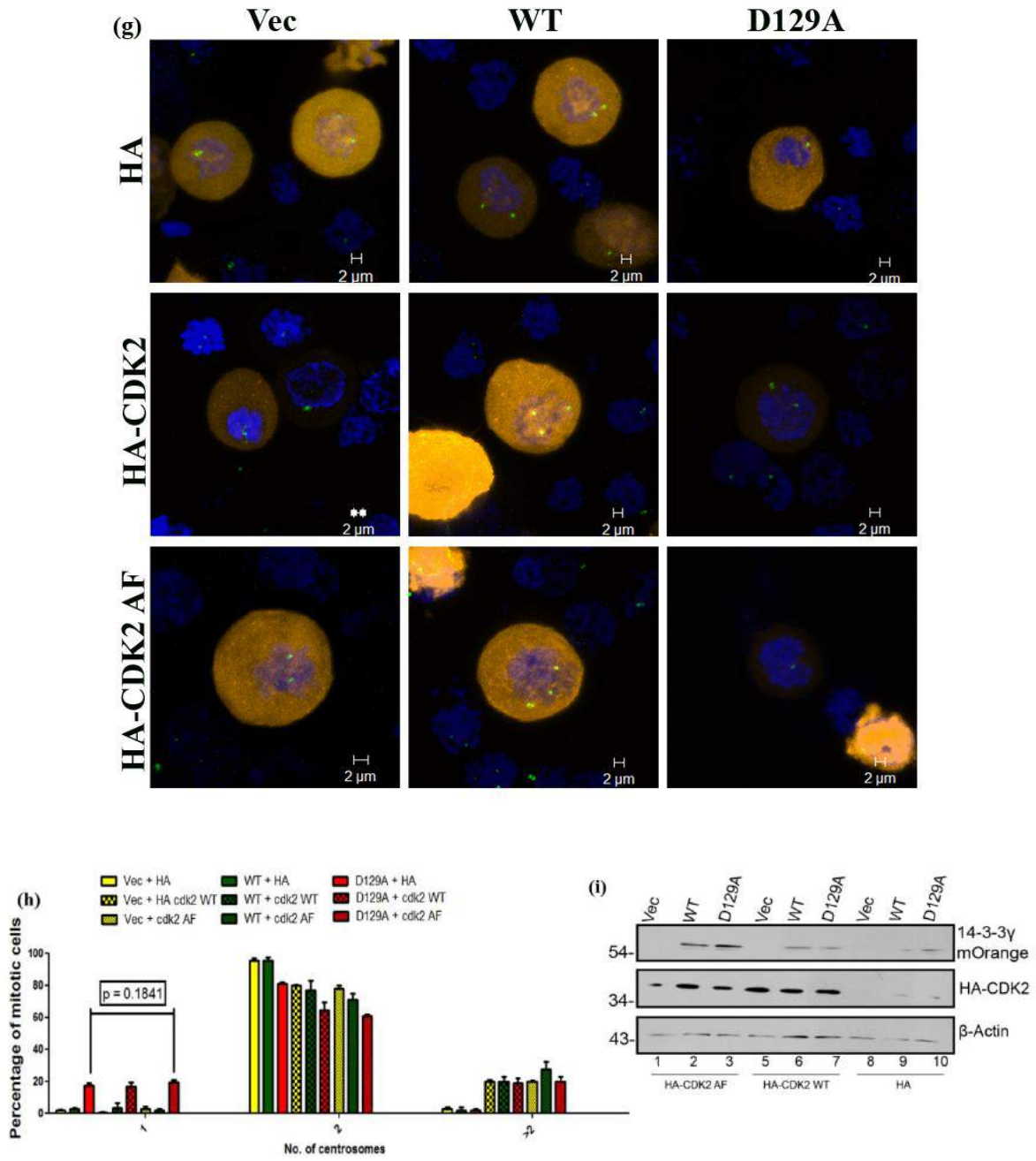

Fig. 4.40. Effect of overxpression of Plk4, CDK1 and CDK2 on the single centrosome phenotype. *HCT116 cells were transfected with the indicated 14-3-3γ and myc-tagged Plk4 (a-c), WT CDK1 or constitutively active CDK1 (CDK1AF) (d-f) and HA-tagged WT CDK2 or constitutively active CDK2 (CDK2AF) (g-i) and centrosome number determined as described. Note that none of these kinases can reverse the single centrosome phenotype, though they can all induce the production of supernumerary centrosomes. Original*

magnification 630X with 4X optical zoom (a and d). Original magnification 400X with 4X optical zoom (g). Scale bar indicates 2 µm unless mentioned.

4.1.11.14 Reversal of the centrosome phenotype by NPM1.

Nucleophosmin1 (NPM1) is a nucleolar protein that has roles in ribosome biogenesis, DNA replication, mitosis, centrosome duplication and chromatin remodeling (326,449-451). NPM1 is known to be a substrate of CDK2 and CDK6 (56,325,451). It has been demonstrated that phosphorylation of NPM1 at a Threonine 199 (T199) residue by CDK2 releases NPM1 from the centrosome (325). This acts as a licensing factor for centriole duplication and triggers centriole biogenesis. We have obtained mutants of NPM1; T199A (this mutant cannot be phosphorylated), T199D (this is a phosphomimetic mutant) (326) (fig. 4.41).

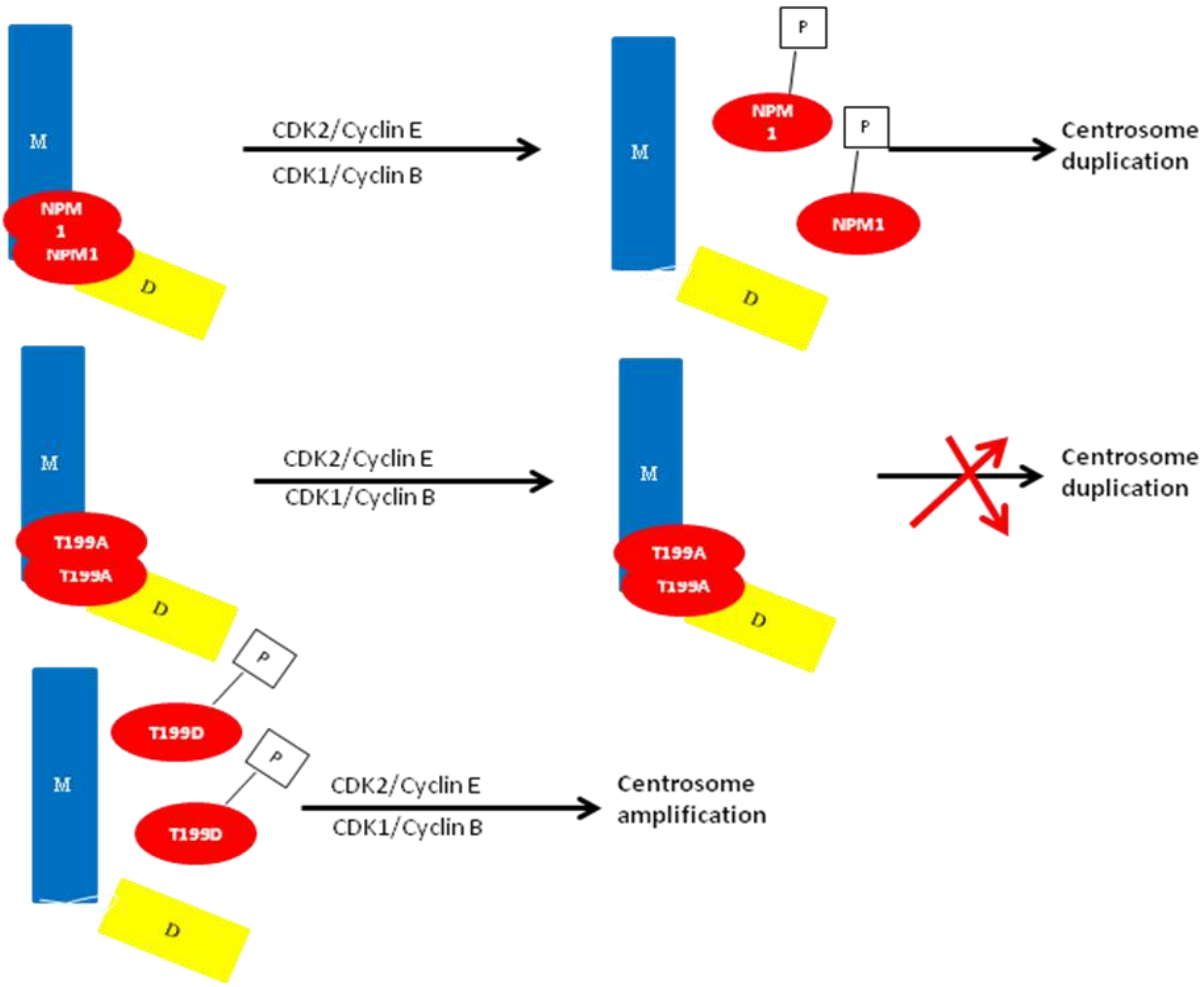

Fig. 4.41 Role of T199 mutants of NPM1 in the centrosome cycle. *Upon phosphorylation of NPM1 at the T199 residue, it dissociates from the centrosome and licenses centrosome duplication. Expression of a T199 mutant inhibits centrosome duplication, whereas the T199D mutant contributes to centrosome amplification.*

We co-transfected HCT116 cells with each of the mOrange tagged 14-3-3γ mutants and each of the NPM1 constructs. 24 hours post transfection, we added nocodazole to synchronize the cells in mitosis (fig. 4.42). 100 transfected, mitotic cells were counted. We observed that expression of the T199D mutant was able to completely rescue the single centrosome phenotype seen in cells expressing the D129A mutant. NPM1 wild type (WT) was also able to partially rescue the single centrosome phenotype. Conversely, expression of the T199A mutant was able to rescue the multiple centrosome phenotype in cells expressing the E136A construct.

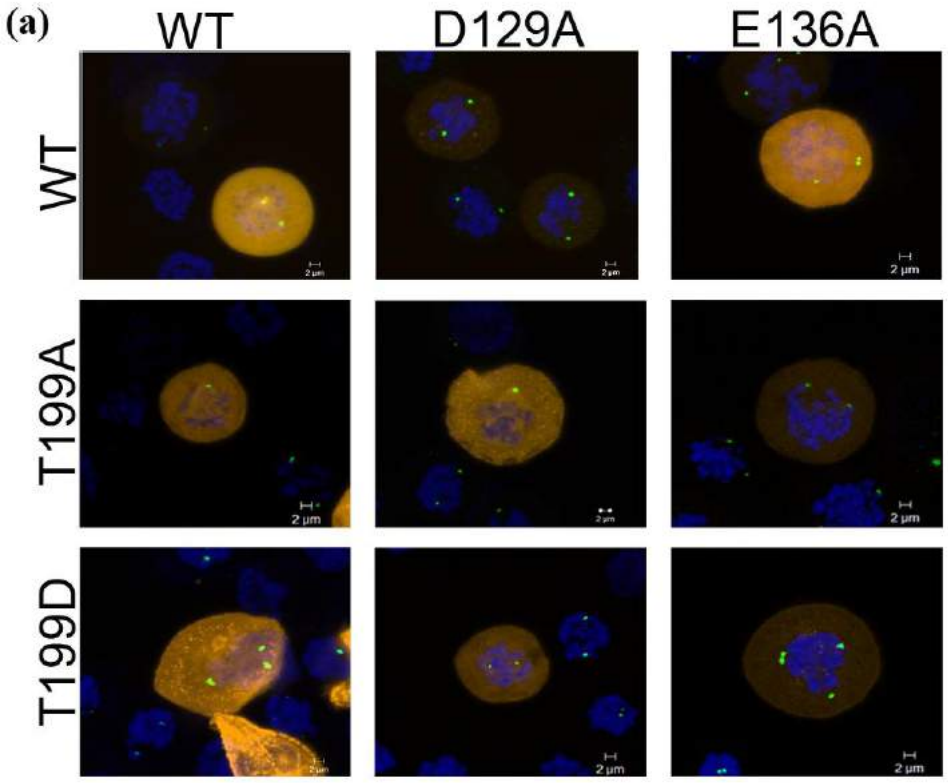

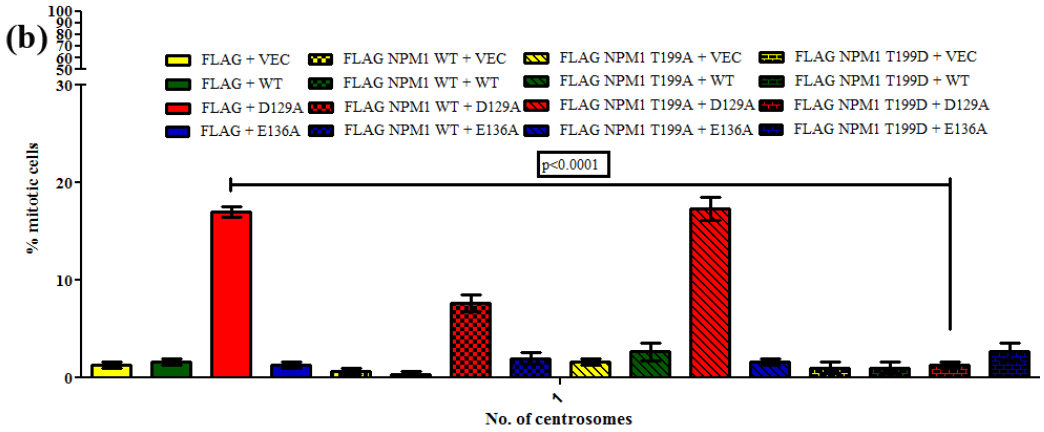
(b)
FLAG + VEC
FLAG + WT
FLAG + D129A
FLAG + E136A
FLAG NPM1 WT + VEC
FLAG NPM1 WT + WT
FLAG NPM1 WT + D129A
FLAG NPM1 WT + E136A
FLAG NPM1 T199A + VEC
FLAG NPM1 T199A + WT
FLAG NPM1 T199A + D129A
FLAG NPM1 T199A + E136A
FLAG NPM1 T199D + VEC
FLAG NPM1 T199D + WT
FLAG NPM1 T199D + D129A
FLAG NPM1 T199D + E136A
p<0.0001
% mitotic cells
No. of centrosomes

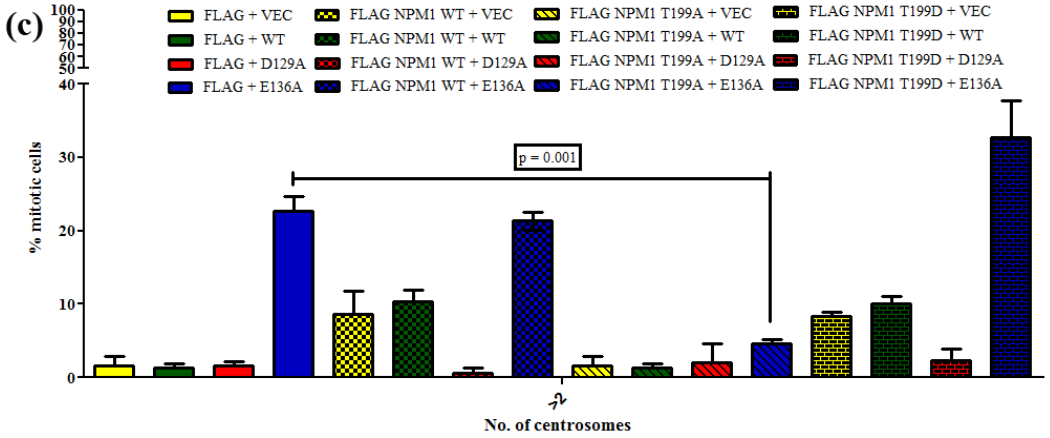
(c)
FLAG + VEC
FLAG + WT
FLAG + D129A
FLAG + E136A
FLAG NPM1 WT + VEC
FLAG NPM1 WT + WT
FLAG NPM1 WT + D129A
FLAG NPM1 WT + E136A
FLAG NPM1 T199A + VEC
FLAG NPM1 T199A + WT
FLAG NPM1 T199A + D129A
FLAG NPM1 T199A + E136A
FLAG NPM1 T199D + VEC
FLAG NPM1 T199D + WT
FLAG NPM1 T199D + D129A
FLAG NPM1 T199D + E136A
p = 0.001
% mitotic cells
No. of centrosomes

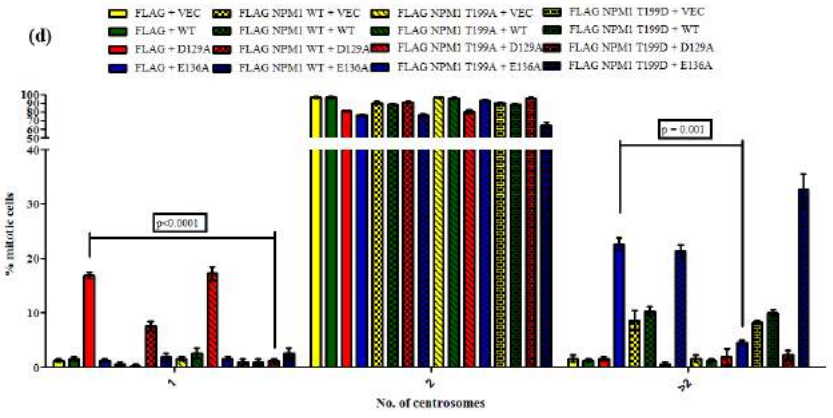
(d)
p<0.0001
p = 0.001
% mitotic cells
No. of centrosomes

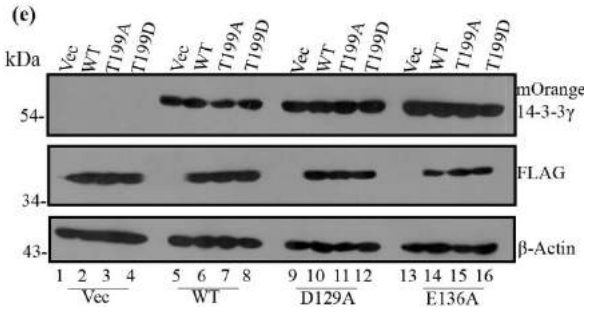
(e)
kDa
Vec
WT
T199A
T199D
54-
34-
43-
mOrange
14-3-3γ
FLAG
β-Actin
1 2 3 4
5 6 7 8
9 10 11 12
13 14 15 16
Vec
WT
D129A
E136A

Fig. 4.42 Reversal of the centrosome phenotype by NPM1. *HCT116 cells were transfected with the indicated 14-3-3γ and NPM1 constructs. Post-transfection the cells were arrested in mitosis and stained with antibodies to Pericentrin and counter-stained with DAPI and centrosome number was determined in mitotic cells. In all the experiments the mean and standard error from at least three independent experiments were plotted, error bars denote standard error of mean and p-values are obtained using Student's t test. Molecular weight markers in kDa are indicated. (a) Representative images from each transfection. Original magnification 630X with 4X optical zoom, (b) Quantitation of % of mitotic cells with a single centrosome, (c) Quantitation of % of cells with multiple centrosomes, (d) Total quantitation and (e) Western blot analysis demonstrates that all proteins are present at equivalent levels.*

4.1.11.15 The reversal of the D129A phenotype is specific to expression of T199D.

NPM1 has been demonstrated to function as a decamer (418). Defects in the oligomerization ability of NPM1 have been shown to affect its function (418). NPM1 is phosphorylated by Aurora B during at a Serine 125 residue during mitosis (449). The overexpression of a mutant, NPM1 S125A results in the centrosome amplification and mitotic defects possibly due to cytokinesis failure (449). We wanted to know if expression of S125 mutants of NPM1 can also affect the single centrosome phenotype. Further, we tested if the oligomerization status of NPM1 can modulate centrosome number. We co-transfected an NPM1 oligomerization defective mutant (L18Q) with mOrange, 14-3-3γ WT and 14-3-3γ D129A (personal communication, Dr. Tapas Kundu). We observed the rescue of the single centrosome phenotype was only possible upon co-expression of the T199D mutant (fig. 4.43).

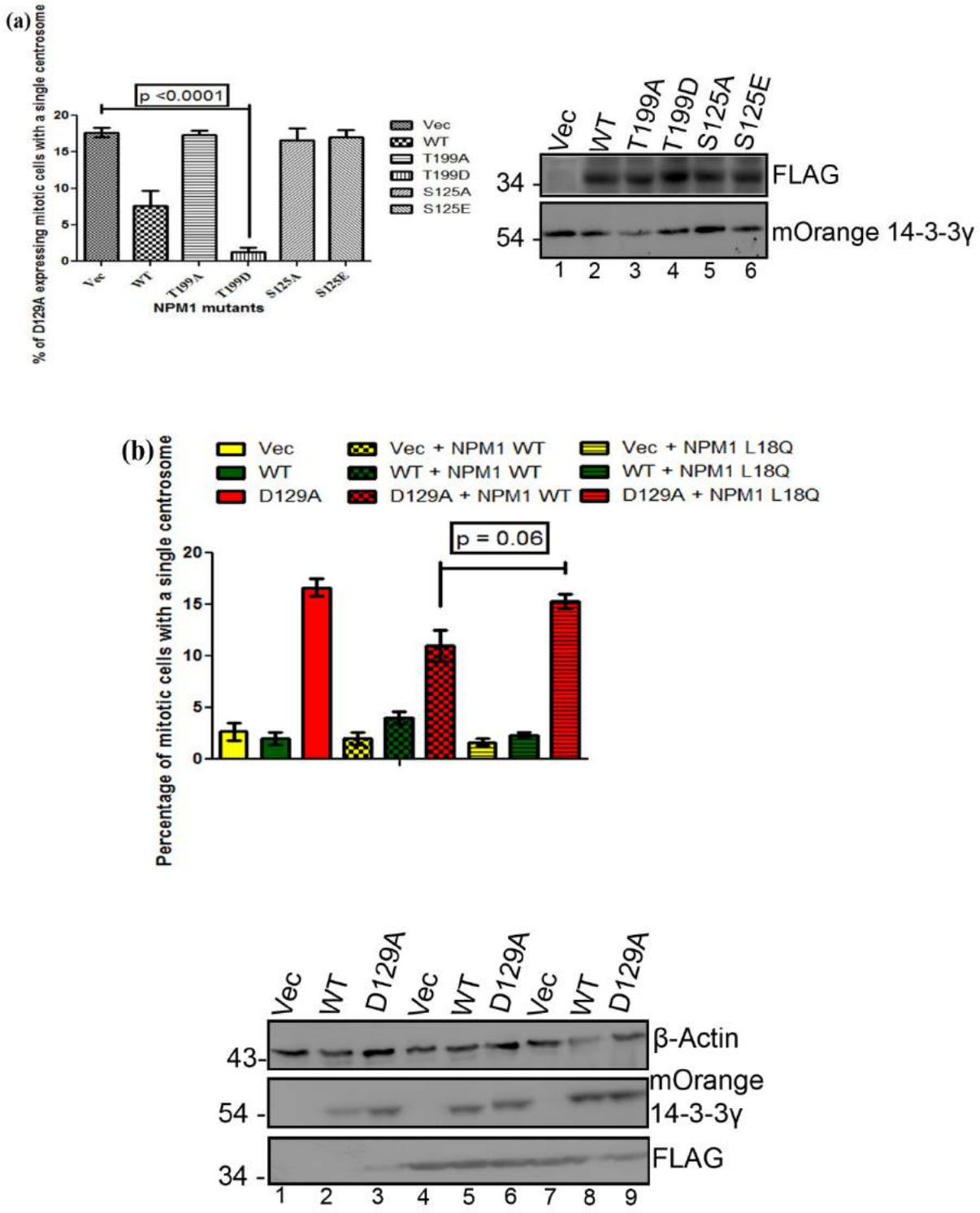

Fig. 4.43 Reversal of the single centrosome phenotype is specific to the T199D mutant of NPM1. *HCT116 cells were transfected with the indicated 14-3-3γ and NPM1 constructs. Post-transfection the cells were arrested in mitosis and stained with antibodies to Pericentrin and counter-stained with DAPI and centrosome number was determined in mitotic cells. In*

all the experiments the mean and standard error from at least three independent experiments were plotted, error bars denote standard error of mean and p-values are obtained using Student's t test. Molecular weight markers in kDa are indicated. Western blot analysis demonstrates that all proteins are present at equivalent levels.

4.1.11.16 Interaction of NPM1 and 14-3-3γ

Given that the overexpression of an NPM1 phosphomimetic mutant is able to rescue the single centrosome phenotype in cells expressing the 14-3-3γ D129A construct, we decided to test for an interaction between 14-3-3γ and NPM1. We performed a GST pulldown assay using GST and GST tagged 14-3-3γ WT. Upon performing a western blot for NPM1, we found that NPM1 interacts with GST 14-3-3γ WT (fig. 4.44).

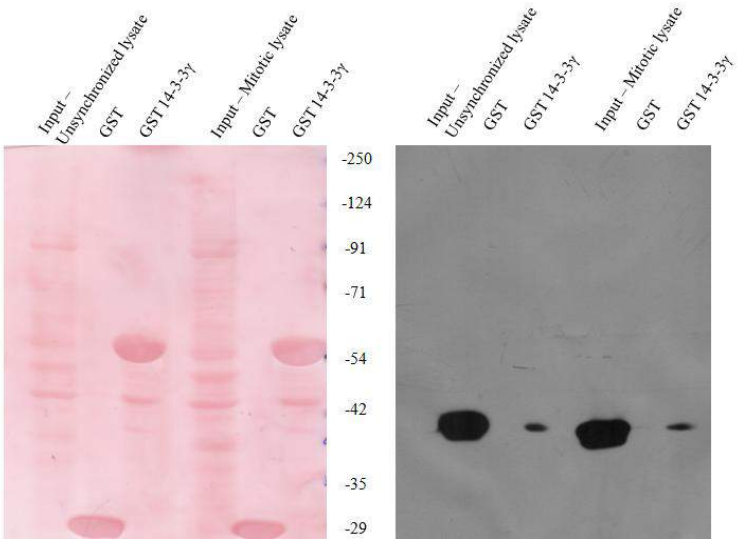

Fig. 4.44 Interaction of GST-14-3-3γ with NPM1. *Unsynchronized and mitotic EBC extracts of HCT116 cells were incubated with the various GST fusion proteins. The complexes were resolved on a 10% SDS-PAGE gel and western blots performed with antibodies against NPM1. The position of molecular weight markers in kDa is indicated. The left panel indicates a Ponceau staining of the memebrane and on the right is the Western blot.*

Further, we wanted to test if all the mutants of 14-3-3γ were able to interact with NPM1. To this end, we cloned the 14-3-3γ mutants into HA pcDNA3 and performed a co-immunoprecipitation. We found that the D129A mutant bound to more of NPM1 as compared to the WT protein while the E136A mutant did not bind to NPM1 at all. The D129AE136A mutant bound to NPM1 with a lower affinity as compared to WT. This suggests that the different mutants of 14-3-3γ bind to NPM1 differentially (fig. 4.45). Further, we used Centrin2 as a positive control for binding to 14-3-3γ (452). We have demonstrated that the binding of Centrin2 to 14-3-3γ is phospho-independent. Here, we observe that all the mutants bind to Centrin2 with the same efficiency (fig. 4.45). This suggests that the binding of NPM1 with 14-3-3γ might be phospho-dependent.

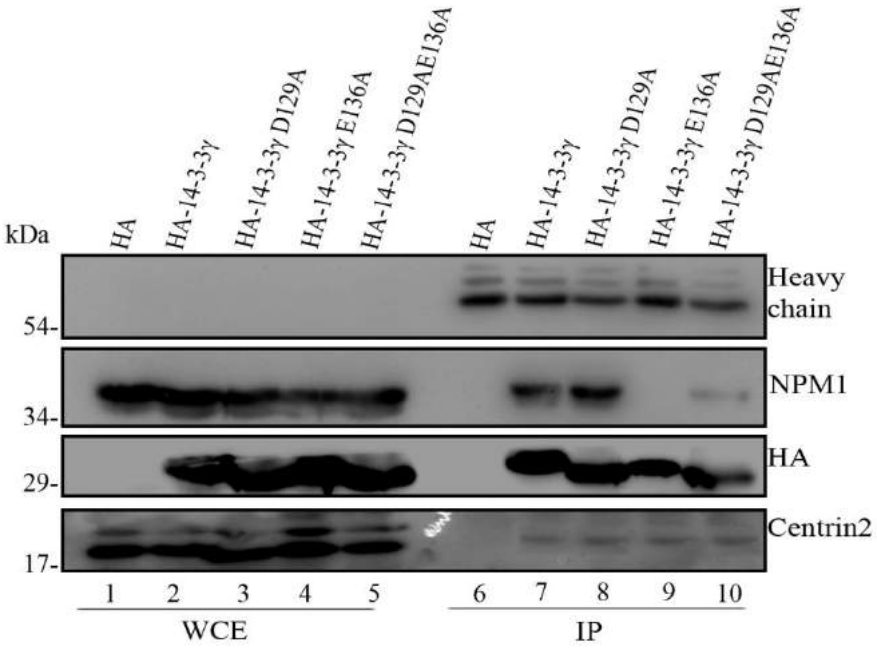

Fig. 4.45 The 14-3-3γ mutants interact differentially with NPM1. *HCT116 cells transfected with the indicated HA tagged constructs were lysed in EBC lysis buffer and subjected to immunoprecipitation with antibodies against the HA epitope. The reactions were resolved on SDS-PAGE gels followed by western blotting with the indicated antibodies. Note that while 14-3-3γ WT forms a complex with NPM1, E136A fails to form a complex with NPM1. D129A*

shows increased complex formation with NPM1 while D129A-E136A forms a complex with NPM1 at reduced efficiency.

4.1.11.17 Mapping the binding site of 14-3-3 on NPM1

In order to map the 14-3-3γ binding site on NPM1, we performed a motif scan to identify putative 14-3-3 binding sites on NPM1 using a web-based prediction tool (403). We found three possible 14-3-3 binding sites; S48, S143 and S293. We performed site directed mutagenesis to convert each of the Serine residues to Alanine so that they can no longer be phosphorylated. Upon testing their binding to 14-3-3γ using a GST pulldown assay, we determined that only the S48A mutant was unable to bind to 14-3-3γ. This suggests that 14-3-3γ binds to NPM1 in a phosphorylation dependent manner via the Ser48 residue (fig. 4.46).

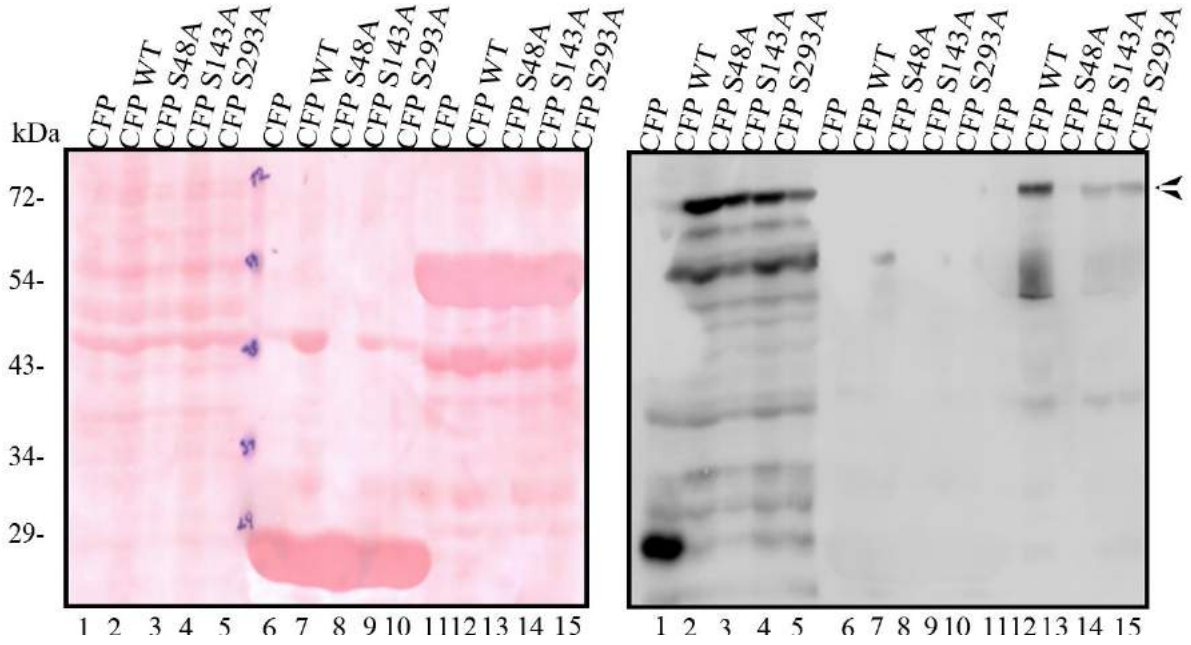

Fig. 4.46 Mapping the 14-3-3 binding site of NPM1. *HCT116 cells were transfected with the indicated NPM1 constructs. 48 hours post-transfection, protein extracts prepared from these cells were incubated with recombinant GST or GST-14-3-3γ immobilized on glutathione-Sepharose beads. The reactions were resolved on SDS-PAGE gels followed by Western*

blotting with GFP antibody. The panel on the left shows the Ponceau-S stain of the same membrane. Lanes 1-5 indicate the WCE, lanes 6-10 indicate pulldown with GST and lanes 11-15 indicate pulldown with GST 14-3-3γ.

Previous results suggest that phosphorylation of NPM1 at S48 by Akt leads to an inhibition of the ability of NPM1 to form oligomers and that a phospho-mimetic mutant (S48E) is unable to form oligomers *in vitro* (418,453). We wished to determine if an S48E mutant of NPM1 could form a complex with 14-3-3γ. Therefore, constructs expressing CFP fusions of WT, S48A, and S48E NPM1 were transfected into HCT116 cells followed by GST pulldown assays as described above. WT and S48E NPM1 formed a complex with GST-14-3-3γ but not GST alone, in contrast to S48A, which failed to form a complex with GST-14-3-3γ (fig. 4.47).

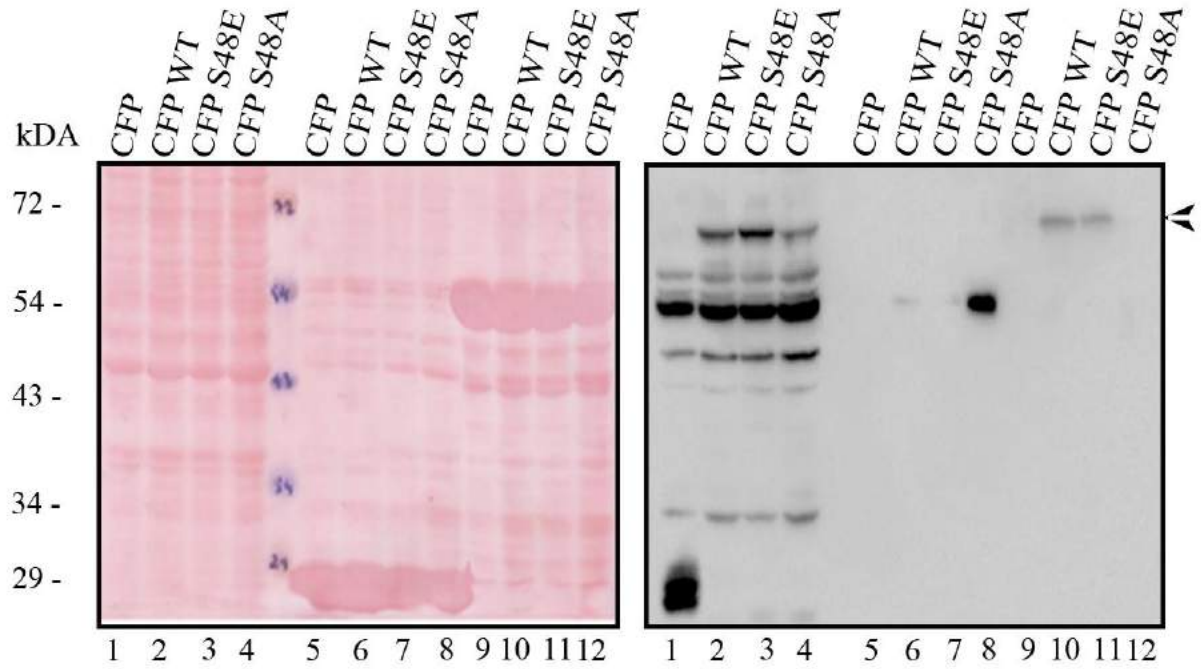

Fig. 4.47 Interaction of the S48 mutants with 14-3-3γ. *HCT116 cells were transfected with the indicated NPM1 constructs. 48 hours post-transfection, protein extracts prepared from these cells were incubated with recombinant GST or GST-14-3-3γ immobilized on glutathione-Sepharose beads. The reactions were resolved on SDS-PAGE gels followed by*

Western blotting with GFP antibody. The panel on the left shows the Ponceau-S stain of the same membrane. Lanes 1-4 indicate the WCE, lanes 5-8 indicate pulldown with GST and lanes 9-12 indicate pulldown with GST 14-3-3γ. S48A fails to form a complex with 14-3-3γ, while S48E forms a complex with 14-3-3γ.

4.1.11.18 Localisation of the S48 mutants of NPM1

NPM1 is a nucleolar protein and its localisation is phosphorylation dependent, as it has been demonstrated that the S48E mutant of NPM1 has a nuclear localisation (453). In order to confirm the same, we transfected HCT116 cells with CFP, CFP-NPM1 WT and S48 mutants. 48 hours post transfection, we fixed and stained the cells with antibodies against pericentrin and counterstained for DNA using DAPI. We observed that as shown previously, the NPM1 WT and S48A mutants displayed a nucleolar localization, whereas the S48E mutant had a nuclear localization. We were unable to observe any NPM1 at the centrosome for any of the constructs (fig. 4.48).

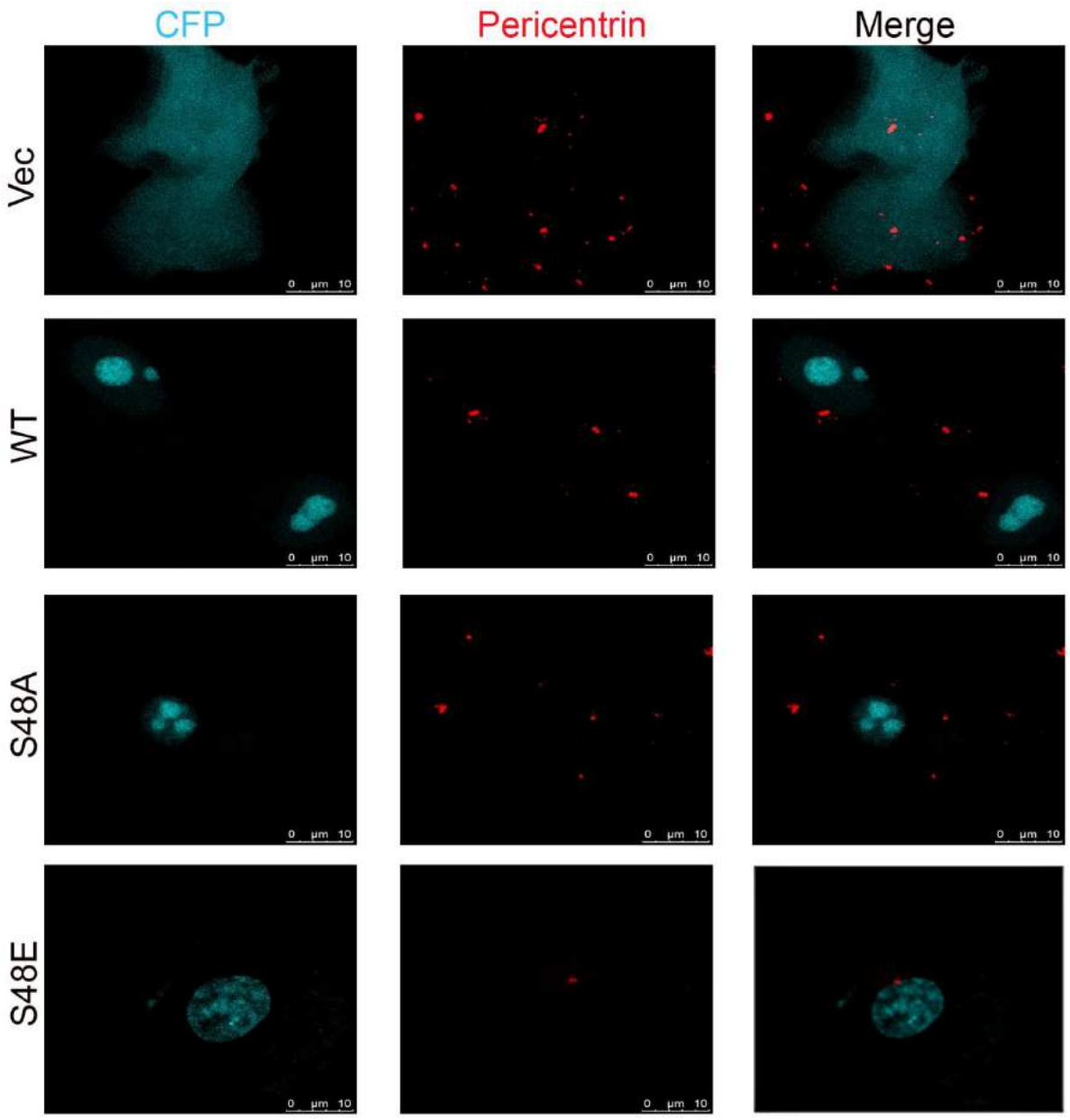

Fig. 4.48 *The indicated CFP-tagged NPM1 constructs were transfected into HCT116 cells and imaged using confocal microscopy. Note that none of the proteins expressed from the constructs localized to the centrosome. Original magnification 630X with 4X optical zoom. Scale bar indicates 10 µm unless mentioned.*

4.1.11.19 Effect of S48 mutants of NPM1 on centrosome number

We have shown that the 14-3-3γ mutants bind to NPM1 differentially and that binding occurs via a phosphorylated S48 residue. We wished to determine if 14-3-3γ binding mutants of NPM1 had any effect on the observed centrosome phenotype. We co-transfected HCT116 cells with each of the NPM1 S48 mutants and each of the 14-3-3γ mutants. Upon counting centrosome number in a 100 transfected mitotic cells 48 hours post transfection, we found that the S48A is able to rescue the single centrosome phenotype seen after expression of D129A (fig. 4.50).. However, we did not observe the presence of multiple centrosomes upon its expression. The S48E mutant reverses the multiple centrosome phenotype observed upon expression of E136A (fig. 4.49). This suggests that the centrosome phenotypes observed upon expression of the 14-3-3γ mutants occur due to their differential binding to NPM1. The phenotype can be reversed by co-expression of 14-3-3γ binding mutants of NPM1.

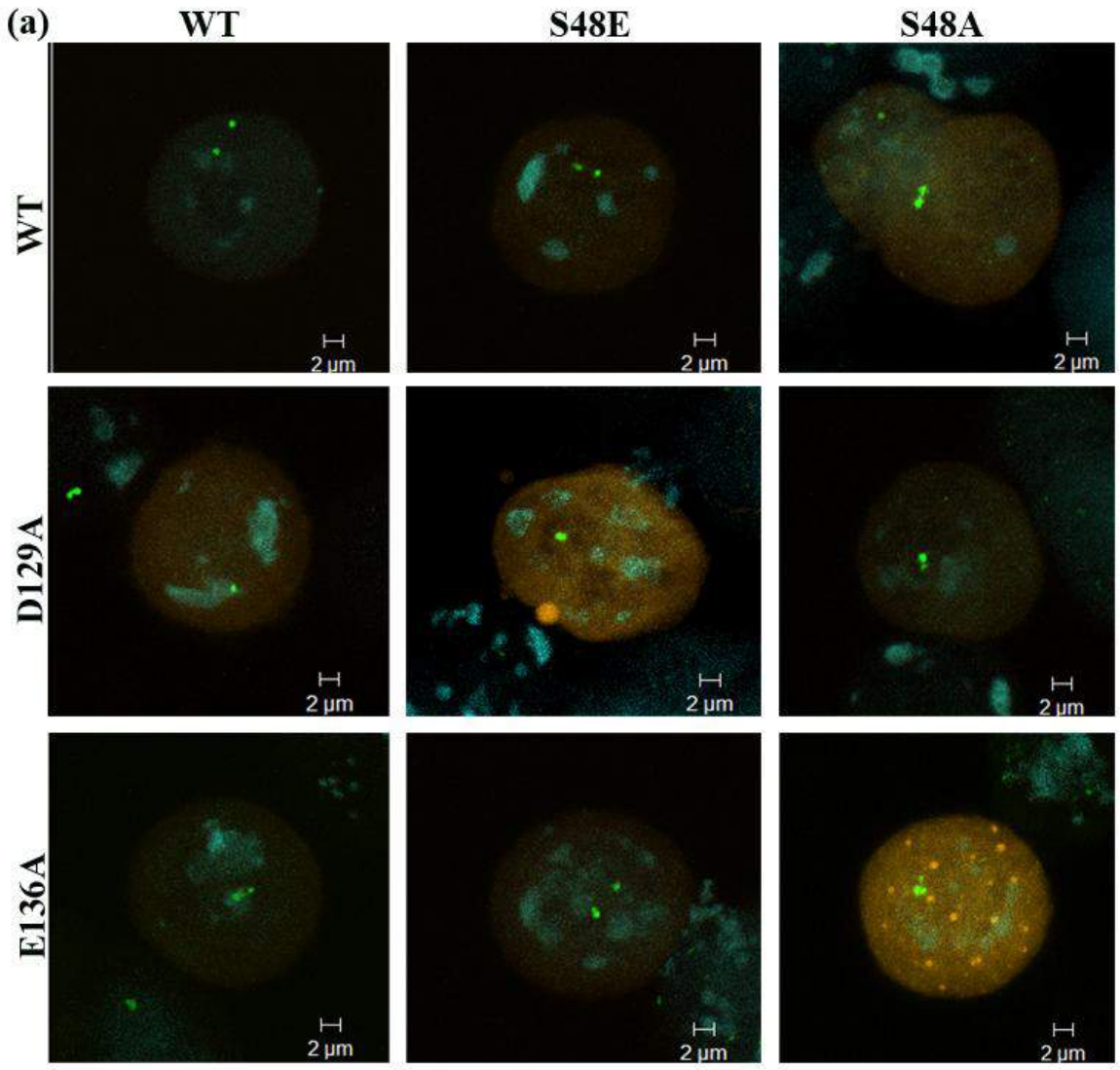
(a)
WT
S48E
S48A
WT
D129A
E136A
2 µm

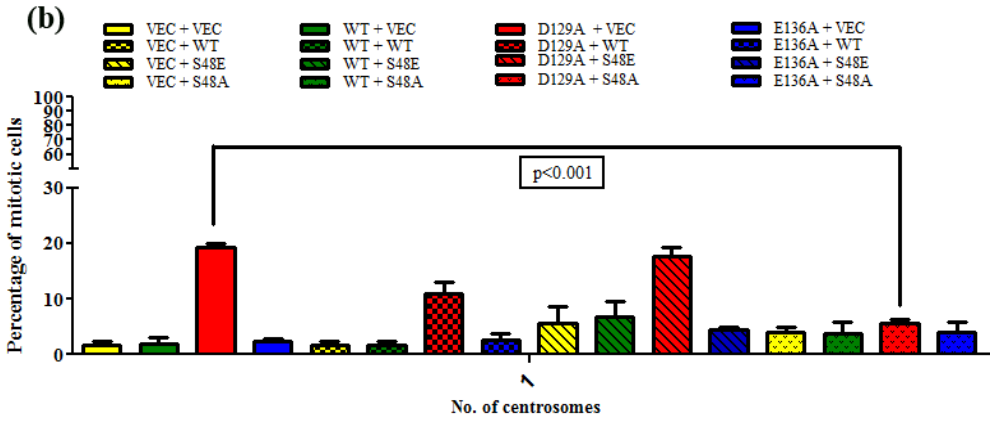
(b)
VEC + VEC
VEC + WT
VEC + S48E
VEC + S48A
WT + VEC
WT + WT
WT + S48E
WT + S48A
D129A + VEC
D129A + WT
D129A + S48E
D129A + S48A
E136A + VEC
E136A + WT
E136A + S48E
E136A + S48A
Percentage of mitotic cells
100
90
80
70
60
30
20
10
0
p<0.001
No. of centrosomes

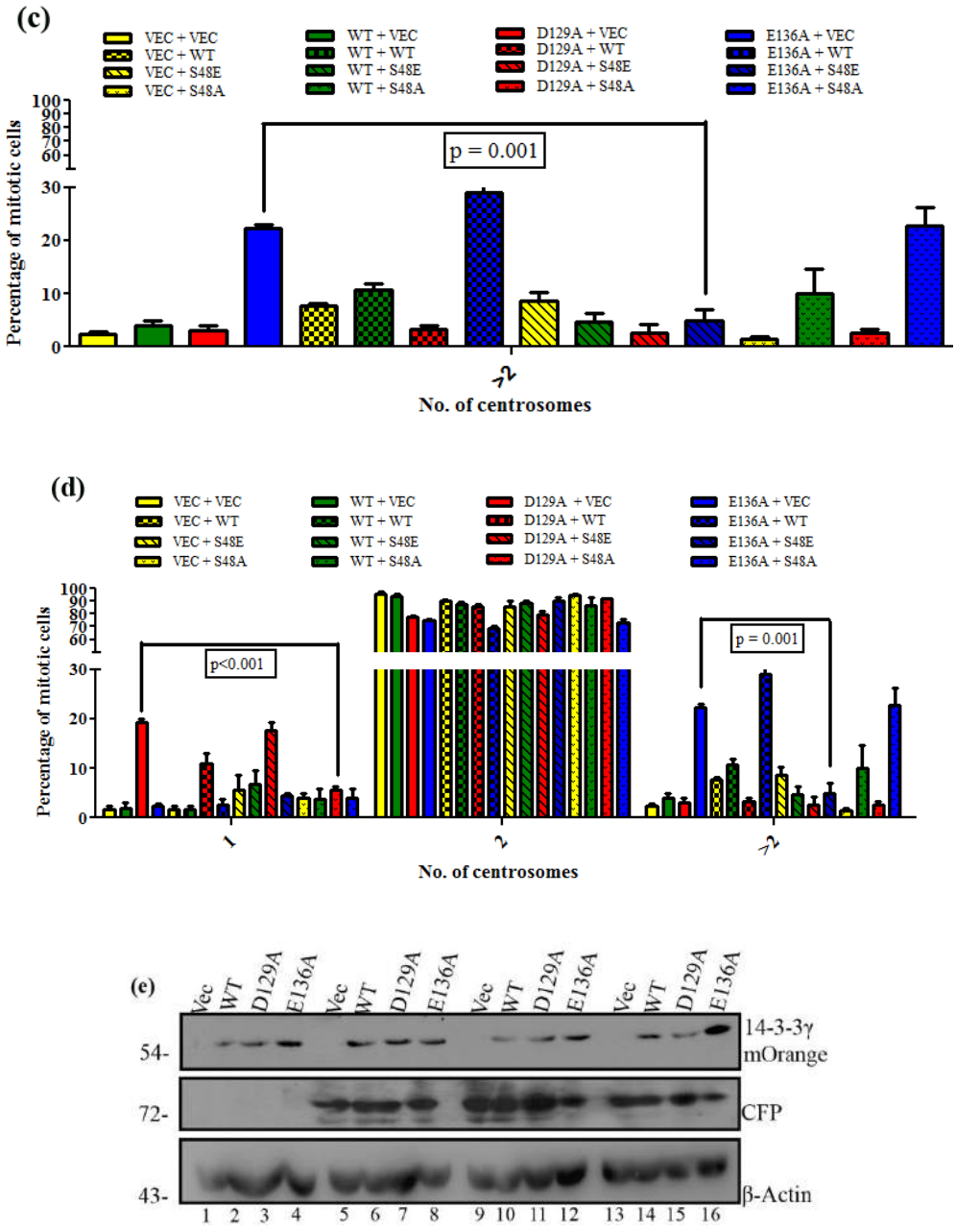

Fig. 4.49 Effect of S48 mutants of NPM1 on centrosome number. *HCT116 cells were transfected with the indicated NPM1 and 14-3-3γ constructs. 48 hours post transfection and synchronization in mitosis, cells were processed for IF or Western blots. Cells were fixed and stained for Pericentrin to determine centrosome number. (a) Representative images of the transfections. Original magnification 630X with 4X optical zoom, scale bar indicates 2µm, (b) Quantitation of % of mitotic cells with a single centrosome, (c) Quantitation of % of mitotic cells with multiple centrosomes, (d) Total quantitation, and (e) Protein extracts were*

*prepared from the transfected cells, resolved on SDS-PAGE gels and Western blots were performed with the indicated antibodies. Lanes 1-4 indicate transfection with CFP vector, lanes 5-8 indicate transfection with CFP NPM1 WT, lanes 9-12 indicate transfection with CFP NPM1 S48E and lanes 13-16 indicate transfection with CFP NPM1 S48A***.**

4.1.11.20 T199 phosphorylation status of the S48 mutants of NPM1

Previous results have demonstrated that NPM1 phosphorylation at T199 acts as a licensing factor for centrosome duplication (56,325). Expression of the phosphor-mimetic T199D was able to rescue the single centrosome phenotype. Given that the S48A mutant was also able to reverse the single centrosome phenotype and the S48E mutant was able to rescue the multiple centrosome phenotype, we wished to determine the T199 phosphorylation status of the NPM1 WT, S48A and S48E mutants. We transfected HCT116 cells with each of the ECFP tagged NPM1 constructs. We also used T199A as a negative control for T199 phosphorylation. We hypothesized that since the S48A mutant is able to rescue the single centrosome phenotype, it should be highly phosphorylated at T199. Conversely, since the S48E mutant is able to rescue the multiple centrosome phenotype, it should have T199 phospho levels comparable to that seen upon expression of NPM1 T199A. And that is what we observed (4.50).

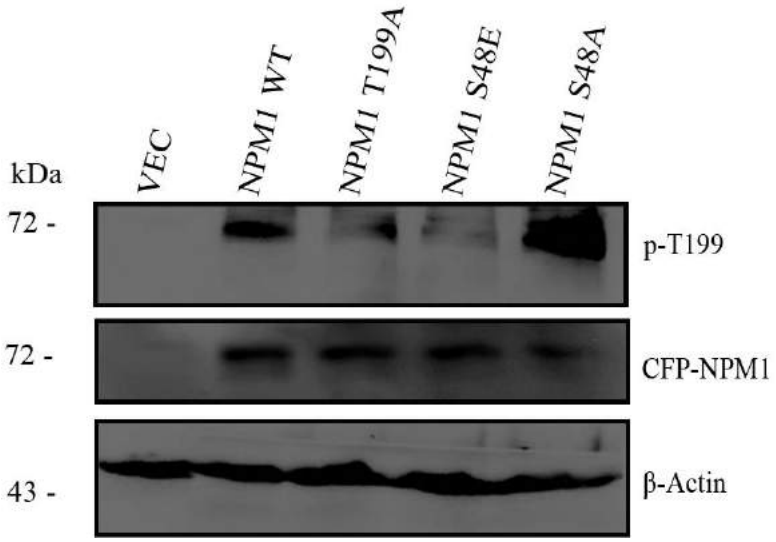

Fig. 4.50 p-T199 status of the S48 mutants of NPM1. *HCT116 cells were transfected with the indicated NPM1 constructs. 48 hours post-transfection, protein extracts prepared from these cells were resolved on SDS-PAGE gels followed by Western blotting. β-actin serve as the loading control. Note that S48A shows increased phosphorylation on T199 while the phosphorylation is significantly reduced in the S48E mutant.*

4.1.11.21 NPM1 and ROCKII

It has been demonstrated that upon phosphorylation of NPM1 by CDK2, it binds to ROCKII (454). ROCKII then phosphorylates proteins that initiate centrosome duplication (454). In order to further confirm the role of NPM1 in this pathway, we used a doxycycline inducible constitutively active construct of ROCKII (ROCKII CA). In HCT116 cells transfected with each of the 14-3-3γ mutants, we co-transfected the ROCKII construct and then added doxycline 24 hours after transfection. 48 hours after transfection, we counted centrosome number in a 100 transfected, mitotic cells. We observed that induction of ROCKII CA lead to the presence of multiple centrosomes. It also reversed the single centrosome phenotype seen upon expression of the D129A mutant (fig. 4.51 (a)). We also tested the effect of ROCKII by

using Calpeptin, a chemical activator of ROCKII. Addition of Calpeptin also reversed the effect of D129A (fig. 4.51 (b)).

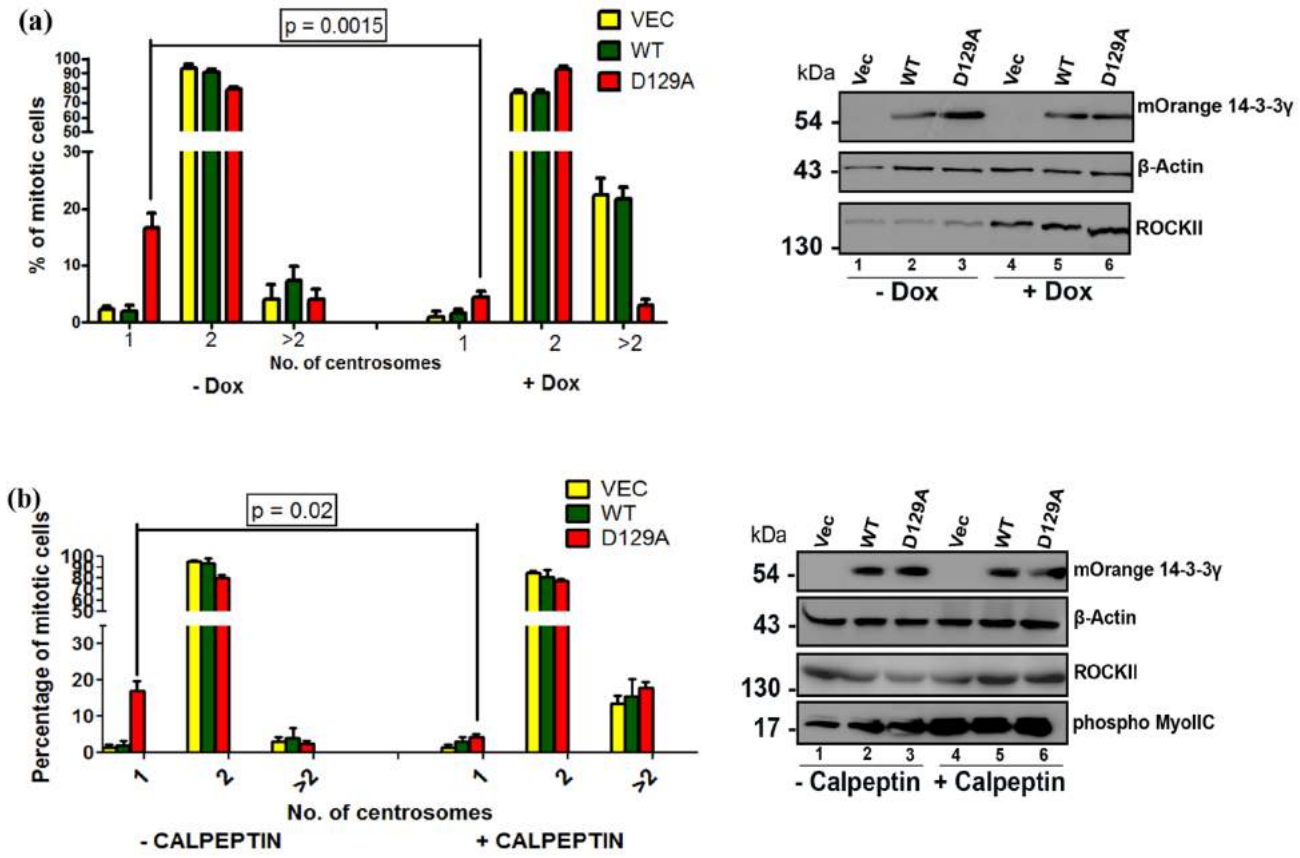

Fig. 4.51 14-3-3γ inhibits the ability of NPM1 to activate ROCKII. *(a) HCT116 cells were transfected with the indicated 14-3-3γ constructs and a doxycycline-inducible constitutively active ROCKII construct. The cells were cultured in the presence and absence of doxycycline and centrosome number determined in mitotic cells as described above. Note that the constitutively active ROCKII construct only induces centrosome duplication in the presence of doxycycline. Western blot indicates overexpression of ROCKII upon doxycycline induction. (b)HCT116 cells were transfected with the indicated 14-3-3γ constructs and treated with either the vector control or the ROCKII activator Calpeptin and centrosome number determined in mitotic cells. Note that Calpeptin reverses the single centrosome phenotype in cells expressing D129A. In all the experiments the mean and standard error from at least three independent experiments were plotted, error bars denote standard error of mean and p-values are obtained using Student's t test. Molecular weight markers in kDa are indicated.*

Our results suggest that the centrosome phenotypes observed upon expression of the different 14-3-3γ mutants are due to differential binding of these mutants to NPM1. In case of the D129A mutant, it binds to NPM1 with a high affinity. This inhibits the ability of NPM1 to dissociate from the centrosome upon phosphorylation by CDK2 at T199. Expression of 14-3-3γ binding deficient mutant, NPM1 S48A, is therefore able to reverse this phenotype. In case of the E136A mutant, which is unable to bind to NPM1, NPM1 dissociates from the centrosome prematurely, which leads to centrosome amplification. Expression of the S48E mutant, which binds to 14-3-3γ, is thus able to reverse this phenotype. The D129AE136A mutant behaves like WT 14-3-3γ due to intragenic complementation.

4.2 How do 14-3-3 proteins regulate centrosome clustering?

Non-transformed cells with multiple centrosomes undergo a multipolar mitosis, which results in massive aneuploidy and eventual apoptosis (391). Centrosome amplification is therefore, not beneficial to cells. Paradoxically, several reports demonstrate that centrosome amplification is common in most forms of cancer [reviewed in (455)]. Several proteins that are involved in the centrosome cycle are deregulated in cancer [reviewed in (384)]. One mechanism to avoid cell death, utilized by transformed cells with multiple centrosomes, is the organization of a pseudo-bipolar or clustered spindle (360). It has been demonstrated using human cell lines and *Drosophila* models, that in this process, from prophase onwards the multiple centrosomes gather so as to form only two functional poles (456). The cells go through a transient multipolar phase that eventually coalesces into a clustered mitosis (385,445,457). Due to the transient multipolar phase, there are merotelic attachments between the kinetochore and the microtubules, which contribute towards Chromosomal Instability

(CIN). However, the CIN is low enough that the resultant daughter cells are still viable. This confers a growth advantage on the daughter cells (359,360).

Loss of 14-3-3γ leads to centrosome amplification (326). When sh-14-3-3γ cells from passage 15 to passage 55 were compared, it was observed that with an increase in passage, there is an increase in aneuploidy and the ability to form soft agar colonies. This is accompanied by an increase in the percentage of cells with clustered centrosomes in the sh-14-3-3γ cells as compared to the vector control. Further, upon expression of the 14-3-3γ binding defective CDC25C S216A across passages, there is still an increase in the percentage of cells with a pseudobipolar spindle (326). However, there is a concomitant increase in the percentage of cells with a multipolar spindle. This also results in a decrease in tumour volume.

4.2.1 Generation of HeLa Kyoto EGFP-α-tubulin/ H2B-mCherry cells with a knockdown of 14-3-3γ

In order to understand how a loss of 14-3-3γ increases the frequency of cells with clustered centrosomes, it is important to study the dynamics of the process in live cells. Clustering is a process that begins in prophase but can be visualized only in metaphase or anaphase cells. When a cell with multiple centrosomes is in prophase, it could proceed in two ways – a multipolar mitosis or a clustered mitosis. If we observe cells only in mitosis, we would underestimate the correct number of cells undergoing a multipolar vs a clustered mitosis. Therefore, in order to visualize the centrosomal dynamics in cells with multiple centrosomes, we obtained the HeLa Kyoto EGFP-α-tubulin/ H2B-mCherry cell line (405). This clonal stable cell line was generated by transfecting HeLa cells with a single circular plasmid followed by G418 and Puromycin drug resistance selection. The advantage of using this cell line was that it would let us visualize spindle architecture and track chromosome dynamics.

This is essential, given that centrosome clustering gives rise to merotelic attachments and chromosome lagging (359).

In order to generate a knockdown of 14-3-3γ in the HeLa Kyoto cell line, we cloned previously tested shRNA targeting 14-3-3γ in a pLKO Hygro vector (234). After selection in Hygromycin, we were able to obtain Hygromycin resistant colonies. In order to test for a knockdown in these colonies, we prepared lysates and performed Western blots using antibodies against 14-3-3γ, with β-Actin as a loading control. We were able to verify that a number of the isolated colonies harboured a knockdown of 14-3-3γ. However, upon culturing the cells further, we observed that the cells were unhealthy and were unable to grow. Also, after a few passages, the cells reverted to WT levels of 14-3-3γ. We observed the same phenotype after repeated transfection and selection (fig. 4.53).

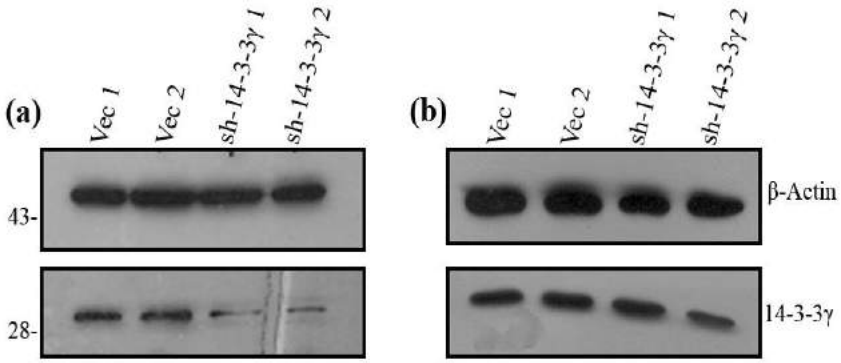

Fig. 4.52 Generation of a knockdown of 14-3-3γ in the HeLa Kyoto cell line. *Clones selected in Hygromycin were tested for a knockdown of 14-3-3γ by performing western blots. (a) Two vector control clones and two sh-14-3-3γ clones. Note the knockdown of 14-3-3γ in the sh-14-3-3γ clones. (b) The same clones after further culturing. Note the reversal in the levels of 14-3-3γ in the sh-14-3-3γ clones.*

Recently, a paper was published where it was demonstrated using HeLa cells, that 14-3-3 proteins shield Cdt2 from proteasomal degradation (235). Cdt2 is the substrate recognition adaptor of $CRL4^{Cdt2}$ E3 ubiquitin ligase complex. CRL^{Cdt2} is essential for the proteasomal degradation of several cell cycle proteins, such as Cdt1, E2F1, p21and Set8, for the maintenance of genomic stability [reviewed in (236)]. FbxO11 mediated proteasomal degradation of Cdt2 leads to cell cycle exit (236). This degradation can be inhibited by its phosphorylation at a Thr464 residue by CDK1 and CDK2. This phosphorylation also generates a binding site for 14-3-3γ, which then shields Cdt2 from degradation and stabilizes it. Upon depletion of 14-3-3γ, there is an increase in the levels of substrates of $CRL4^{Cdt2}$, such as p21 and Set8 (235). This leads to an arrest of the cells at the G2/M phase due to accumulation of Set8. This could explain why we were unable to generate a knockdown of 14-3-3γ in the HeLa cell line.

It is unclear whether this is a cell line specific phenotype, as transient knockdown of 14-3-3γ has been created in HEK293 and U2OS cell lines (326). Moreover, HCT116 cells harbouring a stable knockdown of 14-3-3γ have been generated (234). But given the data from this publication, we decided to change our model cell line and used the previously generated HCT116 derived vector control and 14-3-3γ knockdown cells for our experiments. Therefore, we wished to generate a single construct expressing γ-tubulin-GFP and H2B-mCherry. Tagging γ-tubulin, which is a PCM protein, would help us track the centrosome and study centrosome clustering better.

In order to be able to express two proteins using a single promoter, we first cloned an Internal Ribosome Entry Site (IRES) sequence into the MCS of the pcDNA3.1 Puromycin vector (fig. 4.54 (a)). An IRES is an RNA sequence that forms a complex secondary structure that allows the initiation of translation from any position within an mRNA immediately downstream from where the IRES is located. We first cloned mCherry H2B downstream of an (IRES)

sequence into a pcDNA3.1 Puromycin vector. The expression of the pcDNA3.1 H2B-mCherry-IRES construct was tested by transfecting this construct into HCT116 cells and observing the localization of the H2B-mCherry under a microscope 48 hours post transfection. We observed that the construct expressed correctly, with the H2B-mCherry being expressed in the nucleus (fig. 4.54 (b)). Then, we cloned γ-tubulin GFP upstream of the IRES sequence and tested the expression of the pcDNA3.1 Puro γ-tubulin-GFP-IRES-H2B-mCherry construct. We observed that the H2B-mCherry localized as observed before, in the nucleus. However, we also observed that the γ-tubulin-GFP formed several large puncta within cells, which is not the correct localisation of γ-tubulin (4.54 (c)). This could be due to very high overexpression of the γ-tubulin-GFP protein.

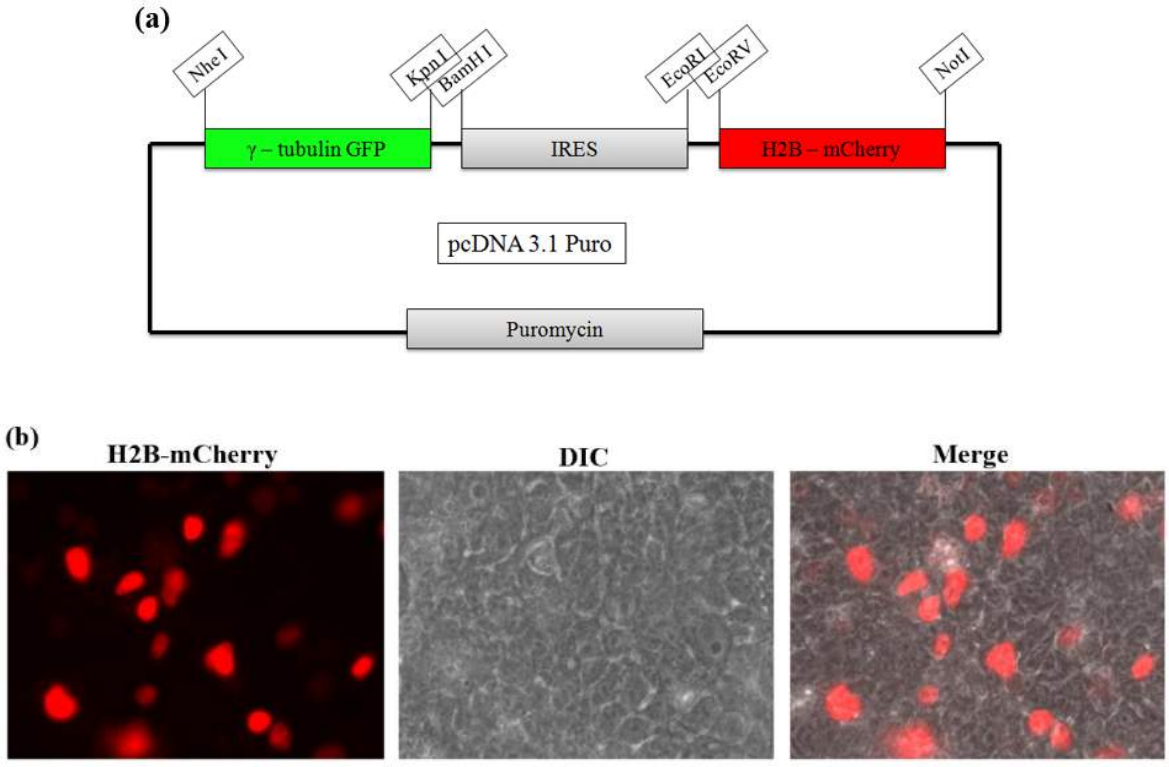

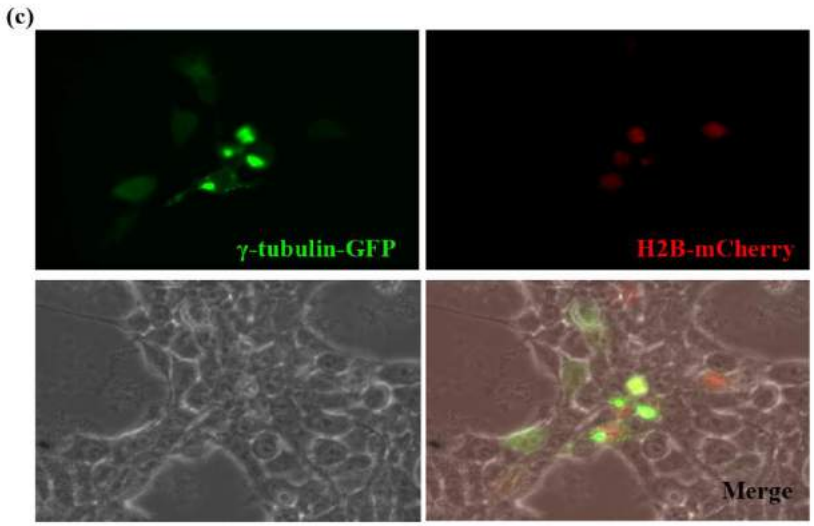

Fig. 4.53. Generation of the pcDNA3.1 –γ-tubulin-GFP-IRES-H2B-mCherry construct. *(a) Design of the live cell construct, (b) HCT116 cells were transfected with the pcDNA3.1 – IRES- H2B – mCherry construct. 48 hours post transfection, the cells were visualised using an inverted microscope, (c) HCT116 cells transfected with the pcDNA3.1 – γ-tubulin-GFP-IRES-H2B-mCherry construct. Note the defective localization of the γ-tubulin GFP.*

It has been reported that, when using an IRES sequence to drive the expression of two genes, the gene downstream of the IRES sequence is expressed at levels 20-50% as that of the upstream gene (458,459). This depends on the gene of interest or the efficiency of the upstream promoter (458,459). Given this data and our observations, we decided to interchange the order in which the two genes were cloned around the IRES sequence. Therefore, we cloned the H2B-mCherry upstream of the IRES sequence and the γ-tubulin-GFP downstream of the IRES sequence. When we tested the expression of the pcDNA3.1 Puro-H2B-mCherry-IRES-γ-tubulin-GFP construct, we observed that both the proteins localized correctly (fig. 4.54). Further, this construct can be used to study centrosome clustering.

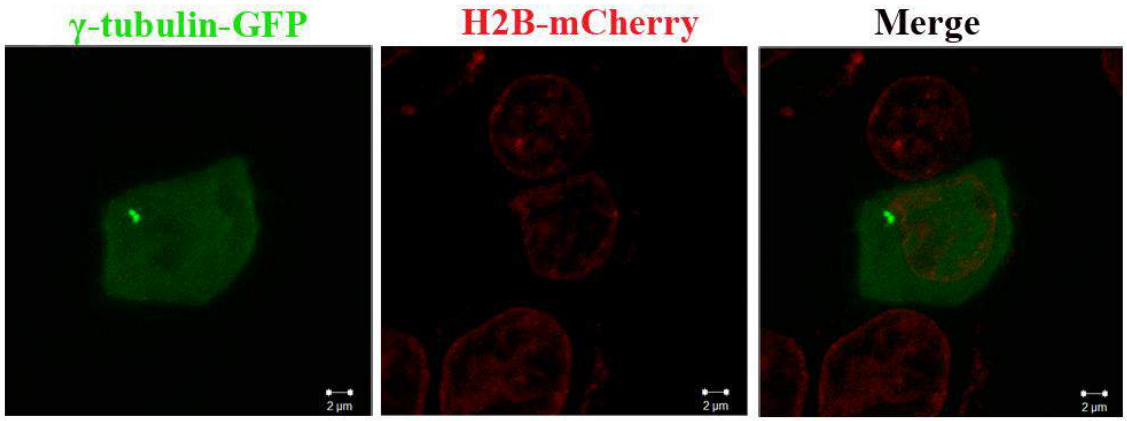

Fig. 4.54. Expression of the pcDNA3.1H2B-mCherry-IRES-γ-tubulin-GFP. *HCT116 cells were transfected with the pcDNA3.1 – γ-tubulin-GFP-IRES-H2B-mCherry construct.48 hours post transfection, the cells were imaged under a Confocal microscope at 630X magnification with 4X optical zoom. Scale bar indicates 2µm. Note the correct localization of the γ-tubulin GFP. Also, cells express H2B-mCherry before they express γ-tubulin-GFP. This is probably due to the γ-tubulin-GFP being cloned downstream of the IRES sequence.*

5. Discussion

5. Discussion.

The results presented in this thesis suggest that 14-3-3 proteins perform several functions in the centrosome cycle. Binding to 14-3-3γ and 14-3-3ε is essential for the centrosomal localization of the Centrin2 (452). The functional consequences of this loss of localization remain to be determined. 14-3-3 proteins are also involved in the centrosome cycle by inhibiting the premature activation of CDC25C (326). The loss of 14-3-3γ results in centrosome amplification due to increased phosphorylation of the T199 residue in NPM1 by CDK1 (326). Further, negatively charged residues within the peptide binding groove of 14-3-3γ can affect binding of 14-3-3 to NPM1. This binding plays an inhibitory role on centrosome duplication, as expression of the E136A mutant, which cannot bind to NPM1 leads to centrosome amplification, and expression of the D129A mutant, which binds with higher affinity to NPM1, inhibits centrosome duplication.

5.1 The centrosome amplification observed upon a knockdown of 14-3-3γ is accompanied by an increase in the levels of p-T288 Aurora A kinase.

The primary function of Aurora-A is to promote bipolar spindle assembly but it also has roles in centrosome maturation and separation, acentrosomal and centrosomal spindle assembly, kinetochore function, cytokinesis and cell fate determination (341,344,345,366,398,415,460-466). Aurora-A activation is dependent on its phosphorylation on residue T288 in the activation loop (467). Our results indicate that Aurora A pT288 levels are higher in the sh-14-3-3γ cells as compared to the vector control cells. Centrosome amplification in the sh-14-3-3γ cells is due to premature CDC25C and CDK1 activation. The connection between premature CDK1 activation and increased Aurora A activation is not clear. Aurora A has not been shown to play a role in centriole biogenesis, although it has roles in centrosome separation. It is possible that its increased activation is an outcome of the centrosome amplification

observed in the sh-14-3-3γ cells. The increase in AuroraA activity might lead to separation of the duplicated centrosomes and thus facilitate centrosome duplication.

5.2 Binding to 14-3-3γ and 14-3-3ε is essential for the centrosomal localization of Centrin2.

Centrin2 is a protein that localizes to the distal lumen of both centrioles (423). Loss of Centrin2 results in centriole "dilution", with the generation of daughter cells with only a single centriole (422). These daughter cells do not survive beyond the fourth cell division (422). Centrin2 also has functions in DNA damage repair; being a part of the Xeroderma Pigmentosum Complex (XPC) it is necessary for nucleotide excision repair (369).

Previous reports have demonstrated that the C terminal region of Centrin2, which consists of the EF3 and EF4 domains (aa. 94-172), are necessary and sufficient for its centrosomal localization and binding to XPC (424). 14-3-3 proteins have been shown to modulate the sub-cellular localization of their ligands (219,226,240,468). Results from this thesis demonstrate that 14-3-3 proteins bind to Centrin2 and that this binding is important for its centrosomal localization. Expression of a 14-3-3 binding deficient mutant of Centrin2 results in a pan-cytoplasmic, punctate localization of Centrin2, but none of the puncta localize to the centrosome. This mutant is not dominant negative, as its expression does not interfere with mitotic progression or spindle formation. While we have been unable to identify the precise site of 14-3-3 and Centrin2 interaction, our results suggest that the binding is indpendent of phosphorylation on Centrin2. There could also be at least two possible regions within Centrin2 that mediate its binding to 14-3-3 proteins; amino acids 29-37 and amino acids 48-63. These could form an as yet uncharacterized 14-3-3 binding site. The other possibility is that the interaction is indirect and that other proteins are required to mediate the interaction of 14-3-3 proteins and Centrin2. The interaction of these proteins and Centrin2 might be

stabilized by 14-3-3 binding and thus help in recruiting Centrin2 to the centrosome. 14-3-3 proteins and Centrin2 may be part of a multi-protein complex, which might be essential for centriole biogenesis and for the accurate localization of Centrin2 at the centrosome.

Several approaches have been taken to explain how the localization of Centrin2 to the centrosome is regulated (424,469,470). Dantas, et. al., used chicken DT40 cells expressing Centrin2 mutants that were unable to bind to Calcium. Their results suggest that the centrosomal localization of Centrin2 depends on its ability to bind to Calcium, as the Alanine mutants of D41, D77, D114 and D150, do not localize at the centrosome (470). Based on or results, this does not seem to be the case. The construct expressing aa. 1-37, which does not contain any of the four calcium binding residues, is able to localize to the centrosome. These discrepancies could be due to differences in centriole biogenesis between species. Experiments in XP4PASV cells, a human fibroblast cell line deficient for XPC, have demonstrated that both, its localization at the centrosome and binding to XPC are dependent upon three amino acids in EF3 and one amino acid in EF4 of Centrin2 (424). Yet, all the C-terminal deletion constructs used in this thesis accumulate at the centrosome and co-localize with Pericentrin, although not with the characteristic 2 or 4 dot organization. This suggests that after Centrin2 is directed to the centrosome, other factors might bind to its C-terminal end and mediate its accurate localization at the centriolar lumen.

X-ray crystallographic studies of mouse Centrin1 indicate that the N-terminus of one Centrin1 monomer might form a complex with the C-terminus of another Centrin1 monomer (471). This suggests that the N-terminal mutants of Centrin2 might form a complex with the endogenous Centrin2. However, the entire EF1 domain in Centrin1 is required for dimerization with the C-terminal EF hands in Centrin1 and the 1-37 mutant does not have the entire EF1 hand. Therefore, it is unlikely that the 1-37 mutant localizes to the centrosome by forming a dimer with the endogenous Centrin2. Further, the 14-3-3 binding defective mutant,

64-172, showed no nuclear localization. This could be due to the fact that nuclear localization of Centrin2 has been linked to its modification by SUMOylation (472). Three putative SUMOylation sites are present within the first 64 amino acid region of Centrin2. It is possible that one of these sites could be responsible for SUMOylation and that is why deletion of this region results in loss of its nuclear localization.

We propose the following model to illustrate the role of 14-3-3 proteins in mediating the localization of Centrin2 at the centrosome (Fig. 5.1). In cells expressing Centrin2 with an intact 14-3-3 binding site, Centrin2 is targeted to the centrosome via its interaction with 14-3-3 and possibly other proteins. Once it is present at the centrosome, other factors regulate its correct localization at the centrosome. In cells expressing a 14-3-3 binding defective mutant of Centrin2, Centrin2 can no longer be targeted to the centrosome and is thus not observed at the centrosome.

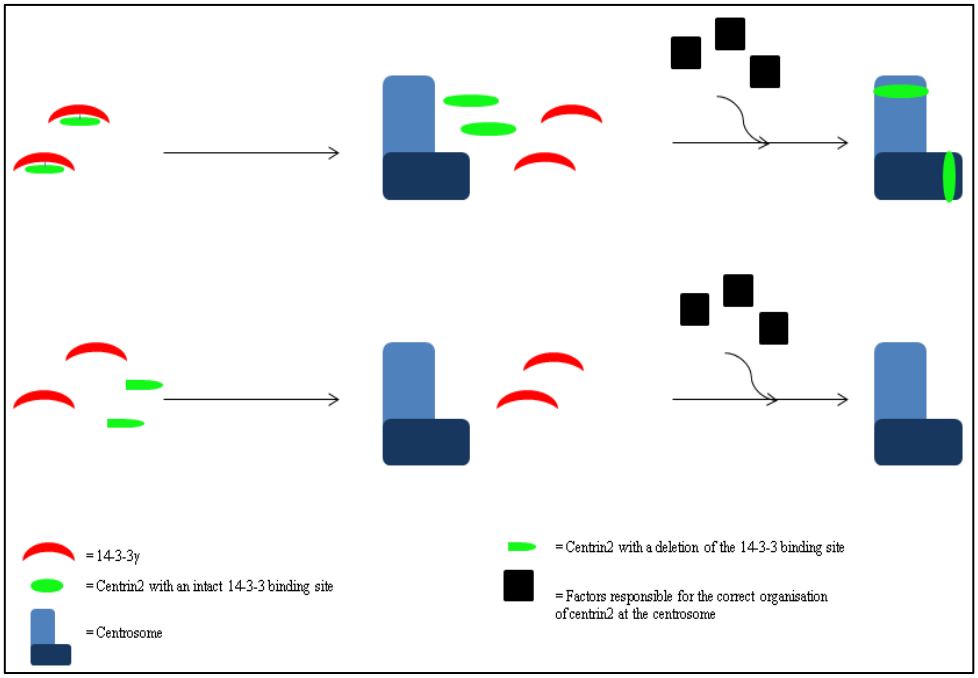

Fig. 5.1 Model describing the role of 14-3-3 proteins in regulating the centrosomal localization of Centrin2.

5.3 The centrosomal localization of γ-tubulin depends on its middle Tubulin/FtsZ, 2 layer sandwich domain.

γ-tubulin is essential for microtubule nucleation, being a part of the γ-Tubulin Small Complex (γ-TuSC) and the γ-Tubulin Ring Complex (γ-TURC). Several reports have focussed on its activity at the centrosome and its connection to various microtubule nucleation pathways (reviewed in (473)). The results in this thesis indicate that its middle Tubulin/FtsZ, 2 layer sandwich domain is essential for its centrosomal localization, as its deletion results in loss of the centrosomal localization of γ-tubulin. This domain might not be essential for binding to 14-3-3γ, as the G1 mutant is still able to bind to 14-3-3γ, although it is possible that there are multiple 14-3-3 binding sites on γ-tubulin. Further experiments are needed to understand which other proteins might be necessary for its centrosomal localization.

5.4 Cep170 levels decrease in the sh-14-3-3γ cells.

Cep170 is a sub-distal appendage protein that is specific to the mother centriole. Our results indicate that both mRNA as well as protein levels of Cep170 decrease in the sh-14-3-3γ cells as compared to the vector control cells. Given that this decrease does not seem to affect the intensity of Cep170 at the centrosome, it is difficult to understand its functional significance. Experiments in the mouse F9 cell line with a knockout of Odf2, another sub-distal appendage protein show that these cells lack sub-distal appendages and are unable to form primary cilia (312). Odf2 has been demonstrated to be one of the first proteins that is recruited to the sub-distal appendages (437). It is possible that this is why its loss has such a severe phenotype. Further, it is not possible to study the formation of primary cilia in HCT116 cells as these are actively cycling cells and do not undergo quiescence.

14-3-3γ can bind to and modulate the centrosomal localization of some centrosomal proteins (fig. 5.2). A better understanding of the consequences of this binding and its specificity is needed.

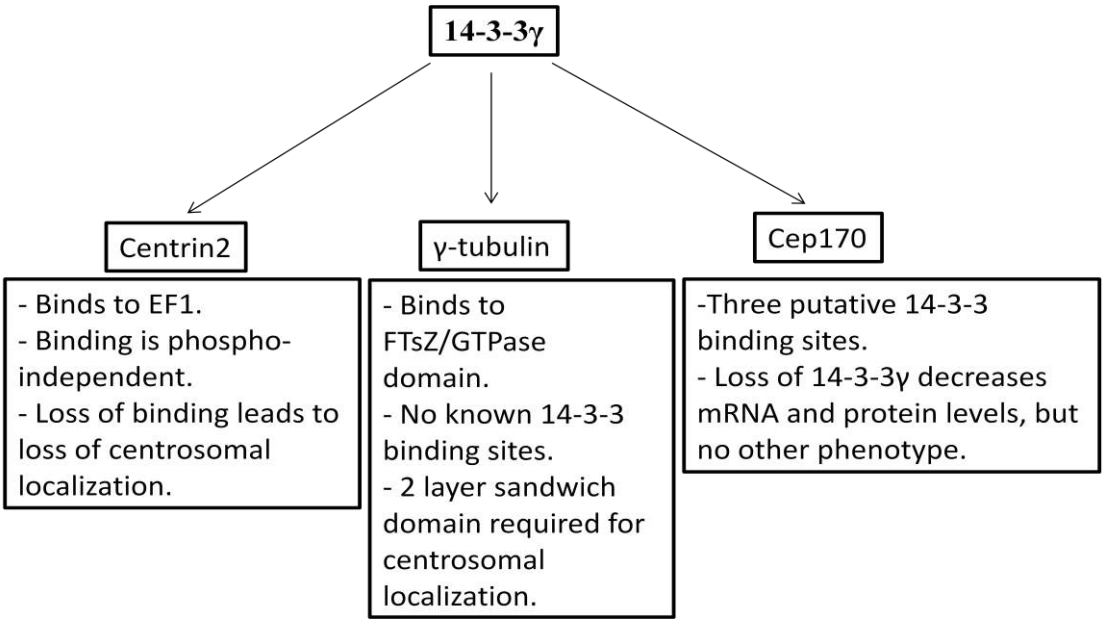

Fig. 5.2 Representation of the connection between 14-3-3 and centrosomal proteins.

5.5 Expression of mutants of the peptide binding grove of 14-3-3γ affects centrosome number.

14-3-3 proteins are dimeric, cup-shaped molecules that can bind to phosphorylated Serine or Threonine residues in a mode specific manner (173,180). Each monomer forms a highly conserved amphipathic groove that is the phosphorylation-binding pocket. A number of positively charged Lysine and Arginine residues (K49, K120, R56, and R127) within this groove mediate the interaction with the phosphate group of the ligand (172). We have demonstrated that negatively charged residues within this peptide binding amphipathic groove of 14-3-3γ can affect centrosome number. Expression of the D129A mutant in HCT116, HaCat and HEK293 cell lines leads to a significant percentage of mitotic cells harbouring single centrosomes (19%). Expression of the E136A mutant in the same cell lines

results in the presence of multiple centrosomes in mitotic cells (21%). Interestingly, expression of the D129AE136A mutant did not result in any change in centrosome number. This suggests that this mutant shows intragenic complementation. We also observed a similar phenotype in the HCT116 derived vector control and sh-14-3-3γ cells. This implies that the phenotype is actually dominant over the endogenous protein in the cells. Further, knock-in experiments are needed to test the effect of the mutants. Also, given that these residues are highly conserved across isoforms and that different 14-3-3 isoforms can have overlapping functions, it is possible that similar mutations in other isoforms might result in a similar phenotype. It would be interesting to study the effect of altering these residues in other isoforms and determine their affect on isoform function.

5.6 The single centrosome phenotype is due to a failure of centriole duplication.

By performing dual staining for centrosomes, using GFP Centrin2, Pericentrin, Cep68 and Ninein as markers, we were able to demonstrate that the single and multiple centrosomes observed are due to defects in centriole duplication. Under normal conditions, mitotic cells would have 4 Centrin2 dots and 2 Pericentrin clouds, a ratio of 4:2 for Centrin2:Pericentrin, indicative of two mature centrosomes. Cells expressing the WT 14-3-3γ show Centrin2:Pericentrin staining in the ratio of 4:2 in mitosis, while the single centrosome observed in cells expressing the D129A mutant shows Centrin2:Pericentrin staining in the ratio of 2:1 in mitosis. As described in section 4.1.11.6 and figure 4.32, this could be due to a defect in separation, disengagement or duplication. In order to understand the phenotype better, we performed dual staining using Centrin2:Cep68 and Centrin2:Ninein. In normal cells in G2, there would be 4 Centrin2 dots and 2 Cep68 dots, indicative of centrosomes that had undergone disengagement and duplication. In cells expressing the WT 14-3-3γ construct, we observed Centrin2:Cep68 staining in the ration of 4:2, which is expected. In cells expressing the D129A construct, with a single centrosome, we observed Centrin2:cep68

staining in the ratio 2:2, which is indicative of a centrosome that has undergone disengagement but is unable to duplicate. Further, a normal G2 cell would stain for Centrin2:Ninein in the ratio of 4:1, indicative of 4 centrioles, of which only one is the grandmother centriole staining positively for Ninein, which is what we observed in cells expressing the WT 14-3-3γ construct. In cells expressing the D129A construct, with a single centrosome, we observed Centrin2:Ninein staining in the ratio 2:1. Taken together with the Cep68 staining, this is indicative of a centrosome that has undergone disengagement but is unable to initiate duplication. Previous reports in RPE1 cells indicate that a 2:2 ratio of Centrin:C-Nap1 exists in cells with disengaged centrioles (334). C-Nap1 is an intercentrosomal linker protein that has been shown to localize to MTOC competent centrioles (334,474). In the same report, hSas-6, which is a protein that localizes to the central cartwheel, has been shown to associate exclusively with daughter centrioles that are MTOC incompetent. It might be useful to study the pattern of hSas-6 in cells expressing these 14-3-3γ mutants. Also, it will be intersting to further characterize the multiple centrosome phenotype using daughter centriole specific markers such as hSas-6 and Centrobin (475). This would help us understand whether the daughter centrioles are formed *de novo* or using the mother centriole as the template.

5.7 Cells expressing the 14-3-3γ mutants exhibit mitotic defects.

Cells expressing the WT 14-3-3γ complete mitosis in ~40 minutes. We observed that cells expressing the D129A mutant, that have a single centrosome in mitosis, are unable to complete mitosis even after 120 minutes in mitosis. In HeLa cells, a knockdown of Centrin2 leads to the presence of a unicentriolar spindle pole. Here, due to "centriole dilution", the two centrioles split, migrate to each pole and nucleate spindle microtubules and complete mitosis (422). In the next round of mitosis, acentriolar spindle poles are formed and eventually, the cells are unable to complete cytokinesis and undergo apoptosis (422). Inspite of having only

two centrioles in a mitosis, the cell is able to complete at least one round of mitosis. A similar phenotype is not observed in cells expressing the D129A mutant. This could be explained by the fact that the duration of mitosis is not specified in this report (422). It is possible that cells expressing the D129A mutant, with a single centrosome in mitosis might also be able to complete mitosis, if observed for a longer duration and this needs to be tested. Also, if these cells are undergo apoptosis eventually, it might be difficult to generate a stable cells overexpressing these constructs. in this case, a conditional knock-in system would be useful. The other possibility is that activation of the Spindle Assembly Checkpoint (SAC) occurs when cells expressing the D129A mutant, with a single MTOC, are in mitosis. As described in section 1.1.2, the SAC is activated upon loss of spindle pole tension, unattached kinetochores at metaphase or by certain spindle poisons such as nocodazole (137). When a single MTOC is present, syntelic attachments can occur, where both sister chromatids are attached to a single spindle pole (476). It might be interesting to study what happens when cells expressing the D129A mutant, with a single centrosome, are treated with a SAC inhibitor such as CFI-402257 (477). If treatment with the SAC inhibitor is able to promote mitosis in these cells, the resulting daughter cells will harbour significant levels of CIN and this might further affect their viability.

Transformed cells with multiple centrosomes usually undergo a clustered mitosis (360,385,391,445,478). Extra centrosomes can add upto 30 minutes to the duration of mitosis, depending on the cell line being used (457). This is in line with our observation that cells expressing the E136A mutant, that possess multiple centrosomes, take a little more than 40 minute to complete mitosis by clustering centrosomes. We have been unable to detect the occurrence of a multipolar mitosis in cells expressing E136A. It is possible that these cells have a very efficient clustering mechanism. Loss of 14-3-3γ leads to an increase in centrosome number, clustering and aneuploidy with an increase in passage (326). The

centrosome clustering can be reversed to a multipolar mitosis upon co-expresssion of CDC25C (326) The multiple centrosome phenotype that we observe upon expression of the E136A mutant mirrors that seen upon loss of 14-3-3γ. Expression of this construct in the sh-14-3-3γ cells actually enhances the centrosome amplification observed upon loss of 14-3-3γ. It would be of interest to test the effect of CDC25C overexpression on centrosome number and clustering in these cells.

5.8 14-3-3γ inhibits centriole duplication by inhibiting NPM1 function.

The single centrosome phenotype cannot be reversed by overexpression of Plk4, CDK1 or CDK2. This is interesting because these proteins are extremely essential for procentriole biogenesis. Plk4 is first recruited at the proximal end of the mother centriole by Cep152, Cep192 and Plk1 (291). Given that overexpression of Plk4 is unable to rescue the single centrosome phenotype, it would be intersting to study the localization of Cep152, Cep63 and Cep192 at these centrosomes. This would help us further understand the dynamics of the recruitment of these centrosomal proteins at the centrosome and how this recruitment is affected in cells expressing the 14-3-3γ mutants.

Our results indicate that the single centrosome phenotype observed upon expression of the D129A mutant can be partially reversed by the NPM1 WT protein or completely reversed upon expression of the NPM1 T199D mutant, which is a phospho-mimetic mutant, or the S48A mutant, which is unable to bind to 14-3-3γ (section 4.1.11.14). Whereas, the multiple centrosome phenotype observed upon expression of the E136A mutant can be reversed upon expression of the NPM1 T199A mutant or the S48E mutant, which we propose is another phospho-mimetic site, necessary for 14-3-3 binding (section 4.1.11.14). Further, the single centrosome phenotype can be reversed upon activation of ROCK2. It has been demonstrated that NPM1 phosphorylated at T199 by CDK2 is displaced from the intercentrosomal linker

and activates ROCK2. Upon ROCK2 activation, centrosome duplication is initiated (454,479). However, using both antibodies against NPM1 and a fluorescently tagged construct of NPM1, we have been unable to detect the presence of NPM1 at the centrosome in both interphase and mitotic cells. Even the CFP NPM1 S48E mutant which localizes to the nucleus is not detected at the centrosome. 14-3-3γ has been shown to localize to the centrosome (326). There are no studies that indicate the presence of ROCK2 at the centrosome. We have demonstrated that 14-3-3γ interacts with NPM1. It is possible that the interaction of 14-3-3γ and NPM1 does not occur at the centrosome. It is clear, however, that the binding of 14-3-3γ to NPM1 inhibits NPM1 function. It is possible that the interaction between NPM1 and 14-3-3γ is not direct. 14-3-3 proteins have been shown to form ternary complexes due to the presence of two ligand binding sites within the dimer (215).

Oligomerization is essential for most NPM1 functions (418). It has been demonstrated previously, that phosphorylation at the S48 residue by Akt destabilizes NPM1 oligomerization (418). Our results indicate that this S48 residue is actually a mode 2 14-3-3 binding site. Mutation of the S48 to Alanine abrogates binding to 14-3-3γ, whereas, the S48E mutant is still able to bind to 14-3-3γ. NPM1 phosphorylated at the S48 residue is unable to oligomerize, therefore, the generation of the 14-3-3 binding site actually inhibits NPM1 oligomer formation. We also need to find out the kinase that phosphorylates NPM1 at S48 and generates a 14-3-3 binding site. It is possible that it could be Akt, in which case, we need to understand the role of Akt in the centrosome cycle.

Based upon our results, we propose the following mechanism (Fig. 5.3). Under normal conditions, in the presence of 14-3-3γ, NPM1 is bound to WT 14-3-3γ and remains at the centrosome and inhibits centrosome duplication. Upon phosphorylation of NPM1 at T199 by the CDK2/Cyclin E complex, NPM1 dissociates from the centrosome, and activates ROCK2, which licenses centrosome duplication (Fig. 5.3 (a)). On expression of the D129A mutant,

which binds to NPM1 with a stronger affinity as compared to WT 14-3-3γ, the NPM1 remains bound to 14-3-3, despite phosphorylation by CDK2/Cyclin E (Fig. 5.3 (b)). This inhibits centrosome duplication. This phenotype can be reversed by the expression of the NPM1 S48A mutant, which is unable to bind to 14-3-3γ. Upon expression of the E136A mutant, which is unable to bind to 14-3-3, NPM1 is untethered at the centrosome and is thus free to activate ROCK2 and leads to centrosome amplification (Fig. 5.3 (c)). This phenotype can be reversed upon expression of NPM1 S48E, which binds to 14-3-3γ. We have not able to understand the dynamics of 14-3-3γ and NPM1 binding and dissociation. It remains to be understood whether 14-3-3 binds to NPM1 before NPM1 is phosphorylated by CDK2/Cyclin E or is it vice versa. It is possible that phosphorylation of T199 acts as a positive feedback loop and makes the S48 site more accessible to 14-3-3 for binding. This is also suggested by the fact that the S48A mutant is more phosphorylated at T199 as compared to WT 14-3-3γ. However, this needs to be tested.

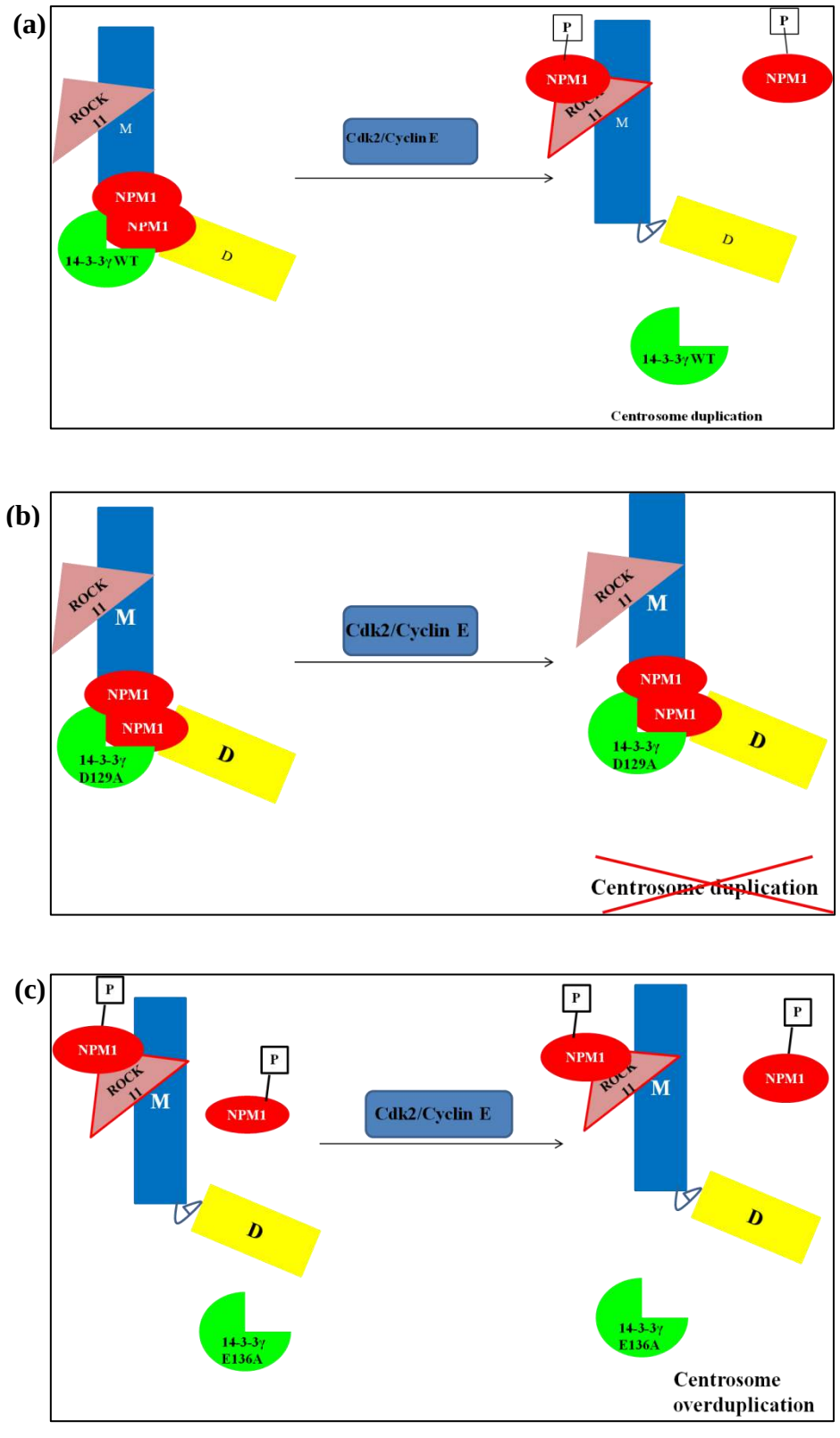

Fig. 5.3 Model explaining the regulation of NPM1 function by 14-3-3γ.

5.9 Mutants of 14-3-3 and oligomerization.

14-3-3 proteins function as homo- or heterodimers (197). It has been demonstrated that dimerization is essential for the function of 14-3-3 proteins, as dimerization defective mutants of 14-3-3 proteins cannot bind to ligands (200). It is possible that each of these mutants dimerize with the endogenous WT 14-3-3γ. This could explain why the phenotype is observable in only a percentage of the transfected cells. To test this hypothesis, a conditional knock-in cell line will have to be generated. It has also been reported that the D129A mutant oligomerizes more efficiently than the WT protein (249). Whether oligomerization contributes to the centrosome phenotype needs to be determined. In order to do this, the oligomerization potential of the E136A and the D129AE136A mutant will also have to be estimated. It is possible that the E136A mutant is unable to bind to NPM1 because it is unable to dimerize.

5.10 The different contributions of 14-3-3 proteins in the centrosome cycle.

Based on the results presented in this thesis, we suggest that 14-3-3 proteins have several roles in the centrosome cycle (fig. 5.4). 14-3-3γ prevents premature CDC25C activation and centrosome amplification in S phase (326). 14-3-3 proteins are also required for the centrosomal localization of the protein Centrin2 (452). Further, 14-3-3γ binding to NPM1 inhibits both the ability of NPM1 to form higher order oligomers and the phosphorylation of NPM1 on T199 by CDK2.

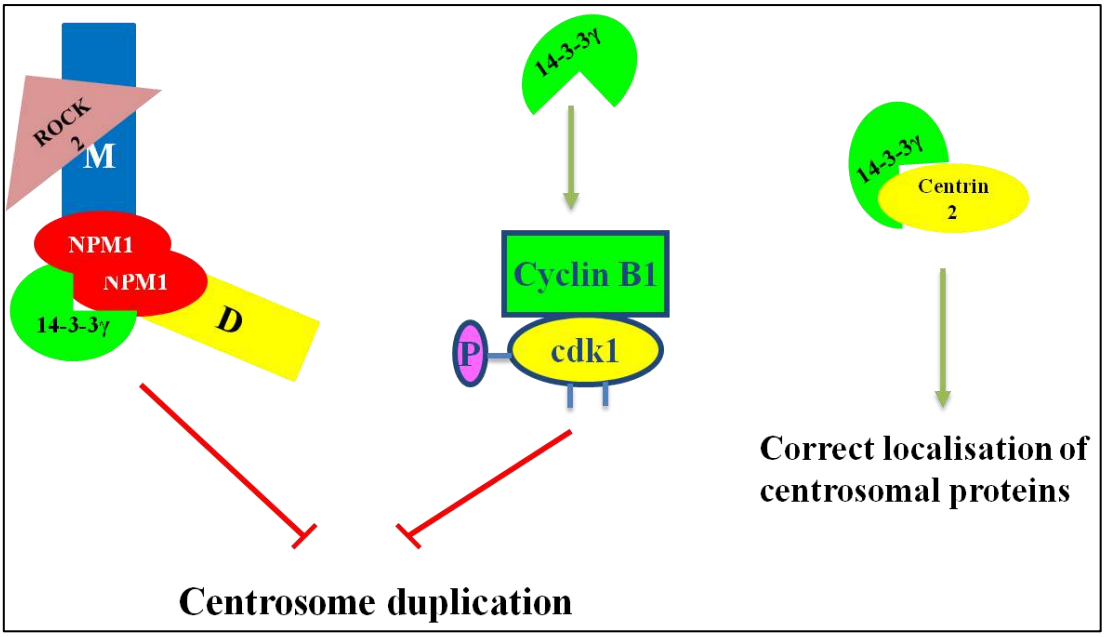

Fig. 5.4 Model representing the different contributions of 14-3-3 proteins to the centrosome cycle.

5.11 Conclusion.

The results in this thesis demonstrate that 14-3-3 proteins perform different functions in the centrosome cycle. These functions rely on the abilities of 14-3-3 proteins to act as adaptor proteins, molecular switches and shuttling proteins. Most of the results in this thesis focus on the γ isoform of 14-3-3 proteins, but as has been described before, it is possible that other isoforms can also perform compensatory functions.

6. Bibliography

1. Piwnica-Worms, H. (1999) Cell cycle. Fools rush in. *Nature* **401**, 535, 537
2. Nurse, P. (2000) A long twentieth century of the cell cycle and beyond. *Cell* **100**, 71-78
3. Mitchison, J. M. (1971) *The biology of the cell cycle [by] J. M. Mitchison*, University Press, Cambridge [Eng.]
4. Morgan, D. (2007) The Cell Cycle : Principles of Control. (Lawrence, E. ed.), New Science Press, UK. pp
5. Elledge, S. J. (1996) Cell cycle checkpoints: preventing an identity crisis. *Science* **274**, 1664-1672
6. Pardee, A. B. (1974) A restriction point for control of normal animal cell proliferation. *Proceedings of the National Academy of Sciences of the United States of America* **71**, 1286-1290
7. Coller, H. A. (2007) What's taking so long? S-phase entry from quiescence versus proliferation. *Nature reviews. Molecular cell biology* **8**, 667-670
8. Hirai, H., Roussel, M. F., Kato, J. Y., Ashmun, R. A., and Sherr, C. J. (1995) Novel INK4 proteins, p19 and p18, are specific inhibitors of the cyclin D-dependent kinases CDK4 and CDK6. *Mol Cell Biol* **15**, 2672-2681
9. Chan, F. K., Zhang, J., Cheng, L., Shapiro, D. N., and Winoto, A. (1995) Identification of human and mouse p19, a novel CDK4 and CDK6 inhibitor with homology to p16ink4. *Mol Cell Biol* **15**, 2682-2688
10. Reynisdottir, I., Polyak, K., Iavarone, A., and Massague, J. (1995) Kip/Cip and Ink4 Cdk inhibitors cooperate to induce cell cycle arrest in response to TGF-beta. *Genes & development* **9**, 1831-1845
11. Ohtani, K., DeGregori, J., and Nevins, J. R. (1995) Regulation of the cyclin E gene by transcription factor E2F1. *Proceedings of the National Academy of Sciences of the United States of America* **92**, 12146-12150
12. Desai, D., Gu, Y., and Morgan, D. O. (1992) Activation of human cyclin-dependent kinases in vitro. *Molecular biology of the cell* **3**, 571-582
13. van den Heuvel, S., and Harlow, E. (1993) Distinct roles for cyclin-dependent kinases in cell cycle control. *Science* **262**, 2050-2054
14. Planas-Silva, M. D., and Weinberg, R. A. (1997) The restriction point and control of cell proliferation. *Current opinion in cell biology* **9**, 768-772
15. Vijayaraghavan, M. R., and Prabhakar, K. . (1984) The endosperm. in *Embryology of Angiosperms* (Johri, B. M. ed.), Berlin: Springer-Verlag. pp 319-376
16. Alberts B, J. A., Lewis J, et al. . (2002) Drosophila and the Molecular Genetics of Pattern Formation: Genesis of the Body Plan. in *Molecular biology of the cell*, 4th Ed., Garland Science, New York. pp
17. Zhimulev, I. F., Belyaeva, E. S., Semeshin, V. F., Koryakov, D. E., Demakov, S. A., Demakova, O. V., Pokholkova, G. V., and Andreyeva, E. N. (2004) Polytene chromosomes: 70 years of genetic research. *International review of cytology* **241**, 203-275
18. Frade, J. M., and Ovejero-Benito, M. C. (2015) Neuronal cell cycle: the neuron itself and its circumstances. *Cell cycle (Georgetown, Tex.)* **14**, 712-720
19. Harper, J. W., and Adams, P. D. (2001) Cyclin-dependent kinases. *Chemical reviews* **101**, 2511-2526
20. De Bondt, H. L., Rosenblatt, J., Jancarik, J., Jones, H. D., Morgan, D. O., and Kim, S. H. (1993) Crystal structure of cyclin-dependent kinase 2. *Nature* **363**, 595-602
21. Jeffrey, P. D., Russo, A. A., Polyak, K., Gibbs, E., Hurwitz, J., Massague, J., and Pavletich, N. P. (1995) Mechanism of CDK activation revealed by the structure of a cyclinA-CDK2 complex. *Nature* **376**, 313-320

22. Frouin, I., Montecucco, A., Biamonti, G., Hubscher, U., Spadari, S., and Maga, G. (2002) Cell cycle-dependent dynamic association of cyclin/Cdk complexes with human DNA replication proteins. *The EMBO journal* **21**, 2485-2495
23. John, P. C., Mews, M., and Moore, R. (2001) Cyclin/Cdk complexes: their involvement in cell cycle progression and mitotic division. *Protoplasma* **216**, 119-142
24. Viallard, J. F., Lacombe, F., Belloc, F., Pellegrin, J. L., and Reiffers, J. (2001) Molecular mechanisms controlling the cell cycle: fundamental aspects and implications for oncology. *Cancer radiotherapie : journal de la Societe francaise de radiotherapie oncologique* **5**, 109-129
25. Nigg, E. A. (1996) Cyclin-dependent kinase 7: at the cross-roads of transcription, DNA repair and cell cycle control? *Current opinion in cell biology* **8**, 312-317
26. Morgan, D. O. (1997) Cyclin-dependent kinases: engines, clocks, and microprocessors. *Annual review of cell and developmental biology* **13**, 261-291
27. Ekholm, S. V., and Reed, S. I. (2000) Regulation of G(1) cyclin-dependent kinases in the mammalian cell cycle. *Current opinion in cell biology* **12**, 676-684
28. Sherr, C. J., and Roberts, J. M. (1999) CDK inhibitors: positive and negative regulators of G1-phase progression. *Genes & development* **13**, 1501-1512
29. Serrano, M., Hannon, G. J., and Beach, D. (1993) A new regulatory motif in cell-cycle control causing specific inhibition of cyclin D/CDK4. *Nature* **366**, 704-707
30. Hannon, G. J., and Beach, D. (1994) p15INK4B is a potential effector of TGF-beta-induced cell cycle arrest. *Nature* **371**, 257-261
31. Guan, K. L., Jenkins, C. W., Li, Y., Nichols, M. A., Wu, X., O'Keefe, C. L., Matera, A. G., and Xiong, Y. (1994) Growth suppression by p18, a p16INK4/MTS1- and p14INK4B/MTS2-related CDK6 inhibitor, correlates with wild-type pRb function. *Genes & development* **8**, 2939-2952
32. Pavletich, N. P. (1999) Mechanisms of cyclin-dependent kinase regulation: structures of Cdks, their cyclin activators, and Cip and INK4 inhibitors. *Journal of molecular biology* **287**, 821-828
33. Chen, J., Jackson, P. K., Kirschner, M. W., and Dutta, A. (1995) Separate domains of p21 involved in the inhibition of Cdk kinase and PCNA. *Nature* **374**, 386-388
34. Chen, J., Saha, P., Kornbluth, S., Dynlacht, B. D., and Dutta, A. (1996) Cyclin-binding motifs are essential for the function of p21CIP1. *Mol Cell Biol* **16**, 4673-4682
35. Nakanishi, M., Robetorye, R. S., Adami, G. R., Pereira-Smith, O. M., and Smith, J. R. (1995) Identification of the active region of the DNA synthesis inhibitory gene p21Sdi1/CIP1/WAF1. *The EMBO journal* **14**, 555-563
36. Warbrick, E., Lane, D. P., Glover, D. M., and Cox, L. S. (1995) A small peptide inhibitor of DNA replication defines the site of interaction between the cyclin-dependent kinase inhibitor p21WAF1 and proliferating cell nuclear antigen. *Current biology : CB* **5**, 275-282
37. Lin, J., Reichner, C., Wu, X., and Levine, A. J. (1996) Analysis of wild-type and mutant p21WAF-1 gene activities. *Mol Cell Biol* **16**, 1786-1793
38. Besson, A., Dowdy, S. F., and Roberts, J. M. (2008) CDK inhibitors: cell cycle regulators and beyond. *Developmental cell* **14**, 159-169
39. Bakiri, L., Lallemand, D., Bossy-Wetzel, E., and Yaniv, M. (2000) Cell cycle-dependent variations in c-Jun and JunB phosphorylation: a role in the control of cyclin D1 expression. *The EMBO journal* **19**, 2056-2068
40. Filmus, J., Robles, A. I., Shi, W., Wong, M. J., Colombo, L. L., and Conti, C. J. (1994) Induction of cyclin D1 overexpression by activated ras. *Oncogene* **9**, 3627-3633

41. Malumbres, M., and Pellicer, A. (1998) RAS pathways to cell cycle control and cell transformation. *Frontiers in bioscience : a journal and virtual library* **3**, d887-912
42. Lavoie, J. N., L'Allemain, G., Brunet, A., Muller, R., and Pouyssegur, J. (1996) Cyclin D1 expression is regulated positively by the p42/p44MAPK and negatively by the p38/HOGMAPK pathway. *The Journal of biological chemistry* **271**, 20608-20616
43. Brehm, A., Miska, E. A., McCance, D. J., Reid, J. L., Bannister, A. J., and Kouzarides, T. (1998) Retinoblastoma protein recruits histone deacetylase to repress transcription. *Nature* **391**, 597-601
44. Magnaghi-Jaulin, L., Groisman, R., Naguibneva, I., Robin, P., Lorain, S., Le Villain, J. P., Troalen, F., Trouche, D., and Harel-Bellan, A. (1998) Retinoblastoma protein represses transcription by recruiting a histone deacetylase. *Nature* **391**, 601-605
45. Kozar, K., Ciemerych, M. A., Rebel, V. I., Shigematsu, H., Zagozdzon, A., Sicinska, E., Geng, Y., Yu, Q., Bhattacharya, S., Bronson, R. T., Akashi, K., and Sicinski, P. (2004) Mouse development and cell proliferation in the absence of D-cyclins. *Cell* **118**, 477-491
46. Ciemerych, M. A., Kenney, A. M., Sicinska, E., Kalaszczynska, I., Bronson, R. T., Rowitch, D. H., Gardner, H., and Sicinski, P. (2002) Development of mice expressing a single D-type cyclin. *Genes & development* **16**, 3277-3289
47. Tsutsui, T., Hesabi, B., Moons, D. S., Pandolfi, P. P., Hansel, K. S., Koff, A., and Kiyokawa, H. (1999) Targeted disruption of CDK4 delays cell cycle entry with enhanced p27(Kip1) activity. *Mol Cell Biol* **19**, 7011-7019
48. Rane, S. G., Dubus, P., Mettus, R. V., Galbreath, E. J., Boden, G., Reddy, E. P., and Barbacid, M. (1999) Loss of Cdk4 expression causes insulin-deficient diabetes and Cdk4 activation results in beta-islet cell hyperplasia. *Nature genetics* **22**, 44-52
49. Hu, M. G., Deshpande, A., Enos, M., Mao, D., Hinds, E. A., Hu, G. F., Chang, R., Guo, Z., Dose, M., Mao, C., Tsichlis, P. N., Gounari, F., and Hinds, P. W. (2009) A requirement for cyclin-dependent kinase 6 in thymocyte development and tumorigenesis. *Cancer Res* **69**, 810-818
50. Botz, J., Zerfass-Thome, K., Spitkovsky, D., Delius, H., Vogt, B., Eilers, M., Hatzigeorgiou, A., and Jansen-Durr, P. (1996) Cell cycle regulation of the murine cyclin E gene depends on an E2F binding site in the promoter. *Mol Cell Biol* **16**, 3401-3409
51. Guichard, P., Hamel, V., Le Guennec, M., Banterle, N., Iacovache, I., Nemcikova, V., Fluckiger, I., Goldie, K. N., Stahlberg, H., Levy, D., Zuber, B., and Gonczy, P. (2017) Cell-free reconstitution reveals centriole cartwheel assembly mechanisms. *Nat Commun* **8**, 14813
52. Zhang, H. S., Postigo, A. A., and Dean, D. C. (1999) Active transcriptional repression by the Rb-E2F complex mediates G1 arrest triggered by p16INK4a, TGFbeta, and contact inhibition. *Cell* **97**, 53-61
53. Yu, Q., and Sicinski, P. (2004) Mammalian cell cycles without cyclin E-CDK2. *Cell cycle (Georgetown, Tex.)* **3**, 292-295
54. Teixeira, L. K., Wang, X., Li, Y., Ekholm-Reed, S., Wu, X., Wang, P., and Reed, S. I. (2015) Cyclin E deregulation promotes loss of specific genomic regions. *Current biology : CB* **25**, 1327-1333
55. Hu, W., Nevzorova, Y. A., Haas, U., Moro, N., Sicinski, P., Geng, Y., Barbacid, M., Trautwein, C., and Liedtke, C. (2014) Concurrent deletion of cyclin E1 and cyclin-dependent kinase 2 in hepatocytes inhibits DNA replication and liver regeneration in mice. *Hepatology (Baltimore, Md.)* **59**, 651-660
56. Okuda, M., Horn, H. F., Tarapore, P., Tokuyama, Y., Smulian, A. G., Chan, P. K., Knudsen, E. S., Hofmann, I. A., Snyder, J. D., Bove, K. E., and Fukasawa, K. (2000)

Nucleophosmin/B23 is a target of CDK2/cyclin E in centrosome duplication. *Cell* **103**, 127-140
57. Sheaff, R. J., Groudine, M., Gordon, M., Roberts, J. M., and Clurman, B. E. (1997) Cyclin E-CDK2 is a regulator of p27Kip1. *Genes & development* **11**, 1464-1478
58. Dealy, M. J., Nguyen, K. V., Lo, J., Gstaiger, M., Krek, W., Elson, D., Arbeit, J., Kipreos, E. T., and Johnson, R. S. (1999) Loss of Cul1 results in early embryonic lethality and dysregulation of cyclin E. *Nature genetics* **23**, 245-248
59. Nakayama, K., Nagahama, H., Minamishima, Y. A., Matsumoto, M., Nakamichi, I., Kitagawa, K., Shirane, M., Tsunematsu, R., Tsukiyama, T., Ishida, N., Kitagawa, M., Nakayama, K., and Hatakeyama, S. (2000) Targeted disruption of Skp2 results in accumulation of cyclin E and p27(Kip1), polyploidy and centrosome overduplication. *The EMBO journal* **19**, 2069-2081
60. Singer, J. D., Gurian-West, M., Clurman, B., and Roberts, J. M. (1999) Cullin-3 targets cyclin E for ubiquitination and controls S phase in mammalian cells. *Genes & development* **13**, 2375-2387
61. Wang, Y., Penfold, S., Tang, X., Hattori, N., Riley, P., Harper, J. W., Cross, J. C., and Tyers, M. (1999) Deletion of the Cul1 gene in mice causes arrest in early embryogenesis and accumulation of cyclin E. *Current biology : CB* **9**, 1191-1194
62. Berthet, C., Aleem, E., Coppola, V., Tessarollo, L., and Kaldis, P. (2003) Cdk2 knockout mice are viable. *Current biology : CB* **13**, 1775-1785
63. Barrière, C., Santamaría, D., Cerqueira, A., Galán, J., Martín, A., Ortega, S., Malumbres, M., Dubus, P., and Barbacid, M. (2007) Mice thrive without Cdk4 and Cdk2. *Molecular oncology* **1**, 72-83
64. Geng, Y., Yu, Q., Sicinska, E., Das, M., Schneider, J. E., Bhattacharya, S., Rideout, W. M., Bronson, R. T., Gardner, H., and Sicinski, P. (2003) Cyclin E ablation in the mouse. *Cell* **114**, 431-443
65. Parisi, T., Beck, A. R., Rougier, N., McNeil, T., Lucian, L., Werb, Z., and Amati, B. (2003) Cyclins E1 and E2 are required for endoreplication in placental trophoblast giant cells. *The EMBO journal* **22**, 4794-4803
66. Connell-Crowley, L., Solomon, M. J., Wei, N., and Harper, J. W. (1993) Phosphorylation independent activation of human cyclin-dependent kinase 2 by cyclin A in vitro. *Molecular biology of the cell* **4**, 79-92
67. Russo, A. A., Jeffrey, P. D., and Pavletich, N. P. (1996) Structural basis of cyclin-dependent kinase activation by phosphorylation. *Nature structural biology* **3**, 696-700
68. Krude, T., Jackman, M., Pines, J., and Laskey, R. A. (1997) Cyclin/Cdk-dependent initiation of DNA replication in a human cell-free system. *Cell* **88**, 109-119
69. Hua, X. H., and Newport, J. (1998) Identification of a preinitiation step in DNA replication that is independent of origin recognition complex and cdc6, but dependent on cdk2. *J Cell Biol* **140**, 271-281
70. Coverley, D., Laman, H., and Laskey, R. A. (2002) Distinct roles for cyclins E and A during DNA replication complex assembly and activation. *Nat Cell Biol* **4**, 523-528
71. Mitra, J., and Enders, G. H. (2004) Cyclin A/Cdk2 complexes regulate activation of Cdk1 and Cdc25 phosphatases in human cells. *Oncogene* **23**, 3361-3367
72. Vigneron, S., Sundermann, L., Labbe, J. C., Pintard, L., Radulescu, O., Castro, A., and Lorca, T. (2018) Cyclin A-cdk1-Dependent Phosphorylation of Bora Is the Triggering Factor Promoting Mitotic Entry. *Developmental cell* **45**, 637-650.e637
73. Dumitru, A. M. G., Rusin, S. F., Clark, A. E. M., Kettenbach, A. N., and Compton, D. A. (2017) Cyclin A/Cdk1 modulates Plk1 activity in prometaphase to regulate kinetochore-microtubule attachment stability. *eLife* **6**

74. Luca, F. C., Shibuya, E. K., Dohrmann, C. E., and Ruderman, J. V. (1991) Both cyclin A delta 60 and B delta 97 are stable and arrest cells in M-phase, but only cyclin B delta 97 turns on cyclin destruction. *The EMBO journal* **10**, 4311-4320
75. Kalaszczynska, I., Geng, Y., Iino, T., Mizuno, S., Choi, Y., Kondratiuk, I., Silver, D. P., Wolgemuth, D. J., Akashi, K., and Sicinski, P. (2009) Cyclin A is redundant in fibroblasts but essential in hematopoietic and embryonic stem cells. *Cell* **138**, 352-365
76. Murphy, M., Stinnakre, M. G., Senamaud-Beaufort, C., Winston, N. J., Sweeney, C., Kubelka, M., Carrington, M., Brechot, C., and Sobczak-Thepot, J. (1997) Delayed early embryonic lethality following disruption of the murine cyclin A2 gene. *Nature genetics* **15**, 83-86
77. Diril, M. K., Ratnacaram, C. K., Padmakumar, V. C., Du, T., Wasser, M., Coppola, V., Tessarollo, L., and Kaldis, P. (2012) Cyclin-dependent kinase 1 (Cdk1) is essential for cell division and suppression of DNA re-replication but not for liver regeneration. *Proceedings of the National Academy of Sciences* **109**, 3826-3831
78. Pines, J., and Hunter, T. (1989) Isolation of a human cyclin cDNA: evidence for cyclin mRNA and protein regulation in the cell cycle and for interaction with p34cdc2. *Cell* **58**, 833-846
79. Brandeis, M., Rosewell, I., Carrington, M., Crompton, T., Jacobs, M. A., Kirk, J., Gannon, J., and Hunt, T. (1998) Cyclin B2-null mice develop normally and are fertile whereas cyclin B1-null mice die in utero. *Proceedings of the National Academy of Sciences of the United States of America* **95**, 4344-4349
80. Ubersax, J. A., Woodbury, E. L., Quang, P. N., Paraz, M., Blethrow, J. D., Shah, K., Shokat, K. M., and Morgan, D. O. (2003) Targets of the cyclin-dependent kinase Cdk1. *Nature* **425**, 859-864
81. Crasta, K., Huang, P., Morgan, G., Winey, M., and Surana, U. (2006) Cdk1 regulates centrosome separation by restraining proteolysis of microtubule-associated proteins. *The EMBO journal* **25**, 2551-2563
82. McHugh, B., and Heck, M. M. (2003) Regulation of chromosome condensation and segregation. *Current opinion in genetics & development* **13**, 185-190
83. Harper, J. W., Burton, J. L., and Solomon, M. J. (2002) The anaphase-promoting complex: it's not just for mitosis any more. *Genes & development* **16**, 2179-2206
84. Peters, J. M. (2002) The anaphase-promoting complex: proteolysis in mitosis and beyond. *Molecular cell* **9**, 931-943
85. Enserink, J. M., and Kolodner, R. D. (2010) An overview of Cdk1-controlled targets and processes. *Cell division* **5**, 11
86. Swaffer, M. P., Jones, A. W., Flynn, H. R., Snijders, A. P., and Nurse, P. (2016) CDK Substrate Phosphorylation and Ordering the Cell Cycle. *Cell* **167**, 1750-1761.e1716
87. Wiesmüller, L., Ford, J. M., and Schiestl, R. H. (2002) DNA Damage, Repair, and Diseases. *Journal of biomedicine & biotechnology* **2**, 45
88. Hartwell, L. H., and Weinert, T. A. (1989) Checkpoints: controls that ensure the order of cell cycle events. *Science* **246**, 629-634
89. Cortez, D., Wang, Y., Qin, J., and Elledge, S. J. (1999) Requirement of ATM-dependent phosphorylation of brca1 in the DNA damage response to double-strand breaks. *Science* **286**, 1162-1166
90. Lim, D. S., Kim, S. T., Xu, B., Maser, R. S., Lin, J., Petrini, J. H., and Kastan, M. B. (2000) ATM phosphorylates p95/nbs1 in an S-phase checkpoint pathway. *Nature* **404**, 613-617
91. Gatei, M., Young, D., Cerosaletti, K. M., Desai-Mehta, A., Spring, K., Kozlov, S., Lavin, M. F., Gatti, R. A., Concannon, P., and Khanna, K. (2000) ATM-dependent

phosphorylation of nibrin in response to radiation exposure. *Nature genetics* **25**, 115-119
92. Bakhoum, S. F., Silkworth, W. T., Nardi, I. K., Nicholson, J. M., Compton, D. A., and Cimini, D. (2014) The mitotic origin of chromosomal instability. *Current biology : CB* **24**, R148-149
93. LaBaer, J., Garrett, M. D., Stevenson, L. F., Slingerland, J. M., Sandhu, C., Chou, H. S., Fattaey, A., and Harlow, E. (1997) New functional activities for the p21 family of CDK inhibitors. *Genes & development* **11**, 847-862
94. Ikeda, Y., Oda, K., Hiraike-Wada, O., Koso, T., Miyasaka, A., Kashiyama, T., Tanikawa, M., Sone, K., Nagasaka, K., Maeda, D., Kawana, K., Nakagawa, S., Fukayama, M., Tetsu, O., Fujii, T., Yano, T., and Kozuma, S. (2013) Cyclin D1 harboring the T286I mutation promotes oncogenic activation in endometrial cancer. *Oncology reports* **30**, 584-588
95. Jeong, S. B., Im, J. H., Yoon, J. H., Bui, Q. T., Lim, S. C., Song, J. M., Shim, Y., Yun, J., Hong, J., and Kang, K. W. (2018) Essential Role of Polo-like Kinase 1 (Plk1) Oncogene in Tumor Growth and Metastasis of Tamoxifen-Resistant Breast Cancer. *Mol Cancer Ther* **17**, 825-837
96. Jackman, J., and O'Connor, P. M. (2001) Methods for synchronizing cells at specific stages of the cell cycle. *Current protocols in cell biology* **Chapter 8**, Unit 8.3
97. Fox, M. H. (2004) Methods for synchronizing mammalian cells. *Methods in molecular biology (Clifton, N.J.)* **241**, 11-16
98. Javanmoghadam-Kamrani, S., and Keyomarsi, K. (2008) Synchronization of the cell cycle using lovastatin. *Cell cycle (Georgetown, Tex.)* **7**, 2434-2440
99. Maréchal, A., and Zou, L. (2013) DNA damage sensing by the ATM and ATR kinases. *Cold Spring Harbor perspectives in biology* **5**
100. Falck, J., Mailand, N., Syljuasen, R. G., Bartek, J., and Lukas, J. (2001) The ATM-Chk2-Cdc25A checkpoint pathway guards against radioresistant DNA synthesis. *Nature* **410**, 842-847
101. Bartek, J., and Lukas, J. (2003) Chk1 and Chk2 kinases in checkpoint control and cancer. *Cancer Cell* **3**, 421-429
102. Donzelli, M., and Draetta, G. F. (2003) Regulating mammalian checkpoints through Cdc25 inactivation. *EMBO reports* **4**, 671-677
103. Morgan, S. E., and Kastan, M. B. (1997) p53 and ATM: cell cycle, cell death, and cancer. *Advances in cancer research* **71**, 1-25
104. Cheng, Q., and Chen, J. (2010) Mechanism of p53 stabilization by ATM after DNA damage. *Cell cycle (Georgetown, Tex.)* **9**, 472-478
105. Tibbetts, R. S., Brumbaugh, K. M., Williams, J. M., Sarkaria, J. N., Cliby, W. A., Shieh, S. Y., Taya, Y., Prives, C., and Abraham, R. T. (1999) A role for ATR in the DNA damage-induced phosphorylation of p53. *Genes & development* **13**, 152-157
106. He, G., Siddik, Z. H., Huang, Z., Wang, R., Koomen, J., Kobayashi, R., Khokhar, A. R., and Kuang, J. (2005) Induction of p21 by p53 following DNA damage inhibits both Cdk4 and Cdk2 activities. *Oncogene* **24**, 2929-2943
107. Benson, E. K., Mungamuri, S. K., Attie, O., Kracikova, M., Sachidanandam, R., Manfredi, J. J., and Aaronson, S. A. (2014) p53-dependent gene repression through p21 is mediated by recruitment of E2F4 repression complexes. *Oncogene* **33**, 3959-3969
108. Diehl, J. A., Zindy, F., and Sherr, C. J. (1997) Inhibition of cyclin D1 phosphorylation on threonine-286 prevents its rapid degradation via the ubiquitin-proteasome pathway. *Genes & development* **11**, 957-972

109. Russo, A. A., Jeffrey, P. D., Patten, A. K., Massague, J., and Pavletich, N. P. (1996) Crystal structure of the p27Kip1 cyclin-dependent-kinase inhibitor bound to the cyclin A-Cdk2 complex. *Nature* **382**, 325-331
110. Roussel, M. F. (1999) The INK4 family of cell cycle inhibitors in cancer. *Oncogene* **18**, 5311-5317
111. Grallert, B., and Boye, E. (2008) The multiple facets of the intra-S checkpoint. *Cell cycle (Georgetown, Tex.)* **7**, 2315-2320
112. Frum, R. A., Chastain, P. D., 2nd, Qu, P., Cohen, S. M., and Kaufman, D. G. (2008) DNA replication in early S phase pauses near newly activated origins. *Cell cycle (Georgetown, Tex.)* **7**, 1440-1448
113. Karnani, N., and Dutta, A. (2011) The effect of the intra-S-phase checkpoint on origins of replication in human cells. *Genes & development* **25**, 621-633
114. Hanks, S. K., and Rao, P. N. (1980) Initiation of DNA synthesis in the prematurely condensed chromosomes of G1 cells. *J Cell Biol* **87**, 285-291
115. Zhou, B. B., and Elledge, S. J. (2000) The DNA damage response: putting checkpoints in perspective. *Nature* **408**, 433-439
116. Friedberg, E. C., Walker, G. C. & Siede, W. . (1995) *DNA Repair and Mutagenesis*, ASM Press, Washington DC
117. Chen, M. S., Ryan, C. E., and Piwnica-Worms, H. (2003) Chk1 kinase negatively regulates mitotic function of Cdc25A phosphatase through 14-3-3 binding. *Mol Cell Biol* **23**, 7488-7497
118. Hassepass, I., Voit, R., and Hoffmann, I. (2003) Phosphorylation at serine 75 is required for UV-mediated degradation of human Cdc25A phosphatase at the S-phase checkpoint. *The Journal of biological chemistry* **278**, 29824-29829
119. Mailand, N., Podtelejnikov, A. V., Groth, A., Mann, M., Bartek, J., and Lukas, J. (2002) Regulation of G(2)/M events by Cdc25A through phosphorylation-dependent modulation of its stability. *The EMBO journal* **21**, 5911-5920
120. Matsuoka, S., Huang, M., and Elledge, S. J. (1998) Linkage of ATM to cell cycle regulation by the Chk2 protein kinase. *Science* **282**, 1893-1897
121. Peng, C. Y., Graves, P. R., Thoma, R. S., Wu, Z., Shaw, A. S., and Piwnica-Worms, H. (1997) Mitotic and G2 checkpoint control: regulation of 14-3-3 protein binding by phosphorylation of Cdc25C on serine-216. *Science* **277**, 1501-1505
122. Schmitt, E., Boutros, R., Froment, C., Monsarrat, B., Ducommun, B., and Dozier, C. (2006) CHK1 phosphorylates CDC25B during the cell cycle in the absence of DNA damage. *J Cell Sci* **119**, 4269-4275
123. Sorensen, C. S., Syljuasen, R. G., Falck, J., Schroeder, T., Ronnstrand, L., Khanna, K. K., Zhou, B. B., Bartek, J., and Lukas, J. (2003) Chk1 regulates the S phase checkpoint by coupling the physiological turnover and ionizing radiation-induced accelerated proteolysis of Cdc25A. *Cancer Cell* **3**, 247-258
124. Uto, K., Inoue, D., Shimuta, K., Nakajo, N., and Sagata, N. (2004) Chk1, but not Chk2, inhibits Cdc25 phosphatases by a novel common mechanism. *The EMBO journal* **23**, 3386-3396
125. Xiao, Z., Chen, Z., Gunasekera, A. H., Sowin, T. J., Rosenberg, S. H., Fesik, S., and Zhang, H. (2003) Chk1 mediates S and G2 arrests through Cdc25A degradation in response to DNA-damaging agents. *The Journal of biological chemistry* **278**, 21767-21773
126. Xu, B., Kim, S. T., Lim, D. S., and Kastan, M. B. (2002) Two molecularly distinct G(2)/M checkpoints are induced by ionizing irradiation. *Mol Cell Biol* **22**, 1049-1059

127. Nyberg, K. A., Michelson, R. J., Putnam, C. W., and Weinert, T. A. (2002) Toward maintaining the genome: DNA damage and replication checkpoints. *Annual review of genetics* **36**, 617-656
128. Russell, K. J., Wiens, L. W., Demers, G. W., Galloway, D. A., Plon, S. E., and Groudine, M. (1995) Abrogation of the G2 checkpoint results in differential radiosensitization of G1 checkpoint-deficient and G1 checkpoint-competent cells. *Cancer Res* **55**, 1639-1642
129. Lindsey-Boltz, L. A., Bermudez, V. P., Hurwitz, J., and Sancar, A. (2001) Purification and characterization of human DNA damage checkpoint Rad complexes. *Proceedings of the National Academy of Sciences* **98**, 11236-11241
130. Mullee, L. I., and Morrison, C. G. (2016) Centrosomes in the DNA damage response--the hub outside the centre. *Chromosome research : an international journal on the molecular, supramolecular and evolutionary aspects of chromosome biology* **24**, 35-51
131. Peng, C. Y., Graves, P. R., Ogg, S., Thoma, R. S., Byrnes, M. J., 3rd, Wu, Z., Stephenson, M. T., and Piwnica-Worms, H. (1998) C-TAK1 protein kinase phosphorylates human Cdc25C on serine 216 and promotes 14-3-3 protein binding. *Cell growth & differentiation : the molecular biology journal of the American Association for Cancer Research* **9**, 197-208
132. Molinari, M., Mercurio, C., Dominguez, J., Goubin, F., and Draetta, G. F. (2000) Human Cdc25 A inactivation in response to S phase inhibition and its role in preventing premature mitosis. *EMBO reports* **1**, 71-79
133. Kumagai, A., and Dunphy, W. G. (1999) Binding of 14-3-3 proteins and nuclear export control the intracellular localization of the mitotic inducer Cdc25. *Genes & development* **13**, 1067-1072
134. Lee, J., Kumagai, A., and Dunphy, W. G. (2001) Positive regulation of Wee1 by Chk1 and 14-3-3 proteins. *Molecular biology of the cell* **12**, 551-563
135. O'Connell, M. J., Raleigh, J. M., Verkade, H. M., and Nurse, P. (1997) Chk1 is a wee1 kinase in the G2 DNA damage checkpoint inhibiting cdc2 by Y15 phosphorylation. *The EMBO journal* **16**, 545-554
136. Lara-Gonzalez, P., Westhorpe, F. G., and Taylor, S. S. (2012) The spindle assembly checkpoint. *Current biology : CB* **22**, R966-980
137. Marcozzi, C., and Pines, J. (2018) Assays for the spindle assembly checkpoint in cell culture. *Methods in cell biology* **144**, 1-13
138. Moyle, M. W., Kim, T., Hattersley, N., Espeut, J., Cheerambathur, D. K., Oegema, K., and Desai, A. (2014) A Bub1–Mad1 interaction targets the Mad1–Mad2 complex to unattached kinetochores to initiate the spindle checkpoint. *The Journal of Cell Biology* **204**, 647-657
139. Zhang, G., Mendez, B. L., Sedgwick, G. G., and Nilsson, J. (2016) Two functionally distinct kinetochore pools of BubR1 ensure accurate chromosome segregation. *Nature Communications* **7**, 12256
140. Overlack, K., Primorac, I., Vleugel, M., Krenn, V., Maffini, S., Hoffmann, I., Kops, G. J., and Musacchio, A. (2015) A molecular basis for the differential roles of Bub1 and BubR1 in the spindle assembly checkpoint. *eLife* **4**, e05269
141. Hwang, L. H., Lau, L. F., Smith, D. L., Mistrot, C. A., Hardwick, K. G., Hwang, E. S., Amon, A., and Murray, A. W. (1998) Budding yeast Cdc20: a target of the spindle checkpoint. *Science* **279**, 1041-1044
142. Baker, D. J., Dawlaty, M. M., Galardy, P., and van Deursen, J. M. (2007) Mitotic regulation of the anaphase-promoting complex. *Cellular and molecular life sciences : CMLS* **64**, 589-600

143. Vanoosthuyse, V., and Hardwick, K. G. (2005) Bub1 and the multilayered inhibition of Cdc20-APC/C in mitosis. *Trends in cell biology* **15**, 231-233
144. Tang, Z., Shu, H., Oncel, D., Chen, S., and Yu, H. (2004) Phosphorylation of Cdc20 by Bub1 provides a catalytic mechanism for APC/C inhibition by the spindle checkpoint. *Molecular cell* **16**, 387-397
145. Uhlmann, F., Lottspelch, F., and Nasmyth, K. (1999) Sister-chromatid separation at anaphase onset is promoted by cleavage of the cohesin subunit Scc1. *Nature* **400**, 37-42
146. Yanagida, M. (2000) Cell cycle mechanisms of sister chromatid separation; roles of Cut1/separin and Cut2/securin. *Genes to cells : devoted to molecular & cellular mechanisms* **5**, 1-8
147. Chestukhin, A., Pfeffer, C., Milligan, S., DeCaprio, J. A., and Pellman, D. (2003) Processing, localization, and requirement of human separase for normal anaphase progression. *Proceedings of the National Academy of Sciences of the United States of America* **100**, 4574-4579
148. Aitken, A. (2006) 14-3-3 proteins: a historic overview. *Seminars in cancer biology* **16**, 162-172
149. Moore, B., Perez, Vj P. . (1967) *Specific acidic proteins of the nervous system.* , Prentice-Hall, Englewood Cliffs, NJ
150. Kleppe, R., Martinez, A., Doskeland, S. O., and Haavik, J. (2011) The 14-3-3 proteins in regulation of cellular metabolism. *Seminars in cell & developmental biology* **22**, 713-719
151. van Hemert, M. J., Steensma, H. Y., and van Heusden, G. P. (2001) 14-3-3 proteins: key regulators of cell division, signalling and apoptosis. *BioEssays : news and reviews in molecular, cellular and developmental biology* **23**, 936-946
152. Dalal, S. N., Yaffe, M. B., and DeCaprio, J. A. (2004) 14-3-3 family members act coordinately to regulate mitotic progression. *Cell cycle (Georgetown, Tex.)* **3**, 672-677
153. Ling, C., Zuo, D., Xue, B., Muthuswamy, S., and Muller, W. J. (2010) A novel role for 14-3-3sigma in regulating epithelial cell polarity. *Genes & development* **24**, 947-956
154. Sehgal, L., Mukhopadhyay, A., Rajan, A., Khapare, N., Sawant, M., Vishal, S. S., Bhatt, K., Ambatipudi, S., Antao, N., Alam, H., Gurjar, M., Basu, S., Mathur, R., Borde, L., Hosing, A. S., Vaidya, M. M., Thorat, R., Samaniego, F., Kolthur-Seetharam, U., and Dalal, S. N. (2014) 14-3-3gamma-Mediated transport of plakoglobin to the cell border is required for the initiation of desmosome assembly in vitro and in vivo. *J Cell Sci* **127**, 2174-2188
155. Tzivion, G., Gupta, V. S., Kaplun, L., and Balan, V. (2006) 14-3-3 proteins as potential oncogenes. *Seminars in cancer biology* **16**, 203-213
156. Freeman, A. K., and Morrison, D. K. (2011) 14-3-3 Proteins: diverse functions in cell proliferation and cancer progression. *Seminars in cell & developmental biology* **22**, 681-687
157. Muslin, A. J., Tanner, J. W., Allen, P. M., and Shaw, A. S. (1996) Interaction of 14-3-3 with signaling proteins is mediated by the recognition of phosphoserine. *Cell* **84**, 889-897
158. Morrison, D. K., Heidecker, G., Rapp, U. R., and Copeland, T. D. (1993) Identification of the major phosphorylation sites of the Raf-1 kinase. *The Journal of biological chemistry* **268**, 17309-17316
159. Aitken, A., Howell, S., Jones, D., Madrazo, J., and Patel, Y. (1995) 14-3-3 alpha and delta are the phosphorylated forms of raf-activating 14-3-3 beta and zeta. In vivo

stoichiometric phosphorylation in brain at a Ser-Pro-Glu-Lys MOTIF. *The Journal of biological chemistry* **270**, 5706-5709
160. Ichimura, T., Isobe, T., Okuyama, T., Takahashi, N., Araki, K., Kuwano, R., and Takahashi, Y. (1988) Molecular cloning of cDNA coding for brain-specific 14-3-3 protein, a protein kinase-dependent activator of tyrosine and tryptophan hydroxylases. *Proceedings of the National Academy of Sciences of the United States of America* **85**, 7084-7088
161. Toker, A., Sellers, L. A., Amess, B., Patel, Y., Harris, A., and Aitken, A. (1992) Multiple isoforms of a protein kinase C inhibitor (KCIP-1/14-3-3) from sheep brain. Amino acid sequence of phosphorylated forms. *European journal of biochemistry* **206**, 453-461
162. Rosenquist, M., Sehnke, P., Ferl, R. J., Sommarin, M., and Larsson, C. (2000) Evolution of the 14-3-3 protein family: does the large number of isoforms in multicellular organisms reflect functional specificity? *Journal of molecular evolution* **51**, 446-458
163. van Heusden, G. P. H., Wenzel, T. J., Lagendijk, E. L., de Steensma, H. Y., and van den Berg, J. A. (1992) Characterization of the yeast BMH1 gene encoding a putative protein homologous to mammalian protein kinase II activators and protein kinase C inhibitors. *FEBS letters* **302**, 145-150
164. Rosenquist, M., Alsterfjord, M., Larsson, C., and Sommarin, M. (2001) Data mining the Arabidopsis genome reveals fifteen 14-3-3 genes. Expression is demonstrated for two out of five novel genes. *Plant physiology* **127**, 142-149
165. van Heusden, G. P., Griffiths, D. J., Ford, J. C., Chin, A. W. T. F., Schrader, P. A., Carr, A. M., and Steensma, H. Y. (1995) The 14-3-3 proteins encoded by the BMH1 and BMH2 genes are essential in the yeast Saccharomyces cerevisiae and can be replaced by a plant homologue. *European journal of biochemistry* **229**, 45-53
166. Prasad, G. L., Valverius, E. M., McDuffie, E., and Cooper, H. L. (1992) Complementary DNA cloning of a novel epithelial cell marker protein, HME1, that may be down-regulated in neoplastic mammary cells. *Cell growth & differentiation : the molecular biology journal of the American Association for Cancer Research* **3**, 507-513
167. Bonnefoy-Bérard, N., Liu, Y. C., von Willebrand, M., Sung, A., Elly, C., Mustelin, T., Yoshida, H., Ishizaka, K., and Altman, A. (1995) Inhibition of phosphatidylinositol 3-kinase activity by association with 14-3-3 proteins in T cells. *Proceedings of the National Academy of Sciences* **92**, 10142-10146
168. Benzinger, A., Popowicz, G. M., Joy, J. K., Majumdar, S., Holak, T. A., and Hermeking, H. (2005) The crystal structure of the non-liganded 14-3-3sigma protein: insights into determinants of isoform specific ligand binding and dimerization. *Cell research* **15**, 219-227
169. Chaudhri, M., Scarabel, M., and Aitken, A. (2003) Mammalian and yeast 14-3-3 isoforms form distinct patterns of dimers in vivo. *Biochemical and biophysical research communications* **300**, 679-685
170. Yang, X., Lee, W. H., Sobott, F., Papagrigoriou, E., Robinson, C. V., Grossmann, J. G., Sundstrom, M., Doyle, D. A., and Elkins, J. M. (2006) Structural basis for protein-protein interactions in the 14-3-3 protein family. *Proceedings of the National Academy of Sciences of the United States of America* **103**, 17237-17242
171. Xiao, B., Smerdon, S. J., Jones, D. H., Dodson, G. G., Soneji, Y., Aitken, A., and Gamblin, S. J. (1995) Structure of a 14-3-3 protein and implications for coordination of multiple signalling pathways. *Nature* **376**, 188-191

172. Liu, D., Bienkowska, J., Petosa, C., Collier, R. J., Fu, H., and Liddington, R. (1995) Crystal structure of the zeta isoform of the 14-3-3 protein. *Nature* **376**, 191-194
173. Rittinger, K., Budman, J., Xu, J., Volinia, S., Cantley, L. C., Smerdon, S. J., Gamblin, S. J., and Yaffe, M. B. (1999) Structural analysis of 14-3-3 phosphopeptide complexes identifies a dual role for the nuclear export signal of 14-3-3 in ligand binding. *Molecular cell* **4**, 153-166
174. Yaffe, M. B. (2002) How do 14-3-3 proteins work?-- Gatekeeper phosphorylation and the molecular anvil hypothesis. *FEBS letters* **513**, 53-57
175. Obsil, T., Ghirlando, R., Klein, D. C., Ganguly, S., and Dyda, F. (2001) Crystal structure of the 14-3-3zeta:serotonin N-acetyltransferase complex. a role for scaffolding in enzyme regulation. *Cell* **105**, 257-267
176. Obsilova, V., Herman, P., Vecer, J., Sulc, M., Teisinger, J., and Obsil, T. (2004) 14-3-3zeta C-terminal stretch changes its conformation upon ligand binding and phosphorylation at Thr232. *The Journal of biological chemistry* **279**, 4531-4540
177. Truong, A. B., Masters, S. C., Yang, H., and Fu, H. (2002) Role of the 14-3-3 C-terminal loop in ligand interaction. *Proteins* **49**, 321-325
178. Wang, W., and Shakes, D. C. (1996) Molecular evolution of the 14-3-3 protein family. *Journal of molecular evolution* **43**, 384-398
179. Bridges, D., and Moorhead, G. B. (2005) 14-3-3 proteins: a number of functions for a numbered protein. *Science's STKE : signal transduction knowledge environment* **2005**, re10
180. Yaffe, M. B., Rittinger, K., Volinia, S., Caron, P. R., Aitken, A., Leffers, H., Gamblin, S. J., Smerdon, S. J., and Cantley, L. C. (1997) The structural basis for 14-3-3:phosphopeptide binding specificity. *Cell* **91**, 961-971
181. Uhart, M., Iglesias, A. A., and Bustos, D. M. (2011) Structurally constrained residues outside the binding motif are essential in the interaction of 14-3-3 and phosphorylated partner. *Journal of molecular biology* **406**, 552-557
182. Brunet, A., Bonni, A., Zigmond, M. J., Lin, M. Z., Juo, P., Hu, L. S., Anderson, M. J., Arden, K. C., Blenis, J., and Greenberg, M. E. (1999) Akt promotes cell survival by phosphorylating and inhibiting a Forkhead transcription factor. *Cell* **96**, 857-868
183. Cahill, C. M., Tzivion, G., Nasrin, N., Ogg, S., Dore, J., Ruvkun, G., and Alexander-Bridges, M. (2001) Phosphatidylinositol 3-kinase signaling inhibits DAF-16 DNA binding and function via 14-3-3-dependent and 14-3-3-independent pathways. *The Journal of biological chemistry* **276**, 13402-13410
184. Zhao, X., Gan, L., Pan, H., Kan, D., Majeski, M., Adam, S. A., and Unterman, T. G. (2004) Multiple elements regulate nuclear/cytoplasmic shuttling of FOXO1: characterization of phosphorylation- and 14-3-3-dependent and -independent mechanisms. *The Biochemical journal* **378**, 839-849
185. Conklin, D. S., Galaktionov, K., and Beach, D. (1995) 14-3-3 proteins associate with cdc25 phosphatases. *Proceedings of the National Academy of Sciences of the United States of America* **92**, 7892-7896
186. Zha, J., Harada, H., Yang, E., Jockel, J., and Korsmeyer, S. J. (1996) Serine phosphorylation of death agonist BAD in response to survival factor results in binding to 14-3-3 not BCL-X(L). *Cell* **87**, 619-628
187. Masters, S. C., Yang, H., Datta, S. R., Greenberg, M. E., and Fu, H. (2001) 14-3-3 inhibits Bad-induced cell death through interaction with serine-136. *Molecular pharmacology* **60**, 1325-1331
188. Coblitz, B., Shikano, S., Wu, M., Gabelli, S. B., Cockrell, L. M., Spieker, M., Hanyu, Y., Fu, H., Amzel, L. M., and Li, M. (2005) C-terminal recognition by 14-3-3 proteins

for surface expression of membrane receptors. *The Journal of biological chemistry* **280**, 36263-36272
189. Wang, B., Yang, H., Liu, Y. C., Jelinek, T., Zhang, L., Ruoslahti, E., and Fu, H. (1999) Isolation of high-affinity peptide antagonists of 14-3-3 proteins by phage display. *Biochemistry* **38**, 12499-12504
190. Campbell, J. K., Gurung, R., Romero, S., Speed, C. J., Andrews, R. K., Berndt, M. C., and Mitchell, C. A. (1997) Activation of the 43 kDa inositol polyphosphate 5-phosphatase by 14-3-3zeta. *Biochemistry* **36**, 15363-15370
191. Baunsgaard, L., Fuglsang, A. T., Jahn, T., Korthout, H. A., de Boer, A. H., and Palmgren, M. G. (1998) The 14-3-3 proteins associate with the plant plasma membrane H(+)-ATPase to generate a fusicoccin binding complex and a fusicoccin responsive system. *The Plant journal : for cell and molecular biology* **13**, 661-671
192. Richter, A., Rose, R., Hedberg, C., Waldmann, H., and Ottmann, C. (2012) An optimised small-molecule stabiliser of the 14-3-3-PMA2 protein-protein interaction. *Chemistry (Weinheim an der Bergstrasse, Germany)* **18**, 6520-6527
193. Rose, R., Erdmann, S., Bovens, S., Wolf, A., Rose, M., Hennig, S., Waldmann, H., and Ottmann, C. (2010) Identification and structure of small-molecule stabilizers of 14-3-3 protein-protein interactions. *Angewandte Chemie (International ed. in English)* **49**, 4129-4132
194. Gu, M., and Du, X. (1998) A novel ligand-binding site in the zeta-form 14-3-3 protein recognizing the platelet glycoprotein Ibalpha and distinct from the c-Raf-binding site. *The Journal of biological chemistry* **273**, 33465-33471
195. Ichimura, T., Uchiyama, J., Kunihiro, O., Ito, M., Horigome, T., Omata, S., Shinkai, F., Kaji, H., and Isobe, T. (1995) Identification of the Site of Interaction of the 14-3-3 Protein with Phosphorylated Tryptophan Hydroxylase. *Journal of Biological Chemistry* **270**, 28515-28518
196. Luo, Z. J., Zhang, X. F., Rapp, U., and Avruch, J. (1995) Identification of the 14.3.3 zeta domains important for self-association and Raf binding. *The Journal of biological chemistry* **270**, 23681-23687
197. Tzivion, G., Luo, Z., and Avruch, J. (1998) A dimeric 14-3-3 protein is an essential cofactor for Raf kinase activity. *Nature* **394**, 88-92
198. Shen, Y. H., Godlewski, J., Bronisz, A., Zhu, J., Comb, M. J., Avruch, J., and Tzivion, G. (2003) Significance of 14-3-3 self-dimerization for phosphorylation-dependent target binding. *Molecular biology of the cell* **14**, 4721-4733
199. Zhang, L., Wang, H., Liu, D., Liddington, R., and Fu, H. (1997) Raf-1 kinase and exoenzyme S interact with 14-3-3zeta through a common site involving lysine 49. *The Journal of biological chemistry* **272**, 13717-13724
200. Brunet, A., Kanai, F., Stehn, J., Xu, J., Sarbassova, D., Frangioni, J. V., Dalal, S. N., DeCaprio, J. A., Greenberg, M. E., and Yaffe, M. B. (2002) 14-3-3 transits to the nucleus and participates in dynamic nucleo-cytoplasmic transport. *J. Cell Biol.* **156**, 817-828
201. Craparo, A., Freund, R., and Gustafson, T. A. (1997) 14-3-3 (ϵ) Interacts with the Insulin-like Growth Factor I Receptor and Insulin Receptor Substrate I in a Phosphoserine-dependent Manner. *Journal of Biological Chemistry* **272**, 11663-11669
202. Ogihara, T., Isobe, T., Ichimura, T., Taoka, M., Funaki, M., Sakoda, H., Onishi, Y., Inukai, K., Anai, M., Fukushima, Y., Kikuchi, M., Yazaki, Y., Oka, Y., and Asano, T. (1997) 14-3-3 protein binds to insulin receptor substrate-1, one of the binding sites of which is in the phosphotyrosine binding domain. *The Journal of biological chemistry* **272**, 25267-25274

203. Liu, Y.-C., Liu, Y., Elly, C., Yoshida, H., Lipkowitz, S., and Altman, A. (1997) Serine Phosphorylation of Cbl Induced by Phorbol Ester Enhances Its Association with 14-3-3 Proteins in T Cells via a Novel Serine-rich 14-3-3-binding Motif. *Journal of Biological Chemistry* **272**, 9979-9985
204. Ku, N. O., Liao, J., and Omary, M. B. (1998) Phosphorylation of human keratin 18 serine 33 regulates binding to 14-3-3 proteins. *The EMBO journal* **17**, 1892-1906
205. Honda, R., Ohba, Y., and Yasuda, H. (1997) 14-3-3 zeta protein binds to the carboxyl half of mouse wee1 kinase. *Biochemical and biophysical research communications* **230**, 262-265
206. Woodcock, J. M., Coolen, C., Goodwin, K. L., Baek, D. J., Bittman, R., Samuel, M. S., Pitson, S. M., and Lopez, A. F. (2015) Destabilisation of dimeric 14-3-3 proteins as a novel approach to anti-cancer therapeutics. *Oncotarget* **6**, 14522-14536
207. Moorhead, G., Douglas, P., Morrice, N., Scarabel, M., Aitken, A., and MacKintosh, C. (1996) Phosphorylated nitrate reductase from spinach leaves is inhibited by 14-3-3 proteins and activated by fusicoccin. *Current biology : CB* **6**, 1104-1113
208. Lambeck, I. C., Fischer-Schrader, K., Niks, D., Roeper, J., Chi, J. C., Hille, R., and Schwarz, G. (2012) Molecular mechanism of 14-3-3 protein-mediated inhibition of plant nitrate reductase. *The Journal of biological chemistry* **287**, 4562-4571
209. Bachmann, M., Huber, J. L., Liao, P. C., Gage, D. A., and Huber, S. C. (1996) The inhibitor protein of phosphorylated nitrate reductase from spinach (Spinacia oleracea) leaves is a 14-3-3 protein. *FEBS letters* **387**, 127-131
210. Obsil, T., and Obsilova, V. (2011) Structural basis of 14-3-3 protein functions. *Seminars in cell & developmental biology* **22**, 663-672
211. Weiner, H., and Kaiser, W. M. (1999) 14-3-3 proteins control proteolysis of nitrate reductase in spinach leaves. *FEBS letters* **455**, 75-78
212. Zhang, L., Chen, J., and Fu, H. (1999) Suppression of apoptosis signal-regulating kinase 1-induced cell death by 14-3-3 proteins. *Proceedings of the National Academy of Sciences* **96**, 8511-8515
213. Petrvalska, O., Kosek, D., Kukacka, Z., Tosner, Z., Man, P., Vecer, J., Herman, P., Obsilova, V., and Obsil, T. (2016) Structural Insight into the 14-3-3 Protein-dependent Inhibition of Protein Kinase ASK1 (Apoptosis Signal-regulating kinase 1). *The Journal of biological chemistry* **291**, 20753-20765
214. Masone, D., Uhart, M., and Bustos, D. M. (2017) On the role of residue phosphorylation in 14-3-3 partners: AANAT as a case study. *Scientific Reports* **7**, 46114
215. Braselmann, S., and McCormick, F. (1995) Bcr and Raf form a complex in vivo via 14-3-3 proteins. *The EMBO journal* **14**, 4839-4848
216. Datta, S. R., Katsov, A., Hu, L., Petros, A., Fesik, S. W., Yaffe, M. B., and Greenberg, M. E. (2000) 14-3-3 proteins and survival kinases cooperate to inactivate BAD by BH3 domain phosphorylation. *Molecular cell* **6**, 41-51
217. Lizcano, J. M., Morrice, N., and Cohen, P. (2000) Regulation of BAD by cAMP-dependent protein kinase is mediated via phosphorylation of a novel site, Ser155. *The Biochemical journal* **349**, 547-557
218. Tan, Y., Demeter, M. R., Ruan, H., and Comb, M. J. (2000) BAD Ser-155 phosphorylation regulates BAD/Bcl-XL interaction and cell survival. *The Journal of biological chemistry* **275**, 25865-25869
219. Li, F. Q., Mofunanya, A., Harris, K., and Takemaru, K. (2008) Chibby cooperates with 14-3-3 to regulate beta-catenin subcellular distribution and signaling activity. *J Cell Biol* **181**, 1141-1154

220. Chene, P. (2001) The role of tetramerization in p53 function. *Oncogene* **20**, 2611-2617
221. Schumacher, B., Mondry, J., Thiel, P., Weyand, M., and Ottmann, C. (2010) Structure of the p53 C-terminus bound to 14-3-3: implications for stabilization of the p53 tetramer. *FEBS letters* **584**, 1443-1448
222. Waterman, M. J., Stavridi, E. S., Waterman, J. L., and Halazonetis, T. D. (1998) ATM-dependent activation of p53 involves dephosphorylation and association with 14-3-3 proteins. *Nature genetics* **19**, 175-178
223. Yang, H. Y., Wen, Y. Y., Chen, C. H., Lozano, G., and Lee, M. H. (2003) 14-3-3 sigma positively regulates p53 and suppresses tumor growth. *Mol Cell Biol* **23**, 7096-7107
224. Rajagopalan, S., Jaulent, A. M., Wells, M., Veprintsev, D. B., and Fersht, A. R. (2008) 14-3-3 activation of DNA binding of p53 by enhancing its association into tetramers. *Nucleic Acids Res* **36**, 5983-5991
225. Graves, P. R., Lovly, C. M., Uy, G. L., and Piwnica-Worms, H. (2001) Localization of human Cdc25C is regulated both by nuclear export and 14-3-3 protein binding. *Oncogene* **20**, 1839-1851
226. Dalal, S. N., Schweitzer, C. M., Gan, J., and DeCaprio, J. A. (1999) Cytoplasmic localization of human cdc25C during interphase requires an intact 14-3-3 binding site. *Mol. Cell. Biol.* **19**, 4465-4479
227. Dansen, T. B., and Burgering, B. M. (2008) Unravelling the tumor-suppressive functions of FOXO proteins. *Trends in cell biology* **18**, 421-429
228. Obsil, T., Ghirlando, R., Anderson, D. E., Hickman, A. B., and Dyda, F. (2003) Two 14-3-3 binding motifs are required for stable association of Forkhead transcription factor FOXO4 with 14-3-3 proteins and inhibition of DNA binding. *Biochemistry* **42**, 15264-15272
229. Rena, G., Prescott, A. R., Guo, S., Cohen, P., and Unterman, T. G. (2001) Roles of the forkhead in rhabdomyosarcoma (FKHR) phosphorylation sites in regulating 14-3-3 binding, transactivation and nuclear targetting. *The Biochemical journal* **354**, 605-612
230. Brownawell, A. M., Kops, G. J., Macara, I. G., and Burgering, B. M. (2001) Inhibition of nuclear import by protein kinase B (Akt) regulates the subcellular distribution and activity of the forkhead transcription factor AFX. *Mol Cell Biol* **21**, 3534-3546
231. Isobe, T., Ichimura, T., Sunaya, T., Okuyama, T., Takahashi, N., Kuwano, R., and Takahashi, Y. (1991) Distinct forms of the protein kinase-dependent activator of tyrosine and tryptophan hydroxylases. *Journal of molecular biology* **217**, 125-132
232. Horie, M., Suzuki, M., Takahashi, E., and Tanigami, A. (1999) Cloning, expression, and chromosomal mapping of the human 14-3-3gamma gene (YWHAG) to 7q11.23. *Genomics* **60**, 241-243
233. Margolis, S. S., Walsh, S., Weiser, D. C., Yoshida, M., Shenolikar, S., and Kornbluth, S. (2003) PP1 control of M phase entry exerted through 14-3-3-regulated Cdc25 dephosphorylation. *The EMBO journal* **22**, 5734-5745
234. Hosing, A. S., Kundu, S. T., and Dalal, S. N. (2008) 14-3-3 Gamma is required to enforce both the incomplete S phase and G2 DNA damage checkpoints. *Cell cycle (Georgetown, Tex.)* **7**, 3171-3179
235. Dar, A., Wu, D., Lee, N., Shibata, E., and Dutta, A. (2014) 14-3-3 proteins play a role in the cell cycle by shielding cdt2 from ubiquitin-mediated degradation. *Mol Cell Biol* **34**, 4049-4061
236. Abbas, T., and Dutta, A. (2011) CRL4Cdt2: master coordinator of cell cycle progression and genome stability. *Cell cycle (Georgetown, Tex.)* **10**, 241-249

237. Furnari, B., Rhind, N., and Russell, P. (1997) Cdc25 mitotic inducer targeted by chk1 DNA damage checkpoint kinase. *Science* **277**, 1495-1497
238. Sanchez, Y., Wong, C., Thoma, R. S., Richman, R., Wu, Z., Piwnica-Worms, H., and Elledge, S. J. (1997) Conservation of the Chk1 checkpoint pathway in mammals: linkage of DNA damage to Cdk regulation through Cdc25. *Science* **277**, 1497-1501
239. Kasahara, K., Goto, H., Enomoto, M., Tomono, Y., Kiyono, T., and Inagaki, M. (2010) 14-3-3gamma mediates Cdc25A proteolysis to block premature mitotic entry after DNA damage. *The EMBO journal* **29**, 2802-2812
240. Vishal, S. S., Tilwani, S., and Dalal, S. N. (2018) Plakoglobin localization to the cell border restores desmosome function in cells lacking 14-3-3gamma. *Biochemical and biophysical research communications* **495**, 1998-2003
241. Han, S. I., Kawano, M. A., Ishizu, K., Watanabe, H., Hasegawa, M., Kanesashi, S. N., Kim, Y. S., Nakanishi, A., Kataoka, K., and Handa, H. (2004) Rep68 protein of adeno-associated virus type 2 interacts with 14-3-3 proteins depending on phosphorylation at serine 535. *Virology* **320**, 144-155
242. Nash, K., Chen, W., Salganik, M., and Muzyczka, N. (2009) Identification of cellular proteins that interact with the adeno-associated virus rep protein. *Journal of virology* **83**, 454-469
243. Autieri, M. V., Haines, D. S., Romanic, A. M., and Ohlstein, E. H. (1996) Expression of 14-3-3 gamma in injured arteries and growth factor- and cytokine-stimulated human vascular smooth muscle cells. *Cell growth & differentiation : the molecular biology journal of the American Association for Cancer Research* **7**, 1453-1460
244. Autieri, M. V., and Carbone, C. J. (1999) 14-3-3Gamma interacts with and is phosphorylated by multiple protein kinase C isoforms in PDGF-stimulated human vascular smooth muscle cells. *DNA and cell biology* **18**, 555-564
245. Stavridi, E. S., Chehab, N. H., Malikzay, A., and Halazonetis, T. D. (2001) Substitutions That Compromise the Ionizing Radiation-induced Association of p53 with 14-3-3 Proteins Also Compromise the Ability of p53 to Induce Cell Cycle Arrest. *Cancer Research* **61**, 7030-7033
246. Rajagopalan, S., Sade, R. S., Townsley, F. M., and Fersht, A. R. (2010) Mechanistic differences in the transcriptional activation of p53 by 14-3-3 isoforms. *Nucleic Acids Res* **38**, 893-906
247. Radhakrishnan, V. M., Putnam, C. W., Qi, W., and Martinez, J. D. (2011) P53 suppresses expression of the 14-3-3 gamma oncogene. *BMC Cancer* **11**, 378
248. Chen, D. Y., Dai, D. F., Hua, Y., and Qi, W. Q. (2015) p53 suppresses 14-3-3gamma by stimulating proteasome-mediated 14-3-3gamma protein degradation. *International journal of oncology* **46**, 818-824
249. Ramteke, M. P., Shelke, P., Ramamoorthy, V., Somavarapu, A. K., Gautam, A. K., Nanaware, P. P., Karanam, S., Mukhopadhyay, S., and Venkatraman, P. (2014) Identification of a novel ATPase activity in 14-3-3 proteins--evidence from enzyme kinetics, structure guided modeling and mutagenesis studies. *FEBS letters* **588**, 71-78
250. Shirakashi, Y., Kawamoto, Y., Tomimoto, H., Takahashi, R., and Ihara, M. (2006) alpha-Synuclein is colocalized with 14-3-3 and synphilin-1 in A53T transgenic mice. *Acta neuropathologica* **112**, 681-689
251. Yacoubian, T. A., Slone, S. R., Harrington, A. J., Hamamichi, S., Schieltz, J. M., Caldwell, K. A., Caldwell, G. A., and Standaert, D. G. (2010) Differential neuroprotective effects of 14-3-3 proteins in models of Parkinson's disease. *Cell death & disease* **1**, e2
252. Muda, K., Bertinetti, D., Gesellchen, F., Hermann, J. S., von Zweydorf, F., Geerlof, A., Jacob, A., Ueffing, M., Gloeckner, C. J., and Herberg, F. W. (2014) Parkinson-

related LRRK2 mutation R1441C/G/H impairs PKA phosphorylation of LRRK2 and disrupts its interaction with 14-3-3. *Proceedings of the National Academy of Sciences of the United States of America* **111**, E34-43
253. Schapansky, J., Khasnavis, S., DeAndrade, M. P., Nardozzi, J. D., Falkson, S. R., Boyd, J. D., Sanderson, J. B., Bartels, T., Melrose, H. L., and LaVoie, M. J. (2018) Familial knockin mutation of LRRK2 causes lysosomal dysfunction and accumulation of endogenous insoluble alpha-synuclein in neurons. *Neurobiology of disease* **111**, 26-35
254. Takahashi, H., Iwata, T., Kitagawa, Y., Takahashi, R. H., Sato, Y., Wakabayashi, H., Takashima, M., Kido, H., Nagashima, K., Kenney, K., Gibbs, C. J., Jr., and Kurata, T. (1999) Increased levels of epsilon and gamma isoforms of 14-3-3 proteins in cerebrospinal fluid in patients with Creutzfeldt-Jakob disease. *Clinical and diagnostic laboratory immunology* **6**, 983-985
255. Van Everbroeck, B. R. J., Boons, J., and Cras, P. (2005) 14-3-3γ isoform detection distinguishes sporadic Creutzfeldt–Jakob disease from other dementias. *Journal of Neurology, Neurosurgery & Psychiatry* **76**, 100-102
256. Zannis-Hadjopoulos, M., Yahyaoui, W., and Callejo, M. (2008) 14-3-3 cruciform-binding proteins as regulators of eukaryotic DNA replication. *Trends in biochemical sciences* **33**, 44-50
257. Brázda, V., Čechová, J., Coufal, J., Rumpel, S., and Jagelská, E. B. (2012) Superhelical DNA as a preferential binding target of 14-3-3γ protein. *Journal of Biomolecular Structure and Dynamics* **30**, 371-378
258. Xu, Z., Fulop, Z., Wu, G., Pone, E. J., Zhang, J., Mai, T., Thomas, L. M., Al-Qahtani, A., White, C. A., Park, S. R., Steinacker, P., Li, Z., Yates, J., 3rd, Herron, B., Otto, M., Zan, H., Fu, H., and Casali, P. (2010) 14-3-3 adaptor proteins recruit AID to 5'-AGCT-3'-rich switch regions for class switch recombination. *Nature structural & molecular biology* **17**, 1124-1135
259. Lam, T., Thomas, L. M., White, C. A., Li, G., Pone, E. J., Xu, Z., and Casali, P. (2013) Scaffold functions of 14-3-3 adaptors in B cell immunoglobulin class switch DNA recombination. *PLoS One* **8**, e80414
260. Raungrut, P., Wongkotsila, A., Lirdprapamongkol, K., Svasti, J., Geater, S. L., Phukaoloun, M., Suwiwat, S., and Thongsuksai, P. (2014) Prognostic significance of 14-3-3gamma overexpression in advanced non-small cell lung cancer. *Asian Pacific journal of cancer prevention : APJCP* **15**, 3513-3518
261. Song, Y., Yang, Z., Ke, Z., Yao, Y., Hu, X., Sun, Y., Li, H., Yin, J., and Zeng, C. (2012) Expression of 14-3-3gamma in patients with breast cancer: correlation with clinicopathological features and prognosis. *Cancer epidemiology* **36**, 533-536
262. Hodgkinson, V. C., Agarwal, V., Elfadl, D., Fox, J. N., McManus, P. L., Mahapatra, T. K., Kneeshaw, P. J., Drew, P. J., Lind, M. J., and Cawkwell, L. (2012) Pilot and feasibility study: comparative proteomic analysis by 2-DE MALDI TOF/TOF MS reveals 14-3-3 proteins as putative biomarkers of response to neoadjuvant chemotherapy in ER-positive breast cancer. *Journal of Proteomics* **75**, 2745-2752
263. Qi, W., Liu, X., Qiao, D., and Martinez, J. D. (2005) Isoform-specific expression of 14-3-3 proteins in human lung cancer tissues. *International journal of cancer* **113**, 359-363
264. Wu, Q., Liu, C. Z., Tao, L. Y., Yu, L., Liu, W., Chen, S. S., and He, X. D. (2012) The clinicopathological and prognostic impact of 14-3-3 protein isoforms expression in human cholangiocarcinoma by immunohistochemistry. *Asian Pacific journal of cancer prevention : APJCP* **13**, 1253-1259

265. Ko, B. S., Lai, I. R., Chang, T. C., Liu, T. A., Chen, S. C., Wang, J., Jan, Y. J., and Liou, J. Y. (2011) Involvement of 14-3-3gamma overexpression in extrahepatic metastasis of hepatocellular carcinoma. *Human pathology* **42**, 129-135
266. Lv, J., Zhu, X., Dong, K., Lin, Y., Hu, Y., and Zhu, C. (2008) Reduced expression of 14-3-3 gamma in uterine leiomyoma as identified by proteomics. *Fertility and Sterility* **90**, 1892-1898
267. Steinacker, P., Schwarz, P., Reim, K., Brechlin, P., Jahn, O., Kratzin, H., Aitken, A., Wiltfang, J., Aguzzi, A., Bahn, E., Baxter, H. C., Brose, N., and Otto, M. (2005) Unchanged survival rates of 14-3-3gamma knockout mice after inoculation with pathological prion protein. *Mol Cell Biol* **25**, 1339-1346
268. Wachi, T., Cornell, B., Marshall, C., Zhukarev, V., Baas, P. W., and Toyo-oka, K. (2016) Ablation of the 14-3-3gamma Protein Results in Neuronal Migration Delay and Morphological Defects in the Developing Cerebral Cortex. *Developmental neurobiology* **76**, 600-614
269. Cornell, B., Wachi, T., Zhukarev, V., and Toyo-Oka, K. (2016) Overexpression of the 14-3-3gamma protein in embryonic mice results in neuronal migration delay in the developing cerebral cortex. *Neurosci Lett* **628**, 40-46
270. Scheer, U. (2014) Historical roots of centrosome research: discovery of Boveri's microscope slides in Würzburg. *Philosophical transactions of the Royal Society of London. Series B, Biological sciences* **369**
271. Rios, R. M. (2014) The centrosome-Golgi apparatus nexus. *Philosophical transactions of the Royal Society of London. Series B, Biological sciences* **369**
272. Arquint, C., Gabryjonczyk, A. M., and Nigg, E. A. (2014) Centrosomes as signalling centres. *Philosophical transactions of the Royal Society of London. Series B, Biological sciences* **369**
273. Stinchcombe, J. C., and Griffiths, G. M. (2014) Communication, the centrosome and the immunological synapse. *Philosophical transactions of the Royal Society of London. Series B, Biological sciences* **369**
274. Reina, J., and Gonzalez, C. (2014) When fate follows age: unequal centrosomes in asymmetric cell division. *Philosophical transactions of the Royal Society of London. Series B, Biological sciences* **369**
275. Nigg, E. A., and Holland, A. J. (2018) Once and only once: mechanisms of centriole duplication and their deregulation in disease. *Nature reviews. Molecular cell biology* **19**, 297-312
276. Tanos, B. E., Yang, H. J., Soni, R., Wang, W. J., Macaluso, F. P., Asara, J. M., and Tsou, M. F. (2013) Centriole distal appendages promote membrane docking, leading to cilia initiation. *Genes & development* **27**, 163-168
277. Uzbekov, R., and Alieva, I. (2018) Who are you, subdistal appendages of centriole? *Open biology* **8**
278. Piel, M., Meyer, P., Khodjakov, A., Rieder, C. L., and Bornens, M. (2000) The respective contributions of the mother and daughter centrioles to centrosome activity and behavior in vertebrate cells. *J Cell Biol* **149**, 317-330
279. Sonnen, K. F., Schermelleh, L., Leonhardt, H., and Nigg, E. A. (2012) 3D-structured illumination microscopy provides novel insight into architecture of human centrosomes. *Biol Open* **1**, 965-976
280. Lawo, S., Hasegan, M., Gupta, G. D., and Pelletier, L. (2012) Subdiffraction imaging of centrosomes reveals higher-order organizational features of pericentriolar material. *Nat Cell Biol* **14**, 1148-1158
281. Mennella, V., Keszthelyi, B., McDonald, K. L., Chhun, B., Kan, F., Rogers, G. C., Huang, B., and Agard, D. A. (2012) Subdiffraction-resolution fluorescence

microscopy reveals a domain of the centrosome critical for pericentriolar material organization. *Nat Cell Biol* **14**, 1159-1168
282. Fu, J., and Glover, D. M. (2012) Structured illumination of the interface between centriole and peri-centriolar material. *Open biology* **2**, 120104
283. Gonczy, P. (2012) Towards a molecular architecture of centriole assembly. *Nature reviews. Molecular cell biology* **13**, 425-435
284. Kitagawa, D., Vakonakis, I., Olieric, N., Hilbert, M., Keller, D., Olieric, V., Bortfeld, M., Erat, M. C., Fluckiger, I., Gonczy, P., and Steinmetz, M. O. (2011) Structural basis of the 9-fold symmetry of centrioles. *Cell* **144**, 364-375
285. Guichard, P., Chretien, D., Marco, S., and Tassin, A. M. (2010) Procentriole assembly revealed by cryo-electron tomography. *The EMBO journal* **29**, 1565-1572
286. Aydogan, M. G., Wainman, A., Saurya, S., Steinacker, T. L., Caballe, A., Novak, Z. A., Baumbach, J., Muschalik, N., and Raff, J. W. (2018) A homeostatic clock sets daughter centriole size in flies. *J Cell Biol* **217**, 1233-1248
287. Lin, Y. C., Chang, C. W., Hsu, W. B., Tang, C. J. C., Lin, Y. N., Chou, E. J., Wu, C. T., and Tang, T. K. (2013) Human microcephaly protein CEP135 binds to hSAS-6 and CPAP, and is required for centriole assembly. *The EMBO journal* **32**, 14
288. Inanç, B., Pütz, M., Lalor, P., Dockery, P., Kuriyama, R., Gergely, F., and Morrison, C. G. (2013) Abnormal centrosomal structure and duplication in Cep135-deficient vertebrate cells. *Molecular biology of the cell* **24**, 2645-2654
289. Greenan, G. A., Keszthelyi, B., Vale, R. D., and Agard, D. A. (2018) Insights into centriole geometry revealed by cryotomography of doublet and triplet centrioles. *eLife* **7**, e36851
290. Winey, M., and O'Toole, E. (2014) Centriole structure. *Philosophical transactions of the Royal Society of London. Series B, Biological sciences* **369**
291. Kim, T. S., Park, J. E., Shukla, A., Choi, S., Murugan, R. N., Lee, J. H., Ahn, M., Rhee, K., Bang, J. K., Kim, B. Y., Loncarek, J., Erikson, R. L., and Lee, K. S. (2013) Hierarchical recruitment of Plk4 and regulation of centriole biogenesis by two centrosomal scaffolds, Cep192 and Cep152. *Proceedings of the National Academy of Sciences of the United States of America* **110**, E4849-4857
292. Dzhindzhev, N. S., Tzolovsky, G., Lipinszki, Z., Abdelaziz, M., Debski, J., Dadlez, M., and Glover, D. M. (2017) Two-step phosphorylation of Ana2 by Plk4 is required for the sequential loading of Ana2 and Sas6 to initiate procentriole formation. *Open biology* **7**
293. Ohta, M., Watanabe, K., Ashikawa, T., Nozaki, Y., Yoshiba, S., Kimura, A., and Kitagawa, D. (2018) Bimodal Binding of STIL to Plk4 Controls Proper Centriole Copy Number. *Cell Reports* **23**, 3160-3169.e3164
294. Leda, M., Holland, A. J., and Goryachev, A. B. (2018) Autoamplification and Competition Drive Symmetry Breaking: Initiation of Centriole Duplication by the PLK4-STIL Network. *iScience* **8**, 222-235
295. Takao, D., Yamamoto, S., and Kitagawa, D. (2018) A theory of centriole duplication based on self-organized spatial pattern formation. *bioRxiv*, 424754
296. Yamamoto, S., and Kitagawa, D. (2018) Self-organization of Plk4 regulates symmetry breaking in centriole duplication. *bioRxiv*, 313635
297. Lin, Y. C., Chang, C. W., Hsu, W. B., Tang, C. J., Lin, Y. N., Chou, E. J., Wu, C. T., and Tang, T. K. (2013) Human microcephaly protein CEP135 binds to hSAS-6 and CPAP, and is required for centriole assembly. *The EMBO journal* **32**, 1141-1154
298. Tang, C. J., Fu, R. H., Wu, K. S., Hsu, W. B., and Tang, T. K. (2009) CPAP is a cell-cycle regulated protein that controls centriole length. *Nat Cell Biol* **11**, 825-831

299. Mariappan, A., Soni, K., Schorpp, K., Zhao, F., Minakar, A., Zheng, X., Mandad, S., Macheleidt, I., Ramani, A., Kubelka, T., Dawidowski, M., Golfmann, K., Wason, A., Yang, C., Simons, J., Schmalz, H. G., Hyman, A. A., Aneja, R., Ullrich, R., Urlaub, H., Odenthal, M., Buttner, R., Li, H., Sattler, M., Hadian, K., and Gopalakrishnan, J. (2019) Inhibition of CPAP-tubulin interaction prevents proliferation of centrosome-amplified cancer cells. *The EMBO journal* **38**
300. Gönczy, P. (2012) Towards a molecular architecture of centriole assembly. *Nature Reviews Molecular Cell Biology* **13**, 11
301. Joo, K., Kim, C. G., Lee, M. S., Moon, H. Y., Lee, S. H., Kim, M. J., Kweon, H. S., Park, W. Y., Kim, C. H., Gleeson, J. G., and Kim, J. (2013) CCDC41 is required for ciliary vesicle docking to the mother centriole. *Proceedings of the National Academy of Sciences of the United States of America* **110**, 5987-5992
302. Sillibourne, J. E., Hurbain, I., Grand-Perret, T., Goud, B., Tran, P., and Bornens, M. (2013) Primary ciliogenesis requires the distal appendage component Cep123. *Biol Open* **2**, 535-545
303. Graser, S., Stierhof, Y. D., Lavoie, S. B., Gassner, O. S., Lamla, S., Le Clech, M., and Nigg, E. A. (2007) Cep164, a novel centriole appendage protein required for primary cilium formation. *J Cell Biol* **179**, 321-330
304. Kodani, A., Salome Sirerol-Piquer, M., Seol, A., Garcia-Verdugo, J. M., and Reiter, J. F. (2013) Kif3a interacts with Dynactin subunit p150 Glued to organize centriole subdistal appendages. *The EMBO journal* **32**, 597-607
305. Ou, Y. Y., Mack, G. J., Zhang, M., and Rattner, J. B. (2002) CEP110 and ninein are located in a specific domain of the centrosome associated with centrosome maturation. *J Cell Sci* **115**, 1825-1835
306. Guarguaglini, G., Duncan, P. I., Stierhof, Y. D., Holmstrom, T., Duensing, S., and Nigg, E. A. (2005) The forkhead-associated domain protein Cep170 interacts with Polo-like kinase 1 and serves as a marker for mature centrioles. *Molecular biology of the cell* **16**, 1095-1107
307. Casenghi, M., Meraldi, P., Weinhart, U., Duncan, P. I., Korner, R., and Nigg, E. A. (2003) Polo-like kinase 1 regulates Nlp, a centrosome protein involved in microtubule nucleation. *Developmental cell* **5**, 113-125
308. Schweizer, S., and Hoyer-Fender, S. (2009) Mouse Odf2 localizes to centrosomes and basal bodies in adult tissues and to the photoreceptor primary cilium. *Cell and tissue research* **338**, 295-301
309. Mazo, G., Soplop, N., Wang, W. J., Uryu, K., and Tsou, M. F. (2016) Spatial Control of Primary Ciliogenesis by Subdistal Appendages Alters Sensation-Associated Properties of Cilia. *Developmental cell* **39**, 424-437
310. Kanie, T., Abbott, K. L., Mooney, N. A., Plowey, E. D., Demeter, J., and Jackson, P. K. (2017) The CEP19-RABL2 GTPase Complex Binds IFT-B to Initiate Intraflagellar Transport at the Ciliary Base. *Developmental cell* **42**, 22-36.e12
311. Schmidt, K. N., Kuhns, S., Neuner, A., Hub, B., Zentgraf, H., and Pereira, G. (2012) Cep164 mediates vesicular docking to the mother centriole during early steps of ciliogenesis. *J Cell Biol* **199**, 1083-1101
312. Ishikawa, H., Kubo, A., Tsukita, S., and Tsukita, S. (2005) Odf2-deficient mother centrioles lack distal/subdistal appendages and the ability to generate primary cilia. *Nat Cell Biol* **7**, 517-524
313. Delgehyr, N., Sillibourne, J., and Bornens, M. (2005) Microtubule nucleation and anchoring at the centrosome are independent processes linked by ninein function. *J Cell Sci* **118**, 1565-1575

314. Bahe, S., Stierhof, Y. D., Wilkinson, C. J., Leiss, F., and Nigg, E. A. (2005) Rootletin forms centriole-associated filaments and functions in centrosome cohesion. *J Cell Biol* **171**, 27-33
315. Vlijm, R., Li, X., Panic, M., Rüthnick, D., Hata, S., Herrmannsdörfer, F., Kuner, T., Heilemann, M., Engelhardt, J., Hell, S. W., and Schiebel, E. (2018) STED nanoscopy of the centrosome linker reveals a CEP68-organized, periodic rootletin network anchored to a C-Nap1 ring at centrioles. *PNAS* **115**, 8
316. He, R., Huang, N., Bao, Y., Zhou, H., Teng, J., and Chen, J. (2013) LRRC45 is a centrosome linker component required for centrosome cohesion. *Cell Rep* **4**, 1100-1107
317. Fry, A. M., Meraldi, P., and Nigg, E. A. (1998) A centrosomal function for the human Nek2 protein kinase, a member of the NIMA family of cell cycle regulators. *The EMBO journal* **17**, 470-481
318. Nigg, E. A., and Stearns, T. (2011) The centrosome cycle: Centriole biogenesis, duplication and inherent asymmetries. *Nat Cell Biol* **13**, 1154-1160
319. Tsou, M. F., Wang, W. J., George, K. A., Uryu, K., Stearns, T., and Jallepalli, P. V. (2009) Polo kinase and separase regulate the mitotic licensing of centriole duplication in human cells. *Developmental cell* **17**, 344-354
320. Matsuo, K., Ohsumi, K., Iwabuchi, M., Kawamata, T., Ono, Y., and Takahashi, M. (2012) Kendrin is a novel substrate for separase involved in the licensing of centriole duplication. *Current biology : CB* **22**, 915-921
321. Lee, K., and Rhee, K. (2012) Separase-dependent cleavage of pericentrin B is necessary and sufficient for centriole disengagement during mitosis. *Cell cycle (Georgetown, Tex.)* **11**, 2476-2485
322. Schockel, L., Mockel, M., Mayer, B., Boos, D., and Stemmann, O. (2011) Cleavage of cohesin rings coordinates the separation of centrioles and chromatids. *Nat Cell Biol* **13**, 966-972
323. Shinmura, K., Tarapore, P., Tokuyama, Y., George, K. R., and Fukasawa, K. (2005) Characterization of centrosomal association of nucleophosmin/B23 linked to Crm1 activity. *FEBS letters* **579**, 6621-6634
324. Peter, M., Nakagawa, J., Doree, M., Labbe, J. C., and Nigg, E. A. (1990) Identification of major nucleolar proteins as candidate mitotic substrates of cdc2 kinase. *Cell* **60**, 791-801
325. Tokuyama, Y., Horn, H. F., Kawamura, K., Tarapore, P., and Fukasawa, K. (2001) Specific phosphorylation of nucleophosmin on Thr(199) by cyclin-dependent kinase 2-cyclin E and its role in centrosome duplication. *The Journal of biological chemistry* **276**, 21529-21537
326. Mukhopadhyay, A., Sehgal, L., Bose, A., Gulvady, A., Senapati, P., Thorat, R., Basu, S., Bhatt, K., Hosing, A. S., Balyan, R., Borde, L., Kundu, T. K., and Dalal, S. N. (2016) 14-3-3 gamma Prevents Centrosome Amplification and Neoplastic Progression. *Sci Rep* **6**, 26580
327. Engle, K. M. M., T-S.; Wasa, M.; Yu, J-Q. (2008) Anomalous centriole configurations are detected in Drosophila wing disc cells upon Cdk1 inactivation. *Accounts of Chemical Research* **45**, 5
328. Gottardo, M., Callaini, G., and Riparbelli, M. G. (2014) Procentriole assembly without centriole disengagement - a paradox of male gametogenesis. *J Cell Sci* **127**, 3434-3439
329. Shukla, A., Kong, D., Sharma, M., Magidson, V., and Loncarek, J. (2015) Plk1 relieves centriole block to reduplication by promoting daughter centriole maturation. *Nat Commun* **6**, 8077

330. Tsou, M. F., and Stearns, T. (2006) Mechanism limiting centrosome duplication to once per cell cycle. *Nature* **442**, 947-951
331. Arquint, C., and Nigg, E. A. (2014) STIL microcephaly mutations interfere with APC/C-mediated degradation and cause centriole amplification. *Current biology : CB* **24**, 351-360
332. Izquierdo, D., Wang, W. J., Uryu, K., and Tsou, M. F. (2014) Stabilization of cartwheel-less centrioles for duplication requires CEP295-mediated centriole-to-centrosome conversion. *Cell Rep* **8**, 957-965
333. Hatch, E. M., Kulukian, A., Holland, A. J., Cleveland, D. W., and Stearns, T. (2010) Cep152 interacts with Plk4 and is required for centriole duplication. *J Cell Biol* **191**, 721-729
334. Wang, W. J., Soni, R. K., Uryu, K., and Tsou, M. F. (2011) The conversion of centrioles to centrosomes: essential coupling of duplication with segregation. *J Cell Biol* **193**, 727-739
335. Bettencourt-Dias, M., Rodrigues-Martins, A., Carpenter, L., Riparbelli, M., Lehmann, L., Gatt, M. K., Carmo, N., Balloux, F., Callaini, G., and Glover, D. M. (2005) SAK/PLK4 Is Required for Centriole Duplication and Flagella Development. *Current Biology* **15**, 9
336. Zitouni, S., Francia, M. E., Leal, F., Montenegro Gouveia, S., Nabais, C., Duarte, P., Gilberto, S., Brito, D., Moyer, T., Kandels-Lewis, S., Ohta, M., Kitagawa, D., Holland, A. J., Karsenti, E., Lorca, T., Lince-Faria, M., and Bettencourt-Dias, M. (2016) CDK1 Prevents Unscheduled PLK4-STIL Complex Assembly in Centriole Biogenesis. *Current biology : CB* **26**, 1127-1137
337. Nakazawa, Y., Hiraki, M., Kamiya, R., and Hirono, M. (2007) SAS-6 is a cartwheel protein that establishes the 9-fold symmetry of the centriole. *Current biology : CB* **17**, 2169-2174
338. Kleylein-Sohn, J., Westendorf, J., Le Clech, M., Habedanck, R., Stierhof, Y. D., and Nigg, E. A. (2007) Plk4-induced centriole biogenesis in human cells. *Developmental cell* **13**, 190-202
339. Schmidt, T. I., Kleylein-Sohn, J., Westendorf, J., Le Clech, M., Lavoie, S. B., Stierhof, Y.-D., and Nigg, E. A. (2009) Control of Centriole Length by CPAP and CP110. *Current Biology* **19**, 1005-1011
340. Azimzadeh, J., Hergert, P., Delouvee, A., Euteneuer, U., Formstecher, E., Khodjakov, A., and Bornens, M. (2009) hPOC5 is a centrin-binding protein required for assembly of full-length centrioles. *J Cell Biol* **185**, 101-114
341. Joukov, V., Walter, J. C., and De Nicolo, A. (2014) The Cep192-organized aurora A-Plk1 cascade is essential for centrosome cycle and bipolar spindle assembly. *Molecular cell* **55**, 578-591
342. Haren, L., Stearns, T., and Luders, J. (2009) Plk1-dependent recruitment of gamma-tubulin complexes to mitotic centrosomes involves multiple PCM components. *PLoS One* **4**, e5976
343. Zhang, X., Chen, Q., Feng, J., Hou, J., Yang, F., Liu, J., Jiang, Q., and Zhang, C. (2009) Sequential phosphorylation of Nedd1 by Cdk1 and Plk1 is required for targeting of the gammaTuRC to the centrosome. *J Cell Sci* **122**, 2240-2251
344. Berdnik, D., and Knoblich, J. A. (2002) Drosophila Aurora-A is required for centrosome maturation and actin-dependent asymmetric protein localization during mitosis. *Current biology : CB* **12**, 640-647
345. Hannak, E., Kirkham, M., Hyman, A. A., and Oegema, K. (2001) Aurora-A kinase is required for centrosome maturation in Caenorhabditis elegans. *J Cell Biol* **155**, 1109-1116

346. Mogensen, M. M., Malik, A., Piel, M., Bouckson-Castaing, V., and Bornens, M. (2000) Microtubule minus-end anchorage at centrosomal and non-centrosomal sites: the role of ninein. *J Cell Sci* **113 (Pt 17)**, 3013-3023
347. Fry, A. M., Mayor, T., Meraldi, P., Stierhof, Y. D., Tanaka, K., and Nigg, E. A. (1998) C-Nap1, a novel centrosomal coiled-coil protein and candidate substrate of the cell cycle-regulated protein kinase Nek2. *J Cell Biol* **141**, 1563-1574
348. Faragher, A. J., and Fry, A. M. (2003) Nek2A kinase stimulates centrosome disjunction and is required for formation of bipolar mitotic spindles. *Molecular biology of the cell* **14**, 2876-2889
349. Pagan, J. K., Marzio, A., Jones, M. J., Saraf, A., Jallepalli, P. V., Florens, L., Washburn, M. P., and Pagano, M. (2015) Degradation of Cep68 and PCNT cleavage mediate Cep215 removal from the PCM to allow centriole separation, disengagement and licensing. *Nat Cell Biol* **17**, 31-43
350. Cole, D. G., Saxton, W. M., Sheehan, K. B., and Scholey, J. M. (1994) A "slow" homotetrameric kinesin-related motor protein purified from Drosophila embryos. *The Journal of biological chemistry* **269**, 22913-22916
351. Sawin, K. E., LeGuellec, K., Philippe, M., and Mitchison, T. J. (1992) Mitotic spindle organization by a plus-end-directed microtubule motor. *Nature* **359**, 540-543
352. Gonczy, P., Pichler, S., Kirkham, M., and Hyman, A. A. (1999) Cytoplasmic dynein is required for distinct aspects of MTOC positioning, including centrosome separation, in the one cell stage Caenorhabditis elegans embryo. *J Cell Biol* **147**, 135-150
353. Tanenbaum, M. E., Macurek, L., Galjart, N., and Medema, R. H. (2008) Dynein, Lis1 and CLIP-170 counteract Eg5-dependent centrosome separation during bipolar spindle assembly. *The EMBO journal* **27**, 3235-3245
354. Wang, L., and Dynlacht, B. D. (2018) The regulation of cilium assembly and disassembly in development and disease. *Development* **145**
355. Ishikawa, T. (2017) Axoneme Structure from Motile Cilia. *Cold Spring Harbor perspectives in biology* **9**
356. Ishikawa, H., and Marshall, W. F. (2017) Intraflagellar Transport and Ciliary Dynamics. *Cold Spring Harbor perspectives in biology* **9**
357. Kollman, J. M., Merdes, A., Mourey, L., and Agard, D. A. (2011) Microtubule nucleation by gamma-tubulin complexes. *Nature reviews. Molecular cell biology* **12**, 709-721
358. Sir, J. H., Putz, M., Daly, O., Morrison, C. G., Dunning, M., Kilmartin, J. V., and Gergely, F. (2013) Loss of centrioles causes chromosomal instability in vertebrate somatic cells. *J Cell Biol* **203**, 747-756
359. Ganem, N. J., Godinho, S. A., and Pellman, D. (2009) A mechanism linking extra centrosomes to chromosomal instability. *Nature* **460**, 278-282
360. Kwon, M., Godinho, S. A., Chandhok, N. S., Ganem, N. J., Azioune, A., Thery, M., and Pellman, D. (2008) Mechanisms to suppress multipolar divisions in cancer cells with extra centrosomes. *Genes & development* **22**, 2189-2203
361. Marthiens, V., Rujano, M. A., Pennetier, C., Tessier, S., Paul-Gilloteaux, P., and Basto, R. (2013) Centrosome amplification causes microcephaly. *Nature cell biology* **15**, 731-740
362. Matsumoto, Y., and Maller, J. L. (2004) A centrosomal localization signal in cyclin E required for Cdk2-independent S phase entry. *Science* **306**, 885-888
363. Ferguson, R. L., Pascreau, G., and Maller, J. L. (2010) The cyclin A centrosomal localization sequence recruits MCM5 and Orc1 to regulate centrosome reduplication. *J Cell Sci* **123**, 2743-2749

364. Hachet, V., Canard, C., and Gönczy, P. (2007) Centrosomes promote timely mitotic entry in C. elegans embryos. *Developmental cell* **12**, 531-541
365. Portier, N., Audhya, A., Maddox, P. S., Green, R. A., Dammermann, A., Desai, A., and Oegema, K. (2007) A microtubule-independent role for centrosomes and aurora a in nuclear envelope breakdown. *Developmental cell* **12**, 515-529
366. Zhao, P., Teng, X., Tantirimudalige, S. N., Nishikawa, M., Wohland, T., Toyama, Y., and Motegi, F. (2019) Aurora-A Breaks Symmetry in Contractile Actomyosin Networks Independently of Its Role in Centrosome Maturation. *Developmental cell* **48**, 631-645.e636
367. Jackman, M., Lindon, C., Nigg, E. A., and Pines, J. (2003) Active cyclin B1-cdk1 first appears on centrosomes in prophase. *Nat. Cell Biol.* **5**, 143-148
368. Doxsey, S., McCollum, D., and Theurkauf, W. (2005) Centrosomes in cellular regulation. *Annual review of cell and developmental biology* **21**, 411-434
369. Araki, M., Masutani, C., Takemura, M., Uchida, A., Sugasawa, K., Kondoh, J., Ohkuma, Y., and Hanaoka, F. (2001) Centrosome protein centrin 2/caltractin 1 is part of the xeroderma pigmentosum group C complex that initiates global genome nucleotide excision repair. *The Journal of biological chemistry* **276**, 18665-18672
370. Dantas, T. J., Wang, Y., Lalor, P., Dockery, P., and Morrison, C. G. (2011) Defective nucleotide excision repair with normal centrosome structures and functions in the absence of all vertebrate centrins. *J Cell Biol* **193**, 307-318
371. Griffith, E., Walker, S., Martin, C. A., Vagnarelli, P., Stiff, T., Vernay, B., Al Sanna, N., Saggar, A., Hamel, B., Earnshaw, W. C., Jeggo, P. A., Jackson, A. P., and O'Driscoll, M. (2008) Mutations in pericentrin cause Seckel syndrome with defective ATR-dependent DNA damage signaling. *Nature genetics* **40**, 232-236
372. Tibelius, A., Marhold, J., Zentgraf, H., Heilig, C. E., Neitzel, H., Ducommun, B., Rauch, A., Ho, A. D., Bartek, J., and Kramer, A. (2009) Microcephalin and pericentrin regulate mitotic entry via centrosome-associated Chk1. *J Cell Biol* **185**, 1149-1157
373. Chaki, M., Airik, R., Ghosh, A. K., Giles, R. H., Chen, R., Slaats, G. G., Wang, H., Hurd, T. W., Zhou, W., Cluckey, A., Gee, H. Y., Ramaswami, G., Hong, C. J., Hamilton, B. A., Cervenka, I., Ganji, R. S., Bryja, V., Arts, H. H., van Reeuwijk, J., Oud, M. M., Letteboer, S. J., Roepman, R., Husson, H., Ibraghimov-Beskrovnaya, O., Yasunaga, T., Walz, G., Eley, L., Sayer, J. A., Schermer, B., Liebau, M. C., Benzing, T., Le Corre, S., Drummond, I., Janssen, S., Allen, S. J., Natarajan, S., O'Toole, J. F., Attanasio, M., Saunier, S., Antignac, C., Koenekoop, R. K., Ren, H., Lopez, I., Nayir, A., Stoetzel, C., Dollfus, H., Massoudi, R., Gleeson, J. G., Andreoli, S. P., Doherty, D. G., Lindstrad, A., Golzio, C., Katsanis, N., Pape, L., Abboud, E. B., Al-Rajhi, A. A., Lewis, R. A., Omran, H., Lee, E. Y., Wang, S., Sekiguchi, J. M., Saunders, R., Johnson, C. A., Garner, E., Vanselow, K., Andersen, J. S., Shlomai, J., Nurnberg, G., Nurnberg, P., Levy, S., Smogorzewska, A., Otto, E. A., and Hildebrandt, F. (2012) Exome capture reveals ZNF423 and CEP164 mutations, linking renal ciliopathies to DNA damage response signaling. *Cell* **150**, 533-548
374. Farina, F., Gaillard, J., Guérin, C., Couté, Y., Sillibourne, J., Blanchoin, L., and Théry, M. (2016) The centrosome is an actin-organizing centre. *Nature cell biology* **18**, 65-75
375. Obino, D., Farina, F., Malbec, O., Saez, P. J., Maurin, M., Gaillard, J., Dingli, F., Loew, D., Gautreau, A., Yuseff, M. I., Blanchoin, L., Thery, M., and Lennon-Dumenil, A. M. (2016) Actin nucleation at the centrosome controls lymphocyte polarity. *Nat Commun* **7**, 10969

376. Farina, F., Ramkumar, N., Brown, L., Samander-Eweis, D., Anstatt, J., Waring, T., Bithell, J., Scita, G., Thery, M., Blanchoin, L., Zech, T., and Baum, B. (2019) Local actin nucleation tunes centrosomal microtubule nucleation during passage through mitosis. *The EMBO journal*
377. Gotlieb, A. I., May, L. M., Subrahmanyan, L., and Kalnins, V. I. (1981) Distribution of microtubule organizing centers in migrating sheets of endothelial cells. *The Journal of Cell Biology* **91**, 589-594
378. Burute, M., Prioux, M., Blin, G., Truchet, S., Letort, G., Tseng, Q., Bessy, T., Lowell, S., Young, J., Filhol, O., and Thery, M. (2017) Polarity Reversal by Centrosome Repositioning Primes Cell Scattering during Epithelial-to-Mesenchymal Transition. *Developmental cell* **40**, 168-184
379. Januschke, J., Llamazares, S., Reina, J., and Gonzalez, C. (2011) Drosophila neuroblasts retain the daughter centrosome. *Nat Commun* **2**, 243
380. Yamashita, Y. M., Mahowald, A. P., Perlin, J. R., and Fuller, M. T. (2007) Asymmetric inheritance of mother versus daughter centrosome in stem cell division. *Science* **315**, 518-521
381. Schnerch, D., and Nigg, E. A. (2016) Structural centrosome aberrations favor proliferation by abrogating microtubule-dependent tissue integrity of breast epithelial mammospheres. *Oncogene* **35**, 2711-2722
382. Ganier, O., Schnerch, D., Oertle, P., Lim, R. Y., Plodinec, M., and Nigg, E. A. (2018) Structural centrosome aberrations promote non-cell-autonomous invasiveness. *The EMBO journal* **37**
383. Nigg, E. A. (2006) Origins and consequences of centrosome aberrations in human cancers. *International journal of cancer* **119**, 2717-2723
384. Godinho, S. A., and Pellman, D. (2014) Causes and consequences of centrosome abnormalities in cancer. *Philosophical transactions of the Royal Society of London. Series B, Biological sciences* **369**
385. Basto, R., Brunk, K., Vinadogrova, T., Peel, N., Franz, A., Khodjakov, A., and Raff, J. W. (2008) Centrosome amplification can initiate tumorigenesis in flies. *Cell* **133**, 1032-1042
386. Castellanos, E., Dominguez, P., and Gonzalez, C. (2008) Centrosome dysfunction in Drosophila neural stem cells causes tumors that are not due to genome instability. *Current biology : CB* **18**, 1209-1214
387. Vitre, B., Holland, A. J., Kulukian, A., Shoshani, O., Hirai, M., Wang, Y., Maldonado, M., Cho, T., Boubaker, J., Swing, D. A., Tessarollo, L., Evans, S. M., Fuchs, E., and Cleveland, D. W. (2015) Chronic centrosome amplification without tumorigenesis. *Proceedings of the National Academy of Sciences of the United States of America* **112**, E6321-6330
388. Coelho, P. A., Bury, L., Shahbazi, M. N., Liakath-Ali, K., Tate, P. H., Wormald, S., Hindley, C. J., Huch, M., Archer, J., Skarnes, W. C., Zernicka-Goetz, M., and Glover, D. M. (2015) Over-expression of Plk4 induces centrosome amplification, loss of primary cilia and associated tissue hyperplasia in the mouse. *Open biology* **5**, 150209
389. Sercin, O., Larsimont, J. C., Karambelas, A. E., Marthiens, V., Moers, V., Boeckx, B., Le Mercier, M., Lambrechts, D., Basto, R., and Blanpain, C. (2016) Transient PLK4 overexpression accelerates tumorigenesis in p53-deficient epidermis. *Nat Cell Biol* **18**, 100-110
390. Levine, M. S., Bakker, B., Boeckx, B., Moyett, J., Lu, J., Vitre, B., Spierings, D. C., Lansdorp, P. M., Cleveland, D. W., Lambrechts, D., Foijer, F., and Holland, A. J. (2017) Centrosome Amplification Is Sufficient to Promote Spontaneous Tumorigenesis in Mammals. *Developmental cell* **40**, 313-322.e315

391. Ring, D., Hubble, R., and Kirschner, M. (1982) Mitosis in a cell with multiple centrioles. *J Cell Biol* **94**, 549-556
392. Dzafic, E., Strzyz, P. J., Wilsch-Brauninger, M., and Norden, C. (2015) Centriole Amplification in Zebrafish Affects Proliferation and Survival but Not Differentiation of Neural Progenitor Cells. *Cell Rep* **13**, 168-182
393. Marthiens, V., Rujano, M. A., Pennetier, C., Tessier, S., Paul-Gilloteaux, P., and Basto, R. (2013) Centrosome amplification causes microcephaly. *Nature Cell Biology* **15**, 731-740
394. Quintyne, N. J., Reing, J. E., Hoffelder, D. R., Gollin, S. M., and Saunders, W. S. (2005) Spindle multipolarity is prevented by centrosomal clustering. *Science (New York, N.Y.)* **307**, 3
395. Cosenza, M. R., Cazzola, A., Rossberg, A., Schieber, N. L., Konotop, G., Bausch, E., Slynko, A., Holland-Letz, T., Raab, M. S., Dubash, T., Glimm, H., Poppelreuther, S., Herold-Mende, C., Schwab, Y., and Kramer, A. (2017) Asymmetric Centriole Numbers at Spindle Poles Cause Chromosome Missegregation in Cancer. *Cell Rep* **20**, 1906-1920
396. Leber, B., Maier, B., Fuchs, F., Chi, J., Riffel, P., Anderhub, S., Wagner, L., Ho, A. D., Salisbury, J. L., Boutros, M., and Kramer, A. (2010) Proteins required for centrosome clustering in cancer cells. *Sci Transl Med* **2**, 33ra38
397. Rhys, A. D., Monteiro, P., Smith, C., Vaghela, M., Arnandis, T., Kato, T., Leitinger, B., Sahai, E., McAinsh, A., Charras, G., and Godinho, S. A. (2018) Loss of E-cadherin provides tolerance to centrosome amplification in epithelial cancer cells. *The Journal of cell biology* **217**, 195-209
398. Navarro-Serer, B., Childers, E. P., Hermance, N. M., Mercadante, D., and Manning, A. L. (2018) Aurora A inhibition limits centrosome clustering and promotes mitotic catastrophe in cells with supernumerary centrosomes. *bioRxiv*, 401661
399. Rebacz, B., Larsen, T. O., Clausen, M. H., Ronnest, M. H., Loffler, H., Ho, A. D., and Kramer, A. (2007) Identification of griseofulvin as an inhibitor of centrosomal clustering in a phenotype-based screen. *Cancer Res* **67**, 6342-6350
400. Konotop, G., Bausch, E., Nagai, T., Turchinovich, A., Becker, N., Benner, A., Boutros, M., Mizuno, K., Kramer, A., and Raab, M. S. (2016) Pharmacological Inhibition of Centrosome Clustering by Slingshot-Mediated Cofilin Activation and Actin Cortex Destabilization. *Cancer Res* **76**, 6690-6700
401. Telles, E., Hosing, A. S., Kundu, S. T., Venkatraman, P., and Dalal, S. N. (2009) A novel pocket in 14-3-3epsilon is required to mediate specific complex formation with cdc25C and to inhibit cell cycle progression upon activation of checkpoint pathways. *Exp Cell Res* **315**, 1448-1457
402. Habedanck, R., Stierhof, Y. D., Wilkinson, C. J., and Nigg, E. A. (2005) The Polo kinase Plk4 functions in centriole duplication. *Nat Cell Biol* **7**, 1140-1146
403. Madeira, F., Tinti, M., Murugesan, G., Berrett, E., Stafford, M., Toth, R., Cole, C., MacKintosh, C., and Barton, G. J. (2015) 14-3-3-Pred: improved methods to predict 14-3-3-binding phosphopeptides. *Bioinformatics (Oxford, England)* **31**, 2276-2283
404. Vishal, S. (2018) *Regulation of cell to cell adhesion and differentiation of spermatogonial stem cells by 14-3-3γ.* PhD, Homi Bhabha National Institute (H.B.N.I.)
405. Neumann, B., Walter, T., Heriche, J. K., Bulkescher, J., Erfle, H., Conrad, C., Rogers, P., Poser, I., Held, M., Liebel, U., Cetin, C., Sieckmann, F., Pau, G., Kabbe, R., Wunsche, A., Satagopam, V., Schmitz, M. H., Chapuis, C., Gerlich, D. W., Schneider, R., Eils, R., Huber, W., Peters, J. M., Hyman, A. A., Durbin, R., Pepperkok, R., and

Ellenberg, J. (2010) Phenotypic profiling of the human genome by time-lapse microscopy reveals cell division genes. *Nature* **464**, 721-727
406. Boukamp, P., Petrussevska, R. T., Breitkreutz, D., Hornung, J., Markham, A., and Fusenig, N. E. (1988) Normal keratinization in a spontaneously immortalized aneuploid human keratinocyte cell line. *J Cell Biol* **106**, 761-771
407. Kundu, S. T., Gosavi, P., Khapare, N., Patel, R., Hosing, A. S., Maru, G. B., Ingle, A., Decaprio, J. A., and Dalal, S. N. (2008) Plakophilin3 downregulation leads to a decrease in cell adhesion and promotes metastasis. *International journal of cancer* **123**, 2303-2314
408. Khapare, N., Kundu, S. T., Sehgal, L., Sawant, M., Priya, R., Gosavi, P., Gupta, N., Alam, H., Karkhanis, M., Naik, N., Vaidya, M. M., and Dalal, S. N. (2012) Plakophilin3 loss leads to an increase in PRL3 levels promoting K8 dephosphorylation, which is required for transformation and metastasis. *PLoS One* **7**, e38561
409. Gosavi, P., Kundu, S. T., Khapare, N., Sehgal, L., Karkhanis, M. S., and Dalal, S. N. (2011) E-cadherin and plakoglobin recruit plakophilin3 to the cell border to initiate desmosome assembly. *Cellular and molecular life sciences : CMLS* **68**, 1439-1454
410. Krek, W., and DeCaprio, J. A. (1995) Cell synchronization. *Methods Enzymol* **254**, 114-124
411. Vassilev, L. T. (2006) Cell cycle synchronization at the G2/M phase border by reversible inhibition of CDK1. *Cell cycle (Georgetown, Tex.)* **5**, 2555-2556
412. Widengren, J., Chmyrov, A., Eggeling, C., Löfdahl, P.-Å., and Seidel, C. A. M. (2007) Strategies to Improve Photostabilities in Ultrasensitive Fluorescence Spectroscopy. *The Journal of Physical Chemistry A* **111**, 429-440
413. Guo, L., and Gai, F. (2013) Simple method to enhance the photostability of the fluorescence reporter R6G for prolonged single-molecule studies. *The journal of physical chemistry. A* **117**, 6164-6170
414. Peel, N., Stevens, N. R., Basto, R., and Raff, J. W. (2007) Overexpressing centriole-replication proteins in vivo induces centriole overduplication and de novo formation. *Current biology : CB* **17**, 834-843
415. Meraldi, P., Honda, R., and Nigg, E. A. (2002) Aurora-A overexpression reveals tetraploidization as a major route to centrosome amplification in p53-/- cells. *The EMBO journal* **21**, 483-492
416. Ohashi, S., Sakashita, G., Ban, R., Nagasawa, M., Matsuzaki, H., Murata, Y., Taniguchi, H., Shima, H., Furukawa, K., and Urano, T. (2006) Phospho-regulation of human protein kinase Aurora-A: analysis using anti-phospho-Thr288 monoclonal antibodies. *Oncogene* **25**, 7691-7702
417. Box, J. K., Paquet, N., Adams, M. N., Boucher, D., Bolderson, E., O'Byrne, K. J., and Richard, D. J. (2016) Nucleophosmin: from structure and function to disease development. *BMC molecular biology* **17**, 19
418. Mitrea, D. M., Grace, C. R., Buljan, M., Yun, M. K., Pytel, N. J., Satumba, J., Nourse, A., Park, C. G., Madan Babu, M., White, S. W., and Kriwacki, R. W. (2014) Structural polymorphism in the N-terminal oligomerization domain of NPM1. *Proceedings of the National Academy of Sciences of the United States of America* **111**, 4466-4471
419. Mukhopadhyay, A. (2012) *REGULATION OF CELL CYCLE CHECKPOINT PATHWAYS BY 14-3-3ε AND 14-3-3γ.* PhD, University of Mumbai
420. Obenauer, J. C., Cantley, L. C., and Yaffe, M. B. (2003) Scansite 2.0: Proteome-wide prediction of cell signaling interactions using short sequence motifs. *Nucleic Acids Res* **31**, 3635-3641

421. Dantas, T. J., Daly, O. M., and Morrison, C. G. (2012) Such small hands: the roles of centrins/caltractins in the centriole and in genome maintenance. *Cellular and molecular life sciences : CMLS* **69**, 2979-2997
422. Salisbury, J. L., Suino, K. M., Busby, R., and Springett, M. (2002) Centrin-2 is required for centriole duplication in mammalian cells. *Current biology : CB* **12**, 1287-1292
423. Paoletti, A., Moudjou, M., Paintrand, M., Salisbury, J. L., and Bornens, M. (1996) Most of centrin in animal cells is not centrosome-associated and centrosomal centrin is confined to the distal lumen of centrioles. *J Cell Sci* **109 (Pt 13)**, 3089-3102
424. Nishi, R., Sakai, W., Tone, D., Hanaoka, F., and Sugasawa, K. (2013) Structure-function analysis of the EF-hand protein centrin-2 for its intracellular localization and nucleotide excision repair. *Nucleic Acids Res* **41**, 6917-6929
425. Acu, I. D., Liu, T., Suino-Powell, K., Mooney, S. M., D'Assoro, A. B., Rowland, N., Muotri, A. R., Correa, R. G., Niu, Y., Kumar, R., and Salisbury, J. L. (2010) Coordination of centrosome homeostasis and DNA repair is intact in MCF-7 and disrupted in MDA-MB 231 breast cancer cells. *Cancer Res* **70**, 3320-3328
426. Tourbez, M., Firanescu, C., Yang, A., Unipan, L., Duchambon, P., Blouquit, Y., and Craescu, C. T. (2004) Calcium-dependent self-assembly of human centrin 2. *The Journal of biological chemistry* **279**, 47672-47680
427. Yang, A., Miron, S., Duchambon, P., Assairi, L., Blouquit, Y., and Craescu, C. T. (2006) The N-terminal domain of human centrin 2 has a closed structure, binds calcium with a very low affinity, and plays a role in the protein self-assembly. *Biochemistry* **45**, 880-889
428. Mukhopadhyay, A., Sehgal, L., Bose, A., Gulvady, A., Parijat, S., Rahul, T., Basu, S., Bhatt, K., Amol S., H., Renu, B., Lalit, B., Tapas K., K., and Dalal, S. N. (2016) 14-3-3γ Prevents Centrosome Amplification and Neoplastic Progression. *Scientific Reports* **6**, 20
429. Fischer, A., Baljuls, A., Reinders, J., Nekhoroshkova, E., Sibilski, C., Metz, R., Albert, S., Rajalingam, K., Hekman, M., and Rapp, U. R. (2009) Regulation of RAF activity by 14-3-3 proteins: RAF kinases associate functionally with both homo- and heterodimeric forms of 14-3-3 proteins. *The Journal of biological chemistry* **284**, 3183-3194
430. Yang, C. H., Kasbek, C., Majumder, S., Yusof, A. M., and Fisk, H. A. (2010) Mps1 phosphorylation sites regulate the function of centrin 2 in centriole assembly. *Molecular biology of the cell* **21**, 4361-4372
431. Conduit, P. T., Wainman, A., and Raff, J. W. (2015) Centrosome function and assembly in animal cells. *Nature reviews. Molecular cell biology* **16**, 611-624
432. Farache, D., Emorine, L., Haren, L., and Merdes, A. (2018) Assembly and regulation of gamma-tubulin complexes. *Open biology* **8**
433. Yuba-Kubo, A., Kubo, A., Hata, M., and Tsukita, S. (2005) Gene knockout analysis of two gamma-tubulin isoforms in mice. *Developmental biology* **282**, 361-373
434. Murphy, S. M., Urbani, L., and Stearns, T. (1998) The mammalian gamma-tubulin complex contains homologues of the yeast spindle pole body components spc97p and spc98p. *J Cell Biol* **141**, 663-674
435. Nakamura, M., and Hashimoto, T. (2009) A mutation in the Arabidopsis gamma-tubulin-containing complex causes helical growth and abnormal microtubule branching. *J Cell Sci* **122**, 2208-2217
436. Draberova, E., D'Agostino, L., Caracciolo, V., Sladkova, V., Sulimenko, T., Sulimenko, V., Sobol, M., Maounis, N. F., Tzelepis, E., Mahera, E., Kren, L., Legido, A., Giordano, A., Mork, S., Hozak, P., Draber, P., and Katsetos, C. D. (2015)

Overexpression and Nucleolar Localization of gamma-Tubulin Small Complex Proteins GCP2 and GCP3 in Glioblastoma. *Journal of neuropathology and experimental neurology* **74**, 723-742
437. Huang, N., Xia, Y., Zhang, D., Wang, S., Bao, Y., He, R., Teng, J., and Chen, J. (2017) Hierarchical assembly of centriole subdistal appendages via centrosome binding proteins CCDC120 and CCDC68. *Nat Commun* **8**, 15057
438. Pillai, S., Nguyen, J., Johnson, J., Haura, E., Coppola, D., and Chellappan, S. (2015) Tank binding kinase 1 is a centrosome-associated kinase necessary for microtubule dynamics and mitosis. *Nat Commun* **6**, 10072
439. Nigg, E. A., and Raff, J. W. (2009) Centrioles, centrosomes, and cilia in health and disease. *Cell* **139**, 663-678
440. Graser, S., Stierhof, Y. D., and Nigg, E. A. (2007) Cep68 and Cep215 (Cdk5rap2) are required for centrosome cohesion. *J Cell Sci* **120**, 4321-4331
441. Vassilev, L. T., Tovar, C., Chen, S., Knezevic, D., Zhao, X., Sun, H., Heimbrook, D. C., and Chen, L. (2006) Selective small-molecule inhibitor reveals critical mitotic functions of human CDK1. *Proceedings of the National Academy of Sciences of the United States of America* **103**, 10660-10665
442. Chen, C. H., Howng, S. L., Cheng, T. S., Chou, M. H., Huang, C. Y., and Hong, Y. R. (2003) Molecular characterization of human ninein protein: two distinct subdomains required for centrosomal targeting and regulating signals in cell cycle. *Biochemical and biophysical research communications* **308**, 975-983
443. Kong, D., Farmer, V., Shukla, A., James, J., Gruskin, R., Kiriyama, S., and Loncarek, J. (2014) Centriole maturation requires regulated Plk1 activity during two consecutive cell cycles. *J Cell Biol* **206**, 855-865
444. Sir, J. H., Pütz, M., Daly, O., Morrison, C. G., Dunning, M., Kilmartin, J. V., and Gergely, F. (2013) Loss of centrioles causes chromosomal instability in vertebrate somatic cells. *Journal of Cell Biology* **203**, 10
445. Quintyne, N. J., Reing, J. E., Hoffelder, D. R., Gollin, S. M., and Saunders, W. S. (2005) Spindle multipolarity is prevented by centrosomal clustering. *Science* **307**, 127-129
446. Mantel, C., Braun, S. E., Reid, S., Henegariu, O., Liu, L., Hangoc, G., and Broxmeyer, H. E. (1999) p21(cip-1/waf-1) deficiency causes deformed nuclear architecture, centriole overduplication, polyploidy, and relaxed microtubule damage checkpoints in human hematopoietic cells. *Blood* **93**, 1390-1398
447. Adon, A. M., Zeng, X., Harrison, M. K., Sannem, S., Kiyokawa, H., Kaldis, P., and Saavedra, H. I. (2010) Cdk2 and Cdk4 regulate the centrosome cycle and are critical mediators of centrosome amplification in p53-null cells. *Mol Cell Biol* **30**, 694-710
448. Matsumoto, Y., Hayashi, K., and Nishida, E. (1999) Cyclin-dependent kinase 2 (Cdk2) is required for centrosome duplication in mammalian cells. *Current biology : CB* **9**, 429-432
449. Shandilya, J., Senapati, P., Dhanasekaran, K., Bangalore, S. S., Kumar, M., Hari Kishore, A., Bhat, A., Kodaganur, G. S., and Kundu, T. K. (2014) Phosphorylation of multifunctional nucleolar protein nucleophosmin (NPM1) by aurora kinase B is critical for mitotic progression. *FEBS letters* **588**, 2198-2205
450. Okuwaki, M., Sumi, A., Hisaoka, M., Saotome-Nakamura, A., Akashi, S., Nishimura, Y., and Nagata, K. (2012) Function of homo- and hetero-oligomers of human nucleoplasmin/nucleophosmin family proteins NPM1, NPM2 and NPM3 during sperm chromatin remodeling. *Nucleic Acids Res* **40**, 4861-4878

451. Cuomo, M. E., Knebel, A., Morrice, N., Paterson, H., Cohen, P., and Mittnacht, S. (2008) p53-Driven apoptosis limits centrosome amplification and genomic instability downstream of NPM1 phosphorylation. *Nat Cell Biol* **10**, 723-730
452. Bose, A., and Dalal, S. N. (2019) 14-3-3 proteins mediate the localization of Centrin2 to centrosome. *Journal of Biosciences* **44**, 42
453. Hamilton, G., Abraham, A. G., Morton, J., Sampson, O., Pefani, D. E., Khoronenkova, S., Grawenda, A., Papaspyropoulos, A., Jamieson, N., McKay, C., Sansom, O., Dianov, G. L., and O'Neill, E. (2014) AKT regulates NPM dependent ARF localization and p53mut stability in tumors. *Oncotarget* **5**, 6142-6167
454. Ma, Z., Kanai, M., Kawamura, K., Kaibuchi, K., Ye, K., and Fukasawa, K. (2006) Interaction between ROCK II and nucleophosmin/B23 in the regulation of centrosome duplication. *Mol Cell Biol* **26**, 9016-9034
455. Chan, J. Y. (2011) A clinical overview of centrosome amplification in human cancers. *International journal of biological sciences* **7**, 1122-1144
456. Marthiens, V., Piel, M., and Basto, R. (2012) Never tear us apart--the importance of centrosome clustering. *J Cell Sci* **125**, 3281-3292
457. Yang, Z., Lončarek, J., Khodjakov, A., and Rieder, C. L. (2008) Extra centrosomes and/or chromosomes prolong mitosis in human cells. *Nature Cell Biology* **8**, 4
458. Mizuguchi, H., Xu, Z., Ishii-Watabe, A., Uchida, E., and Hayakawa, T. (2000) IRES-dependent second gene expression is significantly lower than cap-dependent first gene expression in a bicistronic vector. *Molecular therapy : the journal of the American Society of Gene Therapy* **1**, 376-382
459. Ibrahimi, A., Vande Velde, G., Reumers, V., Toelen, J., Thiry, I., Vandeputte, C., Vets, S., Deroose, C., Bormans, G., Baekelandt, V., Debyser, Z., and Gijsbers, R. (2009) Highly efficient multicistronic lentiviral vectors with peptide 2A sequences. *Human gene therapy* **20**, 845-860
460. Bury, L., Coelho, P. A., Simeone, A., Ferries, S., Eyers, C. E., Eyers, P. A., Zernicka-Goetz, M., and Glover, D. M. (2017) Plk4 and Aurora A cooperate in the initiation of acentriolar spindle assembly in mammalian oocytes. *J Cell Biol* **216**, 3571-3590
461. Cowley, D. O., Rivera-Perez, J. A., Schliekelman, M., He, Y. J., Oliver, T. G., Lu, L., O'Quinn, R., Salmon, E. D., Magnuson, T., and Van Dyke, T. (2009) Aurora-A kinase is essential for bipolar spindle formation and early development. *Mol Cell Biol* **29**, 1059-1071
462. Marumoto, T., Honda, S., Hara, T., Nitta, M., Hirota, T., Kohmura, E., and Saya, H. (2003) Aurora-A kinase maintains the fidelity of early and late mitotic events in HeLa cells. *The Journal of biological chemistry* **278**, 51786-51795
463. Hirota, T., Kunitoku, N., Sasayama, T., Marumoto, T., Zhang, D., Nitta, M., Hatakeyama, K., and Saya, H. (2003) Aurora-A and an interacting activator, the LIM protein Ajuba, are required for mitotic commitment in human cells. *Cell* **114**, 585-598
464. Anand, S., Penrhyn-Lowe, S., and Venkitaraman, A. R. (2003) AURORA-A amplification overrides the mitotic spindle assembly checkpoint, inducing resistance to Taxol. *Cancer Cell* **3**, 51-62
465. Goepfert, T. M., Adigun, Y. E., Zhong, L., Gay, J., Medina, D., and Brinkley, W. R. (2002) Centrosome amplification and overexpression of aurora A are early events in rat mammary carcinogenesis. *Cancer Res* **62**, 4115-4122
466. Kimura, M., Kotani, S., Hattori, T., Sumi, N., Yoshioka, T., Todokoro, K., and Okano, Y. (1997) Cell cycle-dependent expression and spindle pole localization of a novel human protein kinase, Aik, related to Aurora of Drosophila and yeast Ipl1. *The Journal of biological chemistry* **272**, 13766-13771

467. Littlepage, L. E., Wu, H., Andresson, T., Deanehan, J. K., Amundadottir, L. T., and Ruderman, J. V. (2002) Identification of phosphorylated residues that affect the activity of the mitotic kinase Aurora-A. *Proceedings of the National Academy of Sciences of the United States of America* **99**, 15440-15445
468. Dunaway, S., Liu, H. Y., and Walworth, N. C. (2005) Interaction of 14-3-3 protein with Chk1 affects localization and checkpoint function. *J Cell Sci* **118**, 39-50
469. Lutz, W., Lingle, W. L., McCormick, D., Greenwood, T. M., and Salisbury, J. L. (2001) Phosphorylation of centrin during the cell cycle and its role in centriole separation preceding centrosome duplication. *The Journal of biological chemistry* **276**, 20774-20780
470. Dantas, T. J., Daly, O. M., Conroy, P. C., Tomas, M., Wang, Y., Lalor, P., Dockery, P., Ferrando-May, E., and Morrison, C. G. (2013) Calcium-binding capacity of centrin2 is required for linear POC5 assembly but not for nucleotide excision repair. *PLoS One* **8**, e68487
471. Kim, S. Y., Kim, D. S., Hong, J. E., and Park, J. H. (2017) Crystal Structure of Wild-Type Centrin 1 from Mus musculus Occupied by Ca2. *Biochemistry. Biokhimiia* **82**, 1129-1139
472. Klein, U. R., and Nigg, E. A. (2009) SUMO-dependent regulation of centrin-2. *J Cell Sci* **122**, 3312-3321
473. Petry, S., and Vale, R. D. (2015) Microtubule nucleation at the centrosome and beyond. *Nat Cell Biol* **17**, 1089-1093
474. Mayor, T., Stierhof, Y. D., Tanaka, K., Fry, A. M., and Nigg, E. A. (2000) The centrosomal protein C-Nap1 is required for cell cycle-regulated centrosome cohesion. *J Cell Biol* **151**, 837-846
475. Zou, C., Li, J., Bai, Y., Gunning, W. T., Wazer, D. E., Band, V., and Gao, Q. (2005) Centrobin: a novel daughter centriole-associated protein that is required for centriole duplication. *J Cell Biol* **171**, 437-445
476. Godek, K. M., Kabeche, L., and Compton, D. A. (2015) Regulation of kinetochore-microtubule attachments through homeostatic control during mitosis. *Nature reviews. Molecular cell biology* **16**, 57-64
477. Szymiczek, A., Carbone, M., Pastorino, S., Napolitano, A., Tanji, M., Minaai, M., Pagano, I., Mason, J. M., Pass, H. I., Bray, M. R., Mak, T. W., and Yang, H. (2017) Inhibition of the spindle assembly checkpoint kinase Mps-1 as a novel therapeutic strategy in malignant mesothelioma. *Oncogene* **36**, 6501-6507
478. Kwon, M., Godinho, S. A., Chandhok, N. S., Gergely, F., Basto, R., Ganem, N. J., Azioune, A., Thery, M., and Pellman, D. (2008) Mechanisms to suppress multipolar divisions in cancer cells with extra centrosomes. *Genes and Development* **22**, 16
479. Kanai, M., Crowe, M. S., Zheng, Y., Vande Woude, G. F., and Fukasawa, K. (2010) RhoA and RhoC are both required for the ROCK II-dependent promotion of centrosome duplication. *Oncogene* **29**, 6040-6050

J Biosci (2019)44:42
DOI: 10.1007/s12038-019-9867-5

Brief communication

14-3-3 proteins mediate the localization of Centrin2 to centrosome

ARUNABHA BOSE[1,2] and SORAB N DALAL[1,2]*

[1]*KS230, Advanced Centre for Treatment Research and Education in Cancer (ACTREC), Tata Memorial Centre, Kharghar Node, Navi Mumbai 410210, India*

[2]*Homi Bhabha National Institute, Training School complex, Anushakti Nagar, Mumbai 400085, India*

**Corresponding author (Email, sdalal@actrec.gov.in)*

MS received 15 December 2018; accepted 7 March 2019

14-3-3ε and 14-3-3γ localize to the centrosome and regulate centrosome duplication, by inhibiting cdc25C function. As 14-3-3γ and 14-3-3ε form a complex with centrosomal proteins, we asked if this ability was required to regulate centrosome duplication. The results in this report demonstrate that 14-3-3ε and 14-3-3γ form a complex with Centrin2 and that the binding site is located in the N-terminal EF hand in Centrin2, EF1. A Centrin2 mutant that does not form a complex with 14-3-3 proteins displays a punctate cytoplasmic localization and does not localize to the centrosome. These results suggest that in addition to negatively regulating centrosome duplication as previously reported, 14-3-3 proteins might also be required for centriole biogenesis by regulating the localization of Centrin2 at the centrosome.

Keywords. Centrosome; centriole; Centrin2; 14-3-3

1. Introduction

The 14-3-3 protein family comprises a group of small, dimeric, acidic proteins that regulate multiple cellular pathways (Aitken 2006; Tzivion *et al.* 2006; Gardino and Yaffe 2011). 14-3-3 proteins bind to ligands such as cdc25C, Raf-1, IRS-1, via two consensus motifs (modes I and II) containing a phosphorylated serine/threonine residue (Muslin *et al.* 1996; Ogihara *et al.* 1997; Yaffe *et al.* 1997). Alternatively, they also recognize ligands via a phosphorylation independent mode III sequence (Coblitz *et al.* 2005). 14-3-3 proteins can function as molecular scaffolds and association of ligands with 14-3-3 proteins can affect ligand function (Tzivion *et al.* 2001). 14-3-3γ and 14-3-3ε have been demonstrated to localize to centrosomes and the spindle apparatus (Pietromonaco *et al.* 1996) and loss of either 14-3-3ε or 14-3-3γ leads to centrosome amplification (Mukhopadhyay *et al.* 2016).

The centrosome is a membrane-less organelle, which is the primary microtubule organizing centre in mammalian cells (Conduit *et al.* 2015). It consists of a pair of centrioles; the mother centriole and the daughter centriole and a proteinaceous cloud, the pericentriolar matrix (PCM) (reviewed in Azimzadeh and Marshall 2010). The centrosome undergoes a duplication cycle that is coupled with DNA replication. In G1, the mother and daughter centrioles disengage, procentriole synthesis is initiated in S-phase, the new mother centriole acquires distal and sub-distal appendages and procentrioles elongate during G2, and prior to mitosis the two centrosomes migrate to the two poles resulting in formation of the spindle and chromosome segregation (reviewed in Nigg and Holland 2018).

Centrin2, which is the most ubiquitously expressed of the centrin family of proteins (Wolfrum and Salisbury 1998), localizes to the distal end of the centriolar lumen (Paoletti *et al.* 1996) and is absolutely required for centriole duplication (Salisbury *et al.* 2002). Centrin2 is a calcium binding protein and contains four EF hand domains that are essential for calcium binding (Nishi *et al.* 2013). Experiments in different model systems have shown that Centrin2 is essential for basal body development (Dantas *et al.* 2012). Centrin2 is phosphorylated differentially through the cell cycle, and this phosphorylation is said to play a key role in its ability to induce centrosome duplication (Lutz *et al.*

Electronic supplementary material: The online version of this article (https://doi.org/10.1007/s12038-019-9867-5) contains supplementary material, which is available to authorized users.

2001). The N-terminal 25 amino acids of Centrin2 that lie upstream of the EF1 domain are required for self-assembly and this property might be important for the ability of Centrin2 to contribute to centriole formation (Tourbez *et al.* 2004; Yang *et al.* 2006). In addition to the functions required for centrosome formation, Centrin2 mediates nucleotide excision repair through complex formation with XPC (Wood 1996; de Laat *et al.* 1999; Araki *et al.* 2001).

Previous results have demonstrated that 14-3-3ε and 14-3-3γ localize to the centrosome and form a complex with various centrosomal proteins (Pietromonaco *et al.* 1996; Mukhopadhyay *et al.* 2016). The results in this report indicate that these 14-3-3 proteins form a complex with Centrin2 and Centrin2 mutants that do not form a complex with 14-3-3 proteins fail to localize to the centrosome. These results indicate that in addition to negatively regulating centrosome duplication (Mukhopadhyay *et al.* 2016), 14-3-3 proteins might regulate the intra-cellular localization of centrosomal proteins, thus regulating centriole biogenesis.

2. Materials and methods

2.1 *Plasmids and constructs*

All plasmids used in this report are described in supplementary materials and methods.

2.2 *Cell lines and transfection*

The HCT116 cell line was cultured as described previously (Kundu *et al.* 2008). The various EGFP Centrin2 constructs were transfected into HCT116 cells using polyethyleneimine (Polysciences, Inc.). At 48 h post transfection, cells were harvested for western blotting or fixed for immunofluorescence assays as described below. For staining mitotic cells, the cells were synchronized with nocadozole as described (Mukhopadhyay *et al.* 2016). At 18 h post incubation, the nocadozole was removed, cells were allowed to enter mitosis and fixed, stained and imaged using confocal microscopy. For performing live cell imaging, at 48 h post transfection, the cells were treated with nocadozole for 2 h. An hour before imaging, cells were treated with ascorbic acid to reduce phototoxicity. To test the effect of reduced levels of both 14-3-3γ and 14-3-3ε on Centrin2 localization, shRNA constructs designed previously in the laboratory were used (Hosing *et al.* 2008; Telles *et al.* 2009). HCT116 cells were co-transfected with 1 μg of the pTU6-based shRNA constructs, a suitable vector control and EGFP-Centrin2 using Lipofectamine 3000. At 72 h post transfection, the cells were fixed and stained for pericentrin and DAPI and imaged. To count the percentage of mitotic cells with multiple centrosomes, the transfected cells were synchronized with nocadozole as described (Mukhopadhyay *et al.* 2016) and centrosome number determined in three independent experiments.

2.3 *Antibodies and western blotting*

Protein extracts were prepared in SDS sample buffer and protein estimations were performed as described previously (Kundu *et al.* 2008). Details of the antibodies used in this study are provided in supplementary materials and methods.

2.4 *Immunofluorescence and confocal microscopy*

Transfected cells were fixed with 4% paraformaldehyde. The protocol for staining has been previously described (Mukhopadhyay *et al.* 2016). The secondary antibodies used in immunofluorescence assays were conjugated with Alexa Fluor 633 or Alexa Fluor 568, to avoid spectral overlap with GFP. All images were captured using Leica SP8 confocal microscope. Thin sections of 0.8 μm of the entire cell were captured. Images are represented as a projection of the entire Z stack. Cells were imaged at either a 630× magnification with a 4× digital zoom or 1000× with a 4× digital zoom. Images were processed using the Leica LASX software.

2.5 *GST pulldown*

HCT116 cells were transfected with GFP tagged WT or mutant Centrin2 constructs or GFP as a control. At 48 h post transfection, EBC extracts of HCT116 cells were incubated with various GST fusion proteins as indicated. The complexes were resolved on a 10% SDS-PAGE gel and western blotted with antibodies against GFP.

3. Results

3.1 *Centrin2 EF1 is sufficient for complex formation with 14-3-3γ*

Mass spectrometry analysis and fluorescence resonance energy transfer (FRET) assays demonstrated that 14-3-3γ potentially formed a complex with centrosomal proteins (Mukhopadhyay *et al.* 2016). GST pulldown assays demonstrated that 14-3-3γ formed a complex with Centrin2 (figure 1A) and pulldowns for cdc25C (Peng *et al.* 1997), served as a positive control (figure 1A). Centrin2 consists of four EF hand domains and an N-terminal region required for oligomerization (Tourbez *et al.* 2004; Yang *et al.* 2005). To identify the region in Centrin2 required for complex formation with 14-3-3γ, a number of C-terminal domain deletions of Centrin2 were generated and cloned downstream of GFP (figure 1B). The constructs were transfected into HCT116 cells and protein extracts were prepared from the transfected cells and subjected to GST pulldown assays as described in the materials and methods. It was observed that WT GFP-Centrin2 and all the GFP-tagged C terminal deletion mutants formed a complex with 14-3-3γ in contrast

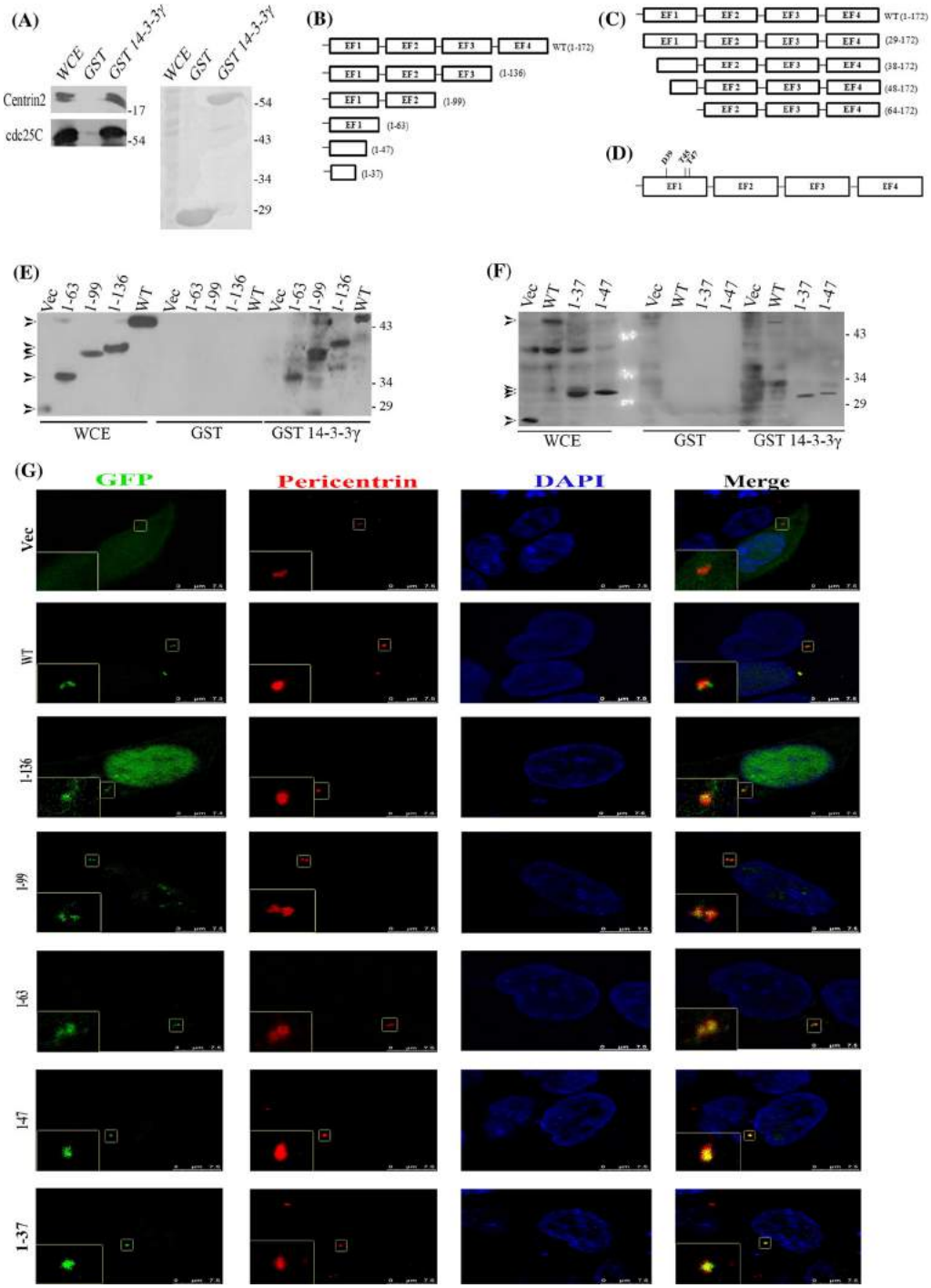

Figure 1. The first EF hand domain of Centrin2 interacts with 14-3-3γ. (**A**) Protein extracts prepared from HCT116 cells were incubated with the indicated GST fusion proteins. The complexes were resolved on 10% SDS-PAGE gels and western blots performed with antibodies against Centrin2 and cdc25C. Note that Centrin2 forms a complex with GST-14-3-3γ but not GST alone. (**B**–**D**) Cartoon of the various Centrin2 mutants used in this study. (**E**, **F**) HCT116 cells were transfected with each of the GFP tagged Centrin2 C-terminal deletion constructs and GFP as a vector control. At 48 h post transfection, EBC extracts of HCT116 cells were incubated with the various GST fusion proteins as indicated. The complexes were resolved on a 10% SDS-PAGE gel and western blotted with antibodies against GFP. Note that the WT and mutant proteins formed a complex with GST-14-3-3γ but not GST alone. Arrows indicate the positions of the GFP fusion proteins and the position of molecular weight markers in kDa is indicated. (**G**) HCT116 cells were transfected with each of the GFP tagged Centrin2 constructs. At 48 h post transfection, the cells were fixed and stained for pericentrin and counterstained with DAPI. The inset is a zoomed image of the box in the main field. Note that the mutant constructs do not show the typical orthogonal arrangement observed with the WT construct. Magnification was a 1000× with 4× digital zoom and scale bars indicate distance in micrometres

to GFP alone (figure 1E). Therefore, we concluded that the N-terminal 63 amino acids of Centrin2 are essential for complex formation with 14-3-3γ. Shorter C-terminal deletions of Centrin2 expressing amino acids 1-37 and 1-47, were tested for their ability to form a complex with 14-3-3γ and it was observed that both 1-37 and 1-47 formed a complex with 14-3-3γ (figure 1F).

In order to assess the localization of the C-terminal mutants of Centrin2, they were transfected in HCT116 cells. Post-transfection, the cells were stained with antibodies to pericentrin and counter-stained with DAPI. It was observed that all the C-terminal mutants localized to the centrosome as demonstrated by their co-localization with pericentrin, in a manner similar to that observed for the WT Centrin2 protein (figure 1G). However, as opposed to what was observed in the WT Centrin2 construct, none of the C-terminal mutants appeared as two (G1 and S phase) or four (G2 and M phase) distinct Centrin2 dots (Paoletti *et al.* 1996). This could imply that the fourth EF hand domain might be involved in the accurate self-assembly of Centrin2 at the centrosome. In addition, one mutant, 1-136, showed a significant enrichment in nuclear localization that was not observed with either the other mutants or the WT protein (figure 1G). This is similar to the localization of only the C terminal region of Centrin2 (aa. 95-172) observed previously (Nishi *et al.* 2013). This region has been implicated in the binding to XPC and the nuclear localization of Centrin2. Nuclear sequestration of Centrin2 is suggested to play a role in the DNA damage response (Acu *et al.* 2010). It is possible that the third EF hand domain of Centrin2 alone is sufficient for its nuclear localization.

3.2 *Deletion of EF1 in Centrin2 abrogates binding with 14-3-3γ and leads to loss of the centrosomal localization of Centrin2*

As the construct with the longest C terminal deletion (1-37) of Centrin2 formed a complex with 14-3-3γ, there were two possibilities. One, that the 14-3-3γ binding site in Centrin2 lies in the first 37 amino acids and second, that there are multiple 14-3-3 binding sites in Centrin2. To test this hypothesis, two types of N-terminal deletion mutants were generated (figure 1C). One lacked the first 28 amino acids (29-172) that are required for the self-assembly of Centrin2 (Tourbez *et al.* 2004; Yang *et al.* 2006). The second type were mutants that had sequential deletions in EF1 or deleted EF1 entirely. These mutants were transfected into HCT116 cells and WT Centrin2 and GFP alone served as positive and negative controls, respectively. GST pull-down assays demonstrated that deletion of the N-terminal region and EF1, abrogated binding to 14-3-3γ (figure 2A). A deletion of the first 28 amino acids (29-172) formed a complex with 14-3-3γ (figure 2A) suggesting that the 14-3-3γ binding site was present in EF1. However, further N-terminal deletions (38-172 and 48-172) formed a complex with 14-3-3γ (figure 2A). These results were surprising as the C-terminal deletion mutants, 1-47 and 1-37, also formed a complex with 14-3-3γ (figure 1F). These results suggest that there might be multiple 14-3-3γ binding sites in the N-terminal 63 amino acids of Centrin2.

The prediction web server (*http://www.compbio.dundee.ac.uk/1433pred*) was used to identify potential 14-3-3 binding sites in Centrin2 (Madeira *et al.* 2015). Two potential 14-3-3 binding sites were identified within EF1 in Centrin2; T45 and T47. The threonine residues that were the putative phosphate acceptors in these potential 14-3-3 binding sites were altered to alanine (T45A and T47A). In addition, we hypothesized that an aspartic acid residue at position 39 (D39) could potentially serve as a phosphomimetic residue in a potential 14-3-3 binding site. This residue was altered to alanine (D39A). All these point mutants were tested for their ability to form a complex with 14-3-3γ in GST pull-down assays. It was observed that all of the point mutants were able to form a complex with 14-3-3γ (figure 2B). A double mutant (T45/47A) also formed a complex with 14-3-3γ (figure 2B). These results suggested that none of these potential 14-3-3γ binding sites in Centrin2 was required for complex formation with 14-3-3γ.

All the N-terminal Centrin2 mutants that formed a complex with 14-3-3γ localized to the centrosome as demonstrated by the observation that the GFP signal co-localized with the pericentrin signal (figure 2C). Interestingly, the organization of these mutants at the centrosome was similar to that of the C-terminal mutants, i.e. unable to form the 2 or 4 dots typical of Centrin2 localization, but accumulated strongly at the centrosome. The single amino acid mutants also localized to the centrosome, in a pattern similar to the full-length construct (supplementary figure 1A). However, the 64-172 mutant that failed to form a complex with 14-3-3γ did not localize to the centrosome or the nucleus (figure 2C) and showed a punctate pattern throughout the cytoplasm. This was observed in all cells transfected with the mutant 64-172 and suggests that 14-3-3γ binding to Centrin2 is required for the localization of Centrin2 to the centrosome.

3.3 *Centrin2 binds to both 14-3-3ε and 14-3-3γ*

Our previous results had indicated that both 14-3-3ε and 14-3-3γ can regulate centrosome duplication and that loss of 14-3-3γ did not lead to a disruption of centrin localization to the centrosome (Mukhopadhyay *et al.* 2016). This raised the possibility that multiple 14-3-3 proteins can bind to Centrin2 and regulate its localization to the centrosome. To test this hypothesis, protein extracts from HCT116 cells were incubated with either GST alone or GST tagged 14-3-3ε or 14-3-3γ, the reactions resolved on SDS-PAGE gels followed by western blotting with antibodies to Centrin2 and cdc25C. As shown in figure 3A, both 14-3-3ε and 14-3-3γ formed a complex with Centrin2. To determine if 14-3-3ε bound to the

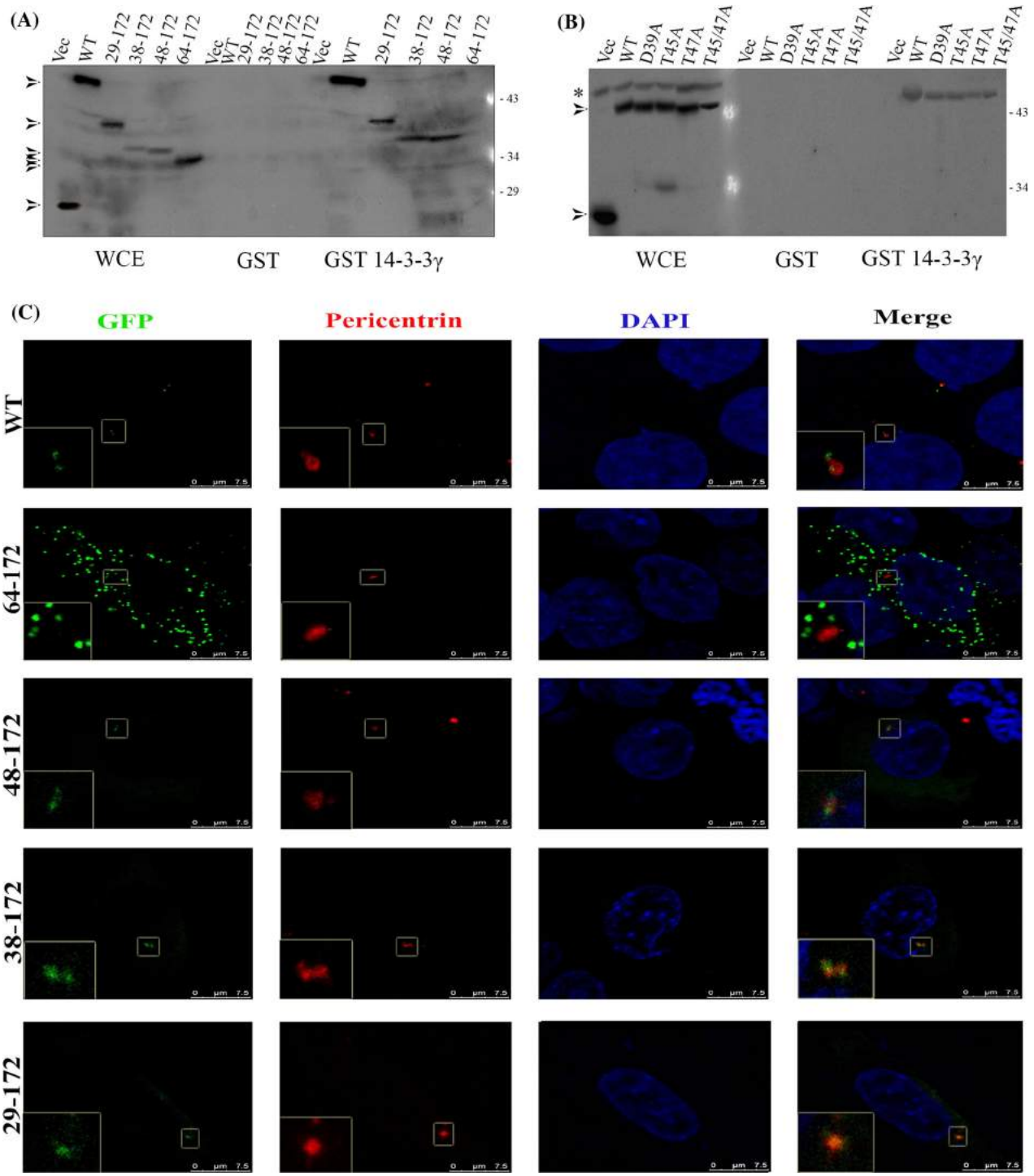

Figure 2. Deletion of the first EF hand domain of Centrin2 abrogates binding with 14-3-3γ and leads to loss of the centrosomal localization of Centrin2. (**A**, **B**) HCT116 cells were transfected with the indicated GFP tagged WT or Centrin2 mutant constructs and GFP as a vector control. At 48 h post transfection, EBC extracts of HCT116 cells were incubated with the various GST fusion proteins as indicated. The complexes were resolved on a 10% SDS-PAGE gel and western blots performed with antibodies against GFP. Note that 64-172 does not form a complex with GST-14-3-3γ in contrast to the WT or other Centrin2 mutants. * Indicates a non-specific band. Arrows indicate the positions of the GFP fusion proteins and the position of molecular weight markers in kDa is indicated. (**C**) HCT116 cells seeded on coverslips were transfected with the GFP tagged WT or mutant Centrin2 constructs. At 48 h post transfection, the cells were fixed and stained for pericentrin and DAPI. The inset is a zoomed image of the box in the main field. Note that the 64-172 construct does not localize to the centrosome unlike the WT or other mutant constructs. The deletion mutants do not show the typical orthogonal arrangement observed with the WT construct. Magnification was a 1000× with 4× digital zoom and scale bars indicate distance in micrometres

same sequence in Centrin2, GFP tagged WT or Centrin2 deletion mutants were transfected into HCT116 cells and the lysates incubated with either GST alone or GST tagged 14-3-3ε or 14-3-3γ, the reactions resolved on SDS-PAGE gels followed by western blotting with antibodies to GFP and β-actin. As shown in figure 3B, both 14-3-3 proteins formed a complex with the 1-63 mutant, but not the 64-172 mutant. These results suggest that both 14-3-3 proteins bind to the same region in Centrin2. Neither of the 14-3-3 proteins bound to β-actin, which served as a negative control.

To determine if loss of 14-3-3ε, 14-3-3γ or both proteins results in a defect in Centrin2 localization, previously characterized shRNA constructs for 14-3-3ε (Telles *et al.* 2009) and 14-3-3γ (Hosing *et al.* 2008) were transfected into HCT116 cells along with GFP-Centrin2. At 72 h post transfection, the cells were stained with antibodies to pericentrin, counter-stained with DAPI and Centrin2 localization determined. Loss of either 14-3-3ε, 14-3-3γ or both proteins did not result in an alteration in the localization of Centrin2 (figure 3C). A decrease in the levels of both proteins was observed in a western blot suggesting that the constructs were functional (figure 3D). In addition, centrosome amplification was observed upon loss of these proteins as previously reported, suggesting that these constructs are functional and the knockdown was effective in inhibiting cdc25C function (Mukhopadhyay *et al.* 2016). Due to the absence of a complete knockdown of both 14-3-3ε and 14-3-3γ, it is possible that sufficient 14-3-3 protein is available to mediate Centrin2 localization. Alternatively, it is possible that Centrin2, like Raf (Fischer *et al.* 2009) binds to all the 14-3-3 isoforms and therefore loss of one ormore isoforms is not sufficient to induce a defect in Centrin2 localization.

3.4 *Centrin2 mutants that do not bind to 14-3-3 proteins do not affect mitotic progression*

Since the 14-3-3 binding deficient mutant of Centrin2 was unable to localize to the centrosome, we wished to determine whether its expression could inhibit spindle formation and mitotic progression. As a first step, we wished to determine if these structures could anchor microtubules. HCT116 cells transfected with either the GFP control, WT Centrin2 or 64-172 mutant constructs were stained with antibodies to pericentrin and α-tubulin. We observed that spindle formation in these cells was comparable to that seen in cells expressing the WT or the vector control constructs (supplementary figure 1B). However, the puncta formed by the 64-172 mutant did not anchor microtubules or serve as spindle poles (supplementary figure 1B). Therefore, expression of a 14-3-3γ binding-deficient mutant of Centrin2 does not interfere with spindle organization. Further, we observed that expression of this mutant has no effect on mitotic timing, with cells expressing both the WT and the 64-172 constructs completing mitosis in ∼40 min (supplementary figure 1C). These results suggest that the 64-172 mutant does not function as a dominant-negative mutant and does not inhibit WT Centrin2 function. These results suggest that 14-3-3γ binds to multiple sites in the first EF hand domain of Centrin2 and that this interaction is required for the accumulation of Centrin2 at the centrosome.

4. Discussion

14-3-3 proteins have been demonstrated to regulate the subcellular localization of their ligands (Dalal *et al.* 1999; Toshima *et al.* 2001; Dunaway *et al.* 2005; Li *et al.* 2008; Vishal *et al.* 2018). The results in this report indicate that 14-3-3 proteins form a complex with Centrin2 and regulate Centrin2 localization to the centrosome. While we have been unable to identify the exact residues in Centrin2 required for 14-3-3 binding, our results indicate that there could be at least two possible regions within Centrin2 that mediate its binding to 14-3-3 proteins; amino acids 29-37 and amino acids 48-63. As there are no consensus 14-3-3 binding sites within either sequence, it is possible that these amino acids form an as yet unreported 14-3-3 binding site and that complex formation is required for the localization of Centrin2 at the centrosome. Alternatively, it is possible that this is not a direct interaction and that the 14-3-3 proteins bind to Centrin2 via another protein or proteins that are required for the recruitment of Centrin2 to the newly synthesized centriole and 14-3-3 proteins and Centrin2 may be part of a multi-protein complex, which might be essential for centriole biogenesis and for the accurate localization of Centrin2 at the centrosome. Therefore, the association between 14-3-3 proteins and Centrin2 might be indirect and depend on proteins that bind to two different domains in Centrin2 leading to the presence of two different regions in Centrin2 that serve as 14-3-3 binding sites.

Multiple reports have attempted to decipher how Centrin2 localizes to the centrosome, given its essential role in centriole biogenesis (Lutz *et al.* 2001; Dantas *et al.* 2013; Nishi *et al.* 2013). Experiments in XP4PASV cells, a human fibroblast cell line deficient for XPC, have demonstrated that three amino acids in EF3 and one amino acid in EF4 of Centrin2 are essential for both, its localization at the centrosome and binding to XPC (Nishi *et al.* 2013). However, all the C-terminal deletion constructs used in this report exhibit an accumulation at the centrosome and co-localize with pericentrin, albeit not in the characteristic 2 or 4 dot organization. It is possible that other factors might bind to the C-terminal end of Centrin2 and mediate the accurate localization of Centrin2 at the centriolar lumen, after it is initially directed to the centrosome. Experiments in chicken DT40 cells suggest that localization of Centrin2 at the centrosome depends upon its binding to calcium, as mutation of the four residues (D41, D77, D114 and D150) essential for calcium binding to alanine, results in a loss of Centrin2 signal at the centriole (Dantas *et al.* 2013). However, we have not observed similar results as the mutant expressing

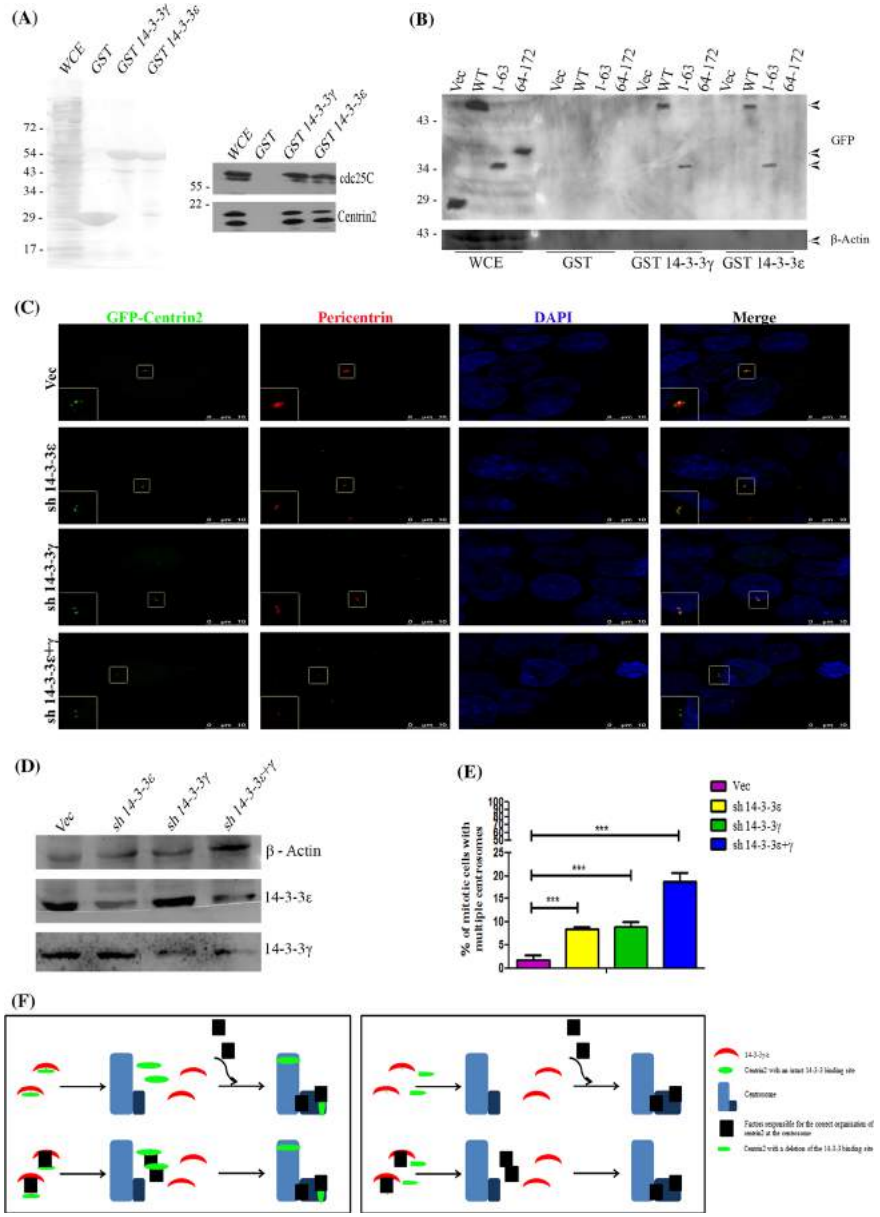

Figure 3. Loss of both 14-3-3ε and 14-3-3γ does not alter the localization of Centrin2. (**A**) Protein extracts from HCT116 cells were incubated with GST, GST-14-3-3ε or GST-14-3-3γ. The reactions were resolved on SDS-PAGE gels followed by western blotting with the indicated antibodies. Note that both 14-3-3ε and 14-3-3γ form a complex with Centrin2. (**B**) HCT116 cells were transfected with the indicated GFP tagged WT or Centrin2 mutant constructs and GFP as a vector control. At 48 h post transfection, EBC extracts of HCT116 cells were incubated with the various GST fusion proteins as indicated. The complexes were resolved on a 10% SDS-PAGE gel and western blots performed with antibodies against GFP or actin. Note that 64-172 does not form a complex with GST-14-3-3ε or GST-14-3-3γ in contrast to the WT or the 1-63 mutant. Arrows indicate the positions of the GFP fusion proteins and the position of molecular weight markers in kDa is indicated. β-Actin serves as a negative control. (**C**, **D**) HCT116 cells seeded on coverslips were transfected with the GFP tagged WT Centrin2 and either the vector control or the indicated 14-3-3 shRNA constructs. At 72 h post transfection, the cells were fixed and stained for pericentrin and DAPI. The inset is a zoomed image of the box in the main field. Magnification was a 630× with 4× digital zoom and scale bars indicate distance in micrometres. Note that loss of both 14-3-3ε and 14-3-3γ does not lead to an alteration in Centrin2 localization. Western blots indicated that the knockdown constructs were effective (**D**). (**E**) HCT116 cells transfected with the indicated shRNA constructs were synchronized in mitosis with nocodazole and centrosome number determined by staining the cells with antibodies to pericentrin and counterstaining with DAPI. Note that loss of either 14-3-3ε or 14-3-3γ leads to centrosome amplification with an additive increase in centrosome amplification when the expression of both genes is inhibited. *** Indicates a p-value <0.001 and all p values were generated using the Student's t-test. (**F**) Model illustrating the significance of 14-3-3γ binding to Centrin2. In cells expressing Centrin2 with an intact 14-3-3 binding site, Centrin2 is targeted to the centrosome via its interaction with 14-3-3 and possibly other proteins. Once it is present at the centrosome, other factors regulate its correct localization at the centrosome. In cells expressing a 14-3-3 binding defective mutant of Centrin2, Centrin2 can no longer be targeted to the centrosome and is thus not observed at the centrosome

the shortest Centrin2 fragment, 1-37, does not possess any of the four calcium binding residues, but still localizes to the centrosome. These differences might reflect minor differences in centriole biogenesis between species. It has been reported that the N-terminus of Centrin1 might form a complex with the C-terminus of Centrin1 (Kim *et al.* 2017), which suggests that the N-terminal mutants of Centrin2 might form a complex with the endogenous Centrin2. However, the entire EF1 domain in Centrin1 is required for dimerization with the C-terminal EF hands in Centrin1 and the 1-37 mutant does not have the entire EF hand. Therefore, it is unlikely that the 1-37 mutant localizes to the centrosome by forming a dimer with the endogenous Centrin2. Further, the 14-3-3γ binding defective mutant, 64-172, showed no nuclear localization. This could be due to the fact that nuclear localization of Centrin2 has been linked to its modification by SUMOylation (Klein and Nigg 2009). Three putative SUMOylation sites are present within the first 64 amino acid region of Centrin2. It is possible that one of these sites could be responsible for SUMOylation and that is why deletion of this region results in loss of its nuclear localization.

Our previous results have demonstrated that 14-3-3ε and 14-3-3γ can inhibit premature centrosome duplication by inhibiting cdc25C function (Mukhopadhyay *et al.* 2016). Cdc25C has a mode I 14-3-3 binding site (Muslin *et al.* 1996; Yaffe *et al.* 1997) and association between cdc25C and 14-3-3 proteins requires an intact serine residue at position 216 (S216) in cdc25C (Peng *et al.* 1997; Dalal *et al.* 1999, 2004). However, while cdc25C binds to only 14-3-3ε and 14-3-3γ (Dalal *et al.* 2004), Raf, which also contains a mode I 14-3-3 binding site forms a complex with all the 14-3-3 isoforms (Fischer *et al.* 2009). Therefore, some redundancy exists in the requirement for 14-3-3 binding to ligands. In this report, we demonstrate that both 14-3-3ε and 14-3-3γ form a complex with Centrin2, however, a decrease in the levels of both proteins does not affect Centrin2 localization but does result in centrosome amplification (figure 3), possibly due to an increase in cdc25C function as previously reported (Mukhopadhyay *et al.* 2016). 14-3-3 proteins bind to Centrin2 via a non-canonical 14-3-3 binding site while they form a complex with cdc25C through a mode I 14-3-3 binding site. Therefore, it is possible that even though the levels of 14-3-3ε and 14-3-3γ are lowered upon the knockdown of these proteins, sufficient protein is available to mediate localization to the centrosome. Alternatively, it is possible that like Raf (Fischer *et al.* 2009), Centrin2 can form a complex with all the 14-3-3 isoforms suggesting that the role of 14-3-3 proteins in regulating the localization of Centrin2 could be shared by multiple 14-3-3 isoforms. This redundancy is consistent with the observation that Centrin2 is essential for centrosome duplication and cell viability (Salisbury *et al.* 2002). Therefore, multiple 14-3-3 proteins might be required to regulate the localization of Centrin2 to the centrosome.

On the basis of our results, we propose the following model (figure 3F). We have demonstrated previously, that 14-3-3ε and 14-3-3γ localize to the centrosome (Mukhopadhyay *et al.* 2016). In cells expressing Centrin2 with an intact 14-3-3 binding site, Centrin2 is targeted to the centrosome via its binding to 14-3-3γ. Once there, it self assembles at the centriole permitting centriole biogenesis. Given that mutation of all potential phosphorylated residues in EF1 that could serve as 14-3-3 binding sites does not abolish complex formation with 14-3-3 proteins, it is possible that the interaction between 14-3-3 proteins and Centrin2 is either independent of phosphorylation or complex formation between 14-3-3 proteins and Centrin2 is dependent on other proteins required for centriole biogenesis. Once it is present at the centrosome, presumably, other factors which might bind to the C-terminal region of Centrin2, direct the organization of Centrin2 to form the centriolar lumen. In cells expressing a mutant of Centrin2 that either fails to form a complex with 14-3-3 proteins or an adaptor protein that bridges the interaction with 14-3-3 proteins, 14-3-3ε and 14-3-3γ are no longer able to target either Centrin2 or the Centrin2 protein complex to the centrosome resulting in the absence of Centrin2 at the centrosome. Thus, in addition to inhibiting premature centrosome duplication in late S and G2 phase by inactivating cdc25C function (Mukhopadhyay *et al.* 2016), 14-3-3ε and 14-3-3γ might promote centriole biogenesis by mediating the localization of Centrin2 to the centrosome.

Acknowledgements

We thank Dr Erich Nigg, for his kind gift of the EGFP C2 Centrin2 construct and the ACTREC microscopy facility for help with the imaging experiments in this report. The work was funded by grants from the Department of Biotechnology, Govt. of India (BT/PR4181/BRB/10/1147/2012 and BT/PR8351/MED/30/995/2013) to SND.

References

Acu ID, Liu T, Suino-Powell K, Mooney SM, D'Assoro AB, Rowland N, Muotri AR, Correa RG, Niu Y, Kumar R and Salisbury JL 2010 Coordination of centrosome homeostasis and DNA repair is intact in MCF-7 and disrupted in MDA-MB 231 breast cancer cells. *Cancer Res.* **70** 3320–3328

Aitken A 2006 14-3-3 proteins: A historic overview. *Semin. Cancer Biol.* **16** 162–172

Araki M, Masutani C, Takemura M, Uchida A, Sugasawa K, Kondoh J, Ohkuma Y and Hanaoka F 2001 Centrosome protein centrin 2/caltractin 1 is part of the xeroderma pigmentosum group C complex that initiates global genome nucleotide excision repair. *J. Biol. Chem.* **276** 18665–18672

Azimzadeh J and Marshall WF 2010 Building the centriole. *Curr. Biol.* **20** R816–R825

Coblitz B, Shikano S, Wu M, Gabelli SB, Cockrell LM, Spieker M, Hanyu Y, Fu H, Amzel LM and Li M 2005 C-terminal recognition by 14-3-3 proteins for surface expression of membrane receptors. *J. Biol. Chem.* **280** 36263–36272

Conduit PT, Wainman A and Raff JW 2015 Centrosome function and assembly in animal cells. *Nat. Rev. Mol. Cell Biol.* **16** 611–624

Dalal SN, Schweitzer CM, Gan J and DeCaprio JA 1999 Cytoplasmic localization of human cdc25C during interphase requires an intact 14-3-3 binding site. *Mol. Cell. Biol.* **19** 4465–4479

Dalal SN, Yaffe MB and DeCaprio JA 2004 14-3-3 family members act coordinately to regulate mitotic progression. *Cell Cycle* **3** 672–677

Dantas TJ, Daly OM and Morrison CG 2012 Such small hands: The roles of centrins/caltractins in the centriole and in genome maintenance. *Cell. Mol. Life Sci.* **69** 2979–2997

Dantas TJ, Daly OM, Conroy PC, Tomas M, Wang Y, Lalor P, Dockery P, Ferrando-May E and Morrison CG 2013 Calcium-binding capacity of centrin2 is required for linear POC5 assembly but not for nucleotide excision repair. *PLoS One* **8** e68487

de Laat WL, Jaspers NG and Hoeijmakers JH 1999 Molecular mechanism of nucleotide excision repair. *Genes Dev.* **13** 768–785

Dunaway S, Liu HY and Walworth NC 2005 Interaction of 14-3-3 protein with Chk1 affects localization and checkpoint function. *J. Cell Sci.* **118** 39–50

Fischer A, Baljuls A, Reinders J, Nekhoroshkova E, Sibilski C, Metz R, Albert S, Rajalingam K, Hekman M and Rapp UR 2009 Regulation of RAF activity by 14-3-3 proteins: RAF kinases associate functionally with both homo- and heterodimeric forms of 14-3-3 proteins. *J. Biol. Chem.* **284** 3183–3194

Gardino AK and Yaffe MB 2011 14-3-3 proteins as signaling integration points for cell cycle control and apoptosis. *Semin. Cell Dev. Biol.* **22** 688–695

Hosing AS, Kundu ST and Dalal SN 2008 14-3-3 gamma is required to enforce both the incomplete S phase and G2 DNA damage checkpoints. *Cell Cycle* **7** 3171–3179

Kim SY, Kim DS, Hong JE and Park JH 2017 Crystal structure of wild-type centrin 1 from *Mus musculus* occupied by Ca2. *Biochemistry (Mosc)* **82** 1129–1139

Klein UR and Nigg EA 2009 SUMO-dependent regulation of centrin-2. *J. Cell Sci.* **122** 3312–3321

Kundu ST, Gosavi P, Khapare N, Patel R, Hosing AS, Maru GB, Ingle A, Decaprio JA and Dalal SN 2008 Plakophilin3 downregulation leads to a decrease in cell adhesion and promotes metastasis. *Int. J. Cancer* **123** 2303–2314

Li FQ, Mofunanya A, Harris K and Takemaru K 2008 Chibby cooperates with 14-3-3 to regulate beta-catenin subcellular distribution and signaling activity. *J. Cell Biol.* **181** 1141–1154

Lutz W, Lingle WL, McCormick D, Greenwood TM and Salisbury JL 2001 Phosphorylation of centrin during the cell cycle and its role in centriole separation preceding centrosome duplication. *J. Biol. Chem.* **276** 20774–20780

Madeira F, Tinti M, Murugesan G, Berrett E, Stafford M, Toth R, Cole C, MacKintosh C and Barton GJ 2015 14-3-3-Pred: Improved methods to predict 14-3-3-binding phosphopeptides. *Bioinformatics* **31** 2276–2283

Mukhopadhyay A, Sehgal L, Bose A, Gulvady A, Senapati P, Thorat R, Basu S, Bhatt K, Hosing AS, Balyan R, Borde L, Kundu TK and Dalal SN 2016 14-3-3 gamma prevents centrosome amplification and neoplastic progression. *Sci. Rep.* **6**. https://doi.org/10.1038/srep26580

Muslin AJ, Tanner JW, Allen PM and Shaw AS 1996 Interaction of 14-3-3 with signaling proteins is mediated by recognition of phosphoserine. *Cell* **84** 889–897

Nigg EA and Holland AJ 2018 Once and only once: Mechanisms of centriole duplication and their deregulation in disease. *Nat. Rev. Mol. Cell Biol.* **19** 297–312

Nishi R, Sakai W, Tone D, Hanaoka F and Sugasawa K 2013 Structure-function analysis of the EF-hand protein centrin-2 for its intracellular localization and nucleotide excision repair. *Nucleic Acids Res.* **41** 6917–6929

Ogihara T, Isobe T, Ichimura T, Taoka M, Funaki M, Sakoda H, Onishi Y, Inukai K, Anai M, Fukushima Y, Kikuchi M, Yazaki Y, Oka Y and Asano T 1997 14-3-3 protein binds to insulin receptor substrate-1, one of the binding sites of which is in the phosphotyrosine binding domain. *J. Biol. Chem.* **272** 25267–25274

Paoletti A, Moudjou M, Paintrand M, Salisbury JL and Bornens M 1996 Most of centrin in animal cells is not centrosome-associated and centrosomal centrin is confined to the distal lumen of centrioles. *J. Cell Sci.* **109** 3089–3102

Peng CY, Graves PR, Thoma RS, Wu Z, Shaw AS and Piwnica-Worms H 1997 Mitotic and G2 checkpoint control: Regulation of 14-3-3 protein binding by phosphorylation of Cdc25C on serine-216. *Science* **277** 1501–1505

Pietromonaco SF, Seluja GA, Aitken A and Elias L 1996 Association of 14-3-3 proteins with centrosomes. *Blood Cells Mol. Dis.* **22** 225–237

Salisbury JL, Suino KM, Busby R and Springett M 2002 Centrin-2 is required for centriole duplication in mammalian cells. *Curr. Biol.* **12** 1287–1292

Telles E, Hosing AS, Kundu ST, Venkatraman P and Dalal SN 2009 A novel pocket in 14-3-3e is required to mediate specific complex formation with cdc25C and to inhibit cell cycle progression upon activation of checkpoint pathways. *Exp. Cell Res.* **315** 1448–1457

Toshima JY, Toshima J, Watanabe T and Mizuno K 2001 Binding of 14-3-3beta regulates the kinase activity and subcellular localization of testicular protein kinase 1. *J. Biol. Chem.* **276** 43471–43481

Tourbez M, Firanescu C, Yang A, Unipan L, Duchambon P, Blouquit Y and Craescu CT 2004 Calcium-dependent self-assembly of human centrin 2. *J. Biol. Chem.* **279** 47672–47680

Tzivion G, Shen YH and Zhu J 2001 14-3-3 proteins; bringing new definitions to scaffolding. *Oncogene* **20** 6331–6338

Tzivion G, Gupta VS, Kaplun L and Balan V 2006 14-3-3 proteins as potential oncogenes. *Semin. Cancer Biol.* **16** 203–213

Vishal SS, Tilwani S and Dalal SN 2018 Plakoglobin localization to the cell border restores desmosome function in cells lacking 14-3-3gamma. *Biochem. Biophys. Res. Commun.* **495** 1998–2003

Wolfrum U and Salisbury JL 1998 Expression of centrin isoforms in the mammalian retina. *Exp. Cell Res.* **242** 10–17

Wood RD 1996 DNA repair in eukaryotes. *Annu. Rev. Biochem.* **65** 135–167

Yaffe MB, Rittinger K, Volinia S, Caron PR, Aitken A, Leffers H, Gamblin SJ, Smerdon SJ and Cantley LC 1997 The structural basis for 14-3-3: Phosphopeptide binding specificity. *Cell* **91** 961–971

Yang A, Miron S, Duchambon P, Assairi L, Blouquit Y and Craescu CT 2005 The N-terminal domain of human Centrin 2 has a closed structure, binds calcium with a very low affinity, and plays a role in the protein self assembly. *Biochemistry* **45** 10

Yang A, Miron S, Duchambon P, Assairi L, Blouquit Y and Craescu CT 2006 The N-terminal domain of human centrin 2 has a closed structure, binds calcium with a very low affinity, and plays a role in the protein self-assembly. *Biochemistry* **45** 880–889

Corresponding editor: KUNDAN SENGUPTA

Metadata of the chapter that will be visualized online

Chapter Title	Centrosome Amplification and Tumorigenesis: Cause or Effect?	
Copyright Year	2019	
Copyright Holder	Springer Nature Switzerland AG	
Author	Family Name	**Bose**
	Particle	
	Given Name	**Arunabha**
	Suffix	
	Organization	KS215, Advanced Centre for Treatment Research and Education in Cancer (ACTREC), Tata Memorial Centre
	Address	Navi Mumbai, Maharashtra, India
	Organization	Homi Bhabha National Institute
	Address	Mumbai, Maharashtra, India
Corresponding Author	Family Name	**Dalal**
	Particle	
	Given Name	**Sorab N.**
	Suffix	
	Organization	KS215, Advanced Centre for Treatment Research and Education in Cancer (ACTREC), Tata Memorial Centre
	Address	Navi Mumbai, Maharashtra, India
	Organization	Homi Bhabha National Institute
	Address	Mumbai, Maharashtra, India
	Email	sdalal@actrec.gov.in
Abstract	Centrosome amplification is a feature of multiple tumour types and has been postulated to contribute to both tumour initiation and tumour progression. This chapter focuses on the mechanisms by which an increase in centrosome number might lead to an increase or decrease in tumour progression and the role of proteins that regulate centrosome number in driving tumorigenesis.	
Keywords (separated by '-')	Centrosome - Centriole - Aneuploidy - Chromosomal instability	

Chapter 18
Centrosome Amplification and Tumorigenesis: Cause or Effect?

Arunabha Bose and Sorab N. Dalal

Abstract Centrosome amplification is a feature of multiple tumour types and has been postulated to contribute to both tumour initiation and tumour progression. This chapter focuses on the mechanisms by which an increase in centrosome number might lead to an increase or decrease in tumour progression and the role of proteins that regulate centrosome number in driving tumorigenesis.

Abbreviations

AKAP450	A-kinase-anchoring protein 450
cdc25C	Cell division cycle 25C
CDK	Cyclin-dependent kinase
CDK5RAP2	CDK5 regulatory Subunit-associated protein 2
CENP-E	CENtrosome-associated **Protein** E
Cep	Centrosomal protein
CLIP-70	Cytoplasmic LInker **Protein** 170
C-NAP1	Centrosomal Nek2-associated protein 1
CP110	Centriolar coiled-coil **protein** of 110 kDa
CPAP	Centrosomal P4.1-associated **protein**
EGFR	Epidermal growth factor receptor
FBF1	Fas-binding factor 1
GCP	γ-tubulin complex protein
hPOC5	human Proteome of Centriole 5
INCENP	Inner CENtromere **Protein**
LRRC45	Leucine-rich repeat containing 45
NEDD1	Neural precursor cell expressed developmentally down-regulated **protein** 1

A. Bose · S. N. Dalal (✉)
KS215, Advanced Centre for Treatment Research and Education in Cancer (ACTREC), Tata Memorial Centre, Navi Mumbai, Maharashtra, India

Homi Bhabha National Institute, Mumbai, Maharashtra, India
e-mail: sdalal@actrec.gov.in

M. Kloc (ed.), *The Golgi apparatus and Centriole*, Results and Problems in Cell Differentiation 67, https://doi.org/10.1007/978-3-030-23173-6_18

ODF2	Outer dense fiber **protein 2**
SAS-6	Spindle assembly abnormal protein 6
SCLT1	Sodium channel and clathrin linker 1
SMC3	Structural maintenance of chromosomes **protein 3**
STIL	SCL interrupting locus protein
TACC2	Transforming acidic coiled-coil-containing protein 2
TRF1	Telomeric repeat-binding factor 1

18.1 Introduction

The cell cycle is a carefully orchestrated process that leads to the accurate segregation of chromosomes into two daughter cells (Malumbres and Barbacid 2007). Accurate genome segregation is accomplished by aligning the paired sister chromatids along the metaphase plate and attachment of the sister chromatids to the mitotic spindle (Reber and Hyman 2015; Walczak and Heald 2008). Following attachment to the spindle, the sister chromatids are 'pulled' apart by forces generated by spindle microtubules that originate from the two poles. Nucleation of the microtubules at the two poles, such that they are organized into a spindle, is mediated by a cellular organelle, called the centrosome (Fu et al. 2016).

The centrosome is a membrane-less organelle, which is the primary microtubule organizing centre (MTOC) in most eukaryotic cells. Its ability to organize microtubules results in it being essential for multiple cellular functions including the generation of the mitotic spindle, regulation of cell cycle progression, the biogenesis of and signalling from cilia, the determination of cell fate, cellular trafficking and the generation of an effective immune response (Arquint et al. 2014; Reina and Gonzalez 2014; Rios 2014; Stinchcombe and Griffiths 2014). Each centrosome consists of a pair of centrioles surrounded by an amorphous structure called the pericentriolar matrix (Luders 2012) (Fig. 18.1). The two centrioles are arranged orthogonally, and each centriole is organized in a typical 9+3 structure, which alludes to the nine sets of triplet microtubules arranged around a central cartwheel (Gonczy 2012). This cartwheel consists of a hub and radial spokes which are made of nine homodimers of Sas-6 (Kitagawa et al. 2011). The spokes emanating from the hub bind to the first microtubule of each triplet through an interaction between Cep135 and the first microtubule of the triplet (Guichard et al. 2017).

In human cells, a mature centriole is a cylinder, ~450 nm in length, with inner and outer diameters of ~130 nm and ~250 nm, respectively (Winey and O'Toole 2014). The centriole is said to have a polarized structure, with a proximal end (the base), and a distal end (the tip). The two centrioles in the centrosome are a mother centriole, which is inherited from the previous cell cycle, and a daughter centriole, whose synthesis is initiated in the current cell cycle during S phase (Fu et al. 2015). The mother centriole can be distinguished from the daughter centriole, by the presence of distal and sub-distal appendages (Fig. 18.1). The distal appendage proteins such as

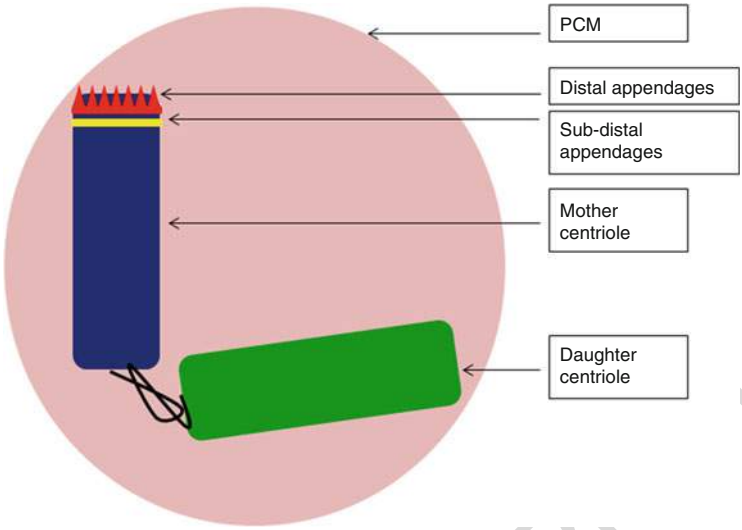

Fig. 18.1 The centrosome. A centrosome consists of a pair of centrioles (represented here in blue and green). The two centrioles differ in age, with one being the mother centriole (in blue) and the other, the daughter (in green). The mother centriole is identified by the presence of distal and sub-distal appendages (red). This centriolar pair is surrounded by an ordered matrix of proteins called the pericentriolar matrix (PCM) (in pink). The PCM contributes towards the nucleation of microtubules and spindle assembly

Cep164, Cep83 and SCLT1 are required to help dock the centrioles at the cell membrane during the formation of cilia (Tanos et al. 2013). Sub-distal appendages are made of proteins such as ninein, Cep170 and centriolin (Jana et al. 2014), and these are associated with nucleating and anchoring microtubules, which contribute to the organization of the mitotic spindle (Piel et al. 2000).

The microtubule organization function of the centrosome is dependent on the presence of the pericentriolar matrix (PCM). The PCM is a multi-protein amorphous structure and contains proteins such as γ-tubulin, pericentrin, CDK5RAP2, CPAP, AKAP450, TACC2, Cep192 and Cep152 (Dictenberg et al. 1998; Gergely et al. 2000; Gomez-Ferreria et al. 2007; Keryer et al. 2003; Woodruff et al. 2014). On the basis of experiments in different model systems, the current consensus is that initially, a scaffold of proteins such as Cep192, Cep152, pericentrin and CDK5RAP2 is formed around the paired centrioles (Hatch et al. 2010; Keryer et al. 2003). The activity of kinases such as polo-like kinase-1 (Plk1) and Aurora A stimulates the recruitment of γ-tubulin, TACC2 and other effector proteins to this ring (Gergely et al. 2000; Hannak et al. 2001; Kong et al. 2014). γ-tubulin forms a complex with GCP proteins to form γ-tubulin ring complexes (γ-TURCs), which are required for nucleating microtubules.

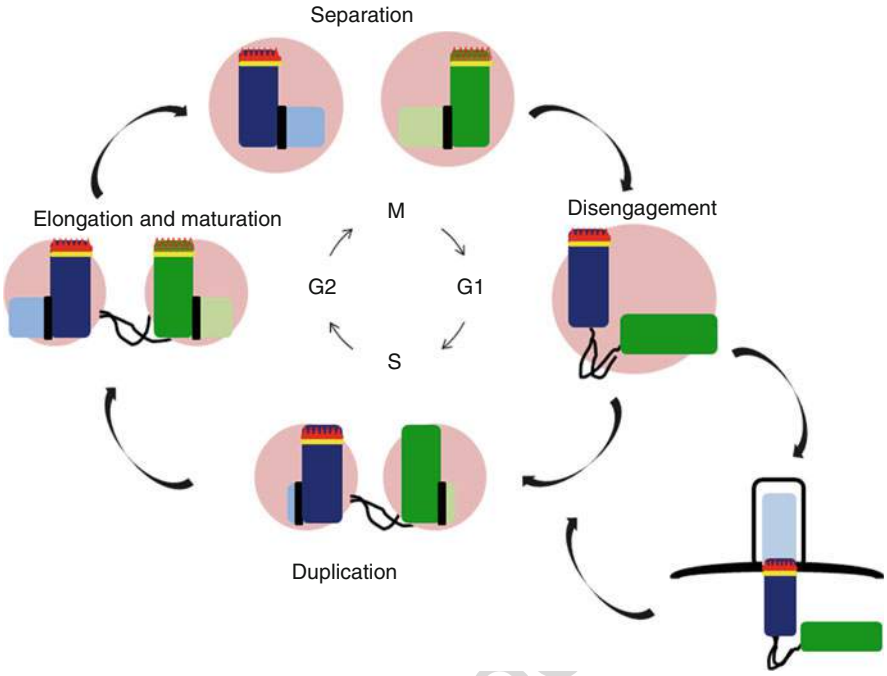

Fig. 18.2 The centrosome cycle. Each daughter cell inherits one centrosome post-mitosis from the mother cell, which consists of two orthogonally arranged centrioles, a mother and daughter centriole. In cycling cells during G1, a new centrosome duplication cycle is initiated by the disengagement of the two centrioles, during G1, which results in a loss of their orthogonal conformation and triggers pro-centriole biogenesis. The two centrioles are now held together by a proteinaceous linker, called the G1-G2 tether. During S phase, the newly formed pro-centrioles are attached to their respective mother centriole, at their proximal end, by the S-M linker. As the cell enters G2, the newly formed pro-centrioles elongate and the new mother centriole matures, so as to be able to nucleate microtubules. As the cell enters mitosis, the G1-G2 tether is degraded and the two centrosomes separate to organize each end of the mitotic spindle. If a cell withdraws from cycle and enters G0, the disengaged centrioles can also participate in the formation of cilia, where the mother centriole is attached to the plasma membrane via distal appendages

18.2 The Centrosome Cycle

The canonical centrosome duplication cycle is synchronized with the DNA replication cycle, thereby ensuring accurate segregation of the genetic material to the two daughter cells. The centrosome duplication cycle consists of four different phases: (1) Disengagement, (2) Duplication, (3) Maturation and (4) Separation (Fig. 18.2). The four steps are discussed below.

18.2.1 Disengagement

From the beginning of the S phase to the onset of mitosis, each mother centriole and its corresponding daughter centriole are orthogonally attached to each other via an S-M linker (Nigg and Stearns 2011). This orthogonal arrangement of the two centrioles is referred to as centriole engagement. The exact composition of the S-M linker has not yet been elucidated; however, studies from *Drosophila* spermatocytes suggest that Sas proteins might be a part of this linker (Stevens et al. 2010). As a cell exits mitosis, the orthogonal arrangement of centrioles in each mature centrosome in the daughter cells is disrupted by proteins such as separase and Plk1, resulting in the degradation of the S-M linker (Tsou et al. 2009). Loss of the S-M linker and establishment of a G1-G2 tether between the two centrioles serves as a licensing event for the initiation of centrosome duplication. Inhibition of Plk1 activity using the small-molecule BI2536 inhibits centriole disengagement during late G2 or early mitosis (Tsou et al. 2009). Knockdown experiments in HeLa cells have demonstrated that cleavage of pericentrin by separase, during anaphase onset, leads to its dissociation from the centrosome, and thus, disengagement (Matsuo et al. 2012). Separase is active only during anaphase onset, and this ensures that centriole duplication occurs only once during the cell cycle (Tsou et al. 2009). Once the centrioles are 'disengaged', they are licensed for the initiation of centriole duplication.

An additional event required for disengagement is the phosphorylation of nucleophosmin 1 (NPM1) by cyclin-dependent kinases. Phosphorylation of NPM1 at a threonine residue at position 199 by CDK2 or CDK1 results in dissociation of NPM1 from the centrosome, thus licensing the centrosome for duplication (Okuda et al. 2000; Peter et al. 1990). Expression of a phospho-deficient mutant of NPM1 (T199A) has been demonstrated to inhibit centrosome duplication (Tokuyama et al. 2001) while a phospho-mimetic mutant (T199D) promotes centrosome amplification (Mukhopadhyay et al. 2016). Further, NPM1 has been demonstrated to localize between the paired centrioles of unduplicated centrosomes (Shinmura et al. 2005). Plk1 phosphorylates NPM1 at Ser-4, and inhibition of this phosphorylation results in mitotic defects such as abnormal centrosome number and the presence of fragmented nuclei in these cells (Zhang et al. 2004b).

Loss of the orthogonal configuration is not the only licensing event for centriolar duplication (Engle et al. 2008; Gottardo et al. 2014; Shukla et al. 2015), and another factor that governs competency for duplication is the distance between the mother and the daughter centrioles. Plk1 can promote maturation and distancing of the orthogonally arranged daughter centriole, leading to reduplication of the mother centriole (Shukla et al. 2015). Further, another event that occurs during the disengagement process is termed 'centriole to centrosome conversion'. It is essential for the newly formed daughter centriole to become duplication competent and for it to able to function as an MTOC. In vertebrates, this begins with the initial loss of the central cartwheel, which is mediated by CDK1 activity (Arquint and Nigg 2014). An increase in Plk1 activity 'modifies' the daughter centriole inherited from the mother

cell and stabilization of the cartwheel-less centriole occurs via its recruitment of Cep295 (Izquierdo et al. 2014). Cep152 and Cep192 are further acquired by the daughter centriole, and the centriole is now competent for duplication and can mature to form the new mother centriole (Hatch et al. 2010; Kim et al. 2013; Wang et al. 2011).

18.2.2 Duplication

Following disengagement, in each cell, there is exactly one mother centriole linked to a daughter centriole via a proteinaceous linker called the G1-G2 tether. The disengaged centrioles are now licensed for duplication (Wang et al. 2011). When cells enter S phase, exactly one pro-centriole must form adjacent to each of the pre-existing centrioles. This process is regulated by proteins such as Plk4 (polo-like kinase 4), Cep192, Cep152, STIL, SAS6 and CDK2. Initially, Cep152 and Cep192 act as scaffolding proteins that recruit Plk4 to the mother centriole (Kim et al. 2013). This results in the ring-like organization of Plk4 around the mother centriole as observed by super-resolution microscopy (Dzhindzhev et al. 2017; Ohta et al. 2018). Plk4 initiates centriole duplication by first marking the site of daughter centriole assembly which is dependent on the interaction between Plk4 and STIL (Ohta et al. 2018; Sonnen et al. 2012). STIL is recruited to the centriole by Cep85 (Liu et al. 2018) and upon recruitment to the mother centriole, STIL further activates and stabilizes Plk4 (Ohta et al. 2018). After recruitment of Plk4 and STIL marks the site of pro-centriole formation, SAS6 localizes to the same site and initiates pro-centriole assembly by assembling into higher order oligomers (Nakazawa et al. 2007). SAS6 oligomerization is the building block for the ninefold symmetrical centriole. Gorab, a trans-golgi protein, interacts with Sas6 and contributes to the establishment of the ninefold symmetry of the centriole and to centriole duplication in *Drosophila* (Kovacs et al. 2018).

Plk4 is initially observed as a ring around the mother centriole, and this ring coalesces into a single spot (Dzhindzhev et al. 2017; Ohta et al. 2018). Several attempts have been made to understand how this transition might occur and how it might regulate centrosome duplication. Currently, there are two proposed models for how the transition occurs. According to a biophysical model proposed by Leda et al. (2018), the activity of Plk4 is dynamic and transiently peaks at several points around the mother centriole. It has been demonstrated previously that complex formation between Plk4 and its substrate, STIL, stabilizes active Plk4 (Moyer et al. 2015). The Plk4–STIL complex could be retained at the centriole due to the binding of STIL to other components of the centriole. This model predicts that there could be multiple points within the ring surrounding the mother centriole, at which this Plk4–STIL complex is stabilized. An exchange of the Plk4–STIL complex occurs between the mother centriole and the cytoplasm, which determines the concentration of the complex at any point. Initially, there is a concentration-based competition between all the Plk4–STIL complexes. The cluster with the highest concentration of Plk4–

STIL is predicted to mark the site of new centriole formation (Leda et al. 2018). The second model suggests that first, Plk4 self-assembles into a ring around the mother centriole. Both inactive and active forms of Plk4 coexist at the centriole. Once it is recruited to the centriole, due to the ability of Plk4 to both laterally inhibit neighbouring molecules of Plk4 and undergo auto-activation, there is a localized increase in Plk4 activity at some points in the ring around the mother centriole. This localized activity is enhanced by complex formation of Plk4 with STIL and SAS6, thus leading to the formation of a single pro-centriole (Takao et al. 2018; Yamamoto and Kitagawa 2018). The formation of the new pro-centriole adjacent to each mother centriole results in the re-establishment of the S-M linker (Nigg and Stearns 2011).

18.2.3 Elongation and Maturation

During late S to G2, once Plk4 has marked the site of pro-centriole biogenesis, centriole elongation is stimulated by proteins such as CPAP, CP110 and SAS6, all of whom play important roles in this process (Kleylein-Sohn et al. 2007). SAS6, the ninefold symmetrical cartwheel protein, acts as a scaffold around which microtubules are assembled (Nakazawa et al. 2007). CPAP is a tubulin dimer-binding capping protein that, along with CP110, promotes microtubule assembly and controls centriolar length (Tang et al. 2009). It has been postulated that Cep135 links SAS6 with CPAP and the microtubule triplet (Lin et al. 2013). Centrin and hPOC5 localize to the distal lumen of centrioles and are essential for elongation at the distal end (Azimzadeh et al. 2009).

Elongation of the pro-centrioles is accompanied by expansion of the PCM. According to one model, pericentrin recruits the Cep192-Plk1-Aurora A kinase complex to the centrosome. Plk1 has been demonstrated to trigger the accumulation of the scaffolding protein, Cep192 (Joukov et al. 2014). Plk1 phosphorylates Cep192, which creates attachment sites for γ-TURCs (Joukov et al. 2014). Plk1 activity also recruits Cep215, a PCM protein, to the two centrosomes (Haren et al. 2009). It is postulated that Aurora A kinase, in conjunction with Plk1, phosphorylates components of the γ-TURCs, thus making them competent for the recruitment of microtubules. Experiments in *C. elegans* and *D. melanogaster* have demonstrated that loss of Aurora A leads to defects in centrosome maturation, with a reduction in the accumulation of α-tubulin and γ-tubulin at the centrosome (Berdnik and Knoblich 2002; Hannak et al. 2001). This step is essential to ensure that the four centrioles are able to function as two competent MTOCs. Centriole maturation also involves the acquisition of distal and sub-distal appendages by the newly formed mother centriole. Centriole maturation begins with the recruitment of ODF2 as a sub-distal appendage (Ishikawa et al. 2005). Ninein and Cep170 also function as sub-distal appendages and bind microtubules (Mogensen et al. 2000). Distal appendages such as Cep164, Cep89, Cep83, FBF1 and SCLT1 are essential for membrane docking and ciliogenesis (Tanos et al. 2013).

18.2.4 Separation

Before entry into mitosis, the G1-G2 tether that connects the two centrosomes is targeted for degradation. This tether is composed of proteins like C-NAP1 (Cep250), rootletin, Cep68 and LRRC45 (Bahe et al. 2005; Faragher and Fry 2003; Fry et al. 1998a, b; Pagan et al. 2015). C-NAP1 is connected to the mother centriole via Cep135 (Kim et al. 2008). C-NAP1 is present at the proximal end of the mother centrioles and the two pools of C-NAP1 are connected by rootletin fibres (Bahe et al. 2005; Vlijm et al. 2018). Super-resolution microscopy experiments have demonstrated that Cep68 binds to rootletin and increases the thickness of rootletin fibres (Vlijm et al. 2018). LRRC45 might link the rootletin fibres with C-NAP1 (He et al. 2013). The degradation of the tether is initiated by the activity of the NIMA-related kinase, Nek2 (Fry et al. 1998b). Nek2 phosphorylates C-NAP1 and rootletin, leading to their displacement from the proximal end of the mother centrioles (Bahe et al. 2005; Fry et al. 1998a). Plk1-mediated degradation of Cep68 further displaces Cep215, a PCM protein, from the centrosome, contributing to centrosome separation (Pagan et al. 2015).

Once the G1-G2 tether has undergone dissolution, the two centrosomes have to be separated so as to form the mitotic spindle. This occurs primarily via the antiparallel sliding action of Eg5, a motor protein (Cole et al. 1994; Sawin et al. 1992). Additionally, proteins such as dynein, Lis1 and CLIP-70 contribute to spindle formation by inducing microtubule sliding in the opposite direction to Eg5. The combined action of these motor proteins and their binding partners promotes migration of the centrosomes to the two poles (Gonczy et al. 1999; Tanenbaum et al. 2008). Each centrosome migrates towards a different pole in mitotic cells, leading to the formation of a mitotic spindle. The bipolar spindle further contributes towards the accurate segregation of DNA into two daughter cells, thus maintaining ploidy.

18.3 Centrosome Defects and Tumour Progression

Two rules govern the centrosome duplication cycle: cell cycle control and copy number control.

- Cell cycle control ensures that the centrosome replicates only once per cell cycle.
- Copy number control ascertains that only one pro-centriole forms adjacent to each mother centriole.

Therefore, deregulation of any step of the centrosome cycle can give rise to centrosome abnormalities. These can be classified into two types: (a) structural and (b) numerical.

(a) **Structural abnormalities**. Structural abnormalities in centrosomes are errors in the organization of the centrosome. This leads to aberrations in centrosome size or shape and these structural alterations are present at high levels in tumour

tissues and have been postulated to contribute to tumour progression (Lingle et al. 1998; Lingle and Salisbury 1999). Recently, it has been demonstrated that overexpression of Ninein-like protein (Nlp) in MCF10A-derived 3D acini leads to the formation of centrosome-related bodies (CRB) harbouring large patches of Nlp, resulting in excessive cell proliferation. The cells in the lumen, which are normally cleared by apoptosis, are not cleared, microtubule organization is altered and this phenotype is associated with cellular transformation and neoplastic progression (Schnerch and Nigg 2016). Further, it has been demonstrated that overexpression of Nlp weakens E-cadherin-based adherens junctions in the epithelium. The weakening of adherens junctions results in increased mechanical stress when a cell in the epithelial tissue enters mitosis. The mitotic programme results in 'budding' of the new daughter cell from the original site and could contribute to metastatic progression in tumour cells (Ganier et al. 2018). In addition to the changes in invasiveness, alterations in centrosome structure could lead to aneuploidy which often contributes to tumour progression (Nigg 2006). However, further studies are needed to investigate the extent of aneuploidy that is induced by structural centrosome aberrations. Moreover, given that the centrosome is the hub of several cellular signalling events, it would be interesting to study how signalling pathways are affected by defects in centrosome structure.

(b) **Numerical abnormalities**. Errors in cell cycle control of centrosome duplication contribute to numerical centrosome abnormalities. They can occur due to centrosome over-duplication, defects in cytokinesis and the de novo formation of centrosomes. These result in the presence of more than two centrosomes in a mitotic cell which is also referred to as centrosome amplification. They are the more extensively studied of the two types of centrosome abnormalities, especially in the context of tumour progression. Given that centrosomes organize microtubules and form the mitotic spindle leading to DNA segregation, any numerical errors in centrosome organization are strongly correlated with chromosomal instability and aneuploidy, which is a hallmark of most tumours. Most tumour cells show an increase in the number of centrosomes, suggesting that the change in centrosome number could drive aneuploidy and thus, tumour progression (Godinho and Pellman 2014).

Cells with multiple centrosomes form a multipolar spindle leading to a multipolar mitosis resulting in aneuploidy (Ring et al. 1982). However, a multipolar mitosis in most tumour cells leads to cell death, probably due to loss of genes that are absolutely required for cell viability. Experiments in Zebrafish demonstrate that neuroepithelial cells harbouring centrosome amplification undergo apoptosis (Dzafic et al. 2015). Similarly, experiments in mice have shown that centrosome amplification leads to microcephaly, due to increased apoptosis (Marthiens et al. 2013). These data suggest that cells harbouring multiple centrosomes must avoid the massive aneuploidy resulting from multipolar mitoses, which raises the interesting question of how tumour cells manage to survive and thrive in the presence of multiple centrosomes. In order to tolerate the burden of extra centrosomes, transformed

cells have developed a mechanism called clustering (Ring et al. 1982). In transformed cells with multiple centrosomes, at prophase, centrosomes are not present at only two distinct poles in tumour cells, thus forming a multipolar spindle. During prophase, the centrosomes migrate to and cluster at two different poles leading to the formation of a pseudo-bipolar spindle during metaphase (Basto et al. 2008; Ganem et al. 2009; Kwon et al. 2008; Quintyne et al. 2005). This formation of pseudo-bipolar spindles leads to errors in kinetochore–microtubule attachments, especially the formation of merotelic attachments, which contributes to the presence of lagging chromosomes and an increase in chromosome instability (CIN) (Cosenza et al. 2017; Ganem et al. 2009). The increase in CIN permits the generation of clones with a growth advantage leading to tumour progression.

Multiple studies have attempted to identify gene products/molecular pathways that are required for centrosome clustering. This could lead to the identification of small molecules that inhibit clustering, which could lead to multipolar mitoses resulting in killing of tumour cells. A screen developed by Kwon et al. attempted to identify genes required for clustering in *Drosophila* S2 cells (Kwon et al. 2008). Depletion of HSET, a motor protein, has been demonstrated to induce the formation of multipolar spindles in human cancer cells harbouring multiple centrosomes (Kwon et al. 2008). Depletion of components of the spindle assembly checkpoint (SAC), Mad2, BubR1 (human Bub1) and CENP-E, also leads to the generation of multipolar spindles in S2 cells (Kwon et al. 2008). Several actin-binding proteins were also identified in these screens suggesting that disruption of actin dynamics could inhibit centrosome clustering (Kwon et al. 2008; Leber et al. 2010). This is consistent with recent data from the Godinho laboratory, which suggests that adherens junction functions that are required for maintaining cortical actin organization and cell stiffness can inhibit centrosome clustering (Rhys et al. 2018).

A genome-wide RNAi screen in UPCI:SCC114, a human oral squamous cell carcinoma (OSCC) cell line, has demonstrated that proteins that are a part of the chromosomal passenger complex (CPC), proteins of the Ndc80 complex, Cep164 and Aurora B, which all contribute to spindle tension, are also required for centrosome clustering (Leber et al. 2010). Depletion of Aurora A in a panel of acute myeloid leukaemia (AML) cell lines also results in formation of a multipolar spindle and non-proliferation (Navarro-Serer et al. 2019). Drugs such as Griseofulvin, CP-673451 and Crenolanib that bind to cytoskeletal elements and inhibit clustering demonstrate the contribution of the cytoskeleton towards clustering (Konotop et al. 2016; Rebacz et al. 2007).

Previous results have suggested that loss of 14-3-3γ leads to premature cdc25C, and hence CDK1 activation, which leads to an increase in centrosome number. This is accompanied by an increase in the number of cells with pseudo-bipolar spindles with passage, an increase in aneuploidy and tumour formation (Mukhopadhyay et al. 2016). However, expression of a 14-3-3γ binding defective mutant of cdc25C in 14-3-3γ knockdown cells leads to a reversal of the clustering phenotype and a decrease in tumour growth and cell viability, presumably due to prematurely high levels of CDK1 activity in interphase and mitosis (Mukhopadhyay et al. 2016). These results are consistent with the hypothesis outlined above which suggests that

small molecules that might disrupt centrosome clustering in tumour cells could lead to tumour cell killing and cell death. All of these results suggest that centrosome clustering is a complex phenotype that requires multiple cellular pathways.

Given the strong correlation between centrosome amplification, CIN and cancer, it has been a long-standing question of whether centrosome number dysregulation is sufficient to promote tumorigenesis. One of the mechanisms leading to cells acquiring extra centrosomes is a failure in cytokinesis. Therefore, it has been difficult to assess the causal link between centrosome amplification and tumorigenesis. However, several recent studies have addressed this question and have offered multiple solutions of how centrosome amplification might lead to tumour progression. In this chapter, we aim to highlight several recent observations that shed some light on the correlation between the presence of multiple centrosomes and transformation. We have focused on proteins that are essential for different steps of the centrosome cycle and how their aberrant expression has been demonstrated to contribute to centrosome amplification and tumorigenesis.

18.3.1 Polo-Like Kinase 1

Polo-like kinase 1 (Plk1) is a member of the polo-like kinase family of proteins that are serine/threonine kinases. It was initially identified in *Drosophila* embryos as a kinase, active during the late anaphase–telophase transition (Llamazares et al. 1991). Plk1 localization changes throughout the cell cycle, with it localizing at the centrosome throughout interphase, and then moving to the kinetochore, the spindle and the spindle mid-body during mitosis (Golsteyn et al. 1995; Kishi et al. 2009). Plk1 performs multiple functions that contribute to mitotic progression. Plk1 phosphorylates multiple residues in the N-terminus of cdc25C resulting in an increase in cdc25C activity and mitotic progression (Toyoshima-Morimoto et al. 2002). Plk1 phosphorylates BubR1 and INCENP, thus stimulating kinetochore assembly (Arnaud et al. 1998; Elowe et al. 2007; Goto et al. 2006). Inhibition of Plk1 in U-2OS cells decreases the robustness of the SAC, which decreases accurate chromosome segregation and could, hence, contribute to CIN (O'Connor et al. 2015). Plk1 contributes to centrosome maturation by phosphorylating NEDD1, which leads to recruitment of γ-TURCs to centrosomes during centrosome maturation (Haren et al. 2009; Zhang et al. 2009). Depletion of Plk1 using siRNA in HeLa cells leads to a lack of phosphorylation of NPM1, which has been demonstrated to lead to defects in nuclear size, cytokinesis and centrosome amplification (Zhang et al. 2004b). The activity of Plk1 is required for centrosome disengagement, as inhibition of Plk1 using a small molecule prevents centrosome disengagement (Tsou et al. 2009).

Protein levels of Plk1 are elevated in a number of tumour types, including gliomas, breast cancers, oesophageal squamous cell carcinomas, non-small cell lung carcinomas, melanoma, renal cancer, prostate and colorectal cancer (Feng et al. 2009; Liu et al. 2017; Ramani et al. 2015). Plk1 levels are high in tamoxifen-resistant MCF-7 cells, and inhibition of Plk1 leads to a decrease in cell

proliferation (Jeong et al. 2018). A decrease in Plk1 levels confers sensitivity to gemcitabine in pancreatic cancer cell lines (Jimeno et al. 2010). Plk1 silencing can also enhance the sensitivity of rectal cancer and medulloblastoma cell lines to radiotherapy (Harris et al. 2012; Rodel et al. 2010). Interestingly, several missense and truncation mutations in the C-terminus of Plk1 have been identified in tumour cell lines such as HepG2, A431, MKN74 and A549 (Simizu and Osada 2000). Given that levels of Plk1 are found to be both overexpressed and reduced in tumour cell lines, it is difficult to actually assess the role of Plk1 in neoplastic progression or cellular transformation.

Recent experiments performed in mouse models of Plk1 overexpression suggest that Plk1 may have different effects on neoplastic transformation and tumour progression depending on the presence of other genetic alterations or the tissue type in which Plk1 expression is elevated. Mouse embryonic fibroblasts (MEFs) isolated from mice carrying a doxycycline-inducible transgene for Plk1 exhibit a variety of mitotic defects such as multiple centrosomes, monopolar and multipolar spindles in pro-metaphase, as well as lagging chromosomes and anaphase bridges resulting in an increased duration of mitosis (de Carcer et al. 2018). Despite the defects in mitosis, when Plk1 overexpressing mice were crossed with mice containing a constitutively active K-Ras allele, K-Ras^{G12D}, which is only expressed in the mammary gland, a decrease in tumour progression was observed in the presence of doxycycline (de Carcer et al. 2018). Another study by Li et al. also found chromosomal instability, lagging and misaligned chromosomes and apoptosis in MEFs isolated from mice conditionally overexpressing Plk1 (Li et al. 2017). No malignant transformation was observed in these mice; however, hypersensitivity to ionizing radiation was observed in the liver. Treatment with ionizing radiation led to an increase in the number of liver tumours and the presence of lymphomas, which was accompanied by inhibition in the expression of genes required for DNA repair (Li et al. 2017). In both cases, despite defects in mitosis that lead to aneuploidy, overexpression of Plk1 alone did not lead to tumorigenesis in mice, suggesting that other mechanisms might contribute to tumour formation upon Plk1 overexpression. It is possible that Plk1 overexpression affects other proteins that influence transformation, such as p53 (Smith et al. 2017).

In contrast to its expression levels in most transformed cell lines, loss of Plk1 has been demonstrated to accelerate tumour formation in mice (Lu et al. 2008). Plk1 null mice show embryonic lethality due to the inability of the embryonic cells to divide. However, a significant proportion of Plk1 heterozygous mice develop tumours in various organs suggesting that haploinsufficiency of Plk1 could drive tumour progression. Splenocytes isolated from these mice harboured a higher incidence of aneuploidy, which could contribute to CIN (Lu et al. 2008). Given all of the data on Plk1, it seems likely that Plk1 can act as either an oncogene or a tumour suppressor in a context-dependent manner.

18.3.2 Separase

Separase or separin is a cysteine protease that promotes anaphase entry in mitotic cells by cleaving Ssc1, which is part of the synaptonemal complex. This relaxes the tension in the spindle and leads to anaphase progression (Uhlmann et al. 1999). Inhibiting separase expression using RNAi in HeLa cells leads to genomic instability (Cucco et al. 2018). Separase forms a complex with the MCM2-7 helicase and loss of separase leads to an increase in replication fork speed, probably due to an increase in the levels of acetylated SMC3 (Cucco et al. 2018). Antisense oligonuleotide-mediated reduction of separase gives rise to aberrant mitoses with lagging chromosomes (Chestukhin et al. 2003). Apart from its function in relieving sister chromatid cohesion, separase also plays a role in ensuring centrosome disengagement (Tsou and Stearns 2006; Tsou et al. 2009). Knockout of separase in HCT116 and HeLa cell lines inhibits centriole disengagement and subsequent duplication (Tsou et al. 2009). Pericentrin is a potential substrate for separase and expression of a pericentrin mutant that cannot be cleaved by separase suppresses centriole disengagement and duplication (Matsuo et al. 2012). Aki1 and cohesin have also been implicated as substrates of separase at the centrosome (Nakamura et al. 2009). Separase also functions in double-strand break repair, where it cleaves cohesin (Hellmuth et al. 2018). Activation of separase in interphase has been demonstrated to aid in DNA double-strand break repair in HEK293 cells (Hellmuth et al. 2018). All of these results suggest that separase is required for maintaining genomic integrity either by regulating genome organization and duplication or by regulating centrosome duplication.

Separase is significantly overexpressed in osteosarcoma, breast and prostate tumour samples as per tissue immunofluorescence analysis (Meyer et al. 2009). An increased nuclear localization of separase was also observed in these tissue samples (Meyer et al. 2009). This unusual localization of separase shows a correlation with tumour status, although the mechanism underlying the correlation between separase levels and tumour progression remains to be elucidated (Meyer et al. 2009). Increased separase activity with aberrant centrosome numbers has been observed in bone marrow samples of patients with myelodysplastic syndrome (MDS) (Ruppenthal et al. 2018). IHC staining of breast tumours samples from patients has demonstrated a strong correlation between abnormal separase expression and impaired survival (Gurvits et al. 2017). These results suggest that an increase in separase levels can drive tumour progression.

A mutation in the zebrafish separase gene results in embryos with abnormal mitotic spindles, aneuploidy, polyploidy and multiple centrosomes (Shepard et al. 2007). Adult zebrafish heterozygous for separase treated with the carcinogen *N*-methyl-*N*-nitro-*N*-nitrosoguanidine (MNNG) were observed to be more susceptible to developing tumours (Shepard et al. 2007). This implies that separase could act as a tumour suppressor. A knockout of separase leads to embryonic lethality in mice (Kumada et al. 2006). Experiments in mouse models suggest that separase haploinsufficiency can lead to tumorigenesis in a p53 mutant background. MEFs isolated from mice heterozygous for separase were found to exhibit a compromised

response to damage induced DNA repair (Hellmuth et al. 2018). Mice with a hypomorphic separase allele display an increased rate of tumorigenesis with a decrease in survival in a p53 mutant background (Mukherjee et al. 2011). Normal splenocytes isolated from these mice exhibited aneuploidy which might contribute to genomic instability (Mukherjee et al. 2011). In contrast to the results described above, conditional overexpression of separase in a mouse mammary epithelial cell line leads to increased aneuploidy and tumorigenesis in a p53 mutant background (Zhang et al. 2008). These data suggest that either an increase or a decrease in separase levels might not be enough to initiate tumour formation, though it might lead to aneuploidy followed by a second genetic event, which could drive tumorigenesis. It might be interesting to observe the effect of separase knockout or overexpression in tissue-specific, conditional mouse models.

18.3.3 Polo-Like Kinase 4

Polo-like kinase 4 (Plk4), a member of the polo family of kinases, is a master regulator of centriole biogenesis (Swallow et al. 2005). Plk4 was initially identified in mice, because of its sequence homology to polo in *Drosophila* (Fode et al. 1994). Further experiments in NIH3T3 cells ascertained that Plk4 is associated with the centrosome throughout the cell cycle (Hudson et al. 2001). Experiments in both *Drosophila* and mammalian cell lines using siRNA demonstrated that decrease in Plk4 levels leads to a loss of centrioles (Bettencourt-Dias et al. 2005; Habedanck et al. 2005). Overexpression of Plk4 increases centriole numbers, with multiple pro-centrioles forming from a single mother centriole (Habedanck et al. 2005; Kleylein-Sohn et al. 2007). These results indicate the importance of Plk4 levels in controlling centrosome numbers. Recent experiments in *Drosophila* have demonstrated that Plk4 also plays a role in controlling centriolar length (Aydogan et al. 2018). Plk4 overexpression can also induce de novo centriole and MTOC formation in *Drosophila* embryos and *Xenopus* egg extracts, respectively (Eckerdt et al. 2011; Rodrigues-Martins et al. 2007). This occurs due to the ability of Plk4 condensates to recruit STIL, α-, β-tubulin and γ-tubulin, leading to the formation of acentriolar MTOCs (Gouveia et al. 2018).

Plk4 levels are elevated in several cancers, such as breast, acute lymphoblastic leukaemia, prostate, pediatric medulloblastomas and embryonal brain tumours (Korzeniewski et al. 2012; Li et al. 2016, 2018; Pezuk et al. 2017). An increase in Plk4 levels has also been observed in human lung cancer and gastric cancer cell lines (Shinmura et al. 2014). Inhibition of Plk4 expression in neuroblastoma cell lines has been shown to suppress invasion and migration (Tian et al. 2018). Further, inhibition of Plk4 using CFI-400945 induces aneuploidy in lung cancer cell lines (Kawakami et al. 2018). In contrast to the results described above, Plk4 levels are decreased in colorectal cancer cell lines and hepatocellular cancers suggesting that a decrease in Plk4 levels might contribute to tumour progression (Kuriyama et al. 2009; Liu et al. 2012; Rosario et al. 2010). Mutations in Plk4, including loss of function mutations,

cause microcephaly and growth failure with impaired centriole biogenesis (Martin et al. 2014). These data suggest that changes in Plk4 expression lead to defects in centrosome biogenesis leading to neoplastic progression.

As overexpression of Plk4 leads to an increase in centrosome number, it has been the focus of multiple experiments to help understand the role of centrosome amplification in tumour formation and progression. Basto et al. demonstrated for the first time that centrosome amplification could drive tumorigenesis (Basto et al. 2008). Using an assay wherein brain tissue from fruit flies overexpressing Sak (the *Drosophila* homologue of Plk4) was transplanted into the abdomen of WT hosts, they demonstrated that a significant percentage of the hosts developed tumours with multiple centrosomes and a number of the tumours formed metastatic colonies (Basto et al. 2008). Using the same transplantation assay, Castellanos et al. screened for the ability of mutants of different centrosomal proteins to affect tumour formation, in *Drosophila* (Castellanos et al. 2008). They were able to demonstrate that 2% of the WT hosts with wing discs from flies overexpressing Sak transplanted into their abdomen could develop tumours (Castellanos et al. 2008). They were unable to assess the degree of CIN due to the small size of the tumours.

Mice with a homozygous deletion of Plk4 displayed embryonic lethality at E7.5 (Hudson et al. 2001). Plk4+/– MEFs had increased centrosomal amplification, multipolar spindle formation and aneuploidy when compared with WT cells (Ko et al. 2005). Nestin-Cre-driven conditional overexpression of Plk4 in the developing mouse brain led to centrosome amplification, aneuploidy and microcephaly; however, no tumours were observed in the brains of these mice (Marthiens et al. 2013). MEFs isolated from mice conditionally overexpressing Plk4, where a lox stop cassette for Plk4 expression was driven by a chicken β-actin promoter, were found to harbour multiple, functional centrosomes which contribute to mitotic errors such as lagging chromosomes and multipolar mitosis (Vitre et al. 2015). Skin fibroblasts derived from mice overexpressing Plk4 had multiple centrosomes, a reduced proliferation rate and poor long-term survival (Vitre et al. 2015). Even when mice overexpressing Plk4 were crossed with p53–/– mice, an increase in the rate of tumour development was not observed, suggesting that Plk4 overexpression in p53–/– mice did not accelerate tumour progression (Vitre et al. 2015). Similar results were obtained in a skin carcinogenesis model, in which mice overexpressing Plk4 were treated with 7,12-dimethylbenz(*a*)anthracene (DMBA), followed by application of the tumour promoter 12-*O*-tetradecanoyl-phorbol-13-acetate (TPA). There was no significant difference in tumour burden between the control and treated mice (Vitre et al. 2015). However, mice carrying a similar Plk4 overexpression allele, where expression was epidermis specific, showed differentiation and barrier defects in the epidermis leading to death in a number of mice at postnatal day one (P1) (Sercin et al. 2016). Mice overexpressing Plk4 that survived past P1 showed a decrease in Plk4 levels suggesting a strong selection pressure against Plk4 overexpression. When these mice were crossed with p53 null mice, the barrier defects were abrogated; however, cells overexpressing Plk4 were not detected post-P1 as in the wild-type mice. Surprisingly, the transient overexpression of Plk4 in the p53–/– mice led to the development of spontaneous skin tumours in

these mice with complete penetrance (Sercin et al. 2016). Thus, using essentially the same overexpression model for Plk4 leads to different outcomes for tumorigenesis in the same tissue. One possible difference is that in the first report (Vitre et al. 2015), Plk4 expression is not turned off in the tissues, whereas in the second report (Sercin et al. 2016), Plk4 overexpression is transient and is selected against in mice after P1. This suggests that constant centrosome amplification might lead to cell death due to the presence of multipolar mitoses, while a transient increase in Plk4 levels might allow for the selection of cells that tolerate the initial aneuploidy and then the loss of Plk4 leads to the stable inheritance of the aneuploid genome. This might also depend on the strain of mice used in these experiments, as the first set of experiments were done in C57/Bl6 mice while the second set were performed in a mixed background as the three transgenes were all in different strains. In another set of experiments, a doxycycline-inducible allele of Plk4 was introduced into the Rosa26 locus (Coelho et al. 2015). When mice homozygous for the inducible Plk4 allele were crossed with p53 null mice, hyperproliferation and defects in developmental programmes were observed in tissues such as the pancreas and the epidermis, as compared to mice which were p53 null alone (Coelho et al. 2015). The hyperproliferation could be a precursor to tumour development. The results described herein suggest that the experimental protocols used to generate mice with overexpression of Plk4 and the strain of mice in which these experiments are performed could lead to differences in tumour initiation and development.

In contrast to the results described above, overexpression of Plk4 initiates tumorigenesis, in a mouse intestinal neoplasia model (Levine et al. 2017). These mice harbour an APC^{min} mutation, which causes them to develop multiple adenomas throughout the intestinal tract (Moser et al. 1990). These mice displayed an increase in tumour initiation, with the tumours showing an increase in centrosome number, suggesting that centrosome amplification led to an increase in tumour initiation. MEFs isolated from mice overexpressing Plk4, in combination with an APC^{min} allele, displayed increased centrosome numbers. In the absence of p53, these cells could proliferate in spite of harbouring multiple centrosomes, even after 12 days of doxycycline treatment. After long-term treatment with doxycycline (8 months), they were able to observe severe aneuploidy in splenocytes isolated from mice overexpressing Plk4, due to increased centrosome amplification. In addition to an increase in the intestinal tumour burden, these mice also developed spontaneous lymphomas, squamous cell carcinomas and sarcomas starting at 36 weeks of age. When assayed for centrosome number, it was observed that these tumours exhibited centrosome amplification. It was also observed that these tumours harboured varied levels of p53 target genes, indicating that the p53 pathway might be at least partially compromised in these tissues (Levine et al. 2017).

Driving genomic instability is not the only way centrosome amplification via Plk4 can drive tumorigenesis. Transient overexpression of Plk4 in a three-dimensional organoid breast cancer model leads to centrosome amplification that promotes invasion (Godinho et al. 2014). This was not due to an increase in aneuploidy, but rather the increase in invasion was due to increased RacI activation which contributes to greater microtubule nucleation (Godinho et al. 2014). Plk4 has also been

demonstrated to phosphorylate Arp2 in the Arp2/3 complex in tumour cell lines, leading to activation of the complex and an increase in migration (Kazazian et al. 2017). Phosphorylation of Plk4 at S305 leads to an increase in migration and cell spreading and increased co-localization with RhoA at cell protrusions, while a decrease in Plk4 expression in MEFs or tumour cells leads to a decrease in migration and invasion, respectively (Rosario et al. 2015). These data suggest that Plk4 expression might lead to tumour progression by regulating cell migration and invasion, in addition to its ability to stimulate centrosome duplication and thus genomic instability.

18.3.4 Aurora A kinase

The Aurora family of kinases consists of three members, A, B and C (Nigg 2001). Aurora A localizes to the centrosome during G2 and the spindle during mitosis (Kimura et al. 1997). Its functions include centrosome maturation, centrosome separation, organization of spindle assembly, chromatin protein modification, chromatid separation and cytokinesis (Fu et al. 2007). Aurora A also localizes to the mitochondria in several cancer cell lines, where it affects mitochondrial dynamics and energy production (Bertolin et al. 2018). Aurora A is recruited to the centrosome by Cep192, which results in its autophosphorylation and activation (Joukov et al. 2014). Aurora A has been demonstrated to contribute to the centrosomal accumulation of γ-tubulin (Hannak et al. 2001). Its centrosomal substrates include γ-tubulin, Centrin1 and D-TACC (Giet et al. 2002; Sardon et al. 2010). Aurora A regulates microtubule growth by organizing the acentriolar spindle in mammalian oocytes during meiosis I (Bury et al. 2017).

Experiments in HeLa cells have shown that increased Aurora A levels can induce centrosome amplification by inhibiting cytokinesis, leading to the formation of tetraploid cells (Meraldi et al. 2002). This effect is augmented in the absence of p53, with 80% of p53–/– MEFs overexpressing Aurora A harbouring extra centrosomes (Meraldi et al. 2002). Knockdown of Aurora A in HeLa cells gives rise to cells with misaligned chromosomes, defective spindle organization, lagging chromosomes, defects in centriole separation and delay in mitotic entry (Hirota et al. 2003; Marumoto et al. 2003). Aurora A also plays a role in the cell cycle; knockdown of Aurora A in HeLa leads to arrest of the cells in G2-M and eventually, apoptosis (Du and Hannon 2004).

Aurora A is overexpressed in several cancers, including breast (where it was first identified), ovarian, human gliomas, colon, pancreatic and lung (Kollareddy et al. 2008). The expression of Aurora A results in an inhibition of apoptosis in lung cancer cell lines treated with the EGFR inhibitor, thus ensuring their survival (Shah et al. 2019). Further, a loss of Aurora A in gastrointestinal cell lines with activated KRAS leads to increased cell death due to an increase in the levels of proteins required for apoptosis (Wang-Bishop et al. 2018). Aurora A might also affect epithelial to mesenchymal transition, as demonstrated in OSCC cell lines (Dawei

et al. 2018). Silencing of Aurora A leads to an increase in the expression of E-cadherin and a decrease in the levels of vimentin in OSCC cells accompanied by an increase in the levels of reactive oxygen species (ROS) (Dawei et al. 2018).

MEFs from Aurora A null mice display monopolar spindles, with a single γ-tubulin focus (Cowley et al. 2009). A knockdown of Aurora A in OSCC cell lines led to a decrease in tumour volume in xenograft assays in nude mice. The decrease in tumour volume was accompanied by pronounced apoptosis in tumour tissues (Dawei et al. 2018). However, Aurora A overexpression in primary MEFs is not enough to induce transformation (Anand et al. 2003). Overexpression of Aurora A in a rat mammary carcinogenesis model, where the mice are treated with methylnitrosourea, results in centrosome amplification, but tumours developed at a point much after centrosome amplification was first observed (Goepfert et al. 2002). In contrast to some of the results described above, conditional overexpression of Aurora A in the mammary gland led to increased apoptosis which was reversed upon depletion of p53 (Zhang et al. 2004a). These results indicate that dysregulation of Aurora A levels alone is insufficient to drive transformation. Given the many defects associated with dysregulation of Aurora A kinase, several attempts have been made to target it in cancers. These inhibitors are being used extensively to gain a better understanding of Aurora A biology.

18.3.5 Nek2A

Nek2 kinase is the human homologue of the *Aspergillus nidulans* protein NIMA (never in mitosis). Its expression varies through the cell cycle, with its levels being the highest during the G2 and M phases (Fry et al. 1998b; Schultz et al. 1994). It is a serine/threonine kinase that phosphorylates inter-centrosomal linker proteins such as CNAP-1 and rootletin (Bahe et al. 2005; Fry et al. 1998a, b). Phosphorylation of these proteins leads to the dissolution of the inter-centrosomal linker and thus, centrosomal separation. The centrosomes can now migrate to the two ends of the cell, form a spindle and participate in cell division (Bahe et al. 2005; Fry et al. 1998a, b). Overexpression of Nek2 leads to premature centrosome splitting and a loss of focused microtubules, as demonstrated in U-2OS cells (Fry et al. 1998b). However, these cells are able to enter mitosis despite the presence of unfocused microtubules (Fry et al. 1998b). Nek2 overexpression in MDA-MB 231 and MCF-7 leads to centrosome amplification. However, CIN occurs only upon a concurrent depletion of its interacting partner, TRF1 (Lee and Gollahon 2013).

Several reports suggest an increase in Nek2 levels in different cancers. These include tumours of the breast, B-cell lymphoma, multiple myeloma, bladder cancer and glioblastoma (Fang and Zhang 2016). This change in expression levels is associated with a poor prognosis, drug resistance and tumour progression (Hayward et al. 2004; Lee and Gollahon 2013; Zhou et al. 2013). However, it is not known exactly what leads to the change in Nek2 levels in these multiple cancer types. Nek2 protein levels decrease when CDK4 expression is inhibited using RNA interference

(Pitner et al. 2013). Knockdown of Nek2 in a Her2+ breast cancer model reduced centrosome amplification (Pitner et al. 2013). There is no direct evidence that demonstrates that the centrosome amplification observed upon Nek2 overexpression alone actually contributes to tumorigenesis. Given the large number of cancers that harbour high levels of Nek2, and the poor prognosis associated with it, several attempts have been made to develop Nek2 as a potential therapeutic target in cancer. These drugs include ATP-binding site blockers, siRNA-mediated approaches and drugs that affect the binding of Nek2 to its substrates (Hayward et al. 2010; Suzuki et al. 2010). Nek2 inhibition, in combination with chemotherapeutic drugs, might provide a better treatment approach to target cancer (Meng et al. 2014; Suzuki et al. 2010).

18.4 Conclusion

Centrosome amplification is a major feature of most cancer cells. Recent evidence in different model systems has finally established it to be one of the causes and a potential initiator of tumorigenesis. However, centrosome amplification doesn't always lead to tumour formation and might inhibit or promote tumorigenesis depending on the cell/tissue of origin or the presence of other genetic changes that might contribute to tumour progression. A distinct possibility for why centrosome amplification doesn't always lead to tumorigenesis might be the requirement for the activation or inhibition of pathways that promote or prevent centrosome clustering. While most research has focused on the effects of numerical centrosomal abnormalities on tumour progression, it will be interesting to study the contribution of structural centrosomal defects to neoplastic progression.

References

Anand S, Penrhyn-Lowe S, Venkitaraman AR (2003) AURORA-A amplification overrides the mitotic spindle assembly checkpoint, inducing resistance to Taxol. Cancer Cell 3:51–62

Arnaud L, Pines J, Nigg EA (1998) GFP tagging reveals human Polo-like kinase 1 at the kinetochore/centromere region of mitotic chromosomes. Chromosoma 107:424–429

Arquint C, Nigg EA (2014) STIL microcephaly mutations interfere with APC/C-mediated degradation and cause centriole amplification. Curr Biol 24:351–360. https://doi.org/10.1016/j.cub.2013.12.016

Arquint C, Gabryjonczyk AM, Nigg EA (2014) Centrosomes as signalling centres. Philos Trans R Soc Lond B Biol Sci 369 (1650). pii: 20130464. https://doi.org/10.1098/rstb.2013.0464

Aydogan MG et al (2018) A homeostatic clock sets daughter centriole size in flies. J Cell Biol 217:1233–1248. https://doi.org/10.1083/jcb.201801014

Azimzadeh J, Hergert P, Delouvee A, Euteneuer U, Formstecher E, Khodjakov A, Bornens M (2009) hPOC5 is a centrin-binding protein required for assembly of full-length centrioles. J Cell Biol 185:101–114. https://doi.org/10.1083/jcb.200808082

Bahe S, Stierhof YD, Wilkinson CJ, Leiss F, Nigg EA (2005) Rootletin forms centriole-associated filaments and functions in centrosome cohesion. J Cell Biol 171:27–33. https://doi.org/10.1083/jcb.200504107

Basto R, Brunk K, Vinadogrova T, Peel N, Franz A, Khodjakov A, Raff JW (2008) Centrosome amplification can initiate tumorigenesis in flies. Cell Rep 133:11

Berdnik D, Knoblich JA (2002) Drosophila Aurora-A is required for centrosome maturation and actin-dependent asymmetric protein localization during mitosis. Curr Biol 12:640–647

Bertolin G et al (2018) Aurora kinase A localises to mitochondria to control organelle dynamics and energy production. Elife 7. https://doi.org/10.7554/eLife.38111

Bettencourt-Dias M et al (2005) SAK/PLK4 is required for centriole duplication and flagella development. Curr Biol 15:9

Bury L et al (2017) Plk4 and Aurora A cooperate in the initiation of acentriolar spindle assembly in mammalian oocytes. J Cell Biol 216:3571–3590. https://doi.org/10.1083/jcb.201606077

Castellanos E, Dominguez P, Gonzalez C (2008) Centrosome dysfunction in Drosophila neural stem cells causes tumors that are not due to genome instability. Curr Biol 18:1209–1214. https://doi.org/10.1016/j.cub.2008.07.029

Chestukhin A, Pfeffer C, Milligan S, DeCaprio JA, Pellman D (2003) Processing, localization, and requirement of human separase for normal anaphase progression. Proc Natl Acad Sci USA 100:4574–4579. https://doi.org/10.1073/pnas.0730733100

Coelho PA et al (2015) Over-expression of Plk4 induces centrosome amplification, loss of primary cilia and associated tissue hyperplasia in the mouse. Open Biol 5:150209. https://doi.org/10.1098/rsob.150209

Cole DG, Saxton WM, Sheehan KB, Scholey JM (1994) A "slow" homotetrameric kinesin-related motor protein purified from Drosophila embryos. J Biol Chem 269:22913–22916

Cosenza MR et al (2017) Asymmetric centriole numbers at spindle poles cause chromosome missegregation in cancer. Cell Rep 20:1906–1920. https://doi.org/10.1016/j.celrep.2017.08.005

Cowley DO et al (2009) Aurora-A kinase is essential for bipolar spindle formation and early development. Mol Cell Biol 29:1059–1071. https://doi.org/10.1128/mcb.01062-08

Cucco F et al (2018) Separase prevents genomic instability by controlling replication fork speed. Nucleic Acids Res 46:267–278. https://doi.org/10.1093/nar/gkx1172

Dawei H, Honggang D, Qian W (2018) AURKA contributes to the progression of oral squamous cell carcinoma (OSCC) through modulating epithelial-to-mesenchymal transition (EMT) and apoptosis via the regulation of ROS. Biochem Biophys Res Commun 507:83–90. https://doi.org/10.1016/j.bbrc.2018.10.170

de Carcer G et al (2018) Plk1 overexpression induces chromosomal instability and suppresses tumor development. Nat Commun 9:3012. https://doi.org/10.1038/s41467-018-05429-5

Dictenberg JB et al (1998) Pericentrin and gamma-tubulin form a protein complex and are organized into a novel lattice at the centrosome. J Cell Biol 141:163–174

Du J, Hannon GJ (2004) Suppression of p160ROCK bypasses cell cycle arrest after Aurora-A/STK15 depletion. Proc Natl Acad Sci USA 101:8975–8980. https://doi.org/10.1073/pnas.0308484101

Dzafic E, Strzyz PJ, Wilsch-Brauninger M, Norden C (2015) Centriole amplification in zebrafish affects proliferation and survival but not differentiation of neural progenitor cells. Cell Rep 13:168–182. https://doi.org/10.1016/j.celrep.2015.08.062

Dzhindzhev NS, Tzolovsky G, Lipinszki Z, Abdelaziz M, Debski J, Dadlez M, Glover DM (2017) Two-step phosphorylation of Ana2 by Plk4 is required for the sequential loading of Ana2 and Sas6 to initiate procentriole formation. Open Biol 7(12). pii: 170247. https://doi.org/10.1098/rsob.170247

Eckerdt F, Yamamoto TM, Lewellyn AL, Maller JL (2011) Identification of a polo-like kinase 4-dependent pathway for de novo centriole formation. Curr Biol 21:428–432. https://doi.org/10.1016/j.cub.2011.01.072

Elowe S, Hummer S, Uldschmid A, Li X, Nigg EA (2007) Tension-sensitive Plk1 phosphorylation on BubR1 regulates the stability of kinetochore microtubule interactions. Genes Dev 21:2205–2219. https://doi.org/10.1101/gad.436007

Engle KMM, T-S; Wasa M, Yu J-Q (2008) Anomalous centriole configurations are detected in Drosophila wing disc cells upon Cdk1 inactivation Acc Chem Res 45:5 AU3

Fang Y, Zhang X (2016) Targeting NEK2 as a promising therapeutic approach for cancer treatment. Cell Cycle 15:895–907. https://doi.org/10.1080/15384101.2016.1152430

Faragher AJ, Fry AM (2003) Nek2A kinase stimulates centrosome disjunction and is required for formation of bipolar mitotic spindles. Mol Biol Cell 14:2876–2889. https://doi.org/10.1091/mbc.e03-02-0108

Feng YB et al (2009) Overexpression of PLK1 is associated with poor survival by inhibiting apoptosis via enhancement of survivin level in esophageal squamous cell carcinoma. Int J Cancer 124:578–588. https://doi.org/10.1002/ijc.23990

Fode C, Motro B, Yousefi S, Heffernan M, Dennis JW (1994) Sak, a murine protein-serine/threonine kinase that is related to the Drosophila polo kinase and involved in cell proliferation. Proc Natl Acad Sci USA 91:6388–6392

Fry AM, Mayor T, Meraldi P, Stierhof YD, Tanaka K, Nigg EA (1998a) C-Nap1, a novel centrosomal coiled-coil protein and candidate substrate of the cell cycle-regulated protein kinase Nek2. J Cell Biol 141:1563–1574

Fry AM, Meraldi P, Nigg EA (1998b) A centrosomal function for the human Nek2 protein kinase, a member of the NIMA family of cell cycle regulators. EMBO J 17:470–481. https://doi.org/10.1093/emboj/17.2.470

Fu J, Bian M, Jiang Q, Zhang C (2007) Roles of Aurora kinases in mitosis and tumorigenesis. Mol Cancer Res 5:1–10. https://doi.org/10.1158/1541-7786.mcr-06-0208

Fu J, Hagan IM, Glover DM (2015) The centrosome and its duplication cycle. Cold Spring Harb Perspect Biol 7:a015800. https://doi.org/10.1101/cshperspect.a015800

Fu J et al (2016) Conserved molecular interactions in centriole-to-centrosome conversion. Nat Cell Biol 18:87–99. https://doi.org/10.1038/ncb3274

Ganem NJ, Godinho SA, Pellman D (2009) A mechanism linking extra centrosomes to chromosomal instability. Nature 460:5

Ganier O, Schnerch D, Oertle P, Lim RY, Plodinec M, Nigg EA (2018) Structural centrosome aberrations promote non-cell-autonomous invasiveness. EMBO J 37. https://doi.org/10.15252/embj.201798576

Gergely F, Karlsson C, Still I, Cowell J, Kilmartin J, Raff JW (2000) The TACC domain identifies a family of centrosomal proteins that can interact with microtubules. Proc Natl Acad Sci USA 97:14352–14357. https://doi.org/10.1073/pnas.97.26.14352

Giet R, McLean D, Descamps S, Lee MJ, Raff JW, Prigent C, Glover DM (2002) Drosophila Aurora A kinase is required to localize D-TACC to centrosomes and to regulate astral microtubules. J Cell Biol 156:437–451. https://doi.org/10.1083/jcb.200108135

Godinho SA, Pellman D (2014) Causes and consequences of centrosome abnormalities in cancer. Philos Trans R Soc Lond B Biol Sci 369. pii: 20130467. https://doi.org/10.1098/rstb.2013.0467

Godinho SA et al (2014) Oncogene-like induction of cellular invasion from centrosome amplification. Nature 510:18

Goepfert TM, Adigun YE, Zhong L, Gay J, Medina D, Brinkley WR (2002) Centrosome amplification and overexpression of aurora A are early events in rat mammary carcinogenesis. Cancer Res 62:4115–4122

Golsteyn RM, Mundt KE, Fry AM, Nigg EA (1995) Cell cycle regulation of the activity and subcellular localization of Plk1, a human protein kinase implicated in mitotic spindle function. J Cell Biol 129:1617–1628

Gomez-Ferreria MA, Rath U, Buster DW, Chanda SK, Caldwell JS, Rines DR, Sharp DJ (2007) Human Cep192 is required for mitotic centrosome and spindle assembly. Curr Biol 17:1960–1966. https://doi.org/10.1016/j.cub.2007.10.019

Gonczy P (2012) Towards a molecular architecture of centriole assembly. Nat Rev Mol Cell Biol 13:425–435. https://doi.org/10.1038/nrm3373
Gonczy P, Pichler S, Kirkham M, Hyman AA (1999) Cytoplasmic dynein is required for distinct aspects of MTOC positioning, including centrosome separation, in the one cell stage Caenorhabditis elegans embryo. J Cell Biol 147:135–150
Goto H et al (2006) Complex formation of Plk1 and INCENP required for metaphase-anaphase transition. Nat Cell Biol 8:180–187. https://doi.org/10.1038/ncb1350
Gottardo M, Callaini G, Riparbelli MG (2014) Procentriole assembly without centriole disengagement—a paradox of male gametogenesis. J Cell Sci 127:3434–3439. https://doi.org/10.1242/jcs.152843
Gouveia SM et al (2018) PLK4 is a microtubule-associated protein that self assembles promoting *de novo* MTOC formation. J Cell Sci. https://doi.org/10.1242/jcs.219501
Guichard P et al (2017) Cell-free reconstitution reveals centriole cartwheel assembly mechanisms. Nat Commun 8:14813. https://doi.org/10.1038/ncomms14813
Gurvits N, Loyttyniemi E, Nykanen M, Kuopio T, Kronqvist P, Talvinen K (2017) Separase is a marker for prognosis and mitotic activity in breast cancer. Br J Cancer 117:1383–1391. https://doi.org/10.1038/bjc.2017.301
Habedanck R, Stierhof YD, Wilkinson CJ, Nigg EA (2005) The Polo kinase Plk4 functions in centriole duplication. Nat Cell Biol 7:1140–1146. https://doi.org/10.1038/ncb1320
Hannak E, Kirkham M, Hyman AA, Oegema K (2001) Aurora-A kinase is required for centrosome maturation in Caenorhabditis elegans. J Cell Biol 155:1109–1116. https://doi.org/10.1083/jcb.200108051
Haren L, Stearns T, Luders J (2009) Plk1-dependent recruitment of gamma-tubulin complexes to mitotic centrosomes involves multiple PCM components. PLoS One 4:e5976. https://doi.org/10.1371/journal.pone.0005976
Harris PS et al (2012) Polo-like kinase 1 (PLK1) inhibition suppresses cell growth and enhances radiation sensitivity in medulloblastoma cells. BMC Cancer 12:80. https://doi.org/10.1186/1471-2407-12-80
Hatch EM, Kulukian A, Holland AJ, Cleveland DW, Stearns T (2010) Cep152 interacts with Plk4 and is required for centriole duplication. J Cell Biol 191:721–729. https://doi.org/10.1083/jcb.201006049
Hayward DG, Clarke RB, Faragher AJ, Pillai MR, Hagan IM, Fry AM (2004) The centrosomal kinase Nek2 displays elevated levels of protein expression in human breast cancer. Cancer Res 64:7370–7376. https://doi.org/10.1158/0008-5472.can-04-0960
Hayward DG et al (2010) Identification by high-throughput screening of viridin analogs as biochemical and cell-based inhibitors of the cell cycle-regulated nek2 kinase. J Biomol Screen 15:918–927. https://doi.org/10.1177/1087057110376537
He R, Huang N, Bao Y, Zhou H, Teng J, Chen J (2013) LRRC45 is a centrosome linker component required for centrosome cohesion. Cell Rep 4:1100–1107. https://doi.org/10.1016/j.celrep.2013.08.005
Hellmuth S, Gutierrez-Caballero C, Llano E, Pendas AM, Stemmann O (2018) Local activation of mammalian separase in interphase promotes double-strand break repair and prevents oncogenic transformation. EMBO J 37. pii: e99184. https://doi.org/10.15252/embj.201899184
Hirota T et al (2003) Aurora-A and an interacting activator, the LIM protein Ajuba, are required for mitotic commitment in human cells. Cell 114:585–598
Hudson JW, Kozarova A, Cheung P, Macmillan JC, Swallow CJ, Cross JC, Dennis JW (2001) Late mitotic failure in mice lacking Sak, a polo-like kinase. Curr Biol 11:441–446
Ishikawa H, Kubo A, Tsukita S, Tsukita S (2005) Odf2-deficient mother centrioles lack distal/subdistal appendages and the ability to generate primary cilia. Nat Cell Biol 7:517–524. https://doi.org/10.1038/ncb1251
Izquierdo D, Wang WJ, Uryu K, Tsou MF (2014) Stabilization of cartwheel-less centrioles for duplication requires CEP295-mediated centriole-to-centrosome conversion. Cell Rep 8:957–965. https://doi.org/10.1016/j.celrep.2014.07.022

Jana SC, Marteil G, Bettencourt-Dias M (2014) Mapping molecules to structure: unveiling secrets of centriole and cilia assembly with near-atomic resolution. Curr Opin Cell Biol 26:96–106. https://doi.org/10.1016/j.ceb.2013.12.001

Jeong SB et al (2018) Essential role of polo-like kinase 1 (Plk1) oncogene in tumor growth and metastasis of tamoxifen-resistant breast cancer. Mol Cancer Ther 17:825–837. https://doi.org/10.1158/1535-7163.mct-17-0545

Jimeno A, Rubio-Viqueira B, Rajeshkumar NV, Chan A, Solomon A, Hidalgo M (2010) A fine-needle aspirate-based vulnerability assay identifies polo-like kinase 1 as a mediator of gemcitabine resistance in pancreatic cancer. Mol Cancer Ther 9:311–318. https://doi.org/10.1158/1535-7163.mct-09-0693

Joukov V, Walter JC, De Nicolo A (2014) The Cep192-organized aurora A-Plk1 cascade is essential for centrosome cycle and bipolar spindle assembly. Mol Cell 55:578–591. https://doi.org/10.1016/j.molcel.2014.06.016

Kawakami M et al (2018) Polo-like kinase 4 inhibition produces polyploidy and apoptotic death of lung cancers. Proc Natl Acad Sci USA 115:1913–1918. https://doi.org/10.1073/pnas.1719760115

Kazazian K et al (2017) Plk4 promotes cancer invasion and metastasis through Arp2/3 complex regulation of the actin cytoskeleton. Cancer Res 77:434–447. https://doi.org/10.1158/0008-5472.can-16-2060

Keryer G, Witczak O, Delouvée A, Kemmner WA, Rouillard D, Tasken K, Bornens M (2003) Dissociating the centrosomal matrix protein AKAP450 from centrioles impairs centriole duplication and cell cycle progression. Mol Biol Cell 14:2436–2446. https://doi.org/10.1091/mbc.e02-09-0614

Kim K, Lee S, Chang J, Rhee K (2008) A novel function of CEP135 as a platform protein of C-NAP1 for its centriolar localization. Exp Cell Res 314:3692–3700. https://doi.org/10.1016/j.yexcr.2008.09.016

Kim TS et al (2013) Hierarchical recruitment of Plk4 and regulation of centriole biogenesis by two centrosomal scaffolds, Cep192 and Cep152. Proc Natl Acad Sci USA 110:E4849–E4857. https://doi.org/10.1073/pnas.1319656110

Kimura M, Kotani S, Hattori T, Sumi N, Yoshioka T, Todokoro K, Okano Y (1997) Cell cycle-dependent expression and spindle pole localization of a novel human protein kinase, Aik, related to Aurora of Drosophila and yeast Ipl1. J Biol Chem 272:13766–13771

Kishi K, van Vugt MA, Okamoto K, Hayashi Y, Yaffe MB (2009) Functional dynamics of Polo-like kinase 1 at the centrosome. Mol Cell Biol 29:3134–3150. https://doi.org/10.1128/mcb.01663-08

Kitagawa D et al (2011) Structural basis of the 9-fold symmetry of centrioles. Cell 144:364–375. https://doi.org/10.1016/j.cell.2011.01.008

Kleylein-Sohn J, Westendorf J, Le Clech M, Habedanck R, Stierhof YD, Nigg EA (2007) Plk4-induced centriole biogenesis in human cells. Dev Cell 13:190–202. https://doi.org/10.1016/j.devcel.2007.07.002

Ko MA, Rosario CO, Hudson JW, Kulkarni S, Pollett A, Dennis JW, Swallow CJ (2005) Plk4 haploinsufficiency causes mitotic infidelity and carcinogenesis. Nat Genet 37:883–888. https://doi.org/10.1038/ng1605

Kollareddy M, Dzubak P, Zheleva D, Hajduch M (2008) Aurora kinases: structure, functions and their association with cancer. Biomed Pap Med Fac Univ Palacky Olomouc Czech Repub 152:27–33

Kong D, Farmer V, Shukla A, James J, Gruskin R, Kiriyama S, Loncarek J (2014) Centriole maturation requires regulated Plk1 activity during two consecutive cell cycles. J Cell Biol 206:855–865. https://doi.org/10.1083/jcb.201407087

Konotop G et al (2016) Pharmacological inhibition of centrosome clustering by slingshot-mediated cofilin activation and actin cortex destabilization. Cancer Res 76:6690–6700. https://doi.org/10.1158/0008-5472.can-16-1144

928 Korzeniewski N, Hohenfellner M, Duensing S (2012) CAND1 promotes PLK4-mediated centriole
929 overduplication and is frequently disrupted in prostate cancer. Neoplasia (New York, NY)
930 14:799–806
931 Kovacs L et al (2018) Gorab is a Golgi protein required for structure and duplication of Drosophila
932 centrioles. Nat Genet 50:1021–1031. https://doi.org/10.1038/s41588-018-0149-1
933 Kumada K et al (2006) The selective continued linkage of centromeres from mitosis to interphase in
934 the absence of mammalian separase. J Cell Biol 172:835–846. https://doi.org/10.1083/jcb.
935 200511126
936 Kuriyama R, Bettencourt-Dias M, Hoffmann I, Arnold M, Sandvig L (2009) Gamma-tubulin-
937 containing abnormal centrioles are induced by insufficient Plk4 in human HCT116 colorectal
938 cancer cells. J Cell Sci 122:2014–2023. https://doi.org/10.1242/jcs.036715
939 Kwon M, Godinho SA, Chandhok NS, Ganem NJ, Azioune A, Thery M, Pellman D (2008)
940 Mechanisms to suppress multipolar divisions in cancer cells with extra centrosomes. Genes
941 Dev 22:2189–2203. https://doi.org/10.1101/gad.1700908
942 Leber B et al (2010) Proteins required for centrosome clustering in cancer cells. Sci Transl Med
943 2:33ra38. https://doi.org/10.1126/scitranslmed.3000915
944 Leda M, Holland AJ, Goryachev AB (2018) Autoamplification and competition drive symmetry
945 breaking: initiation of centriole duplication by the PLK4-STIL network. iScience 8:222–235.
946 https://doi.org/10.1016/j.isci.2018.10.003
947 Lee J, Gollahon L (2013) Mitotic perturbations induced by Nek2 overexpression require interaction
948 with TRF1 in breast cancer cells. Cell Cycle 12:3599–3614. https://doi.org/10.4161/cc.26589
949 Levine MS et al (2017) Centrosome amplification is sufficient to promote spontaneous tumorigen-
950 esis in mammals. Dev Cell 40:313–322.e315. https://doi.org/10.1016/j.devcel.2016.12.022
951 Li Z, Dai K, Wang C, Song Y, Gu F, Liu F, Fu L (2016) Expression of polo-like kinase 4(PLK4) in
952 breast cancer and its response to taxane-based neoadjuvant chemotherapy. J Cancer
953 7:1125–1132. https://doi.org/10.7150/jca.14307
954 Li Z et al (2017) Polo-like kinase 1 (Plk1) overexpression enhances ionizing radiation-induced
955 cancer formation in mice. J Biol Chem 292:17461–17472. https://doi.org/10.1074/jbc.M117.
956 810960
957 Li S, Wang C, Wang W, Liu W, Zhang G (2018) Abnormally high expression of POLD1, MCM2,
958 and PLK4 promotes relapse of acute lymphoblastic leukemia. Medicine 97:e10734. https://doi.
959 org/10.1097/md.0000000000010734
960 Lin YC et al (2013) Human microcephaly protein CEP135 binds to hSAS-6 and CPAP, and is
961 required for centriole assembly. EMBO J 32:1141–1154. https://doi.org/10.1038/emboj.2013.
962 56
963 Lingle WL, Salisbury JL (1999) Altered centrosome structure is associated with abnormal mitoses
964 in human breast tumors. Am J Pathol 155:1941–1951. https://doi.org/10.1016/s0002-9440(10)
965 65513-7
966 Lingle WL, Lutz WH, Ingle JN, Maihle NJ, Salisbury JL (1998) Centrosome hypertrophy in human
967 breast tumors: implications for genomic stability and cell polarity. Proc Natl Acad Sci USA
968 95:2950–2955
969 Liu L, Zhang CZ, Cai M, Fu J, Chen GG, Yun J (2012) Downregulation of polo-like kinase 4 in
970 hepatocellular carcinoma associates with poor prognosis. PLoS One 7:e41293. https://doi.org/
971 10.1371/journal.pone.0041293
972 Liu Z, Sun Q, Wang X (2017) PLK1, a potential target for cancer therapy. Transl Oncol 10:22–32.
973 https://doi.org/10.1016/j.tranon.2016.10.003
974 Liu Y et al (2018) Direct binding of CEP85 to STIL ensures robust PLK4 activation and efficient
975 centriole assembly. Nat Commun 9:15
976 Llamazares S et al (1991) Polo encodes a protein kinase homolog required for mitosis in Drosoph-
977 ila. Genes Dev 5:2153–2165
978 Lu LY, Wood JL, Minter-Dykhouse K, Ye L, Saunders TL, Yu X, Chen J (2008) Polo-like kinase
979 1 is essential for early embryonic development and tumor suppression. Mol Cell Biol
980 28:6870–6876. https://doi.org/10.1128/mcb.00392-08

Luders J (2012) The amorphous pericentriolar cloud takes shape. Nat Cell Biol 14:1126–1128. https://doi.org/10.1038/ncb2617
Malumbres M, Barbacid M (2007) Cell cycle kinases in cancer. Curr Opin Genet Dev 17:60–65. https://doi.org/10.1016/j.gde.2006.12.008
Marthiens V, Rujano MA, Pennetier C, Tessier S, Paul-Gilloteaux P, Basto R (2013) Centrosome amplification causes microcephaly. Nat Cell Biol 15:731–740. https://doi.org/10.1038/ncb2746
Martin CA et al (2014) Mutations in PLK4, encoding a master regulator of centriole biogenesis, cause microcephaly, growth failure and retinopathy. Nat Genet 46:1283–1292. https://doi.org/10.1038/ng.3122
Marumoto T, Honda S, Hara T, Nitta M, Hirota T, Kohmura E, Saya H (2003) Aurora-A kinase maintains the fidelity of early and late mitotic events in HeLa cells. J Biol Chem 278:51786–51795. https://doi.org/10.1074/jbc.M306275200
Matsuo K, Ohsumi K, Iwabuchi M, Kawamata T, Ono Y, Takahashi M (2012) Kendrin is a novel substrate for separase involved in the licensing of centriole duplication. Curr Biol 22:915–921. https://doi.org/10.1016/j.cub.2012.03.048
Meng L et al (2014) Inhibition of Nek2 by small molecules affects proteasome activity. BioMed Res Int 2014:13. https://doi.org/10.1155/2014/273180
Meraldi P, Honda R, Nigg EA (2002) Aurora-A overexpression reveals tetraploidization as a major route to centrosome amplification in p53-/- cells. EMBO J 21:483–492
Meyer R, Fofanov V, Panigrahi A, Merchant F, Zhang N, Pati D (2009) Overexpression and mislocalization of the chromosomal segregation protein separase in multiple human cancers. Clin Cancer Res 15:2703–2710. https://doi.org/10.1158/1078-0432.ccr-08-2454
Mogensen MM, Malik A, Piel M, Bouckson-Castaing V, Bornens M (2000) Microtubule minus-end anchorage at centrosomal and non-centrosomal sites: the role of ninein. J Cell Sci 113(Pt 17):3013–3023
Moser AR, Pitot HC, Dove WF (1990) A dominant mutation that predisposes to multiple intestinal neoplasia in the mouse. Science 247:322–324
Moyer TC, Clutario KM, Lambrus BG, Daggubati V, Holland AJ (2015) Binding of STIL to Plk4 activates kinase activity to promote centriole assembly. J Cell Biol 209:863–878. https://doi.org/10.1083/jcb.201502088
Mukherjee M et al (2011) Separase loss of function cooperates with the loss of p53 in the initiation and progression of T- and B-cell lymphoma, leukemia and aneuploidy in mice. PLoS One 6:e22167. https://doi.org/10.1371/journal.pone.0022167
Mukhopadhyay A et al (2016) 14-3-3gamma prevents centrosome amplification and neoplastic progression. Sci Rep 6:26580. https://doi.org/10.1038/srep26580
Nakamura A, Arai H, Fujita N (2009) Centrosomal Aki1 and cohesin function in separase-regulated centriole disengagement. J Cell Biol 187:607–614. https://doi.org/10.1083/jcb.200906019
Nakazawa Y, Hiraki M, Kamiya R, Hirono M (2007) SAS-6 is a cartwheel protein that establishes the 9-fold symmetry of the centriole. Curr Biol 17:2169–2174. https://doi.org/10.1016/j.cub.2007.11.046
Navarro-Serer B, Childers EP, Hermance NM, Mercadante D, Manning AL (2019) Aurora A inhibition limits centrosome clustering and promotes mitotic catastrophe in cells with supernumerary centrosomes. Oncotarget 10(17):1649–1659
Nigg EA (2001) Mitotic kinases as regulators of cell division and its checkpoints. Nat Rev Mol Cell Biol 2:21–32. https://doi.org/10.1038/35048096
Nigg EA (2006) Origins and consequences of centrosome aberrations in human cancers. Int J Cancer 119:2717–2723. https://doi.org/10.1002/ijc.22245
Nigg EA, Stearns T (2011) The centrosome cycle: centriole biogenesis, duplication and inherent asymmetries. Nat Cell Biol 13:1154–1160. https://doi.org/10.1038/ncb2345
O'Connor A, Maffini S, Rainey MD, Kaczmarczyk A, Gaboriau D, Musacchio A, Santocanale C (2015) Requirement for PLK1 kinase activity in the maintenance of a robust spindle assembly checkpoint. Biol Open 5:11–19. https://doi.org/10.1242/bio.014969

1033 Ohta M, Watanabe K, Ashikawa T, Nozaki Y, Yoshiba S, Kimura A, Kitagawa D (2018) Bimodal
1034 binding of STIL to Plk4 controls proper centriole copy number. Cell Rep 23:3160–3169.e3164.
1035 https://doi.org/10.1016/j.celrep.2018.05.030
1036 Okuda M et al (2000) Nucleophosmin/B23 is a target of CDK2/cyclin E in centrosome duplication.
1037 Cell 103:127–140
1038 Pagan JK et al (2015) Degradation of Cep68 and PCNT cleavage mediate Cep215 removal from the
1039 PCM to allow centriole separation, disengagement and licensing. Nat Cell Biol 17:31–43.
1040 https://doi.org/10.1038/ncb3076
1041 Peter M, Nakagawa J, Doree M, Labbe JC, Nigg EA (1990) Identification of major nucleolar
1042 proteins as candidate mitotic substrates of cdc2 kinase. Cell 60:791–801
1043 Pezuk JA, Brassesco MS, de Oliveira RS, Machado HR, Neder L, Scrideli CA, Tone LG (2017)
1044 PLK1-associated microRNAs are correlated with pediatric medulloblastoma prognosis. Childs
1045 Nerv Syst 33:609–615. https://doi.org/10.1007/s00381-017-3366-5
1046 Piel M, Meyer P, Khodjakov A, Rieder CL, Bornens M (2000) The respective contributions of the
1047 mother and daughter centrioles to centrosome activity and behavior in vertebrate cells. J Cell
1048 Biol 149:317–330
1049 Pitner H, Kathryn M, Saavedra HI (2013) Cdk4 and Nek2 signal binucleation and centrosome
1050 amplification in a Her2+ breast cancer model. PLoS One 8:4
1051 Quintyne NJ, Reing JE, Hoffelder DR, Gollin SM, Saunders WS (2005) Spindle multipolarity is
1052 prevented by centrosomal clustering. Science 307:3
1053 Ramani P, Nash R, Sowa-Avugrah E, Rogers C (2015) High levels of polo-like kinase 1 and
1054 phosphorylated translationally controlled tumor protein indicate poor prognosis in neuroblas-
1055 tomas. J Neurooncol 125:103–111. https://doi.org/10.1007/s11060-015-1900-4
1056 Rebacz B, Larsen TO, Clausen MH, Ronnest MH, Loffler H, Ho AD, Kramer A (2007) Identifi-
1057 cation of griseofulvin as an inhibitor of centrosomal clustering in a phenotype-based screen.
1058 Cancer Res 67:6342–6350. https://doi.org/10.1158/0008-5472.can-07-0663
1059 Reber S, Hyman AA (2015) Emergent properties of the metaphase spindle. Cold Spring Harb
1060 Perspect Biol 7:a015784. https://doi.org/10.1101/cshperspect.a015784
1061 Reina J, Gonzalez C (2014) When fate follows age: unequal centrosomes in asymmetric cell
1062 division. Philos Trans R Soc Lond B Biol Sci 369. https://doi.org/10.1098/rstb.2013.0466
1063 Rhys AD et al (2018) Loss of E-cadherin provides tolerance to centrosome amplification in
1064 epithelial cancer cells. J Cell Biol 217:195–209. https://doi.org/10.1083/jcb.201704102
1065 Ring D, Hubble R, Kirschner M (1982) Mitosis in a cell with multiple centrioles. J Cell Biol
1066 94:549–556
1067 Rios RM (2014) The centrosome-Golgi apparatus nexus. Philos Trans R Soc Lond B Biol Sci 369.
1068 https://doi.org/10.1098/rstb.2013.0462
1069 Rodel F et al (2010) Polo-like kinase 1 as predictive marker and therapeutic target for radiotherapy
1070 in rectal cancer. Am J Pathol 177:918–929. https://doi.org/10.2353/ajpath.2010.100040
1071 Rodrigues-Martins A, Riparbelli M, Callaini G, Glover DM, Bettencourt-Dias M (2007) Revisiting
1072 the role of the mother centriole in centriole biogenesis. Science 316:1046–1050. https://doi.org/
1073 10.1126/science.1142950
1074 Rosario CO et al (2010) Plk4 is required for cytokinesis and maintenance of chromosomal stability.
1075 Proc Natl Acad Sci USA 107:6888–6893. https://doi.org/10.1073/pnas.0910941107
1076 Rosario CO et al (2015) A novel role for Plk4 in regulating cell spreading and motility. Oncogene
1077 34:3441–3451. https://doi.org/10.1038/onc.2014.275
1078 Ruppenthal S, Kleiner H, Nolte F, Fabarius A, Hofmann WK, Nowak D, Seifarth W (2018)
1079 Increased separase activity and occurrence of centrosome aberrations concur with transforma-
1080 tion of MDS. PLoS One 13:e0191734. https://doi.org/10.1371/journal.pone.0191734
1081 Sardon T, Pache RA, Stein A, Molina H, Vernos I, Aloy P (2010) Uncovering new substrates for
1082 Aurora A kinase. EMBO Rep 11:977–984. https://doi.org/10.1038/embor.2010.171
1083 Sawin KE, LeGuellec K, Philippe M, Mitchison TJ (1992) Mitotic spindle organization by a plus-
1084 end-directed microtubule motor. Nature 359:540–543. https://doi.org/10.1038/359540a0

Schnerch D, Nigg EA (2016) Structural centrosome aberrations favor proliferation by abrogating microtubule-dependent tissue integrity of breast epithelial mammospheres. Oncogene 35:2711–2722. https://doi.org/10.1038/onc.2015.332

Schultz SJ, Fry AM, Sutterlin C, Ried T, Nigg EA (1994) Cell cycle-dependent expression of Nek2, a novel human protein kinase related to the NIMA mitotic regulator of Aspergillus nidulans. Cell Growth Differ 5:625–635

Sercin O et al (2016) Transient PLK4 overexpression accelerates tumorigenesis in p53-deficient epidermis. Nat Cell Biol 18:100–110. https://doi.org/10.1038/ncb3270

Shah KN et al (2019) Aurora kinase A drives the evolution of resistance to third-generation EGFR inhibitors in lung cancer. Nat Med 25:111–118. https://doi.org/10.1038/s41591-018-0264-7

Shepard JL et al (2007) A mutation in separase causes genome instability and increased susceptibility to epithelial cancer. Genes Dev 21:55–59. https://doi.org/10.1101/gad.1470407

Shinmura K, Tarapore P, Tokuyama Y, George KR, Fukasawa K (2005) Characterization of centrosomal association of nucleophosmin/B23 linked to Crm1 activity. FEBS Lett 579:6621–6634. https://doi.org/10.1016/j.febslet.2005.10.057

Shinmura K, Kurabe N, Goto M, Yamada H, Natsume H, Konno H, Sugimura H (2014) PLK4 overexpression and its effect on centrosome regulation and chromosome stability in human gastric cancer. Mol Biol Rep 41:6635–6644. https://doi.org/10.1007/s11033-014-3546-2

Shukla A, Kong D, Sharma M, Magidson V, Loncarek J (2015) Plk1 relieves centriole block to reduplication by promoting daughter centriole maturation. Nat Commun 6:8077. https://doi.org/10.1038/ncomms9077

Simizu S, Osada H (2000) Mutations in the Plk gene lead to instability of Plk protein in human tumour cell lines. Nat Cell Biol 2:852–854. https://doi.org/10.1038/35041102

Smith L, Farzan R, Ali S, Buluwela L, Saurin AT, Meek DW (2017) The responses of cancer cells to PLK1 inhibitors reveal a novel protective role for p53 in maintaining centrosome separation. Sci Rep 7:16115. https://doi.org/10.1038/s41598-017-16394-2

Sonnen KF, Schermelleh L, Leonhardt H, Nigg EA (2012) 3D-structured illumination microscopy provides novel insight into architecture of human centrosomes. Biol Open 1:965–976. https://doi.org/10.1242/bio.20122337

Stevens NR, Roque H, Raff JW (2010) DSas-6 and Ana2 coassemble into tubules to promote centriole duplication and engagement. Dev Cell 19:913–919. https://doi.org/10.1016/j.devcel.2010.11.010

Stinchcombe JC, Griffiths GM (2014) Communication, the centrosome and the immunological synapse. Philos Trans R Soc Lond B Biol Sci 369. https://doi.org/10.1098/rstb.2013.0463

Suzuki K, Kokuryo T, Senga T, Yokoyama Y, Nagino M, Hamaguchi M (2010) Novel combination treatment for colorectal cancer using Nek2 siRNA and cisplatin. Cancer Sci 101:1163–1169. https://doi.org/10.1111/j.1349-7006.2010.01504.x

Swallow CJ, Ko MA, Siddiqui NU, Hudson JW, Dennis JW (2005) Sak/Plk4 and mitotic fidelity. Oncogene 24:306–312. https://doi.org/10.1038/sj.onc.1208275

Takao D, Yamamoto S, Kitagawa D (2018) A theory of centriole duplication based on self-organized spatial pattern formation. bioRxiv 424754. https://doi.org/10.1101/424754

Tanenbaum ME, Macurek L, Galjart N, Medema RH (2008) Dynein, Lis1 and CLIP-170 counteract Eg5-dependent centrosome separation during bipolar spindle assembly. EMBO J 27:3235–3245. https://doi.org/10.1038/emboj.2008.242

Tang CJ, Fu RH, Wu KS, Hsu WB, Tang TK (2009) CPAP is a cell-cycle regulated protein that controls centriole length. Nat Cell Biol 11:825–831. https://doi.org/10.1038/ncb1889

Tanos BE, Yang HJ, Soni R, Wang WJ, Macaluso FP, Asara JM, Tsou MF (2013) Centriole distal appendages promote membrane docking, leading to cilia initiation. Genes Dev 27:163–168. https://doi.org/10.1101/gad.207043.112

Tian X et al (2018) Polo-like kinase 4 mediates epithelial-mesenchymal transition in neuroblastoma via PI3K/Akt signaling pathway. Cell Death Dis 9:54. https://doi.org/10.1038/s41419-017-0088-2

Tokuyama Y, Horn HF, Kawamura K, Tarapore P, Fukasawa K (2001) Specific phosphorylation of nucleophosmin on Thr(199) by cyclin-dependent kinase 2-cyclin E and its role in centrosome duplication. J Biol Chem 276:21529–21537. https://doi.org/10.1074/jbc.M100014200

Toyoshima-Morimoto F, Taniguchi E, Nishida E (2002) Plk1 promotes nuclear translocation of human Cdc25C during prophase. EMBO Rep 3:341–348. https://doi.org/10.1093/embo-reports/kvf069

Tsou MF, Stearns T (2006) Mechanism limiting centrosome duplication to once per cell cycle. Nature 442:947–951. https://doi.org/10.1038/nature04985

Tsou MF, Wang WJ, George KA, Uryu K, Stearns T, Jallepalli PV (2009) Polo kinase and separase regulate the mitotic licensing of centriole duplication in human cells. Dev Cell 17:344–354. https://doi.org/10.1016/j.devcel.2009.07.015

Uhlmann F, Lottspelch F, Nasmyth K (1999) Sister-chromatid separation at anaphase onset is promoted by cleavage of the cohesin subunit Scc1. Nature 400:37–42. https://doi.org/10.1038/21831

Vitre B et al (2015) Chronic centrosome amplification without tumorigenesis. Proc Natl Acad Sci USA 112:11

Vlijm R et al (2018) STED nanoscopy of the centrosome linker reveals a CEP68-organized, periodic rootletin network anchored to a C-Nap1 ring at centrioles. Proc Natl Acad Sci USA 115:8

Walczak CE, Heald R (2008) Mechanisms of mitotic spindle assembly and function. Int Rev Cytol 265:111–158. https://doi.org/10.1016/s0074-7696(07)65003-7

Wang WJ, Soni RK, Uryu K, Tsou MF (2011) The conversion of centrioles to centrosomes: essential coupling of duplication with segregation. J Cell Biol 193:727–739. https://doi.org/10.1083/jcb.201101109

Wang-Bishop L et al (2018) Inhibition of AURKA reduces proliferation and survival of gastrointestinal cancer cells with activated KRAS by preventing activation of RPS6KB1. Gastroenterology. https://doi.org/10.1053/j.gastro.2018.10.030

Winey M, O'Toole E (2014) Centriole structure. Philos Trans R Soc Lond B Biol Sci 369. https://doi.org/10.1098/rstb.2013.0457

Woodruff JB, Wueseke O, Hyman AA (2014) Pericentriolar material structure and dynamics. Philos Trans R Soc Lond B Biol Sci 369. https://doi.org/10.1098/rstb.2013.0459

Yamamoto S, Kitagawa D (2018) Self-organization of Plk4 regulates symmetry breaking in centriole duplication. bioRxiv 313635. https://doi.org/10.1101/313635

Zhang D et al (2004a) Cre-loxP-controlled periodic Aurora-A overexpression induces mitotic abnormalities and hyperplasia in mammary glands of mouse models. Oncogene 23:8720–8730. https://doi.org/10.1038/sj.onc.1208153

Zhang H, Shi X, Paddon H, Hampong M, Dai W, Pelech S (2004b) B23/nucleophosmin serine 4 phosphorylation mediates mitotic functions of polo-like kinase 1. J Biol Chem 279:35726–35734. https://doi.org/10.1074/jbc.M403264200

Zhang N et al (2008) Overexpression of Separase induces aneuploidy and mammary tumorigenesis. Proc Natl Acad Sci USA 105:13033–13038. https://doi.org/10.1073/pnas.0801610105

Zhang X et al (2009) Sequential phosphorylation of Nedd1 by Cdk1 and Plk1 is required for targeting of the gammaTuRC to the centrosome. J Cell Sci 122:2240–2251. https://doi.org/10.1242/jcs.042747

Zhou W et al (2013) NEK2 induces drug resistance mainly through activation of efflux drug pumps and is associated with poor prognosis in myeloma and other cancers. Cancer Cell 23:48–62. https://doi.org/10.1016/j.ccr.2012.12.001

Author Queries

Chapter No.: 18 461942_1_En

Query Refs.	Details Required	Author's response
AU1	Please check whether affiliations are ok	
AU2	Citation "Engle 2008" has been changed to "Engle et al. 2008" in order to match with the reference list. Please check.	
AU3	Please check the author names in ref. Engle et al. (2008)	

SCIENTIFIC REPORTS

OPEN

14-3-3γ Prevents Centrosome Amplification and Neoplastic Progression

Received: 08 October 2015
Accepted: 04 May 2016
Published: 02 June 2016

Amitabha Mukhopadhyay[1,†], Lalit Sehgal[1,*,‡], Arunabha Bose[1,*], Anushree Gulvady[1,#], Parijat Senapati[2], Rahul Thorat[1], Srikanta Basu[1], Khyati Bhatt[1], Amol S. Hosing[1], Renu Balyan[3], Lalit Borde[4], Tapas K. Kundu[2] & Sorab N. Dalal[1]

More than 80% of malignant tumors show centrosome amplification and clustering. Centrosome amplification results from aberrations in the centrosome duplication cycle, which is strictly coordinated with DNA-replication-cycle. However, the relationship between cell-cycle regulators and centrosome duplicating factors is not well understood. This report demonstrates that 14-3-3γ localizes to the centrosome and 14-3-3γ loss leads to centrosome amplification. Loss of 14-3-3γ results in the phosphorylation of NPM1 at Thr-199, causing early centriole disjunction and centrosome hyper-duplication. The centrosome amplification led to aneuploidy and increased tumor formation in mice. Importantly, an increase in passage of the 14-3-3γ-knockdown cells led to an increase in the number of cells containing clustered centrosomes leading to the generation of pseudo-bipolar spindles. The increase in pseudo-bipolar spindles was reversed and an increase in the number of multi-polar spindles was observed upon expression of a constitutively active 14-3-3-binding-defective-mutant of cdc25C (S216A) in the 14-3-3γ knockdown cells. The increase in multi-polar spindle formation was associated with decreased cell viability and a decrease in tumor growth. Our findings uncover the molecular basis of regulation of centrosome duplication by 14-3-3γ and inhibition of tumor growth by premature activation of the mitotic program and the disruption of centrosome clustering.

The centrosome is the major microtubule nucleating and organizing center in mammalian cells, consisting of two cylindrical centrioles, surrounded by multi-layered toroid of pericentriolar matrix (PCM)[1,2]. Resting cells contain one centrosome which duplicates strictly once in a cell cycle, synchronized with DNA replication cycle, giving rise to two daughter centrosomes before the onset of mitosis [reviewed in[3]]. Deregulation of the centrosome duplication cycle leads to centrosome amplification, which is commonly observed in multiple human tumors [reviewed in[4]]. Normal cells with supernumerary centrosomes generally die, due to the formation of multipolar spindles leading to severe aneuploidy and prolonged checkpoint arrest and mitotic catastrophe. In contrast, tumor cells with multiple centrosomes are able to cluster centrosomes at opposite poles thus generating pseudo-bipolar spindles. Generation of pseudo-bipolar spindles prevents mitotic catastrophe and promotes limited aneuploidy resulting in an increase in cell survival and also resulting in the generation of invasive tumors[5–7].

Two centrioles remain closely connected with each other through a proteinaceous linker, during G1[8]. Biogenesis of the nascent daughter centriole (procentriole) begins with the relaxation of the inter-centriolar tether, resulting in separation of the mother centrioles, termed as centriole disjunction[9,10]. Centriole disjunction is regulated by orchestrated phosphorylation of various linker proteins including NPM1, β-catenin, Nek2, C-Nap1 (CEP250), rootletin, Cep68, causing their displacement from the linker[11–16]. After steric relaxation, procentriole biogenesis proceeds with step-wise assembly of the central "cart-wheel"[17–19]. Procentrioles mature, through the

[1]Advanced Centre for Treatment Research and Education in Cancer, Tata Memorial Center, Mumbai 410210, India. [2]Transcription and Disease Laboratory, Molecular Biology and Genetics Unit, Jawaharlal Nehru Centre for Advanced Scientific Research, Bangalore 560064, India. [3]National Institute of Immunology, New Delhi 110067, India. [4]Department of Biological Sciences, Tata Institute of Fundamental Research, Mumbai 400005, India. [†]Present address: Institute of Biophysical Dynamics, University of Chicago, Chicago, IL 60637, USA. [‡]Present address: Department of Lymphoma and Myeloma, MD Anderson Cancer Center, Texas, TX 77030, USA. [#]Present address: Department of Cell and Developmental Biology, State University of New York Upstate Medical University, Syracuse NY 13210, USA. [*]These authors contributed equally to the work. Correspondence and requests for materials should be addressed to S.N.D. (email: sdalal@actrec.gov.in)

S and G2 phase, from the proximal end of the mother centriole. If centriole disjunction is blocked, in spite of continued nuclear duplication, centriole duplication remains stalled due to inhibition in cartwheel-templating from mother centriole[20].

Current studies indicate that, activation of the cdk1/cyclinB complex is involved in generation of altered centrosome number. However, the centrosomal targets of cdk1 and underlying mechanism of cdk1-mediated regulation of centrosome duplication are largely unknown[21–26]. The cdk1/cyclinB1 complex is activated by cdc25C, whose activity is inhibited during interphase by complex formation with 14-3-3 proteins[27,28]. Here, we report a novel role of the 14-3-3-protein family[29] in regulating centrosome number. We demonstrate that, 14-3-3γ and 14-3-3ε localize to the centrosome and control centrosome duplication by preventing premature activation of cdc25C, the cdk1/cyclinB1 complex and the centrosomal protein Nucleophosmin (NPM1)[30]. Loss of 14-3-3γ results in an increase in aneuploidy, cellular transformation and the formation of larger tumors in nude mice. Surprisingly, the expression of a 14-3-3-binding-deficient mutant of cdc25C (S216A) in 14-3-3γ-knockdown cells, at high passage, led to an extensive increase in spindle multi-polarity, a decrease in centrosome clustering, a decrease in cell survival and a reversal of tumor formation in nude mice. These results suggest that 14-3-3γ-mediated premature activation of the mitotic program during interphase results in an induction in spindle multi-polarity, a decrease in centrosome clustering and an inhibition of tumor formation.

Results

Loss of 14-3-3γ leads to centrosome amplification. Loss of 14-3-3γ (Fig. 1a,b) results in an override of the S and G2 cell cycle check-points in HCT116 cells, leading to premature mitotic progression[31]. In addition to the loss of checkpoint control, an increase in mitotic index was also observed in 14-3-3γ-knockdown cells (Supplementary Fig. S1a,b), a phenotype often associated with centrosome amplification[32,33]. To determine if loss of 14-3-3γ lead to an increase in centrosome number, we determined centrosome number in cells that lack only the 14-3-3γ isoform (Supplementary Fig. S1c and Fig. 1c,d). An increase in number of cells containing supernumerary centrosomes in mitotic phase was observed in the 14-3-3γ-knockdown cells as compared to the vector controls, using antibodies specific to γ-Tubulin [pericentriolar marker[34]], Ninein [mother centriole marker[35]] and Cep-170 [mother centriole marker[36]] (Fig. 1c,d). In addition, cells were also transfected with GFP-Centrin [centriole specific marker[37]] to confirm that loss of 14-3-3γ led to an increase in centrosome number (Fig. 1c,d). Similarly, loss of 14-3-3γ in HEK293 and U2OS cells also led to increased centrosome amplification (Fig. 1e,f). Expression of an shRNA-resistant 14-3-3γ construct resulted in a reversal of centrosome amplification in the 14-3-3γ-knockdown cells (Supplementary Fig. S1d–f), suggesting that centrosome amplification was solely due to loss of 14-3-3γ.

To determine whether the centrosome foci observed in 14-3-3γ-knockdown cells, are intact or fragmented centrosomes, the 14-3-3γ-knockdown and vector control cells were transfected with GFP-Centrin followed by immuno-staining with antibodies to Pericentrin[38]. All the amplified centrosome foci stained for both the centrosomal markers, thus ruling out the possibility that the structures we observe upon 14-3-3γ-loss are centrosome fragments (Supplementary Fig. S1g,h). To determine whether the additional centrosomes can anchor spindles, 14-3-3γ-knockdown cells were transfected with mCherry-α-Tubulin and GFP-Centrin or stained with antibodies to γ-Tubulin, followed by confocal microscopy. All the centrosomes present in 14-3-3γ-knockdown cells act as spindle generation centers (Fig. 1g–i). A minor increase in protein levels was observed for the centrosome protein required for cartwheel formation, h-SAS6 and an increase in the activation of the centrosome associated kinase Aurora A was observed upon loss of 14-3-3γ (Supplementary Fig. S5a,b).

To determine if the increase in centrosome number is observed in other cell cycle phases, centrosome number was estimated in interphase cells. An increase in centrosome number during interphase was also observed in 14-3-3γ-knockdown cells as compared to the vector control, using immunofluorescence with antibodies to Cep-170 and Centrin (Figs 1j–l and 2). To further confirm that we were observing intact centrioles, centrioles were examined using transmission electron microscopy. 14-3-3γ-knockdown cells showed the presence of more than two centrioles during interphase in comparison to the vector-control cells (Fig. 1m).

Centrosome over-duplication is the cause of centrosome amplification. Centrosome amplification can occur in two ways — (i) by *de novo* synthesis without using an existing centriole as template or, (ii) due to defects in template dependent centriole duplication process, which is termed as centriole over-duplication or hyper-duplication[39,40]. To determine the time-point in the cell cycle at which centrosome amplification takes place, cells were synchronized in late G1 with mimosine, prior to the initiation of centrosome duplication, released from the mimosine block and then followed over time. We have quantitated the number of cells with >2 centrosomes in these figures so as to provide a comparison with the experiments shown in Fig. 1. We have not determined the number of cells with only one centrosome, which would be the standard centrosome number during G1 and early S phase. The quantitation shown in this figure does not take into account the number of centrosome amplification events that have occurred in the previous cycle and therefore, the increase in centrosome number upon loss of 14-3-3γ is not observed at early time points in the cell cycle. An alternative explanation is that cells with multiple centrosomes demonstrate an increased sensitivity to mimosine. However, it was observed that centrosome number increases during S-phase between 6–10 hours post release from mimosine and coincides with an increase in the expression of cyclinB1 (Fig. 2a–d). Thus, centrosome amplification, caused by the loss of 14-3-3γ occurs due to centriole over-duplication during interphase.

14-3-3γ-mediated centrosome over-duplication leads to increased aneuploidy and early tumor formation. Cells with multiple spindle poles either die due to a failure to complete mitosis, or survive after a multi-polar mitosis. On occasion, these cells cluster multiple centrosomes at two spindle poles leading to (i) an increase in aneuploidy, (ii) a favorable microtubule organization and (iii) often tumor progression[39]. To test

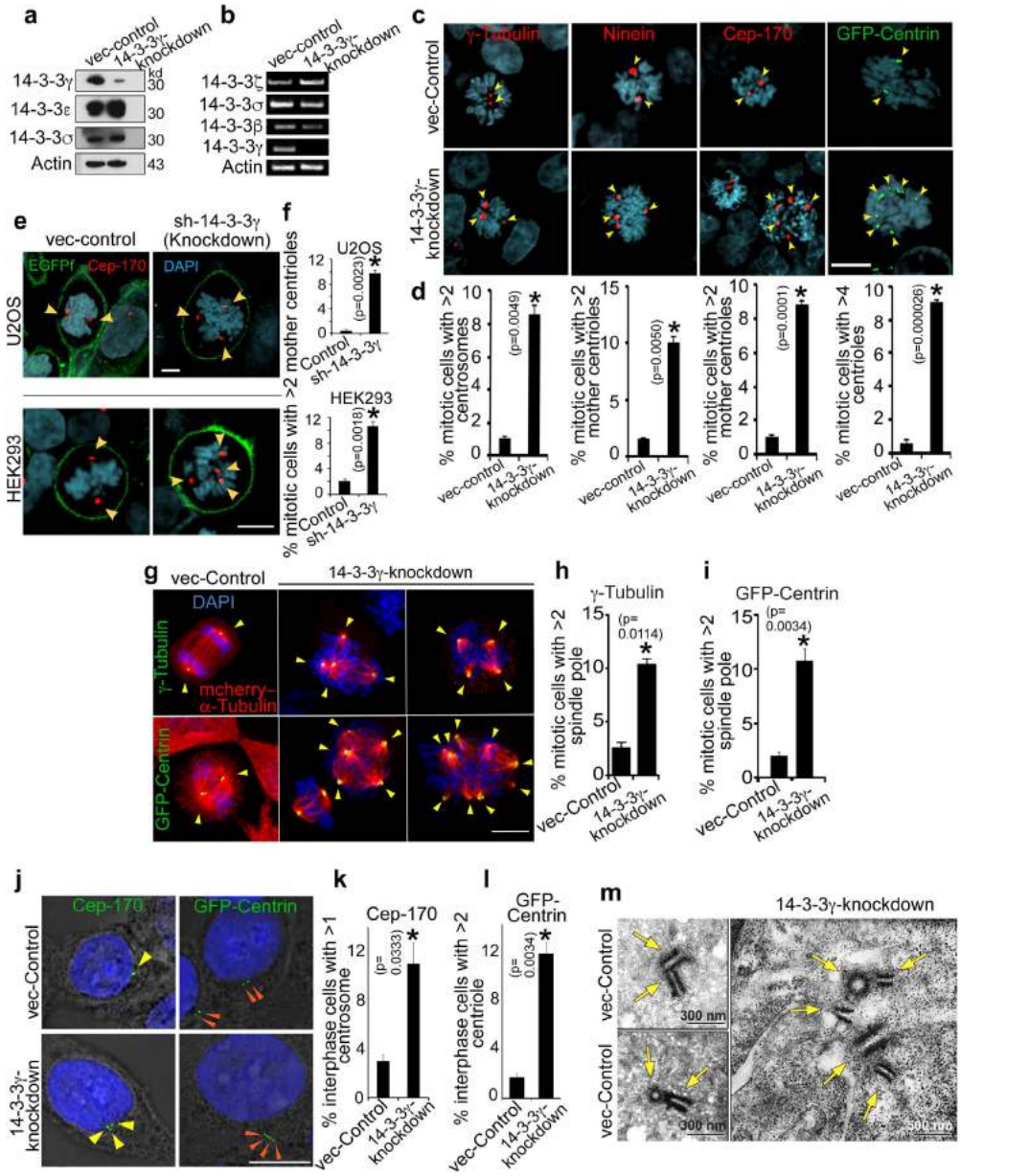

Figure 1. Loss of 14-3-3γ causes centrosome amplification in human cells. (**a–b**) The protein (**a**) and mRNA (**b**) levels of the indicated gene products in 14-3-3γ-knockdown and vector-control cells were determined as described. Actin and GAPDH served as loading controls. (**c–d**) Centrosomes of 14-3-3γ-knockdown and vector-control cells were stained with antibodies specific to γ-Tubulin, Ninein and Cep170, or the cells were transfected with GFP-Centrin as indicated (**c**). Cells were co-stained with DAPI to visualize the nuclei and analyzed by confocal microscopy. Representative images are shown (**c**). The percentage of mitotic cells with more than 2 centrosomes or more than four centrioles was determined in three independent experiments (**d**). (**e–f**) HEK293 or U2OS cells were transfected with plasmids encoding EGFP-f (control) or EGFP-f and shRNA-14-3-3γ. Cells were stained with anti-Cep-170 antibodies, to determine centrosome number. (**g–i**) Multiple spindle poles associated with supernumerary centrosomes were observed by transfecting the cells with mCherry-α-tubulin and GFP-Centrin, or transfection of mCherry-α-tubulin followed by immuno-staining for γ-Tubulin (**g**). The number of spindle poles was determined as indicated in the materials and methods (**h–i**). Note that all the centrosomes anchor the mitotic spindle. (**j–l**) The indicated cells were stained with antibodies to Cep-170 or transfected with GFP-Centrin followed by co-staining with DAPI and the number of centrosomes determined. The images shown are merged with DIC image. (**k**) The number of cells with more than 1 centrosome (for Cep-170) and (**l**) more than 2 centrioles (for Centrin) were determined in three independent experiments. (**m**) Osmium tetroxide stained 14-3-3γ-knockdown and vector-control cells were visualized at 25000x magnification under scanning Electron Microscope. Centrioles are indicated by arrows. All the Western blots were run under the same experimental conditions and the full length blots are in Supplementary Fig. 6. In all the experiments the mean and standard error from at least three independent experiments were plotted, error bars denote standard error of mean and p-values are obtained using Student's t test (2 sample unequal variance) and the asterisk (*) represents a p value <0.05. Original magnification 630X with 2X optical zoom. Scale bar indicate 10 μm, unless mentioned.

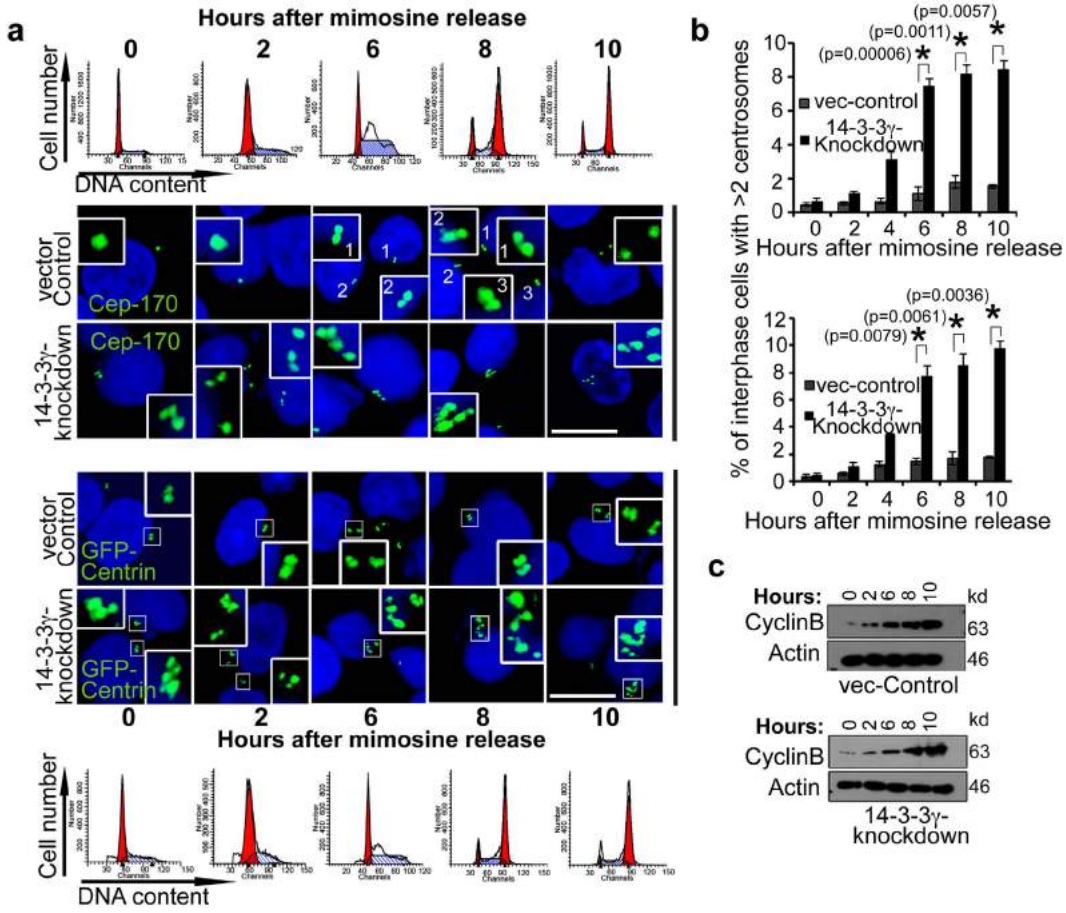

d

Time point (hours)	vec-control			14-3-3γ-knockdown		
	% G0/G1	% S	% G2/GM	% G0/G1	% S	% G2/GM
0	76.79	23.21	0.00	69.96	29.42	0.00
2	62.63	30.37	0.00	69.28	30.72	0.00
6	30.89	69.04	0.07	45.64	54.29	0.07
8	14.13	20.87	65.01	12	21.31	66.69
10	13.94	27.38	58.68	10.61	20.39	69.00

Figure 2. Depletion of 14-3-3γ leads to centrosome over-duplication during S-phase. (**a,b**) 14-3-3γ-knockdown and vector-control cells were transfected with GFP-Centrin and synchronized with mimosine. Another similar set of un-transfected cells were used for staining with anti-Cep-170 antibody. At various time points post mimosine withdrawal (0 hours), cells were either processed for FACS analysis, or were stained with anti-Cep-170 antibody to visualize centrioles and co-stained with DAPI for nuclei. The cells transfected with GFP-Centrin were counter-stained with DAPI. The cell cycle histograms and associated representative confocal images are shown (**a**). The percentage of cells with centrosome amplification was determined at each time point in each experiment and the mean and standard error are plotted (**b**); Student's t test (2 sample unequal variance) was used to determine p-value; $p < 0.05$ (*). (**c**) Protein extracts were resolved on SDS-PAGE gels followed by Western blotting for cyclinB1. Note that an increase in CyclinB1 level is coincident with an increase in centrosome number. Western blots for actin served as a loading control. (**d**) Table showing the percentages of cells in different cell cycle phases at each time point. All the Western blots were run under the same experimental conditions and the full length blots are in Supplementary Fig. 6.

if centrosome over-duplication leads to increased aneuploidy, chromosome number was determined in the 14-3-3γ-knockdown and vector-control cells by counting chromosomes in metaphase plates; HCT116 cells are near diploid and have a normal chromosomal complement (ATCC). Loss of 14-3-3γ-led to an increase in the number of cells with more or less than 46 chromosomes as compared to the vector control (Fig. 3a,b). Moreover, the extent of aneuploidy was increased with sub-culturing ("passage") of the 14-3-3γ-knockdown cells (Fig. 3c,d); cells in passage-55 showing a greater increase in aneuploidy as compared to cell in passage-15. Aneuploidy leads to chromosome instability and chromosome lagging during anaphase, which often results in cells containing

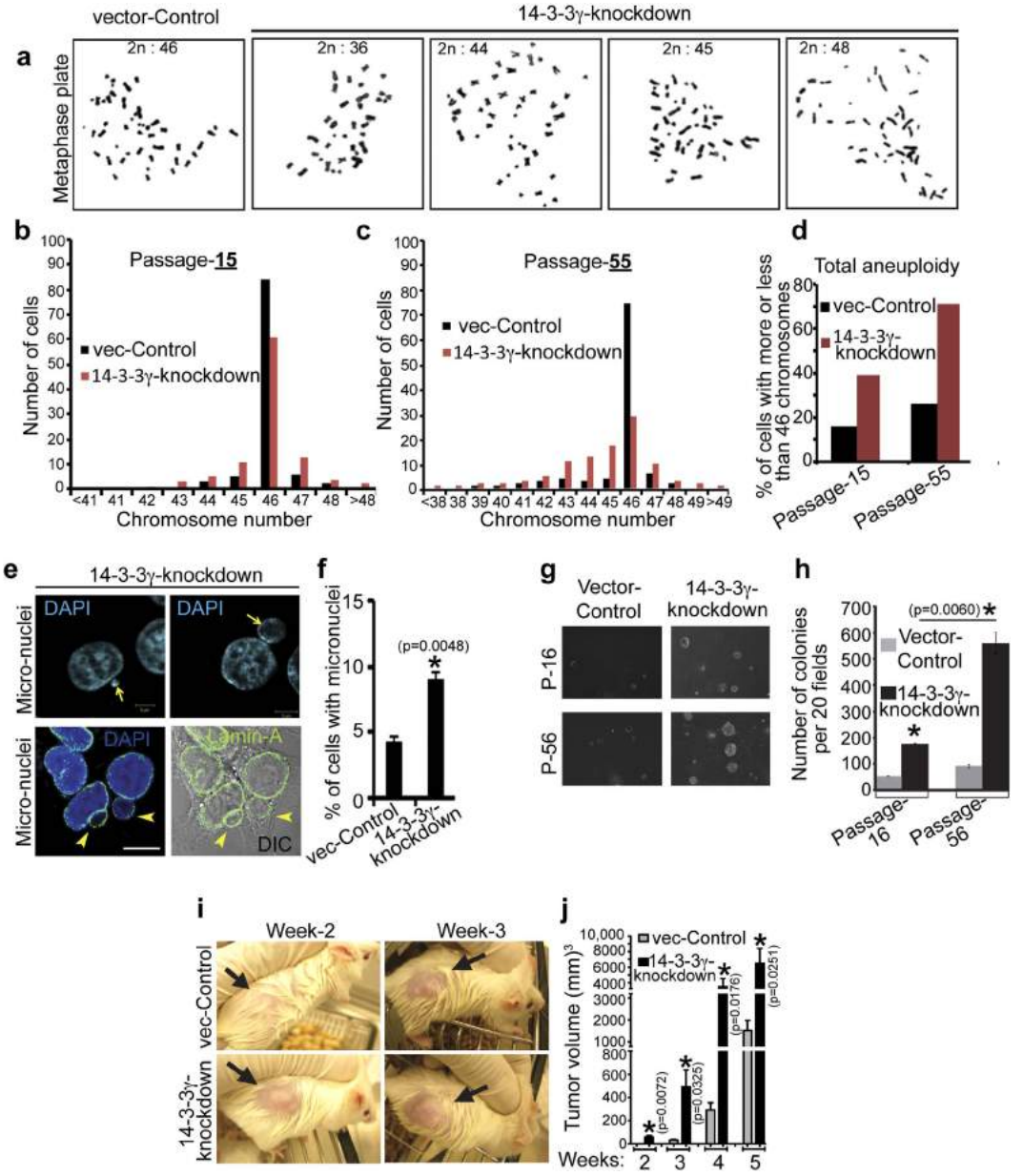

Figure 3. Centrosome amplification, resulted by depletion of 14-3-3γ, leads to higher aneuploidy and increased tumor formation. (**a–d**) Chromosome counts from 14-3-3γ-knockdown cells show an increase in aneuploidy in comparison to the vector control cells. (**a**) Representative metaphase plates (visualized under 1000x magnification of upright fluorescence microscope) with different chromosome numbers from 14-3-3γ -knockdown and vector control cells are shown. (**b,c**) Chromosome numbers from one hundred 14-3-3γ -knockdown and vector control cells were counted at early (15) or late (55) passage. Aneuploidy increases with loss of 14-3-3γ and rise in cellular passage. (**d**) Difference in overall aneuploidy (total number of cells with more or less than 46 chromosomes) between knockdown and control line, at passage-15 and 55, is plotted. (**e**) Micronuclei were observed by DAPI staining or transfection with GFP-Lamin-A. Scale bar is 10 μm unless mentioned. (**f**) The number of cells showing micronuclei formation was determined in the 14-3-3γ-knockdown and vector control cells. 100 cells were counted in three independent experiments and the mean and standard error are plotted. (**g,h**) Early and late passage 14-3-3γ-knockdown and vector control cells were plated in soft agar and colonies counted formed after 2-3 weeks from 20 fields (at 10X magnification) and the mean and standard deviation from three independent experiments is plotted. (**i**) 5 NOD-SCID mice were subcutaneously injected with 10^6 cells of 14-3-3γ-knockdown and control line, and tumor size determined every week as described. (**J**) Tumor volume is plotted on the Y-axis and the time in weeks on the X-axis. The corresponding mean tumor volumes in mm^3 are: Week 2 vec-Control 0, 14-3-3γ knockdown 58.8; Week 3 vec-Control 33.5, 14-3-3γ knockdown 492.5; Week 4 vec-Control 293, 14-3-3γ knockdown 3510; Week 5 vec-Control 1,519, 14-3-3γ knockdown 6,497. An asterisk (*) indicates a p value <0.05. p-values were determined using a Students t-test (2 sample unequal variance).

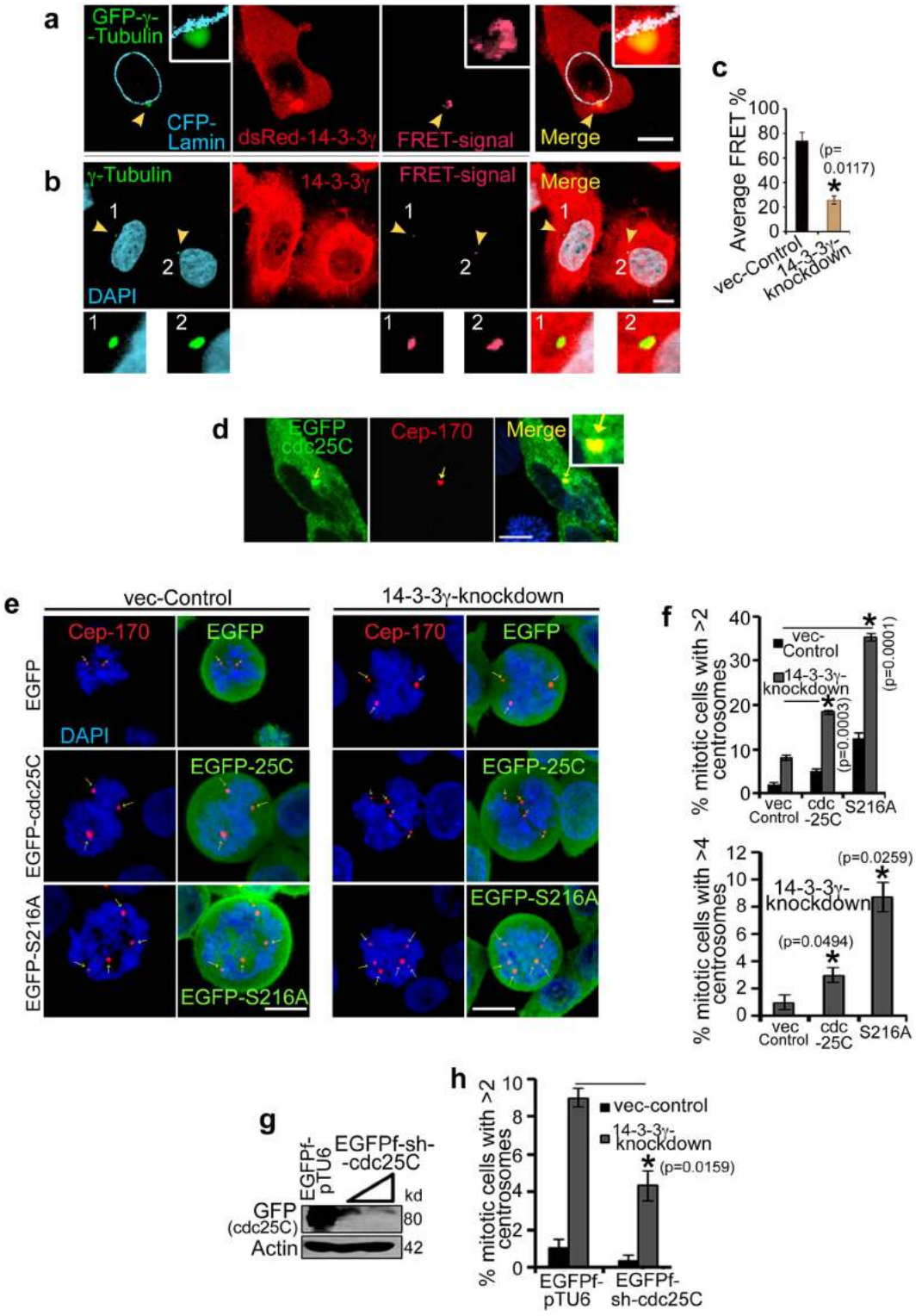

Figure 4. Cdc25C activity stimulates centrosome over-duplication in 14-3-3γ-knockdown cells. (**a–c**) HCT116 cells were transfected with CFP-Lamin-A (cyan), GFP-γ-Tubulin (donor) and dsRed-14-3-3γ (acceptor) (**a**) or stained with antibodies to γ-Tubulin (green) and 14-3-3γ (red) (**b**) and counter-stained with DAPI (blue) followed by sensitized emission FRET analysis. The FRET images are shown in the third panel from the left, while the fourth image from the left shows the merged image as indicated. The smaller panels show a magnified image of the boxed region. (**c**) A comparison of FRET signal intensities obtained from antibody based FRET was performed in 14-3-3γ-knockdown and control line. The graph shows the mean and standard deviation for percentage FRET efficiency from ten different cells. p values indicated were obtained using a student's t-test (2 sample unequal variance) and the asterisk indicates $p < 0.05$. (**d**) Co-localization of cdc25C at centrosome is determined by transfecting HCT116 cells with EGFP-cdc25C (green) and staining with anti Cep-170 (red) antibody. (**e–g**) 14-3-3γ-knockdown cells were transfected with the vector control (EGFP),

EGFP-cdc25C or EGFP-S216A and stained with antibodies to Cep-170 (red) (**e**). (**f,g**) Centrosome number was determined and the mean and standard error from three different experiments is plotted (**h**) 14-3-3γ -knockdown and control cells were co-transfected with GFP-cdc25C and increasing concentration of EGFPf-sh-cdc25C. Western blot is showing the reduction in GFP-cdc25C upon expression of sh-cdc25C. (**i**) Vector control and 14-3-3γ knockdown cells were transfected with the vector control (EGFPf-pTU6) or EGFP-f-shcdc25C. The transfected cells were stained with antibodies to Cep170 and centrosome number was determined in a 100 transfected cells (identified by GFP expression) in three independent experiments. In all cases p values were obtained using a student's t-test. Scale bars are 10 μm unless mentioned. All the Western blots were run under the same experimental conditions and the full length blots are in Supplementary Fig. 6.

micronuclei that appear as extra-nuclear satellite around the nucleus[41,42]. An increase in micronuclei formation was observed in 14-3-3γ-knockdown cells by staining with nuclear specific stain DAPI. Micronuclei also remain surrounded by nuclear membrane, which was observed with antibody specific to nuclear membrane protein, Lamin-A (Fig. 3e,f).

As increase in aneuploidy often leads to neoplastic transformation, soft agar assays were performed to determine if loss of 14-3-3γ could lead to an increase in cellular transformation. 14-3-3γ-knockdown cells showed significantly higher number of colonies with increased diameter in soft agarose assay, in comparison to the control line (Fig. 3g,h and Supplementary Fig. S1i). The number of colonies formed by the 14-3-3γ-knockdown cells showed a greater increase with an increase in passage as compared to the vector control cells. The 14-3-3γ-knockdown cells develop tumors at an early time point and form larger tumors in immune-deficient (NOD-SCID) mice, in comparison to the vector-control cells (Fig. 3i,j). The tumors formed by 14-3-3γ-knockdown cells showed an increased centrosome number in comparison to the tumor tissue sections of vector-control (Supplementary Fig. S1j).

14-3-3γ localizes to the centrosome and interacts with centrosomal proteins. To determine whether 14-3-3γ localizes to the centrosome and forms complex with centrosomal proteins, we performed sensitized emission fluorescence resonance energy transfer (FRET) assays, as described in the materials and methods section[43]. FRET analysis using fluorescently tagged versions of 14-3-3γ and γ-Tubulin demonstrated that 14-3-3γ and γ-Tubulin are in close physical proximity at the centrosome (Fig. 4a). FRET analysis, using immuno-staining with antibodies specific to 14-3-3γ and γ-Tubulin, showed a significantly reduced FRET signal from the 14-3-3γ-knockdown cells as compared to the vector controls, suggesting that 14-3-3γ binds to γ-Tubulin and localizes to the centrosome (Fig. 4b,c). As 14-3-3γ often forms a dimer with 14-3-3ε[44], we determined if 14-3-3ε localized to the centrosome using the PCM marker γ-Tubulin. Confocal microscopy demonstrated that 14-3-3ε localized to the centrosome, however, no FRET was observed between 14-3-3ε and γ-Tubulin (Supplementary Fig. S2d). Similarly, biochemical analyses using bacterially purified 14-3-3 proteins or co-immunoprecipitation assays demonstrated that 14-3-3γ forms a complex with γ-Tubulin, whereas 14-3-3ε showed very little to no interaction with γ-Tubulin (Supplementary Fig. S2e,f). Few other putative centrosomal interactors of 14-3-3γ such as, GCP2[45], KIF5B[46], KLC2[47] were also identified in GST-pulldown coupled mass spectrometric (MALDI-TOF) analysis (Supplementary Fig. S2g). As 14-3-3γ and 14-3-3ε localize to the centrosome, we tested the effect of combined loss of both the isoforms on centrosome amplification. Expression of both 14-3-3γ and 14-3-3ε was inhibited using vector driven RNAi and centrosome number was determined in mitotic cells. Loss of either 14-3-3ε or 14-3-3γ led to a similar increase in centrosome number in HCT116 cells, in comparison to the vector control (Supplementary Fig. S2a–c). However, inhibiting the expression of both 14-3-3γ and 14-3-3ε resulted in an additive effect in the increase in centrosome number. Therefore, these results suggest that 14-3-3ε and 14-3-3γ localize to the centrosome and prevent centrosome re-duplication in HCT116 cells.

14-3-3γ prevents centrosome amplification by inhibiting cdc25C function. 14-3-3γ and 14-3-3ε form a complex with cdc25C and resulting in an inhibition of cdc25C function by preventing it from activating the substrate cdk1/cyclinB[27,48,49]. Cdc25C localizes to centrosome[50,51] and activates the centrosomal cdk1/cyclinB1 complex, resulting in activation of the mitotic cascade[52,53]. Therefore it is possible that increased cdc25C activation, upon loss of 14-3-3γ, could be responsible for centrosome amplification in the 14-3-3γ knockdown cells. As previously reported by this laboratory[31], immuno-blotting with phospho-S216-cdc25C specific antibodies demonstrate that cdc25C is constitutively active in the 14-3-3γ knockdown cells due to a decrease in the levels of cdc25C phosphorylated on S216 when compared to the vector control (Supplementary Fig. S3a). GFP-tagged cdc25C co-localizes with the centrosome during interphase as demonstrated by immuno-staining with antibodies to Cep170 (Fig. 4d). Over-expression of cdc25C or the 14-3-3-binding-defective mutant cdc25C-S216A in 14-3-3γ-knockdown cells resulted in a greater increase in centrosome amplification than that observed with the vector control cells (Fig. 4e,f and Supplementary Fig. S3b) and the increase was similar to that observed when the expression of both 14-3-3γ and 14-3-3ε were inhibited in these cells. Inhibition of cdc25C expression using vector driven RNAi reduced the extent of centriole over duplication (Fig. 4g,h and Supplementary Fig. S3c). These results suggest that an increase in cdc25C activity leads to centrosome over-duplication. As other cdc25 isoforms also form a complex with 14-3-3 proteins though not with 14-3-3γ[54,55], the effect of over-expressing cdc25A and cdc25B on centrosome number was determined in the vector control and 14-3-3γ-knockdown cells. Epitope tagged cdc25A, cdc25B and cdc25C were transfected into the vector control and 14-3-3γ-knockdown cells and centrosome number determined as described in materials and methods. Expression of the individual cdc25 isoforms resulted in 10–20% increase in 14-3-3γ-knockdown cells containing multiple centrosomes, in comparison to the vector-control cells (Supplementary Fig. S3e). Similarly, a knockdown of cdc25A, B and C by individual shRNA constructs reduced the percentage of multiple centrosome containing 14-3-3γ-knockdown

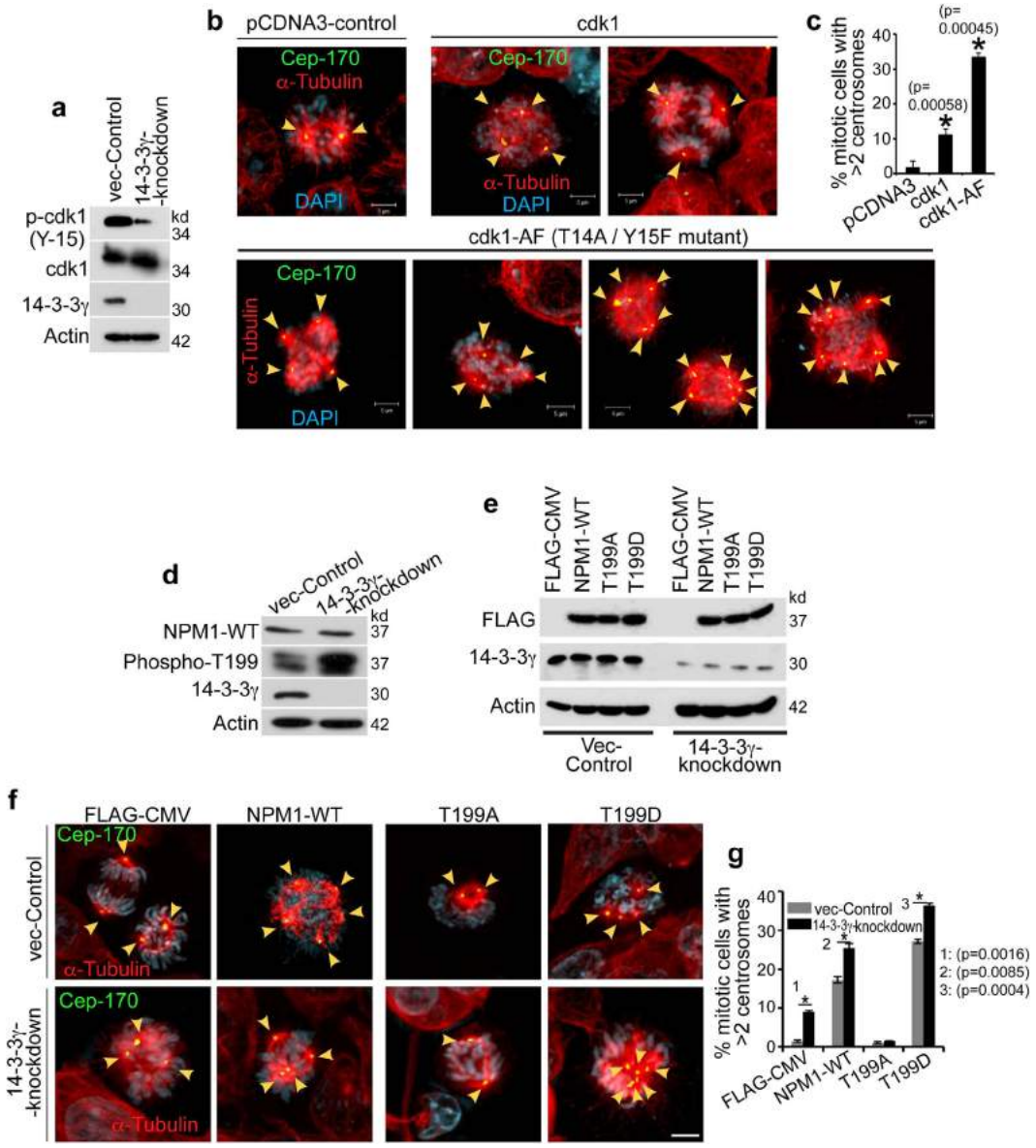

Figure 5. Increased NPM1 phosphorylation at T199 leads to centrosome duplication in 14-3-3γknockdown cells. (**a**) Protein extracts from vector control or 14-3-3γ knockdown cells were resolved on SDS-PAGE followed by immuno-blotting with the indicated antibodies. Actin served as loading control. (**b,c**) HCT116 cells were transfected with mCherry-α-tubulin and co-transfected with either the control plasmid (pCDNA3) or plasmids encoding wild type cdk1 (cdk1) or constitutively active cdk1 (cdk1AF). Post-transfection the cells were stained with antibodies to Cep170 (green) and DAPI (blue) (**b**). The percentage of mitotic cells with >2 centrosomes was determined in three independent experiments (**c**). (**d**) Protein extracts from the vector control and 14-3-3γ knockdown cells were resolved by SDS-PAGE, followed by Western blotting with the indicated antibodies. Note that NPM1 is phosphorylated on T199 to a greater degree in the 14-3-3γ knockdown cells. Actin served as loading control. (**e**) The 14-3-3γ -knockdown and vector control cells were transfected with either the vector control or FLAG-epitope tagged versions of WT NPM1 or the NPM1 mutants (T199A and T199D). Post transfections, protein extracts prepared from these cells were resolved by SDS-PAGE followed by Western blotting with the indicated antibodies. Western blots for actin serves as loading controls. (**f,g**) 14-3-3γ-knockdown and vector-control cells, transfected with mCherry-α-tubulin and FLAG-NPM1 constructs, were stained with antibodies to Cep-170, co-stained with DAPI and followed by confocal microscopy (**f**) to determine the percentage of cells containing >2 centrosomes. The mean and standard deviation of three independent cells is plotted (**g**) p values were determined using a Student's t-test (2 sample unequal variance) with $p < 0.05$. Scale bars indicate 5 μm. All the Western blots were run under the same experimental conditions and the full length blots are in Supplementary Fig. 6.

cells (Supplementary Fig. S3f). These results suggest that all the cdc25 isoforms contribute to centrosome amplification in this cell type.

Premature activation of cdk1 during interphase results in centrosome amplification. Cdc25C activates cdk1/CyclinB1, by dephosphorylating Thr14 and Tyr15 residues of cdk1 [reviewed in[56]] and therefore we determined if the increase in centrosome amplification observed upon cdc25C activation was due to an increase in cdk1 activity. A reduction in Tyr-15 phosphorylation of cdk1 in 14-3-3γ-knockdown cells indicated that cdk1 was active in 14-3-3γ-knockdown cells (Fig. 5a). If cdk1 activation is responsible for the centrosome over-duplication upon loss of 14-3-3γ, over-expression of cdk1 or the constitutively active mutant, cdk1AF[57], should result in an increase in centrosome number. Over-expression of either cdk1 or cdk1-AF resulted in an increase in centrosome over-duplication in HCT116 cells, a phenotype similar to that observed upon the over-expression of cdc25C (Fig. 5b,c and Supplementary Fig. S4a,b). The increase in centrosome duplication by over-expression of cdk1-AF was comparable to that observed with cdc25C-S216A expression in 14-3-3γ-knockdown cells (Figs 4g and 5c). Inhibition of cdk1 expression reduced centrosome amplification in 14-3-3γ-knockdown cells (Supplementary Fig. S4c,d). Similar results were obtained when we inhibited the expression of cdk2, which has previously been shown to be essential for centrosome duplication[11]. Depletion of both the cdks resulted in an additive decrease in centrosome duplication. These results suggest that the presence of an active cdk1 complex is responsible for centrosome over-duplication and are consistent with our data that centrosome over-duplication is co-incident with the expression of CyclinB1 in these cells (Fig. 2d).

Cdk1 phosphorylates the centriolar linker protein NPM1 leading to centrosome amplification. Phosphorylation of the inter-centriolar linker protein Nucleophosmin (or NPM1, also known as B23, Numatrin or NO38) at T199 residue causes its detachment from the centriolar linker, thus increasing the distance between two centrioles and providing the spatial signal for procentriole biogenesis, templating from the mother centriole[16,58,59]. *In vitro* kinase assays demonstrated that the T199 residue of NPM1 could be phosphorylated by cdk1/cyclinB1 complex, while the phospho-deficient mutant, NPM1-T199A does not serve as an efficient substrate for cdk1 (Supplementary Fig. S4e,f). In addition, an increase in T199 phosphorylation of NPM1 was also observed in the 14-3-3γ-knockdown cells upon immuno-blotting with phospho-specific antibodies recognizing NPM1 phosphorylated on T199 (Fig. 5c). To test the effect of cdk1-mediated T199-phosphorylation of NPM1 on centrosome over-duplication, we expressed the phospho-mimetic (T199D) and phospho-deficient (T199A) mutants of NPM1 in 14-3-3γ-knockdown cells (Fig. 5d). The extent of centrosome amplification was significantly reduced with the expression of NPM1-T199A, while the centrosome amplification was increased upon T199D expression (Fig. 5e,f). To confirm that the increase in NPM1 phosphorylation occurs during S-phase, a cell cycle synchrony experiment was performed as described earlier. Western blot analyses demonstrated that NPM1 phosphorylation in the vector control cells first appears at 10 hours post release from mimosine when the majority of the cells are in G2 phase, while in the 14-3-3γ knockdown cells NPM1 phosphorylation appears at the six hour time point and coincides with the increased expression of cyclin B1 (Supplementary Fig. S5c). These results are consistent with our observation that cdk1 is prematurely active upon loss of 14-3-3γ (Fig. 5a), suggesting that cdk1 might be the major NPM1 kinase in cells lacking 14-3-3 γ. Therefore, premature activation of cdk1 in 14-3-3γ-knockdown cells causes hyper-phosphorylation of T199 residue of NPM1 and possibly other centrosomal proteins resulting in centrosome amplification.

Premature cdc25C activation reduces centrosome clustering and inhibits tumor growth. Normal cells cannot tolerate centrosome amplification and die eventually due to spindle asymmetry, mitotic catastrophe, unfavorable aneuploidy or defects in interphase cytoskeletal organization[60,61]. In contrast, aggressive tumor cells have evolved a mechanism to cluster multiple centrosomes and thus generating a pseudo-bipolar spindle during mitosis to maintain a lower level of aneuploidy thus preventing mitotic catastrophe[62–64]. Tumorigenic potential and aggressiveness of cultured cells generally increase with the increase in sub-culturing or "passage"[65,66]. A gradual increase in centrosome clustering with progressive sub-culturing was observed in the 14-3-3γ-knockdown cells as compared to the vector control (Fig. 6a–c). While an increase in multi-polar spindle formation was also observed in 14-3-3γ-knockdown cells, the increase in the number cells with clustered centrosomes is greater in the 14-3-3γ knockdown cells. This suggests that loss of 14-3-3γ leads to the selection of a population of cells that are capable of clustering their supernumerary centrosomes.

Inhibition of centrosome clustering has been shown to result in tumor cell death by generating multipolar mitoses, or by leading to abnormalities in cell polarization, focal adhesion and migration[64,67]. As over-expression of cdc25C in the 14-3-3γ-knockdown cells led to an increase in centrosome number, we wished to determine if the increase in centrosome number affected cell survival and tumor formation. MTT assays demonstrated that expression of both WT cdc25C and the cdc25C-mutant (S216A) in the 14-3-3γ-knockdown cells resulted in a significant decrease in cell viability (Supplementary Fig. S3d). We tested if over-expression of cdc25C-S216A in 14-3-3γ-knockdown cells could reverse centrosome clustering observed in the 14-3-3γ knockdown cells. Expression of either cdc25C or cdc25C-S216A in 14-3-3γ-knockdown cells at different passages led to a decrease in centrosome clustering and increase in spindle-multipolarity (Fig. 6d,e). To determine if this decrease in centrosome clustering and cell viability is associated with a decrease in neoplastic transformation, doxycycline inducible constructs for cdc25C or cdc25C-S216A were expressed in the 14-3-3γ-knockdown cells (Fig. 6f). Cells were selected in puromycin and soft agar assays performed in the presence or absence of doxycycline. A significant reduction in soft agar colony formation was observed in 14-3-3γ-knockdown cells expressing cdc25C-S216A (Fig. 6g). To find if over-expression of cdc25C-S216A in the 14-3-3γ-knockdown cells could lead to a decrease in tumor formation, 14-3-3γ-knockdown cells were transfected with the inducible constructs of cdc25C-S216A described above. 48 hours post transfection cells were enriched by puromycin selection and then injected

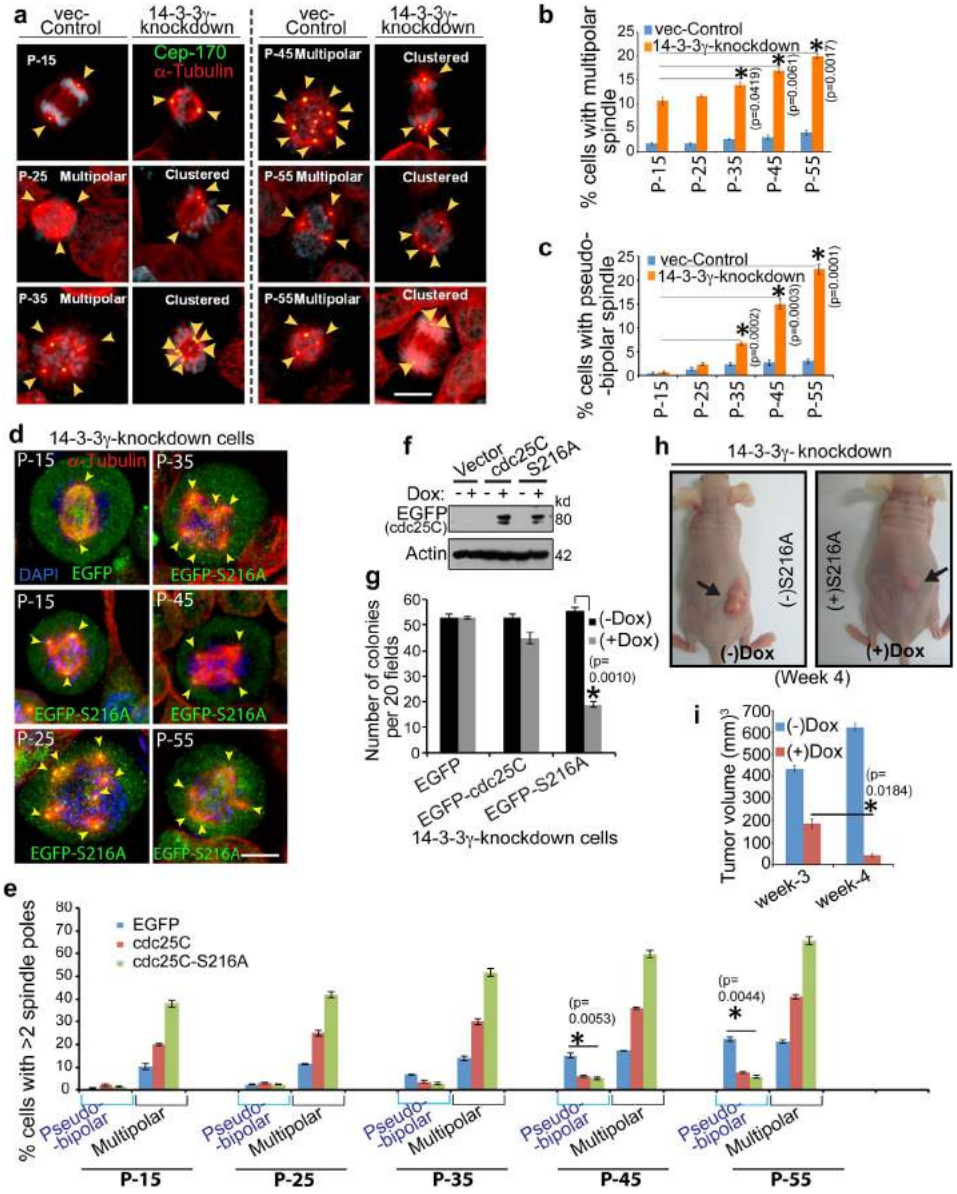

Figure 6. Over-expression of cdc25C-S216A leads to an increase in multipolar mitoses and a decrease in neoplastic progression. (**a**) 14-3-3γ-knockdown and vector control cells at different passages (P) were fixed and stained with antibodies to α-tubulin and Cep-170 and co-stained with DAPI. Arrows indicate centrosome poles. (**b,c**) The percentage of cells with multi-polar spindles and pseudo bi-polar spindles was determined in three independent experiments and the mean and standard error plotted. (**d**) 14-3-3γ-knockdown cells were transfected with EGFP, EGFP-cdc25C or EGFP-S216A constructs. Cells were fixed and stained with anti-α -Tubulin antibody and co-stained with DAPI. Arrows indicate spindle poles. (**e**) The percentage of cells with multi-polar spindles and pseudo bi-polar spindles was determined in three independent experiments and the mean and standard deviation plotted. A significant increase in the number of cells with multi-polar spindles and a corresponding decrease in the number of cells with pseudo-bipolar spindles was observed in cells expressing the two cdc25C constructs at all passages. (**f,g**) 14-3-3γ-knockdown cells were transfected with doxycycline (Dox) inducible constructs expressing either GFP or EGFP-cdc25C or EGFP-cdc25C-S216A. Post transfection the cells were selected in puromycin to select transfected cells. Transfected cells were grown in the presence or absence of doxycycline and protein extracts were resolved on SDS-PAGE gels followed by Western blotting with the indicated antibodies (**f**) or the cells were embedded in soft agar in the presence or absence of doxycycline and colony formation determined in three independent experiments. The mean and standard deviation are plotted (**g**). (**h,i**) 14-3-3γ-knockdown cells were transfected with doxycycline (Dox) inducible constructs expressing EGFP-cdc25C-S216A. Post selection, cells were injected subcutaneously in Nude mice. One set was given doxycycline in the drinking water (+Dox) and the other set received no doxycycline (−Dox). Tumor volume was measured and the mean and standard error are plotted from 4 × 2 sets of mice at different times post injection. p values were obtained using Student's t test (2 sample unequal variance). p values <0.05 are indicated by asterisk. All the Western blots were run under the same experimental conditions and the full length blots are in Supplementary Fig. 6.

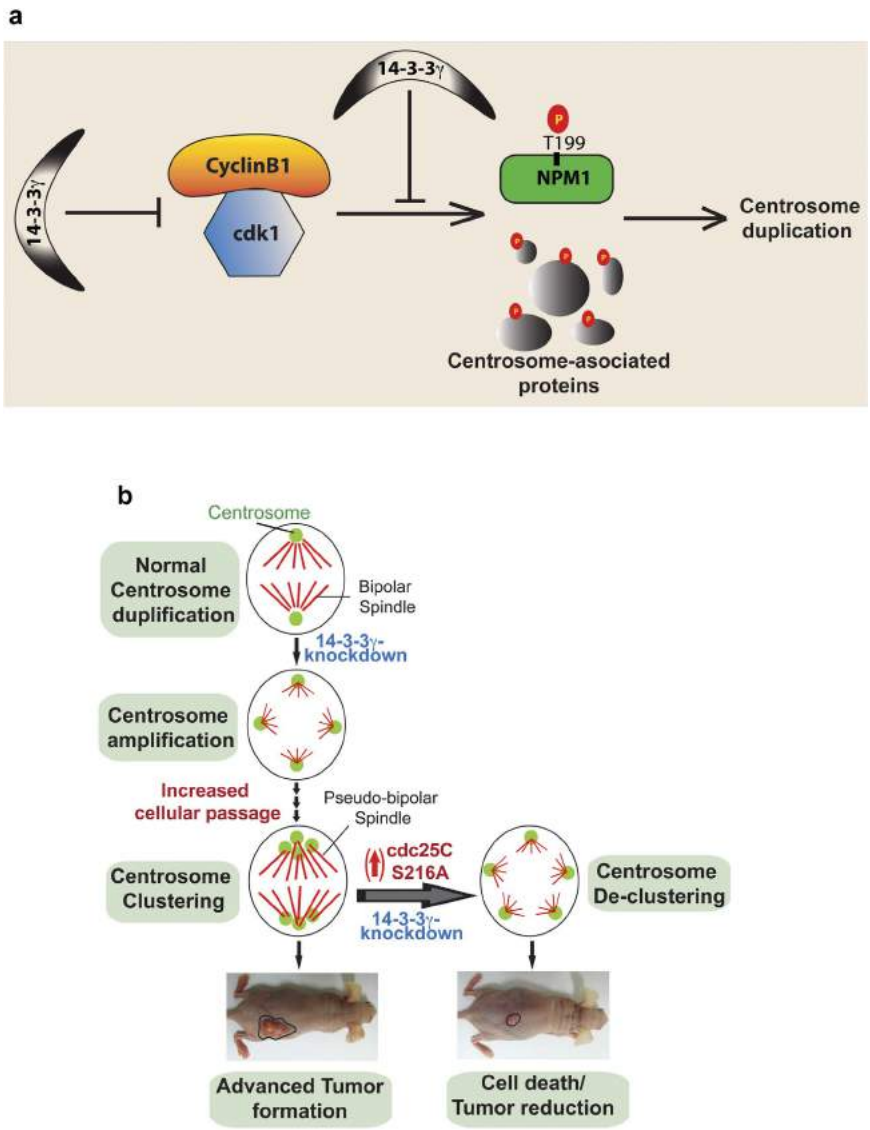

Figure 7. Model for centrosome duplication and reduced tumor formation upon activation of cdc25C. (**a**) 14-3-3γ sequesters cdc25C in cytoplasm during S phase and thus cdk1 remains inactive due to the inhibitory phosphorylation at Thr-14 and Tyr-15. As a consequence, NPM1 is not phosphorylated at T199 and remains associated with inter-centriolar linker. (**b**) Loss of 14-3-3γ causes activation of cdc25C resulting in dephosphorylation and activation of cdk1. Active cdk1 phosphorylates T199 of NPM1. T199 phosphorylation of NPM1 results in its dissociation from centriolar linker. Dissociation of NPM1 from centriolar linker leads to centriole separation (disjunction) and thus provides steric permission for procentriole nucleation and maturation. (**c**) Expression of active-cdc25C (cdc25C-S216A), in 14-3-3γ-knockdown cells prematurely activates cdk1, which leads to centrosome hyper-duplication through increased phosphorylation of residue T199 in NPM1. (**d**) Centrosomes cluster with the increase in passage in the 14-3-3γ knockdown cells leading to increased transformation. A decrease in centrosome clustering is observed upon premature activation of cdc25C, resulting in a decrease in tumor growth.

subcutaneously into nude mice. The mice were segregated into two groups and one group was given doxycycline in the drinking water to induce S216A expression. Mice given doxycycline in the drinking water developed smaller tumors than mice that were not given doxycycline, suggesting that cdc25C-S216A expression leads to a decrease in tumor formation (Fig. 6h,i). Therefore we conclude that, depletion of 14-3-3γ and the premature hyper-activation of cdc25C, causes hyper-activation in cdk1 and hyper-phosphorylation of NPM1 at T199 residue and other centrosome associated proteins (Fig. 7a) during interphase leading to (i) reversal of centrosome clustering, (ii) generation of extensive spindle multipolarity, (iii) cell death in culture and (iv) inhibition of tumorigenesis in mice (Fig. 7b).

Discussion

We report for the first time that, loss of 14-3-3γ causes centrosome over-duplication, centrosome clustering and tumor formation in mice. Although 14-3-3 proteins have been isolated from centrosomal fractions[68], the molecular basis and isoform specific role of 14-3-3 in centrosome duplication remained unknown. In this study, we have demonstrated that 14-3-3ε and 14-3-3γ localize to the centrosome and form complexes with centrosomal proteins. Our results demonstrate a mechanism by which 14-3-3γ restricts centrosome duplication to once per cell cycle, by inhibiting cdc25C function, thus preventing premature activation of cdk1 during interphase and resulting in a decrease in phosphorylation of T199 residue of the centriolar linker protein NPM1. Identification of the molecular basis of 14-3-3γ-mediated centrosome duplication helped to design a way to reduce centrosome clustering, leading subsequently to a decrease in tumor formation in nude mice by over-expression of constitutively active (14-3-3-binding-deficient) cdc25C in 14-3-3γ-knockdown cells. This also suggests that complete disruption of the cdc25C-14-3-3 complex during interphase might be a way to inhibit tumor growth and selective tumor cell killing.

In *S. pombe*, cdc25 activates the cdc2 (cdk1-ortholog)/cyclinB complex, which phosphorylates a spindle pole body protein Cut12 (Stf1). Gain of function mutation in Cut12 is sufficient to drive mitosis in the absence of cdc25C, and loss of Cut12 results in the failure in microtubule nucleation, failure to associate Spindle Pole Bodies to the nuclear membrane and failure in mitotic entry leading to mitotic arrest. The defects observed upon Cut12 deletion could be rescued by enhancing cdc25C or cdk1 function suggesting that cdc25C and cdk1 have a role to play in centrosome duplication[24,69,70]. However, experiments in other cell systems have suggested that loss of cdk1 leads to an increase in centrosome number due to the induction of multiple rounds of S-phase[71,72]. One of these studies[71] reported that, while inhibition of cdk1 in rodent cells causes centrosome amplification due to endo-reduplication, the same phenotype was not observed in human cell lines including HCT116 and U-2OS, similar to the results reported here. The differences observed between experiments performed in *Drosophila* or rodent cell lines in culture and in human cell lines might be due to species specific differences in centrosome duplication. Altogether, these observations support the fact that increased cdk1-activation can lead to centrosome amplification in human cells. Cdk1 overexpression leads to genomic instability, centrosome separation[22,23,73] and centrosome amplification[74]. Nam and van Deursen recently showed that cyclin B overexpression in the mouse leads to accelerated centrosome separation, chromosome mis-segregation and tumor formation through a Plk1−Nek2−C-NAP1/rootletin mediated pathway[26,75]. Therefore, it is evident that increased activation of the cyclin B/cdk1 complex leads to centrosome amplification, aneuploidy and tumor formation. Further, activation of cdk1 leads to the activation of Plk1 by the Aurora-A and Bora kinases[76]. Plk1 activation is responsible for Cep-152/Cep-192 mediated activation of Plk-4, which drives centriolar cartwheel formation through 9-fold assembly of Sas-6 dimers[77–79]. Thus, a positive feedback loop of cdk1 is required for the commitment of M phase progression[80] and initiation of centriole biogenesis.

Although NPM1 is phosphorylated by the G1/S checkpoint regulator cdk2[16], it was not clear if NPM1 could also serve as a cdk1 substrate for centriole disjunction during S-phase[12,59]. In this study, we have demonstrated that T199 residue of NPM1 is a target of cdk1, and early phosphorylation of NPM1 by cdk1 leads to a premature increase in centrosome number. Further, our results suggest that in HCT116 cells cdk1 is the major NPM1 kinase and that the increase in NPM1 phosphorylation upon loss of 14-3-3γ is due to a premature increase in cdk1 activity. Our data does not exclude the possibility that cdk1 phosphorylates other centrosomal proteins, in addition to NPM1, and that these substrates might also contribute to the increase in centrosome number observed upon loss of 14-3-3γ (Fig. 7a). Interestingly, loss of either cdk1 or cdk2 in the 14-3-3γ knockdown cells leads to a decrease in centrosome number, suggesting that cdk1 is not phosphorylating the same set of substrates as cdk2. Therefore, when cdk1 is prematurely activated during S-phase in the 14-3-3γ-knockdown cells, it stimulates centrosome over-duplication and this requires cdk2 activity suggesting that the activity of both proteins is required for centrosome amplification.

Our work also demonstrates that the mitotic phosphatase cdc25C is required for the increase in centrosome number observed upon loss of 14-3-3γ. However, over-expression of all the cdc25 isoforms in HCT116 cells results in an increase in centrosome number and a knockdown of the individual isoforms reduces centrosome number (Supplementary Fig. S3e,f). While both cdc25A and cdc25B have been reported to bind to 14-3-3 proteins, neither forms a complex with 14-3-3γ and have been shown to bind other 14-3-3 isoforms[54,55]. It is possible that all of the cdc25 isoforms can regulate the increase in centrosome duplication, indeed it has been reported that all of them are required for the complete activation of cdk1/cyclinB[81] and that multiple isoforms need to be inactivated to generate a cell cycle arrest[82]. These are also consistent with our results that over-expression of cdk1 or an active form of cdk1 could lead to an increase in centrosome duplication, as the increased activity of the cdc25 family members would remove the inhibitory phosphates from the over-expressed cdk1. However, the increase in centrosome number upon loss of 14-3-3γ is dependent on the expression of cyclin B, as suggested by the data in Fig. 2, suggesting that the effects we observe are dependent on cdk1.

Our work also demonstrates that in addition to regulating cdc25C function, 14-3-3γ also binds to other centrosomal or centrosome associate proteins that regulate centrosome function. It is also possible that the interaction of 14-3-3γ with centrosomal proteins prevents their phosphorylation by cdks, thus preventing centrosome amplification (Fig. 7a). These results suggest the probable existence of other mechanisms by which 14-3-3γ regulates centrosome duplication and biogenesis by regulating PLK4/Sas-6 mediated centriole cartwheel formation[83,84], or regulating the assembly of pericentriolar matrix[85,86], or the formation of γ-Tubulin-ring complex to regulate microtubule nucleation[19]. Further work is required to clarify the mechanisms by which 14-3-3 proteins regulate centrosome biogenesis, as 14-3-3 proteins are broad-spectrum phospho-Ser/Thr-binding adaptor proteins that act as signal integration nodes for multiple biochemical pathways[29].

Multipolar cell divisions are rare and multipolar spindles are often unstable short-lived intermediates. Tumor cells have evolved mechanisms to induce centrosome clustering leading to the formation of a pseudo-bipolar

spindle during mitosis. Pseudo-bipolar mitoses result in the formation merotelic chromosome attachments leading to a favorable aneuploidy and acquisition of the neoplastic phenotype[61]. However, a hypothesis that is being currently promulgated in the literature suggests that promoting excessive genetic instability could be a potential target for anti-tumor therapeutics[61,87], as tumor cells are programmed to be genetically unstable due to the inactivation of checkpoint pathways [reviewed in[88–90]]. Thus, exploiting the addiction to genetic instability could result in increased cell death even in tumors that are normally resistant to several cytotoxic agents used in cancer therapy. Our work demonstrates that rather than inhibiting cdk1 activity, a novel way of inhibiting tumor growth might be the premature activation of cdk1 in interphase cells. This is in contrast to the paradigm generally accepted in the literature where several studies have attempted to use inhibitors of the cell-cycle kinases to inhibit tumor growth, an approach that has not achieved significant success. While our observation is based on data generated in a xenograft mouse model that lacks an intact immune system, similar experiments could not be performed in mouse genetic models as mouse cdc25C lacks the 14-3-3 binding site and does not form a complex with 14-3-3 proteins (our unpublished data). However, given the data suggesting that over-expression of B cyclins in the mouse results in tumor progression[26] and the number of papers suggesting that cyclin B is over-expressed in human tumors as compared to normal tissue[91–96], we believe that our data suggesting that the premature activation of cdk1 is a potent way of killing tumor cells, certainly has broad significance for the field of tumor therapeutics (Fig. 7b).

Overall, this study provides a conceptual framework to understand the role of 14-3-3 proteins in centrosome duplication by regulating the activity of cdc25C, cdk1 and NPM1. Our work also indicates the future possibility of development of therapeutic methods to reduce tumor growth by targeting the disruption of 14-3-3-cdc25C complex in the interphase cells, without affecting normal cells. The novel molecular basis of 14-3-3-mediated centrosome duplication and harnessing this concept to inhibit centrosome-clustering and subsequent tumor reduction opens the door towards understanding the regulation of centrosome biogenesis by myriad roles of 14-3-3 proteins, and creating novel avenues for preventing tumor growth by centrosome de-clustering.

Materials and Methods

Ethics Statement. Maintenance of the animal facility is as per the national guidelines provided by the Committee for the Purpose of Control and Supervision of the Experiments on Animals (CPCSEA), Ministry of Environment and Forest, Government of India. All the experiments in this manuscript have been carried out according to the approved guidelines. The animals were housed in a controlled environment with the temperature and relative humidity being maintained at 23 ± 2 °C and 40–70% respectively and a day night cycle of 12 hrs each (7:00 to 19:00 light; 19:00 to 7:00 dark). The animals were received an autoclaved balanced diet prepared in-house as per the standard formula and sterile water *ad libitum*. Mice were housed in the Individually Ventilated Cage (IVC) system (M/S Citizen, India) provided with autoclaved corn cob bedding material (Natgrit 406) procured from Natural Organics, Satara, MS, India. Protocols for the experiments were approved by the Institutional Animal Ethics Committee (IAEC) of the Advanced Centre for Treatment Research and Education in Cancer (ACTREC). The animal study proposal number is 11/2008 dated August 19, 2008.

Cell culture and transfections. HCT116, U-2OS and HEK293 cells and the HCT116 derived vector control and 14-3-3γ-knockdown cells were cultured as described[31]. Cells were transfected with lipofectamine-LTX (Invitrogen) according to the manufacturer's instructions. HCT116 cells transfected with the pTRIPZ constructs expressing either WT cdc25C or S216A were maintained in media containing 1 μg/ml of puromycin. Expression of cdc25C was induced by adding doxycycline to the medium at a concentration of 2 μg/ml. To perform the rescue experiments GFP14-3-3γ-R (shRNA resistant 14-3-3γ cDNA) was transfected into 14-3-3γ-knockdown cells and subsequently the cells expressing GFP construct were sorted using flow cytometry as described[97]. Centrosome number was determined as described below.

Estimation of centrosome and spindle pole number, and determination of centrosome clustering and multi-polarity. To enrich cells in mitosis, the 14-3-3γ-knockdown and vector control cells were synchronized using 400 μM mimosine for 20 hours as described[98], released and fixed with 4% para-formaldehyde after 12–14 hours, to allow them to enter mitosis. To determine the percentage of cells containing more than two centrosomes or spindle poles, centrosomes or spindle poles of 100 mitotic cells were counted from three independent experiments. As over-expression of cdc25C or cdc25C-S216A in 14-3-3γ-knockdown cell causes death in culture gradually after 48 hours of expression, centrosome counts were performed immediately after 48 hours of transfection. The spindle poles from 100(x3) mitotic cells were counted in 3 independent experiments to determine the number of cells with pseudo-bipolar, multi-polar or truly bipolar spindles.

Immunofluorescence, FRET analysis and confocal microscopy. To determine the localization of proteins, different cell types were grown on glass cover slips. Cells were transfected with combinations of fluorescence proteins or labeled with fluorophore-conjugated antibodies. Cells were fixed with 4% para-formaldehyde and permiabilized with 0.3% tritonX-100. 0.05% DAPI was used to stain nuclei. Argon, Helium/Neon and diode lasers were used to capture images on a Carl Zeiss LSM 510 Meta confocal microscope. Images were captured under the oil immersion objectives of LSM510 meta (Carl Zeiss) confocal microscope, at 630X or 1000X magnification with 2X to 4X digital zoom. All the images were captured after background nullification with secondary antibodies. Images were processed using the LSM510 software. FRET measurements were performed using the sensitized emission method in fixed cells using samples: Donor only (GFP or Alexa-Fluor-488), Acceptor only (dsRed or Alexa-Fluor-546) and FRET sample. Following images were acquired for FRET corrections and efficiency calculations: (1) Acceptor Only using Acceptor filter set. (2) Acceptor Only using FRET filter set. (3) Donor Only using Donor filter set. (4) Donor Only using FRET filter set. (5) FRET Specimen Only using FRET

Oligonucleotide	Sequence
cdk1a	CCGGATGGGGATTCAGAAATTGATCAGTTCTCGATCAATTTCTGAATCCCCATTTTTTTC
cdk1b	TCGAGAAAAAAATGGGGATTCAGAAATTGATCGAGAACTGATCAATTTCTGAATCCCCAT
cdk2a	CCGGAGCTGTGGACATCTGGAGCCTAGTTCTCAGGCTCCAGATGTCCACAGCTTTTTTTC
cdk2b	TCGAGAAAAAAAGCTGTGGACATCTGGAGCCTGAGAACTAGGCTCCAGATGTCCACAGCT
14-3-3β Fwd	GGTATCTTTCTGAAGTGGC
14-3-3β Rev	GCTACAGGCCTTTTC
14-3-3γFwd	GAGCCACTGTCGAATG
14-3-3γ Rev	CGCTGCAATTCTTGATC
14-3-3σ Fwd	GCAGCCTTCATGAAAG
14-3-3σ Rev	CCCTTCATCTTCAGGTAG
14-3-3ζ Fwd	GTTCTTGATCCCCAATGC
14-3-3ζ Rev	CTCTGGGGAGTTCAGAATC
GAPDH Fwd	TGCATCCTGCACCACCAACT
GAPDH Rev	CGCCTGCTTCACCACCTTC
Cdc25C-1a (shRNA)	CCGGTGAAGAGAATAATCATCGTGTTTTCAAGAGAAACACGATGATTATTCTCTTCTTTTTC
Cdc25C-1b (shRNA)	TCGAGAAAAAGAAGAGAATAATCATCGTGTTTCTCTTGAAAACACGATGATTATTCTCTTCA
Cdc25B-1a (shRNA)	CCGGTAATCCTCCCTGTCGTCTGAATTTCAAGAGAATTCAGACGACAGGGAGGATTTTTTTC
Cdc25B-1b (shRNA)	TCGAGAAAAAAATCCTCCCTGTCGTCTGAATTCTCTTGAAATTCAGACGACAGGGAGGATTA
Cdc25A-1a (shRNA)	CCGGTAGCAACCACTGGAGGTGAAGTTCAAGAGACTTCACCTCCAGTGGTTGCTTTTTTC
Cdc25A-1b (shRNA)	TCGAGAAAAAAGCAACCACTGGAGGTGAAGTCTCTTGAACTTCACCTCCAGTGGTTGCTA

Table 1. Sequences of oligonucleotide primers. Sequences of oligonucleotide primers used for designing shRNA constructs and performing RT-PCR assays.

filter set. All the images were captured at X630 magnification in 12-bit format using Zeiss LSM 510 Meta confocal laser scanning microscope. The images were acquired using following lasers: Donor excitation using 488 nm Argon laser line while acceptor excitation using 543 nm Helium Neon laser line. Images acquired were further processed using LSM 510 image examiner software. The nomenclature and equations for FRET calculations are as previously described[43] and the FRET protocol was obtained from the Centre for Optical Instrumentation laboratory, Wellcome Trust Centre, University of Edinburg[99]. FRET Corrections: (i) Acceptor in FRET channel (Co-efficient A) = Average intensity of Acceptor only using FRET set/Average intensity of Acceptor only using acceptor set. (ii) Donor in FRET channel (Co-efficient B) = Average intensity of Donor only using FRET filter set/Average intensity of Donor only using Donor filter set. (iii) Average FRET efficiency = FRET Specimen − (A * FRET Specimen using Acceptor filter set) − (B * FRET Specimen using Donor filter set) * 100.

Electron microscopy. To study centrosome amplification and organization in higher magnification 14-3-3γ-knockdown and vector-control cells were visualized under transmission electron microscope. Synchronized cells in S-phase were fixed with 3% glutaraldehyde, washed with 0.1 M of sodium cacodylate and post fixed with 1% osmium tetra oxide (Tedpella). Cultures were dehydrated and processed. Grids were contrasted with alcoholic uranyl acetate for 1 minute and lead citrate for half a minute. The grids were observed under a Carl Zeiss LIBRA120 EFTEM transmission electron microscope, at an accelerating voltage of 120KV and at 25000X magnification. Images were captured using a Slow Scan CCD camera (TRS, Germany).

Preparation of metaphase plates. Cells were arrested in mitosis by growing them in Colcemid (0.1 μg/ml) for 2 hours and were incubated in a hypotonic solution (0.075 M KCl) for 15–25 minutes at 37 °C. Metaphase spreads were generated by dropping the cells from a height on frosted glass slides and chromosomes were stained with Giemsa and imaged under 100X objective of the AxioImager Z1 upright microscope (Carl Zeiss).

Soft Agar Assays. Soft agar assays for the 14-3-3γ-knockdown and vector-control cells were performed as previously described[100]. To determine whether cdc25C over-expression led to a decrease in transformation, the 14-3-3γ-knockdown cells were transfected with doxycycline inducible constructs for EGFP, EGFP-cdc25C and EGFP-S216A. Transfected cells were selected in 0.5 μg/ml puromycin. 72 hours post selection, the cells were harvested by trypsinization and 10,000 cells plated in soft agar containing puromycin at a concentration of 0.5 μg/ml in the presence or absence of 2 μg/ml doxycycline in triplicate. The remaining cells were cultured in regular media containing puromycin at a concentration of 0.5 μg/ml in the presence or absence of 2 μg/ml doxycycline. The cells were harvested and protein extracts were prepared as described[27] and resolved on SDS-PAGE gels for Western blot analysis with antibodies to GFP.

Tumour formation in immunocompromised mice. For the present study, we used NOD.CB17-*Prkdc*^{scid}/NCrCrl (NOD-SCID mice) or BALB/c Nude mice (CAnN.Cg-*Foxn1nu*/Crl). The foundation stock of the immuno-compromised mice was procured from Charles River Laboratories, Willington, USA. All animal studies were approved by the Institutional Animal Ethics committee (IAEC) constituted under the guidelines of the CPCSEA, Government of India. 10^6 HCT116 derived 14-3-3γ-knockdown and vector-control cells were re-suspended in DMEM medium without serum and injected subcutaneously in the dorsal flank of 6–8 weeks

old NOD-SCID mice (obtained from ACTREC animal house facility). Five mice were injected for each clone. Tumor formation was monitored at intervals of 2–3 days and tumor size was measured by Vernier calipers. Tumor volume (mm^3) was calculated by the formula ½ LV^2 where L is the largest dimension and V its perpendicular dimension, as previously reported[100]. For the tumor reversal experiment, nude mice were injected with 10^6 cells and tumor volumes measure as mentioned above. One set of mice were given 2 mg/ml dox + 5% sucrose in drinking water (protected from light). The water was changed every 3 days.

Plasmids and constructs. The shRNA constructs targeting 14-3-3ε and 14-3-3γ and the shRNA resistant 14-3-3γ cDNA were described previously[31,101]. Published shRNA sequences for cdc25C[102], cdc25B[103], cdc25A[104], cdk1[105] and cdk2[106] (Table 1) were cloned in pTU6IIA[100] digested with AgeI and XhoI (New England Biolabs). The 5′ and 3′ oligonucleotides were annealed and phosphorylated at both the ends using T4 polynucleotide kinase (Fermentas). Oligos were designed in such a way that AgeI and XhoI restriction sites remained at the two termini. The annealed oligos were cloned into the pTU6 vector digested with AgeI and XhoI The shRNA cassettes was excised with EcoRI and XhoI and cloned into pEGFP-f (Clontech). The GFP-centrin construct[107], the cdk1 expression constructs[108] and the CFP-lamin construct[109] have been described previously. DsRed-14-3-3γ was generated by removing stop-codon from 14-3-3γ cDNA by PCR and cloned between Nhe1 and BamH1 of the pDsRedN1 vector (Clontech). Cdc25C and cdc25C-S216A mutant were cloned into pEGFPN1 (Clontech) and subsequently sub-cloned as EGFP fusions into pTRIPZ (Open Biosystems). WT NPM1 was cloned into the HindIII/XbaI sites of the pFLAG-CMV2 vector and the T199A and T199D mutants were generated by site-directed mutagenesis (Stratagene). Reverse transcriptase coupled polymerase chain reactions (RT-PCR) for the different 14-3-3 genes or GAPDH as a loading control were performed as described[100].

Antibodies. Primary antibodies for 14-3-3γ (CG31; Abcam ab76525; dilution 1:2500), 14-3-3ε (T16; Santacruz sc1020; dilution 1:1000), 14-3-3σ (CS112 tissue culture supernatant 1:50), β-actin (Sigma A5316; dilution 1:5000), GFP (Clontech 632375; dilution 1:15,000), NPM1 (Invitrogen 325200; dilution 1:5000), phospho-T199 NPM1 (Abcam ab81551; dilution 1:2000), Aurora A (Invitrogen 458900, dilution 1:1000), p-T288 Aurora A (Cell signaling technology 3079, dilution 1:1000) and h-Sas6 ([110] dilution 1:3000) were used for Western blot experiments. The secondary goat anti-mouse HRP (Pierce) and goat anti-rabbit HRP (Pierce) antibodies were used at a dilution of 1:2500 for Western blot analysis. Primary antibodies for Cep-170 (Invitrogen 41-3200; dilution 1:50), γ-Tubulin (Sigma T3559; dilution 1:200), α-tubulin (Abcam ab7291; dilution 1:500), centrin1 (Abcam ab11257; dilution 1:50), Ninein (Abcam ab4447; dilution 1:50), 14-3-3γ (CG31; Abcam ab76525; dilution 1:200) antibodies were used for immunofluorescence. Secondary antibodies (conjugated with Alexafluor-568, Alexafluor-546, Alexafluor-455 from Molecular probes, Invitrogen; dilution 1:100) were used for immunofluorescence studies.

Cell cycle analysis. To determine the time point of centrosome duplication, 14-3-3γ-knockdown and vector-control cells were arrested at G1/S boundary and released at different intervals afterwards. Cells were synchronized at G1/S phase by 400 μMM mimosine for 20 hours[98]. Cells were washed twice with PBS and then fed with complete medium. Cells were harvested by trypsinization at 0, 2, 4, 6, 8 and 10 hours post release, fixed with 100% ethanol and stained with propidium iodide (Sigma) and the cell cycle profiles were acquired on a FACS Calibur (BD Biosciences) and analyzed using MODFIT software[31]. Protein extracts prepared from another aliquot of cells were used to determine the levels of CyclinB1, 14-3-3γ and actin by Western blot analysis. At each time point, cells were stained with antibodies to centrosome proteins and centrosome number determined as described above.

MALDI-TOF/TOF mass spectrometry. Lysates 14-3-3γ-knockdown and vector-control cells were used in GST-pulldown using GST-14-3-3γ (pGEX-3X, GE) as bait. Pulldown fractions were resolved in 6–12% gradient SDS-PAGE and gels were visualized by colloidal coomassie stain (PAGE blue, Fermentas). Bands of differential intensities were excised and treated with 30 mM potassium ferricyanide and 100 mM sodium thiosulfate solution. The gel pieces were reduced with 10 mM DTT. Rehydrated and reduced gel pieces were trypsinized in 20 μg/ml Trypsin (proteomics grade, Sigma, 5266) in 25 mM ammonium bicarbonate at 37 °C overnight. Extraction of the in-gel digested peptides was performed with 5% v/v trifluoro acetic acid in 50% v/v acetonitrile. 1 μl of recovered peptides and 1 μl of peptide matrix solution (20 mg/ml HCCA in 0.1% v/v TFA in 50% v/v acetonitrile) were spotted onto sample target plate. External calibration was prepared by mixing peptide standard mixture and peptide matrix solution similarly. Mass spectra were acquired by MALDI-TOF/TOF mass spectrometer (Bruker Daltonics, Ultraflex II) on reflector ion positive mode. MASCOT database search engine (version 2.2.03) was used for comparing peptide masses with those in NCBInr protein database (database version: NCBInr_20080812.fasta) in *Homo sapiens*. Searches were carried out with trypsin digestion, one missed cleavage, fixed carbamidomethylation of cysteine residues and optional oxidation of methionine with 100-ppm mass tolerance for mono-isotopic peptide masses.

***In vitro* kinase assays.** The cdk1/cyclinB1 enzyme was purchased from ProQinase. 1 μg of bacterially expressed recombinant WT NPM1-his_6 or T199A-NPM1-his_6 was incubated along with about 4 ng of cdk1/cyclinB1 enzyme in a 20 μl reaction mixture containing 50 mM Tris-HCl, 100 mM NaCl, 0.1 mM EGTA, 10 mM $MgCl_2$, 0.2% β-mercaptoethanol, and [γ-^{32}P] ATP. The reaction mixture was resolved on a 12% SDS-PAGE and autoradiography was performed.

MTT assays. To determine the viability of vector control and 14-3-3γ-knockdown cells expressing cdc25C or cdc25C-S216A, the colorimetric MTT metabolic activity assay was performed. The control and knockdown

cells were transfected with doxycycline inducible (and Puromycin resistant) EGFP, EGFP-cdc25C WT and EGFP-cdc25C-S216A constructs. 24 hours post transfection, cells were washed with PBS and fed with fresh media containing selection antibiotic (DMEM + Puromycin). 60 hours post selection, 2000 cells of each lines were seeded in 96-well microtiter plate. After the cells had adhered (~24 hours), media was changed to DMEM + Puromycin + Doxycycline, in order to induce the expression of cdc25C. The day of addition of doxycycline was considered as day 0 and the MTT assay was performed across 6 days. For the MTT assay, 20 μL of 5 μg/mL MTT [3-(4,5-Dimethylthiazol-2-yl)-2,5-Diphenyltetrazolium Bromide)] reagent was added to each well. 4 hours post addition of MTT, 100 μL of 10% SDS in HCl was added to the wells and incubated overnight. Absorbance of each well was measured at 540 nm/690 nm to assess viability. Percentage of cell viability is depicted as relative to that of day 0.

References

1. Fu, J., Hagan, I. M. & Glover, D. M. The centrosome and its duplication cycle. *Cold Spring Harb Perspect Med* **5,** a015800 (2015).
2. Mennella, V. *et al.* Subdiffraction-resolution fluorescence microscopy reveals a domain of the centrosome critical for pericentriolar material organization. *Nat Cell Biol* **14,** 1159–1168, doi: 10.1038/ncb2597 (2012).
3. Nigg, E. A. & Stearns, T. The centrosome cycle: Centriole biogenesis, duplication and inherent asymmetries. *Nat Cell Biol* **13,** 1154–1160, doi: 10.1038/ncb2345 (2011).
4. Cunha-Ferreira, I. *et al.* The SCF/Slimb ubiquitin ligase limits centrosome amplification through degradation of SAK/PLK4. *Current biology: CB* **19,** 43–49, doi: 10.1016/j.cub.2008.11.037 (2009).
5. Godinho, S. A. *et al.* Oncogene-like induction of cellular invasion from centrosome amplification. *Nature* **510,** 167–171, doi: 10.1038/nature13277 (2014).
6. Ogden, A. *et al.* Quantitative multi-parametric evaluation of centrosome declustering drugs: centrosome amplification, mitotic phenotype, cell cycle and death. *Cell Death Dis* **5,** e1204, doi: 10.1038/cddis.2014.164 (2014).
7. Vitale, I., Galluzzi, L., Castedo, M. & Kroemer, G. Mitotic catastrophe: a mechanism for avoiding genomic instability. *Nat Rev Mol Cell Biol* **12,** 385–392, doi: 10.1038/nrm3115 (2011).
8. Mardin, B. R. & Schiebel, E. Breaking the ties that bind: new advances in centrosome biology. *J Cell Biol* **197,** 11–18, doi: 10.1083/jcb.201108006 (2012).
9. Fang, G. *et al.* Centlein mediates an interaction between C-Nap1 and Cep68 to maintain centrosome cohesion. *J Cell Sci* **127,** 1631–1639, doi: 10.1242/jcs.139451 (2014).
10. Hardy, T. *et al.* Multisite phosphorylation of C-Nap1 releases it from Cep135 to trigger centrosome disjunction. *J Cell Sci* **127,** 2493–2506, doi: 10.1242/jcs.142331 (2014).
11. Adon, A. M. *et al.* Cdk2 and Cdk4 regulate the centrosome cycle and are critical mediators of centrosome amplification in p53-null cells. *Mol Cell Biol* **30,** 694–710, doi: 10.1128/MCB.00253-09 (2010).
12. Colombo, E., Alcalay, M. & Pelicci, P. G. Nucleophosmin and its complex network: a possible therapeutic target in hematological diseases. *Oncogene* **30,** 2595–2609, doi: 10.1038/onc.2010.646 (2011).
13. Cuomo, M. E. *et al.* p53-Driven apoptosis limits centrosome amplification and genomic instability downstream of NPM1 phosphorylation. *Nat Cell Biol* **10,** 723–730, doi: 10.1038/ncb1735 (2008).
14. Ling, H., Hanashiro, K., Luong, T. H., Benavides, L. & Fukasawa, K. Functional relationship among PLK2, PLK4 and ROCK2 to induce centrosome amplification. *Cell Cycle* **14,** 544–553, doi: 10.4161/15384101.2014.989121 (2015).
15. Mbom, B. C., Nelson, W. J. & Barth, A. beta-catenin at the centrosome: discrete pools of beta-catenin communicate during mitosis and may co-ordinate centrosome functions and cell cycle progression. *Bioessays* **35,** 804–809, doi: 10.1002/bies.201300045 (2013).
16. Tokuyama, Y., Horn, H. F., Kawamura, K., Tarapore, P. & Fukasawa, K. Specific phosphorylation of nucleophosmin on Thr(199) by cyclin-dependent kinase 2-cyclin E and its role in centrosome duplication. *J Biol Chem* **276,** 21529–21537, doi: 10.1074/jbc.M100014200 (2001).
17. Guichard, P. *et al.* Native architecture of the centriole proximal region reveals features underlying its 9-fold radial symmetry. *Current biology: CB* **23,** 1620–1628, doi: 10.1016/j.cub.2013.06.061 (2013).
18. Guillet, V. *et al.* Crystal structure of gamma-tubulin complex protein GCP4 provides insight into microtubule nucleation. *Nature structural & molecular biology* **18,** 915–919, doi: 10.1038/nsmb.2083 (2011).
19. Kollman, J. M., Merdes, A., Mourey, L. & Agard, D. A. Microtubule nucleation by gamma-tubulin complexes. *Nat Rev Mol Cell Biol* **12,** 709–721, doi: 10.1038/nrm3209 (2011).
20. Fong, C. S., Kim, M., Yang, T. T., Liao, J. C. & Tsou, M. F. SAS-6 assembly templated by the lumen of cartwheel-less centrioles precedes centriole duplication. *Dev cell* **30,** 238–245, doi: 10.1016/j.devcel.2014.05.008 (2014).
21. Blangy, A. *et al.* Phosphorylation by p34cdc2 regulates spindle association of human Eg5, a kinesin-related motor essential for bipolar spindle formation *in vivo*. *Cell* **83,** 1159–1169 (1995).
22. Carter, S. L., Eklund, A. C., Kohane, I. S., Harris, L. N. & Szallasi, Z. A signature of chromosomal instability inferred from gene expression profiles predicts clinical outcome in multiple human cancers. *Nat Genet* **38,** 1043–1048, doi: 10.1038/ng1861 (2006).
23. Crasta, K., Huang, P., Morgan, G., Winey, M. & Surana, U. Cdk1 regulates centrosome separation by restraining proteolysis of microtubule-associated proteins. *EMBO J* **25,** 2551–2563, doi: 10.1038/sj.emboj.7601136 (2006).
24. Grallert, A. & Hagan, I. M. Schizosaccharomyces pombe NIMA-related kinase, Fin1, regulates spindle formation and an affinity of Polo for the SPB. *EMBO J* **21,** 3096–3107, doi: 10.1093/emboj/cdf294 (2002).
25. Loffler, H. *et al.* Cep63 recruits Cdk1 to the centrosome: implications for regulation of mitotic entry, centrosome amplification, and genome maintenance. *Cancer Res* **71,** 2129–2139, doi: 10.1158/0008-5472.CAN-10-2684 (2011).
26. Nam, H. J. & van Deursen, J. M. Cyclin B2 and p53 control proper timing of centrosome separation. *Nat Cell Biol* **16,** 538–549, doi: 10.1038/ncb2952 (2014).
27. Dalal, S. N., Schweitzer, C. M., Gan, J. & DeCaprio, J. A. Cytoplasmic localization of human cdc25C during interphase requires an intact 14-3-3 binding site. *Mol Cell Biol* **19,** 4465–4479 (1999).
28. Peng, C. Y. *et al.* Mitotic and G2 checkpoint control: regulation of 14-3-3 protein binding by phosphorylation of Cdc25C on serine-216. *Science* **277,** 1501–1505 (1997).
29. Yaffe, M. B. How do 14-3-3 proteins work? - Gatekeeper phosphorylation and the molecular anvil hypothesis. *FEBS Letters* **513,** 53–57 (2002).
30. Tsou, M. F. & Stearns, T. Controlling centrosome number: licenses and blocks. *Curr Opin Cell Biol* **18,** 74–78, doi: 10.1016/j.ceb.2005.12.008 (2006).
31. Hosing, A. S., Kundu, S. T. & Dalal, S. N. 14-3-3 Gamma is required to enforce both the incomplete S phase and G2 DNA damage checkpoints. *Cell Cycle* **7,** 3171–3179 (2008).
32. Chan, J. Y. A clinical overview of centrosome amplification in human cancers. *Int J Biol Sci* **7,** 1122–1144 (2011).
33. Castiel, A. *et al.* The Stil protein regulates centrosome integrity and mitosis through suppression of Chfr. *J. Cell Sci* **124,** 532–539, doi: 10.1242/jcs.079731 (2011).
34. Moudjou, M., Bordes, N., Paintrand, M. & Bornens, M. gamma-Tubulin in mammalian cells: the centrosomal and the cytosolic forms. *J Cell Sci* **109** (Pt 4), 875–887 (1996).

35. Mogensen, M. M., Malik, A., Piel, M., Bouckson-Castaing, V. & Bornens, M. Microtubule minus-end anchorage at centrosomal and non-centrosomal sites: the role of ninein. *J Cell Sci* **113** (Pt 17), 3013–3023 (2000).
36. Guarguaglini, G. *et al.* The forkhead-associated domain protein Cep170 interacts with Polo-like kinase 1 and serves as a marker for mature centrioles. *Mol Biol Cell* **16,** 1095–1107, doi: 10.1091/mbc.E04-10-0939 (2005).
37. Tollenaere, M. A., Mailand, N. & Bekker-Jensen, S. Centriolar satellites: key mediators of centrosome functions. *Cell Mol Life Sci* **72,** 11–23, doi: 10.1007/s00018-014-1711-3 (2015).
38. Rosario, C. O. *et al.* Plk4 is required for cytokinesis and maintenance of chromosomal stability. *Proc Natl Acad Sci USA* **107,** 6888–6893, doi: 10.1073/pnas.0910941107 (2010).
39. Godinho, S. A. & Pellman, D. Causes and consequences of centrosome abnormalities in cancer. *Philosophical transactions of the Royal Society of London. Series B, Biological sciences* **369,** doi: 10.1098/rstb.2013.0467 (2014).
40. Hut, H. M. *et al.* Centrosomes split in the presence of impaired DNA integrity during mitosis. *Mol Biol Cell* **14,** 1993–2004, doi: 10.1091/mbc.E02-08-0510 (2003).
41. Hatch, E. M., Fischer, A. H., Deerinck, T. J. & Hetzer, M. W. Catastrophic nuclear envelope collapse in cancer cell micronuclei. *Cell* **154,** 47–60, doi: 10.1016/j.cell.2013.06.007 (2013).
42. Tucker, J. D. & Preston, R. J. Chromosome aberrations, micronuclei, aneuploidy, sister chromatid exchanges, and cancer risk assessment. *Mutation Res* **365,** 147–159 (1996).
43. Gordon, G. W., Berry, G., Liang, X. H., Levine, B. & Herman, B. Quantitative fluorescence resonance energy transfer measurements using fluorescence microscopy. *Biophysical J* **74,** 2702–2713, doi: 10.1016/S0006-3495(98)77976-7 (1998).
44. Yang, X. *et al.* Structural basis for protein-protein interactions in the 14-3-3 protein family. *Proc Natl Acad Sci USA* **103,** 17237–17242, doi: 10.1073/pnas.0605779103 (2006).
45. Moritz, M. & Agard, D. A. Gamma-tubulin complexes and microtubule nucleation. *Curr Opin Struct Biol* **11,** 174–181 (2001).
46. McNally, K. L. *et al.* Kinesin-1 prevents capture of the oocyte meiotic spindle by the sperm aster. *Dev Cell* **22,** 788–798, doi: 10.1016/j.devcel.2012.01.010 (2012).
47. Splinter, D. *et al.* Bicaudal D2, dynein, and kinesin-1 associate with nuclear pore complexes and regulate centrosome and nuclear positioning during mitotic entry. *PLoS Biol* **8,** e1000350, doi: 10.1371/journal.pbio.1000350 (2010).
48. Peng, C. Y. *et al.* C-TAK1 protein kinase phosphorylates human Cdc25C on serine 216 and promotes 14-3-3 protein binding. *Cell Growth Differ* **9,** 197–208 (1998).
49. Dalal, S. N., Yaffe, M. B. & DeCaprio, J. A. 14-3-3 family members act coordinately to regulate mitotic progression. *Cell Cycle* **3,** 672–677 (2004).
50. Bonnet, J., Coopman, P. & Morris, M. C. Characterization of centrosomal localization and dynamics of Cdc25C phosphatase in mitosis. *Cell Cycle* **7,** 1991–1998, doi: 6095 (2008).
51. Busch, C. *et al.* The G2/M checkpoint phosphatase cdc25C is located within centrosomes. *The international journal of biochemistry & cell biology* **39,** 1707–1713, doi: 10.1016/j.biocel.2007.04.022 (2007).
52. Jackman, M., Lindon, C., Nigg, E. A. & Pines, J. Active cyclin B1-Cdk1 first appears on centrosomes in prophase. *Nat Cell Biol* **5,** 143–148, doi: 10.1038/ncb918 (2003).
53. Kramer, A., Lukas, J. & Bartek, J. Checking out the centrosome. *Cell Cycle* **3,** 1390–1393 (2004).
54. Conklin, D. S., Galaktionov, K. & Beach, D. 14-3-3 proteins associate with cdc25 phosphatases. *Proc Natl Acad Sci USA* **92,** 7892–7896 (1995).
55. Mils, V. *et al.* Specific interaction between 14-3-3 isoforms and the human CDC25B phosphatase. *Oncogene* **19,** 1257–1265, doi: 10.1038/sj.onc.1203419 (2000).
56. Deibler, R. W. & Kirschner, M. W. Quantitative reconstitution of mitotic CDK1 activation in somatic cell extracts. *Mol Cell* **37,** 753–767, doi: 10.1016/j.molcel.2010.02.023 (2010).
57. Krek, W. & Nigg, E. A. Mutations of p34cdc2 phosphorylation sites induce premature mitotic events in HeLa cells: evidence for a double block to p34cdc2 kinase activation in vertebrates. *EMBO J* **10,** 3331–3341 (1991).
58. Okuda, M. *et al.* Nucleophosmin/B23 is a target of CDK2/cyclin E in centrosome duplication. *Cell* **103,** 127–140 (2000).
59. Peter, M., Nakagawa, J., Doree, M., Labbe, J. C. & Nigg, E. A. Identification of major nucleolar proteins as candidate mitotic substrates of cdc2 kinase. *Cell* **60,** 791–801 (1990).
60. Zyss, D. & Gergely, F. Centrosome function in cancer: guilty or innocent? *Trends Cell Biol* **19,** 334–346, doi: 10.1016/j.tcb.2009.04.001 (2009).
61. Ganem, N. J., Godinho, S. A. & Pellman, D. A mechanism linking extra centrosomes to chromosomal instability. *Nature* **460,** 278–282, doi: 10.1038/nature08136 (2009).
62. Lingle, W. L., Lukasiewicz, K. & Salisbury, J. L. Deregulation of the centrosome cycle and the origin of chromosomal instability in cancer. *Adv Exp Med Biol* **570,** 393–421, doi: 10.1007/1-4020-3764-3_14 (2005).
63. Marthiens, V., Piel, M. & Basto, R. Never tear us apart--the importance of centrosome clustering. *J Cell Sci* **125,** 3281–3292, doi: 10.1242/jcs.094797 (2012).
64. Pannu, V. *et al.* Centrosome-declustering drugs mediate a two-pronged attack on interphase and mitosis in supercentrosomal cancer cells. *Cell Death Dis* **5,** e1538, doi: 10.1038/cddis.2014.505 (2014).
65. Gregoire, L. *et al.* Spontaneous malignant transformation of human ovarian surface epithelial cells *in vitro*. *Clin Cancer Res* **7,** 4280–4287 (2001).
66. Pronsato, L. *et al.* High passage numbers induce resistance to apoptosis in C2C12 muscle cells. *Biocell* **37,** 1–9 (2013).
67. Pannu, V. *et al.* HSET overexpression fuels tumor progression via centrosome clustering-independent mechanisms in breast cancer patients. *Oncotarget* **6,** 6076–6091 (2015).
68. Pietromonaco, S. F., Seluja, G. A., Aitken, A. & Elias, L. Association of 14-3-3 proteins with centrosomes. *Blood Cells Mol Dis* **22,** 225–237, doi: S1079-9796(96)90103-5 10.1006/bcmd.1996.0103 (1996).
69. Tallada, V. A., Bridge, A. J., Emery, P. A. & Hagan, I. M. Suppression of the Schizosaccharomyces pombe cut12.1 cell-cycle defect by mutations in cdc25 and genes involved in transcriptional and translational control. *Genetics* **176,** 73–83, doi: 10.1534/genetics.107.072090 (2007).
70. Tallada, V. A., Tanaka, K., Yanagida, M. & Hagan, I. M. The S. pombe mitotic regulator Cut12 promotes spindle pole body activation and integration into the nuclear envelope. *J Cell Biol* **185,** 875–888, doi: 10.1083/jcb.200812108 (2009).
71. Steere, N. *et al.* Centrosome amplification in CHO and DT40 cells by inactivation of cyclin-dependent kinases. *Cytoskeleton (Hoboken)* **68,** 446–458, doi: 10.1002/cm.20523 (2011).
72. Vidwans, S. J., Wong, M. L. & O'Farrell, P. H. Anomalous centriole configurations are detected in Drosophila wing disc cells upon Cdk1 inactivation. *J Cell Sci* **116,** 137–143 (2003).
73. Blangy, A. *et al.* Phosphorylation by p34cdc2 regulates spindle association of human Eg5, a kinesin-related motor essential for bipolar spindle formation *in vivo*. *Cell* **83,** 1159–1169 (1995).
74. Löffler, H. *et al.* Cep63 recruits Cdk1 to the centrosome: implications for regulation of mitotic entry, centrosome amplification, and genome maintenance. *Cancer Res* **71,** 2129–2139, doi: 10.1158/0008-5472.can-10-2684 (2011).
75. Zhang, B. *et al.* Never in mitosis gene A-related kinase 6 promotes cell proliferation of hepatocellular carcinoma via cyclin B modulation. *Oncology letters* **8,** 1163–1168, doi: 10.3892/ol.2014.2300 (2014).
76. Seki, A., Coppinger, J. A., Jang, C.-Y., Yates, J. R. & Fang, G. Bora and the kinase Aurora a cooperatively activate the kinase Plk1 and control mitotic entry. *Science* **320,** 1655–1658, doi: 10.1126/science.1157425 (2008).

77. Park, S.-Y. *et al.* Molecular basis for unidirectional scaffold switching of human Plk4 in centriole biogenesis. *Nature structural & molecular biology* **21,** 696–703, doi: 10.1038/nsmb.2846 (2014).
78. Joukov, V., Walter, J. C. & De Nicolo, A. The Cep192-organized aurora A-Plk1 cascade is essential for centrosome cycle and bipolar spindle assembly. *Mol Cell* **55,** 578–591, doi: 10.1016/j.molcel.2014.06.016 (2014).
79. Sonnen, K. F., Gabryjonczyk, A.-M., Anselm, E., Stierhof, Y.-D. & Nigg, E. A. Human Cep192 and Cep152 cooperate in Plk4 recruitment and centriole duplication. *J Cell Sci* **126,** 3223–3233, doi: 10.1242/jcs.129502 (2013).
80. Santos, S. D. M., Wollman, R., Meyer, T. & Ferrell, J. E. Spatial positive feedback at the onset of mitosis. *Cell* **149,** 1500–1513, doi: 10.1016/j.cell.2012.05.028 (2012).
81. Mailand, N. *et al.* Regulation of G(2)/M events by Cdc25A through phosphorylation-dependent modulation of its stability. *EMBO J* **21,** 5911–5920 (2002).
82. Lindqvist, A., Kallstrom, H., Lundgren, A., Barsoum, E. & Rosenthal, C. K. Cdc25B cooperates with Cdc25A to induce mitosis but has a unique role in activating cyclin B1-Cdk1 at the centrosome. *J Cell Biol* **171,** 35–45, doi: jcb.200503066 10.1083/jcb.200503066 (2005).
83. Avidor-Reiss, T. & Gopalakrishnan, J. Cell Cycle Regulation of the Centrosome and Cilium. *Drug Discov Today Dis Mech* **10,** e119–e124, doi: 10.1016/j.ddmec.2013.03.002 (2013).
84. Matsuzawa, A. *et al.* The BRCA1/BARD1-interacting protein OLA1 functions in centrosome regulation. *Mol cell* **53,** 101–114, doi: 10.1016/j.molcel.2013.10.028 (2014).
85. Woodruff, J. B., Wueseke, O. & Hyman, A. A. Pericentriolar material structure and dynamics. *Philosophical transactions of the Royal Society of London. Series B, Biological sciences* **369,** doi: 10.1098/rstb.2013.0459 (2014).
86. Woodruff, J. B. *et al.* Centrosomes. Regulated assembly of a supramolecular centrosome scaffold *in vitro*. *Science* **348,** 808–812, doi: 10.1126/science.aaa3923 (2015).
87. Janssen, A. & Medema, R. H. Genetic instability: tipping the balance. *Oncogene* **32,** 4459–4470, doi: 10.1038/onc.2012.576 (2013).
88. Nurse, P. Checkpoint pathways come of age. *Cell* **91,** 865–867 (1997).
89. Zhou, B. B. & Elledge, S. J. The DNA damage response: putting checkpoints in perspective. *Nature* **408,** 433–439, doi: 10.1038/35044005 (2000).
90. Nurse, P., Masui, Y. & Hartwell, L. Understanding the cell cycle. *Nat Med* **4,** 1103–1106, doi: 10.1038/2594 (1998).
91. Androic, I. *et al.* Targeting cyclin B1 inhibits proliferation and sensitizes breast cancer cells to taxol. *BMC cancer* **8,** 391, doi: 10.1186/1471-2407-8-391 (2008).
92. Gomez, L. A., de Las Pozas, A., Reiner, T., Burnstein, K. & Perez-Stable, C. Increased expression of cyclin B1 sensitizes prostate cancer cells to apoptosis induced by chemotherapy. *Mol cancer therapeutics* **6,** 1534–1543, doi: 10.1158/1535-7163.MCT-06-0727 (2007).
93. Gong, J., Ardelt, B., Traganos, F. & Darzynkiewicz, Z. Unscheduled expression of cyclin B1 and cyclin E in several leukemic and solid tumor cell lines. *Cancer Res* **54,** 4285–4288 (1994).
94. Huang, V. *et al.* Upregulation of Cyclin B1 by miRNA and its implications in cancer. *Nucleic acids research* **40,** 1695–1707, doi: 10.1093/nar/gkr934 (2012).
95. Shen, M. *et al.* Detection of cyclin b1 expression in g(1)-phase cancer cell lines and cancer tissues by postsorting Western blot analysis. *Cancer Res* **64,** 1607–1610 (2004).
96. Soria, J. C. *et al.* Overexpression of cyclin B1 in early-stage non-small cell lung cancer and its clinical implication. *Cancer Res* **60,** 4000–4004 (2000).
97. Khapare, N. *et al.* Plakophilin3 Loss Leads to an Increase in PRL3 Levels Promoting K8 Dephosphorylation, Which Is Required for Transformation and Metastasis. *Plos One* **7,** e38561, doi: 10.1371/journal.pone.0038561PONE-D-11-23082 (2012).
98. Krek, W. & DeCaprio, J. A. Cell synchronization. *Methods Enzymol* **254,** 114–124 (1995).
99. Flory, M. R., Carson, A. R., Muller, E. G. & Aebersold, R. An SMC-domain protein in fission yeast links telomeres to the meiotic centrosome. *Mol cell* **16,** 619–630, doi: 10.1016/j.molcel.2004.10.027 (2004).
100. Kundu, S. T. *et al.* Plakophilin3 downregulation leads to a decrease in cell adhesion and promotes metastasis. *Int J Cancer* **123,** 2303–2314, doi: 10.1002/ijc.23797 (2008).
101. Telles, E., Hosing, A. S., Kundu, S. T., Venkatraman, P. & Dalal, S. N. A novel pocket in 14-3-3epsilon is required to mediate specific complex formation with cdc25C and to inhibit cell cycle progression upon activation of checkpoint pathways. *Exp Cell Res* **315,** 1448–1457, doi: 10.1016/j.yexcr.2009.01.018 (2009).
102. Wei, S. *et al.* A critical role for phosphatase haplodeficiency in the selective suppression of deletion 5q MDS by lenalidomide. *Proc Natl Acad Sci USA* **106,** 12974–12979, doi: 10.1073/pnas.0811267106 (2009).
103. Lindqvist, A., Kallstrom, H. & Karlsson Rosenthal, C. Characterisation of Cdc25B localisation and nuclear export during the cell cycle and in response to stress. *J Cell Sci* **117,** 4979–4990, doi: 10.1242/jcs.01395 (2004).
104. Ray, D. *et al.* Hemizygous disruption of Cdc25A inhibits cellular transformation and mammary tumorigenesis in mice. *Cancer Res* **67,** 6605–6611, doi: 10.1158/0008-5472.CAN-06-4815 (2007).
105. Lindqvist, A., van Zon, W., Karlsson Rosenthal, C. & Wolthuis, R. M. Cyclin B1-Cdk1 activation continues after centrosome separation to control mitotic progression. *PLoS Biol* **5,** e123, doi: 10.1371/journal.pbio.0050123 (2007).
106. Molenaar, J. J. *et al.* Inactivation of CDK2 is synthetically lethal to MYCN over-expressing cancer cells. *Proc Natl Acad Sci USA* **106,** 12968–12973, doi: 10.1073/pnas.0901418106 (2009).
107. Piel, M., Nordberg, J., Euteneuer, U. & Bornens, M. Centrosome-dependent exit of cytokinesis in animal cells. *Science* **291,** 1550–1553, doi: 10.1126/science.291.5508.1550 (2001).
108. Hagting, A., Karlsson, C., Clute, P., Jackman, M. & Pines, J. MPF localization is controlled by nuclear export. *EMBO J.* **17,** 4127–4138 (1998).
109. Ivorra, C. *et al.* A mechanism of AP-1 suppression through interaction of c-Fos with lamin A/C. *Genes & Dev* **20,** 307–320, doi: 10.1101/gad.349506 (2006).
110. Tang, C. J., Fu, R. H., Wu, K. S., Hsu, W. B. & Tang, T. K. CPAP is a cell-cycle regulated protein that controls centriole length. *Nat Cell Biol* **11,** 825–831, doi: 10.1038/ncb1889 (2009).

Acknowledgements

The authors would like to thank M. Bornens for the gift of the GFP-Centrin construct, J. Pines for the cdk1 expression constructs, T. A. Wittmann for the mCherry-α-tubulin construct, J. Larner for the TripZ construct, V. A. Garcia for the GFP-LaminA and CFP-LaminA construct, Odile Mondesert for HA-cdc25B (pCDNA3-HA-cdc25B3-human) construct, Helen Piwnica-Worms for myc-cdc25A (pCDNA3-myc-cdc25A-human) construct, T. K. Tang for the h-Sas6 antibody and J. Joseph for the Aurora antibodies, V. Kailaje for help with microscopy and M. Mahimkar and A. Srikant for help with the metaphase plate analysis. We would also like to thank the ACTREC imaging faculty and the electron microscope facilities at ACTREC and TIFR. AM was supported by a fellowship from the University Grants Commission, Govt. of India and SB and ASH were supported by fellowships from the Council for Scientific and Industrial Research. The work was funded by grants from the Department of Biotechnology and ACTREC to SND.

Author Contributions

A.M. designed and performed all centrosome amplification, aneuploidy and clustering related experiments and wrote the paper. L.S. performed cdk1 knockdown and mouse tumor reversal experiments. A.B. carried out dual staining of centrosomes, MTT and anchorage independent growth assays. A.G. performed time-lapse centrosome duplication experiments. A.G. and L.B. performed electron microscopy of centrosomes. R.T. and R.B. performed mouse maintenance, injections, and surgeries. S.B. tested expression levels of 14-3-3 isoforms. K.B. cloned ds-Red 14-3-3γ. A.S.H. generated 14-3-3γ knockdown clones, counted mitotic index. P.S. conducted cdk1/NPM1 kinase assay. T.K.K. supervised NPM1 collaboration. S.N.D. supervised the entire project.

Additional Information

Supplementary information accompanies this paper at http://www.nature.com/srep

Competing financial interests: The authors declare no competing financial interests.

How to cite this article: Mukhopadhyay, A. *et al.* 14-3-3γ Prevents Centrosome Amplification and Neoplastic Progression. *Sci. Rep.* **6**, 26580; doi: 10.1038/srep26580 (2016).